Right Ventricular Physiology, Adaptation and Failure in Congenital and Acquired Heart Disease

Mark K. Friedberg
Andrew N. Redington
Editors

EXTRAS ONLINE

Springer

Right Ventricular Physiology, Adaptation and Failure in Congenital and Acquired Heart Disease

Mark K. Friedberg
Andrew N. Redington
Editors

Right Ventricular Physiology, Adaptation and Failure in Congenital and Acquired Heart Disease

Springer

Editors
Mark K. Friedberg
Paediatric Cardiology
Labatt Family Heart Center
Hospital for Sick Children
Toronto, Ontario
Canada

Andrew N. Redington
Heart Institute
Cincinnati Children's Hosp Med Center
Cincinnati, OH
USA

ISBN 978-3-319-67094-2 ISBN 978-3-319-67096-6 (eBook)
https://doi.org/10.1007/978-3-319-67096-6

Library of Congress Control Number: 2017960174

Printed on acid-free paper

This Springer imprint is published by Springer Nature
The registered company is Springer International Publishing AG
The registered company address is: Gewerbestrasse 11, 6330 Cham, Switzerland

Preface

The inspiration for 'Right Ventricular Physiology, Adaptation and Failure in Congenital and Acquired Heart Disease' stemmed from the 3rd International RV Symposium held in Toronto. Many of its authors were invited speakers in that symposium, and all are leaders in their areas of expertise.

Paediatric cardiologists and cardiovascular surgeons have been well aware of the importance of the right ventricle (RV) for many years, yet the RV is still sometimes characterised as the 'forgotten ventricle'. However, it is evident from the explosion of research in the past decade or two that the RV is 'coming of age' and its importance increasingly recognised. Indeed, there have been substantial advances in basic research, diagnosis and management of a diverse array of conditions that affect the RV, and although our understanding of the RV is far from complete, it is considerably more comprehensive than just a few years ago.

Despite these advances in knowledge, to date, there has not been a written framework that provides a comprehensive review of RV embryology, physiology, function, failure and disease. This text aims to fill that gap, with state-of-the-art contributions from thought leaders in the field. The book incorporates a wide variety of topics including chapters that relate to early development, molecular adaptation to stress, interactions between the right and left ventricles, imaging, RV failure, neonatal conditions, congenital heart disease, interventional management and surgery. We hope these will be of interest to a wide audience of professionals including basic scientists, neonatologists, intensive care physicians, paediatric cardiologists, surgeons, heart failure specialists and specialists in adult congenital heart disease.

It is our hope that this 'translational' approach will not only be new and informative but will place the RV at the centre of discussion and research across disciplines that will bridge between scientists and clinicians to enrich and advance our field for the betterment of our patients.

The saying 'it takes a village' is particularly appropriate when producing a book such as this. Many people deserve our gratitude in helping this book come to fruition, including colleagues at the Hospital for Sick Children in Toronto; family, friends and colleagues from across the globe; and Noreen Adatia and Elektra McDermott for their administrative support.

Toronto, ON, Canada — Mark K. Friedberg
Cincinnati, OH, USA — Andrew N. Redington

Contents

Contributors

Theo Arts Biomedical Engineering, Maastricht University Medical Center, Maastricht, The Netherlands

Lee Benson Paediatric Cardiology, Labatt Family Heart Center, Hospital for Sick Children, Toronto, ON, Canada

Daniel Bernstein Pediatric Cardiology, Lucile Packard Children's Hospital, Stanford University, Palo Alto, CA, USA

Christopher A. Caldarone Cardiovascular Surgery, The Hospital for Sick Children, Toronto, ON, Canada

Paul Delgado-Olguin Physiology and Experimental Medicine, Peter Gilgan Center for Research and Learning, The Hospital for Sick Children, Toronto, ON, Canada

Tammo Delhaas Biomedical Engineering, Maastricht University Medical Center, Maastricht, The Netherlands

Anne I. Dipchand Paediatric Cardiology, Labatt Family Heart Centre, Hospital for Sick Children, Toronto, ON, Canada

Adam L. Dorfman University of Michigan, Congenital Heart Center, Department of Pediatrics, C.S. Mott Children's Hospital, University of Michigan, Ann Arbor, MI, USA

Mark K. Friedberg Paediatric Cardiology, Labatt Family Heart Center Hospital for Sick Children, Toronto, ON, Canada

Lars Grosse-Wortmann Paediatric Cardiology, Labatt Family Heart Center, Hospital for Sick Children, Toronto, ON, Canada

Christoph Haller Cardiovascular Surgery, The Hospital for Sick Children, Toronto, ON, Canada

Nicholas E. Hobson Bioengineering, Children's Hospital Colorado, Aurora, CO, USA

Marina L. Hughes Paediatric Cardiology, Hospital for Sick Children, London, UK

Kendall S. Hunter Bioengineering, Children's Hospital Colorado, Aurora, CO, USA

Robert P. Jankov, MBBS, PhD, FRACP Neonatologist, Children's Hospital of Eastern Ontario (CHEO), The Ottawa Hospital, Ottawa, ON, Canada

Department of Pediatrics, University of Ottawa, Ottawa, ON, Canada

Senior Scientist, CHEO Research Institute, Ottawa, ON, Canada

Yvette Koeken Biomedical Engineering, Maastricht University Medical Center, Maastricht, The Netherlands

Joost Lumens Biomedical Engineering, Maastricht University Medical Center, Maastricht, The Netherlands

Jan Marek Paediatric Cardiology, Hospital for Sick Children, London, UK

Jacob Mathew Cardiology Transplant, Hospital for Sick Children, Toronto, ON, Canada

Luc L. Mertens Paediatric Cardiology, The Hospital for Sick Children, Toronto, ON, Canada

Seema Mital Pediatrics, The Hospital for Sick Children, Toronto, ON, Canada

Georgina Palau-Caballero Biomedical Engineering, Maastricht University Medical Center, Maastricht, The Netherlands

Sushma Reddy Paediatric Cardiology, Lucille Packard Children's Hospital, Stanford University, Palo Alto, CA, USA

Andrew N. Redington Heart Institute, Cincinnati Children's Hospital Medical Center, Cincinnati, OH, USA

S. Lucy Roche The Peter Munk Cardiac Center, University Health Network, Toronto Congenital Cardiac Center for Adults, Toronto, ON, Canada

Dietmar Schranz Pediatric Cardiology, Hesse Pediatric Heart Center, Frankfurt, Germany

Norman H. Silverman Division of Pediatric Cardiology, Stanford University, Stanford, CA, USA

Division of Pediatric Cardiology, University of California San Francisco, Palo Alto, CA, USA

Harsimran S. Singh Weill Cornell Medicine—New York Presbyterian Hospital, Internal Medicine and Pediatrics, New York, NY, USA

A. Keith Tanswell Neonatology, Translational Medicine, The Hospital for Sick Children, Toronto, ON, Canada

Victor Tsang Cardiothoracic Surgery, Hospital for Sick Children, London, UK

Norbert F. Voelkel Virginia Commonwealth University, Richmond, VA, USA

John Walmsley Biomedical Engineering, Maastricht University Medical Center, Maastricht, The Netherlands

Embryological Origins: How Does the Right Ventricle Form

1

Paul Delgado-Olguin

Abstract

The heart originates from a group of cardiac progenitor cells that form the cardiac tube, which develops into a complex four-chambered beating organ. Several tissues signal to stimulate cardiac progenitors to acquire cell fate and differentiate. The timing of differentiation of cardiac progenitors defines the first and second heart fields. The first heart field gives rise to the left ventricle. The second heart field, located anterior to the first heart field, is added to the cardiac tube to give rise mainly to the outflow tract and the right ventricle. Several epigenetic mechanisms including histone and DNA methylation stabilize the transcriptional programs controlling cardiac development.

Keywords

Cardiac development • Second heart field • Cardiac progenitors • Right ventricle • Cardiomyocyte differentiation • Transcriptional regulation

Introduction

The heart develops from cardiac progenitor cells that originate during gastrulation and which move through the primitive streak and emerge as a bilateral cardiac field that fuses in the embryonic midline to form the cardiac crescent and the heart tube later on. The cardiac tube, in which cardiac progenitors start differentiating into cardiomyocytes, serves as a scaffold for addition of cardiac progenitors through the arterial and venous poles. The cardiac tube undergoes complex morphogenetic movements including looping and septation that result in the division of the heart into chambers [1, 2]. Understanding how these processes occur has been the goal of very active research. Early experiments aimed at identifying the cells acting as the building blocks that form the heart identified the population of progenitors cells that are added to the cardiac tube

P. Delgado-Olguin
Translational Medicine, Peter Gilgan Center for Research and Learning, The Hospital for Sick Children, 686 Bay St Room 10-9715, Toronto, ON, Canada, M5G 0A4
e-mail: paul.delgadoolguin@sickkids.ca

M.K. Friedberg, A.N. Redington (eds.), *Right Ventricular Physiology, Adaptation and Failure in Congenital and Acquired Heart Disease*, https://doi.org/10.1007/978-3-319-67096-6_1

[3]. These observations fueled further research that confirmed the existence of two groups of cardiac progenitors, known as the first and second heart fields. The first heart field forms the cardiac crescent and the cardiac tube, and gives rise mainly to the left ventricle. The second heart field, added to the cardiac tube, contributes the totality of outflow tract and the right ventricle [4]. A recent finding of a group of progenitors regulated by canonical Wnt signaling that gives rise to pacemaker cells in chicken led to proposing the existence of a "tertiary" heart field [5]. The exact nature of the molecular cues that induce segregation of these progenitors is not clear, however extensive research using mainly animal and cellular model systems has made significant progress in uncovering the transcriptional pathways that regulate differentiation of cardiac progenitors and cardiogenesis.

This chapter provides an overview of the process of cardiac development, starting with a concise explanation of the morphogenetic events that transform the cardiac crescent into the four-chambered heart. Then, the events that led to the identification of the cardiac fields are discussed, emphasizing the discovery of the second heart field and its contribution to cardiogenesis. The transition from proliferating to differentiating cardiac progenitors and its relevance for development of the second heart field and right ventricle is discussed. Finally, recent findings on the molecular mechanisms controlling differentiation and maturation of cardiac myocytes are summarized.

Overview of Cardiac Development

Early Cardiac Development

The heart is the first organ to function during embryogenesis. The formation of the heart is a complex process that starts very early during development. The earliest cardiac progenitors arise during gastrulation [6, 7], during which the three embryonic layers ectoderm, mesoderm and endoderm are patterned. Multipotent cardiac progenitors arise from a cell population expressing mesoderm posterior 1 homolog, or Mesp1. Mesp1-expressing progenitors give rise first to the first heart field, and then to the second heart field at E6.75 in the gastrulating mouse embryo. Progenitors of the first heart field give rise to either cardiomyocytes or endothelial cells. Progenitors of the second heart field give rise to cardiomyocytes, endothelial cells, and smooth muscle cells [7]. Thus, cardiac progenitors are hierarchically segregated early during gastrulation. Studies using stem cell models of cardiac differentiation, as well as cell lineage tracing in animal models have shed light on some of the intermediate stages in the progression from stem cells to specialized differentiated cardiac lineages (Fig. 1.1) [8].

The cardiac progenitors emerge through the primitive streak and they take position cranially to the forming neural tube and surrounding the neural plate at approximately 18 days of human development. The cardiac progenitors aggregate to form two bilateral primitive heart fields, which fuse in the midline to form a horse shoe-shaped tube from splanchnic mesoderm known as the cardiac crescent. The cardiac crescent harbors a population of cardiac progenitors known as the first heart field, which contributes to the formation of the left ventricle and portions of the atria. As a result of ventral folding of the embryo in a cranial to caudal direction, the limbs of the cardiac crescent coalesce and fuse in the midline to form the linear heart tube (Fig. 1.2). Co-migration of cardiac and vascular progenitors allows for the formation of the endothelial heart tube, which is separated from the primitive myocardium by cardiac jelly, and which will form the endocardium. At this stage, day 22 of development, dilations and constrictions of the heart tube define the *truncus arteriosus*, *bulbus cordis*, primitive ventricle and atrium, and the *sinus venosus* (Fig. 1.3). The transition from cardiac progenitors into differentiating cardiomyocytes results in coordinated contraction of the linear heart tube and blood flow from the *sinus venosus* towards the cranial portion of the embryo. The linear heart tube is then extended by proliferation of resident differentiating cardiac progenitors and by contribution of additional ones

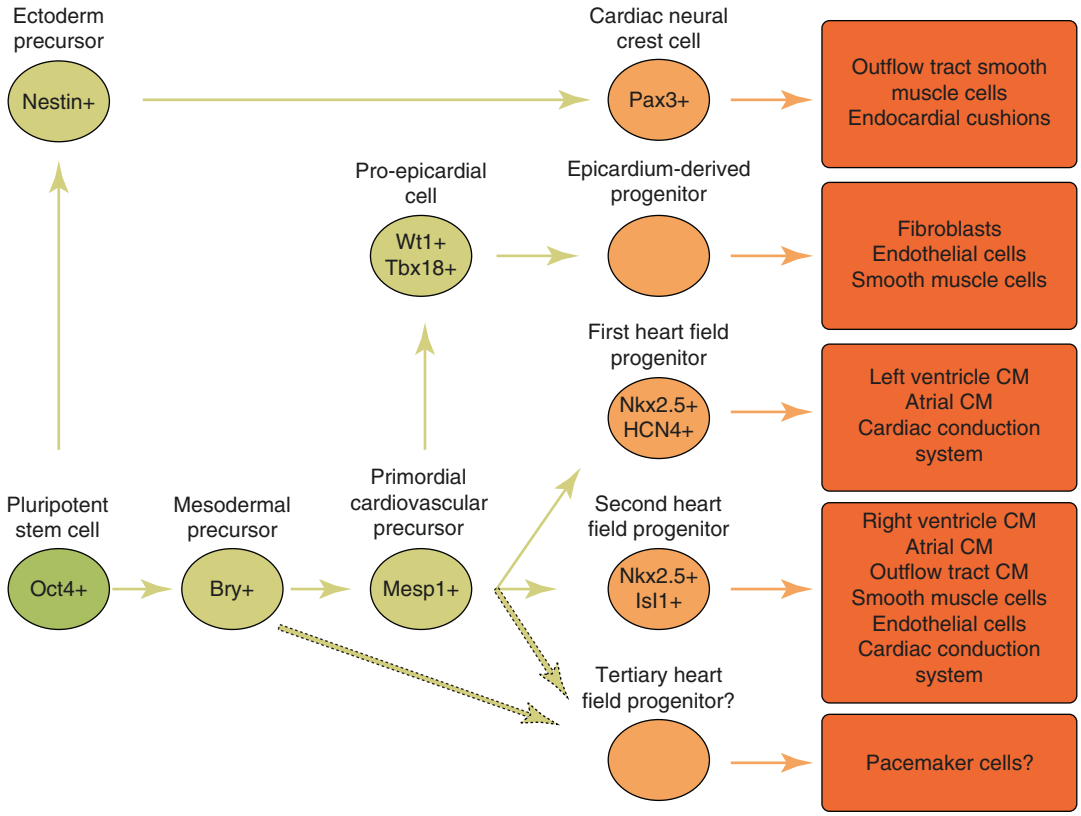

Fig. 1.1 Cardiac cell lineage progression. Intermediate stages generated from pluripotent stem cells towards differentiated cardiac lineages. Markers expressed in the intermediate progenitors are indicated. *CM* cardiomyocytes. Progression towards tertiary heart progenitors is speculative and is indicated with *dotted arrows*. Modified from [8]

originated from splanchnic and pharyngeal mesoderm, which migrate into the linear heart through the arterial and venous poles. This population of cardiac progenitors added to the linear heart is known as the second heart field. Cardiac progenitors of the second heart field give rise to the totality of the right ventricular myocardium, the outflow tract and an important proportion of the atria (Fig. 1.2) [4, 9, 10].

Cardiac Looping

Looping of the heart tube is the first visual evidence of embryonic asymmetry. Progenitors of the second heart field continue to be added during the process of looping, in which torsion forces cause the elongating heart tube to simultaneously twist and rotate rightwards, resulting in the formation of a C-shaped cardiac tube at embryonic day 23 (Fig. 1.3). These morphogenetic movements push the ventral portion of the linear tube towards the right outer curvature of the C-shaped tube, while the dorsal portion of the linear heart separates from the dorsal pericardial wall and forms the inner left curvature. Elongation continues at the arterial and venous poles, and the cardiac tube arranges into and S-shape structure, in which the outflow and inflow tracts come closer together cranially. Displacement of the *bulbus cordis* caudally, ventrally and rightwards, leftwards displacement of the primitive ventricle, and dorsal and cranial displacement of the primitive atrium by embryonic day 28, results in the proper spatial arrangement of the future cardiac chambers (Fig. 1.3). The rightwards movement

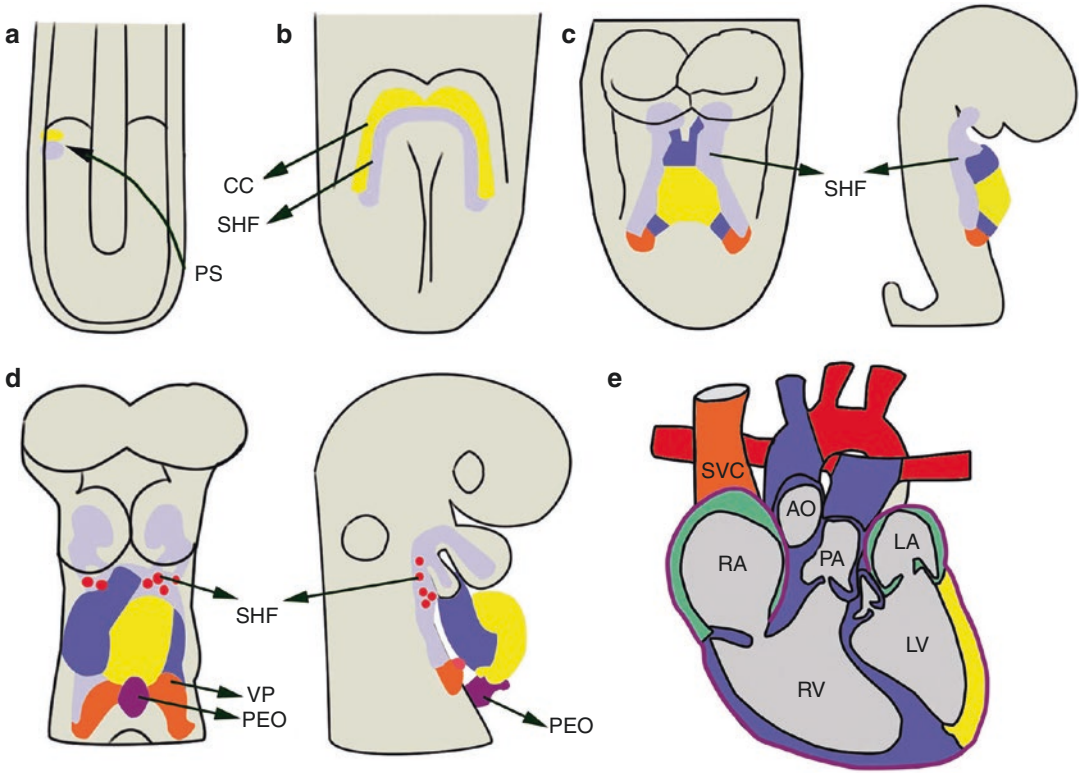

Fig. 1.2 Cardiac development. (**a**) Cardiac progenitors migrate anteriorly from the primitive streak (PS) to form two bilateral cardiac fields that (**b**) fuse in the midline to form the cardiac crescent (*yellow*) with the second heart field (*purple*) located medially. (**c**, **d**) Front (*left*) and lateral (*right*) views of the (**c**) linear, and (**d**) looping heart tube. Progenitors of the second heart field and the neural crest (*red*) migrate into the looping heart. (**e**) Fully developed heart. *Green colored atria* represent contribution of first and second heart field progenitors. The proepicardial organ gives rise to the epicardium. *AO* aorta, *CC* cardiac crescent, *LA* left atrium, *LV* left ventricle, *PEO* proepicardial organ, *PA* pulmonary artery, *SHF* second heart field, *RA* right atrium, *RV* right ventricle, *SVC* superior vena cava, *VP* venous pole. (**a**–**d**) modified from [10]. (**e**) Modified from [126]

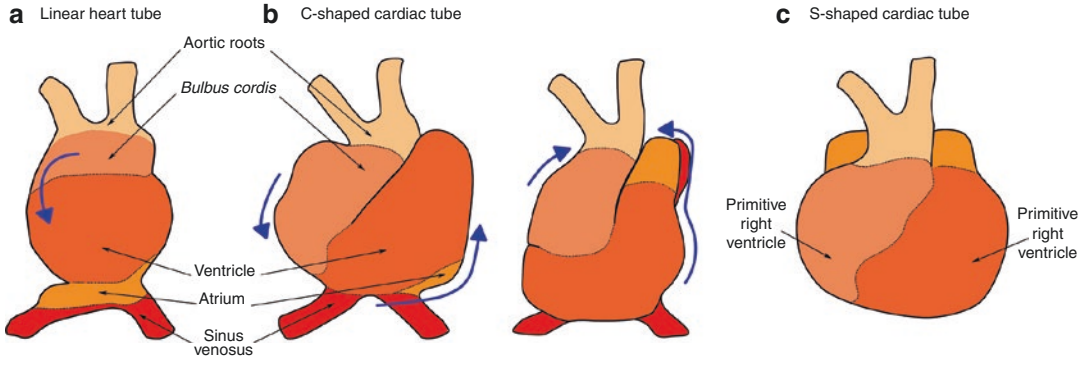

Fig. 1.3 Cardiac looping. The linear heart tube (**a**) twists and rotates rightwards resulting in the formation of the C-shaped tube (**b**). Elongation at the arterial and venous poles force arrangement into the S-shape tube (**c**), in which the outflow and inflow tracts come closer together cranially. Displacement of the *bulbus cordis* caudally, ventrally and rightwards, leftwards displacement of the primitive ventricle, and dorsal and cranial displacement of the primitive atrium, results in the proper spatial arrangement of the future cardiac chambers. Modified from [127]

of the heart tube and the establishment of asymmetry is regulated by leftwards flow in the node, which is a structure formed at the distal tip of the primitive streak containing motile cilia. The leftwards flow in the node elicits asymmetrical activation of diverse signaling pathways controlling left-right asymmetry, and include Ssh, Notch, Wnt, and FGF signaling. Nodal signaling activates expression of *FoxH1*, resulting in downstream asymmetric activation of left-right determinants *Nodal*, *Lefty* and *Pitx2c* [11].

After looping is complete, cells from the pro-epicardial organ (Fig. 1.2), which is a transient group of cells originated from lateral plate mesoderm and located ventro-caudally to the base of the heart [12], migrate towards the surface of the heart to form the epicardium and later contribute to formation of the coronary vasculature, early *sinus venosus*, and endocardium [13].

Cardiac Septation

The process of cardiac septation has been extensively reviewed [1, 14, 15]. Cardiac septation occurs during the fourth to the seventh week of embryogenesis and completely defines the cardiac chambers, separating the left from the right side and establishing the pulmonary and systemic circulatory systems. Studies on animal models have identified numerous molecular pathways that regulate cardiac septation and valve development, highlighting the complexity of the process. TFG, BMP, SMAD, Notch, Wnt, EGF, calcineurin/NFAT and VEGF signaling pathways are important regulators of cardiac septation. Transcription factors also required for the process are Pax3, Pbx and Meis, GATA, and T-box factors. In addition, epigenetic mechanisms controlling the expression of genes, including microRNAs and chromatin regulators also play central roles [16].

Ventricular Septation

Septation of the common ventricle occurs during the fifth week of development, and is completed by the ninth week. The muscular projection that will separate the ventricle starts forming during the looping process, when the walls of the future right and left ventricles grow concomitantly and coalesce resulting in the formation of the primitive interventricular septum, or interventricular ridge, at the base of the common ventricle [17]. The interventricular septum grows and extends posteriorly towards the endocardial atrioventricular cushions, leaving a space known as interventricular foramen. The interventricular foramen is closed when the interventricular septum fuses with the conotruncal septum, which forms from the fusion of conotruncal ridges derived from the endocardial cushions [18, 19].

The molecular processes patterning the ventricles are poorly understood. Comparative studies of the expression of the developmental regulator *Tbx5*, which is a key transcription factor regulating cardiac differentiation, have provided interesting insight. While *Tbx5* is homogenously expressed in the early developing single ventricle of turtle and lizard, it is restricted to precursors of the left ventricle in chicken and mouse. In later stages of development, *Tbx5* is preferentially expressed in a left to right gradient in the turtle ventricle, which by then develops an interventricular primary septum-like structure. Consistent with a key function for *Tbx5* in cardiac septation, genetically modified mice that mimic the reptilian *Tbx5* expression pattern develop a single ventricle. Thus, expression of *Tbx5* may constitute a patterning cue for ventricular septation [20].

Atrial Septation

The process of atrial septation has also been extensively reviewed [1, 14, 21]. Cardiac septation starts in the atrioventricular (AV) canal, a constriction of the looped cardiac tube that defines the primitive ventricle and atria. A subset of endothelial cells on the ventral and dorsal surface of the AV canal undergo endothelial to mesenchymal transition and migrate into the underlying cardiac jelly to form the endocardial cushions, which grow and fuse separating the right and left sides of the AV canal and partially separating the primitive atria from the ventricle. Then, the primitive atrium starts septation through the growth of the *septum primum*, which is a muscular appendage arising from the roof of

the left side of the chamber that grows towards, but does not reach the endocardial cushion [21], leaving an orifice known as the *ostium primum* or atrial foramen (Fig. 1.4). Apoptosis in the elongating *septum primum* creates a perforation known as the *ostium secundum*. The mesenchymal cap at the end of the growing *septum primum* fuses with the endocardial cushion in the AV canal. Before fusion of the *septum primum* with the endocardial cushion, another muscular appendage grows from the roof of the atrial chamber in the right side of the *septum primum* [21], known as *septum secundum*, which grows downwards overlapping the *ostium secundum* but does not reach the endocardial cushion. The partial overlap of the *septum secundum* with the *septum primum* and *ostium secundum* results in incomplete septation of the embryonic atria, which communicate through the *foramen ovale* (Fig. 1.4). This communication allows oxygenated blood coming from the placenta to reach the fetal circulation. Atrial septation is completed after birth, when increased pressure in the left atrium pushes the *septum primum* laterally towards the *septum secundum* closing the *foramen ovale*.

Outflow Tract Septation

Given the relevant function of the outflow tract in development of the right ventricle, its early stages of development will be discussed in more detail later in the "Development of the second heart field" section.

The process of septation of the outflow tract has been extensively reviewed [15, 16]. Septation of the outflow tract starts during the fifth week of development, and consists in the division of the common outflow chamber and *truncus arteriosus* to form the outlets and valves of the right and left ventricles, the pulmonary trunk and the aorta, respectively (Fig. 1.4). At the fifth week of human development, the outflow tract myocardium extends from the aortic sac [22]. At this stage, the proximal (conal) and distal (truncal) portions of the outflow tract can be distinguished by the presence of the conotruncal curvature, also known as the "dog-leg bend" [23]. Two pairs of endocardial ridges, the conotruncal and intercalated ridges, follow a spiral path and give rise to cushions that develop along the proximal and distal outflow tract. The spiral arrangement of the endocardial ridges positions the pulmonary trunk around the aorta. These cushions are formed in part with migrating mesenchyme derived from the neural crest. Septation starts with the fusion of the distal cushions, located towards the aortic sac, followed by fusion of the proximal cushions. Fusion of the distal portion of the proximal cushions with distal intercalated cushions will generate the aortic and pulmonary valves [15]. Around the 50th day of gestation, fusion of the proximal part of the outflow tract cushions results in formation of an embryonic outlet septum within the right ventricle. This septum is muscularized by invasion of parietal cardiac myocytes [24]. The septum then fuses with the muscular ventricular septum, confining the outlet of the aorta to the left ventricle and separating the ventricles. Further muscularization of the endocardial cushions [25], contribution of progenitor cells originated in the neural crest, and apoptosis [26] are required for complete separation of the outflow tract into the pulmonary artery and aorta.

Trabeculation

Trabeculae are projections of cardiac myoctes covered by endocardium that extend into the ventricle. Trabeculae are very important in the developing heart, as they extend the surface area favoring cardiac oxygenation and nutrient uptake before development of the coronary vasculature [27]. Trabeculae begin to form after looping of the cardiac tube by delamination of myocytes from the ventricular wall into the cardiac jelly [28]. Coordinated myocardial proliferation and differentiation results in the definition of two myocardial layers, the compact and trabecular myocardium. This process requires reciprocal communication between myocardium and endocardium via NOTCH and bone morphogenetic protein (BMP) signaling. NOTCH is activated exclusively in endocardial

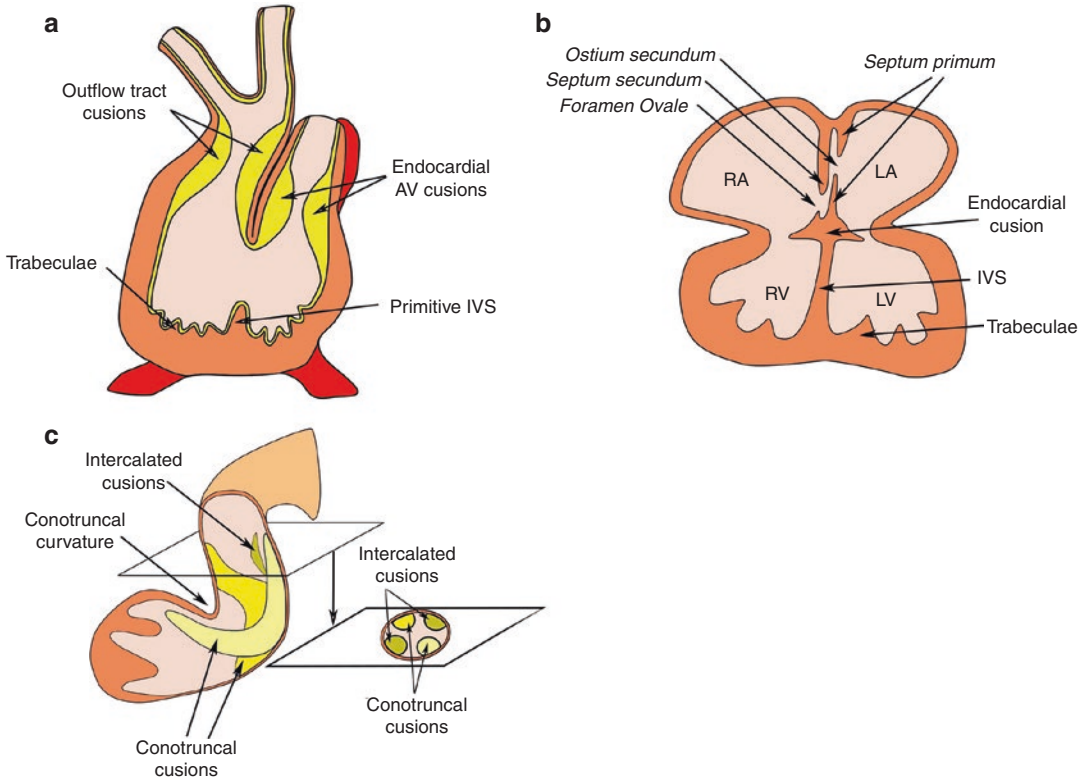

Fig. 1.4 Cardiac septation. (**a**) The primitive interventricular septum (IVS) is formed as a result of concomitant growth of the walls of the future ventricles colliding at the base of the common ventricle. The primitive IVS grows towards and fuses with the endocardial atrio ventricular cushions. (**b**) Septation of the atria results from the growth of the *septum primum* and *septum secundum* from the roof the common ventricle towards the endocardial cushion. Apoptosis in the elongating *septum primum* creates the *ostium secundum.* The septum secundum grows downwards overlapping the *ostium secundum* but does not reach the endocardial cushion. The partial overlap of the *septum secundum* with the *septum primum* and *ostium secundum* results in incomplete septation of the embryonic atria, which communicate through the *foramen ovale.* Modified from [127] (**c**) The proximal (conal) and distal (truncal) portions of the outflow tract can be distinguished by the presence of the conotruncal curvature. Two pairs of endocardial ridges, the conotruncal and intercalated ridges, follow a spiral path and give rise to cushions that develop along the proximal and distal outflow tract. Septation starts with the fusion of the distal cushions, located towards the aortic sac, followed by fusion of the proximal cushions. Fusion of the distal portion of the proximal cushions with distal intercalated cushions will generate the aortic and pulmonary valves. Modified from [16]

cells at the base of the trabeculae, resulting in expression of ephrin B2 (EPHB2) and subsequent expression of the secreted ligand neuregulin (NRG1) which stimulates differentiation of adjacent trabecular myocytes. Simultaneously, endocardial NOTCH stimulates proliferation of adjacent cardiomyocytes by activating BMP10 [29]. Trabeculae then undergo extensive maturation. Trabeculae stop growing towards the ventricles and thicken radially; causing them to compact to the point that trabecular myocardium is indistinguishable from compact myocardium and forms the complex trabecular network observed in the mature heart [30].

The Cardiac Fields

The previous sections highlight the fact that development of the heart entails complex morphogenetic processes involving multiple cell types, but how the cellular complexity of the

heart is generated during embryogenesis has not been discussed. As mentioned at the beginning of this chapter, cardiac progenitor cells developing during gastrulation give rise to the multiple cardiac cell types (Fig. 1.1), however the precise mechanisms that specify the fate of cardiac progenitors or the molecular cues that restrict their anatomical identity during development are not completely understood.

The first evidence for the existence of a group of cells giving rise to cardiac structures, or a cardiac field, was provided by the demonstration that lateral plate mesoderm located bilaterally to the primitive node of head-process stage chick embryos can generate myocardium and beating tissue in transplantation experiments [31]. Cells in this primitive bilateral cardiac field express the transcription factors Nk2 homebox 2, or *Nkx2-5*, and *Isl* Lim homeobox 1, or *Isl1*, contain progenitors of the first and second heart fields [32, 33] and migrate as a cohesive group and fuse at the midline. However, the location and timing for specification of such progenitors is poorly understood. A study shed light on this issue. Analysis of the expression of markers of early cardiac differentiation and the VEGF-1 receptor *Flk1* [6], which marks a multipotent progenitor population that differentiates into hematopoietic, endothelial, smooth muscle and cardiac myocytes [34, 35], demonstrated that cardiac progenitors are specified from mesoderm very early during gastrulation before formation of the bilateral cardiac field [6]. This study identified a molecular signature for the progression of mesoderm towards commitment to the cardiac lineage. A subpopulation of mesoderm cells expressing *Mesp1* during early gastrulation activate expression of *Smarcd3*, *Flk1*, and a marker of the anterior portion of the second heart field (AHF): the *Mef2cAHF* enhancer [36], followed by expression of specific markers of the cardiac lineage *Tbx5* and *Isl1* [6]. Therefore, expression of *Smarcd3* could be a very early marker of specification of the cardiac field from mesoderm during gastrulation. The endoderm adjacent to the lateral splanchnic mesoderm, the overlying endoderm, and the neural tube and notochord, signal positively and negatively to regulate cardiac differentiation through bone morphogenetic protein (BMP), fibroblast growth factor (FGF), and canonical and noncanonical Wnt pathways [37]. This signaling induces mesodermal progenitors expressing Mesp1 to activate transcription factors including *Isl1*, *Tbx5*, *Nkx2-5* and *Gata4*, and the chromatin remodeler *Baf60c*, which induce downstream expression of cardiac differentiation markers [38–41].

Once the cardiac progenitors in the primitive heart field converge in the midline, they form the cardiac crescent, which corresponds to the first heart field (Fig. 1.2). Cells in the cardiac crescent are labeled by expression of the ion channel *Hcn4*, which is also a marker of the conduction system [42], myosin light chain 2a or *Mlc2a* [43], *Tbx5* [44], and myosin light chain 1 [45], encoded by *MLC3F* [46]. The limbs of the cardiac crescent fuse in the midline to form the linear heart tube, in which cardiac myocytes start differentiating, as evidenced by expression of muscle-specific proteins and the presence of beating [47–49]. Lineage tracing experiments for *Hcn4*-expressing cells have shown that the first heart field contributes myocardium to portions of the left ventricle and atria [43].

Isl1 expression is turned off as progenitors start differentiating [47] and is absent in the heart tube, but remains present in undifferentiated cardiac progenitors located in the splanchnic mesoderm posterior to the first heart field [4], therefore *Isl1* is considered as a marker of cardiac progenitors [4, 50]. This population of *Isl1* positive cells includes the second heart field. Cells in the second heart field are more proliferative, and their differentiation is delayed compared to first heart field progenitors [51, 52]. Progenitors of the second heart field are added to the linear and looping heart tube through the arterial pole anteriorly, and through the venous pole posteriorly to form the outflow tract, the right ventricle and a proportion of the atria [4].

A recent study traced the origin of chicken pacemaker cells to a field outside the first and second heart fields, a so-called tertiary heart field [5]. However, the origin of pacemaker cells remains controversial.

The Second Heart Field

Progenitors of the second heart field contribute the totality of the right ventricular myocardium, the outflow tract and the majority of the atria [9]. In addition, defects during its development cause several congenital cardiac diseases. The origin and development of the second heart field will be discussed in more detail in the following sections.

Discovery of the Second Heart Field and Its Contribution to Cardiogenesis

Cell labeling experiments using iron oxide performed by Victoria de la Cruz and colleagues in 1977 showed that the outflow tract was added after the cardiac tube was formed, leading to the hypothesis that this region originated from a secondary source of myocardium [3]. Later studies defined the identity of this cardiac progenitor population. Lineage tracing analysis for cells expressing a transgene driven by *FGF10* revealed contribution to the right ventricle, *conus* and *truncus* [53]. Other studies in which cells residing in the pharyngeal arches cranial to the cardiac tube were chemically labeled also revealed contribution to the *conus* and *truncus* [54]. The observation that cardiac field markers *Nkx2-5* and *Gata4* are expressed in the pharyngeal mesoderm caudal to the outflow tract, which also express a marker of migratory cells, suggested that this discrete cell population could migrate towards the cardiac tube and contribute to the formation of the heart. Indeed, cell-labeling experiments revealed contribution to the *conus* and *truncus*. This cell population was named the "second heart field" [55], which refers to the progenitors in the splanchnic mesoderm that migrate into to the linear heart through the arterial and venous poles [4] and that contribute myocardium to the distal outflow tract and smooth muscle of the great arteries in the arterial pole [55, 56]. The later discovery of *Isl1*, unified these findings, as it is expressed in the cell population that contributes to the right ventricle, *conus* and *truncus* (Figs. 1.2 and 1.3) [4]. Based on the results from cell labeling and lineage tracing experiments mentioned, the second heart field, labeled by *Isl1* expression, has been divided in "subfields": the anterior heart field, and the second heart field, which refer to the distinct cardiac progenitor populations added to the heart tube at different times [51]. Progenitors in the anterior heart field are labeled by expression of the *FGF10* transgene and migrate into the cardiac tube to at the arterial pole to form the right ventricle and the outflow tract [53]. A transgene driven by the promoter and enhancer of *Mef2c* is also expressed in the anterior heart field, but it is not restricted, as it also labels atrial progenitors and the muscular atrial septa [36, 57], which are contributed posteriorly to the cardiac tube through the venous pole. The differential contribution, and gene expression patterns of second heart field progenitors at the arterial and venous poles of the heart tube suggest that these sub-regions are pre-patterned [10, 58–60]. Retinoic acid signaling might be involved in pre-patterning the second heart field [61], as *Raldh2* encoding retinaldehyde dehydrogenase, an enzyme required for retinoic acid synthesis, functions in establishing the posterior boundary of the second heart field [62, 63] and patterning the embryonic heart [64]. Accordingly, mutation of *Raldh2* results in posterior expansion of second heart field marker genes [62, 63], and abrogation of retinoic acid signaling in pharyngeal mesoderm disrupts alignment and septation of the outflow tract [65].

The relevance of the second heart field in cardiogenesis was demonstrated by studies of the function of *Isl1* in the mouse and subsequently confirmed in *Xenopus* and zebrafish. The heart in homozygous null mice for *Isl1* does not loop and does not develop an outflow tract, right ventricle or an important proportion of the atria. Accordingly, *Isl1* is required for cell proliferation and survival in the pharyngeal endoderm and splanchnic mesoderm, and for migration of cardiac progenitors [4]. Further studies confirmed that impairment of second heart field development impairs cardiac elongation and looping [66, 67]. Similarly, knockdown of *isl1* in *Xenopus* results in abnormal cardiac development and reduced expression of cardiac differentiation

marker genes [68]. Studies in zebrafish revealed a that *isl1* is required for complete cardiomyocyte differentiation [69], and further studies have strengthened the existence of a second heart field in zebrafish [70, 71]. These findings indicate that an important function of *Isl1* in cardiac differentiation and patterning has been conserved during evolution, which is in line with requirement of the second heart field for cardiac morphogenesis and human health. Perturbation of second heart field development resulst in defective alignment of the ascending aorta with the left ventricle [66, 72], which occurs in human conotruncal defects like tetralogy of Fallot, overriding aorta and double outlet right ventricle [73]. Abnormal second heart field development can also cause defective atrial and atrioventricular septation in the venous pole of the heart [57, 74].

Development of the Second Heart Field

Cardiac progenitors segregate from mesodermal cells during gastrulation [6, 75]. After migration of the primitive cardiac field towards the midline, the anterior lateral splanchnic mesoderm forms the cardiac crescent, in which cardiac progenitors start differentiating. Concomitantly, splanchnic mesoderm containing the second heart field locates medially to the cardiac crescent [32, 53, 61]. Separation of the heart tube from the dorsal wall of the pericardial cavity separates the second heart field, leaving the heart tube connected to the pharyngeal mesoderm through the arterial and venous poles [76]. While differentiation starts in the first heart field, the second heart field remains in a proliferative and undifferentiated state in the caudal pharyngeal region [52], however, the mechanisms promoting cell renewal are not understood. A recent finding indicates that the second branchial arch serves as a microenvironment for cardiac progenitor cell expansion, and that a cell autonomous function of *Numb* and *Numb* like (*Numbl*) is required [77]. Active research has uncovered complex interactions between the microenvironment of the second heart field in regulating the balance between proliferation and differentiation of the second heart field, as well as the pathways promoting cell fate acquisition and segregation of progenitors. The microenvironment surrounding second heart field progenitors, include the lateral plate and paraxial mesoderm, adjacent endoderm, overlying ectoderm, dorsal aortas, notochord, and neural tube; which signal through retinoic acid, fibroblast growth factor (FGF), Wnt, bone morphogenetic protein (BMP), and sonic hedgehog (Shh) to regulate the fate, differentiation, and behavior of cardiac progenitors of the second heart field. These proteins activate a hierarchical signaling cascade that ultimately affects the activity of key transcription factors and their downstream targets to establish gene expression patterns [10, 78].

Proliferation and Survival of Second Heart Field Progenitors

Stimulatory and repressive activities of BMP, FGF and canonical Wnt signaling turn on the cardiac gene expression program in anterior lateral splanchnic mesoderm [37] by activating expression of transcriptional regulators including *Isl1*, *Nkx2-5*, *Mef2c* and *Gata4*, and the chromatin remodeler *Baf60c* [1, 38]. During formation of the linear heart tube, proliferation, survival and delayed differentiation of second heart field progenitors is controlled by Notch, Wnt/b-catenin, FGF and Hedgehog (Hh) signaling from the pharyngeal endoderm [78, 79]. Notch signals repress cardiac differentiation by preventing activation of *Mef2c* expression [80], and by activating *Hes1*, which is required for cardiac progenitor cell proliferation, and prevents precocious differentiation [81], upstream Wnt/b-catenin [82]. Wnt/b-catenin signaling activates *Isl1* gene expression by binding to its regulatory region [83], activates *Gata6* expression [84], and promotes expansion of *Isl1*-expressing progenitors [85, 86], and its loss results in defects in outflow tract and right ventricle development [83, 86].

Inactivation of Wnt/b-catenin is accompanied by loss of FGF signaling [86, 87], which regulates second heart field progenitor proliferation in the dorsal pericardial wall mainly through the

ligand Fgf8, with contribution from Fgf3, and Fgf10 [79, 88–91]. Inactivation of *Fgf10* exacerbates cardiac defects in *Fgf8* mutants, and compound inactivation of *Fgf10* and *Fgf3* results in decreased expression of *Isl1*, and unstable *Nkx2-5* expression, leading to shortening of the outflow tract [91]. *Isl1* acts upstream the Wnt and FGF signaling pathways by regulating the expression of *Tbx1*, which regulates FGF ligand expression [4, 92], is required for proliferation of the pharyngeal mesoderm [93], and is mutated in human DiGeorge syndrome, associated with conotruncal congenital cardiac abnormalities [94]. *Tbx1* is an important promoter of progenitor proliferation and suppressor of differentiation. Tbx1 inhibits activation of BMP target genes, interacts with Sp1, which activates cardiac gene expression, targeting it for degradation, and represses the expression of *Mef2c*, which is required for differentiation [95–97]. The homeodomain transcription factor *Six1* and its coactivator *Eya1* act upstream *Fgf8* and downstream *Tbx1* in the regulation of second heart field proliferation and survival [61, 98].

Shh from the pharyngeal mesoderm is also required for proliferation of the second heart field, and for neural crest development [99]. The forkhead box transcription factors *Foxf1a* and *Foxf2* regulate atrioventricular septation, and integrate Tbx5 and Hedgehog pathways by the synergistic activity of the hedgehog transcriptional regulators Tbx5 and Gli1 in activation of *Foxf* gene expression [100].

Differentiation of Cardiac Progenitors and Cardiogenesis

T-box transcription factors regulate the transition from proliferating to differentiating cardiac progenitors by controlling BMP signaling [101]. BMP signaling from the distal outflow tract induces this transition at the arterial pole by inducing neural crest derivatives to express *Msx1*, which represses *FGF* gene expression, thus opposing FGF signaling [102]. Cardiac progenitors start differentiating as they enter the cardiac tube and express cardiogenic transcription factors [38]. It is not clear if progenitors of the second heart field follow a specific differentiation pathway different from that followed by first heart field progenitors. Identifying the transcriptional programs controlling first and second heart field differentiation is subject of active research. In the first heart field, transcription factors including Nkx2-5, Gata4, Tbx5, the basic helix-loop-helix transcription factors Hand1 and 2, and Mef2c regulate cardiac cell differentiation in the cardiac crescent and the developing heart. Gata4 associates with Baf60c/Smarcd3, acting as a link with the BAF chromatin remodeling complex, to activate expression of Nkx2-5, which physically interacts with Gata4 to activate the cardiac gene expression program [40]. Indeed, forced expression of *Gata4*, *Tbx5* and *Baf60c*/*Smarcd3* induces ectopic myocardial differentiation and beating in mesoderm, suggesting these factors might act as master regulators of the cardiac differentiation program [41]. These findings also suggest that chromatin structure dynamics is important for the establishment of the transcriptional program regulating cardiogenesis. Indeed histone acetylation and methylation are key for cardiomyocyte differentiation and cardiogenesis [103].

The histone acetyltransferase P300 regulates the expression of cardiac genes *Nkx2-5*, *Mef2c*, *Hand1/2*, *ANP*, *BNP*, *a-MHC*, and *b-MHC*, at least in part by interacting with Gata4, Nkx2-5 and Mef2c [103]. Accordingly, deficiency of P300 results in abnormal cardiogenesis with decreased trabeculation and defective differentiation [104]. In addition, P300 directly acetylates GATA4 and Mef2c, increasing their transcriptional activity [105, 106]. Removal of acetyl marks also alters cardiac development. The histone deacetylases HDAC5 and 9 interact with Mef2c, suppressing its transcriptional activity, and their inactivation results in lethality with thinning of the myocardial wall [107, 108].

Histone methylation has a key function in the orchestration of the cardiac transcriptional program. Analysis of the global distribution of histone methylation marks in stem cell-derived cardiomyocytes revealed that cardiac differentiation is regulated by coordinated epigenetic

transitions [109]. Furthermore, a chromatin signature distinguishes cardiac genes encoding transcription factors and soluble proteins regulating cardiac differentiation, from lineage-specific genes regulating cardiac function and maintenance. This chromatin signature consists in enrichment of tri-methylation of lysine 4 of histone H3 (H3K4me3) and H3K36me3, which are histone marks associated with gene activation, and lack of H3K27me3, which is a mark of inactive genes [110].

The fundamental role of histone methylation in cardiac differentiation is highlighted by the discovery that de novo mutations in genes involved in H2K4 and H3K27 methylation are enriched in the transcriptome of patients with congenital heart disease [111]. Accordingly, deficiency of histone methyltransferases affects cardiac development. Deficiency of the H3K4 methyltransferase *Smyd1* results in embryonic lethality with defective cardiomyocyte maturation and right ventricular development [112].

Deletion of the H4K36 methyltransferase Wolf-WHSC1 has been found in patients with Wolf-Hirschhorn Syndrome, associated with congenital heart defects [113]. WHSC1 interacts with Nkx2-5 and represses transcription. Accordingly, deficiency of WHSC1 causes lethality with ventricular septal defects [114].

H3K27me3 stabilizes the transcriptional program of differentiating cardiac progenitors by suppressing the expression of the transcription factor *Six1* [115], which is required for development of second heart field progenitors, but is suppressed during differentiation [98]. Inactivation of the H3K27me3 methyltransferase *Ezh2* in cardiac progenitors results in embryonic lethality with decreased cardiomyocyte proliferation and septal defects [116, 117]. Inactivation of *Ezh2* in progenitors of the second heart field does not cause developmental cardiac defects, but results in adult cardiac disease with right ventricular hypertrophy and increased fibrosis due to derepression of a transcriptional program characteristic of skeletal muscle downstream of *Six1* [115]. Therefore, it is possible that altering the epigenetic environment early during early differentiation of cardiac progenitors results in long-term gene expression misregulation that may predispose to postnatal cardiac disease.

The H3K9 mono and di-methyltransferases G9a and GLP act as transcriptional repressors and their combined deficiency causes atrioventricular septal defects [118], and silencing of the H3K9me3 Suv39h1 promotes expression of genes controlling cell cycle progression, resulting in increased proliferation [119].

Thus, repressive histone methylation stabilizes the cardiac gene expression program by repressing non-cardiac gene expression [103, 115].

Given that dynamic histone modification transitions regulate cardiac differentiation [109], it is not unexpected that removal of histone methylations is also important for cardiogenesis. Proteins harboring the Jumonji (Jmj) domain are histone demethylases that regulate gene expression [120], and deficiency of several of them affects cardiac development. Deficiency of the H3 and H4 arginine demethylase Jmjd6 causes perinatal death with ventricular septal defects and double outlet right ventricle. UTX is a H3K27 demethylase encoded in the X chromosome expressed in the developing heart, and its deficiency results in embryonic lethality with reduced expression of *Nkx2-5* and *Tbx5*, defective cardiac tube looping, and lack of chamber development [121]. UTX is recruited to cardiac genes through interaction with Nkx2-5, Tbx5, Gata4 and Baf60c, and influences cardiac enhancer activity by it interaction with the MLL3/4 complex, which mediates H3K4 methylation [121].

Dynamic DNA methylation has recently been shown to regulate the maturation of cardiac myocytes. DNA methylation represses gene expression, and loss of DNA methylation accompanies activation of genes expressed in adult mature cardiomyocytes, like the adult troponin *Tnni3*. In contrast, de novo methylation induced by the DNA methyltransferases DNMT3A/B occurs in genes expressed in immature newborn cardiomyocytes but that are silenced in mature hearts, like the fetal troponin *Tnni1* [122]. DNA methylation acts in concert with histone methylation to regulate the transition from newborn to adult

gene expression program. For instance, *Isl1*, which is expressed embryonically, and silenced upon differentiation, remains demethylated in newborn and adult cardiomyocytes, however it is occupied by the repressive histone mark H3K27me3 [122].

Thus, multiple epigenetic processes coordinate the gene expression programs controlling cardiac differentiation and maturation. However, we still do not completely understand the epigenetic control of cardiovascular development. Furthering this field will be required to uncover the roots of cardiovascular disease and will put us in a better position to design future preventive and therapeutic strategies.

Conclusions and Future Directions

Development of the right ventricle entails complex morphogenetic processes that transform a group of progenitor cells in the cardiac fields into a four-chambered heart. Coordinated signaling pathways instruct key transcription factors to tightly regulate gene expression and orchestrate cardiac development. The study of transcriptional pathways involved in the establishment and differentiation of the cardiac fields has led to important discoveries that could revolutionize the approaches to treat diseases caused by loss of myocardium. Recent studies found a combination of transcription factors that induce the cardiac phenotype in non-cardiac myocytes. These pioneering experiments showed that forced expression of *Gata4*, *Tbx5* and *Baf60c*/*Smarcd3* induces ectopic myocardial differentiation and beating in mesoderm in vivo [41]. Subsequent experiments showed that induction of *Gata4*, *Mef2c* and *Tbx5* can induce a cardiomyocyte-like phenotype in fibroblasts [123, 124]. Furthermore this combination of transcription factors can induce trans-differentiation of cardiac fibroblasts in post-infarction scars into beating cardiomyocytes [125]. These findings suggest that forced expression of key cardiogenic transcription factors holds a potential therapeutic use, however, the efficiency of the induction of the cardiac phenotype is low in the reported protocols. Uncovering the so far unknown molecular cues that induce the cardiac progenitor fate early during gastrulation and that control cardiac development could provide the missing elements required for controlled and efficient induction of cardiomyogenesis, and thus revolutionize the approaches to treat cardiac disease.

Acknowledgements P.D.O. is funded by the Heart and Stroke Foundation of Canada (G-17-0018613), Operational Funds from the Hospital for Sick Children, the Natural Sciences and Engineering Research Council of Canada (NSERC) (500865), and the Canadian Institutes of Health Research (CIHR) (PJT-149046). The author thanks Koroboshka Brand-Arzamendi for graphics.

References

1. Miquerol L, Kelly RG. Organogenesis of the vertebrate heart. Wiley Interdiscip Rev Dev Biol. 2013;2(1):17–29.
2. Harvey RP. Patterning the vertebrate heart. Nat Rev Genet. 2002;3(7):544–56.
3. de la Cruz MV, Sanchez Gomez C, Arteaga MM, Arguello C. Experimental study of the development of the truncus and the conus in the chick embryo. J Anat. 1977;123(Pt 3):661–86.
4. Cai CL, Liang X, Shi Y, Chu PH, Pfaff SL, Chen J, et al. Isl1 identifies a cardiac progenitor population that proliferates prior to differentiation and contributes a majority of cells to the heart. Dev Cell. 2003;5(6):877–89.
5. Bressan M, Liu G, Mikawa T. Early mesodermal cues assign avian cardiac pacemaker fate potential in a tertiary heart field. Science. 2013;340(6133):744–8.
6. Devine WP, Wythe JD, George M, Koshiba-Takeuchi K, Bruneau BG. Early patterning and specification of cardiac progenitors in gastrulating mesoderm. elife. 2014;3:e03848.
7. Lescroart F, Chabab S, Lin X, Rulands S, Paulissen C, Rodolosse A, et al. Early lineage restriction in temporally distinct populations of Mesp1 progenitors during mammalian heart development. Nat Cell Biol. 2014;16(9):829–40.
8. Sahara M, Santoro F, Chien KR. Programming and reprogramming a human heart cell. EMBO J. 2015;34(6):710–38.
9. Buckingham M, Meilhac S, Zaffran S. Building the mammalian heart from two sources of myocardial cells. Nat Rev Genet. 2005;6(11):826–35.
10. Vincent SD, Buckingham ME. How to make a heart. Curr Top Dev Biol. 2010;90:1–41.
11. Chen CM, Norris D, Bhattacharya S. Transcriptional control of left-right patterning in cardiac development. Pediatr Cardiol. 2010;31(3):371–7.

12. Maya-Ramos L, Cleland J, Bressan M, Mikawa T. Induction of the Proepicardium. J Dev Biol. 2013;1(2):82–91.
13. Katz TC, Singh MK, Degenhardt K, Rivera-Feliciano J, Johnson RL, Epstein JA, et al. Distinct compartments of the proepicardial organ give rise to coronary vascular endothelial cells. Dev Cell. 2012;22(3):639–50.
14. Anderson RH, Webb S, Brown NA, Lamers W, Moorman A. Development of the heart: (2) septation of the atriums and ventricles. Heart. 2003;89(8):949–58.
15. Anderson RH, Webb S, Brown NA, Lamers W, Moorman A. Development of the heart: (3) formation of the ventricular outflow tracts, arterial valves, and intrapericardial arterial trunks. Heart. 2003;89(9):1110–8.
16. Lin CJ, Lin CY, Chen CH, Zhou B, Chang CP. Partitioning the heart: mechanisms of cardiac septation and valve development. Development. 2012;139(18):3277–99.
17. Lamers WH, Wessels A, Verbeek FJ, Moorman AF, Viragh S, Wenink AC, et al. New findings concerning ventricular septation in the human heart. Implications for maldevelopment. Circulation. 1992;86(4):1194–205.
18. Allwork SP, Anderson RH. Developmental anatomy of the membranous part of the ventricular septum in the human heart. Br Heart J. 1979;41(3):275–80.
19. Odgers PN. The development of the pars membranacea septi in the human heart. J Anat. 1938;72(Pt 2):247–59.
20. Koshiba-Takeuchi K, Mori AD, Kaynak BL, Cebra-Thomas J, Sukonnik T, Georges RO, et al. Reptilian heart development and the molecular basis of cardiac chamber evolution. Nature. 2009;461(7260):95–8.
21. Webb S, Brown NA, Anderson RH. Formation of the atrioventricular septal structures in the normal mouse. Circ Res. 1998;82(6):645–56.
22. Hiruma T, Nakajima Y, Nakamura H. Development of pharyngeal arch arteries in early mouse embryo. J Anat. 2002;201(1):15–29.
23. Webb S, Qayyum SR, Anderson RH, Lamers WH, Richardson MK. Septation and separation within the outflow tract of the developing heart. J Anat. 2003;202(4):327–42.
24. van den Hoff MJ, Moorman AF, Ruijter JM, Lamers WH, Bennington RW, Markwald RR, et al. Myocardialization of the cardiac outflow tract. Dev Biol. 1999;212(2):477–90.
25. McBride RE, Moore GW, Hutchins GM. Development of the outflow tract and closure of the interventricular septum in the normal human heart. Am J Anat. 1981;160(3):309–31.
26. Poelmann RE, Mikawa T, Gittenberger-de Groot AC. Neural crest cells in outflow tract septation of the embryonic chicken heart: differentiation and apoptosis. Dev Dyn. 1998;212(3):373–84.
27. Minot CS. On a hitherto unrecognised form of blood circulation without capillaries in the organs of Vertebrata. Proc Boston Soc. Nat Hist. 1900;4(6):133–4.
28. Liu J, Bressan M, Hassel D, Huisken J, Staudt D, Kikuchi K, et al. A dual role for ErbB2 signaling in cardiac trabeculation. Development. 2010;137(22):3867–75.
29. High FA, Epstein JA. The multifaceted role of Notch in cardiac development and disease. Nat Rev Genet. 2008;9(1):49–61.
30. Samsa LA, Yang B, Liu J. Embryonic cardiac chamber maturation: Trabeculation, conduction, and cardiomyocyte proliferation. Am J Med Genet C Semin Med Genet. 2013;163C(3):157–68.
31. Rawles ME. The heart-forming areas of the early chick blastoderm. Physiol Zool. 1943;16(1):22–42.
32. Abu-Issa R, Kirby ML. Patterning of the heart field in the chick. Dev Biol. 2008;319(2):223–33.
33. Ma Q, Zhou B, Pu WT. Reassessment of Isl1 and Nkx2-5 cardiac fate maps using a Gata4-based reporter of Cre activity. Dev Biol. 2008;323(1):98–104.
34. Ishitobi H, Wakamatsu A, Liu F, Azami T, Hamada M, Matsumoto K, et al. Molecular basis for Flk1 expression in hemato-cardiovascular progenitors in the mouse. Development. 2011;138(24):5357–68.
35. Kattman SJ, Huber TL, Keller GM. Multipotent flk-1+ cardiovascular progenitor cells give rise to the cardiomyocyte, endothelial, and vascular smooth muscle lineages. Dev Cell. 2006;11(5):723–32.
36. Verzi MP, , McCulley DJ, De Val S, Dodou E, Black BL. The right ventricle, outflow tract, and ventricular septum comprise a restricted expression domain within the secondary/anterior heart field. Dev Biol 2005;287(1):134-145.
37. Evans SM, Yelon D, Conlon FL, Kirby ML. Myocardial lineage development. Circ Res. 2010;107(12):1428–44.
38. Bruneau BG. Signaling and transcriptional networks in heart development and regeneration. Cold Spring Harb Perspect Biol. 2013;5(3):a008292.
39. Chang CP, Bruneau BG. Epigenetics and cardiovascular development. Annu Rev Physiol. 2012;74:41–68.
40. Lickert H, Takeuchi JK, Von Both I, Walls JR, McAuliffe F, Adamson SL, et al. Baf60c is essential for function of BAF chromatin remodelling complexes in heart development. Nature. 2004;432(7013):107–12.
41. Takeuchi JK, Bruneau BG. Directed transdifferentiation of mouse mesoderm to heart tissue by defined factors. Nature. 2009;459(7247):708–0.
42. Vicente-Steijn R, Passier R, Wisse LJ, Schalij MJ, Poelmann RE, Gittenberger-de Groot AC, et al. Funny current channel HCN4 delineates the developing cardiac conduction system in chicken heart. Heart Rhythm. 2011;8(8):1254–63.
43. Spater D, Abramczuk MK, Buac K, Zangi L, Stachel MW, Clarke J, et al. A HCN4+ cardiomyo-

genic progenitor derived from the first heart field and human pluripotent stem cells. Nat Cell Biol. 2013;15(9):1098–106.
44. Bruneau BG, Logan M, Davis N, Levi T, Tabin CJ, Seidman JG, et al. Chamber-specific cardiac expression of Tbx5 and heart defects in Holt-Oram syndrome. Dev Biol. 1999;211(1):100–8.
45. Kelly RG, Zammit PS, Schneider A, Alonso S, Biben C, Buckingham ME. Embryonic and fetal myogenic programs act through separate enhancers at the MLC1F/3F locus. Dev Biol. 1997;187(2):183–9.
46. Cohen-Haguenauer O, Barton PJ, Nguyen VC, Serero S, Gross MS, Jegou-Foubert C, et al. Assignment of the human fast skeletal muscle myosin alkali light chains gene (MLC1F/MLC3F) to 2q 32.1-2qter. Hum Genet. 1988;78(1):65–70.
47. Prall OW, Menon MK, Solloway MJ, Watanabe Y, Zaffran S, Bajolle F, et al. An Nkx2-5/Bmp2/Smad1 negative feedback loop controls heart progenitor specification and proliferation. Cell. 2007;128(5):947–59.
48. Saga Y, Kitajima S, Miyagawa-Tomita S. Mesp1 expression is the earliest sign of cardiovascular development. Trends Cardiovasc Med. 2000;10(8):345–52.
49. Saga Y, Miyagawa-Tomita S, Takagi A, Kitajima S, Miyazaki J, Inoue T. MesP1 is expressed in the heart precursor cells and required for the formation of a single heart tube. Development. 1999;126(15):3437–47.
50. Laugwitz KL, Moretti A, Lam J, Gruber P, Chen Y, Woodard S, et al. Postnatal isl1+ cardioblasts enter fully differentiated cardiomyocyte lineages. Nature. 2005;433(7026):647–53.
51. Dyer LA, Kirby ML. The role of secondary heart field in cardiac development. Dev Biol. 2009;336(2):137–44.
52. Rochais F, Mesbah K, Kelly RG. Signaling pathways controlling second heart field development. Circ Res. 2009;104(8):933–42.
53. Kelly RG, Brown NA, Buckingham ME. The arterial pole of the mouse heart forms from Fgf10-expressing cells in pharyngeal mesoderm. Dev Cell. 2001;1(3):435–40.
54. Mjaatvedt CH, Nakaoka T, Moreno-Rodriguez R, Norris RA, Kern MJ, Eisenberg CA, et al. The outflow tract of the heart is recruited from a novel heart-forming field. Dev Biol. 2001;238(1):97–109.
55. Waldo KL, Kumiski DH, Wallis KT, Stadt HA, Hutson MR, Platt DH, et al. Conotruncal myocardium arises from a secondary heart field. Development. 2001;128(16):3179–88.
56. Waldo KL, Hutson MR, Ward CC, Zdanowicz M, Stadt HA, Kumiski D, et al. Secondary heart field contributes myocardium and smooth muscle to the arterial pole of the developing heart. Dev Biol. 2005;281(1):78–90.
57. Goddeeris MM, Rho S, Petiet A, Davenport CL, Johnson GA, Meyers EN, et al. Intracardiac septation requires hedgehog-dependent cellular contributions from outside the heart. Development. 2008;135(10):1887–95.
58. Galli D, Domínguez JN, Zaffran S, Munk A, Brown NA, Buckingham ME. Atrial myocardium derives from the posterior region of the second heart field, which acquires left-right identity as Pitx2c is expressed. Development. 2008;135(6):1157–67.
59. Snarr BS, O'Neal JL, Chintalapudi MR, Wirrig EE, Phelps AL, Kubalak SW, et al. Isl1 expression at the venous pole identifies a novel role for the second heart field in cardiac development. Circ Res. 2007;101(10):971–4.
60. Dominguez JN, Meilhac SM, Bland YS, Buckingham ME, Brown NA. Asymmetric fate of the posterior part of the second heart field results in unexpected left/right contributions to both poles of the heart. Circ Res. 2012;111(10):1323–35.
61. Zaffran S, Kelly RG. New developments in the second heart field. Differentiation. 2012;84(1):17–24.
62. Ryckebusch L, Wang Z, Bertrand N, Lin SC, Chi X, Schwartz R, et al. Retinoic acid deficiency alters second heart field formation. Proc Natl Acad Sci U S A. 2008;105(8):2913–8.
63. Sirbu IO, Zhao X, Duester G. Retinoic acid controls heart anteroposterior patterning by down-regulating Isl1 through the Fgf8 pathway. Dev Dyn. 2008;237(6):1627–35.
64. Hochgreb T, Linhares VL, Menezes DC, Sampaio AC, Yan CY, Cardoso WV, et al. A caudorostral wave of RALDH2 conveys anteroposterior information to the cardiac field. Development. 2003;130(22):5363–74.
65. Li P, Pashmforoush M, Sucov HM. Retinoic acid regulates differentiation of the secondary heart field and TGFbeta-mediated outflow tract septation. Dev Cell. 2010;18(3):480–5.
66. Park EJ, Ogden LA, Talbot A, Evans S, Cai CL, Black BL, et al. Required, tissue-specific roles for Fgf8 in outflow tract formation and remodeling. Development. 2006;133(12):2419–33.
67. Prall OW, Menon MK, Solloway MJ, Watanabe Y, Zaffran S, Bajolle F, et al. An Nkx2-5/Bmp2/Smad1 negative feedback loop controls heart progenitor specification and proliferation. Cell. 2005;128(5):947–59.
68. Brade T, Gessert S, Kühl M, Pandur P. The amphibian second heart field: Xenopus islet-1 is required for cardiovascular development. Dev Biol. 2007;311(2):297–310.
69. de Pater E, Clijsters L, Marques SR, Lin YF, Garavito-Aguilar ZV, Yelon D, et al. Distinct phases of cardiomyocyte differentiation regulate growth of the zebrafish heart. Development. 2009;136(10):1633–41.
70. Lazic S, Scott IC. Mef2cb regulates late myocardial cell addition from a second heart field-like population of progenitors in zebrafish. Dev Biol. 2011;354(1):123–33.
71. Zhou Y, Cashman TJ, Nevis KR, Obregon P, Carney SA, Liu Y, et al. Latent TGF-beta binding protein 3

identifies a second heart field in zebrafish. Nature. 2011;474(7353):645–8.
72. Ward C, Stadt H, Hutson M, Kirby ML. Ablation of the secondary heart field leads to tetralogy of Fallot and pulmonary atresia. Dev Biol. 2005;284(1):72–83.
73. Moon A. Mouse models of congenital cardiovascular disease. Curr Top Dev Biol. 2008;84:171–248.
74. Hoffmann AD, Peterson MA, Friedland-Little JM, Anderson SA, Moskowitz IP. sonic hedgehog is required in pulmonary endoderm for atrial septation. Development. 2009;136(10):1761–70.
75. Meilhac SM, Esner M, Kelly RG, Nicolas JF, Buckingham ME. The clonal origin of myocardial cells in different regions of the embryonic mouse heart. Dev Cell. 2004;6(5):685–98.
76. Kelly RG, Buckingham ME. The anterior heart-forming field: voyage to the arterial pole of the heart. Trends Genet. 2002;18(4):210–6.
77. Shenje LT, Andersen P, Uosaki H, Fernandez L, Rainer PP, Cho GS, et al. Precardiac deletion of Numb and Numblike reveals renewal of cardiac progenitors. elife. 2014;3:e02164.
78. Kelly RG. The second heart field. Curr Top Dev Biol. 2012;100:33–65.
79. Francou A, Saint-Michel E, Mesbah K, Théveniau-Ruissy M, Rana MS, Christoffels VM, Kelly RG. Second heart field cardiac progenitor cells in the early mouse embryo. Biochim Biophys Acta. 2013;1833(4):795–8.
80. MacGrogan D, Nus M, de la Pompa JL. Notch signaling in cardiac development and disease. Curr Top Dev Biol. 2010;92(92):333–65.
81. Rochais F, Dandonneau M, Mesbah K, Jarry T, Mattei MG, Kelly RG. Hes1 is expressed in the second heart field and is required for outflow tract development. PLoS One. 2009;4(7):e6267.
82. Klaus A, Muller M, Schulz H, Saga Y, Martin JF, Birchmeier W. Wnt/beta-catenin and Bmp signals control distinct sets of transcription factors in cardiac progenitor cells. Proc Natl Acad Sci U S A. 2012;109(27):10921–6.
83. Lu H, Li Y, Wang Y, Liu Y, Wang W, Jia Z, et al. Wnt-promoted Isl1 expression through a novel TCF/LEF1 binding site and H3K9 acetylation in early stages of cardiomyocyte differentiation of P19CL6 cells. Mol Cell Biochem. 2014;391(1-2):183–92.
84. Tian Y, Yuan L, Goss AM, Wang T, Yang J, Lepore JJ, et al. Characterization and in vivo pharmacological rescue of a Wnt2-Gata6 pathway required for cardiac inflow tract development. Dev Cell. 2010;18(2):275–87.
85. Bu L, Jiang X, Martin-Puig S, Caron L, Zhu S, Shao Y, et al. Human ISL1 heart progenitors generate diverse multipotent cardiovascular cell lineages. Nature. 2009;460(7251):113–7.
86. Cohen ED, Wang Z, Lepore JJ, Lu MM, Taketo MM, Epstein DJ, et al. Wnt/beta-catenin signaling promotes expansion of Isl-1-positive cardiac progenitor cells through regulation of FGF signaling. J Clin Invest. 2007;117(7):1794–804.
87. Tzahor E. Wnt/beta-catenin signaling and cardiogenesis: timing does matter. Dev Cell 2007;13(1):10–3.
88. Park EJ, Watanabe Y, Smyth G, Miyagawa-Tomita S, Meyers E, Klingensmith J, et al. An FGF autocrine loop initiated in second heart field mesoderm regulates morphogenesis at the arterial pole of the heart. Development. 2008;135(21):3599–610.
89. Ilagan R, Abu-Issa R, Brown D, Yang YP, Jiao K, Schwartz RJ, et al. Fgf8 is required for anterior heart field development. Development. 2006;133(12):2435–45.
90. Watanabe Y, Miyagawa-Tomita S, Vincent SD, Kelly RG, Moon AM, Buckingham ME. Role of mesodermal FGF8 and FGF10 overlaps in the development of the arterial pole of the heart and pharyngeal arch arteries. Circ Res. 2010;106(3):495–503.
91. Urness LD, Bleyl SB, Wright TJ, Moon AM, Mansour SL. Redundant and dosage sensitive requirements for Fgf3 and Fgf10 in cardiovascular development. Dev Biol. 2011;356(2):383–97.
92. Vitelli F, Taddei I, Morishima M, Meyers EN, Lindsay EA, Baldini A. A genetic link between Tbx1 and fibroblast growth factor signaling. Development. 2002;129(19):4605–11.
93. Zhang Z, Huynh T, Baldini A. Mesodermal expression of Tbx1 is necessary and sufficient for pharyngeal arch and cardiac outflow tract development. Development. 2006;133(18):3587–95.
94. Baldini A. Dissecting contiguous gene defects: TBX1. Curr Opin Genet Dev. 2005;15(3):279–84.
95. Chen L, Fulcoli FG, Tang S, Baldini A. Tbx1 regulates proliferation and differentiation of multipotent heart progenitors. Circ Res. 2009;105(9):842–51.
96. Fulcoli FG, Huynh T, Scambler PJ, Baldini A. Tbx1 regulates the BMP-Smad1 pathway in a transcription independent manner. PLoS One. 2009;4(6):e6049.
97. Pane LS, Zhang Z, Ferrentino R, Huynh T, Cutillo L, Baldini A. Tbx1 is a negative modulator of Mef2c. Hum Mol Genet. 2012;21(11):2485–96.
98. Guo C, Sun Y, Zhou B, Adam RM, Li X, WT P, et al. A Tbx1-Six1/Eya1-Fgf8 genetic pathway controls mammalian cardiovascular and craniofacial morphogenesis. J Clin Invest. 2011;121(4):1585–95.
99. Dyer LA, Kirby ML. Sonic hedgehog maintains proliferation in secondary heart field progenitors and is required for normal arterial pole formation. Dev Biol. 2009;330(2):305–17.
100. Hoffmann AD, Yang XH, Burnicka-Turek O, Bosman JD, Ren X, Steimle JD, Vokes SA, McMahon AP, Kalinichenko VV, Moskowitz IP. Foxf genes integrate tbx5 and hedgehog pathways in the second heart field for cardiac septation. PLoS Genet. 2014;10(10):e1004604.
101. Mesbah K, Rana MS, Francou A, van Duijvenboden K, Papaioannou VE, Moorman AF, et al. Identification of a Tbx1/Tbx2/Tbx3 genetic pathway governing pharyngeal and arterial pole morphogenesis. Hum Mol Genet. 2012;21(6):1217–29.

102. Tirosh-Finkel L, Zeisel A, Brodt-Ivenshitz M, Shamai A, Yao Z, Seger R, et al. BMP-mediated inhibition of FGF signaling promotes cardiomyocyte differentiation of anterior heart field progenitors. Development. 2010;137(18):2989–3000.
103. Oyama K, El-Nachef D, Zhang Y, Sdek P, MacLellan WR. Epigenetic regulation of cardiac myocyte differentiation. Front Genet. 2014;5:375.
104. Yao TP, Oh SP, Fuchs M, Zhou ND, Ch'ng LE, Newsome D, et al. Gene dosage-dependent embryonic development and proliferation defects in mice lacking the transcriptional integrator p300. Cell. 1998;93(3):361–72.
105. Kawamura T, Ono K, Morimoto T, Wada H, Hirai M, Hidaka K, et al. Acetylation of GATA-4 is involved in the differentiation of embryonic stem cells into cardiac myocytes. J Biol Chem. 2005;280(20):19682–8.
106. Ma K, Chan JK, Zhu G, Wu Z. Myocyte enhancer factor 2 acetylation by p300 enhances its DNA binding activity, transcriptional activity, and myogenic differentiation. Mol Cell Biol. 2005;25(9):3575–82.
107. Zhang CL, McKinsey TA, Chang S, Antos CL, Hill JA, Olson EN. Class II histone deacetylases act as signal-responsive repressors of cardiac hypertrophy. Cell. 2002;110(4):479–88.
108. Chang S, McKinsey TA, Zhang CL, Richardson JA, Hill JA, Olson EN. Histone deacetylases 5 and 9 govern responsiveness of the heart to a subset of stress signals and play redundant roles in heart development. Mol Cell Biol. 2004;24(19):8467–76.
109. Wamstad JA, Alexander JM, Truty RM, Shrikumar A, Li F, Eilertson KE, et al. Dynamic and coordinated epigenetic regulation of developmental transitions in the cardiac lineage. Cell. 2012;151(1):206–20.
110. Paige SL, Thomas S, Stoick-Cooper CL, Wang H, Maves L, Sandstrom R, et al. A temporal chromatin signature in human embryonic stem cells identifies regulators of cardiac development. Cell. 2012;151(1):221–32.
111. Zaidi S, Choi M, Wakimoto H, Ma L, Jiang J, Overton JD, et al. De novo mutations in histone-modifying genes in congenital heart disease. Nature. 2013;498(7453):220–3.
112. Gottlieb PD, Pierce SA, Sims RJ, Yamagishi H, Weihe EK, Harriss JV, et al. Bop encodes a muscle-restricted protein containing MYND and SET domains and is essential for cardiac differentiation and morphogenesis. Nat Genet. 2002;31(1):25–32.
113. Bergemann AD, Cole F, Hirschhorn K. The etiology of Wolf-Hirschhorn syndrome. Trends Genet. 2005;21(3):188–95.
114. Nimura K, Ura K, Shiratori H, Ikawa M, Okabe M, Schwartz RJ, et al. A histone H3 lysine 36 trimethyltransferase links Nkx2-5 to Wolf-Hirschhorn syndrome. Nature. 2009;460(7252):287–91.
115. Delgado-Olguin P, Huang Y, Li X, Christodoulou D, Seidman CE, Seidman JG, et al. Epigenetic repression of cardiac progenitor gene expression by Ezh2 is required for postnatal cardiac homeostasis. Nat Genet. 2012;44(3):343–7.
116. He A, Ma Q, Cao J, von Gise A, Zhou P, Xie H, et al. Polycomb repressive complex 2 regulates normal development of the mouse heart. Circ Res. 2012;110(3):406–15.
117. Chen L, Ma Y, Kim EY, Yu W, Schwartz RJ, Qian L, et al. Conditional ablation of Ezh2 in murine hearts reveals its essential roles in endocardial cushion formation, cardiomyocyte proliferation and survival. PLoS One. 2012;7(2):e31005.
118. Inagawa M, Nakajima K, Makino T, Ogawa S, Kojima M, Ito S, et al. Histone H3 lysine 9 methyltransferases, G9a and GLP are essential for cardiac morphogenesis. Mech Dev. 2013;130(11-12):519–31.
119. Sdek P, Zhao P, Wang Y, Huang CJ, Ko CY, Butler PC, et al. Rb and p130 control cell cycle gene silencing to maintain the postmitotic phenotype in cardiac myocytes. J Cell Biol. 2011;194(3):407–23.
120. Klose RJ, Kallin EM, Zhang Y. JmjC-domain-containing proteins and histone demethylation. Nat Rev Genet. 2006;7(9):715–27.
121. Lee S, Lee JW, Lee SK. UTX, a histone H3-lysine 27 demethylase, acts as a critical switch to activate the cardiac developmental program. Dev Cell. 2012;22(1):25–37.
122. Gilsbach R, Preissl S, Gruning BA, Schnick T, Burger L, Benes V, et al. Dynamic DNA methylation orchestrates cardiomyocyte development, maturation and disease. Nat Commun. 2014;5:5288.
123. Fu JD, Stone NR, Liu L, Spencer CI, Qian L, Hayashi Y, et al. Direct reprogramming of human fibroblasts toward a cardiomyocyte-like state. Stem Cell Rep. 2013;1(3):235–47.
124. Ieda M, Fu JD, Delgado-Olguin P, Vedantham V, Hayashi Y, Bruneau BG, et al. Direct reprogramming of fibroblasts into functional cardiomyocytes by defined factors. Cell. 2010;142(3):375–86.
125. Qian L, Huang Y, Spencer CI, Foley A, Vedantham V, Liu L, et al. In vivo reprogramming of murine cardiac fibroblasts into induced cardiomyocytes. Nature. 2012;485(7400):593–8.
126. Gama-Carvalho M, Andrade J, Bras-Rosario L. Regulation of cardiac cell fate by microRNAs: implications for heart regeneration. Cell. 2014;3(4):996–1026.
127. Hill MA. Embryology heart looping sequence.jpg. 2015 [cited 2015 May 17]. Available from: https://embryology.med.unsw.edu.au/embryology/index.php/File:Heart_Looping_Sequence.jpg.

How Does the Pressure-Overloaded Right Ventricle Adapt and Why Does It Fail? Macro-and Micro-Molecular Perspectives

2

Norbert F. Voelkel

Abstract

The right ventricle (RV) eventually fails in most patients with severe chronic pulmonary hypertension, however, the individual myocardial reserve and ability to cope with the increased afterload, inflammation and metabolic derangements are highly variable. Hypertrophy is required for the RV to successfully adapt to the chronically elevated pressure and shear stress in the lung vessels. RV hypertrophy associated with an appropriate myocardial capillary density and normal function of the capillary endothelial cells are hallmarks of successful adaptation. Neuroendocrine hyperactivity or overdrive may contribute and facilitate the transition from adaptive RV hypertrophy to RV failure. Therapeutic strategies that reduce cellular stress and modify damaging failure components such as inflammation, lipotoxicity and proteotoxicity need to be explored in order to evaluate whether they can preserve RV function and improve outcome, even when the afterload of the RV cannot be significantly reduced.

Keywords

Right ventricular hypertrophy • Capillary rarefaction • Myocardial fibrosis • Cardiac MRI • Carvedilol

Introduction

In the early days of pulmonary hypertension research two important observations were made: First, it was recognized that many, perhaps most, patients with severe pulmonary arterial hypertension (PAH) died from right heart failure, many from sudden death. Second, the medical records showed, at a time when there was no treatment for PAH, that there were a few patients with very high pulmonary artery pressures, yet they were none-the-less long-time survivors [1]. Interestingly, when intravenous prostacyclin treatment was established for the treatment of patients with "primary" PAH, and shown to improve survival [2], it was not intuitive that

N.F. Voelkel
Virginia Commonwealth University P.O. Box 980678
Richmond, VA 23298-0678, USA
e-mail: nfvoelkel@gmail.com

M.K. Friedberg, A.N. Redington (eds.), *Right Ventricular Physiology, Adaptation and Failure in Congenital and Acquired Heart Disease*, https://doi.org/10.1007/978-3-319-67096-6_2

improved survival was due to improved right ventricular (RV) function and reversal of right ventricular failure (RVF). An early assessment of inadequate attention to the all-important RV failure component of severe PAH can be found in Michael Bristow's then state-of-the-art presentation at the Aspen Lung Conference in 1997.

> There are excellent data implicating RV function as an important determinant of the natural history of PPH. However, in this disorder, RV dysfunction has not received the kind of investigative scrutiny that pulmonary vascular mechanisms have enjoyed. This is partly because subjects with PPH are cared for by pulmonologists, whose investigative interests are focused on the lung rather than the heart….one of the fundamentally important questions surrounding PPH is that subjects differ substantially in their tendency to develop RVF. This leads to a variable natural history…. therefore mechanistic hypotheses for the development of RVF need to accommodate this biological variability [3].

This call to investigate mechanisms leading to RV failure has been answered in the past decade. The following paragraphs concern the main message of this chapter: In severe PAH, the lung vessels, the heart, the endocrine system and the immune system are involved, and therefore a systems-based approach and analysis are appropriate.

Is Right Ventricular Hypertrophy in Pulmonary Hypertension Bad?

Traditional teaching is that 'all hypertrophy is detrimental'. However, the exception is the RV in the setting of chronic pressure overload. Although never formally investigated, it is safe to say that the successful adaptation to a chronically elevated pulmonary artery pressure, with or without increased blood flow related to a shunt, requires RV hypertrophy. Similarly, in patients with congenitally corrected transposition of the great arteries a sub-aortic RV supports the high resistance systemic circulation.

Experimentally, banding of the main pulmonary artery (PAB) in the rat results in a robust RV hypertrophic response, yet without evidence of RV failure, even when PAB animals are additionally exposed to chronic hypoxia [4].We postulate that a hypertrophied, but well vascularized RV, with development of an adequate capillary bed does not fail. However, RV hypertrophy not adequately supplied by a proportionately developed microcirculation is prone to fail. To some degree, severe PAH associated with congenital heart disease and characterized by Eisenmenger physiology is the clinical example of a well-adapted RV [5]. In these patients, RV wall thickness is greater than in patients with IPAH, and there is less diffuse myocardial fibrosis [6]. In theory, it would be beneficial if the RV in patients with IPAH could be transformed into an "Eisenmenger RV". While cardiac myocytes make up 1/3 of the cells in the myocardium, they account for 80% of the mass; yet, hypertrophy is mainly due to KLF-5-driven up-regulation of IGF-1 in cardiac fibroblasts—a good example of cell-cell interaction [7]. Another characteristic of successful RV hypertrophic adaptation is enhanced fatty acid oxidation (FAO). A microvascular density that matches the increased muscle mass requires that the signaling chain that leads from transcription factor- and growth factor expression to an angiogenic response remains intact. The most important transcription factors involved in the capillary growth response are HIF-1alpha and PGC-1alpha.

Classic studies by Murray and Vatner in conscious dogs showed that blood flow in the hypertrophied RV approximately doubles [8], while the number of capillaries is maintained (Fig. 2.1). Thus, a muscular, well-perfused RV is required to handle an increased pulmonary vascular resistance.

Ischemia

The failing RV in patients with severe PAH is ischemic [9] and the reduced RV blood flow in these patients is likely, at least in part, explained by capillary rarefaction. The association of capillary rarefaction with ventricular failure had previously been elegantly demonstrated by Wolfgang Schaper's group in the hypertrophied LV in patients with aortic valve stenosis [10]. It is of

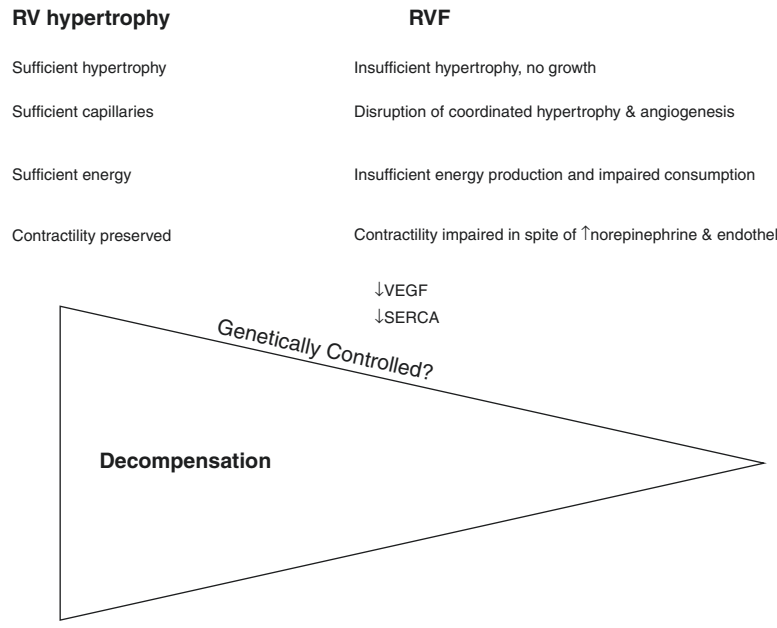

Fig. 2.1 Comparison of the well adapted, hypertrophied right ventricle and the failing right ventricle. The exact sequence of events that initiates the right heart failure program are not well understood. The schematic also postulates that there are genetically determined mechanisms that regulate adaptation to mechanical and oxidative stress

great interest that myocardial blood flow reserve in patients with severe PAH is significantly reduced not only in the pressure overloaded RV, but also in the underfilled LV [11]. Whether in this setting LV capillary rarefaction occurs is unknown. However, decreased LV preload correlates with clinical deterioration in patients with severe PAH.

Reduced RV Ejection Fraction in Severe PAH

It has long been appreciated that in patients with severe PAH a declining cardiac output heralds poor prognosis. The important cardiac magnetic resonance imaging (MRI) study by Van Veerdonk and coworkers [12] has now established that in PAH patients on'targeted' therapy a decline in the RV ejection fraction (RVEF) and not a decrease in the pulmonary vascular resistance (PVR) is a predictor of outcome. While PVR is calculated from hemodynamic variables, measurement of RVEF requires volume measurements by cMRI. The importance of this study is that a temporally treatment-associated decrease in PVR cannot be interpreted as a sign of clinical improvement unless the RVEF is also known. Put more succinctly, a decrease in RVEF while on targeted treatment for severe PAH is a predictor of short-term survival.

Why Does the RV Fail?

If pressure overload per se and RV hypertrophy are insufficient explanations for RV maladaptation and eventual failure, then what causes RV failure? Although RV failure is a clinical syndrome characterized by signs of congestion, there is increasing consensus that RV function can be assessed by measuring RVEF. While RV failure is characterized by RV volume overload, shift of the inter-ventricular septum and dilatation of the inferior vena cava, the factors which push the RV from the compensated state to failure differ perhaps between patients. There are signs of neurohormonal overdrive and of LV underfilling in most patients with progressive RV failure (Fig. 2.2) [13, 14]. Stress hormone production may be triggered by myocardial stress, ischemia and inflammation, all leading to an oxidant/antioxidant imbalance [15, 16] which predisposes cardiomyocytes and capillary endothelial cells to succumb to apoptosis.

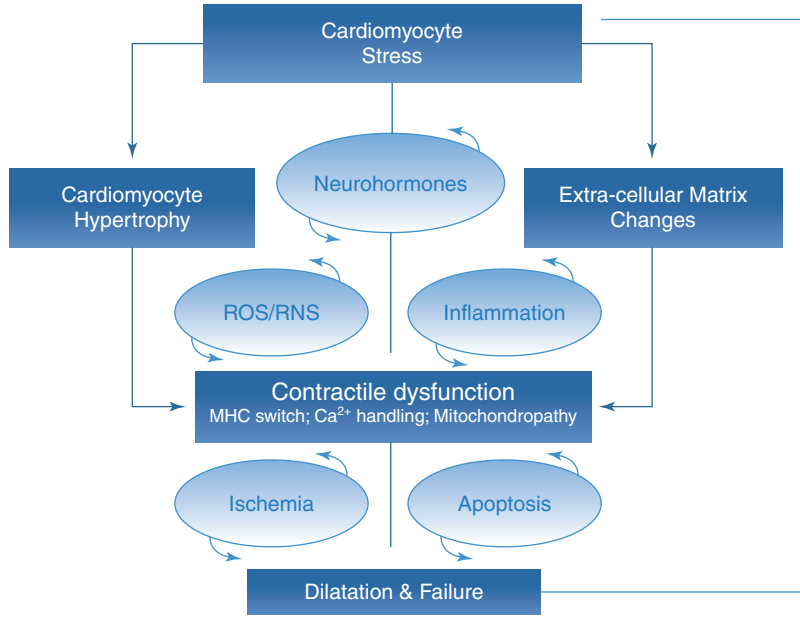

Fig. 2.2 This schematic depicts and integrates various elements of myocardial stress such as ischemia, inflammation and apoptosis that lead to RV dilatation and failure. With permission from Bogaard HJ, Abe K, Vonk Noordegraaf A, Voelkel NF. The right ventricle under pressure: cellular and molecular mechanisms of right-heart failure in pulmonary hypertension. Chest 2009;135:794–804 © Elsevier 2009 [13]

There are several potential ways forward on the journey to investigate the causes of RV failure. Experimentally, one can apply specific strategies designed to provoke the RV into failure. An example of such a strategy has been to treat PAB rats with a pan histone deacetylase inhibitor [17]. These animals develop RV capillary rarefaction, fibrosis and failure. In the Sugen/chronic hypoxia rat model of severe PAH, inhibition of VEGF signaling prevents the proper capillarization of the RV and this circumstance is one explanation for the development of RV failure in this model.

Clinically, one can sample peripheral and pulmonary venous blood and measure circulating mediator molecules such as norepinephrine, endothelin, cortisol, renin, angiotensin and aldosterone [18].

The Sick Lung Circulation Hypothesis

Given the pathological changes in a very large number of small pulmonary arterioles, and in some instances the pulmonary venules, which is the consequence of endothelial cell activation, endothelial cell apoptosis and phenotypic changes in the pulmonary vascular wall, functional changes in the lung circulation are not surprising. Most appreciated perhaps is endothelial cell dysfunction manifested by reduced endothelial cell nitric oxide (NO) and prostacyclin synthesis. We postulate that in addition, 'bad humors' are released from the sick lung circulation and predict that in chronic lung diseases where the lung vessels are involved, these 'bad humors' impact the heart [19–22]. A quantitative assessment of factors released by the sick lung circulation is possible by measuring the pulmonary arterio-venous gradient. To date only a few studies have reported on lung-tissue-dependent release of VEGF m, TGFbeta 1, PDGF-BB and PAI (plasminogen activator inhibitor). Release of MCP-1 and GDF-15 [23, 24] from the pulmonary hypertensive lung is likely, but has not been formally studied. Perros et al. [25] reported increased numbers of circulating cytotoxic cells and granulysin in patients with severe veno-occlusive PAH. In addition, free DNA and micro-RNA encapsulated in microspheres, emitted by the sick lung vessel cells, are likely to influence the structure and function of the myocardial micro-circulation. The postulated effects in the heart (both RV and LV) are activation and injury of the myocardial microvascular endothe-

lial cells and stimulation of endothelial cell-mesenchymal transformation (enMT), a process that can lead to myofibroblast formation and perivascular fibrosis.

The Molecular Gene Expression Signature of RV Failure

It is reasonable to postulate, based on what has been discussed so far, that the pattern of expressed genes and proteins differs between a compensated, hypertrophied RV and a failing RV. Mechanical wall stretch, ischemia and the altered myocardial milieu generated by the factors released by the sick lung circulation may all impact the RV and generate a gene expression signature of RV failure. Experiments were conducted and RNA was extracted from RV and LV tissue samples comparing normal rat hearts with those from PAB rats and rats that had undergone the Sugen/chronic hypoxia protocol [26]. The failing RV in Su/Hx rats was hypertrophied and dilated, TAPSE was significantly decreased and histologically the tissue was characterized by capillary rarefaction, apoptosis and fibrosis [27]. Remaining microvessels showed a lack of expression of the prostacyclin synthase protein. Microarray expression analysis of the four groups of animals elucidated patterns of expressed genes that reflected mechanisms underlying the compensated state versus the failure state. For example, as adaptive RV hypertrophy is driven by IGF-1, it was highly expressed in the PAB RV, but decreased in the Su/Hx failing RV (Fig. 2.3). Phosphorylated Akt expression was decreased in the failing RV (Fig. 2.4), as were VEGFA and apelin [27]. Gene expression of key enzymes encoding fatty acid oxidation, including expression of the transcription factor PGC-1alpha (Figs. 2.5 and 2.6), were decreased and gene expression of enzymes encoding the glycolytic pathway were increased [26]. As expected, we found clear and categorical gene expression patterns, which allow mechanistic explanation of adapted and failing tissue at the level of cell growth/autophagy/apoptosis, inflammation, fibrosis and intact or impaired

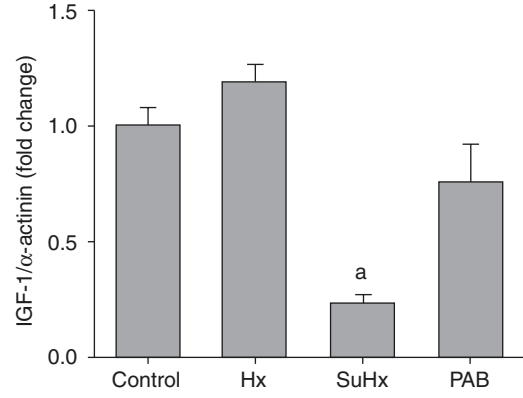

Fig. 2.3 Protein expression of IGF-1 in the RV myocardium, assessed by Western blot is dramatically decreased in the failing RV from rats exposed to the Sugen/chronic hypoxia protocol (SuHx), when compared to rats exposed to chronic hypoxia alone or to the RV from rats weeks following pulmonary artery banding (PAB). With permission from Bogaard HJ, Natarajan R, Mizuno S, Abbate A, Chang PJ, Chau VQ, Hoke NN, Kraskauskas D, Kasper M, Salloum FN, Voelkel NF. Adrenergic receptor blockade reverses right heart remodeling and dysfunction in pulmonary hypertensive rats. Am J Respir Crit Care Med. 2010;182:652–60 © American Thoracic Society 2010 [27]

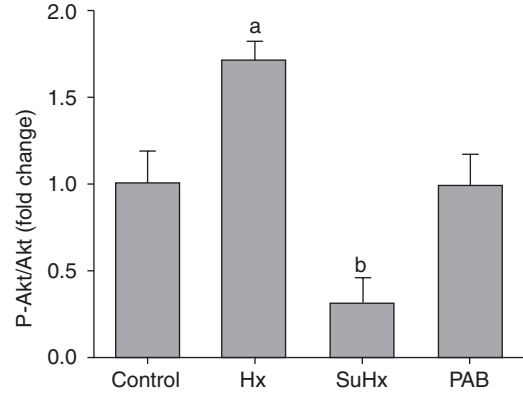

Fig. 2.4 Protein expression of phoshorylated Akt (pAkt), initiated downstream in the signaling cascade after binding of the angiogenic VEGF ligand to its receptors in the RV myocardium, assessed by Western blot, is dramatically decreased in the failing RV from rats exposed to the Sugen/chronic hypoxia protocol (SuHx) when compared to rats exposed to chronic hypoxia alone or to the RV from rats weeks following pulmonary artery banding (PAB). With permission from Bogaard HJ, Natarajan R, Mizuno S, Abbate A, Chang PJ, Chau VQ, Hoke NN, Kraskauskas D, Kasper M, Salloum FN, Voelkel NF. Adrenergic receptor blockade reverses right heart remodeling and dysfunction in pulmonary hypertensive rats. Am J Respir Crit Care Med. 2010;182:652–60 © American Thoracic Society 2010 [27]

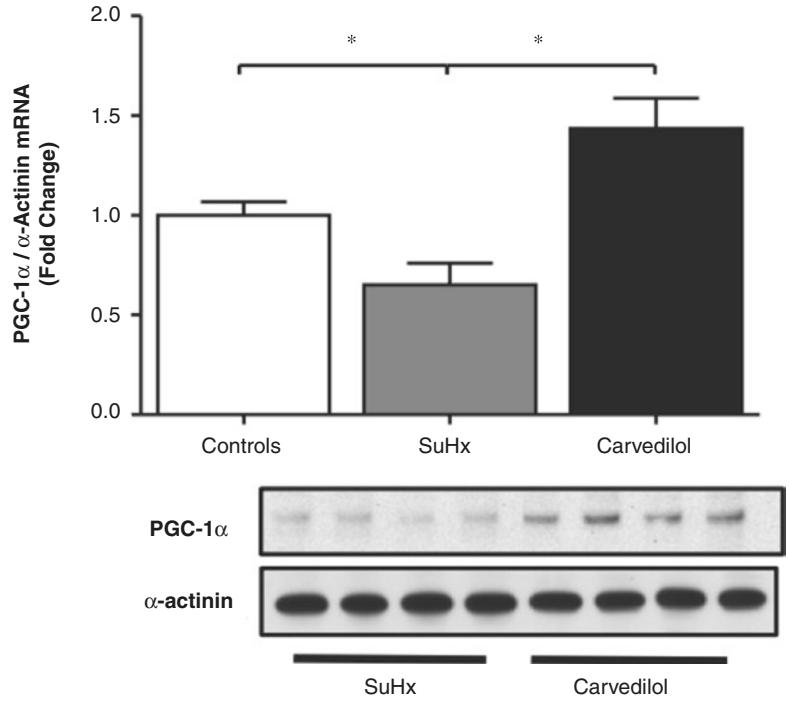

Fig. 2.5 Protein expression of the transcription factor PGC-1alpha, important for VEGF transcription and transcription of genes encoding enzymes of fatty acid oxidation, is reduced in the failing RV from SuHx animals. Treatment of rats with carvedilol after established RV failure reversed the decrease in PGC-1 alpha expression. With permission from Gomez-Arroyo J, Mizuno S, Szczepanek K, Van Tassel B, Natarajan R, dos Remedios C, Drake JI et al. Metabolic remodeling and mitochondrial dysfunction in failing right ventricular hypertrophy secondary to pulmonary arterial hypertension. Cir Heart Failure 2013;6:136–144 © Wolters Kluwer 2013 [29]

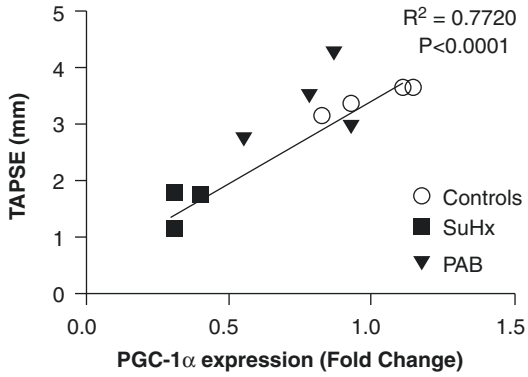

Fig. 2.6 Decreased expression of PGC-1alpha is of functional importance as its expression correlates with TAPSE (tricuspid valve plane systolic excursion). With permission from Gomez-Arroyo J, Mizuno S, Szczepanek K, Van Tassel B, Natarajan R, dos Remedios C, Drake JI et al. Metabolic remodeling and mitochondrial dysfunction in failing right ventricular hypertrophy secondary to pulmonary arterial hypertension. Cir Heart Failure 2013;6:136–144 © Wolters Kluwer 2013 [29]

angiogenesis [26]. Because experimental RV failure in the Su/Hx rats could be reversed by treatment with carvedilol, this lead to testing of the hypothesis that components of the RV failure program or gene expression signature could be changed or normalized. It was found that carvedilol-induced reversal of RV failure was associated with a reduction of RV hypertrophy and return of a capillary density towards normal. Under the influence of chronic carvedilol treatment more than 400 genes were altered in their expression reflecting improved myocardial energy metabolism and reduced myocardial stress, even though RV afterload remained unchanged [27–29]. These experimental data provided the impetus to test carvedilol treatment as add-on therapy to established treatment of patients with severe PAH and assessment of the RVEF after 6 months of carvedilol therapy. The

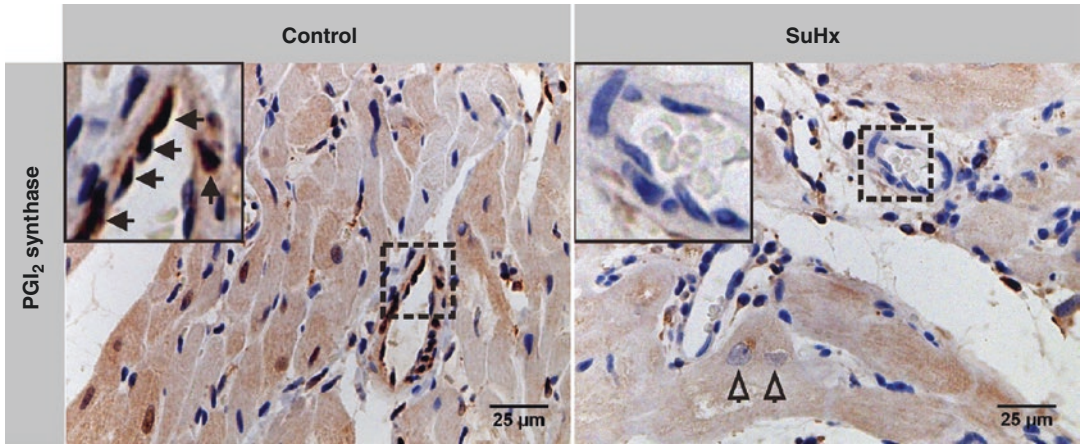

Fig. 2.7 Right ventricle, immuno-histochemistry; staining for an antibody directed against prostacyclin synthase, the terminal enzyme required for prostacyclin synthesis. Right ventricular tissue from a rat exposed to the SuHx protocol with established RV failure. The inserts show capillary endothelial cells. The expression of prostacyclin synthase protein is lost in the capillary from the failing RV. This indicates that there is endothelial cell dysfunction in the remaining RV capillaries, not only loss of capillaries

small pilot study results suggest that carvedilol treatment of PAH patients is safe and increases RVEF as measured by cMRI [30].

Conclusion and New Hypotheses

Hypertrophy is required for the RV to adapt successfully to a chronically elevated afterload and a chronically elevated RV afterload *per se* is insufficient to cause RV failure. One postulate that needs to be investigated is that activation of neuroendocrine pathways is one important mechanism that promotes the transition from a stressed but functional RV to frank RV failure. A second postulate is that a myocardial microangiopathy is critically involved and responsible for the "metabolic remodeling" and an EnMT that leads to perivascular fibrosis. Further, it is intriguing to speculate that the health of the lung vessel endothelium is linked to the health of the myocardial microvascular endothelium and that the function of the microvessel endothelial cells in the heart (Fig. 2.7) is linked to the metabolic reprogramming of the cardiomyocytes. If so, an improvement of endothelial cell function may repair the mitochondriopathy, which likely underlies the myocardial oxidative stress and endoplasmic reticulum stress.

The experimental studies demonstrating reversal of RV failure by carvedilol treatment are encouraging and hopefully will stimulate the search for additional therapeutic strategies to support the right ventricle under pressure [13]. As atrial septostomy does not in any way influence the behavior of the hypertensive lung circulation, but unloads the RV and improves exercise tolerance [31], treatment to reduce cellular stress and modify damaging failure components such as lipotoxicity [32] and proteotoxicity [33] may stabilize the RV under pressure, even when its afterload cannot be significantly reduced.

References

1. Voelkel NF, Reeves JT. Primary pulmonary hypertension. In: Moser KM, editor. Pulmonary vascular diseases. New York: Marcel Dekker; 1979. p. 573–628.
2. Barst RJ, Rubin LJ, Long WA, McGoon MD, Rich S, Badesch DB, Groves BM, et al. A comparison of intravenous epoprostenol (prostacyclin) with conventional therapy_for primary pulmonary hypertension. NEJM. 1996;334:296–301.
3. Bristow MR, Zisman LS, Lowes BD, Abraham WT, Badesch DB, et al. The pressure overloaded right ventricle in pulmonary hypertension. Chest. 1998;114:101S–6S.

4. Bogaard HJ, Natarajan R, Henderson C, Long CS, Kraskauskas D, Smithson L, Ockaili R, McCord JM, Voelkel NF. Chronic pulmonary artery pressure overload is insufficient to explain right heart failure. Circulation. 2009;120:1951–60.
5. Hopkins WE, Ochoa LL, Richardson GW, Trulock EP. Comparison of the hemodynamics and survival of adults with severe primary pulmonary hypertension or Eisenmenger syndrome. J Heart Lung Transplant. 1996;15:100–5.
6. Gomez-Arroyo JG, Santos-Martinez LE, Aranda A, Pullido T, Beltran M, et al. Differences in right ventricular remodeling secondary to pressure overload in patients with pulmonary hypertension. Am J Resp Crit Care Med. 2014;189:603–6.
7. Takeda N, Manabe I, Uchino Y, Eguchi K, Matsumoto S, Nishimura S, Shindo T, Sano M, Otsu K, Snider P, Conway SJ, Nagai R. Cardiac fibroblasts are essential for the adaptive response of the murine heart to pressure overload. J Clin Invest. 2010;120(1):254–65.
8. Murray PA, Baig H, Fishbein MC, Vatner SF. Effects of exerimental right ventricular hypertrophy on myocardial blood flow in conscious dogs. J Clin Invest. 1979;64:421–7.
9. Gómez A, Bialostozky D, Zajarias A, Santos E, Palomar A, Martínez ML, Sandoval J. Right ventricular ischemia in patients with primary pulmonary hypertension. J Am Coll Cardiol. 2001;38:1137–42.
10. Elsässer A, Decker E, Kostin S, Hein S, Skwara W, Müller KD, Greiber S, Schaper W, Klövekorn WP, Schaper JA. self-perpetuating vicious cycle of tissue damage in human hibernating myocardium. Mol. Cell Biochem. 2000;213:17–28.
11. Vogel-Claussen J, Skrok J, Shehata ML, Singh S, Sibley CT, Boyce DM, Lechtzin N, Girgis RE, Mathai SC, Goldstein TA, Zheng J, Lima JA, Bluemke DA, Hassoun PM. Right and left ventricular myocardial perfusion reserves correlate with right ventricular function and pulmonary hemodynamics in patients with pulmonary arterial hypertension. Radiology. 2011;258:119–27.
12. van de Veerdonk MC, Kind T, Marcus JT, Mauritz GJ, Heymans MW, Bogaard HJ, Boonstra A, Marques KM, Westerhof N, Vonk-Noordegraaf A. Progressive right ventricular dysfunction in patients with pulmonary arterial hypertension responding to therapy. J Am Coll Cardiol. 2011;58:2511–9.
13. Bogaard HJ, Abe K, Vonk Noordegraaf A, Voelkel NF. The right ventricle under pressure: cellular and molecular mechanisms of right-heart failure in pulmonary hypertension. Chest. 2009;135:794–804.
14. de Man FS, Handoko ML, Guignabert C, Bogaard HJ, Vonk-Noordegraaf A. Neurohormonal axis in patients with pulmonary arterial hypertension: friend or foe? Am J Respir Crit Care Med. 2013;187:14–9.
15. Voelkel NF, Natarajan R, Drake JI, Bogaard HJ. Right ventricle in pulmonary hypertension. Compr Physiol. 2011;1:525–40.
16. Purnomo Y, Piccart Y, Coenen T, Prihadi JS, Lijnen PJ. Oxidative stress and transforming growth factor beta 1-induced cardiac fibrosis. Cardiovasc Hematol Disord Drug Targets. 2013;13:165–72.
17. Bogaard HJ, Mizuno S, Hussaini AA, Toldo S, Abbate A, Kraskauskas D, Kasper M, Natarajan R, Voelkel NF. Suppression of histone deacetylases worsens right ventricular dysfunction after pulmonary artery banding in rats. Am J Respir Crit Care Med. 2011;183:1402–10.
18. Nolly MB, Caldiz CI, Yeves AM, Villa-Abrille MC, Morgan PE, et al. The signaling pathway for aldosterone-induced mitochondrial production of superoxide anion in the myocardium. J Mol Cell Cardiol. 2014;67:60–8.
19. Voelkel NF, Gomez-Arroyo J, Abbate A, Bogaard HJ, Nicolls MR. Pathobiology of pulmonary arterial hypertension and right ventricular failure. Eur Respir J. 2012;40:1555–65.
20. Voelkel NF. The sick lung circulation and the failing right ventricle. In: Voelkel NF, Schranz D, editors. The right ventricle in health and disease. New York: Springer; 2015. p. 303–13.
21. Voelkel NF, Gomez-Arroyo J, Abbate A, Bogaard HJ. Mechanisms of righheart failure-A work in progress and a plea for failure prevention. Pulm Circ. 2013;3:137–43.
22. Oka T, Hikoso S, Yamaguchi O, Taneike M, Takeda T, et al. Mitochondrial DNA that escapes from autophagy causes inflammation and heart failure. Nature. 2012;485:251–5.
23. Park JE, Lyon AR, Shao D, Hector LR, Xu H, O'Gara P, Pinhu L, Chambers RC, Wort SJ, Griffiths MJ. Pulmonary venous hypertension and mechanical strain stimulate monocyte chemoattractant protein-1 release and structural remodelling of the lung in human and rodent chronic heart failure models. Thorax. 2014;69:1120–7.
24. Nickel N, Kempf T, Tapken H, Tongers J, Laenger F, Lehmann U, Golpon H, Olsson K, Wilkins MR, Gibbs JS, Hoeper MM. Wollert KCGrowth differentiation factor-15 in idiopathic pulmonary arterial hypertension. Am J Respir Crit Care Med. 2008;178:534–41.
25. Perros F, Cohen-Kaminsky S, Gambaryan N, Girerd B, Raymond N, Klingelschmitt I, Huertas A, Mercier O, Fadel E, Simonneau G, Humbert M, Dorfmüller P, Montani D. Cytotoxic cells and granulysin in pulmonary arterial hypertension and pulmonary veno-occlusive disease. Am J Respir Crit Care Med. 2013;187(2):189–96.
26. Drake JI, Bogaard HJ, Mizuno S, Clifton B, Xie B, Gao Y, Dumur CI, Fawcett P, Voelkel NF, Natarajan R. Molecular signature of a right heart failure program in chronic severe pulmonary hypertension. Am J Respir Cell Mol Biol. 2011;45:1239–47.
27. Bogaard HJ, Natarajan R, Mizuno S, Abbate A, Chang PJ, Chau VQ, Hoke NN, Kraskauskas D, Kasper M, Salloum FN, Voelkel NF. Adrenergic receptor blockade reverses right heart remodeling and dysfunction in pulmonary hypertensive rats. Am J Respir Crit Care Med. 2010;182:652–60.
28. Drake JI, Gomez-Arroyo J, Dumur CI, Kraskauskas D, Natarajan R, Bogaard HJ, Fawcett P, Voelkel

NF. Chronic carvedilol treatment partially reverses the right ventricular failure transcriptional profile in experimental pulmonary hypertension. Physiol Genomics. 2013;45:449–61.
29. Gomez-Arroyo J, Mizuno S, Szczepanek K, Van Tassel B, Natarajan R, dos Remedios C, Drake JI, et al. Metabolic remodeling and mitochondrial dysfunction in failing right ventricular hypertrophy secondary to pulmonary arterial hypertension. Cir Heart Fail. 2013;6:136–44.
30. Grinnan D, Bogaard HJ, Grizzard J, Van Tassell B, Abbate A, DeWilde C, Priday A, Voelkel NF. Treatment of group I pulmonary arterial hypertension with carvedilol is safe. Am J Respir Crit Care Med. 2014;189:1562–4.
31. Sandoval J, Torbicki A. Atrial septostomy. In: Voelkel NF, Schranz D, editors. The right ventricle in health and disease. New York: Springer; 2015. p. 419–37.
32. Hemnes AR, Brittain EL, Trammell AW, Fessel JP, Austin ED, Penner N, Maynard KB, Gleaves L, Talati M, Absi T, Disalvo T, West J. Evidence for right ventricular lipotoxicity in heritable pulmonary arterial hypertension. Am J Respir Crit Care Med. 2014;189:325–34.
33. McLendon PM, Robbins J. Proteotoxicity and cardiac dysfunction. Circ Res. 2015;116:1863–82.

Molecular Aspects of Right Ventricular Adaptation to Stress

3

Sushma Reddy and Daniel Bernstein

Abstract

The development of left ventricular (LV) hypertrophy and the progression to LV failure have been extensively studied and have provided valuable insight into the mechanisms of disease progression. However, there is minimal data on the right ventricular (RV) adaptation to pressure and volume loading. These hemodynamic stressors are commonly seen in children and adults after surgery for congenital heart disease (CHD), placing the RV at risk for progression to heart failure. Here, we will highlight some of similarities and differences in the molecular remodeling between the right and left ventricles when subjected to abnormal loading conditions.

Keywords

Heart defects, congenital • Heart failure • Right ventricle • Hypertrophy
Oxidative stress • Angiogenesis

Introduction

Congenital heart disease (CHD) is the single most common class of birth defects and is a leading cause of infant mortality in developing countries [1, 2]. CHD often leads to abnormal loading conditions starting in the neonatal period both before and after surgical palliation leading to a lifetime of chronic pressure and/or volume loading. While numerous animal and human studies have led to valuable insight into the molecular mechanisms of left ventricular (LV) hypertrophy and the progression from a compensated state to one of overt heart failure, [3, 4] little is known about the right ventricular (RV) response to stress [5, 6]. The RV response to pressure overload secondary to pulmonary hypertension (PHTN) and work in animal models of CHD are only now being evaluated. In addition to RV pressure overload seen in CHD patients with single RVs, systemic RVs as in l-transposition or d-transposition

S. Reddy (✉) • D. Bernstein
Pediatric Cardiology, Lucile Packard Children's Hospital, Stanford University, 750 Welch Rd, Ste 305, Palo Alto, CA 94304, USA
e-mail: sureddy@stanford.edu

M.K. Friedberg, A.N. Redington (eds.), *Right Ventricular Physiology, Adaptation and Failure in Congenital and Acquired Heart Disease*, https://doi.org/10.1007/978-3-319-67096-6_3

following atrial switch and PHTN, RV volume overload is a much more common and unique sequelae after repair of many forms of CHD such as tetralogy of Fallot or pulmonary atresia following RV outflow tract reconstruction. There is even less data on RV remodeling following volume overload. With advances in medical and surgical care of these children, they are growing into adolescence and adulthood with the potential for a lifetime of abnormal loading conditions on the RV, predisposing them to early heart failure, arrhythmias, transplantation and death. Their quality of life will ultimately depend on our ability to understand the basic mechanism of disease progression, identify potential drug targets and develop RV-specific therapies. We will highlight our current knowledge of the RV adaptation to the unique hemodynamic stressors seen in the CHD patient while discussing the similarities and differences between right and left ventricular remodeling and addressing novel therapies currently in development.

The Right and Left Ventricles Respond Differently to Increasing Afterload

The RV is uniquely at risk when exposed to chronic afterload. This is best demonstrated in long-term studies of patients with single ventricle physiology, where the systemic RV progresses to heart failure sooner and more often than those with a systemic LV [7]. Similarly, patients with l-transposition of the great arteries or patients who have undergone an atrial switch operation for d-transposition of the great arteries, where the RV functions as the systemic ventricle, have an increased risk of RV failure, even in the absence of atrioventricular valve regurgitation or other lesions. These systemic RVs develop hypertrophy at a very early age or never regress, suggesting that increased wall stress alone cannot be the only factor predisposing these ventricles to failure. In addition, standard left heart failure drugs (β-blockers, ACE inhibitors, angiotensin II receptor blockers), have been shown to not improve function or survival in patients with systemic RV failure due to CHD in multiple clinical trials. Critically, β-blockers appeared to worsen outcomes in patients with a systemic RV in one trial [8–11] suggesting fundamental differences in the mechanisms of right vs. left ventricular failure, particularly when treating systemic RV failure in CHD.

In the past, these differences between the right and left ventricles were thought to be related to changes in shape, structure and loading conditions [12, 13]. We now know that these differences begin early in development, before afterload differences become operative. The primary and secondary heart fields, lead to the differentiation of left or right ventricular cardiomyocytes during early development, with subsequent chamber-specific differences in cell signaling and Ca^{2+} handling, all suggesting fundamental differences between the two ventricles at the cellular level as well [14].

Using animal models of pressure overload stress, we and others have shown that the two ventricles exhibit similar molecular alterations in genes regulating extracellular matrix and cytoskeletal remodeling. However, there are important differences in genes regulating reactive oxygen species (ROS) production and antioxidant protection, angiogenesis, energy production and mitochondrial function (Table 3.1 and Fig. 3.1) [15–18]. These results confirm differences at the cellular and molecular level in the mechanisms leading to heart failure between the two ventricles, which are discussed below.

RV Molecular Remodeling: Adaptive and Maladaptive Responses

ROS Production and Antioxidant Defenses

Under conditions of afterload stress, both ventricles increase overall cellular ROS production; however, the RV antioxidant defenses via superoxide dismutase (SOD) and glutathione peroxidase (GPX) fail early, whereas in the LV they remain intact until a more advanced stage of failure [19, 20]. This results in early ROS-

Table 3.1 Summary of key findings in the right ventricle during rest, hypertrophy and failure

Pathways	Effect of RV hypertrophy and failure	Significance in the RV	LV hypertrophy and failure
Metabolic adaptation	⇓ Fatty acid binding protein (non stressed state) ⇑ Glycolysis ⇓ Mitochondrial complex 1, III, IV ⇓ Resting mitochondrial membrane potential; hyperpolarized with hypertrophy ⇓ Mitochondrial DNA with failure in CHD	⇓ Energy production	- FABP - Resting mitochondrial membrane potential
Oxidative stress	⇑ Hif-1α activation and complex II-mediated ROS production Antioxidant enzymes (SOD, GPX) are not activated with hypertophy ⇓PGC1α	⇑ Mitochondrial ROS production	⇑ NADPH oxidase mediated ROS production ⇑ Antioxidant enzyme activity (SOD, GPX) with hypertrophy NADPH oxidase mediated ROS production
Electrical remodeling	⇓ Kv channel expression, prolonging the action potential and QT interval	⇑ Risk of arrhythmias	
Angiogenesis	⇓ Microvascular bed ⇓ Angiogenic response	⇑ Susceptibility to ischemia	⇑ Microvascular bed and angiogenic response with hypertrophy
Response to hypoxia	⇑ Glycolysis	⇓ Energy production	
Adrenergic receptors	⇓ β-, α1- and DA1 receptors ⇓cAMP levels and ⇑GRK2 activity ⇑ Coupling of β2 receptors to Gs ⇓ Myofilament Ca^{2+} sensitivity through phosphorytation of MLCK (non stress)	⇓ Inotropic response ⇑ β2-receptor mediated inotrophy and lusitropy Negative α1-signaling (non stress) switches to positive (failure)	Positive α1-signaling (non stress) due to ⇑ myofilament Ca^{2+} sensitivity
RAAS	RAAS activation	Hypertrophy	
MicroRNAs	Non-cardiomyocyte origin of some miRs Defect in MiR-126/VEGF pathway	Paracrine effect of cardiomyocytes ⇓ Angiogenesis	

FABP fatty acid binding protein, *CHD* congenital heart disease, *SOD* superoxide dismutase, *GPX* glutathione peroxidase, *GRK* G protein-coupled receptor kinase, *MLCK* myosin light chain, *RAAS* renin-angiotensin-aldosterone system. With permission from Reddy S, Bernstein D. Molecular Mechanisms of Right Ventricular Failure. Circulation. 2015 Nov 03;132 (18):1734–42 © Wolters Kluwer 2015 [17]

related damage and apoptosis [21]. It is encouraging to note that the antioxidant EUK-134 (a superoxide dismutase and catalase mimetic) was shown to reduce oxidative stress and ROS production in the failing RV due to PHTN and to improve RV systolic function [22]. There are also differences between the two ventricles in the primary source of ROS production, with greater mitochondrial ROS generation by NADPH oxidase and mitochondrial complex II in RV failure [23].

PGC1α is a key regulator of both mitochondrial metabolism and mitochondrial biogenesis (the generation of "new" mitochondria) which has been shown to be decreased in animal models of RV failure, leading to impaired fatty acid

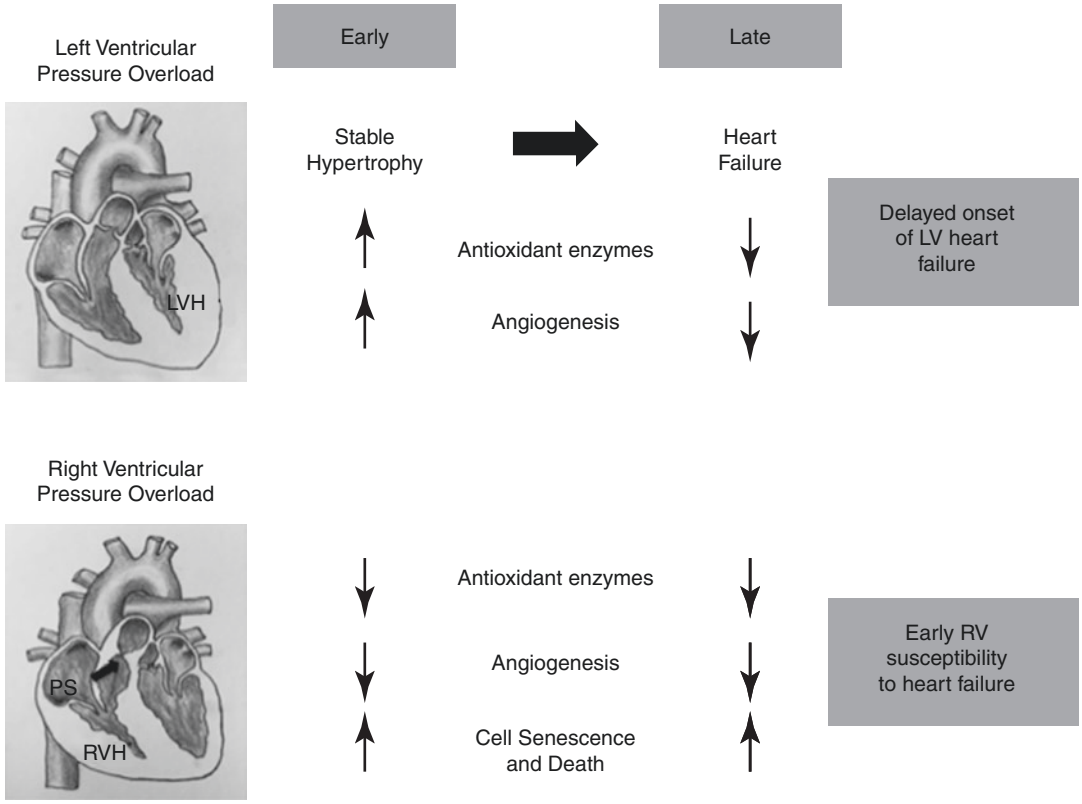

Fig. 3.1 Right ventricular susceptibility to heart failure. Stable LVH is characterized by an increase in antioxidant enzymes and angiogenesis and decreased ROS generation, which protects the LV from early progression to heart failure. However in RVH, there is an early decrease in antioxidant enzymes and failure of angiogenesis along with increased ROS and cell death thereby making the RV more susceptible to early heart failure. *LVH* left ventricular hypertrophy, *RVH* right ventricular hypertrophy, *PS* pulmonary stenosis, *ROS* reactive oxygen species. Cardiac illustrations by Mingming Zhao. With permission from Reddy S, Bernstein D. The vulnerable right ventricle. Current opinion in pediatrics. 2015 Oct;27 (5):563–8 © Wolters Kluwer Health 2015 [18]

oxidation, decreased mitochondrial mass and number, and reduced oxidative capacity. This represents another mechanism leading to increased ROS production, causing mitochondrial DNA damage and impairing mitochondrial biogenesis [20, 24]. These data were confirmed in patients by Karamanlidis et al., who demonstrated a progressive decline in mitochondrial DNA with the progression from RVH to RVF in children with CHD (including those with TOF, pulmonary stenosis, double outlet RV, double chambered RV and single RV). They also showed that mitochondrial DNA-encoded genes responsible for mitochondrial biogenesis fall before the onset of heart failure [24].

Blood Flow and Angiogenesis

The RV has a lower resting oxygen consumption and therefore lower resting coronary blood flow than the LV. In the normal RV, the majority of coronary flow occurs in systole, in contrast to the normal LV where coronary flow is mostly in diastole thereby making the RV more susceptible to ischemia in conditions of afterload stress. Animal data suggests that right coronary artery flow is increased in response to afterload stress. However, whether this is adequate to meet the increased oxygen demand of the hypertrophied RV remains to be determined [25, 26].

As a further insult to the vulnerable RV, there are differences in the RV's ability to induce the

formation of new blood vessels to compensate for myocardial hypertrophy compared to that of the LV [27, 28]. When the LV is exposed to afterload stress, it initially increases the production of new capillaries (angiogenesis), in order to keep up with the increased blood flow requirements of hypertrophied cardiomyocytes. This process is mediated by increased cardiomyocyte production of the pro-angiogenic factors HIF-1α and vascular endothelial growth factor (VEGF) Angiogenesis is only impaired when the LV begins to fail, which is mediated by an increase in p53, which then inhibits pro-angiogenic factors. In contrast, in the RV, even at the onset of pressure overload, VEGF falls and thus capillary density decreases, rendering the stressed RV more susceptible to micro-ischemic injury [23, 27–31]. In compensation, there is right coronary artery vasodilation via endogenous release of NO, thereby helping to improve oxygen demand-supply balance, at least temporarily. This is another feature not seen in the afterload stressed LV [32, 33]. Thus, whether differences in RV vs. LV oxygen delivery and microvascular remodeling are responsible for the differences in stress response between the two ventricles is still an area open to further investigation.

Response to Hypoxia

Hypoxia can be a component of the clinical picture in patients with RV failure, whether due to persistent right-to-left shunts in CHD, or in patients with PHTN. Hypoxia activates Hif1α/VEGF signaling in the RV in the SUGEN-hypoxia animal model of PHTN, but similar to isolated pressure overload, without increasing capillary density. This is particularly relevant in systemic RVs exposed to hypoxia such as in infants with hypoplastic left heart syndrome after a Norwood/Sano or Glenn palliation, and before their Fontan procedure, where the RV is hypertrophied, leading to increased metabolic demand, but fails to increase capillary density to enhance delivery of oxygen and nutrients. This combination of these stressors may be responsible for the increased rate of failure of these single RVs. Hypoxia also triggers glycolysis, which may correlate with the development of RV failure [15].

Neurohormonal Activation: Adrenergic Receptors

β-adrenergic receptor signal regulation is similar in the normal RV and LV, leading to a positive inotropic response in both ventricles. β-adrenergic receptor signal regulation is also similar in animal models of failing RV vs. the LV with downregulation of β1-, α1- and DA1 receptors, decreased cAMP levels and increased G protein-coupled receptor kinase-2 (GRK2) activity, leading to an impaired inotropic response. This downregulation of adrenergic signaling is greater in PHTN-induced than in PAB-induced RV hypertrophy and failure. Interestingly however, the clinical response of the two ventricles to β-adrenergic blockers is quite different [34]. Children with systemic RVs did not benefit from the use of β-blockers, and there is even a suggestion that this class of drugs can worsen heart failure symptoms [10]. Similarly, in adults with RV failure after repaired tetralogy of Fallot, β-blockade showed no improvement in peak VO2, RVEF, ventricular volume or NYHA class [35]. In contrast, one retrospective study of adults with a systemic RV and mild (NYHA class I and II) symptoms did show an improvement if they were taking a β-blocker for at least 4 months [36]. These patients showed an increase in β2-receptor mediated inotropy and lusitropy secondary to enhanced coupling of β2 receptors to Gs [37].

In contrast, there is evidence that α1-adrenergic receptor signaling differs between the non-stressed RV and LV. Stimulation of α1-receptors results in a negative inotropic response in the RV and a positive inotropic response in the LV. This differential response is not mediated by differences in PKC activation, but instead by greater myofilament Ca^{2+} sensitivity through phosphorylation of myosin light chain (MLCK) in the LV versus the RV [38]. However, in a model of the failing RV induced by coronary artery ligation, MLCK increases, resulting in a

greater myofilament Ca^{2+} sensitivity, and α1-signaling then switches from being a negative to being a positive inotrope [39]. The applicability of these findings in RV failure due to non-ischemic heart disease, such as in children with CHD, remains to be determined.

Neurohormonal Activation: Renin-Angiotensin-Aldosterone System (RAAS)

RAAS activation occurs in the setting of low LV cardiac output and or low systemic vascular resistance, causes vasoconstriction and increased tubular sodium reabsorption peripherally and is also a positive mediator of cardiomyocyte fibrosis. There is limited data on RAAS in RV failure other than a few studies in chronic obstructive pulmonary disease and systemic sclerosis causing PHTN [40–42]. RAAS activation is seen in patients with PHTN and treatment with losartan, an angiotensin II receptor antagonist decreases hypertrophy and restores normal RV-pulmonary arterial coupling [43]. Treatment with ACE inhibition in PHTN patients however has conflicting results, which is thought to be related to breakthrough aldosterone signaling from incomplete inhibition [43]. Similarly, whether RAAS is stimulated with RV failure in the setting of CHD remains to be determined, particularly important since ACE inhibitors (enalapril, ramipril) and angiotensin II receptor antagonists (losartan) have failed to improve right heart failure in CHD patients with a systemic RV [11, 44–46]. There are currently clinical trials evaluating the efficacy of losartan in adults with tetralogy of Fallot and RV failure, but a better understanding of the basic mechanisms of RAAS activation in the stressed RV needs to be concurrently undertaken.

Mitochondrial Remodeling

The mitochondrial protein profiles of the RV and LV are similar at rest, with equivalent cellular aerobic capacity, volume of mitochondria, mitochondrial enzyme content (cytochrome c oxidase, complexes 1, 3, 4 and 5, aconitase and Mn-SOD) and mitochondrial enzyme activities [47]. In the LV exposed to afterload stress, antioxidant enzymes such as Mn-SOD increase during the early stages, whereas in the RV Mn-SOD never increases, which may lead to an earlier increase in mitochondrial reactive oxygen species production and subsequent mitochondrial dysfunction and cell death when compared to the LV [21].

Mitochondrial membrane potential, a surrogate of overall mitochondrial function, is lower in the resting RV than in the LV. With RV afterload stress, there is an increase in mitochondrial membrane potential which may be related to activation of the NFAT pathway, and which is reversed by the PDK inhibitor dichloroacetate (discussed below). This difference in mitochondrial remodeling may represent another difference in the stress response between the RV and the LV, and represents another potential target for RV-specific therapy [48].

Metabolic Adaptations to Pressure Overload

The RV and LV differ in their work load, and hence in their energy needs. The LV workload is five times greater than the RV due to the higher systemic vascular resistance when compared to the low resistance pulmonary vascular bed. Due to this decreased workload on the resting RV, both oxygen consumption and metabolic stress are lower than in the LV [25, 49]. Despite this difference, the non-stressed RV and LV are largely similar in their energetic profiles [47].

The metabolic profile of both ventricles is profoundly altered with afterload stress. Both the RV and LV myocardium normally utilize free fatty acids for biosynthesis and energy production. With afterload stress, the myocardium shifts to a greater dependence on glucose for its energy source via increased glucose uptake and glycolysis. While this shift is beneficial during acute stress, chronic dependence on glycolysis for energy production is inadequate to meet the demands of the myocardium, leading to an energy starved state and subsequently to heart failure.

In RV failure secondary to pulmonary artery banding (PAB), this shift in glycolysis is associated with a 50% decrease in energy reserve [50]. Decreased glucose oxidation is also related to the activation of pyruvate dehydrogenase kinases (PDKs), preventing pyruvate from entering the Krebs cycle and decreasing ATP generation. Dichloroacetate inhibits PDKs and improves glucose oxidation and RV function in rat models of PHTN [15]. Partial inhibition of beta-oxidation by trimetazidine has been shown to improve both LV and RV function in patients with diabetic cardiomyopathy [51]. To date, these drugs have not been tested in animal models of CHD. Other mediators increasing glycolysis, Hif-1α and p38-MAPK are also activated when the RV begins to fail. In a murine model of acute, severe PAB-induced RV failure, we showed a downregulation of mitochondrial enzymes (acetyl-coenzyme A acyltransferase 2, NADH dehydrogenase, NADH-ubiquinone oxidoreductase, succinate dehydrogenase complex and ATP synthase). Whereas a decrease in mitochondrial enzymes-complex 1, III and IV are seen in children with tetralogy of Fallot; there is no data on systemic right ventricles as in l-TGA, d-TGA after atrial switch or single right ventricles [52]. There is suggestion that at least some components of RV electrical remodeling may be secondary to metabolic derangements such as the reduced Kv channel expression, prolonging the action potential duration and QT interval and increasing the risk of arrhythmias [15]. Interestingly, these can be reversed by restoration of glucose oxidation using dichloroacetate.

In summary, the RV and LV both undergo major shifts in metabolism in response to acute and chronic afterload stress. However, the switch to glycolysis appears to occur earlier in the pressure loaded RV vs. the pressure loaded LV resulting in an earlier decrease in net ATP production in the RV. If energetic pathways are more at risk in the chronic pressure-loaded RV, then strategies that maintain favorable ATP production and oxygen consumption may be beneficial. Several drugs that increase glucose utilization (ranolazine, trimetazidine, perhexiline) have been tested in animal models of PHTN and in human clinical trials of LV failure and PHTN-induced RV failure, with variable success [53–56]. There is little data on the metabolic derangements in CHD and no data on the utility of drugs to modify these alterations. Cardiac metabolic imaging, e.g. MR spectroscopy, has the potential to shed more light on alterations in RV metabolism in patients with CHD [57]. While important differences in metabolism exist between animal models and patients, thereby limiting direct translation, the use of animal models is the first step toward understanding the mechanism of disease. Patients with right heart failure due to PHTN show a metabolic shift away from fatty acid metabolism to glycolysis. Abnormalities in mitochondrial complexes 1, III and IV have been described in children with tetralogy of Fallot. These results are similar to those demonstrated in animal models of PHTN and pulmonary artery banding, making it feasible to use animal models as the first step in studying the mechanism of RV failure, with subsequent confirmation in patients.

Metabolic Response to Chronic Volume Overload

Our knowledge of the RV response to volume load is limited despite this being common late sequelae after RV outflow tract reconstruction, in single right ventricles with an aortopulmonary shunt, or in l-TGA with atrioventricular valve regurgitation, a major contributor to morbidity and mortality in this population. To address this shortcoming, we developed a murine model of chronic RV volume overload, and used this as a platform to evaluate the transcriptional regulation of the volume loaded RV [58]. Early diastolic dysfunction and preserved systolic function were associated with downregulation of several metabolic pathway regulators, including phosphofructokinase, a rate-limiting enzyme in glycolysis, and aconitase, an upstream TCA cycle enzyme, both important for ATP production. There were also decreases in ATP-binding transporters, genes encoding transport of nutrients across the cell membrane. With the worsening of diastolic dysfunction and the onset of fibrosis, but with

preserved systolic function, there is a shift away from β-oxidation with downregulation of fatty acid binding protein and upregulation of AMP kinases, and increased glycogenolysis with upregulation of GSK3β and glycogen phosphorylase. These adaptations are similar to those described during LV volume overload, however, additional research will be required to determine if more subtle differences exist.

MicroRNAs

miRs are small, non-coding RNAs of 18–25 nucleotides that regulate gene expression by degradation or translational suppression of mRNA. As master regulators of entire gene networks, miRs have received considerable attention in cardiovascular development and in LV hypertrophy and failure and are being developed as therapeutic targets and as biomarkers to monitor disease progression [59–61].

While miR expression is largely similar between the afterload stressed RV and LV, there are interesting differences. We profiled miR expression at various stages of adaptive RVH progressing to RV failure, and identified four RV-specific miRs: miRs 34a, 28, 93 and 148a, none of which are increased in LV hypertrophy and failure induced by transverse aortic constriction (TAC) [62–65]. These miRs cause cell cycle arrest, oxidant damage, impairment of DNA repair as well as inhibition of pro-angiogenic factors [66, 67]. An interesting feature of these four RV-specific miRs is that they are upregulated only in non-cardiomyocytes in the heart (endothelial cells and fibroblasts), but affect cardiomyocytes via paracrine signaling. These four RV-specific miRs may enhance the progression to RV failure by increasing oxidative stress, reducing oxidative defenses, decreasing angiogenesis and activating cell death pathways, the very pathways that differ most between the RV and LV, as shown above. Potus et al. suggest a systemic vascular defect in the miR-126/VEGF pathway in PHTN in pulmonary artery endothelial cells and in the RV. This pathway was upregulated during compensated RVH but transitioned to being downregulated with RV failure [68]. PHTN is also characterized by a downregulation in miR-208 followed by an upregulation of its target Mef2 in RVF [69, 70].

Novel Models of RV Failure Simulating Residual Lesions After Surgery for Right Sided Obstructive Lesions

In order to address the minimal data on the cellular and molecular mechanisms of RV hypertrophy and the progression to RV failure in CHD, we have created murine models of RV pressure overload, volume overload and combined pressure and volume overload to simulate some of the common residual lesions seen after RV outflow tract reconstruction, thereby enabling the assessment of genome-wide changes in the RV. These models reflect the clinical picture seen in children with progression from a compensated, adaptive stage with predominant diastolic dysfunction to decompensated systolic dysfunction with clinical heart failure.

Pressure overload alone was characterized by upregulation of genes regulating phosphate and other inorganic ion transport, cell adhesion and cell death pathways. Although most of these transcriptional changes were similar between the RV and LV, there were several genes that were uniquely upregulated in the pressure loaded RV, including genes involved in Wnt signaling (Dickkopf 3, Sfrp2, and Wif1), annexin A7, clusterin/apolipoprotein J, neuroblastoma suppression of tumorigenicity 1 (Nbl1), formin binding protein (Fnbp4), and LOX. Metabolic pathways dominated the downregulated gene pathways [16]. Whether these differences in the RV vs. LV are related to their different geometric structures, to markedly different afterloads, or to basic differences in cardiomyocyte biology will be the subject of future research.

The gene expression changes in the volume-loaded RV vs. LV are also largely similar [58]. While RV pressure and volume overload led to dysregulation of pathways involved in extracellular matrix remodeling, the actin cytoskeleton

and metabolism, pressure overload led to a greater change in transcripts reflecting a more severe phenotype. Whereas RV diastolic dysfunction is well described in children with CHD with residual pressure and volume overload lesions, the mechanisms underlying diastolic dysfunction are poorly understood. Our novel animal models with chronic RV diastolic function may aid in better understanding the mechanism of diastolic dysfunction.

Development of animal models of chronic RV failure are critical, as they may better represent the clinical course of patients with CHD, as opposed to models where failure occurs within a few weeks. Improving energy efficiency and arresting cell death and fibrosis are areas to target for new therapeutics and utilizing chronic animal models in a stable and compensated state will be ideal for therapeutic trials.

Key Points

- RV failure secondary to CHD does not respond to standard left heart failure medical therapies.
- New models of RV failure highlight differences in the molecular response to stress between the two ventricles.
- Pathways regulating reactive oxygen species production and antioxidant protection, angiogenesis and cell death differ between the two ventricles when exposed to pressure and/or volume loading.

Conclusions

As a testament to the vast advances in medical care and in surgical techniques, the vast majority of children with even complex CHD are growing into adolescence and adulthood. This has dramatically increased the burden of hemodynamic stressors, in particular on the RV, thereby increasing the incidence of RV failure in this population. While the vast number of studies on LV failure has advanced our knowledge of the mechanisms of disease progression from a compensated state to a state of overt heart failure, much less is known about the mechanisms of RV adaptation to pressure and volume load and the progression to RV failure. New animal models of RV failure simulating residual lesions seen after CHD and new models of PHTN are beginning to unravel the molecular mechanisms of disease and the RV's increased susceptibility to failure. These studies will pave the way toward developing RV-specific heart failure therapies.

Acknowledgements Mingming Zhao, Dong-Qing Hu, and Giovanni Fajardo. NIH/NHLBI grant HL061535 (DB); Children's Heart Foundation grant (DB and SR); Packard Children's Hospital Pediatric Research Fund, Heart Center Research Fund and Reddy Foundation grant (SR); NIH/NHLBI 1K08HL127277 (SR). Department of Defense CMDRP in Congenital Heart Disease (DB and SR).

References

1. Hoffman JI, Kaplan S. The incidence of congenital heart disease. J Am Coll Cardiol. 2002;39(12):1890–900.
2. Belmont JW. Recent progress in the molecular genetics of congenital heart defects. Clin Genet. 1998;54(1):11–9.
3. Lund O, Kristensen LH, Baandrup U, Hansen OK, Nielsen TT, Emmertsen K, et al. Myocardial structure as a determinant of pre- and postoperative ventricular function and long-term prognosis after valve replacement for aortic stenosis. Eur Heart J. 1998;19(7):1099–108.
4. Douglas PS, Reichek N, Hackney K, Ioli A, Sutton MG. Contribution of afterload, hypertrophy and geometry to left ventricular ejection fraction in aortic valve stenosis, pure aortic regurgitation and idiopathic dilated cardiomyopathy. Am J Cardiol. 1987;59(15):1398–404.
5. Kaufman BD, Desai M, Reddy S, Osorio JC, Chen JM, Mosca RS, et al. Genomic profiling of left and right ventricular hypertrophy in congenital heart disease. J Card Fail. 2008;14(9):760–7.
6. Buermans HP, Redout EM, Schiel AE, Musters RJ, Zuidwijk M, Eijk PP, et al. Microarray analysis reveals pivotal divergent mRNA expression profiles early in the development of either compensated ventricular hypertrophy or heart failure. Physiol Genomics. 2005;21(3):314–23.
7. Gentles TL, Mayer JE Jr, Gauvreau K, Newburger JW, Lock JE, Kupferschmid JP, et al. Fontan operation in five hundred consecutive patients: factors influencing early and late outcome. J Thorac Cardiovasc Surg. 1997;4(3):376–91.

8. Winter MM, Bouma BJ, Groenink M, Konings TC, Tijssen JG, van Veldhuisen DJ, et al. Latest insights in therapeutic options for systemic right ventricular failure: a comparison with left ventricular failure. Heart. 2009;95(12):960–3.
9. Szymanski P, Klisiewicz A, Hoffman P. Therapeutic options for systemic right ventricular failure. Heart. 2009;95(23):1950–1. Author reply 1.
10. Shaddy RE, Boucek MM, Hsu DT, Boucek RJ, Canter CE, Mahony L, et al. Carvedilol for children and adolescents with heart failure: a randomized controlled trial. JAMA. 2007;298(10):1171–9.
11. Hsu DT, Zak V, Mahony L, Sleeper LA, Atz AM, Levine JC, et al. Enalapril in infants with single ventricle: results of a multicenter randomized trial. Circulation. 2010;122(4):333–40.
12. Buckberg GD, RESTORE Group. The ventricular septum: the lion of right ventricular function, and its impact on right ventricular restoration. Eur J Cardiothorac Surg. 2006;29(Suppl 1):S272–8.
13. Friedberg MK, Redington AN. Right versus left ventricular failure: differences, similarities, and interactions. Circulation. 2014;129(9):1033–44.
14. Kondo RP, Dederko DA, Teutsch C, Chrast J, Catalucci D, Chien KR, et al. Comparison of contraction and calcium handling between right and left ventricular myocytes from adult mouse heart: a role for repolarization waveform. J Physiol. 2006;571(Pt 1):131–46.
15. Piao L, Marsboom G, Archer SL. Mitochondrial metabolic adaptation in right ventricular hypertrophy and failure. J Mol Med. 2010;88(10):1011–20.
16. Urashima T, Zhao M, Wagner R, Fajardo G, Farahani S, Quertermous T, et al. Molecular and physiological characterization of RV remodeling in a murine model of pulmonary stenosis. Am J Physiol Heart Circ Physiol. 2008;295(3):H1351–H68.
17. Reddy S, Bernstein D. Molecular Mechanisms of Right Ventricular Failure. Circulation. 2015;132(18):1734–42.
18. Reddy S, Bernstein D. The vulnerable right ventricle. Curr Opin Pediatr. 2015;27(5):563–8.
19. Tsutsui H, Ide T, Hayashidani S, Suematsu N, Utsumi H, Nakamura R, et al. Greater susceptibility of failing cardiac myocytes to oxygen free radical-mediated injury. Cardiovasc Res. 2001;49(1):103–9.
20. Gomez-Arroyo J, Mizuno S, Szczepanek K, Van Tassell B, Natarajan R, dos Remedios CG, et al. Metabolic gene remodeling and mitochondrial dysfunction in failing right ventricular hypertrophy secondary to pulmonary arterial hypertension. Circ Heart Fail. 2013;6(1):136–44.
21. Ecarnot-Laubriet A, Rochette L, Vergely C, Sicard P, Teyssier JR. The activation pattern of the antioxidant enzymes in the right ventricle of rat in response to pressure overload is of heart failure type. Heart Dis. 2003;5(5):308–12.
22. Redout EM, van der Toorn A, Zuidwijk MJ, van de Kolk CW, van Echteld CJ, Musters RJ, et al. Antioxidant treatment attenuates pulmonary arterial hypertension-induced heart failure. Am J Physiol Heart Circ Physiol. 2010;298(3):H1038–47.
23. Redout EM, Wagner MJ, Zuidwijk MJ, Boer C, Musters RJ, van Hardeveld C, et al. Right-ventricular failure is associated with increased mitochondrial complex II activity and production of reactive oxygen species. Cardiovasc Res. 2007;75(4):770–81.
24. Karamanlidis G, Bautista-Hernandez V, Fynn-Thompson F, Del Nido P, Tian R. Impaired mitochondrial biogenesis precedes heart failure in right ventricular hypertrophy in congenital heart disease. Circ Heart Fail. 2011;4(6):707–13.
25. Zong P, Tune JD, Downey HF. Mechanisms of oxygen demand/supply balance in the right ventricle. Exp Biol Med. 2005;230(8):507–19.
26. Saito D, Tani H, Kusachi S, Uchida S, Ohbayashi N, Marutani M, et al. Oxygen metabolism of the hypertrophic right ventricle in open chest dogs. Cardiovasc Res. 1991;25(9):731–9.
27. Choi YH, Cowan DB, Nathan M, Poutias D, Stamm C, del Nido PJ, et al. Myocardial hypertrophy overrides the angiogenic response to hypoxia. PLoS One. 2008;3(12):e4042.
28. Bogaard HJ, Natarajan R, Henderson SC, Long CS, Kraskauskas D, Smithson L, et al. Chronic pulmonary artery pressure elevation is insufficient to explain right heart failure. Circulation. 2009;120(20):1951–60.
29. Zamir M. The physics of coronary blood flow. New York: Springer; 2005.
30. Sano M, Minamino T, Toko H, Miyauchi H, Orimo M, Qin Y, et al. p53-induced inhibition of Hif-1 causes cardiac dysfunction during pressure overload. Nature. 2007;446(7134):444–8.
31. Partovian C, Adnot S, Eddahibi S, Teiger E, Levame M, Dreyfus P, et al. Heart and lung VEGF mRNA expression in rats with monocrotaline- or hypoxia-induced pulmonary hypertension. Am J Phys. 1998;275(6 Pt 2):H1948–56.
32. Setty S, Tune JD, Downey HF. Nitric oxide contributes to oxygen demand-supply balance in hypoperfused right ventricle. Cardiovasc Res. 2004;64(3):431–6.
33. Tune JD, Richmond KN, Gorman MW, Feigl EO. Role of nitric oxide and adenosine in control of coronary blood flow in exercising dogs. Circulation. 2000;101(25):2942–8.
34. Piao L, Fang YH, Parikh KS, Ryan JJ, D'Souza KM, Theccanat T, et al. GRK2-mediated inhibition of adrenergic and dopaminergic signaling in right ventricular hypertrophy: therapeutic implications in pulmonary hypertension. Circulation. 2012;126(24):2859–69.
35. Norozi K, Bahlmann J, Raab B, Alpers V, Arnhold JO, Kuehne T, et al. A prospective, randomized, double-blind, placebo controlled trial of beta-blockade in patients who have undergone surgical correction of tetralogy of Fallot. Cardiol Young. 2007;17(4):372–9.
36. Doughan AR, McConnell ME, Book WM. Effect of beta blockers (carvedilol or metoprolol XL) in patients with transposition of great arteries and dysfunction of the systemic right ventricle. Am J Cardiol. 2007;99(5):704–6.

37. Molenaar P, Bartel S, Cochrane A, Vetter D, Jalali H, Pohlner P, et al. Both beta(2)- and beta(1)-adrenergic receptors mediate hastened relaxation and phosphorylation of phospholamban and troponin I in ventricular myocardium of Fallot infants, consistent with selective coupling of beta(2)-adrenergic receptors to G(s)-protein. Circulation. 2000;102(15):1814–21.
38. Wang GY, McCloskey DT, Turcato S, Swigart PM, Simpson PC, Baker AJ. Contrasting inotropic responses to alpha1-adrenergic receptor stimulation in left versus right ventricular myocardium. Am J Physiol Heart Circ Physiol. 2006;291(4):H2013–7.
39. Wang GY, Yeh CC, Jensen BC, Mann MJ, Simpson PC, Baker AJ. Heart failure switches the RV alpha1-adrenergic inotropic response from negative to positive. Am J Physiol Heart Circ Physiol. 2010;298(3):H913–20.
40. Anand IS, Chandrashekhar Y, Ferrari R, Sarma R, Guleria R, Jindal SK, et al. Pathogenesis of congestive state in chronic obstructive pulmonary disease. Studies of body water and sodium, renal function, hemodynamics, and plasma hormones during edema and after recovery. Circulation. 1992;86(1):12–21.
41. Farber MO, Roberts LR, Weinberger MH, Robertson GL, Fineberg NS, Manfredi F. Abnormalities of sodium and H2O handling in chronic obstructive lung disease. Arch Intern Med. 1982;142(7):1326–30.
42. Schrier RW, Bansal S. Pulmonary hypertension, right ventricular failure, and kidney: different from left ventricular failure? Clin J Am Soc Nephrol. 2008;3(5):1232–7.
43. Maron BA, Leopold JA. The role of the renin-angiotensin-aldosterone system in the pathobiology of pulmonary arterial hypertension (2013 Grover Conference series). Pulm Circ. 2014;4(2):200–10.
44. van der Bom T, Winter MM, Bouma BJ, Groenink M, Vliegen HW, Pieper PG, et al. Effect of valsartan on systemic right ventricular function: a double-blind, randomized, placebo-controlled pilot trial. Circulation. 2013;127(3):322–30.
45. Dore A, Houde C, Chan KL, Ducharme A, Khairy P, Juneau M, et al. Angiotensin receptor blockade and exercise capacity in adults with systemic right ventricles: a multicenter, randomized, placebo-controlled clinical trial. Circulation. 2005;112(16):2411–6.
46. Robinson B, Heise CT, Moore JW, Anella J, Sokoloski M, Eshaghpour E. Afterload reduction therapy in patients following intraatrial baffle operation for transposition of the great arteries. Pediatr Cardiol. 2002;23(6):618–23.
47. Phillips D, Aponte AM, Covian R, Neufeld E, ZX Y, Balaban RS. Homogenous protein programming in the mammalian left and right ventricle free walls. Physiol Genomics. 2011;43(21):1198–206.
48. Nagendran J, Gurtu V, Fu DZ, Dyck JR, Haromy A, Ross DB, et al. A dynamic and chamber-specific mitochondrial remodeling in right ventricular hypertrophy can be therapeutically targeted. J Thorac Cardiovasc Surg. 2008;136(1):168–78. 78 e1-3.
49. Kusachi S, Nishiyama O, Yasuhara K, Saito D, Haraoka S, Nagashima H. Right and left ventricular oxygen metabolism in open-chest dogs. Am J Phys. 1982;243(5):H761–6.
50. Do E, Baudet S, Verdys M, Touzeau C, Bailly F, Lucas-Heron B, et al. Energy metabolism in normal and hypertrophied right ventricle of the ferret heart. J Mol Cell Cardiol. 1997;29(7):1903–13.
51. Gunes Y, Guntekin U, Tuncer M, Sahin M. Improved left and right ventricular functions with trimetazidine in patients with heart failure: a tissue Doppler study. Heart Vessel. 2009;24(4):277–82.
52. Gu Q, Chen XT, Xiao YB, Chen L, Wang XF, Fang J, et al. Identification of differently expressed genes and small molecule drugs for Tetralogy of Fallot by bioinformatics strategy. Pediatr Cardiol. 2014;35(5):863–9.
53. Rastogi S, Sharov VG, Mishra S, Gupta RC, Blackburn B, Belardinelli L, et al. Ranolazine combined with enalapril or metoprolol prevents progressive LV dysfunction and remodeling in dogs with moderate heart failure. Am J Physiol Heart Circ Physiol. 2008;295(5):H2149–55.
54. Phan TT, Shivu GN, Choudhury A, Abozguia K, Davies C, Naidoo U, et al. Multi-centre experience on the use of perhexiline in chronic heart failure and refractory angina: old drug, new hope. Eur J Heart Fail. 2009;11(9):881–6.
55. Halbirk M, Norrelund H, Moller N, Schmitz O, Gotzsche L, Nielsen R, et al. Suppression of circulating free fatty acids with acipimox in chronic heart failure patients changes whole body metabolism but does not affect cardiac function. Am J Physiol Heart Circ Physiol. 2010;299(4):H1220–5.
56. Nikolaidis LA, Mankad S, Sokos GG, Miske G, Shah A, Elahi D, et al. Effects of glucagon-like peptide-1 in patients with acute myocardial infarction and left ventricular dysfunction after successful reperfusion. Circulation. 2004;109(8):962–5.
57. O'Connor RD, Xu J, Ewald GA, Ackerman JJ, Peterson LR, Gropler RJ, et al. Intramyocardial triglyceride quantification by magnetic resonance spectroscopy: In vivo and ex vivo correlation in human subjects. Magn Reson Med. 2011;65(5):1234–8.
58. Reddy S, Zhao M, Hu DQ, Fajardo G, Katznelson E, Punn R, et al. Physiologic and molecular characterization of a murine model of right ventricular volume overload. Am J Physiol Heart Circ Physiol. 2013;304(10):H1314–27.
59. Cordes KR, Srivastava D. MicroRNA regulation of cardiovascular development. Circ Res. 2009;104(6):724–32.
60. Callis TE, Wang DZ. Taking microRNAs to heart. Trends Mol Med. 2008;14(6):254–60.
61. El-Armouche A, Schwoerer AP, Neuber C, Emmons J, Biermann D, Christalla T, et al. Common microRNA signatures in cardiac hypertrophic and atrophic remodeling induced by changes in hemodynamic load. PLoS One. 2010;5(12):e14263.
62. Yang M, Yao Y, Eades G, Zhang Y, Zhou Q. MiR-28 regulates Nrf2 expression through a Keap1-

independent mechanism. Breast Cancer Res Treat. 2011;129(3):983–91.
63. Smith-Vikos T, Slack FJ. MicroRNAs and their roles in aging. J Cell Sci. 2012;125(Pt 1):7–17.
64. Yu J, Li Q, Xu Q, Liu L, Jiang B. MiR-148a inhibits angiogenesis by targeting ERBB3. J Biomed Res. 2011;25(3):170–7.
65. Reddy S, Zhao M, Hu DQ, Fajardo G, Hu S, Ghosh Z, et al. Dynamic microRNA expression during the transition from right ventricular hypertrophy to failure. Physiol Genomics. 2012;44(10):562–75.
66. Tabuchi T, Satoh M, Itoh T, Nakamura M. MicroRNA-34a regulates the longevity-associated protein SIRT1 in coronary artery disease: effect of statins on SIRT1 and microRNA-34a expression. Clin Sci (Lond). 2012;123(3):161–71.
67. Boon RA, Iekushi K, Lechner S, Seeger T, Fischer A, Heydt S, et al. MicroRNA-34a regulates cardiac ageing and function. Nature. 2013;495(7439):107–10.
68. Potus F, Malenfant S, Graydon C, Mainguy V, Tremblay E, Breuils-Bonnet S, et al. Impaired angiogenesis and peripheral muscle microcirculation loss contribute to exercise intolerance in pulmonary arterial hypertension. Am J Respir Crit Care Med. 2014;190(3):318–28.
69. Thum T, Batkai S. MicroRNAs in right ventricular (dys)function (2013 Grover Conference series). Pulm Circ. 2014;4(2):185–90.
70. Paulin R, Sutendra G, Gurtu V, Dromparis P, Haromy A, Provencher S, et al. A miR-208-Mef2 axis drives the decompensation of right ventricular function in pulmonary hypertension. Circ Res. 2015;116(1):56–69.

Genetic Variation and Outcomes in Right Ventricular Congenital Heart Disease

4

Seema Mital

Abstract

The right ventricle (RV) is exposed to numerous stressors in patients with congenital heart defects. The ability of the RV to adapt to stress is important in maintaining long term structure and function. Genetic factors play an important role in influencing RV adaptation. These include variations in genes involved in hypoxia signaling, metabolic regulation and neurohormonal regulation. Variants in these genes influence the RV response to hypoxia, pressure or volume overload and surgical injury. Knowledge of patient genotype may help identify those at highest risk for adverse RV remodeling and RV failure, and importantly in guiding choice and timing of interventions to preserve RV function.

Keywords

Right ventricle • Personalized medicine • Polymorphisms • Genes • Hypoxia inducible factor • Renin-angiotensin-aldosterone system • Fibrosis

Abbreviations

CHD	Congenital heart disease
HCM	Hypertrophic cardiomyopathy
HIF1A	Hypoxia inducible factor 1α
LV	Left ventricle
RAAS	Renin-angiotensin-aldosterone system
RV	Right ventricle
SNP	Single nucleotide polymorphism
TGFB1	Transforming growth factor β1
TOF	Tetralogy of Fallot

S. Mital
Paediatric Cardiology, The Hospital for Sick Children, 555 University Ave, Toronto, ON, Canada, M5G 1X8
e-mail: seema.mital@sickkids.ca

Introduction

The goal of personalized medicine is to improve prediction of risk, guide pre-emptive interventions aimed at prevention and/or progression of disease, and to improve the precision of interventions by using biology driven therapies targeted to molecular pathways dysregulated in disease. Genome-guided therapies remain the cornerstone

M.K. Friedberg, A.N. Redington (eds.), *Right Ventricular Physiology, Adaptation and Failure in Congenital and Acquired Heart Disease*, https://doi.org/10.1007/978-3-319-67096-6_4

of personalized medicine. Advances in genomics have expedited the discovery of the genetic and genomic basis of Mendelian and complex disorders including congenital heart disease (CHD) [1–4]. The ability of next-generation sequencing to screen the entire human genome has led to the identification of not only single gene defects but also multi-genic disorders as well as biological pathways enriched in pathogenic variants.

The discovery in the last decade that the RV has distinct embryologic origins from the second heart field has opened up a new field of inquiry focused on identifying the role of the second heart field genes in RV development and disease [5]. For example, studies have identified structural and sequence variation in patients with second heart field defects and tetralogy of Fallot (TOF) [6–8]. Here we review genetic variants that modify RV disease severity and outcomes including severity of cardiac and extra-cardiac phenotypes. The most widely studied amongst RV diseases in the context of CHD includes tetralogy of Fallot (TOF) and single ventricle lesions where the RV is the systemic RV e.g. hypoplastic left heart syndrome (HLHS).

The Right Ventricle in Tetralogy of Fallot

Environmental Influences

The RV in TOF faces extraordinary stresses throughout the lifetime of the patient. In the unrepaired state during infancy, the RV is exposed to hypoxia and pressure load, and following complete repair the RV primarily faces volume overload secondary to pulmonary insufficiency and/or other residual hemodynamic lesions. The classic phenotype is progressive RV dilation and dysfunction that, untreated, culminates in RV failure. The rate at which this adverse RV remodeling progresses varies from patient to patient despite similar degree of pulmonary insuffiency. Pulmonary valve replacement is usually performed for moderate to severe RV dilation, RV dysfunction, exercise intolerance, arrhythmias and/or symptomatic heart failure. However, the extent of improvement in RV function and in exercise tolerance following pulmonary valve replacement is somewhat unpredictable, with some patients showing restoration of normal RV function while persistent RV dysfunction occurs in others. This has made clinical determination of the optimal timing for pulmonary valve replacement challenging. The patient to patient variability suggests that there are individual differences in how the RV in TOF adapts to ongoing stresses and that these differences may be genetic in origin. In this regard, hypoxia signaling is an important adaptive pathway in the heart and genetic variation in hypoxia signaling has the potential to influence RV adaptation.

Genetic Influences

There are important adaptive signaling pathways that are activated during periods of stress to maintain cardiovascular homeostasis. These pathways have been widely studied in the context of LV disease and less so in RV disease. Since the pulmonary vascular bed is uniquely sensitive to changes in oxygen tension, there has been particular interest in responses of the RV and the pulmonary vascular bed to hypoxic (and hemodynamic) stress. Hypoxia-inducible factor-1α (*HIF1A*) is an oxygen-sensitive transcription factor that is a central mediator of the response to hypoxia (Fig. 4.1). During acute hypoxia, *HIF1A* translocates to the nucleus to activate angiogenic, glycolytic and antioxidant genes that help with myocardial adaptation to hypoxia [9]. However, chronic HIF1A upregulation can be detrimental by promoting persistent activation of pro-fibrotic genes like transforming growth factor β1 (*TGFB1*) and resultant fibrosis [10]. Therefore *HIF1A* plays a complex role in mediating the cardiac hypoxic response.

Hypoxia Response Genes and RV Adaptation

In a mouse study, Kim et al. identified the importance of *HIF1a* in maintaining low pulmonary vascular tone by decreasing myosin light chain phosphorylation in pulmonary artery smooth muscle cells with, conversely, development of

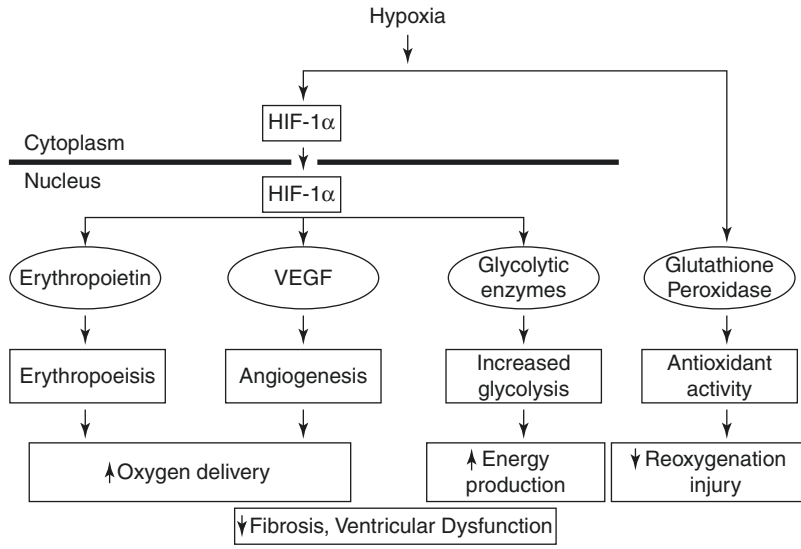

Fig. 4.1 The illustration shows the left ventricular adaptive response to hypoxia. Hypoxia activates HIF1α. This leads to the transcription of target genes that increase erythropoiesis (erythropoietin), angiogenesis (VEGF), glycolysis and anti-oxidant effects (glutathione peroxidase) resulting in improved oxygen delivery and energy production and reduced reoxygenation injury. *HIF1α* hypoxia inducible factor 1α, *VEGF* vascular endothelial growth factor. Reproduced with permission from Reddy S, Osorio JC, Duque AM, Kaufman BD, Phillips AB, Chen JM, et al. Failure of Right Ventricular Adaptation in Children With Tetralogy of Fallot. Circulation. 2006 July 4, 2006;114(1 suppl):I-37–I-42 © Wolters Kluwer 2006 [12]

pulmonary hypertension in *HIF1a* null mice [11]. Reddy et al. investigated the role of hypoxia response genes in RV adaptation in patients with TOF [12]. They found that cyanotic patients had a significantly lower expression of hypoxia response genes regulated by *HIF1a* including vascular endothelial growth factor, glycolytic enzymes, and glutathione peroxidase, and a higher expression of collagen compared with acyanotic patients (Fig. 4.2). Therefore, the hypoxic response of the RV in TOF differed from the LV and was associated with higher postoperative lactate levels suggesting a maladaptive RV response to chronic hypoxia.

HIF1A Genetic Variants and RV Adaptation

We explored the role of genetic variation in this highly conserved *HIF1A* signaling pathway in RV phenotype in TOF. Jeewa et al. studied the influence of three common single nucleotide polymorphisms (SNPs) in *HIF1A* on early and late RV remodeling in 180 TOF patients [13]. They found that patients with a higher number of functioning *HIF1A* alleles had higher TGFB1 expression and more fibrosis at initial repair when compared to patients with <4 functioning *HIF1A* alleles. However, during follow-up, patients with a higher number of functioning *HIF1A* alleles showed less RV dilation, better preservation of RV function (Fig. 4.3), and greater freedom from RV re-interventions (Fig. 4.4). This paper highlighted the importance of the hypoxia response genes in mediating RV adaptation to both hypoxia and hemodynamic stress. In particular, it raised the intriguing possibility that early RV fibrosis in the context of HIF1A upregulation was an adaptive response and may have allowed the RV to better handle long term hemodynamic stress while preserving RV function. The study also demonstrates the interaction of genetic and "environmental" factors in influencing clinical phenotype (Fig. 4.5) [14].

Interestingly, these findings were at odds with data obtained in patients with hypertrophic cardiomyopathy (HCM). Alkon et al. found that pediatric HCM patients with a higher number of *HIF1A* functioning alleles had more myocardial

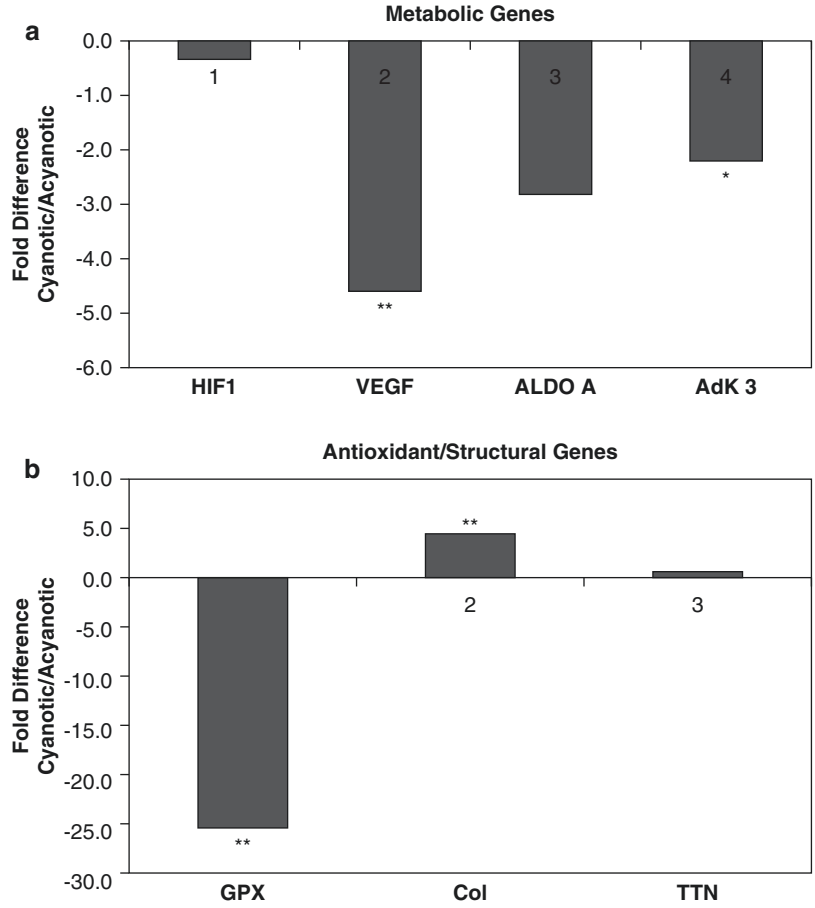

Fig. 4.2 Gene expression in RV of cyanotic vs acyanotic TOF. The bars represent the fold-difference in the gene expression in the RV myocardium of cyanotic compared with acyanotic TOF patients. (**a**) There was lower expression of angiogenic (VEGF) and metabolic (ALDO A, ADK3) genes in the cyanotic RV. (**b**) There was lower expression of antioxidant genes (GPX) and higher expression of collagen in the cyanotic RV. Expression of HIF1α and titin (TTN) was not different. *P < 0.05; **P < 0.01 between cyanotic vs acyanotic TOF. *HIF1* hypoxia-inducible factor 1α, *VEGF* vascular endothelial growth factor, *ALDO A* aldolase A, *ADK3* adenylate kinase 3, *GPX* glutathione peroxidase, *Col* collagen, *TTN* titin. Reproduced with permission from Reddy S, Osorio JC, Duque AM, Kaufman BD, Phillips AB, Chen JM, et al. Failure of Right Ventricular Adaptation in Children With Tetralogy of Fallot. Circulation. 2006 July 4, 2006;114(1 suppl):I-37–I-42 © Wolters Kluwer 2006 [12]

TGFB1 upregulation and endothelial-mesenchymal transition in the LV [15]. These patients also had more severe septal hypertrophy, more diastolic dysfunction and lower freedom from myectomy compared to patients with fewer functioning *HIF1A* alleles. Thus, although chronic HIF1A upregulation was associated with pro-fibrotic TGFB1 upregulation in both TOF and HCM patients, this was associated with less adverse remodeling and dysfunction in the RV in TOF, but with more hypertrophy and dysfunction in the LV in HCM. This suggests that the impact of *HIF1A* genetic variation is dependent on the type of environmental insult and/or ventricular chamber type affected.

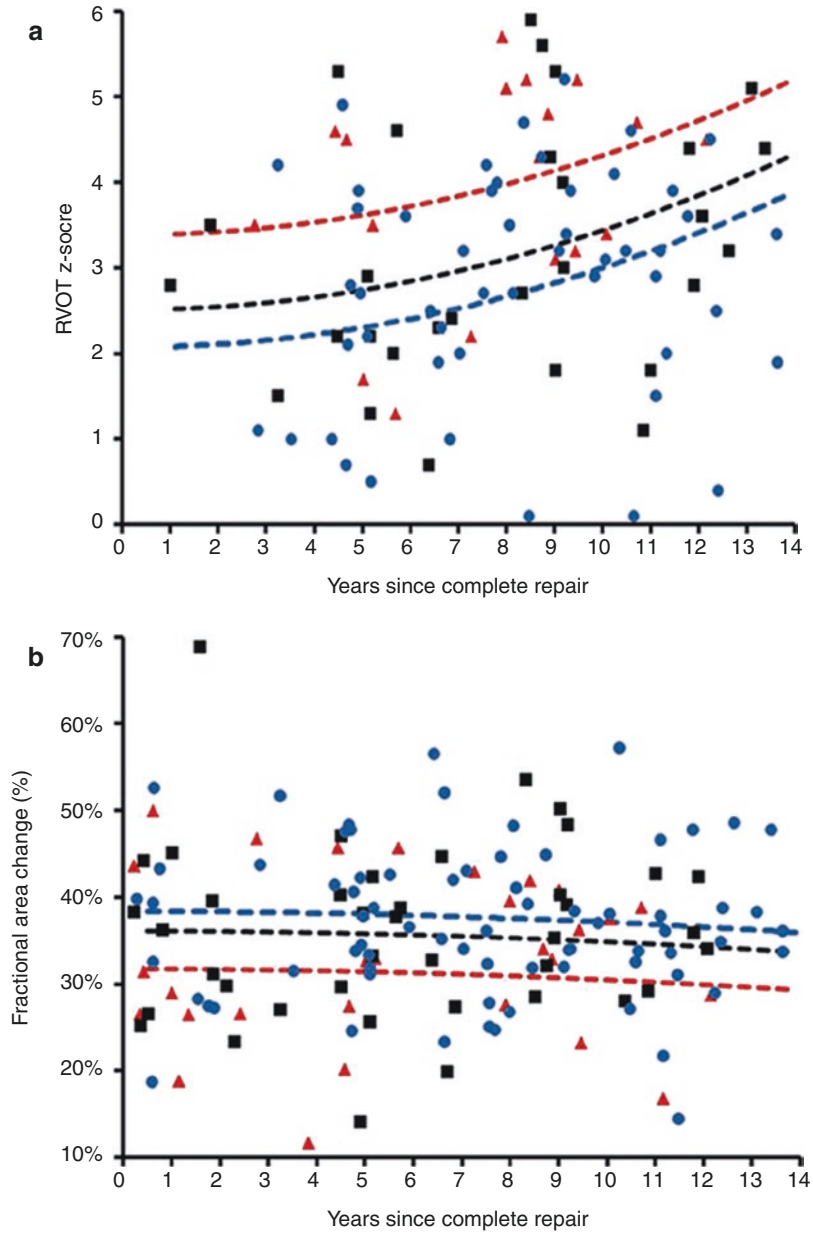

Fig. 4.3 *HIFA* genotype and RV phenotype in TOF. (**a**) *HIF1A* genotype and RVOT dilation: RVOT *z*-score increased progressively after TOF repair but was lower in patients with a higher number of functioning *HIF1A*alleles ($P = 0.002$) ($n = 180$). (**b**) *HIF1A* genotype and RV function: RV systolic function assessed using fractional area of change decreased with time, but the rate of decline of systolic function was lower in TOF patients with a higher number of functioning *HIF1A* alleles ($P = 0.04$). *Red triangles*, one to three functioning *HIF1A* alleles; *black squares*, 4 or 5 functioning *HIF1A* alleles; *blue circles*, six functioning *HIF1A* alleles. The *red*, *black*, and *blue lines* are regression lines showing the relationship between RVOT *z*-score or fractional area change and number of functioning *HIF1A* alleles. *RVOT* right ventricular outflow tract. Reproduced with permission from Jeewa A MA, Mertens L, Manlhiot C, Kinnear C, Mondal. T, Smythe J, Rosenberg H, Lougheed J, McCrindle BW, van Arsdell G, Redington AN, Mital S. Genetic determinants of right-ventricular remodeling after tetralogy of Fallot repair. Pediatr Res. 2012;72(4):407–13 © Nature Publishing Group 2012 [13]

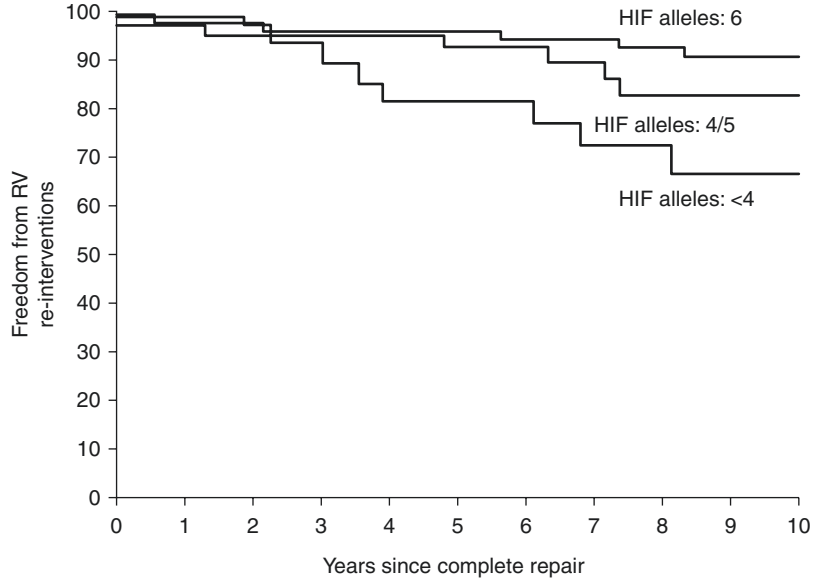

Fig. 4.4 Kaplan–Meier survival curve showing freedom from RV re-interventions (pulmonary valve or conduit replacement) during follow-up. Freedom from re-interventions was significantly lower in patients with four or more functioning *HIF1A* alleles as compared with those with fewer than four alleles. The hazard ratio for re-intervention decreased by 0.78 for every additional functioning allele ($P = 0.04$). *HIF* hypoxia-inducible factor 1α. Reproduced with permission from Jeewa A MA, Mertens L, Manlhiot C, Kinnear C, Mondal T, Smythe J, Rosenberg H, Lougheed J, McCrindle BW, van Arsdell G, Redington AN, Mital S. Genetic determinants of right-ventricular remodeling after tetralogy of Fallot repair. Pediatr Res. 2012;72(4):407–13 © Nature Publishing Group 2012 [13]

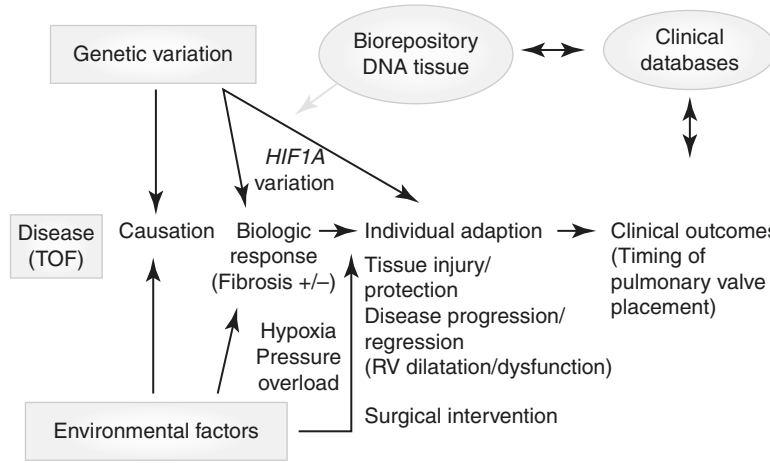

Fig. 4.5 Interaction of "environmental" and genetic factors in determining clinical outcomes. Genetic and environmental factors interact to cause disease and to determine the biologic response to the condition and its treatment. *HIF1A* genetic variants affecting its expression influence the response in tetralogy of Fallot (TOF) to the environmental stresses of hypoxia, pressure overload, and surgical repair. Establishing a chain of evidence from underlying genetic variation to observed clinical outcome relies on the integration of biorepository and clinical database resources as demonstrated by this study. *RV* right ventricular. Reproduced with permission from Russell MW WN. Getting personal: understanding how genetic variation affects clinical outcomes in patients with tetralogy of Fallot. Pediatr Res. 2012;72(4):334–6.© Nature Publishing Group [14]

Genetic Variants and Bypass-mediated Injury

The RV encounters not only hemodynamic stresses but also surgical and bypass mediated injury which is compounded in patients requiring multiple re-operations. Bypass mediated injury is predominantly related to hypoxia-reoxygenation or ischemia-reperfusion that generates oxidative stress that can adversely impact ventricular function postoperatively. The extent of bypass-mediated injury varies considerably from one patient to the next. About 40% of East Asians carry an aldehyde dehydrogenase-2*2 (*ALDH2*2*) allele, an important anti-oxidant gene and metabolic gene. Zhang et al. studied *ALDH2*2* in patients undergoing surgery for TOF repair and identified patients with increased bypass-mediated injury i.e. higher postoperative troponin I elevation, higher inotrope scores, and longer intensive care unit and/or hospital length of stay [16]. In their study, carriers of the *ALDH2*2* allele demonstrated cardioprotection during surgery for TOF repair as seen by lower postoperative troponin I, inotrope score, and shorter postoperative length of intensive care and hospital stay. Thus, knowledge of *ALDH2* genotype can identify patients at higher risk for bypass mediated injury amongst those undergoing TOF repair.

Clinical Significance

Although additional validation studies are needed, these studies emphasize the important gene-environment interactions that influence disease phenotypes and the potential for genetic guided approaches to treatment in TOF patients. For example, physicians may be able to use targeted genetic testing to identify patients at risk for progressive RV dilation or dysfunction and treat them according to risk. This may include better cardio-protective strategies in those at risk for bypass mediated injury i.e. *ALDH2*2* carriers to avoid perioperative injury to the RV, early complete repair to minimize duration of hypoxia exposure during infancy in those with fewer *HIF1A* functioning alleles, and lower threshold for pulmonary valve replacement during follow-up in those with fewer *HIF1A* functioning alleles to preserve long term RV function and avoid irreversible injury.

The Right Ventricle as the "Single" Ventricle

Environmental Influences

Hypoplastic left heart syndrome (HLHS) is one of the commonest forms of single ventricle lesions where the RV serves as the systemic RV. Similar to TOF, the systemic RV in single ventricle lesions is exposed to multiple stressors throughout a patient's lifetime. The RV is exposed to significant volume overload during infancy following stage 1 palliation (Norwood procedure, Sano procedure, hybrid procedure) since the RV supports both the systemic and pulmonary circulation. The RV is unloaded (at least in terms of volume load) after superior cavopulmonary connection (SCPC) and the Fontan procedure) but is still required to support the systemic circulation even after complete palliation. While relatively rare in the first decade or two after successful Fontan palliation, the RV may fail during follow-up resulting in heart failure, death or need for transplant. Which patient will develop RV dysfunction, and how fast, may be related to genetic variation in ability for ventricular adaptation. Early identification of patients who are genetically predisposed to RV failure in single ventricle lesions may guide type and timing of intervention before end-stage heart failure.

Genetic Influences

The renin-angiotensin-aldosterone system (RAAS) is one of the most important neuro-hormonal systems responsible for cardiovascular homeostasis. Similar to hypoxia signaling, RAAS activation in response to acute stress is adaptive or compensatory; however chronic activation can result in adverse effects secondary to persistent elevation in systemic vascular resistance, increased

myocardial oxygen consumption, myocyte injury and death, and myocardial fibrosis. The adverse impact of SNPs that were associated with RAAS upregulation on severity of LV hypertrophy was first reported in patients with HCM [17]. These five SNPs in the RAAS genes were subsequently evaluated in single ventricle infants participating in a Pediatric Heart Network multicenter clinical trial of enalapril (55% with systemic RVs) [18]. In this trial, 230 infants with single ventricle lesions were randomized after stage 1 palliation to receive placebo or enalapril for 14 months. Somatic growth and ventricular function were assessed before stage 2 palliation (usually around 6 months) and at 14 months follow-up. The study revealed that single ventricle patients had significant elevations in ventricular mass and volume prior to SCPC and while this improved after SCPC, it did not normalize in all patients at 14 months follow-up. Importantly, there was no benefit of enalapril therapy on either somatic growth or ventricular function and heart failure severity during 14 mos follow-up. However, a genetic sub-study in 154 trial participants revealed intriguing genetic associations with reverse ventricular remodeling. In the genetic substudy, the same five SNPs associated with RAAS upregulation were evaluated for response to ventricular unloading at the time of stage 2 palliation. While patients with fewer (<2) RAAS upregulation genotypes showed favorable reverse remodeling after stage 2 palliation, this reverse remodeling was not seen in patients with ≥2 RAAS upregulation genotypes. These patients demonstrated persistent elevation in ventricular mass and volume at 14 months follow-up (Fig. 4.6) [19]. This effect was independent of ventricular morphology i.e. systemic LV or RV, and of enalapril treatment. This study highlighted the important influence of RAAS genotype in influencing response to ventricular volume unloading surgery.

Clinical Significance

Similar to patients with TOF, this study highlights the gene-environment interactions that influence cardiac response to environmental stressors like hemodynamic load. While these findings require further validation, it suggests that physicians may be able to do targeted genetic testing in single ventricle patients to identify those that are at risk for progressive and irreversible ventricular remodeling. These patients may benefit from earlier volume unloading surgery before the injury becomes irreversible. This is particularly important in single ventricle patients since high ventricular mass at the time of Fontan can adversely impact Fontan outcomes by reducing ventricular compliance and forward flow through the Fontan circulation.

Genetic Variation and Non-Cardiac Phenotype in Right Ventricular Lesions

Genetic variation can impact not only cardiac but also non-cardiac phenotype in children with heart disease. Children with CHD are at risk for adverse neurodevelopmental outcomes related not only to structural abnormalities but also to cerebral perfusion abnormalities and brain injury related to cardiopulmonary bypass and deep hypothermic circulatory arrest [20]. Gaynor et al. found that genetic variation had a significant impact on neurocognitive outcomes in infants who had cardiac surgery before 6 months of age [21]. Infants carrying the apolipoprotein E epsilon 2 allele (*ApoE €2*) had lower neurocognitive performance at 1 year of age measured using Bayley Scales of Infant Development (BSID). This impairment persisted at 4 years of age [22]. Importantly, Zeltser et al. evaluated the influence of this genotype on neurodevelopmental outcome in 60 children after TOF repair [23]. The presence of a genetic syndrome and of the *ApoE €2* allele was predictive of lower BSID scores at 1 year of age after TOF repair. The influence of this genotype on neurodevelopmental outcomes was replicated in infants with hypoplastic left heart syndrome enrolled in a Pediatric Heart Network trial—the Single Ventricle Reconstruction trial [24]. This suggests that genetic risk stratification may have utility in infants undergoing cardiac surgery to

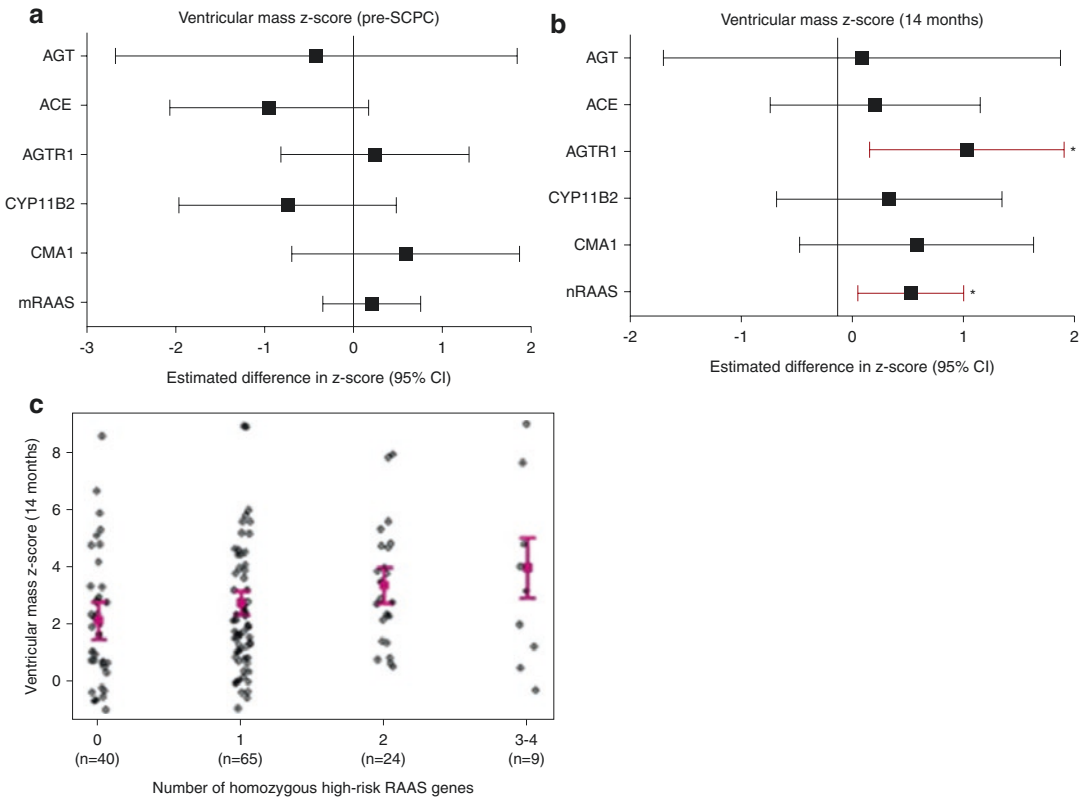

Fig. 4.6 Difference (and 95% confidence intervals) in ventricular mass z-scores at (**a**) pre-SCPC and (**b**) 14 months study visit between individual high risk versus no high risk RAAS genotypes using recessive model (*P < 0.05 versus low-risk genotype) showing a trend toward higher mass z-scores at 14 months in patients with high-risk genotypes with strongest association with *AGTR1*. (**c**) Linear regression model (mean ± 95% confidence limits) showing incremental effect of increasing number of RAAS-upregulation genotypes on ventricular mass z-score at 14 months. *SCPC* superior cavopulmonary connection, *AGT* angiotensinogen, *ACE* angiotensin-converting enzyme, *AGTR1* angiotensin II type 1 receptor, *CYP11B2* aldosterone synthase, *CMA1* chymase, *nRAAS* total number of high-risk renin-angiotensin-aldosterone system genotypes, *CI* confidence interval. Reproduced with permission from Mital S, Chung WK, Colan SD, Sleeper LA, Manlhiot C, Arrington CB, et al. Renin-Angiotensin-Aldosterone Genotype Influences Ventricular Remodeling in Infants With Single Ventricle. Circulation. 2011;123(21):2353–62. © Wolters Kluwer 2011 [19]

identify those at highest risk for neurological injury. These infants may benefit from neuroprotective strategies perioperatively and more importantly, these infants may need to be monitored closely during follow up to provide early intervention strategies in a timely manner.

Future Directions

While the candidate SNP association studies described here provide exciting insights into the importance of genetic factors in CHD outcomes, the search for genomic variants needs to be broadened from candidate SNP association studies to genome wide approaches. The use of next-generation sequencing allows an unbiased search of the patient genome or exome and allows capture of not only common but also rare and novel variants of potential clinical significance. It also allows identification of biological pathways enriched for variants. This approach is rapidly gaining traction with the reduction in sequencing costs and improvements in bioinformatics platforms and pipelines [25]. These discoveries will not only improve the precision of personalized

risk stratification and targeted therapies but also help in the discovery of new therapies, particularly for diseases of the RV for which no therapies currently exist, by identifying potentially "druggable" targets in biologically relevant pathways. Genetic-guided approaches therefore have the potential to improve outcomes through personalized management of patients including tailoring type and timing of medical and surgical management based on predicted genetic risk and prediction of response.

References

1. Purcell SM, Moran JL, Fromer M, Ruderfer D, Solovieff N, Roussos P, et al. A polygenic burden of rare disruptive mutations in schizophrenia. Nature. 2014;506(7487):185–90.
2. Michaelson JJ, Shi Y, Gujral M, Zheng H, Malhotra D, Jin X, et al. Whole-genome sequencing in autism identifies hot spots for de novo germline mutation. Cell. 2012;151(7):1431–42.
3. Zaidi S, Choi M, Wakimoto H, Ma L, Jiang J, Overton JD, et al. De novo mutations in histone-modifying genes in congenital heart disease. Nature. 2013;498(7453):220–3.
4. Al Turki S, Manickaraj AK, Mercer CL, Gerety SS, Hitz MP, Lindsay S, et al. Rare variants in NR2F2 cause congenital heart defects in humans. Am J Hum Genet. 2014;94(4):574–85.
5. Buckingham M, Meilhac S, Zaffran S. Building the mammalian heart from two sources of myocardial cells. Nat Rev Genet. 2005;6(11):826–35.
6. Stevens KN, Hakonarson H, Kim CE, Doevendans PA, Koeleman BP, Mital S, et al. Common variation in ISL1 confers genetic susceptibility for human congenital heart disease. PLoS One. 2010;5(5):e10855.
7. Greenway SC, Pereira AC, Lin JC, DePalma SR, Israel SJ, Mesquita SM, et al. De novo copy number variants identify new genes and loci in isolated sporadic tetralogy of Fallot. Nat Genet. 2009;41(8):931–5.
8. Silversides CK, Lionel AC, Costain G, Merico D, Migita O, Liu B, et al. Rare copy number variations in adults with tetralogy of Fallot implicate novel risk gene pathways. PLoS Genet. 2012;8(8):e1002843.
9. Semenza GL, Agani F, Feldser D, Iyer N, Kotch L, Laughner E, et al. Hypoxia, HIF-1, and the pathophysiology of common human diseases. Adv Exp Med Biol. 2000;475:123–30.
10. Sun S, Ning X, Zhang Y, Lu Y, Nie Y, Han S, et al. Hypoxia-inducible factor-1alpha induces Twist expression in tubular epithelial cells subjected to hypoxia, leading to epithelial-to-mesenchymal transition. Kidney Int. 2009;75(12):1278–87.
11. Kim Y-M, Barnes EA, Alvira CM, Ying L, Reddy S, Cornfield DN. Hypoxia-inducible factor-1α in pulmonary artery smooth muscle cells lowers vascular tone by decreasing myosin light chain phosphorylation. Circ Res. 2013;112(9):1230–3.
12. Reddy S, Osorio JC, Duque AM, Kaufman BD, Phillips AB, Chen JM, et al. Failure of right ventricular adaptation in children with tetralogy of fallot. Circulation. 2006;114(1 Suppl):I37–42.
13. Jeewa A, Manickaraj AK, Mertens L, Manlhiot C, Kinnear C, Mondal T, Smythe J, Rosenberg H, Lougheed J, McCrindle BW, van Arsdell G, Redington AN, Mital S. Genetic determinants of right-ventricular remodeling after tetralogy of Fallot repair. Pediatr Res. 2012;72(4):407–13.
14. Russell MW, Wilder NS. Getting personal: understanding how genetic variation affects clinical outcomes in patients with tetralogy of Fallot. Pediatr Res. 2012;72(4):334–6.
15. Alkon J, Friedberg MK, Manlhiot C, Manickaraj AK, Kinnear C, McCrindle BW, Benson LN, Addonizio LJ, Colan SD, Mital S. Genetic variations in hypoxia response genes influence hypertrophic cardiomyopathy phenotype. Pediatr Res. 2012;72(6):583–92.
16. Zhang H, Gong DX, Zhang YJ, Li SJ, Hu S. Effect of mitochondrial aldehyde dehydrogenase-2 genotype on cardioprotection in patients with congenital heart disease. Eur Heart J. 2012;33(13):1606–14.
17. Ortlepp JR, Vosberg HP, Reith S, Ohme F, Mahon NG, Schroder D, et al. Genetic polymorphisms in the renin-angiotensin-aldosterone system associated with expression of left ventricular hypertrophy in hypertrophic cardiomyopathy: a study of five polymorphic genes in a family with a disease causing mutation in the myosin binding protein C gene. Heart. 2002;87(3):270–5.
18. Hsu DT, Zak V, Mahony L, Sleeper LA, Atz AM, Levine JC, et al. Enalapril in infants with single ventricle: results of a multicenter randomized trial. Circulation. 2010;122(4):333–40.
19. Mital S, Chung WK, Colan SD, Sleeper LA, Manlhiot C, Arrington CB, et al. Renin-angiotensin-aldosterone genotype influences ventricular remodeling in infants with single ventricle. Circulation. 2011;123(21):2353–62.
20. Wypij D, Newburger JW, Rappaport LA, duPlessis AJ, Jonas RA, Wernovsky G, et al. The effect of duration of deep hypothermic circulatory arrest in infant heart surgery on late neurodevelopment: The Boston Circulatory Arrest Trial. J Thorac Cardiovasc Surg. 2003;126(5):1397–403.
21. Gaynor JW, Gerdes M, Zackai EH, Bernbaum J, Wernovsky G, Clancy RR, et al. Apolipoprotein E genotype and neurodevelopmental sequelae of infant cardiac surgery. J Thorac Cardiovasc Surg. 2003;126(6):1736–45.
22. Gaynor JW, Nord AS, Wernovsky G, Bernbaum J, Solot CB, Burnham N, et al. Apolipoprotein E geno-

type modifies the risk of behavior problems after infant cardiac surgery. Pediatrics. 2009;124(1):241–50.
23. Zeltser I, Jarvik GP, Bernbaum J, Wernovsky G, Nord AS, Gerdes M, Zackai E, Clancy R, Nicolson SC, Spray TL, Gaynor JW. Genetic factors are important determinants of neurodevelopmental outcome after repair of tetralogy of Fallot. J Thorac Cardiovasc Surg. 2008;135(1):91–7.
24. Gaynor JW, Kim DS, Arrington CB, Atz AM, Bellinger DC, Burt AA, Ghanayem NS, Jacobs JP, Lee TM, Lewis AB, Mahle WT, Marino BS, Miller SG, Newburger JW, Pizarro C, Ravishankar C, Stolle CA, Wilder NS, Jarvik GP, Mital S, Russell MW. Validation of association of the apo-lipoprotein E (APOE) ε2 allele with neurodevelopmental dysfunction after cardiac surgery in neonates and infants. J Thorac Cardiovasc Surg. 2014;148(6):2560–6.
25. Ashley EA, Hershberger RE, Caleshu C, Ellinor PT, Garcia JGN, Herrington DM, et al. Genetics and cardiovascular disease: a policy statement from the american heart association. Circulation. 2012;126(1):142–57.

Ventricular-Vascular Coupling in the Pulmonary Circulation

5

Nicholas E. Hobson and Kendall S. Hunter

Abstract

Ventricular performance quantities such as the end-systolic pressure-volume relationship (ESPVR) have been the subject of numerous basic science studies, yet their clinical use remains limited, particularly in the right ventricle (RV). This is primarily due to the difficulty of volume measurements in the small, crescent-shaped RV via catheterization. However, such parameters should be a superior indicator of ventricular function compared with other hemodynamic measures used in the prognosis of pulmonary arterial hypertension (PAH), such as pulmonary vascular resistance index (PVRI). Thus, there is clinical interest in methods that estimate ESPVR and related parameters while being minimally invasive. The focus of this chapter is on one such method and its possible non-invasive extensions, a modified single-beat method which estimates the ventricular-vascular coupling ratio (VVCR), or the ratio of end-systolic ventricular elastance (E_{es}) to arterial elastance (E_a). Within the single-beat elastance framework, the maximum isovolumic pressure ($P_{max,iso}$) and end-systolic pressure are found; based on a novel assumption about the slopes of E_{es} and E_a, VVCR is then computed using only pressure. A lower coupling ratio is hypothesized to be a good indicator of RV dysfunction and failure, as represented by the World Health Organization Functional Class (WHO-FC). We also investigate two non-invasive forms of this method using measurements in children: one in which pressure data is obtained from the velocity of the tricuspid regurgitant (TR) jet measured by Doppler ultrasound; and another in which myocardial performance index (MPI) is

N.E. Hobson • K.S. Hunter (✉)
Department of Bioengineering, University of Colorado Anschutz Medical Campus, Aurora, CO 80045, USA
e-mail: nicholas.hobson@ucdenver.edu; kendall.hunter@ucdenver.edu

M.K. Friedberg, A.N. Redington (eds.), *Right Ventricular Physiology, Adaptation and Failure in Congenital and Acquired Heart Disease*, https://doi.org/10.1007/978-3-319-67096-6_5

used to approximate VVCR. Finally, a very new but existing noninvasive method to compute VVCR using only volumes is explored as a predictor of reactivity in children with PH.

Keywords
Ventricular-vascular coupling • Pulmonary circulation

Introduction

Ventricular performance quantities such as the end-systolic pressure-volume relationship (ESPVR) have been the subject of numerous basic science studies, yet their clinical use remains limited, particularly in the right ventricle (RV). This is primarily due to the difficulty of volume measurements in the small, crescent-shaped RV via catheterization. However, such parameters should be a superior indicator of ventricular function compared with other hemodynamic measures used in the prognosis of pulmonary arterial hypertension (PAH), such as pulmonary vascular resistance index (PVRI). Thus, there is clinical interest in methods that estimate ESPVR and related parameters while being minimally invasive.

The focus of this chapter is on one such method and its possible non-invasive extensions, a modified single-beat method, which estimates the ventricular-vascular coupling ratio (VVCR), or the ratio of end-systolic ventricular elastance (E_{es}) to arterial elastance (E_a). Within the single-beat elastance framework, the maximum isovolumic pressure ($P_{max,iso}$) and end-systolic pressure are found; based on a novel assumption about the slopes of E_{es} and E_a, VVCR is then computed using only pressure. A lower coupling ratio is hypothesized to be a good indicator of RV dysfunction and failure, as represented by the World Health Organization Functional Class (WHO-FC). We also investigate two non-invasive forms of this method using measurements in children: one in which pressure data is obtained from the velocity of the tricuspid regurgitant (TR) jet measured by Doppler ultrasound; and another in which myocardial performance index (MPI) is used to approximate VVCR. Finally, a very new but existing noninvasive method to compute VVCR using only volumes is explored as a predictor of reactivity in children with PH.

Concepts and Background

Characterization of the pressure-volume relationship of the heart as a pump dates back to an 1898 paper by Otto Frank [1], in which he presented a P-V diagram of contractions of the isolated frog left ventricle. Frank made two important observations about this diagram: first, peak systolic activity, whether measured by isovolumic pressure or isobaric ejection volume, is related to preloaded end-diastolic volume (EDV); and second, when the ventricle is in ejecting mode, the curve produced by connecting the end-systolic points of different PV loops (known as the end-systolic pressure-volume relationship, or ESPVR) is quite different than the isovolumic (non-ejecting) curve. These observations were well-received in Europe, and in 1914 Ernest Starling published a series of papers that led to the now well-known Frank-Starling law of the heart [1, 2], which describes the ability of the heart to compensate for varying end-diastolic volumes by varying its work output accordingly.

Research on this topic waned until the 1950s, when interest in pressure-volume relationships of the heart experienced a resurgence. Studies by Ullrich et al (1954), Hild and Sick (1955), and Hild and Herz (1956) obtained pressure-volume relationships for mammalian hearts, which proved to be somewhat different than the previous studies using the frog ventricle. These studies revealed the ESPVR displayed only slight curvilinearity within physiologic pressure ranges. Monroe et al. (1960, 1961, 1964) showed similarly that the ESPVR for the dog ventricle under

the control condition was almost linear, contrary to studies of the frog that showed strong dependence of ESPVR on preload and afterload history.

The ESPVR Relationship and Elastance

The near-linearity of the ESPVR curve has been validated in both the left ventricle (Cross et al. 1961, Taylor et al. 1969) and right ventricle (Lafontant et al. 1962). Perhaps the most substantial work on the characterization of ESPVR and PV relationships of the left ventricle come from the 1970's to 1980's in Japan from authors Suga, Sagawa, and Sunagawa. These serial works on the in vivo canine heart further confirmed and refined the linearity of ESPVR in the physiologic range and helped advance understanding of a wide array of other properties of these measurements. Advances in catheter technology and the advent of the conductance catheter allowed instantaneous volume measurements of the left ventricle in vivo [3], meaning ESPVR could be obtained in a cardiac catheter lab by altering preload (EDV) and obtaining a series of PV loops and connecting their end-systolic points (Fig. 5.1). As the end-diastolic volume increases and the loops shift to the right, end-systolic pressure increases along the ESPVR line up to a maximum pressure for isovolumic contraction [4]. Because ESPVR is relatively insensitive to changes in preload, afterload, and heart rate, it provides a valuable index of systolic cardiac function. Specifically, the slope of the ESPVR is a measure of end-systolic elastance (E_{es}) of the ventricle. Furthermore, a second useful measure, effective arterial elastance (E_a), can be obtained as the slope of the line from the pressure-volume loop, from the end-systolic PV point (upper-left of the PV box) to the end-diastolic volume intercept (bottom-right). Arterial elastance was defined as the ratio of end-systolic pressure to stroke volume, P_{es}/SV (Fig. 5.1). This definition, from a 1983 work by Sunagawa and colleagues examining LV-arterial interaction, is based on the assumption that vascular impedance can be modeled as a three-element Windkessel model [5]. By defining SV in terms of mean arterial flow over a single cardiac cycle, the P_{es}-SV relationship in the arteries was described analytically

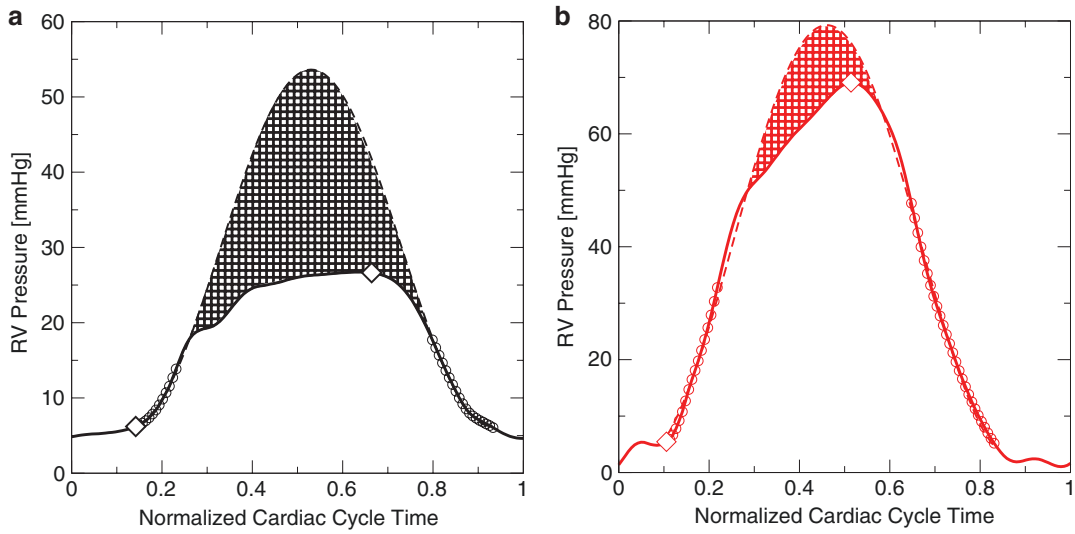

Fig. 5.1 (**a**, **b**) Estimation of VVCR using the pressure only method. A WHO FC 1 patient (*left plot*) has a significantly smaller pressure ejection requirement (i.e. max RVSP, shown as *diamonds* near *end-systole*) than maximum isovolumic pressure, yielding high VVCR-P, while the WHO FC 4 patient (*right plot*) has little "overhead" between these two quantities, yielding low VVCR-P

as a linear relationship when characteristic arterial impedance, peripheral resistance, compliance, and systolic and diastolic durations are constant. The expression describing the slope of that relationship involving those arterial parameters was denoted by E_a (effective arterial elastance). Because both E_{es} and E_a are given in the same units, their ratio can be computed as E_{es}/E_a to provide a measure of ventricular-vascular coupling.

Arterial Elastance and Ventricular-Vascular Coupling

Works by Sunagawa et al. [5, 6] sought to test the hypothesis that ventricular external work would be maximized if the ventricular and arterial elastances are equal. They investigated the optimal arterial resistance under a number of variable parameters such as end-diastolic volume, contractility, heart rate, and arterial compliance, and found that optimal arterial resistance varied only slightly with arterial compliance, while varying widely with contractility and heart rate. These findings suggest that the ratio of ventricular and arterial elastance is optimally nearly unity, which gives rise to the idea that the ventricle and vasculature are coupled from an energetics viewpoint. In other words, optimal flow (and optimal energy transfer from the ventricle through the vasculature) is achieved at an arterial elastance equal to ventricular elastance. Thus, the effects of increased afterload on PV loops and ESPVR should be significant.

Single-Beat Methodology

In 1991, Takeuchi et al. proposed a novel method for the calculation of the slope of the ESPVR (E_{es}) using a single beat [7]. They realized that the maximum pressure the ventricle can produce during isovolumic contraction could be estimated from the pressure trace alone, and the slope of the ESPVR could be obtained by drawing a line from this point tangential to the upper-left corner of a single PV loop (i.e. near the end-systolic point). Sinusoidal curve fitting is performed on the pressure trace of the ventricle using data points which correspond to periods of isovolumic contraction and relaxation in order to estimate P_{max}. This is a much easier method than the previous one for generating the ESPVR, which involved creating at least three PV loops by altering the end-diastolic volume.

This method has also been validated for the right ventricle by Brimioulle et al. in 2003 [8]. A number of assumptions and limitations unique to the RV were addressed in their work. The triangular shape of typical PV loops in the RV means that end-systole and end-ejection often occur at different times. The upper-left corner was used as the end-systolic point, which is valid for the LV but less so for the RV. The assumption that isovolumic beats are sinusoidal, established by Sunagawa by Fourier analysis for the LV, was verified by comparing estimated $P_{max,iso}$ of ejecting beats with observed P_{max} for isovolumic beats of the same starting EDV, which were found to be strongly correlated. Due to the challenges of measuring RV volume in vivo, they determined RV volume changes by integrating flow measured in the proximal pulmonary artery with a widely validated ultrasonic method. They also found expected changes in E_{es} and E_a under a variety of inotropic states.

Pulmonary Hypertension

Pulmonary hypertension was first classified in 1973 in a meeting organized by the World Health Organization. PH is defined as a hemodynamic and pathological condition in which a mean pulmonary arterial pressure (PAP) of 25 mmHg or greater at rest is measured by right heart catheterization. Normal PAP is 14 ± 3 mmHg with an upper limit of about 20 mmHg. The significance of a mean PAP of 21–24 mmHg is unclear [9].

The clinical classification of PH has undergone some changes in international conferences since the initial 1973 WHO classification, but the basic differentiation of primary and secondary PH is still apparent. The broad categories of the classification agreed upon at the fourth World

Symposium for PH at Dana Point, California in 2008 [9] are as follows:

1. Pulmonary arterial hypertension (PAH)
2. Pulmonary veno-occlusive disease and/or pulmonary capillary haemangiomatosis
3. Pulmonary hypertension due to left heart disease
4. Pulmonary hypertension due to lung diseases and/or hypoxia
5. Chronic thromboembolic pulmonary hypertension
6. PH with unclear or multifactorial mechanisms

The focus of the methods discussed in this chapter is primary hypertension (group 1, PAH), or PH not caused by other health problems.

Diagnosis

Diagnosis of PH is a process of exclusion, so often different diagnostic tools and methods need to be employed to eliminate all other possible causes. In the case of PAH, this means ruling out left heart disease, veno-occlusive disease, lung disease, and chronic thromboembolism [10].

Symptoms of PAH are often mild and present mainly during exercise, and can include shortness of breath, fatigue, weakness, angina, syncope, and abdominal distension. Auscultory physical signs that may aide diagnosis are: tricuspid valve regurgitation murmur, a diastolic murmur of pulmonary insufficiency, and an RV third heart sound. Patients with advanced disease may present with signs such as ascites, peripheral edema, and cool extremities [10]. However, these physical signs vary widely and may not present at all.

Echocardiography can provide an estimation of PAP by obtaining velocity measurements of regurgitant tricuspid valve jets, which occur in more than 70% of patients with PAH [11] Velocity of TR jets is measured using Doppler ultrasound. By using a simplified form of Bernoulli's equation, mean PAP can be calculated as $4 \times (\textit{tricuspid regurgitant velocity})^2 + (\textit{estimated right atrial pressure})$. However, echocardiography is limited by the noise inherent in ultrasound imaging, which can lead to faint or inaccurate signals.

The gold standard for the diagnosis of PAH is right heart catheterization (RHC), and it is necessary for confirming such a diagnosis [10]. The following variables must be obtained: PAP, right atrial pressure, RV pressure, pulmonary wedge pressure (PWP), and cardiac output (CO) by either thermodilution or the Fick method. A mean PAP of 25 mmHg or greater with a PWP of 15 mmHg or less in the absence of other causes confirms a diagnosis of PAH [10]. Although RHC is a relatively safe procedure, it is invasive, and therefore carries some risk to the patient.

Assessment of RV function

A number of methods for the assessment of RV function have been proposed and validated over the past 30 years, varying widely in invasiveness as well as efficacy and accuracy. In 1984, Kimchi et al. became the first group to evaluate RV ejection fraction (RVEF) using radionuclide ventriculography [12]. They defined RV failure as RVEF less than 38%. In 1989, Vincent et al. obtained RVEF using a modified PA catheter with a fast-response thermistor, utilizing the thermodilution method [13]. However, these methods are not ideal both because they are either nuclear or invasive, and because RVEF varies widely in normal patients from 30% to 60%.

Cardiac magnetic resonance (CMR) imaging is the gold standard for evaluating RV function and can reliably quantify RV volume and RVEF. Delayed contrast-enhanced CMR has also been shown to detect fibrotic tissue in the RV wall, but can only detect regional changes in myocardial tissue. Contrast-enhanced T1-weighted CMR allows the detection of diffuse fibrosis [14]. However, CMR is expensive and availability is often limited.

Echocardiography is currently the most practical tool for assessing RV function at the bedside. A failed right ventricle is severely dilated, which can be assessed by comparing the area of the chamber with that of the left ventricle. A ratio of RV:LV area less than 0.6 is considered normal,

and greater than 1 is considered failing [10]. In 1995, Masahiro, et al. demonstrated the efficacy of an automated method for obtaining a correlate of the ESPVR based on the area of the chamber from echocardiography, rather than volume measured by catheterization [15]. They showed that the ESPAR responded similarly to ESPVR as RV function declined. Another sign readable from echocardiography is paradoxical septal motion during systole, which indicates RV systolic pressure overload. In Doppler mode, the ejection flow can show pulmonary hypertension by a shortening of the acceleration time of flow (<100 ms). A related parameter proposed by Tei et al. in 1995 takes the ratio of combined isovolumic contraction and relaxation times compared with ejection time, termed the myocardial performance index (MPI) [16]. Longer periods of isovolumic contraction and relaxation yield a higher MPI, and indicate worse RV function. Interestingly, this measure bears a certain similarity to VVCR, because longer isovolumic periods will inevitably yield lower estimated maximum isovolumic pressures.

Advances in 3D echocardiography in the past years have made the non-invasive measurement of RV volume possible. There are several methods for calculating RV volumes from echocardiographic images. One involves the manual tracking of RV area through a series of slices, while the other uses border-detection algorithms to automate this process. These measurements have been shown to correlate well with volume measurements obtained from CMR, but consistently predict volumes 20–34% smaller than those obtained by CMR [14]. Thus, 3D echocardiography requires further refinement and validation, but could become a gold standard in the future.

Mechanical-Mechanistic Links

Despite its origin in the pulmonary vasculature, the proximate cause of death in pulmonary hypertension is often RV failure [17]. In response to pulmonary hypertension, the RV undergoes hypertrophic remodeling reflecting increased myocyte size and altered programs of gene expression. Ultimately this pathologic remodeling leads to wall thinning, chamber dilation, and RV failure [18]; however, therapies that directly target the dysfunctional RV are not currently available [10, 19]. Inflammatory processes in the pulmonary vasculature are increasingly recognized to play a role in the progression of pulmonary hypertension [20], and additional evidence suggests that inflammatory-fibrotic modeling contributes importantly to the progression of heart failure [21]. Together, these observations suggest the need to examine the relationships between RV overload and function, hypertrophic remodeling, and activation of inflammatory-fibrotic processes in the RV, in the setting of pulmonary hypertension.

Animal and Clinical PV Studies

Animal Work

A significant amount of work has been done in recent years to better characterize the role of ventricular adaptation to pulmonary hypertension in animal models. A 2004 interspecies study by Wauthy et al. [22] showed that while E_{es} and E_a both increased during short (10 min) bouts of hypoxia-induced hypertension, VVCR remained optimal in dogs, goats, and pigs. This trend was also observed in induced embolism and proximal pulmonary artery constriction in dogs. In all cases, a proportional increase in E_{es} compensated for elevated E_a, and optimal coupling was maintained.

In a 2007 study by Grignola et al. [23] of an acute PH model in 6 anesthetized sheep in which proximal occlusion and whole-pulmonary vasoconstriction (by phenylephrine) were compared, coupling, as assessed by an energy transmission ratio and the ratio of pulsatile energy to total energy, was better maintained in the vasoconstictive model. Their model showed that activation of smooth muscle cells in the main pulmonary artery helped maintain energy transfer from the RV to the hypertensive pulmonary vasculature by preserving the reflected wave magnitude.

Several models of progressive pressure overload ("chronic" PAH) have shown that the RV in healthy animals operates close to maximum efficiency (VVCR ≈ 2), decreases as afterload increases to operate close to the point of maximal stroke work (VVCR ≈ 1), and finally decouples (VVCR <1) approaching failure. The trend is one of continually increasing E_a, with E_{es} initially increasing and finally returning to baseline values. This was shown in a porcine model by Ghuysen et al. [24] of progressive pulmonary embolism by injection of blood clots. E_a increased continually with each injection, while E_{es} increased after the first two injections, but failed to increase further. Thus, E_{es}/E_a initially decreased to values near optimal stroke work, but the final injection caused values to drop below 1, decreased stroke work, and RV dilation.

Another animal model of interest is a 2007 study by Missant et al. [25] regarding the effects of Levosimendan on RV dysfunction in a porcine model. Levosimendan is a calcium sensitizer—it increases the sensitivity of the heart to calcium, thus increasing cardiac contractility without a rise in intracellular calcium. Levosimendan exerts its positive inotropic effect by increasing calcium sensitivity of myocytes by binding to cardiac troponin C in a calcium-dependent manner. In healthy animals, Levosimendan improved contractility but actually reduced efficiency (i.e. VVCR dropped slightly), with no change in PVR or characteristic impedance. The lack of improvement in efficiency was explained as the RV was already operating at max efficiency (best coupling) in health. In an ischemia/reperfusion model of RV failure along with pressure overload (PA banding), Levosimendan increased inotropy (i.e. E_{es}), thus maintaining or improving coupling.

Finally, a study by Kind et al. sought to better characterize the isovolumic beat in rats using Fourier analysis. They induced stable and progressive acute pulmonary hypertension in the rats by the administration of monocrotaline 40 and 60 mg/kg, respectively. Isovolumic beats were obtained by clamping the pulmonary artery in these rats and controls. The waveforms were then normalized in pressure and time, averaged, and modeled by a Fourier series using six harmonics. This normalized waveform was parameterized and used for curve fitting of single beats, then compared to other isovolumic beat models from the literature, including the sinusoidal method by Sunagawa et al. mentioned earlier in this chapter. It was found that the Fourier-based model was more accurate than the other models at predicting maximum isovolumic pressure from ejecting beats (compared with true isovolumic beats obtained by pulmonary artery clamping during the prior beat), and that the other models generally underestimated maximum isovolumic pressure. This approach holds great promise in improving single-beat methodology in humans.

Clinical Work

Although there has been much work done in the lab characterizing the pressure-volume relationship of the ventricle, and though these works generally strive to emphasize the potential clinical usefulness of PV loops, their use in clinical settings has remained extremely limited for a number of reasons. First, the procedures for obtaining instantaneous pressure and volume measurements require invasive catheterization, optimally with high-fidelity catheters. Techniques for volume measurements in particular have been difficult and imprecise. Measurements of volume of the RV are especially troublesome due to its location, smaller size, and non-uniform geometry. Furthermore, many clinical decisions can be made based on more easily-obtained measures, such as ejection fraction [26].

However, there have emerged a number of clinical studies in recent years demonstrating and validating the usefulness of PV-loop-derived parameters. A study in 1992 by Kelly et al. [27] tested the use of effective arterial elastance of the LV as an index of vascular load in normal and hypertensive humans. The study found that E_a based on PV loops was nearly identical to E_a derived from a three-element Windkessel model for normal patients, and that it exceeded simple resistance by nearly 25% in hypertensive patients, due to decreased compliance and wave reflection. The findings suggest that even E_a alone, not to

speak of full ESPVR or E_{es}/E_a coupling, could provide a convenient assessment of arterial impedance and its effects on ventricular function in hypertensive patients.

The earliest population-based study assessing diagnostic capabilities of LV PV loops comes from Lam et al. from Minnesota in 2007 [28]. This study compared patients exhibiting heart failure with a normal ejection fraction (HFnlEF) with patients with hypertension but no heart failure (HTN), and with patients without cardiovascular disease. The authors characterized left ventricular volume, effective arterial elastance, LV end-systolic elastance, and LVdiastolic elastance and relaxation noninvasively. Their results showed increased E_{es} for hypertensive and HFnlEF patients compared with the control, as well as a shift to the right of the V_0 volume intercept for HFnlEF patients relative to HTN patients, indicating an overall increase in ventricular volume. They observed similar differences in the EDPVR curves for the three groups, with hypertensive patients having a greater EDV than HFnlEF patients. Their work showed a probable role of diastolic dysfunction in HFnlEF patients relative to HTN patients. Furthermore, it shows the potential diagnostic power of ESPVR and EDPVR curves for distinguishing specific cardiovascular disorders.

Furthermore, a 2004 study by Kuehne et al. validated the single-beat method for the RV using cine MRI to obtain RV volume, and also undertook a small clinical study comparing 6 control patients to 6 patients with chronic pulmonary hypertension. They obtained indexes of cardiac pump function, measured as cardiac index or the ratio of cardiac output to body surface area, E_{es} indexed to myocardial mass and ventricular-arterial coupling (E_{es}/E_a). In patients with PAH, RV pump function was decreased, myocardial contractility was enhanced, and VVC was inefficient compared with the control group. These results agree with the expected physiologic impact of PAH on RV function discussed above, and are encouraging for the minimally-invasive prognosis of PAH. Finally, a recent study by Sanz et al. [29] used a different simplification of the single-beat method to use MRI combined with invasive measurement of mPAP to approximate the inverse of VVCR (e.g. E_a/E_{es}) in 143 adults with PH. Their E_a and VVCR both showed increasing group trends when sub-divided by increasing quartiles of PVRI. Unfortunately, their approximation was quickly shown to be incomparable to the gold-standard in that it neglects the zero-pressure intercept of RV volume [30]. This however does not mean that their approximation lacks clinical utility; indeed we show in our work below that this measure clearly distinguishes reactive vs. unreactive children with PAH in terms of their response to pulmonary vascular vasodilators.

Emerging Methods for Assessment of VVCR

It is useful to distinguish between patients with early- and late-stage pulmonary hypertension as "compensated" and "failing," in terms of ventricular function. In early-stage PAH, as the ventricle must overcome greater vascular pressure and impedance, the end-systolic pressure will increase to compensate, which is achieved by an increase in ventricular elastance. This progression will also be reflected in a slightly increased E_a as distal vessels dilate, leading to increased mPAP; and as vascular remodeling gradually stiffens the arterial vasculature, leading to increased pulse pressure. Together these lead to a greater P_{es}. Thus, the coupling ratio between the ventricle and arteries, E_{es}/E_a, may decrease somewhat but should remain above or close to unity. Over time however, the heart becomes overworked, and P_{es} approaches the maximum isovolumic pressure the ventricle can produce, as shown in Fig. 5.1a, b. A patient transitions from compensated to failing when the ventricle and vasculature become uncoupled, and the ventricle begins to dilate to meet cardiac output needs. The PV loop shifts to the right and becomes narrower as end-diastolic volume increases and stroke volume decreases [31–34]. These patients should have a markedly decreased coupling ratio, which signifies uncoupling of the ventricle and vasculature. We have preliminary evidence below that

these patients are unreactive to pulmonary vasodilators in terms of cardiac output, indicating that lack of reactivity in PVR is as suggestive of problems with RV function as much as problems in vascular function.

Invasive Pressure-Only VVCR

The basis for this work is a modification of the single-beat method that estimates VVCR while eliminating the need for volume measurement. Re-examining Fig. 5.1a, it can be seen that:

$$E_{es} \cong \frac{P_{\max,iso} - P_{es}}{SV} \tag{1}$$

and given the definition [6, 27].

$$E_a = \frac{P_{es}}{SV} \tag{2}$$

Inserting Eqs. (1) and (2) into the expression for VVCR, we have:

$$\frac{E_{es}}{E_a} \cong \frac{P_{\max,iso} - P_{es}}{SV} \cdot \frac{SV}{P_{es}} = \frac{P_{\max,iso} - P_{es}}{P_{es}} = \frac{P_{\max,iso}}{P_{es}} - 1 \tag{3}$$

Thus, from Eq. (3) we obtain an expression for VVCR as a simple ratio of maximum isovolumic pressure to end-systolic pressure. The single-beat method can be applied to pressure traces from the RV, estimating $P_{max,iso}$ by sinusoidal curve fitting to periods of isovolumic contraction and relaxation, and comparing this value to the observed end-systolic pressure to obtain an estimate of VVCR.

Based on the above analysis, the coupling ratio E_{es}/E_a actually quantifies the heart's "reserve" capacity, or the ratio of its maximum pressure capability to its current pressure requirement, at a particular inotropic state. As such, we hypothesize that this ratio will be prognostic of RV failure in PH. Our approach computes the ratio using only pressure, allowing us to avoid having to acquire more difficult, less readily available PV loops. By using only clinically feasible standard-of-care measurements, we enable wider clinical applicability of the resulting prognostic, and further open the possibility of non-invasive estimation of the coupling ratio. Our simplified approach promises to enable more routine assessment of RV function. Furthermore, our quantitative approach of describing the system has the potential to better guide future basic science and mechanistic studies of the disease as well as assist in the interpretation of future therapeutic study results.

Pressure Data Analysis

All data analysis was performed in MATLAB. Pressure traces from the right ventricle were divided into single beats by ECG gating. $P_{max,iso}$ was determined by fitting the equation $P = a + b \cdot \sin(c \cdot t + d)$, [8] where P is pressure and t is time, to pressure values from the end-diastolic point up to the point of the maximal value of the first derivative, corresponding to isovolumic contraction, and from the time of the minimal value of the first derivative to the same pressure value as the end-diastolic point, corresponding to isovolumic relaxation. The end-diastolic point was defined as the time at which dP/dt exceeds 200 mmHg/s [7]. Curve fitting was performed using the Levenberg-Marquardt algorithm for non-linear least squares [8].

The coupling ratio E_{es}/E_a was determined from Eq. (3), which required an additional assumption regarding the timing of end-systole. Alyono et al. [31] found that 30 ms before dP/dt_{min} is the best definition for end-systole using pressure data alone, compared with definitions using pressure and volume together. Because the pressure data was obtained with a sampling frequency of 250 Hz, data points were separated by 4 ms, so end-systole was defined as 32 ms, or 8 data points, prior to dP/dt_{min} rather than 30 ms prior. VVCR was also calculated using P_{max} for a given pulse as end-systole in addition to the 32 ms prior to dP/dt_{min} definition for end-systole, and each method was compared. VVCR (P_{max}) was superior to VVCR (P_{es}) for all tests, so results will only be shown for VVCR (P_{max}).

Initial Results for New Techniques

Indirect evidence that VVCR is related to the progression of right heart remodeling processes can be found by comparing it, as well as load parameters such as mPAP, to tissue markers of hypertrophy, inflammation, or fibrosis. Preliminary comparisons were performed with a small set of neonatal male calves (post-natal day 1), exposed to 14 d hypoxia (simulated elevation 4300 m) or ambient atmosphere (Ft. Collins, CO). Hemodynamics were obtained by right heart catheterization via the jugular vein with a solid state catheter to obtain RV and main PA pressures; post study, the RV and LV were excised and Real Time PCR was used to examine gene expression. Although a low-power data set, the results clearly demonstrate (Table 5.1, Fig. 5.2a, b) that gene products reflective of pressure overload of the cardiac myocyte (β-myosin heavy chain (MHC), skeletal α-actin, Brain natriuretic peptide (BNP)) correlated strongly with mean PA pressure, whereas gene products reflective of myocardial inflammation showed greater dependence on VVCR. Further, ECM remodeling gene products also showed equivalent or greater dependence on the coupling ratio rather than developed mPAP. These results suggest that hypertrophic RV remodeling driven by cardiac myocytes is primarily responsive to increasing pulmonary vascular pressure whereas inflammatory and ECM remodeling in the RV are more sensitive to altered mechanical coupling of the cardiopulmonary system, and reinforce the conclusion that RV remodeling encompasses multiple processes responding to non-identical determinants. Thus, understanding and predicting disease progression from the viewpoint of hemodynamics requires a multifactorial approach.

Non-Invasive Methods

We begin by discussing a Doppler ultrasound technique, which makes use of a simplification of Bernoulli's principle in order to approximate RV pressure from the velocity of the regurgitant tricuspid valve (known as a TR jet). This pressure trace is then used to compute VVCR using the single-beat methodology described above. Also noninvasive in nature, two papers have been published that investigate the use of myocardial performance index (MPI, or "Tei index") [32, 33]. The second of these two is particularly interesting; in it, MPI is shown to most strongly correlate to 6 min walk distance, BNP, cardiac index, mPAP, and PVR, better than other echo measures of RV function. Below we present preliminary evidence that MPI is a good predictor of patient outcomes, as well as derive its relationship to VVCR that may explain its predictive power.

TR Jet Technique

Doppler ultrasound data acquired during catheterization was visualized and processed in Matlab. Noise reduction was first applied using the discrete wavelet transform method described

Table 5.1 *R*-squared values characterizing correlations between hemodynamic parameters (mPAP, Coupling Ratio) and tissue markers of myocyte overload, inflammation, and fibrosis ($n = 9$)

Tissue Marker	NPPB (BNP)	ACTA1	MHY7	MCP-1	IL-1b	IL-1RA	TN-C	OPN	COL 1A1	ED-A Fn
mPAP	0.738	0.545	0.581	0.567	0.370	0.413	0.439	0.602	0.247	0.175
VVCR	0.446	0.324	0.242	0.597	0.657	0.506	0.428	0.597	0.700	0.592
Different?	0.140	0.252	0.151	0.458	0.172	0.389	0.487	0.492	0.068	0.100

Generally, mPAP shows best (and most significant) correlation with tissue markers of myocyte overload, while the coupling ratio displays best correlation with inflammation and fibrosis. Only two correlations approached a significant difference

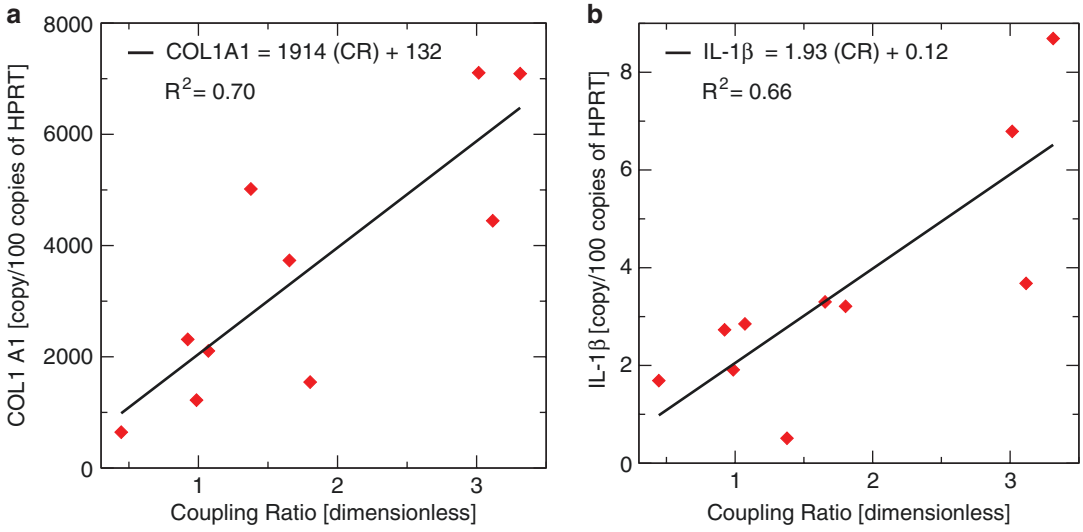

Fig. 5.2 (**a**, **b**) Notable regressions between coupling ratio and inflammatory/fibrotic tissue markers

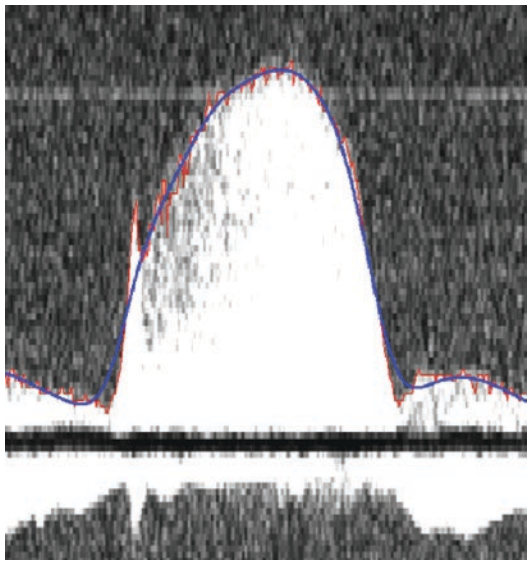

Fig. 5.3 Automatic trace of Doppler US image of TR jet. *Red* raw trace, *Blue* smoothed trace

by Zhang et al. in 2001 [35]. To obtain an envelope of the velocity, traces of the TR jet image were performed by an automatic edge detection routine using an adjustable threshold magnitude. A threshold value was computed automatically based on the noise level, soft thresholding was applied to the detail coefficients, and the image was reconstructed, as shown in Fig. 5.3. The smoothed velocity trace was transformed into approximate right-ventricular pressure by simplification of Bernoulli's principle as $P=4V^2$, as is done in clinical practice, in which P is the ventricular pressure and V is the velocity of the jet. This data was subsequently analyzed again using the techniques described in the Invasive Pressure-Only VVCR section above. Having already performed better in the catheterization cases, the maximal pressure was used in computing the coupling ratio, rather than the end-systolic definition of 30 ms prior to dP/dt_{min}. VVCR was obtained in this fashion for 11 patients, and they follow the same trends (with respect to WHO FC) as with the invasively obtained ratios; however, we have not yet performed outcomes analyses in this small set.

MPI Transformation to VVCR

Given our modeling approach with pressure, we can estimate both P_{es} and $P_{max,iso}$ from merely the isovolumic times and ejection time. These times are routinely collected in our cath lab for the prediction of the myocardial performance index

[MPI—also known as the Tei index [16, 36]], which is computed as $\frac{IVCT + IVRT}{RVET}$, in which IVCT & IVRT are the IsoVolumic Contraction/Relaxation Times, and RVET is the RV Ejection Time. From this time equation, an assumption that P_{es} occurs approximately at the end of ejection time, and the sinusoidal approximation for isovolumic contraction pressure, we can derive the equation.

$$VVCR \approx \cot\left(\pi \frac{MPI}{MPI + 1}\right)^2, \qquad (4)$$

in which π is the constant pi (3.14159…); thus VVCR is approximated by a trigonometric transform of MPI. As MPI varies from low values near zero (indicating good performance) to higher values still less than one (increasing functional limitation), estimated VVCR varies from large values (>5) to values close to zero, predicting the same functional status. To see how well this predicted patient status, we compared MPI, approximated VVCR, and PVRI measured within 48 h in 27 children with PAH to determine how well each predicted WHO FC at follow up, in outcomes categories identical to the three trichotomous groups discussed above. Shown in Fig. 5.4 are box plots of MPI, approximated VVCR, and PVRI for the three outcomes groups (n = 7, 11, 9 for OC1, OC2, OC3, respectively). Clear separation exists in both noninvasive measures between healthy group and severe functional limitation group mean values, whereas due to high variance PVRI has overlap in all three groups. ANOVA showed both noninvasive values differentiated the groups ($p < 0.05$), whereas PVRI did not ($p = 0.08$). Additionally, both noninvasive methods showed better fit to trichotomous and dichotomous WHO-FC based outcomes. While it is currently unclear if the trigonometric transformation of MPI (into VVCR) is advantageous, the transformation does make clear MPI's relation to VVCR; neither have been comprehensively explored as prognostics in pediatric PAH.

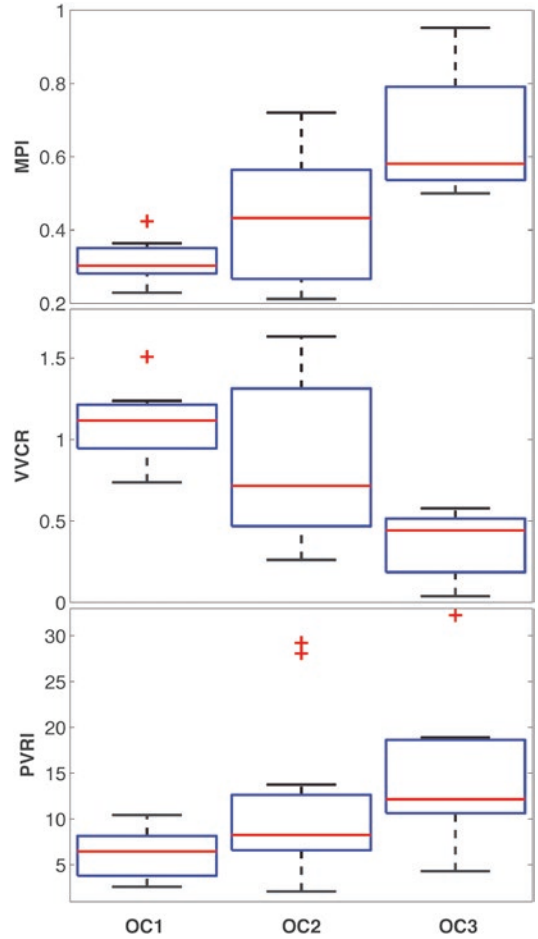

Fig. 5.4 Box plots of MPI, MPI-approximated VVCR, and PVRI. Both noninvasive measures better categorize (and predict) the three WHO FC based outcomes parameters

MRI Technique

As noted above, the Sanz et al. [29] method of computing VVCR, while not comparable to the gold standard, may still possess clinical utility. To explore this possibility, we examined 16 pediatric subjects who underwent MRI and catheterization within month (14 were within 48 h). Age ranged from 3 months to 23 years, with the mean being 11.3 ± 7.4 years. E_a and E_a/E_{max} increased with increasing severity defined by PVR, with $p < 0.001$ for both. E_a/E_{es} steadily increased with increasing PVRI, as might be expected.

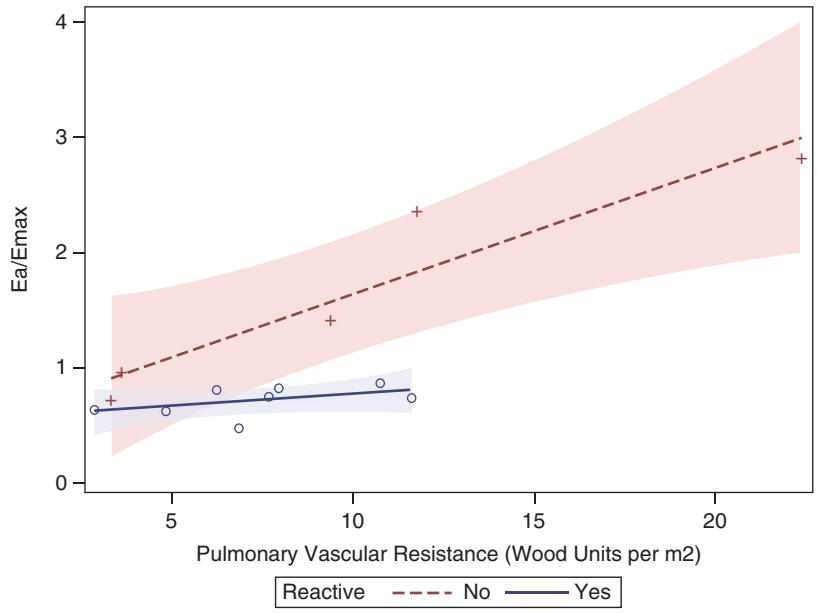

Fig. 5.5 MRI approximated inverse VVCR (with invasive pressure—mPAP), regressed in groups of reactive (*blue*) and non-reactive (*red*) patients vs. PVRI. The sickest patients (with largest inverse VVCR) showed greater decoupling as a function of afterload

Interestingly, patients in the highest quartile were found to be non-reactive to pulmonary vasodilators in PVRI during catheterization. ROC curve analysis determined that an E_a/E_{es} ratio of 0.85 had a sensitivity of 100% and a specificity of 80% of predicting reactivity; further, the AOC of this ROC curve was 0.89 ($p = 0.008$), suggesting quite good discrimination among those who were and were not reactive. Further, preliminary regressions of PVR vs. inverse VVCR in patients grouped by their reactivity in PVR when administered 100% O2 and/or 100% O2 and NO indicated that those unreactive (<20% change) are more uncoupled than those who are reactive (Fig. 5.5). This is in some sense unsurprising, in that PVR reactivity can occur due to reductions in mPAP (vascular reactivity) and increases in cardiac output (RV reactivity).

Limitations

There are a number of limitations associated with the simplified VVCR model. Because VVCR is a ratio of elastances, it can only provide an indirect measurement of ventricular performance as it relates to the state of the vasculature. Thus, parameters involving direct measurement of RV volume, such as ESPVR, will likely always remain better indicators of RV contractility. Furthermore, although the measurement of pressure is much simpler than the measurement of pressure and volume together, our first approximation of VVCR still requires catheterization, meaning it offers no large advantage in terms of invasiveness. Additionally, although it has been shown here to be prognostic, this method for obtaining VVCR requires validation against gold standard measurement. Validation will include pressure-volume studies in both animals and humans, and continual testing should show a strong correlation between VVCR obtained by PV loops and VVCR obtained by pressure alone.

Discussion/Conclusions

Pressure-volume loops and their associated parameters (E_{es}, E_a) are considered the gold-standard measures of ventricular function;

however, the difficult nature of changing ventricular preload and of measuring volume—particularly of the RV—has limited their clinical applicability. Through the 1990s and 2000s a new method—the single beat method—has greatly simplified the process of obtaining PV loops, elastances, and ventricular-vascular coupling ratio. The ratio is a combined measure of contractility and afterload, specifies the efficiency of heart ejection, and is generally a decreasing function of disease worsening. Emerging clinical measurements are providing preliminary evidence that VVCR is a good prognosticator of both left and right-sided heart failure.

By modification of the single beat method equations, we have obtained even simpler and more clinically accessible invasive and noninvasive ways to measure the ventricular-vascular coupling ratio and thereby predict RV function in pediatric PAH. Our invasive data clearly show PVRI and VVCR are independent parameters; thus these VVCR measurements offer new insight into disease progression unavailable from measurements of distal or proximal afterload. Three of the four noninvasive approaches already show high prognostic potential, and all are additionally applicable to adult PH. We conclude that VVCR holds promise for future clinical use in the prognosis of PAH.

References

1. Frank O. Die Grundform des arteriellen Pulses Erste. Z Biol. 1899;37:483–526.
2. Zimmer H. Who discovered the frank-starling mechanism? News Physiol Sci. 2012;17:181–4. https://doi.org/10.1152/nips.01383.2002.
3. Baan J, van der Velde ET, Jong TTA, et al. Continuous stroke volume and cardiac output from intraventricular dimensions obtained with impedance catheter. Cardiovasc Res. 1981;15(6):328–34.
4. Suga H, Sagawa K. Instantaneous pressure-volume relationships and their ratio in the excised, supported canine left ventricle. Circ Res. 1974;35(1):117–26.
5. Sunagawa K, Maughan WL, Burkhoff D, Sagawa K. Left ventricular interaction with arterial load studied in isolated canine ventricle. Am J Phys. 1983;245(5 Pt 1):H773–80.
6. Sunagawa K, Maughan WL, Sagawa K. Optimal arterial resistance for the maximal stroke work studied in isolated canine left ventricle. Circ Res. 1985;56(4):586–95.
7. Takeuchi M, Igarashi Y, Tomimoto S, et al. Single-beat estimation of the slope of the end-systolic pressure-volume relation in the human left ventricle. Circulation. 1991;83(1):202–12.
8. Brimioulle S, January F, Tabima DM, et al. Single-beat estimation of right ventricular end-systolic pressure-volume relationship. Am J Phys. 2003;284(5):H1625–30. https://doi.org/10.1152/ajpheart.01023.2002.
9. Rich S. Primary pulmonary hypertension: executive summary from the World Symposium-Primary Pulmonary Hypertension 1998. Geneva World Health Organization. 1998. http://scholar.google.com/scholar?q=Executive+Summary+from+the+World++Symposium+on+Primary+Pulmonary+Hypertension&btnG=&hl=en&as_sdt=0%2C6##0. Accessed 25 Sept 2013.
10. Galiè N, Hoeper MM, Humbert M, et al. Guidelines for the diagnosis and treatment of pulmonary hypertension: the Task Force for the Diagnosis and Treatment of Pulmonary Hypertension of the European Society of Cardiology (ESC) and the European Respiratory Society (ERS), endorsed by the Internat. Eur Heart J. 2009;30(20):2493–537. https://doi.org/10.1093/eurheartj/ehp297.
11. Yock PG, Popp RL. Noninvasive estimation of right ventricular systolic pressure by Doppler ultrasound in patients with tricuspid regurgitation. Circulation. 1984;70(4):657–62. https://doi.org/10.1161/01.CIR.70.4.657.
12. Kimchi A, Gray Ellrodt A, Berman DS, Riedinger MS, Swan HJC, Murata GH. Right ventricular performance in septic shock: A combined radionuclide and hemodynamic study. J Am Coll Cardiol. 1984;4(5):945–51. https://doi.org/10.1016/S0735-1097(84)80055-8.
13. Vincent JL, Reuse C, Frank N, Contempre B, Kahn RJ. Right ventricular dysfunction in septic shock: assessment by measurements of right ventricular ejection fraction using the thermodilution technique. Acta Anaesthesiol Scand. 1989;33(1):34–8. https://doi.org/10.1111/j.1399-6576.1989.tb02856.x.
14. Mertens LL, Friedberg MK. Imaging the right ventricle--current state of the art. Nat Rev Cardiol. 2010;7(10):551–63. https://doi.org/10.1038/nrcardio.2010.118.
15. Oe M, Gorcsan J, Mandarino WA, Kawai A, Griffith BP, Kormos RL. Automated echocardiographic measures of right ventricular area as an index of volume and end-systolic pressure-area relations to assess right ventricular function. Circulation. 1995;92(4):1026–33. https://doi.org/10.1161/01.CIR.92.4.1026.
16. Tei C, Dujardin K, Hodge D. Doppler index combining systolic and diastolic myocardial performance: clinical value in cardiac amyloidisis. J Am Coll Cardiol. 1996;28(3):658–64.
17. Sandoval J, Bauerle O, Palomar A, et al. Survival in primary pulmonary hypertension. Validation of a prognostic equation. Circulation. 1994;89(4):1733–44. https://doi.org/10.1161/01.CIR.89.4.1733.

18. Voelkel NF, Quaife RA, Leinwand LA, et al. Right ventricular function and failure: report of a National Heart, Lung, and Blood Institute working group on cellular and molecular mechanisms of right heart failure. Circulation. 2006;114(17):1883–91. https://doi.org/10.1161/CIRCULATIONAHA.106.632208.
19. Barst RJ, Gibbs JS, Ghofrani HA, et al. Updated evidence-based treatment algorithm in pulmonary arterial hypertension. J Am Coll Cardiol. 2009;54(1 Suppl):S78–84. https://doi.org/10.1016/j.jacc.2009.04.017.
20. Hassoun PM, Mouthon L, Barberà JA, et al. Inflammation, growth factors, and pulmonary vascular remodeling. J Am Coll Cardiol. 2009;54(1 Suppl):S10–9. https://doi.org/10.1016/j.jacc.2009.04.006.
21. Frantz S, Bauersachs J, Ertl G. Post-infarct remodelling: contribution of wound healing and inflammation. Cardiovasc Res. 2009;81(3):474–81. https://doi.org/10.1093/cvr/cvn292.
22. Wauthy P, Pagnamenta A, Vassalli F, Naeije R, Brimioulle S. Right ventricular adaptation to pulmonary hypertension: an interspecies comparison. Am J Physiol Heart Circ Physiol. 2004;286(4):H1441–7. https://doi.org/10.1152/ajpheart.00640.2003.
23. Grignola JC, Ginés F, Bia D, Armentano R. Improved right ventricular-vascular coupling during active pulmonary hypertension. Int J Cardiol. 2007;115(2):171–82. https://doi.org/10.1016/j.ijcard.2006.03.007.
24. Ghuysen A, Lambermont B, Kolh P, et al. Alteration of right ventricular-pulmonary vascular coupling in a porcine model of progressive pressure overloading. Shock. 2008;29(2):197–204. https://doi.org/10.1097/SHK.0b013e318070c790.
25. Missant C, Rex S, Segers P, Wouters PF. Levosimendan improves right ventriculovascular coupling in a porcine model of right ventricular dysfunction. Crit Care Med. 2007;35(3):707–15.
26. Burkhoff D, Mirsky I, Suga H. Assessment of systolic and diastolic ventricular properties via pressure-volume analysis: a guide for clinical, translational, and basic researchers. Am J Physiol Heart Circ Physiol. 2005;289(2):H501–12. https://doi.org/10.1152/ajpheart.00138.2005.
27. Kelly RP, Ting C, Yang T, et al. Effective arterial elastance as index of arterial vascular load in humans. Circulation. 1992;86:513–21. https://doi.org/10.1161/01.CIR.86.2.513.
28. Lam CSP, Roger VL, Rodeheffer RJ, et al. Cardiac structure and ventricular-vascular function in persons with heart failure and preserved ejection fraction from Olmsted County, Minnesota. Circulation. 2007;115(15):1982–90. https://doi.org/10.1161/CIRCULATIONAHA.106.659763.
29. Sanz J, García-Alvarez A, Fernández-Friera L, et al. Right ventriculo-arterial coupling in pulmonary hypertension: a magnetic resonance study. Heart. 2012;98(3):238–43. https://doi.org/10.1136/heartjnl-2011-300462.
30. Trip P, Kind T, van de Veerdonk MC, et al. Accurate assessment of load-independent right ventricular systolic function in patients with pulmonary hypertension. J Heart Lung Transplant. 2013;32(1):50–5. https://doi.org/10.1016/j.healun.2012.09.022.
31. Alyono D, Larson VE, Anderson RW. Defining end systole for end-systolic pressure-volume ratio. J Surg Res. 1985;39(4):344–50. https://doi.org/10.1016/0022-4804(85)90113-1.
32. Sato T, Tsujino I, Oyama-Manabe N, et al. Simple prediction of right ventricular ejection fraction using tricuspid annular plane systolic excursion in pulmonary hypertension. Int J Card Imaging. 2013;29(8):1799–805. https://doi.org/10.1007/s10554-013-0286-7.
33. Ogihara Y, Yamada N, Dohi K, et al. Utility of right ventricular Tei-index for assessing disease severity and determining response to treatment in patients with pulmonary arterial hypertension. J Cardiol. 2013. http://www.sciencedirect.com/science/article/pii/S0914508713002220. Accessed 16 Sept 2013.
34. Badesch DB, Champion HC, Sanchez MAG, et al. Diagnosis and assessment of pulmonary arterial hypertension. J Am Coll Cardiol. 2009;54(1 Suppl):S55–66. https://doi.org/10.1016/j.jacc.2009.04.011.
35. Zhang Y, Wang Y, Wang W, Liu B. Doppler ultrasound signal denoising based on wavelet frames. IEEE Trans Ultrason Ferroelectr Freq Control. 2001;48(3):709–16.
36. Tei C, Nishimura RA, Seward JB, Tajik AJ. Noninvasive Doppler-derived myocardial performance index: Correlation with simultaneous measurements of cardiac catheterization measurements. J Am Soc Echocardiogr. 1997;10(2):169–78. https://doi.org/10.1016/S0894-7317(97)70090-7.
37. Monroe RG, French GN. Left ventricular pressure-volume relationships and myocardial oxygen consumption in the isolated heart. Circ Res. 1961;9(2):362–73. Available from: http://circres.ahajournals.org/cgi/doi/10.1161/01.RES.9.2.362
38. Monroe RG, French G. Ventricular pressure-volume relationships and oxygen consumption in fibrillation and arrest. Circ Res. 1960;8(1):260–6. Available from: http://circres.ahajournals.org/cgi/doi/10.1161/01.RES.8.1.260
39. Monroe RG, Strang RH, LaFarge CG, Levy J. Ventricular performance, pressure-volume relationships, and O2 consumption during hypothermia. Am J Physiol. 1964;206(1):67–73.
40. Lafontant R, Feinberg H, Katz L. Pressure-volume relationships in right ventricle. Circ Res. 1962;11:699–701. Available from: http://circres.ahajournals.org/content/11/4/699.short
41. Taylor R, Covell J, Ross J Jr. Volume-tension diagrams of ejecting and isovolumic contractions in left ventricle. Am J Physiol. 1969;216:1097–102. http://ajplegacy.physiology.org/content/ajplegacy/216/5/1097.full.pdf
42. Cross C, Rieben P. Influence of coronary perfusion and myocarckd edema on pressure-volume diagram of left ventricle. Am J Physiol. 1961;201:102–8. Available from: http://ajplegacy.physiology.org/content/ajplegacy/201/1/102.full.pdf

43. Hild R, Mechelke K, Nusser E. Über die Beziehungen zwischen dem Druck und der Stromstärke in der Arteria pulmonalis sowie der Leistung des rechten Ventrikels beim "unbeeinflußten Kreislauf" der Katze und im oligämischen Schock. Pflüger's Archiv für die gesamte Physiologie des Menschen und der Tiere. 1956;263(4):401–10. Available from: http://link.springer.com/article/10.1007/BF00380426
44. Hild R, Sick L. Das Druck-Volumen-Diagramm des isolierten spontan schlagenden Katzenherzens. Z Biol. 1955;107:51. Available from http://scholar.google.com/scholar?q=hild+and+sick+1955&btnG=&hl=en&as_sdt=0%2C6#1
45. Ullrich KJ, Riecker G, Kramer K. Das Druckvolumdiagramm des Warmbl terherzens. Pflügers Arch for die Gesamte Physiol des Menschen und der Tiere. 1954;259(6):481–98. Available from: http://link.springer.com/10.1007/BF00412913

Right–Left Ventricular Interactions in RV Afterload and Preload

6

Mark K. Friedberg

Abstract

Ventricular–ventricular interactions refer to the cumulative effect of changes in filling, function, geometry and synchrony of one ventricle on the filling, function, geometry and synchrony of the contra-lateral ventricle. A substantial portion of RV mechanical work under normal circumstances is generated by LV contraction. However, the RV also profoundly influences LV function. These RV to LV and LV to RV interactions, are particularly prominent during increased volume and pressure loading, and affect disease course and outcome. These ventricular–ventricular interactions may also be recruited and targeted for therapeutic benefit. For example, controlled pulmonary artery banding in dilated cardiomyopathy and aortic banding in pulmonary hypertension may augment the function of the failing left and right ventricle respectively. Even in single ventricle physiology, the hypoplastic ventricle can affect the function of the dominant ventricle. In this chapter we review the physiology, pathophysiology and therapeutic benefit of ventricular–ventricular interactions.

Keywords

Ventricular–ventricular interactions • Pulmonary hypertension • Systole Diastole

Introduction

Considerable emphasis has been placed on differentiating between the embryological origins, characteristics, physiology and function of the left (LV) and right (RV) ventricles. However, far less emphasis has been placed on the intimate relations between the two sides of the heart. Yet, these reciprocal relations form an innate and fundamental

M.K. Friedberg
Paediatric Cardiology, Labatt Family Heart Center
Hospital for Sick Children, Toronto, Ontario, Canada
e-mail: mark.friedberg@sickkids.ca

M.K. Friedberg, A.N. Redington (eds.), *Right Ventricular Physiology, Adaptation and Failure in Congenital and Acquired Heart Disease*, https://doi.org/10.1007/978-3-319-67096-6_6

basis for cardiac function in both physiology and disease. Ventricular–ventricular interactions (VVI) refer to the cumulative effect of changes in filling, function, geometry and synchrony of one ventricle on the filling, function, geometry and synchrony of the contra-lateral ventricle. In this chapter we will review the physiology of VVI and provide examples of how they affect cardiac function in specific conditions; and how they may possibly be utilized for therapeutic benefit.

The Physiological Basis of Ventricular–Ventricular Interactions

The RV and LV are intimately attached through a common septum, a common pericardial space and shared myocardial fibers encircling the ventricles [1]. Santamore's laboratory made pivotal discoveries regarding the effects of LV volume loading and dysfunction on RV developed pressure. A decrease in LV volume below its optimal volume caused a 6% decrease in RV developed pressure. LV free wall ischaemia/infarction from coronary artery ligation resulted in an additional 9% decrease in RV developed pressure. In the absence of any LV free wall force development (caused by LV free wall incision), there was a dramatic 45% additional decrease in RV developed pressure [2]. Thus, it appears that a substantial portion of RV mechanical work under normal circumstances is generated by LV contraction and that the LV free wall plays a major role in RV function [2]. In fact, Hoffman demonstrated that even when the RV myocardium is entirely replaced with a non-contractile prosthesis, normal LV shortening lead to virtually normal RV pressure generation [3]. However, these experiments also demonstrated that VVI operate not only from left to right, but also from right to left; and that intact RV geometry is necessary for normal LV function. Progressive enlargement of the non-contractile RV, lead to a progressive reduction in both RV and LV mechanical work [3]. Thus, progressive RV dilatation lead to reduced LV pressure development and stroke work [3].

From Santamore's classic experiments, not only was intact LV free wall function an important contributor to RV function, but at the same time, changes in RV developed pressure were related to septal position, particularly septal bulging into the RV cavity during systole, suggesting an important role for the septum in mediating ventricular–ventricular interactions [3]. While these findings may suggest that changes in RV volume are the cause of decreased RV developed pressure, Shertz showed that even when RV volume is held constant, LV isovolumetric contraction results in simultaneous increases in RV stroke volume and RV developed pressure [4]. Therefore, it seems that additional mechanisms are at play, beyond RV volume and septal shift alone.

These additional mechanisms were also vividly delineated by Santamore's group. In an experimental model of intact but explanted hearts, the investigators disrupted electrical but not mechanical continuity between the RV and LV (Table 6.1) [5]. Thus electrical stimulation of the LV would only lead to LV contraction, and

Table 6.1 Mechanisms of ventricular–ventricular interactions

Mechanism	Pathophysiology	Example
Septal position	Septal displacement reduces contralateral ventricular volume and geometry	LV compression in PAH
Pericardial constraint	Enhances septal displacement mechanism by limiting available space	Tamponade physiology
Shared myofibers	Fibers in the superficial layer traverse both ventricles	Presumed mechanism whereby pulmonary artery band enhances LV function in DCM
Coronary circulation	In some conditions, LV function is dependent on coronary flow originating from the RV cavity through 'sinusoids'	Pulmonary atresia/intact ventricular septum

electrical stimulation of the RV would only lead to LV contraction. This allowed study of the effects of the contraction of one ventricle on developed pressure and flow in the contralateral ventricle. In these experiments, during RV pacing, there was minimal developed pressure in the LV. Conversely, during pacing of the electrically isolated LV, RV pressure development and pulmonary blood flow were almost normal [6]. These ex vivo experimental observations have been elegantly shown in the human heart in vivo during pre-excitation of one ventricle by pacing or during extra-systolic beats [6]. Under normal circumstances, LV and RV electrical activation occur almost simultaneously (with a very short delay) and when measuring developed pressure over time (dP/dT) in either ventricle, only one pressure spike is observed. This makes it difficult to tease out the separate contributions of the contraction of one ventricle to developed pressure in the contralateral ventricle. However, when the LV is activated separately from the RV, by an extra-systolic beat or by left bundle branch block, two distinct pressure spikes can be observed in the RV, one that arises from RV contraction and the other that arises from LV contraction [6].

Up to now, we have emphasized the impact of LV function on the RV. However, the RV also influences LV function. These RV to LV interactions have been shown both during increased RV volume loading, as well as during increased RV pressure loading. We already discussed Hoffman's experiments where a progressively enlarging (even though non-contractile) RV, adversely impacted LV developed pressure [3]. Indeed, during changes in RV volume loading, there can be substantial changes in LV function and even LV contractility, as manifested by a shift in the end systolic pressure-volume relation [7]. How important these effects are in the clinical setting requires further study. In experimental models of acute RV ischemia, which leads to acute RV dysfunction and dilatation; LV dysfunction and reduced contractility is observed [8]. This dysfunction can be reversed by volume-unloading the RV using a superior vena cava to pulmonary artery shunt with disconnection of the PA from the RV. However, the question arises: How does volume unloading the dysfunctional RV, lead to improvement in load-*independent* parameters of LV contractility?

Changes in LV volumes alone following RV dysfunction and acute dilatation may not adequately account for all these effects. During acute right coronary ischemia and RV dilation, there was a decrease in LV size mediated primarily by a leftward septal shift secondary to RV dilatation [9]. However, this was accompanied by reduced LV contractility measured by load-independent indices, which are not influenced by ventricular volumes [9]. Moreover, when pericardial constraint was relieved by opening the pericardium, there was no significant change in LV volume or RV dilation, but an observed improvement of load-independent measures of LV myocardial contractility.

One explanation for these findings is that decreasing RV volume, improving RV dilation or reversing leftward septal shift all improve or restore LV geometry thereby allowing improved myocardial mechanics and contractility [8]. Nonetheless, while septal shift and a non-compliant pericardium are central mediators of right to left ventricular interactions, the load independent nature of LV measures in the experiments described above suggests that changes in LV geometry do not sufficiently account for its improved contractility [10].

An additional explanation for the observed phenomena is through the muscle fibers themselves. It has been well established that there are common muscle tracts that transverse the LV and RV in the superficial and mid layers [11, 12]. An increase in LV contractility for example, may therefore lead to an increase in RV contractility, presumably through the Anrep effect. This concept was demonstrated by Belinkie et al. who demonstrated that acute aortic constriction leads to improvement in the performance and stroke volume of the failing RV, independent of changes in right coronary artery flow [13]. The authors attributed the ventricular–ventricular interactions, at least in part, to a rightward septal shift and change in the inter-ventricular pressure gradient brought about by aortic constriction [13]. We have recently expanded on these concepts as a

possible therapeutic target in increased RV afterload and pulmonary arterial hypertension. However, before detailing these findings, let us first expand on the adverse ventricular–ventricular interactions in pulmonary hypertension and increased RV afterload.

Right to Left Ventricular–Ventricular Interactions in Increased RV Afterload

In patients with PAH, reduced LV filling is secondary to at least two important phenomena. Firstly, due to reduced RV stroke volume and output, LV preload is reduced. This has been demonstrated by Gurudevan et al. [14] before and after pulmonary embolectomy in patients with chronic thromboembolic pulmonary arterial hypertension. In those patients, pulmonary vein and mitral Doppler inflow patterns clearly improved after relief of the pulmonary obstruction. Concomitantly, RV hypertension and dilatation causes leftward displacement of the interventricular septum, which directly reduces LV filling [10, 15–19]. Following this, Gan et al. using MRI, demonstrated that LV end-diastolic volume, more than RV end-diastolic volume is linearly correlated to cardiac output [15]. These RV–LV interactions can be simply assessed using the LV eccentricity index [20, 21]. This is a simple echo index, measured from 2-D imaging which relates the lateral to anterior-posterior dimensions of the LV in the short-axis, thereby reflecting the degree of anterior-posterior LV compression by the distended RV. The importance of this interaction is supported by the finding that the LV eccentricity index is related to survival in PAH [20]. We have recently shown that in children with iPAH, that the LV eccentricity index is associated with death or need for lung transplantation [22]. Thus it seems that in increased RV afterload, the hypertensive RV affects LV geometry and function both in an in-series effect (reduced RV output leading to decreased LV preload); as well as a parallel effect arising from leftward septal shift.

These same ventricular–ventricular interactions were beautifully demonstrated using strain imaging by MRI in patients with tetralogy of Fallot who had outflow tract obstruction [23]. These investigators showed how prolonged leftward shift of the septum secondary to increased RV afterload leads to reduced LV filling when the septum bulges leftward in early LV diastole. Relief of the RV outflow obstruction reversed these findings, with normalization of septal curvature, shortening of RV contraction and improved LV filling [23]. Importantly, improved LV filling was directly related to an improvement in exercise capacity, demonstrating the clinical relevance of these findings [23].

However, the right to left adverse ventricular–ventricular interactions observed in increased RV afterload extend beyond altered geometry alone, and substantially affect myocardial health and performance. Visner demonstrated in dogs that impaired LV systolic function during acute RV hypertension induced by pulmonary artery constriction was accounted for by rearrangements in LV dynamic geometry that primarily resulted from the anatomic contiguity of the two ventricles at the septal insertion points [19]. Septal shift is predominantly determined by the transeptal pressure gradient. Therefore, in the hypertensive RV, not only is septal function impaired, but the configuration of the displaced septum into the LV may increase local wall shear stress and regional injury [17]. Indeed, the RV septal insertion regions may be particularly prone to increased stress and subsequent fibrosis as they are exposed to high shear forces from LV circumferential and RV longitudinal shortening [17, 24, 25]. Recently, MRI delayed gadolinium enhancement, thought to represent fibrosis, at the RV septal insertion points has been found almost universally in adult patients with PAH and correlates with the degree of RV afterload [24, 26, 27]. Fibrosis at the RV septal insertions was associated with reduced RV longitudinal contraction [27] and the extent RV fibrosis in PAH has been inversely related to RV ejection fraction, stroke volume and end-systolic volume; and also with increased mortality [24].

However, from the findings discussed above, and from our own work, it is apparent that it is not only the geometrical consequences of leftward septal shift that induces adverse ventricular interactions, but also the timing of these events.

Temporal Aspects of Adverse Ventricular–Ventricular Interactions in Increased RV Afterload

Not only is the interventricular septum shifted leftward towards the LV, reducing its filling and volume; but this leftward shift is prolonged due to the prolonged RV contraction time observed in PAH and increased RV afterload (Fig. 6.1). Although pulmonary ejection time is short in PAH [28], the duration of RV contraction is prolonged (Fig. 6.1) [29]. At the same time, RV diastole and filling time are shortened (Fig. 6.1) [28]. The prolonged RV systole, extends into the time period where the LV has already started its diastole, thereby compromising LV filling (Fig. 6.1) [7, 14, 15]. This adverse relation is worsened by increasing heart rate as diastole disproportionately shortens more than systole with increasing heart rate. Thus children with PAH have a marked decrease in diastolic duration and increase in the systolic duration when their heart rate increases as compared with controls [29]. The ratio between systolic and diastolic duration measured from tricuspid regurgitation Doppler, reflects the overall prolonged systolic duration and decreased LV filling (Fig. 6.1). We have shown the S:D ratio is temporally related to death or need for lung transplantation in the pediatric PAH population with the highest risk occurring when the S/D ratio was >1.40 [29].

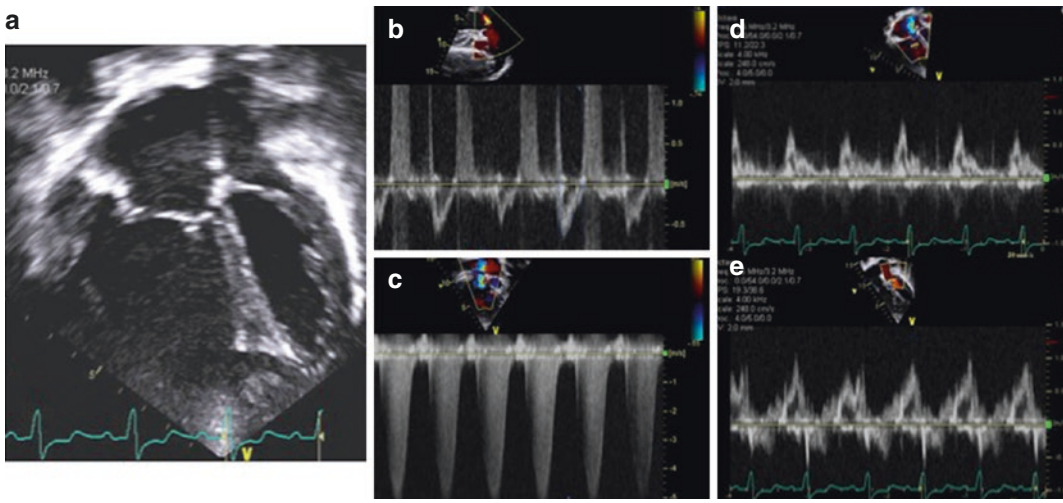

Fig. 6.1 Child with severe idiopathic pulmonary hypertension. Panel (**a**) depicts an apical 4-chamber view showing a markedly dilated right ventricle which compresses the left ventricle in systole and diastole. Panel (**b**) depicts Doppler in the pulmonary artery. Right ventricular ejection is short in duration and reducing volume due to severely increased pulmonary vascular resistance (Panel **b**). However, right ventricular contraction and systole, is actually prolonged as seen by the duration of tricuspid regurgitation (Panel **c**). Thus, Doppler of the tricuspid regurgitation jet is useful not only to measure right ventricular systolic pressure, but also the duration of systole (duration of the tricuspid regurgitation) and diastole (the duration of the interval between tricuspid regurgitation jets). The prolonged right ventricular systole shifts the septum leftward in left ventricular systole and diastole, thereby reflecting ventricular interactions whereby the displaced septum impedes left ventricular filling. Thus, not only is right ventricular diastolic filling compromised (Panel **d**) as seen by monophasic, late diastolic filling of short duration; but left ventricular diastolic filling is compromised as well with abnormal early (**e**) and late (**a**) filling relations occurring late (Panel **e**). Left ventricular diastolic filling is thus compromised by reduced right ventricular output (Panel **a**) and by prolonged right ventricular systole which shifts the septum leftward in left ventricular diastole (Panel **c**)

Thus, prolonged septal shift, reduced LV filling and a prolonged RV systolic to diastolic duration ratio are linked to clinical outcomes [29, 30]. The link between temporal and geometric events is further supported by the inverse relationship between heart rate and LV end-diastolic volume.

Adverse Right to Left Ventricular–Ventricular Interactions in Repaired Tetralogy of Fallot

Interventricular dyssynchrony contributes to prolonged RV contraction in PAH and is also important in other congenital heart disease such as tetralogy of Fallot (TOF) [31], where the delay between left and right isovolumic contraction time, is related to risk of ventricular arrhythmias and also to the patient's exercise capacity [32].

However, interventricular contraction delays are not the only adverse ventricular–ventricular interaction found in tetralogy of Fallot. Several studies have found linear relations between RV and LV systolic indices whether measured by ejection fraction, annular displacement or myocardial strain [33, 34]. Indeed, while TOF is most commonly considered a disorder predominantly affecting RV function, our group and others have shown that not only RV, but also LV myocardial strain is reduced in this population [35, 36]. Investigators from the Toronto General Hospital were among the first to demonstrate reduced LV myocardial strain in adults with more advanced and long-standing RV remodeling and dysfunction, while our group has demonstrated that reduced LV strain, as well as abnormal LV rotation mechanics, are already impaired in children, much earlier in the clinical course after surgical repair of TOF [35, 36]. Impaired LV dysfunction was related to the degree of RV enlargement and dysfunction, suggesting adverse ventricular–ventricular interactions [36, 37]. This is at least in part related to the presence of pulmonary regurgitation as pulmonary valve replacement leads not only to improved RV size and function but also to improved LV function [38, 39].

Findings of impaired LV dysfunction, whether at the myocardial or ventricular level is important as LV dysfunction has been found not only to be prevalent in the TOF population, but to be an important risk factor for functional impairment and even mortality [40]. We also found that not only RV but also LV incoordinate motion is worsened during exercise in children after TOF repair, suggesting that worsening of adverse interactions may be provoked by exercise [41].

While in the current discussion we have concentrated mainly on LV dysfunction in conditions predominantly affecting the RV, RV dysfunction is also apparent in diseases affecting predominantly the LV. PAH secondary to LV dysfunction or left sided obstructive lesions is an obvious example [42]. In LV DCM, concomitant RV dysfunction is a well-recognized risk factor for worse mortality [43]. We have also investigated more subtle examples of adverse left to right ventricular–ventricular interactions. For example, in aortic stenosis, we found reduced RV myocardial strain in a sub-set of patients [44]. In those patients with reduced RV myocardial function during aortic stenosis, RV strain improved after aortic valvuloplasty.

However, relief of valvar stenosis does not automatically lead to improvements in contralateral ventricular function. Li et al. found that following pulmonary valve balloon valvuloplasty for pulmonary stenosis, patients demonstrated persistent LV abnormalities including reduced myocardial strain and increased mechanical dyssynchrony at a mean interval of 18 ± 6 years after the procedure [45]. However, these LV abnormalities, were likely related to persistent RV abnormalities as these patients had larger RV volumes which correlated with the degree of decreased LV circumferential strain and increased dyssynchrony.

Additionally, there are situations where relief of RV afterload may lead to LV dysfunction. One classic example is in pulmonary atresia with intact ventricular septum where in a subset of patients LV myocardial coronary blood supply is dependent on the presence of coronary sinusoids. When LV coronary supply is compromised (e.g when the left coronary system is stenosed), LV coronary supply is dependent on collateral flow originating from the high-pressured, small, RV

cavity, through the sinusoids. In this situation decompressing the RV by opening the atretic RV outflow tract can lead to serious LV ischaemia and compromise. The presence of these sinusoids, even without RV dependence, may be associated with long-term risk for LV regional wall motion abnormalities, dysfunction and possibly increased risk for death [46]. This complex subject is well beyond the scope of this chapter, but demonstrates that coronary abnormalities and even differential RV to LV filling pressures, which affect coronary resistance and flow, can affect ventricular–ventricular interactions [47].

Using Ventricular–Ventricular Interactions for Therapeutic Benefit

Up to now, we have described several examples of adverse ventricular–ventricular interactions. Although shared myofibers and septal position play a role in mediating adverse ventricular–ventricular interactions they also constitute a target for therapeutic intervention. We have developed a rabbit model of sustained increased RV afterload using adjustable pulmonary artery banding. This model allows study of isolated increased RV afterload on the LV, without potential confounding effects of systemic pharmacological agents or hypoxia often used in animal models of PAH. We found that both acute and chronic isolated RV afterload induced by pulmonary artery banding leads to biventricular dysfunction [48–50]. The functional compromise was accompanied in both ventricles by adverse remodeling as manifested by biventricular myocyte hypertrophy, reduced contractility and increased fibrosis [48, 49]. While RV myocyte hypertrophy is an expected finding secondary to isolated RV afterload, similar developments in the otherwise healthy LV is intriguing. Using a similar juvenile rabbit model of pulmonary artery banding, Kitahori found septal apoptosis, fibrosis, and reduced capillary density after 6 to 8 weeks of PAB which extended to the LV free-wall [51]. Interestingly, these animal data are different to findings in human subjects with increased RV afterload secondary to pulmonary hypertension where LV atrophy was present [52]. Whether this is explained by increased apoptosis or other mechanisms requires further investigation.

We further demonstrated in our rabbit pulmonary artery band model, that during isolated acute RV failure, a small increase in LV afterload by systemic epinephrine or norepinephrine or by the addition of mild aortic banding lead to an increase in load-independent indices of LV and RV contractility [48, 49]. In both the RV and LV, collagen deposition following pulmonary artery banding was associated with activation of the fibrosis cascade including TGFβ1, CTGF and endothelin (ET)-1; as well as with upregulation of matrix metalloproteinases which mark increased extra-cellular matrix degeneration. Conversely, the observed improvement in LV and RV contractility induced by addition of mild LV afterload was also beneficial during chronic RV afterload, and was associated with amelioration of biventricular myocyte hypertrophy and fibrosis as well as downregulation of fibrosis signaling [48, 49].

The improvement seen in RV and LV function with addition of a mild aortic band in our rabbit model may stem from amelioration of septal shift induced by the aortic band, improvement in ventricular geometry and also by inducing increased LV contractility through a modest increase in LV afterload. This in turn may lead to increased RV contractility through shared myofibers traversing both ventricles.

In clinical practice, increasing the subpulmonary ventricle's afterload to improve cardiac function is used in patients who have congenitally corrected transposition of the great arteries and tricuspid regurgitation. In ccTGA, the RV is the systemic ventricle and the systemically positioned tricuspid valve is often anatomically abnormal and regurgitant [53]. In this situation, the dilated systemic RV bulges towards the LV, with the septum pulling the tricuspid attachments leftward contributing to tricuspid valve non-coaptation and regurgitation. RV annular dilatation and these geometric abnormalities feed a worsening cycle of tricuspid regurgitation and RV dilation. By placement of a controlled pulmonary band to increase LV afterload (and LV pressures)

on the one hand, while avoiding LV failure on the other, the septum shifts towards the LV and assumes a more neutral position thereby changing TV annular configuration and reducing TR. It is also interesting to postulate whether pulmonary artery banding in this situation increases LV contractility, thereby leading to an increase in systemic RV contractility through shared myocardial fibers; as we hypothesized for the addition of aortic banding in our aforementioned rabbit model.

While we demonstrated, at least in animal models, that increasing LV afterload can be used to enhance RV performance, one may ask whether the RV can be utilized to support the failing LV. One of the most interesting initiatives addressing this idea was promoted by the Giessen group who investigated pulmonary artery banding in children with end stage LV dilated cardiomyopathy [54, 55]. Pulmonary artery banding was applied in 17 infants with dilated cardiomyopathy as compassionate care and was tolerated well. All of these 17 infants could be removed from transplant listing following marked improvements in LV size, function and clinical status [55]. In 12 infants, the pulmonary artery banding was subsequently released by trans-catheter technique with ten continuing to do well. This suggests that either the DCM was reversible, or that therapy through ventricular–ventricular interactions brought about sustained LV reverse remodeling. These 'proof-of-principle' results certainly require validation in larger prospective controlled trials but suggest that utilization of ventricular–ventricular interactions through pulmonary artery banding in LV failure may provide a novel, safe and effective therapeutic alternative; in this high-risk population.

Do Ventricular–Ventricular Interactions Affect Ventricular Function in Single-Ventricle Physiology?

While it is intuitive to discuss ventricular–ventricular interactions when there are two functioning ventricles, ventricular cross-talk may be just as important to ventricular mechanics when there is only one functioning ventricle, as occurs when either the RV or LV is severely under-developed. Using magnetic resonance imaging, Fogel demonstrated in children with a functionally single ventricle that regional myocardial strain, twist, and radial motion are markedly different to that seen in biventricular hearts [56]. In hypoplastic left heart syndrome for example, the absence of a developed LV may alter TV annular configuration and worsen TR, an important risk factor for adverse outcomes in this high-risk population [57]. Using strain imaging, we recently found that asymmetry in septal to lateral contraction at the tricuspid annulus in HLHS is associated with more TR [58]. This asymmetry manifested both in the degree of developed strain at the septal and lateral basal segments, and in the time to peak strain [58]. Likewise, a larger interventricular septum, as a marker of the dysfunctional/hypoplastic LV size, may be a risk factor for death or transplant in this population [59]. This may be yet another manifestation of the effects of ventricular–ventricular interactions on RV function. However, not all authors have found an effect of the size of the hypoplastic LV on RV function or outcomes in HLHS [60]. Thus, wall motion abnormalities, arising at least in part from adverse VVI, may contribute to adverse tricuspid valve geometry and function [61] in addition to the tricuspid valve structural abnormalities that underlie TR in HLHS [62].

Summary

In summary, ventricular–ventricular interactions profoundly affect right and left ventricular function in both normal conditions and in various disease states (Table 6.2), especially those characterized by increased afterload or preload. A better understanding of the pathophysiology of ventricular–ventricular interactions can lead to new therapeutic interventions that target or harness these interactions.

Table 6.2 Examples of conditions where ventricular–ventricular interactions have been shown to be important

Condition	Comment
Right-to-left interactions	
Increased RV afterload	
Pulmonary hypertension	Leftward septal shift, decreased LV preload, LV myocardial injury
RV outflow tract obstruction	Pulmonary stenosis and conduit obstruction after repair of Tetralogy of Fallot
Right ventricular infarction	Acute experimental models of right coronary artery ligation ligation
Increased RV preload	
Repaired Tetralogy of Fallot	RV dilatation leads to LV dysfunction
Left-to-right interactions	
Hypoplastic left heart syndrome	LV geometry and septal dysfunction may affect RV function. LV sinusoids in some patients may affect RV function
Aortic stenosis	Some patients have decreased RV function which improves after aortic balloon valvuloplasty

References

1. Sanchez-Quintana D, Anderson RH, Ho SY. Ventricular myoarchitecture in tetralogy of Fallot. Heart. 1996;76(3):280–6.
2. Santamore WP, et al. Left ventricular effects on right ventricular developed pressure. J Appl Physiol. 1976;41(6):925–30.
3. Hoffman D, et al. Left-to-right ventricular interaction with a noncontracting right ventricle. J Thorac Cardiovasc Surg. 1994;107(6):1496–502.
4. Schertz C, Pinsky MR. Effect of the pericardium on systolic ventricular interdependence in the dog. J Crit Care. 1993;8(1):17–23.
5. Damiano RJ Jr, et al. Significant left ventricular contribution to right ventricular systolic function. Am J Phys. 1991;261(5 Pt 2):H1514–24.
6. Feneley MP, et al. Contribution of left ventricular contraction to the generation of right ventricular systolic pressure in the human heart. Circulation. 1985;71(3):473–80.
7. Taylor RR, et al. Dependence of ventricular distensibility on filling of the opposite ventricle. Am J Phys. 1967;213(3):711–8.
8. Danton MH, et al. Modified Glenn connection for acutely ischemic right ventricular failure reverses secondary left ventricular dysfunction. J Thorac Cardiovasc Surg. 2001;122(1):80–91.
9. Brookes C, et al. Acute right ventricular dilatation in response to ischemia significantly impairs left ventricular systolic performance. Circulation. 1999;100(7):761–7.
10. Moulopoulos SD, et al. Left ventricular performance during by-pass or distension of the right ventricle. Circ Res. 1965;17(6):484–91.
11. Sanchez-Quintana D, et al. Myoarchitecture and connective tissue in hearts with tricuspid atresia. Heart. 1999;81(2):182–91.
12. Smerup M, et al. The three-dimensional arrangement of the myocytes aggregated together within the mammalian ventricular myocardium. Anat Rec (Hoboken). 2009;292(1):1–11.
13. Belenkie I, et al. Effects of aortic constriction during experimental acute right ventricular pressure loading. Further insights into diastolic and systolic ventricular interaction. Circulation. 1995;92(3):546–54.
14. Gurudevan SV, et al. Abnormal left ventricular diastolic filling in chronic thromboembolic pulmonary hypertension: true diastolic dysfunction or left ventricular underfilling? J Am Coll Cardiol. 2007;49(12):1334–9.
15. Gan CT, et al. Impaired left ventricular filling due to right-to-left ventricular interaction in patients with pulmonary arterial hypertension. Am J Physiol Heart Circ Physiol. 2006;290(4):H1528–33.
16. Marcus JT, et al. Impaired left ventricular filling due to right ventricular pressure overload in primary pulmonary hypertension: noninvasive monitoring using MRI. Chest. 2001;119(6):1761–5.
17. Nelson GS, et al. Compression of interventricular septum during right ventricular pressure loading. Am J Physiol Heart Circ Physiol. 2001;280(6):H2639–48.
18. Roeleveld RJ, et al. Interventricular septal configuration at mr imaging and pulmonary arterial pressure in pulmonary hypertension. Radiology. 2005;234(3):710–7.
19. Visner MC, et al. Alterations in left ventricular three-dimensional dynamic geometry and systolic function during acute right ventricular hypertension in the conscious dog. Circulation. 1983;67(2):353–65.
20. Raymond RJ, et al. Echocardiographic predictors of adverse outcomes in primary pulmonary hypertension. J Am Coll Cardiol. 2002;39(7):1214–9.
21. Ryan T, et al. An echocardiographic index for separation of right ventricular volume and pressure overload. J Am Coll Cardiol. 1985;5(4):918–27.
22. Kassem E, Humpl T, Friedberg MK. Prognostic significance of 2-dimensional, M-mode, and Doppler echo indices of right ventricular function in children with pulmonary arterial hypertension. Am Heart J. 2013;165(6):1024–31.
23. Lurz P, et al. Improvement in left ventricular filling properties after relief of right ventricle to pulmonary artery conduit obstruction: contribution of septal motion and interventricular mechanical delay. Eur Heart J. 2009;30(18):2266–74.

24. McCann GP, et al. Extent of MRI delayed enhancement of myocardial mass is related to right ventricular dysfunction in pulmonary artery hypertension. AJR Am J Roentgenol. 2007;188(2):349–55.
25. Beyar R, et al. Ventricular interaction and septal deformation: a model compared with experimental data. Am J Phys. 1993;265(6 Pt 2):H2044–56.
26. Sanz J, et al. Prevalence and correlates of septal delayed contrast enhancement in patients with pulmonary hypertension. Am J Cardiol. 2007;100(4):731–5.
27. Shehata ML, et al. Myocardial delayed enhancement in pulmonary hypertension: pulmonary hemodynamics, right ventricular function, and remodeling. AJR Am J Roentgenol. 2011;196(1):87–94.
28. Duffels MG, et al. Duration of right ventricular contraction predicts the efficacy of bosentan treatment in patients with pulmonary hypertension. Eur J Echocardiogr. 2009;10(3):433–8.
29. Alkon J, et al. Usefulness of the right ventricular systolic to diastolic duration ratio to predict functional capacity and survival in children with pulmonary arterial hypertension. Am J Cardiol. 2010;106(3):430–6.
30. Mahmud E, et al. Correlation of left ventricular diastolic filling characteristics with right ventricular overload and pulmonary artery pressure in chronic thromboembolic pulmonary hypertension. J Am Coll Cardiol. 2002;40(2):318–24.
31. Marcus JT, et al. Interventricular mechanical asynchrony in pulmonary arterial hypertension: left-to-right delay in peak shortening is related to right ventricular overload and left ventricular underfilling. J Am Coll Cardiol. 2008;51(7):750–7.
32. D'Andrea A, et al. Right ventricular myocardial activation delay in adult patients with right bundle branch block late after repair of Tetralogy of Fallot. Eur J Echocardiogr. 2004;5(2):123–31.
33. Davlouros PA, et al. Right ventricular function in adults with repaired tetralogy of Fallot assessed with cardiovascular magnetic resonance imaging: detrimental role of right ventricular outflow aneurysms or akinesia and adverse right-to-left ventricular interaction. J Am Coll Cardiol. 2002;40(11):2044–52.
34. Kempny A, et al. Right ventricular-left ventricular interaction in adults with Tetralogy of Fallot: A combined cardiac magnetic resonance and echocardiographic speckle tracking study. Int J Cardiol. 2012;154(3):259–64.
35. Weidemann F, et al. Quantification of regional right and left ventricular function by ultrasonic strain rate and strain indexes after surgical repair of tetralogy of Fallot. Am J Cardiol. 2002;90(2):133–8.
36. Friedberg MK, et al. Impaired right and left ventricular diastolic myocardial mechanics and filling in asymptomatic children and adolescents after repair of tetralogy of Fallot. Eur Heart J Cardiovasc Imaging. 2012;13(11):905–13.
37. Dragulescu A, et al. Effect of chronic right ventricular volume overload on ventricular interaction in patients after tetralogy of fallot repair. J Am Soc Echocardiogr. 2014;27(8):896–902.
38. Frigiola A, et al. Biventricular response after pulmonary valve replacement for right ventricular outflow tract dysfunction: is age a predictor of outcome? Circulation. 2008;118(14 Suppl):S182–90.
39. Tobler D, et al. The left heart after pulmonary valve replacement in adults late after tetralogy of Fallot repair. Int J Cardiol. 2012;160(3):165–70.
40. Ghai A, et al. Left ventricular dysfunction is a risk factor for sudden cardiac death in adults late after repair of tetralogy of Fallot. J Am Coll Cardiol. 2002;40(9):1675–80.
41. Roche SL, et al. Exercise induces biventricular mechanical dyssynchrony in children with repaired tetralogy of Fallot. Heart. 2010;96(24):2010–5.
42. Thenappan T, Gomberg-Maitland M. Epidemiology of pulmonary hypertension and right ventricular failure in left heart failure. Curr Heart Fail Rep. 2014;11(4):428–35.
43. Gulati A, et al. The prevalence and prognostic significance of right ventricular systolic dysfunction in nonischemic dilated cardiomyopathy. Circulation. 2013;128(15):1623–33.
44. Friedberg MK, Wu S, Slorach C. Left-Right ventricular interactions in pediatric aortic stenosis: right ventricular myocardial strain before and after aortic valvuloplasty. J Am Soc Echocardiogr. 2013;26(4):390–7.
45. Li SJ, et al. Right and left ventricular mechanics and interaction late after balloon valvoplasty for pulmonary stenosis. Eur Heart J Cardiovasc Imaging. 2014;15(9):1020–8.
46. Akagi T, et al. Ventriculo-coronary arterial connections in pulmonary atresia with intact ventricular septum, and their influences on ventricular performance and clinical course. Am J Cardiol. 1993;72(7):586–90.
47. Gentles TL, et al. Right ventricular decompression and left ventricular function in pulmonary atresia with intact ventricular septum. The influence of less extensive coronary anomalies. Circulation. 1993;88(5 Pt 2):II183–8.
48. Apitz C, et al. Beneficial effects of vasopressors on right ventricular function in experimental acute right ventricular failure in a rabbit model. Thorac Cardiovasc Surg. 2012;60(1):17–23.
49. Apitz C, et al. Biventricular structural and functional responses to aortic constriction in a rabbit model of chronic right ventricular pressure overload. J Thorac Cardiovasc Surg. 2012;144(6):1494–501.
50. Friedberg MK, et al. Adverse biventricular remodeling in isolated right ventricular hypertension is mediated by increased transforming growth factor-beta1 signaling and is abrogated by angiotensin receptor blockade. Am J Respir Cell Mol Biol. 2013;49(6):1019–28.
51. Kitahori K, et al. Development of left ventricular diastolic dysfunction with preservation of ejection fraction during progression of infant right ventricular hypertrophy. Circ Heart Fail. 2009;2(6):599–607.

52. Manders E, et al. Contractile dysfunction of left ventricular cardiomyocytes in patients with pulmonary arterial hypertension. J Am Coll Cardiol. 2014;64(1):28–37.
53. Prieto LR, et al. Progressive tricuspid valve disease in patients with congenitally corrected transposition of the great arteries. Circulation. 1998;98(10):997–1005.
54. Schranz D, et al. Pulmonary artery banding for idiopathic dilative cardiomyopathy: a novel therapeutic strategy using an old surgical procedure. J Thorac Cardiovasc Surg. 2007;134(3):796–7.
55. Schranz D, et al. Pulmonary artery banding in infants and young children with left ventricular dilated cardiomyopathy: a novel therapeutic strategy before heart transplantation. J Heart Lung Transplant. 2013;32(5):475–81.
56. Fogel MA, et al. A study in ventricular-ventricular interaction. Single right ventricles compared with systemic right ventricles in a dual-chamber circulation. Circulation. 1995;92(2):219–30.
57. Takahashi K, et al. Real-time 3-dimensional echocardiography provides new insight into mechanisms of tricuspid valve regurgitation in patients with hypoplastic left heart syndrome. Circulation. 2009;120(12):1091–8.
58. Bharucha T, et al. Right ventricular mechanical dyssynchrony and asymmetric contraction in hypoplastic heart syndrome are associated with tricuspid regurgitation. J Am Soc Echocardiogr. 2013;26(10):1214–20.
59. Walsh MA, et al. Left ventricular morphology influences mortality after the Norwood operation. Heart. 2009;95(15):1238–44.
60. Wisler J, Khoury PR, Kimball TR. The effect of left ventricular size on right ventricular hemodynamics in pediatric survivors with hypoplastic left heart syndrome. J Am Soc Echocardiogr. 2008;21(5):464–9.
61. Kutty S, et al. Tricuspid regurgitation in hypoplastic left heart syndrome: mechanistic insights from 3-dimensional echocardiography and relationship with outcomes. Circ Cardiovasc Imaging. 2014;7(5):765–72.
62. Bharucha T, et al. Mechanisms of tricuspid valve regurgitation in hypoplastic left heart syndrome: a case-matched echocardiographic-surgical comparison study. Eur Heart J Cardiovasc Imaging. 2013;14(2):135–41.

7 Computational Study on the Cardiovascular System: Ventricular–Ventricular Interaction and Right Ventricular Failure in Pulmonary Arterial Hypertension

Tammo Delhaas, Theo Arts, Yvette Koeken, Joost Lumens, Georgina Palau-Caballero, and John Walmsley

Abstract

In this chapter, we describe how the CircAdapt model of the heart and circulation has been used to both increase our understanding of the pathophysiology of pulmonary arterial hypertension (PAH) and predict the effects of therapy. Simulation results reproduce key features of mechanical incoordination observed in PAH patients, including early diastolic septal motion and strain abnormalities. Our simulations suggest that septal movement is not dependent solely on the transseptal pressure gradient. Additionally, an imbalance of forces at the right ventricular (RV) attachment points resulting from ongoing RV free wall contraction during the early diastolic phase causes abnormal septal motion. We also demonstrate that atrial septostomy in patients with severe PAH might be beneficial because it increases left ventricular (LV) preload and, consequently, allows better maintenance of systemic arterial blood pressure during exercise. Finally, we show that pacing the RV free wall in severely decompensated PAH results in more synchronous LV and RV pressure decay, more homogeneous distribution of myofiber load over the ventricular walls, and a slight improvement of RV pump function.

T. Delhaas (✉) • T. Arts • Y. Koeken • J. Lumens
G. Palau-Caballero • J. Walmsley
Department of Biomedical Engineering
Cardiovascular Research Institute Maastricht
(CARIM), Maastricht University Medical Center,
Maastricht, The Netherlands
e-mail: tammo.delhaas@maastrichtuniversity.nl

M.K. Friedberg, A.N. Redington (eds.), *Right Ventricular Physiology, Adaptation and Failure in Congenital and Acquired Heart Disease*, https://doi.org/10.1007/978-3-319-67096-6_7

Keywords

PAH • Computer model • Ventricular interaction • Hemodynamics Myocardial deformation • Circadapt • Right ventricular failure • Pacing

Introduction

A wealth of new information about the cardiovascular system in pulmonary arterial hypertension (PAH) has become available due to the technological advances in imaging over the past decades. Considerable insights into right ventricular (RV) function as well as the pathophysiology of PAH have been gained from echocardiography and cardiac magnetic resonance imaging [1, 2]. However, the challenge to interpret these imaging results increases proportionally with the amount of available information, especially in diseases with low prevalence, such as PAH [3]. Mechanistic mathematical modeling based on physics and physiology is a promising alternative approach to the study of physiological and pathophysiological responses in patients. In this chapter, we describe how the CircAdapt model of the heart and circulation has increased our understanding of the pathophysiology of PAH, and how we can use the model to assess the effect of therapy.

The CircAdapt Model

The CircAdapt model was developed in an attempt to reduce the input information required for computational models, and to focus on clinically measurable output data [4–7]. CircAdapt allows rapid simulation of cardiac pump function and cardiovascular system dynamics for both research and educational purposes (www.circadapt.org). The model consists of a network composed of a limited number of module types, i.e., chambers, valves, tubes and resistances (Fig. 7.1a). The CircAdapt model generates tracings of hemodynamic and mechanical variables (such as cardiac and vascular pressures and volumes, flow through cardiac valves, and local tissue mechanics as a function of time over the entire cardiac cycle. When using the educational version, simulation of a single cardiac beat in real-time, can be displayed on a regular PC.

The heart in the CircAdapt model consists of five walls, i.e., the left and right atrial walls, the left and right ventricular wall, and the interventricular septum. Cavity pressures are calculated from cavity volumes as follows. Cavity volumes determine wall area. Wall areas determine strain of the myofibers in the wall. A model of myofiber mechanics is used to calculate myofiber stress from myofiber strain. Myofiber stress then determines wall tension in each cardiac wall. The mechanical equilibrium between the three ventricular walls is used to calculate their shape when encapsulating the two ventricular cavities (Fig. 7.1b) via the TriSeg module [5]. Transmural pressure is calculated for each wall from wall tension and curvature using Laplace' s law. Finally, cavity pressures are found by adding the transmural pressures to the intra-pericardial pressure surrounding the myocardial walls.

Non-linear elastic tube modules with characteristic impedance for pressure-flow waves represent large blood vessels (arteries and veins). Valves with inertia and Bernoulli pressure losses connect tubes and chambers. Effective orifice area of a cardiac valve depends on direction and magnitude of flow through the valve and on pressure drop over the valve. Non-linear resistances that connect the pulmonary and systemic arterial and venous tube modules represent the pulmonary and systemic vascular beds. Finally, a passive elastic sheet surrounding the entire heart (ventricles and atria) is included to represent the pericardium.

An important and unique feature of the CircAdapt model is that it reduces the number of independent parameters through implementation of structural adaptation of cardiac and vascular walls to mechanical load of the tissue. Size and mass of cardiac walls and large blood vessels

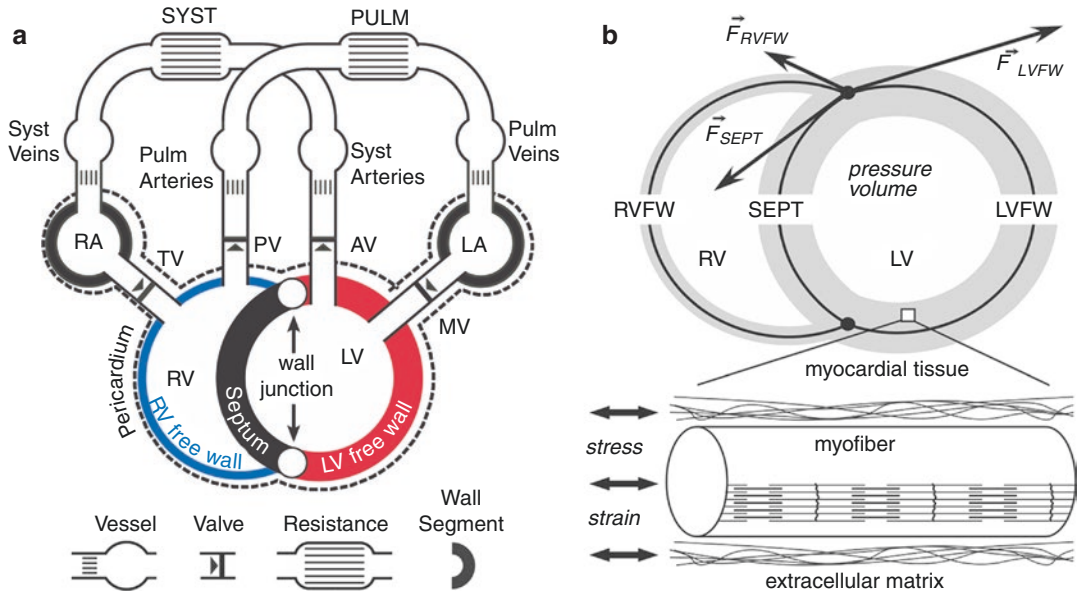

Fig. 7.1 (**a**) The CircAdapt model. (**b**) The TriSeg module of ventricular mechanics. *AV* aortic valve, *F* force, *LA* left atrium, *LV* left ventricle, *LVFW* left ventricular free wall, *MV* mitral valve, *Pulm* pulmonary, *PV* pulmonary valve, *RA* right atrium, *RV* right ventricle, *RVFW* right ventricular free wall, *SEPT* interventricular septum, *Syst* systemic, *TV* tricuspid valve

adapt to normalize local mechanical tissue load to tissue-specific physiological levels [4, 6].

Suitability of the CircAdapt Model for Realistic Modeling of Pulmonary Arterial Hypertension

The multiscale nature of the CircAdapt model allows us to relate global pump mechanics of the cardiac chambers to both systemic hemodynamics and local mechanics of the myocardium. CircAdapt integrates basic physical and physiological principles such as conservation of energy. In the current context, this means that the total amount of contractile work generated by the myofibers should equal the total amount of hydraulic pump work as delivered by the ventricles. Importantly, the model also incorporates ventricular interaction through mutual mechanical and hemodynamic dependence of the LV and the RV. Hemodynamic interaction follows due to the series coupling within the pulmonary and the systemic circulations [8]. CircAdapt also predicts mechanical interaction via the interventricular septum in which a change of shape, size or pressure-volume relation of one ventricle affects the shape, size and pressure-volume relation of the other ventricle through the septum [9]. The modular nature of the CircAdapt model allows us the versatility to introduce additional valves to represent (for example) an atrial septal defect. Finally, the relatively stiff pericardial sac surrounding the heart limits acute cardiac distension and, thereby, modulates mechanical ventricular interaction [10].

Simulation of Normal Cardiovascular Mechanics and Hemodynamics

Normal left and right heart dynamics were simulated during rest and exercise (Fig. 7.2). The methods used to obtain these simulations have been published in detail elsewhere [5]. Major input parameter values were: mean systemic arterial blood pressure of 92 mmHg (rest and exercise), cardiac output 5.1 l/min (rest) and 15.3 l/min (exercise), and heart rate 70 beats/min (rest)

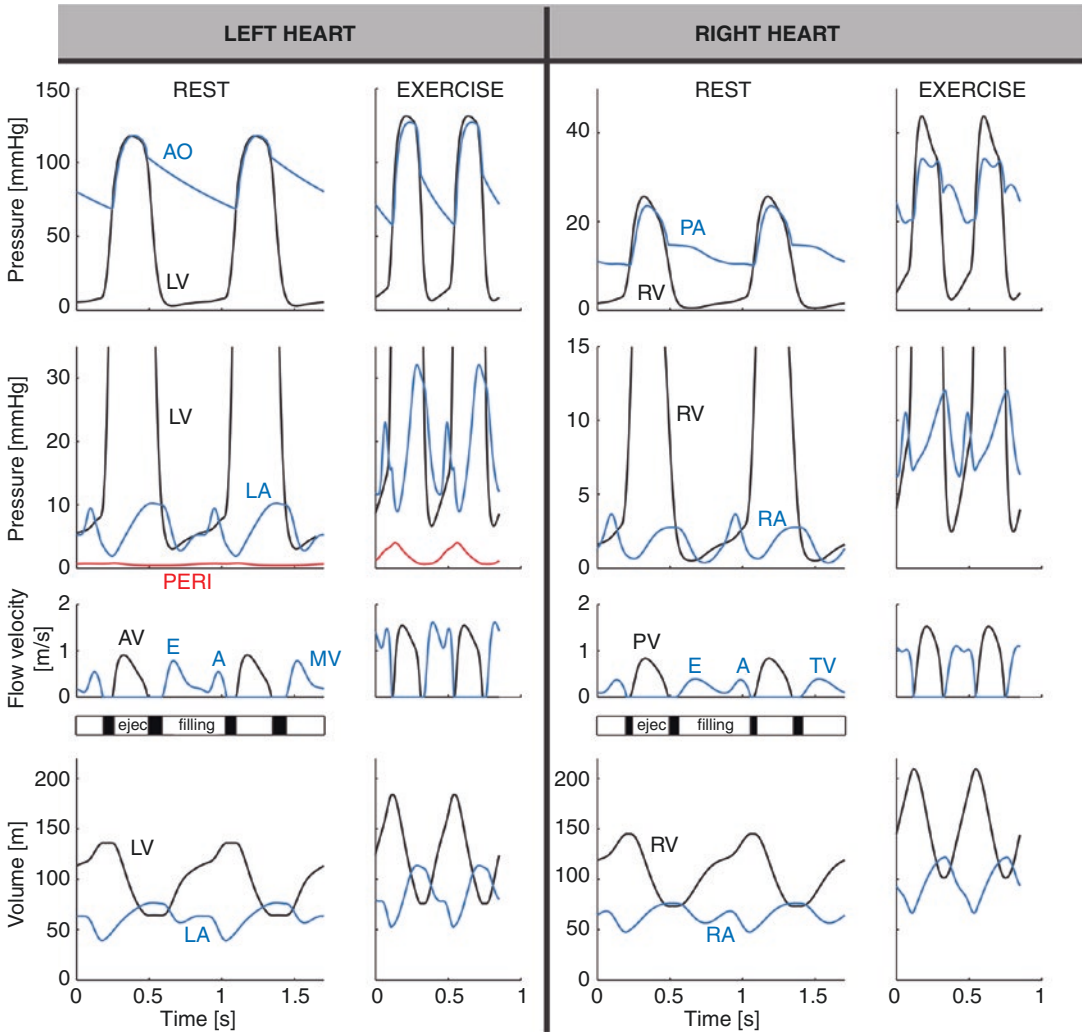

Fig. 7.2 CircAdapt simulation of normal left and right heart dynamics at rest and during exercise. *A* atrial contraction-induced late filling wave, *AV* aortic valve, *E* early mitral filling wave, *ejec* ejection, *LA* left atrium, *LV* left ventricle, *MV* mitral valve, *PERI* pericardial, *PV* pulmonary valve, *RA* right atrium, *RV* right ventricle, *TV* tricuspid valve

and 140 beats/min (exercise). Simulated time courses for pressure and volume were physiologic, both at rest and during exercise: time courses of mitral and tricuspid valve flows showed an early passive filling wave (E) followed by a clearly separated late filling wave (A) that resulted from atrial contraction; atrial contraction induced a rise in LV and RV cavity pressures and volumes towards the end of diastole; inertia effects can be appreciated from the negative pressure gradients across the AV-valves towards the ends of both the E- and A-waves as well from the negative pressure gradient across the aortic and pulmonary valve towards end of the ejection phase; LV and RV end-diastolic volumes were not significantly different; opening of the pulmonary valve occurred earlier than the opening of the aortic valve, whereas its closure was later. The model appropriately simulated the effects of acute alterations in loading conditions that reflected the changes seen during exercise (Fig. 7.2, right panels).

Developmental Stages of PAH

Development of PAH is characterized by progressive remodeling and vasoconstriction of the pulmonary vasculature leading to a gradual increase of pulmonary vascular resistance. RV pressure increases to maintain cardiac output and may finally approach or even exceed LV pressure. During the early stages of the disease, RV free wall mass increases (hypertrophy) to compensate for the increase in RV afterload and to decrease wall stress to within normal physiological ranges [11, 12]. As the disease progresses, RV free wall tissue can no longer adequately adapt to the increased load and, as a result, cardiac myocytes (and presumably also sarcomeres) become over-stretched [13], RV end-diastolic volume increases [14] and RV pump function deteriorates [15]. These morphological and functional changes will ultimately result in decompensated right heart failure, characterized by an increase in RV filling pressures, development of RV diastolic dysfunction, RV dilatation, and decreased cardiac output [16].

CircAdapt Simulation Protocol for PAH

We took the different disease stages of PAH into account in the simulation protocol for the CircAdapt model. Starting from our baseline (NORMAL) simulation at rest, a first simulation of mild compensated PAH (PAH-Comp) was obtained by increasing pulmonary vascular resistance (PVR) while allowing the heart and large blood vessels to structurally adapt to normalize mechanical tissue load. This adaptation process resulted in an increase of the mean pulmonary artery pressure (mPAP) from 18 mmHg, in the NORMAL simulation, to 32 mmHg in the PAH-Comp simulation while RV free wall (RVFW) mass increased by 40% to normalize cardiac stresses and strains to tissue-specific physiological levels [4]. States of moderately and severely decompensated PAH (PAH-DecompMod and PAH-DecompSev, respectively) were achieved by increasing PVR so that mPAP was equal to 55 and 79 mmHg, respectively, while further adaptation of cardiac and vascular walls to mechanical load was prevented.

Ventricular Hemodynamics and Mechanics in Simulated PAH

In the PAH-Comp simulation, the increase of PVR influenced neither the RV end diastolic volume (140 ml) nor the RV ejection fraction (52%). PAH-Decomp simulations showed increases of RV end-diastolic volume towards 169 and 217 ml for the moderately and severely decompensated PAH simulations, respectively. RV systolic pump function deteriorated as is evident from the decrease of RV ejection fraction to 43 and 33% for the moderate and severely decompensated PAH simulation, respectively.

Figure 7.3 shows changes in time courses of simulated ventricular pressures and circumferential strains from normal conditions to PAH-DecompSev. While RV pressures increased during the PAH simulations (Fig. 7.3: top panel row), it only exceeded LV pressure in the PAH-DecompSev simulation during diastole and late systole. When RV pressures were normalized to peak LV pressure (Fig. 7.3: middle panel row), it can be observed that PAH hardly affected the timing of LV pressure rise and decay; however, RV pressure decay was delayed proportionally to PAH severity. The LV-to-RV time difference in pressure decay changed from +28 ms in the NORMAL simulation to −40 ms in PAH-DecompSev. This delay in RV pressure decay was associated with delayed RV isovolumic relaxation as can be appreciated from the time courses of circumferential strains (Fig. 7.3, bottom panel row). Whereas in the NORMAL and PAH-Comp simulations the strain patterns were relatively synchronous and uniform in the three ventricular walls (Fig. 7.3: bottom panel row), in the simulations of decompensated PAH circumferential strain patterns changed. During isovolumic contraction, the initial shortening of the LVFW and SEPT caused a stretch of the RVFW. This stretch resulted in a delay in the onset of RVFW shortening compared with that of the

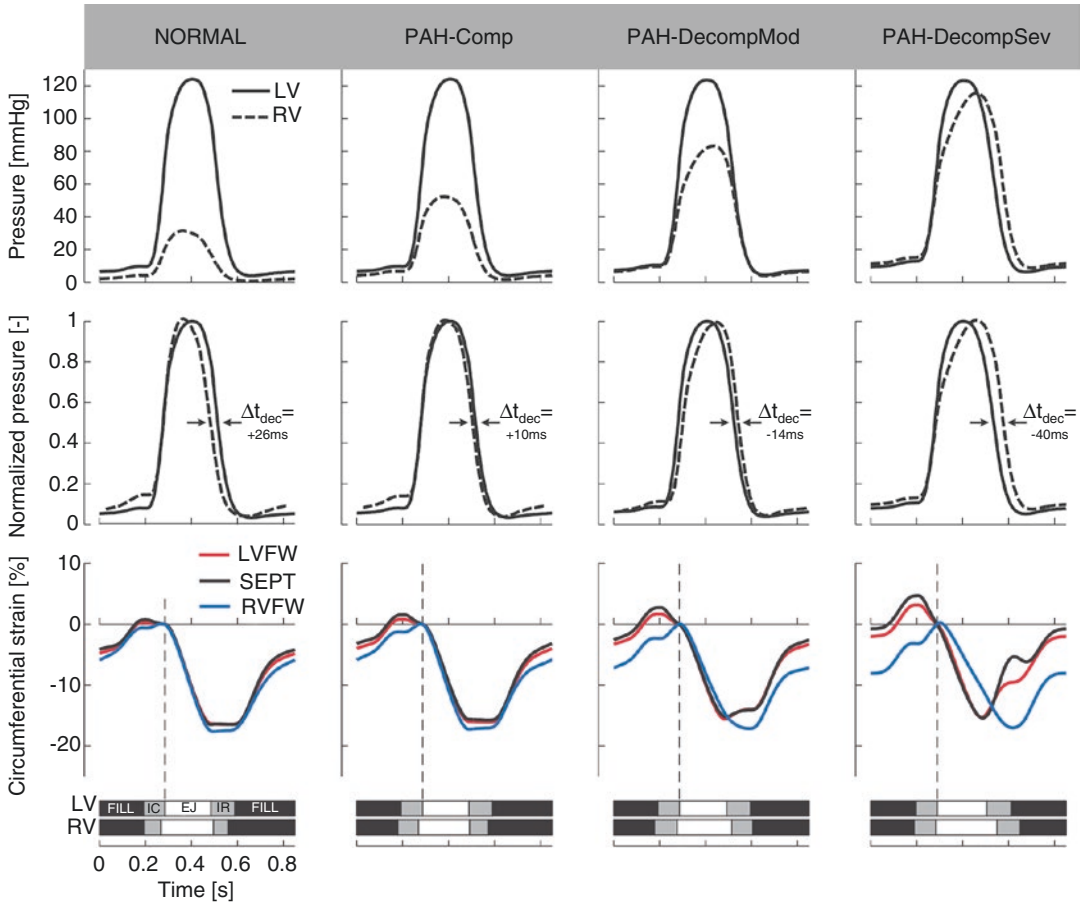

Fig. 7.3 Time courses of simulated ventricular pressures and circumferential strains under normal and PAH conditions. *EJ* ejection phase, *Fill* filling phase, *IC* isovolumic contraction phase, *IR* isovolumic relaxation phase, *LV* left ventricle, *LVFW* left ventricular free wall, *NORMAL* normal ventricular loading conditions at rest, *PAH-Comp* PAH loading conditions with compensation, *PAH-DecompMod* moderately decompensated PAH condition, *PAH-DecompSev* severely decompensated PAH condition, *RV* right ventricle, *RVFW* right ventricular free wall, *SEPT* interventricular septum, Δt_{dec} LV-to-RV time delay in pressure decay. Adapted from [32]

LVFW and SEPT as well as in an on-going RVFW shortening into the isovolumic relaxation phase with peak RVFW shortening occurring at the moment of mitral valve opening. Closure of the pulmonary valve was delayed concomitantly with PAH severity (Fig. 7.3, bars at bottom).

Septal Movement in Simulated PAH

It is well established that septal position is related to transseptal pressure gradient [17]. Our model realistically reproduces the abnormal position and motion pattern of the interventricular septum, which is one of the most characteristic phenomena seen in PAH patients [18]. Figure 7.4 shows tracings of septal curvature throughout the cardiac cycle. In the NORMAL simulation, septal wall curvature is always positive, indicating that the septum always bulges towards the RV. With increasing severity of PAH, hence with decreasing transseptal pressure gradient, septal wall curvature decreases, indicating flattening of the septal wall. In the moderately decompensated PAH simulation, the septal wall apparently decreases its curvature towards the end of the ejection phase and even

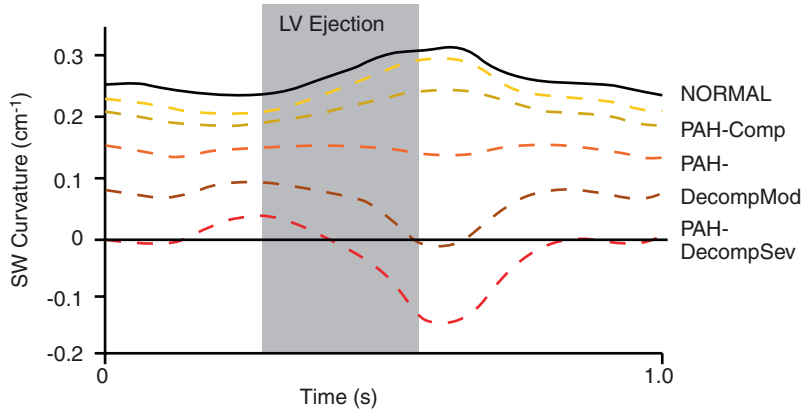

Fig. 7.4 Time courses of septal wall curvature under normal and PAH conditions. *LV* left ventricular, *SW* septal wall, *NORMAL* normal ventricular loading conditions at rest, *PAH-Comp* PAH loading conditions with compensation, *PAH-DecompMod* moderately decompensated PAH condition, *PAH-DecompSev* severely decompensated PAH condition

bulges just towards the LV in early diastole. The septal wall flattening occurs despite the fact that in the PAH-DecompMod simulation LV pressure exceeded RV pressure throughout almost the entire cardiac cycle (see Fig. 7.3), indicating that transseptal pressure gradient does not entirely explain the motion of the septum. In the severely decompensated PAH simulation, the septum clearly bulges towards the LV from midway through the ejection phase until midway through diastole, corresponding with the fact that transseptal pressure gradient also changed direction during this part of the cardiac cycle.

Our results clearly show that septal movement is not dependent solely on the transseptal pressure gradient. We propose that an imbalance of forces at the RV attachment points resulting from ongoing RVFW contraction during the early diastolic phase pulls the septum leftwards, providing an additional source of septal movement.

In Silico Testing of Interventions in PAH

These studies established that the CircAdapt model can produce realistic simulations of cardiac mechanics and hemodynamics under normal and PAH conditions. We therefore set out to use the model to test several therapeutic interventions in PAH.

Atrial Septostomy in PAH

To clarify whether the benefits of atrial septostomy (AS) in PAH patients are explained by increase of oxygen availability in the tissues, the possibility to maintain blood pressure during exercise, or a combination of these factors [19–21], we evaluated effects of AS using CircAdapt [22]. We assessed the immediate effects of a circular AS with diameters ranging from 1 to 16 mm for levels of PAH with mean pulmonary arterial pressure (mPAP) ranging from 50 to 82 mmHg. Mean systemic arterial pressure was set to 61 mmHg to mimic pediatric blood pressure levels. The top panel of Fig. 7.5 shows the ratio of pulmonary to systemic blood flow as a function of shunt size and mPAP. It shows that shunts with a diameter of 1 to 2 mm resulted in almost no flow across the shunt. For shunt sizes of 3 mm and more, the ratio of pulmonary blood flow to systemic blood flow (Qp/Qs) was almost proportional to mPAP. The size and the direction of the shunt flow depended both on mPAP and shunt size. For shunt diameters above 2 mm, Qp/Qs was only proportional to the extent of pulmonary

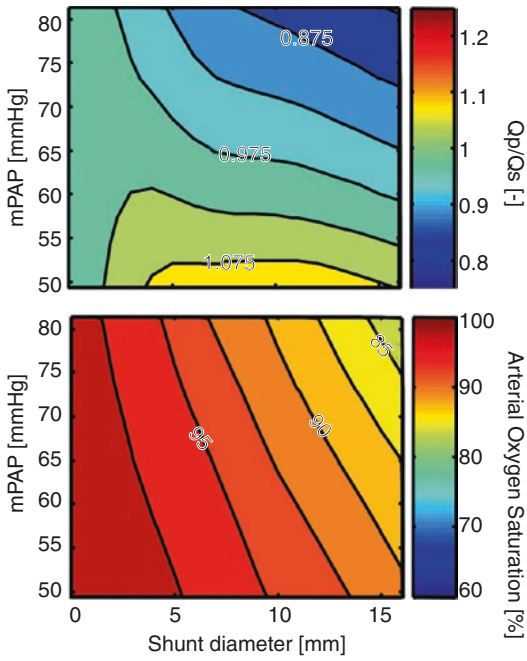

Fig. 7.5 Blood flow distribution and arterial oxygen saturation as a function of PAH severity and atrial septal defect diameter. *ASD* atrial septal defect, *mPAP* mean pulmonary arterial pressure, *Qp* pulmonary blood flow, *Qs* systemic blood flow

hypertension. Atrial septostomy led to a decrease in both upper and lower body arterial oxygen saturation that was proportional to both mPAP and shunt size (Fig. 7.5, lower panel). Simulations of exercise with severe PAH showed that these PAH patients benefit from an ASD because right-to-left atrial shunt flow facilitates maintenance of systemic arterial pressure [22]. Systemic oxygen transport, defined as systemic flow multiplied by the systemic arterial oxygen saturation, increased with exercise because the decrease in arterial oxygen saturation is overcompensated for by the increase in flow [20, 23]. However, in the presence of a right-to-left shunt, desaturated blood will bypass the pulmonary vascular bed and, hence, systemic blood flow does not reflect effective pulmonary blood flow any more, but is the sum of the right-to-left shunt and the effective pulmonary blood flow. Therefore, effective systemic oxygen transport capacity, being the product of effective pulmonary blood flow and pulmonary venous saturation, does not increase after atrial septostomy in PAH patients. We therefore believe that AS might be beneficial to patients with severe PAH because it increases LV preload and, consequently, allows better maintenance of systemic arterial blood pressure during exercise.

RV Free Wall Pacing in PAH

Several studies have shown that morbidity and mortality of PAH patients are determined by the ability of the RV to maintain normal stroke volume and cardiac output [24, 25]. In PAH, structural remodeling (hypertrophy and dilatation) is limited to the RVFW [14], suggesting an inhomogeneous distribution of myocardial tissue load. Local reduction of mechanical load of the RVFW may therefore be another therapeutic option, in addition to conventional reduction of pulmonary vascular resistance [26].

Severe PAH patients have interventricular mechanical dyssynchrony with prolonged duration of shortening and delayed peak shortening in the RV free wall compared with that of the LV free wall and the interventricular septum [27, 28]. RVFW shortening continued even after pulmonary valve closure and appeared to relate to leftward septal motion during LV isovolumic relaxation. As a potential treatment, early RVFW pacing was suggested as a way to improve interventricular mechanical synchrony and, thereby, cardiac pump function [19, 28, 29]. In our opinion, RVFW pacing also seems logical because during ventricular pacing, mechanical myofiber work is significantly decreased in early-activated regions, whereas it is increased in late-activated regions [30, 31].

Using the CircAdapt model, we tested the hypothesis that early pacing of the RV free wall improves ventricular mechanical coordination and, thereby, global RV pump function in PAH [32]. Model simulations also showed interventricular mechanical dyssynchrony in severely decompensated PAH (Fig. 7.6). This mechanical dyssynchrony was associated with prolonged duration of RV free wall shortening and inhomogeneous distribution of myofiber load over the

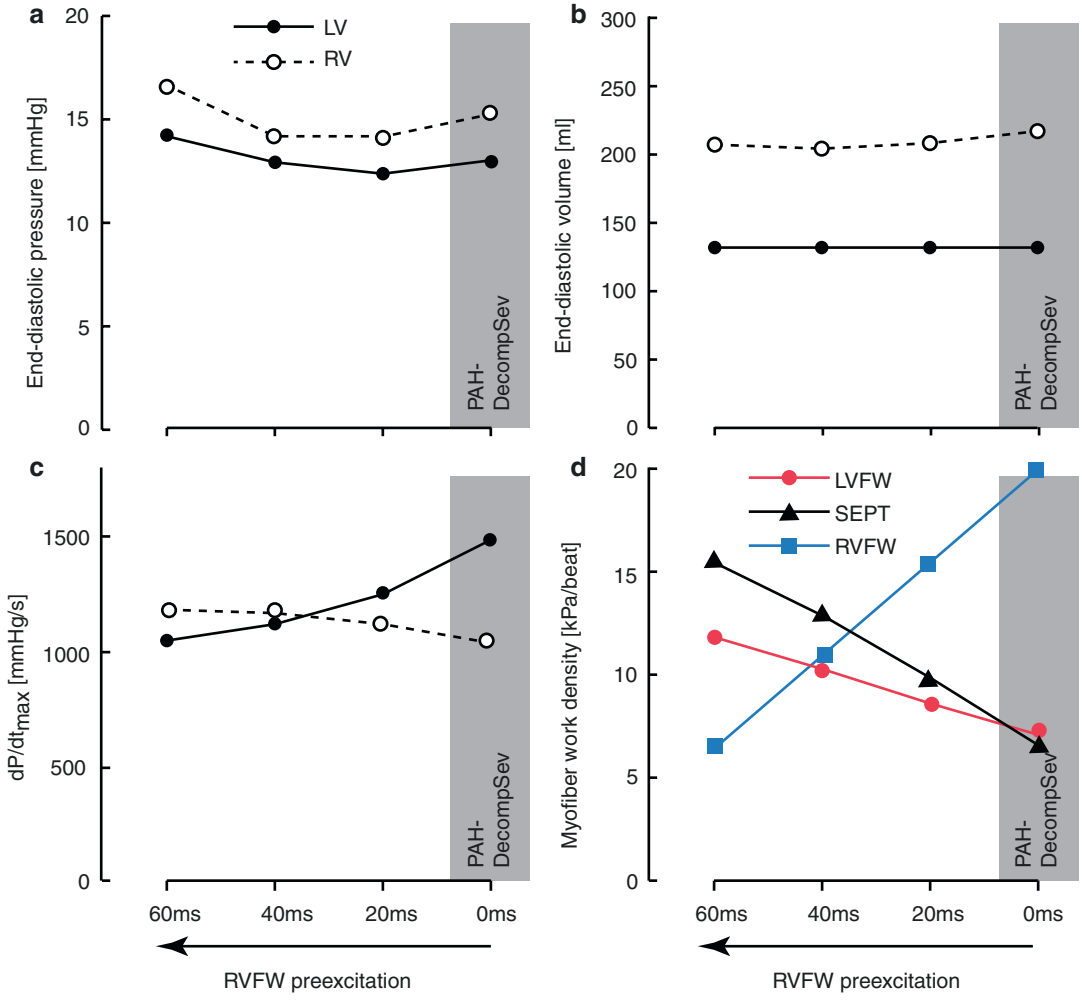

Fig. 7.6 Simulated effect of right ventricular free wall (RVFW) pacing on cardiac pump function in severe PAH. dP/dt_{max} maximal rate of pressure rise, *LV* left ventricle, *LVFW* left ventricular free wall, *RV* right ventricle, *SEPT* interventricular septum, *RVFW* right ventricular free wall, *PAH-DecompSev* severely decompensated PAH condition. Adapted from [32]

ventricular walls. Pre-excitation of the RV free wall resulted in more synchronous LV and RV pressure decay, more homogeneous distribution of myofiber load over the ventricular walls, and slight improvement of RV pump function. Pre-exciting the RV relieved the RV free wall from the extremely high myofiber work at the cost of an increase of myofiber work in the LV free wall and septum. The effects were maximal upon 40 ms pre-excitation of the RV free wall. The redistribution of myofiber work over the ventricular walls and the improvement in RV pump function are apparently due to the mechanical interaction of the ventricular walls.

CircAdapt provided initial theoretical evidence that a therapeutic intervention such as RVFW pacing may improve RV pump function in decompensated PAH. Recent studies in isolated hearts of experimental animals with PAH [19] and in patients with severe chronic thromboembolic pulmonary hypertension [33] have subsequently demonstrated that RV pacing does indeed have beneficial effects on RV pump function.

Conclusion and Future Perspectives

The CircAdapt model of the human heart and circulation produces realistic simulations of global hemodynamic pump function as well as of local mechanical deformation and work distribution in PAH. CircAdapt can be used to investigate *in silico* both the pathophysiological effects of PAH itself and its treatment on cardiac mechanics and hemodynamics. It is therefore a feasible platform to investigate new therapeutic strategies or to generate hypotheses on new therapies. Computer models like CircAdapt are likely to play an important role in the future in helping physicians to practice personalized, predictive and preventive medicine. By integrating the available clinical measurements in a multiscale model of human cardiovascular dynamics, it is anticipated that the hemodynamic status of a patient can be estimated more precisely than by conventional means (i.e., based on individual measurements). We envision that earlier stages of disease are likely to become detectable, which in turn, may lead to better and more preventative medicine. It is interesting to speculate that patient-specific modeling may also reduce the inconvenience of regular monitoring to the patient and reduce direct healthcare costs. A more precise diagnosis, as well as the possibility of *in silico* testing of intended therapeutic interventions, will lead to more successful and efficient treatment of PAH patients, which may improve long-term prognosis and quality of life.

References

1. Forfia PR, Vachiery JL. Echocardiography in pulmonary arterial hypertension. Am J Cardiol. 2012;110(6 Suppl):16S–24S.
2. Vonk-Noordegraaf A, Souza R. Cardiac magnetic resonance imaging: what can it add to our knowledge of the right ventricle in pulmonary arterial hypertension? Am J Cardiol. 2012;110(6 Suppl):25S–31S.
3. Chin KM, Coghlan G. Characterizing the right ventricle: advancing our knowledge. Am J Cardiol. 2012;110(6 Suppl):3S–8S.
4. Arts T, Delhaas T, Bovendeerd P, Verbeek X, Prinzen FW. Adaptation to mechanical load determines shape and properties of heart and circulation: the CircAdapt model. Am J Physiol Heart Circ Physiol. 2005;288(4):H1943–54.
5. Lumens J, Delhaas T, Kirn B, Arts T. Three-wall segment (TriSeg) model describing mechanics and hemodynamics of ventricular interaction. Ann Biomed Eng. 2009;37(11):2234–55.
6. Arts T, Lumens J, Kroon W, Delhaas T. Control of whole heart geometry by intramyocardial mechanofeedback: a model study. PLoS Comput Biol. 2012;8(2):e1002369.
7. Walmsley J, Arts T, Derval N, Bordachar P, Cochet H, Ploux S, et al. Fast simulation of mechanical heterogeneity in the electrically asynchronous heart using the multipatch module. PLoS Comput Biol. 2015;11(7):e1004284.
8. Belenkie I, Smith ER, Tyberg JV. Ventricular interaction: from bench to bedside. Ann Med. 2001;33(4):236–41.
9. Baker AE, Dani R, Smith ER, Tyberg JV, Belenkie I. Quantitative assessment of independent contributions of pericardium and septum to direct ventricular interaction. Am J Phys. 1998;275(2 Pt 2):H476–83.
10. Belenkie I, Sas R, Mitchell J, Smith ER, Tyberg JV. Opening the pericardium during pulmonary artery constriction improves cardiac function. J Appl Physiol (1985). 2004;96(3):917–22.
11. Omens JH. Stress and strain as regulators of myocardial growth. Prog Biophys Mol Biol. 1998;69(2–3):559–72.
12. Russell B, Curtis MW, Koshman YE, Samarel AM. Mechanical stress-induced sarcomere assembly for cardiac muscle growth in length and width. J Mol Cell Cardiol. 2010;48(5):817–23.
13. Olivetti G, Ricci R, Lagrasta C, Maniga E, Sonnenblick EH, Anversa P. Cellular basis of wall remodeling in long-term pressure overload-induced right ventricular hypertrophy in rats. Circ Res. 1988;63(3):648–57.
14. Minami S, Onodera T, Okazaki F, Miyazaki H, Ohsawa S, Mochizuki S. Myocyte morphological characteristics differ between the phases of pulmonary hypertension-induced ventricular hypertrophy and failure. Int Heart J. 2006;47(4):629–37.
15. Hardziyenka M, Campian ME, de Bruin-Bon HA, Michel MC, Tan HL. Sequence of echocardiographic changes during development of right ventricular failure in rat. J Am Soc Echocardiogr. 2006;19(10):1272–9.
16. Voelkel NF, Quaife RA, Leinwand LA, Barst RJ, McGoon MD, Meldrum DR, et al. Right ventricular function and failure: report of a National Heart, Lung, and Blood Institute working group on cellular and molecular mechanisms of right heart failure. Circulation. 2006;114(17):1883–91.
17. Tanaka H, Tei C, Nakao S, Tahara M, Sakurai S, Kashima T, et al. Diastolic bulging of the interventricular septum toward the left ventricle. An echocardiographic manifestation of negative interventricular pressure gradient between left and right ventricles during diastole. Circulation. 1980;62(3):558–63.
18. Mori S, Nakatani S, Kanzaki H, Yamagata K, Take Y, Matsuura Y, et al. Patterns of the interventricular septal motion can predict conditions of patients with

pulmonary hypertension. J Am Soc Echocardiogr. 2008;21(4):386–93.
19. Keogh AM, Mayer E, Benza RL, Corris P, Dartevelle PG, Frost AE, et al. Interventional and surgical modalities of treatment in pulmonary hypertension. J Am Coll Cardiol. 2009;54(1 Suppl):S67–77.
20. Kurzyna M, Dabrowski M, Bielecki D, Fijalkowska A, Pruszczyk P, Opolski G, et al. Atrial septostomy in treatment of end-stage right heart failure in patients with pulmonary hypertension. Chest. 2007;131(4):977–83.
21. Zierer A, Melby SJ, Voeller RK, Moon MR. Interatrial shunt for chronic pulmonary hypertension: differential impact of low-flow vs. high-flow shunting. Am J Physiol Heart Circ Physiol. 2009;296(3):H639–44.
22. Koeken Y, Kuijpers NH, Lumens J, Arts T, Delhaas T. Atrial septostomy benefits severe pulmonary hypertension patients by increase of left ventricular preload reserve. Am J Physiol Heart Circ Physiol. 2012;302(12):H2654–62.
23. Micheletti A, Hislop AA, Lammers A, Bonhoeffer P, Derrick G, Rees P, et al. Role of atrial septostomy in the treatment of children with pulmonary arterial hypertension. Heart. 2006;92(7):969–72.
24. Chin KM, Kim NH, Rubin LJ. The right ventricle in pulmonary hypertension. Coron Artery Dis. 2005;16(1):13–8.
25. Sandoval J, Bauerle O, Palomar A, Gomez A, Martinez-Guerra ML, Beltran M, et al. Survival in primary pulmonary hypertension. Validation of a prognostic equation. Circulation. 1994;89(4):1733–44.
26. Galie N, Hoeper MM, Humbert M, Torbicki A, Vachiery JL, Barbera JA, et al. Guidelines for the diagnosis and treatment of pulmonary hypertension: the Task Force for the Diagnosis and Treatment of Pulmonary Hypertension of the European Society of Cardiology (ESC) and the European Respiratory Society (ERS), endorsed by the International Society of Heart and Lung Transplantation (ISHLT). Eur Heart J. 2009;30(20):2493–537.
27. Bossone E, Avelar E, Bach DS, Gillespie B, Rubenfire M, Armstrong WF. Diagnostic value of resting tricuspid regurgitation velocity and right ventricular ejection flow parameters for the detection of exercise induced pulmonary arterial hypertension. Int J Card Imaging. 2000;16(6):429–36.
28. Marcus JT, Gan CT, Zwanenburg JJ, Boonstra A, Allaart CP, Gotte MJ, et al. Interventricular mechanical asynchrony in pulmonary arterial hypertension: left-to-right delay in peak shortening is related to right ventricular overload and left ventricular underfilling. J Am Coll Cardiol. 2008;51(7):750–7.
29. Beyar R. Heart inefficiency in pulmonary hypertension: a double jeopardy. J Am Coll Cardiol. 2008;51(7):758–9.
30. Delhaas T, Arts T, Prinzen FW, Reneman RS. Regional fibre stress-fibre strain area as an estimate of regional blood flow and oxygen demand in the canine heart. J Physiol. 1994;477(Pt 3):481–96.
31. Prinzen FW, Hunter WC, Wyman BT, McVeigh ER. Mapping of regional myocardial strain and work during ventricular pacing: experimental study using magnetic resonance imaging tagging. J Am Coll Cardiol. 1999;33(6):1735–42.
32. Lumens J, Arts T, Broers B, Boomars KA, van Paassen P, Prinzen FW, et al. Right ventricular free wall pacing improves cardiac pump function in severe pulmonary arterial hypertension: a computer simulation analysis. Am J Physiol Heart Circ Physiol. 2009;297(6):H2196–205.
33. Hardziyenka M, Surie S, de Groot JR, de Bruin-Bon HA, Knops RE, Remmelink M, et al. Right ventricular pacing improves haemodynamics in right ventricular failure from pressure overload: an open observational proof-of-principle study in patients with chronic thromboembolic pulmonary hypertension. Europace. 2011;13(12):1753–9.

Can the Right Ventricle Support the Failing Left Ventricle?

8

Dietmar Schranz

Abstract

Ventricular failure, from cardiomyopathy or adverse loading, is the leading cause of cardiac death in children. In severe pediatric dilated cardiomyopathy of the left ventricle, heart transplant is the only life-saving option, but is limited by donor availability, cost and relatively poor survival. Alternatives are clearly needed. We have made a series of observations regarding therapeutic modification of ventricular afterload to improve contra-lateral ventricular function. These findings demonstrate novel mechanisms of ventricular–ventricular interactions (VVI), the potential to harness them for therapeutic benefit, and may constitute a paradigm shift in the treatment of pediatric heart failure. The pathophysiological rationale is that although left (LV) and right (RV) ventricular function are usually considered separately, they are inextricably linked through a common septum, shared myofibers and pericardium. Using the Anrep effect induced by banding of the pulmonary artery, LV function can be enhanced via VVI. Thus, VVI may hold great potential for treatment of LV failure. Future studies are needed to further delineate the geometrical, temporal and molecular mechanisms of PA-banding-induced ventricular crosstalk; and to examine their potential modulation through mechanical, electrophysiological and pharmacological interventions.

Keywords

Right ventricle • Failing left ventricle • Support • Ventricular–ventricular interactions

Dilated cardiomyopathy (DCM) is a leading cause of cardiac death in children [1, 2]. 'Traditional' medical therapies proven to be of benefit in adults with heart failure such as beta-blockers, ACE inhibitors and angiotensin receptor blockers have failed to benefit children with acquired and congenital heart failure in random-

D. Schranz
Pediatric Cardiology, Hesse Pediatric Heart Center, Theodor-Stern-kai 7, Frankfurt 60590, Germany
e-mail: dietmar.schranz@paediat.med.uni-giessen.de

M.K. Friedberg, A.N. Redington (eds.), *Right Ventricular Physiology, Adaptation and Failure in Congenital and Acquired Heart Disease*, https://doi.org/10.1007/978-3-319-67096-6_8

ized clinical trials [3, 4]. Currently, patients diagnosed with end-stage heart failure despite maximal medical therapy may be listed for heart transplantation (HTx) with or without prior support with a ventricular assist device. While heart transplantation is currently the only proven viable life-saving option, it is limited by donor availability, cost and reduced long-term survival [6, 7]; from a global health perspective, HTx is available to only a very small minority of affected children. Therefore, there is a pressing need for alternative therapies. Indeed, the report from a recent working group of the National Institutes of Health, calls for major new initiatives for the development of new therapies in children with heart failure [5].

Although left (LV) and right (RV) ventricular function is usually considered separately, they are inextricably linked through a common septum, shared myofibers and pericardial space [8]. Consequently it has been shown that LV contraction contributes more than 50% of RV work [9]. However, the full portfolio of ventricular–ventricular (V–V) interactions in either LV or RV failure is incompletely understood and has not been harnessed for therapeutic benefit. Based on novel experimental and clinical observations [9–14], we hypothesized that V–V interactions may have therapeutic potential in general, but in particular for the LV with systolic failure. Therefore, the introduction of reversible pulmonary artery banding (rPAB) to the therapeutic arsenal in left heart failure constitutes a paradigm shift, particularly for infants and children with end-stage DCM [15, 16]. The surgical technique of PAB has a low risk, and is usually used to restrict pulmonary artery blood flow to balance systemic-pulmonary circulations in cases of complex ventricular shunts and, for example, in patients with congenitally corrected TGA who are candidates for an anatomic biventricular repair. In young children suffering LV-DCM, the initial rationale for development of rPAB was leftward mechanical shift of the interventricular septum; thereby improving LV end-diastolic volume and pressure via improved Frank-Starling effects and filling dynamics, respectively (Fig. 8.1). Together with restored ventricular

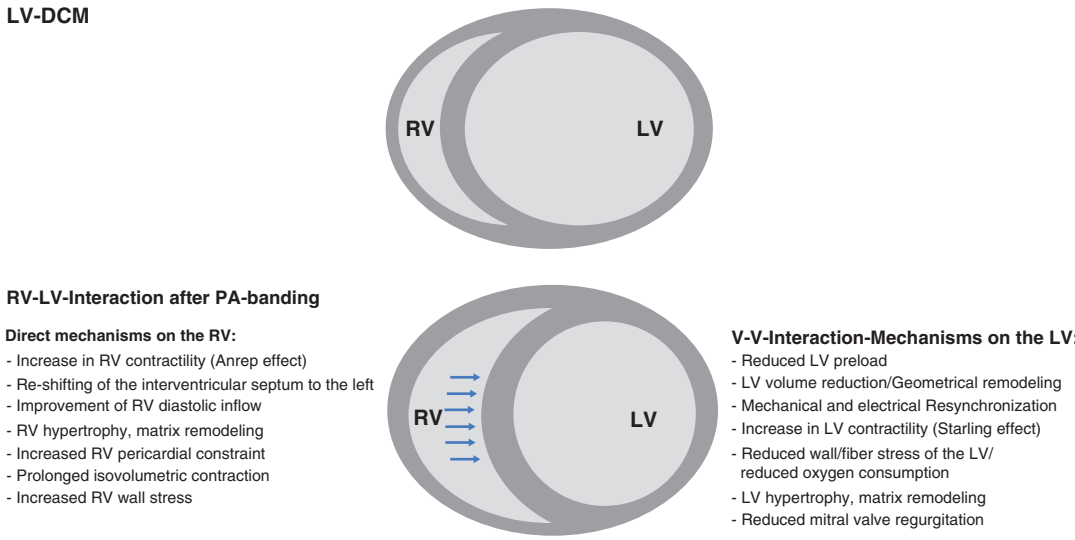

Fig. 8.1 Schematic transverse sectional view on the left (LV) and right (RV) ventricle. The upper panel is showing the changes in LV dilated cardiomyopathy (DCM), leading to LV failure and dilation, bulging of the interventricular septum to the right, thus resulting in impaired RV filling. The lower panel is showing the potential mechanisms how an increase in RV afterload induced by pulmonary banding might modify adverse ventricular–ventricular interactions for therapeutic benefit. We hypothesize that beyond the pure mechanical shift of the interventricular septum (*arrows*) corresponding mechanisms on cellular and molecular levels i.e. neuro-humoral and immunological activation, altered bioenergetics (mitochondrial remodeling) may play an important role

electromechanical synchrony, increased LV ejection fraction led to clinical improvement at rest and during exercise. In this context, rPAB is a promising therapeutic option with the potential to be a clinical 'game changer' [17]. The first rPAB approach in a DCM patient was performed eight years ago in a newborn listed for HTX 2-months after birth without a realistic chance to receive donor heart in a timely manner [15]. By the end of 2014, 26 infants and young children had undergone rPAB with end-stage DCM; six of them during open-heart surgery for concomitant repair of additional cardiac lesions; twenty patients received isolated surgical-PAB by an off-pump open-chest approach. In all patients surgery was well tolerated without perioperative mortality. Remarkable clinical improvements and significant improvements in LV cardiac function and reverse remodeling including LV-size, LV-ejection fraction, and mitral valve regurgitation have been observed (Fig. 8.2). Twenty one of 26 patients could be de-listed from transplant list. Following further improvement in their clinical and hemodynamic status, complete or partial pulmonary artery de-banding was performed by transcatheter technique in 17 patients. Two of 26 patients (8%), both with LV non-compaction morphology, decompensated 4 and 6 months after complete transcatheter de-banding and died 6 and 9 months later, one following complications during support with a ventricular assist device.

These 'proof-of-principle' results imply that rPAB in LV failure provides a novel alternative 'bridge-to-transplant' or destination therapy in children with advanced LV-DCM. Technically rPAB is simple, safe, effective and affordable making it a realistic option for children worldwide, especially where transplant is not an option. However, to date, the pediatric DCM population who may benefit from V–V interaction therapy has not been defined, and we have demonstrated therapeutic benefit only in infants and children whose myocardium may have greater potential for recovery [18, 19]. Therefore, there is a need for a prospective, randomized study of rPAB in LV-DCM, including older children up to 12-years of age. In addition, biochemical profiling is warranted as part of a comprehensive strategy to define patient characteristics, thereby defining mechanisms of response and allowing future prediction and augmentation of response [20].

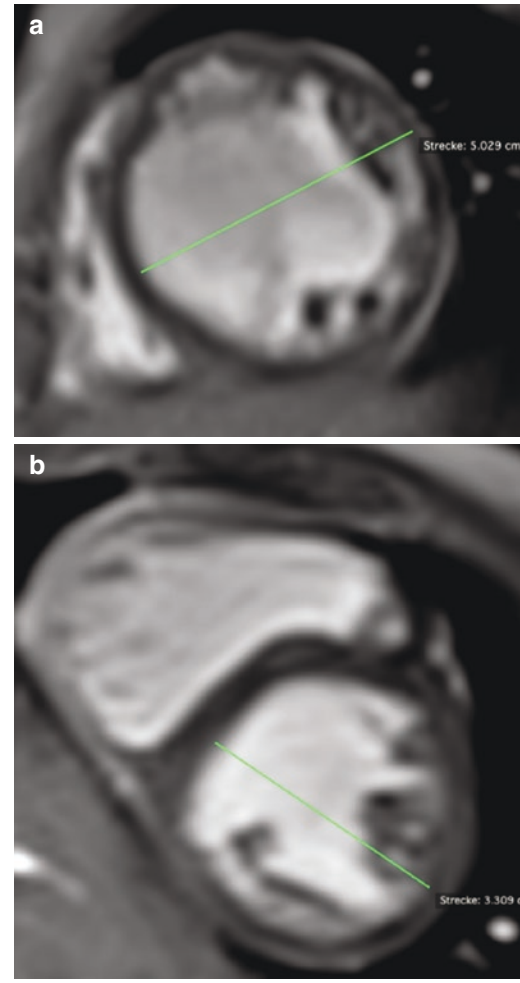

Fig. 8.2 (**a**, **b**) Magnetic resonance tomography in a 15 months old boy with LV-DCM who was admitted to our hospital for heart transplantation. The *upper panel* shows in a short axis view the severe dilation (z-score of left ventricular enddiastolic diameter, LVEDD +7.5) of the LV and the compressed RV. The left ventricular ejection fraction (LV-EF) was only 23%. The *lower panel* demonstrates the remarkable findings 4 months after the PA-banding operation: LV-size (LVEDD z-score + 1.2), geometry and LV-EF (52%) fundamentally improved, respectively

Although anecdotal, based on our single center experience we would emphasize that rPAB needs to be supported by concomitant anticongestive therapy. Considering the neuro-humoral activation

in patients with DCM in general and specifically the beta-adrenergic-receptor-pathophysiological response of pediatric DCM [21], we have treated infants and children who received a rPAB, using a ß1-specific beta-blocker (Bisoprolol), a tissue ACE-inhibitor (Lisinopril) and a mineralocorticoid-blocker (spironolactone) [22].

In summary, the failure of pharmacotherapy alone and the limited availability of heart transplantation for heart failure in children mandate a new approach to treatment. V–V interactions represent novel therapeutic targets in both right heart and left heart disease. In particular, we hypothesize that rPAB can benefit LV failure via enhanced Anrep effects and beneficial modification of biventricular geometry in infants and children with LV-DCM. Future studies are required to examine the mechanisms underlying the observed response in the early proof-of-principle reports, and to establish which children are most likely to benefit from this simple intervention.

Acknowledgements For knowledge exchange and fruitful discussions over the last years, I want to thanks: Mark Friedman and Andrew Redington, Toronto; Tammo Delhaas, Maastricht; Daniel Bernstein, Stanford; My Co-worker Christian Apitz.

References

1. Daubeney PE, Nugent AW, Chondros P, et al. Clinical features and outcomes of childhood dilated cardiomyopathy: results from a national population-based study. Circulation. 2006;114:2671–8.
2. Towbin JA, Lowe AM, Colan SD, et al. Incidence, causes, and outcomes of dilated cardiomyopathy in children. JAMA. 2006;296:1867–76.
3. Shaddy RE, Boucek MM, Hsu DT, Boucek RJ, et al. Pediatric Carvedilol Study Group. Carvedilol for children and adolescents with heart failure: a randomized controlled trial. JAMA. 2007;298(10):1171–9.
4. Roche SL, Redington AN. Right ventricle: wrong targets? Another blow for pharmacotherapy in congenital heart diseases. Circulation. 2013;127(3):314–6.
5. Burns KM, Byrne BJ, Gelb BD, Kühn B, et al. New mechanistic and therapeutic targets for pediatric heart failure: report from a national heart, lung, and blood institute working group. Circulation. 2014;130(1):79–86.
6. Alexander PM, Daubeney PE, Nugent AW, et al. Long-term outcomes of dilated cardiomyopathy diagnosed during childhood: results from a national population-based study of childhood cardiomyopathy. Circulation. 2013;128:2039–46.
7. Canter CE, Shaddy RE, Bernstein D, et al. Indications for heart transplantation in pediatric heart disease: a scientific statement from the American Heart Association Council on Cardiovascular Disease in the Young; the Councils on Clinical Cardiology, Cardiovascular Nursing, and Cardiovascular Surgery and Anesthesia; and the Quality of Care and Outcomes Research Interdisciplinary Working Group. Circulation. 2007;115:658–76.
8. Sanchez-Quintana D, Anderson RH, Ho SY. Ventricular myoarchitecture in tetralogy of Fallot. Heart. 1996;76:280–6.
9. Damiano RJ Jr, La Follette P Jr, Cox JL, Lowe JE, Santamore WP. Significant left ventricular contribution to right ventricular systolic function. Am J Phys. 1991;261:H1514–24.
10. Yamashita H, Onodera S, Imamoto T, et al. Functional and geometrical interference and interdependency between the right and left ventricle in cor pulmonale: an experimental study on simultaneous measurement of biventricular geometry of acute right ventricular pressure overload. Jpn Cir J. 1989;53:1237–44.
11. Belenkie I, Horne SG, Dani R, Smith ER, Tyberg JV. Effects of aortic constriction during experimental acute right ventricular pressure loading. Further insights into diastolic and systolic ventricular interaction. Circulation. 1995;92:546–54.
12. Apitz C, Honjo O, Friedberg MK, et al. Beneficial effects of vasopressors on right ventricular function in experimental acute right ventricular failure in a rabbit model. Thoracic Cardiovasc Surg. 2012;60:17–23.
13. Apitz C, Honjo O, Humpl T, et al. Biventricular structural and functional responses to aortic constriction in a rabbit model of chronic right ventricular pressure overload. J Thoracic Cardiovasc Surg. 2012;144:1494–501.
14. Friedberg M, Cho MY, Li J, et al. Adverse biventricular remodeling in isolated right ventricular hypertension is mediated by increased TGFβ1 signaling and is abrogated by angiotensin receptor blockade. Am J Respir Cell Mol Biol. 2013;49(6):1019–28.
15. Schranz D, Veldman A, Bartram U, Michel-Behnke I, Bauer J, Akinturk H. Pulmonary artery banding for idiopathic dilative cardiomyopathy: a novel therapeutic strategy using an old surgical procedure. J Thoracic Cardiovasc Surg. 2007;134:796–7.
16. Schranz D, Rupp S, Muller M, et al. Pulmonary artery banding in infants and young children with left ventricular dilated cardiomyopathy: A novel therapeutic strategy before heart transplantation. J Heart Lung Transplant. 2013;32:475–81.
17. Bailey LL. Back to the future! Bold new indication for pulmonary artery banding. J Heart Lung Transplant. 2013;32:482–48313.
18. Amir G, Ma X, Reddy VM, et al. Dynamics of human myocardial progenitor cell populations in the neonatal period. Ann Thoracic Surg. 2008;86:1311–9.

19. Mishra R, Vijayan K, Colletti EJ, et al. Characterization and functionality of cardiac progenitor cells in congenital heart patients. Circulation. 2011;123:364–73.
20. Lumens J, Ploux S, Strik M, Gorcsan J 3rd, et al. Comparative electromechanical and hemodynamic effects of left ventricular and biventricular pacing in dyssynchronous heart failure: electrical resynchronization versus left-right ventricular interaction. J Am Coll Cardiol. 2013;62(25):2395–403.
21. Miyamoto SD, Stauffer BL, Nakano S, et al. Beta-adrenergic adaptation in pediatric idiopathic dilated cardiomyopathy. Eur Heart J. 2014;35:33–41.
22. Recla S, Steinbrenner B, Schranz D. Medical therapy in dilated cardiomyopathy and pulmonary arterial banding in children. J Heart Lung Transplant. 2013;32:1045–6.

Echocardiographic Assessment of the Right Ventricle

9

Luc L. Mertens

Abstract

While cardiac magnetic resonance imaging is considered the clinical reference technique for the assessment of right ventricular (RV) size and function, echocardiography remains the first-line imaging technique. Recent guidelines for the use of echocardiography recommend the use of quantitative measures of RV dimensions and function. For functional assessment, a combination of fractional area change, tissue Doppler velocities and tricuspid annular planar systolic excursion (TAPSE) provide practical tools that can be used to monitor RV function serially. Novel techniques including three-dimensional echocardiography and strain imaging provide more detailed information that can be helpful in selected patient groups.

Keywords

Right ventricle • Echocardiography • Three-dimensional echocardiography • Strain imaging

Introduction

The echocardiographic assessment of RV size and function remains a controversial topic. While most echocardiography laboratories rely predominantly upon qualitative assessment of the RV, recent guidelines and recommendations stress the importance of including quantitative assessment of RV size and function in clinical reports [1, 2]. Different studies have demonstrated clearly the limitations of qualitative assessment when compared to cardiac magnetic resonance imaging (MRI). For example, visual estimation of RV size and function is inaccurate and has wide interobserver variability. Adding quantitative echocardiographic parameters significantly improves accuracy and reliability of echocardiographic assessment [3]. Particularly in pediatric patients with more complex congenital heart disease like hypoplastic left heart syndrome, qualitative assessment of RV function often results in misclassification of the

L.L. Mertens
Paediatric Cardiology, The Hospital for Sick Children, 555 University Ave, Toronto, ON M1G 1X8, Canada
e-mail: luc.mertens@sickkids.ca

M.K. Friedberg, A.N. Redington (eds.), *Right Ventricular Physiology, Adaptation and Failure in Congenital and Acquired Heart Disease*, https://doi.org/10.1007/978-3-319-67096-6_9

degree of RV dysfunction, even in the hands of experienced echocardiographers [4]. While these observations do not imply that qualitative evaluation is never useful as the first 'gestalt' for the echocardiographer, it does suggest that quantitative assessment of RV size and function is essential for quality assurance and accuracy.

Echocardiographic RV imaging is limited by different factors [5]. One of the challenges in the assessment of RV function is the more complex geometry of the RV, which significantly differs from the simpler ellipsoid left ventricle (LV) shape. This makes the RV more difficult to describe in a simple geometric model. Different complex mathematical formula for calculating RV volumes based on 2-D measurements have been proposed but all have limitations and are relatively complicated for application in routine clinical practice [6]. The anterior position in the chest further limits visualization of the RV anterior wall as located in the near field of the echo beam. The wrapping of the RV around the LV further limits two-dimensional imaging of the RV and makes it impossible to image the inflow, trabecular and outflow components in a single view. Assessing the size of the different RV components is especially relevant in conditions where regional RV remodelling occurs. For example, in patients after repair of tetralogy of Fallot (TOF), right ventricular outflow tract patch dilatation can lead to aneurysmal enlargement of the right ventricular outflow tract while pulmonary regurgitation tends to result in progressive enlargement of the RV inflow and apical segments [7]. Accurate determination of RV size in these patients will require imaging the different RV components.

When assessing RV function, the specific RV contraction pattern and physiology has to be taken into account. The RV contracts in a more longitudinal direction with a peristaltic wave moving from the RV inflow to the RV outflow, propelling the blood into the pulmonary circulation. This contrasts with the LV which contracts in a more circumferential direction with limited impact of longitudinal shortening on overall ejection.

Despite all these limitations and caveats, echocardiography can provide a reasonable quantitative assessment of RV size and function and should be performed in every patient where assessment of RV function is important.

Measurement of RV Dimensions

Different measurements of RV size have been proposed and are included in several guideline documents [1, 2, 8, 9]. One of the older measurements of RV size that is no longer included in the guidelines, but is still commonly used in clinical practice, is M-mode measurement of RV end-diastolic dimension from the parasternal long-axis or short-axis view used to assess LV size and function. When measuring the LV, the M-mode also cuts through the RV, close to the right ventricular outflow tract (RVOT). The RV can be measured at end-diastole (R-wave of the QRS; Fig. 9.1). The problem with the measurement is that it is not based on specific RV anatomical landmarks and measures the RV trabecular part

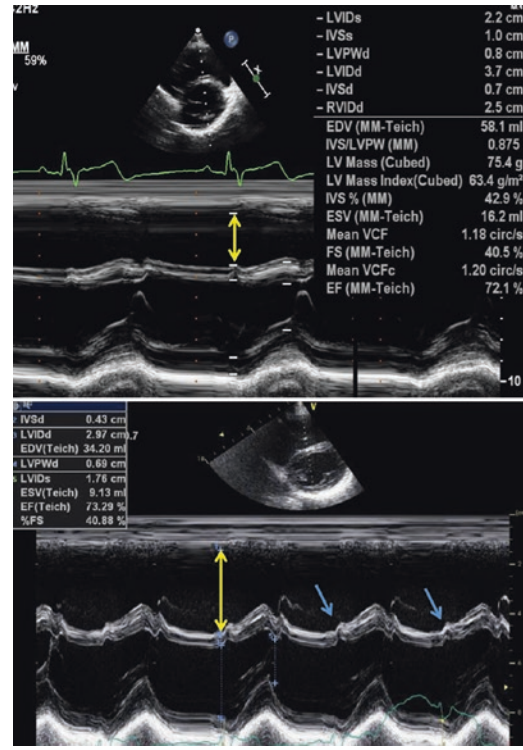

Fig. 9.1 Measurement of RV dimension from the parasternal short axis M-mode in patients after TOF repair. In the *upper panel*, the RV is positioned nicely anterior to the LV and the M-mode is a *straight line* through the RV trabecular part just below the RVOT. In the *lower panel* it is difficult to obtain an image with the RV positioned anterior to the LV. There is abnormal septal motion related to early septal activation and delayed anterior wall activation resulting in the inward septal motion during the R-wave (*small blue arrows*)

just below the RVOT. Thus, it does not really provide an assessment of different RV components and it can be difficult to avoid an oblique scan. Also, the septum can be activated early, related to right bundle branch block, resulting in abnormal septal motion during the R-wave of the QRS (septal flash). The main reason this measurement is still used in clinical practice, is the availability of pediatric z-scores which allows evaluating changes in RV size over time, independent of patient growth. Zervan et al. demonstrated progressive enlargement of this RV M-mode dimension the first 7 years after TOF repair, with regression after pulmonary valve replacement [10]. This suggests the measurement can be used for tracking progressive RV dilatation.

Recent guidelines recommend measuring RV dimensions from the apical RV-centric view. This view is obtained from the standard apical 4-chamber view by sliding the transducer slightly medially on the chest putting the right ventricular (RV) apex in the middle of the imaging sector. Measurements are obtained in mid-diastole (when the ventricle is largest, Fig. 9.2). The RV transverse diameter is measured at the basal one-third below the tricuspid annulus (RV 1) and in the middle third of RV inflow, approximately halfway between the maximal basal diameter and the apex, at the level of papillary muscles at end-diastole (RV2). RV length is measured from the mid-point of the tricuspid valve annulus to the RV apex. In adults, RV1 > 41 mm and RV2 > 35 mm, indicates RV dilatation. Pediatric z-scores for these RV measurements are currently unavailable, which limits the application of these measurements in children. Additionally the apical RV view only images the RV inflow and trabecular parts and does not include the RV outflow. Especially in patients in whom the RVOT is dilated this results in underestimation of overall RV size. Lai et al. demonstrated that echocardiographic RV dimensions as measured from the apical 4-chamber view are smaller compared to MRI measurements [11]. From the parasternal short and long-axis views, proximal RVOT dimensions can be measured (Fig. 9.3). These measurements are similar to the M-mode measurements obtained from the same windows but are less dependent on alignment of the probe.

From the RV-centric apical view, the RV end-diastolic area can be measured at end-diastole. We include the RV trabeculations in the measurement of RV area as we also use a similar approach when measuring MRI RV volumes (Fig. 9.4).

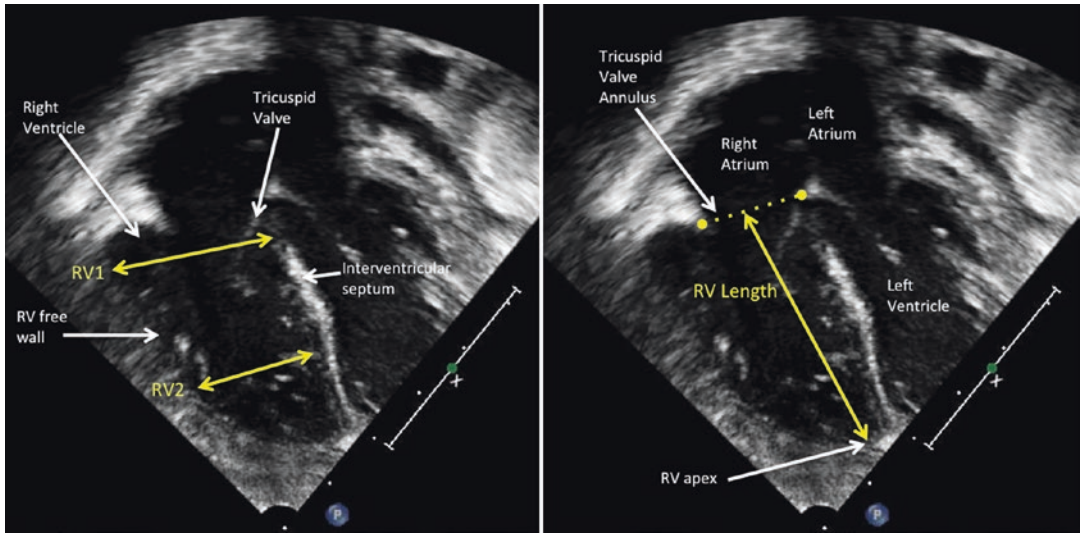

Fig. 9.2 RV width and length measurements from an RV-centric apical view. RV1 is measured at the basal level, from the endocardium of the RV free wall to the interventricular septum (IVS). RV2 is measured in the middle third of RV inflow, approximately halfway between the maximal basal diameter and the apex, at the level of papillary muscles at end-diastole (*left panel*). RV length is measured from the mid-point of the tricuspid valve annulus to the RV apex

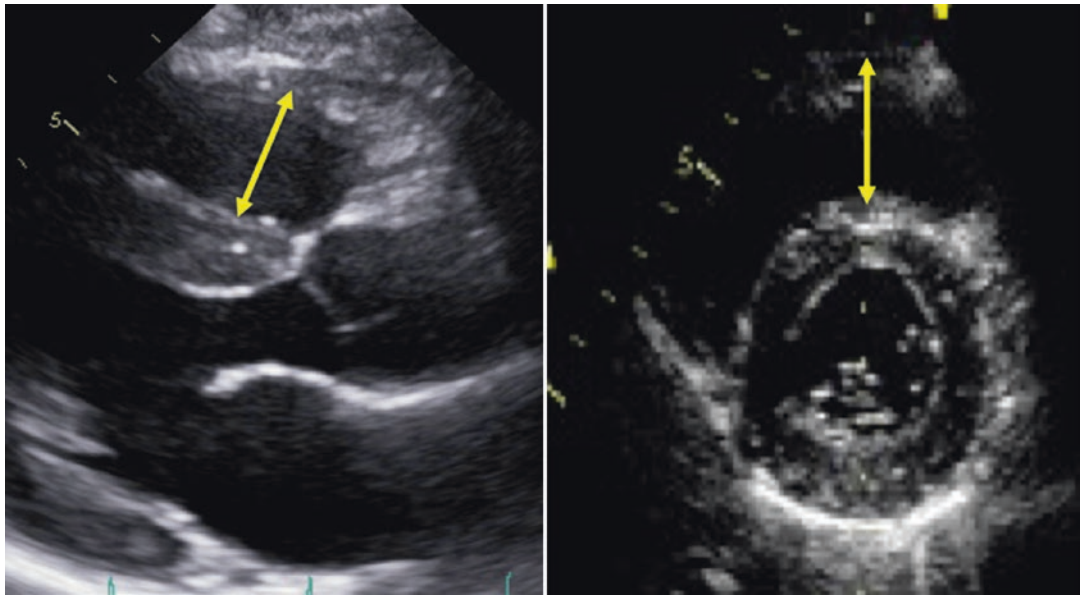

Fig. 9.3 Proximal RVOT dimension as measured from the parasternal long (*left panel*) and short (*right panel*) axis

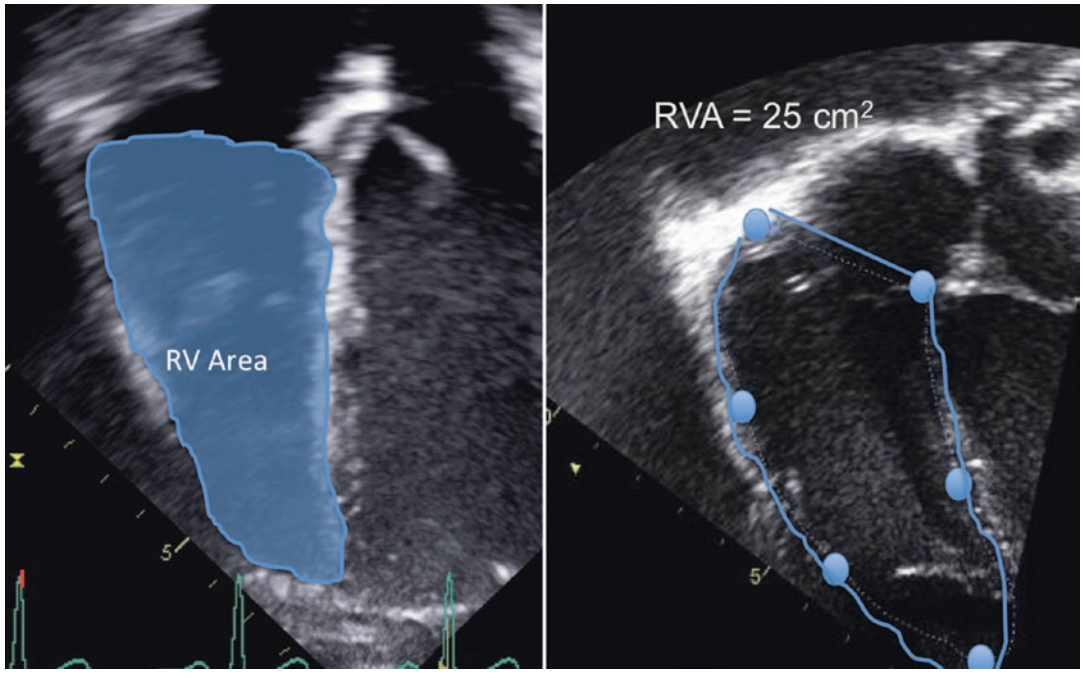

Fig. 9.4 Measurement of end-diastolic RV area from the RV-centric apical 4-chamber view. The *right panel* shows the measurement in post-operative TOF patient. The area indexed for BSA was 29 cm^2/m^2

Especially in adult patients with limited imaging windows, delineation of the RV free wall can be difficult and foreshortening from the RV-centric view should also be avoided. In older patients after TOF repair, RV end-diastolic area indexed for body surface area ($RVEDA_i$) was shown to correlate linearly with indexed RV end-diastolic volume ($RVEDV_i$) as measured by MRI [($RVEDV_i = 11.5 + (7 \times RVEDA_i)$]) [12]. In children after TOF repair $RVEDA_i > 20$ cm^2/m^2 predicts $RVEDV_i > 170$ ml/m^2 with high sensitivity and specificity [13]. This relatively simple measurement can provide guidance for selecting patients for cardiac MRI for assessment of RV volumes and also for the serial follow-up of RV dimensions. Adding 2-dimensional measurements from additional RV views such as the apical RV 2-chamber and RV 3-chamber views further increase the accuracy of RV size assessment. The feasibility of these views is however influenced by the limited visualization of the anterior RV wall segments, certainly in adults. In newborns, however, our group demonstrated a high feasibility and reproducibility of additional RV measurements from these views [14].

Assessment of RV wall thickness in the assessment of RV hypertrophy remains difficult due to lack of reproducible anatomic landmarks that allow standardization of RV wall thickness measurements. It is recommended to assess RV wall thickness in the RV free wall as imaged from subcostal long-axis views at end-diastole below the tricuspid annulus at a distance approximating the length of the anterior tricuspid leaflet when it is full open and parallel to the RV free wall. The measurement should exclude trabeculae, papillary muscles and epicardial fat. In adults, RV thickness >0.5 cm is considered abnormal. However, no normal pediatric data are available. The recommended measurement technique is difficult and prone to measurement variability as it can be challenging to define the endocardial and epicardial borders related to the RV trabeculations.

Measurement of RV Volumes

Three-dimensional echocardiography is being increasingly adopted for measuring RV end-diastolic and end-systolic volumes. Full volumetric RV data acquisition can be performed from the RV-centric apical view focussing on including the entire RV cavity and all RV walls. This can be difficult in adult patients with significant RV dilatation. Additionally as 3-D spatial resolution is lower than 2-D resolution, visualization of all RV endocardial borders can be challenging. This limits its feasibility of 3-D RV volumetric assessment, especially in adult patients after congenital heart surgery. Different studies reported feasibility of only 50–60% [15]. Different software packages are available for RV 3-D volumetric measurements. They require tracing the RV endocardial borders at end-diastole and end-systole. Semi-automated tracing is available but manual adjustments are often required and complicate RV volumetric measurements. RV trabeculations and the moderator band are included in the volume measurements. Intra and interobserver variability between the different methods can be important and should be taken into account when RV 3-D volumes are used. When compared to MRI volumetric data, 3-D echocardiographic volumes generally underestimate RV volumes by 10–25% [15–18]. This difference seems larger in more dilated RVs. These intertechnique differences should be taken into account when decision-making is based on RV volumes such as for pulmonary valve replacement in patients after TOF repair as most of the cut-off values for RV volumes have been based on MRI measurements.

In adults, normal data on echocardiographic RV volumes are available, and are influenced by age and gender [1]. For adults, $RVEDV_i$ of 87 mL/m^2 in men and 74 mL/m^2 are considered the upper limits of normal. With increasing age, $RVEDV_i$ progressively decreases. In children, good, normal echocardiographic 3-D reference data are not available limiting clinical utility of this method in younger age groups.

Other techniques have been proposed such as the 2-D based knowledge reconstruction method which uses magnetic tracking attached to the ultrasound probe for localizing RV 2-D images in 3-D space. On the 2-D images anatomic landmarks are identified and based on a database of RV shapes, RV volumes are reconstructed. While this method has excellent feasibility, reliability and accuracy, its clinical use is limited as image acquisition and analysis is cumbersome and requires specific equipment [16, 19]. Our group found the method difficult to integrate in a high-volume clinical echocardiography laboratory.

Echocardiographic Assessment of RV Systolic Function

Different echocardiographic methods have been proposed for assessing RV systolic function. In most validation studies, RV ejection fraction (RVEF) as measured by MRI is used as the gold-standard reference technique for assessing global RV function. RVEF is influenced by contractile function, size and loading conditions. In the adult population RVEF is also influenced by age and gender. Utilizing RVEF as a parameter for RV function should thus be interpreted carefully, taking the different parameters influencing the measurement into account when used for clinical decision-making.

Three-dimensional echocardiography is the best echocardiographic technique for measuring RVEF, albeit with the limitations mentioned above. Apart from limited feasibility in a post-surgical population, the reproducibility of the method is influenced by variability in measurement of RV systolic volumes. In our experience, RVESV is more difficult to measure, as at end-systole the trabeculations can be difficult to delineate precisely [16]. This influences variability in RVEF calculations. While in adults an RVEF >45% is considered normal, with slightly higher values in women than men, no reliable normative data are available for children. Furthermore, as 3-D echocardiography is not readily available in every laboratory and because the technique is cumbersome, time-consuming and requires specific software and expertise, this method is not widely used in clinical practice and other techniques for assessing RV function have been introduced and validated.

RV fractional area change (FAC) is a reasonable substitute for RVEF. It measures the area change between end-systole and end-diastole from the RV-centric apical 4-chamber view (Fig. 9.5).

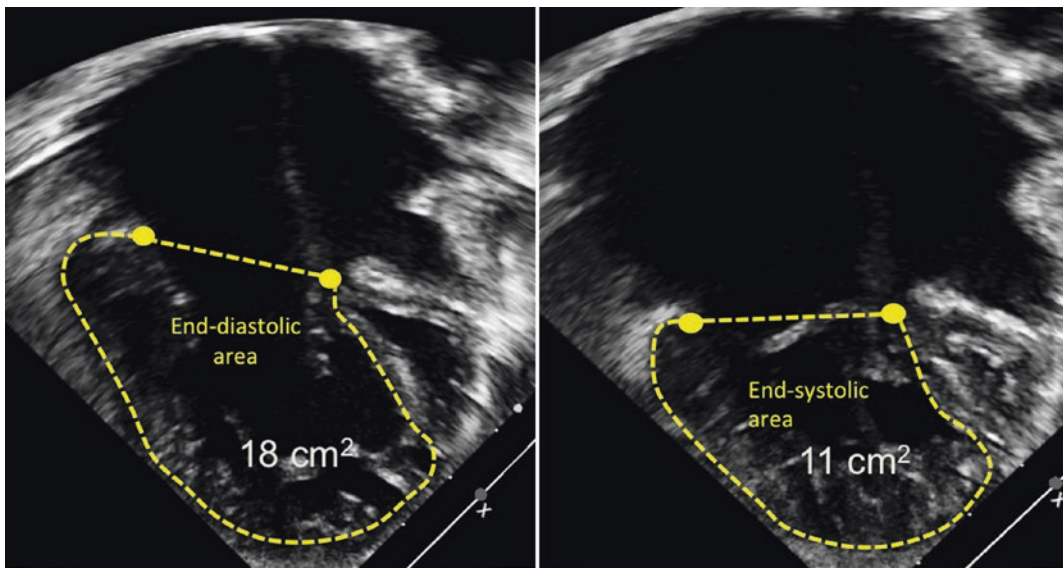

Fig. 9.5 Measurement of fractional area change in patient with hypoplastic left heart syndrome. From the apical RV-centric view, RV end diastolic area (EDA) and end systole areas (ESA) are measured and FAC is calculated by calculating (EDA-ESA)/EDA. For this patient FAC was estimated as 39% which is within normal rage

As for EF, trabeculations are included in the FAC measurement. FAC correlates well with RV EF [20] and for adults FAC >35% is considered normal. No good, normative pediatric data have been established. Our data in newborns suggest that in the neonatal period FAC is lower compared to the adult population with a mean value of 26% for the apical 4-chamber FAC. In this study FAC was also measured from the apical RV 3-chamber view, which resulted in higher values (mean 3-C FAC was 39%). More reference data are required but it is our recommendation to include RV FAC as a standard measurement for assessing RV function.

Tricuspid annular planar systolic excursion or *TAPSE* measures systolic longitudinal displacement of the lateral tricuspid annulus from the RV-centric RV view. It can be measured by placing an M-mode cursor through the tricuspid lateral annulus and measuring the distance the annulus travels from end-diastole to end-systole. The M-mode cursor needs to be well aligned with the longitudinal motion often requiring sliding the probe more rightward and lateral. To standardize timing of the measurement and improve the reproducibility, a color tissue Doppler M-mode tracing can be obtained (Fig. 9.6). TAPSE is a parameter assessing RV longitudinal function. If RV dysfunction is global, it correlates well with RVEF but in case of regional RV dysfunction the correlation between TAPSE and RVEF or FAC is much lower. In TOF patients post-repair for instance, TAPSE correlates only moderately with global RVEF as RVOT and anterior wall dysfunction are not captured by TAPSE [21]. In adults, normal TAPSE is >17 mm. Normal values and z-scores have been published for children and infants [22, 23]. In adults with pulmonary hypertension TAPSE has high prognostic value while in children with pulmonary arterial hypertension the prognostic value of TAPSE is less well established [24, 25]. Measurement of TAPSE is influenced by cardiac translation, RV-LV interactions and tricuspid valve regurgitation.

Tricuspid lateral annulus systolic velocity (s') as measured by tissue Doppler imaging (TDI) is another measurement of RV longitudinal function that is easy to obtain and is highly-reproducible (Fig. 9.7). As for TAPSE alignment with longitudinal motion of the RV lateral wall is important and should be optimized. The pulsed-Doppler cursor is placed at the tricuspid annulus in adults and just below the annulus for children. In adults s' >9.5 cm/s is considered normal. Normal data for children have been obtained including z-scores [26, 27]. TDI-derived s' is a

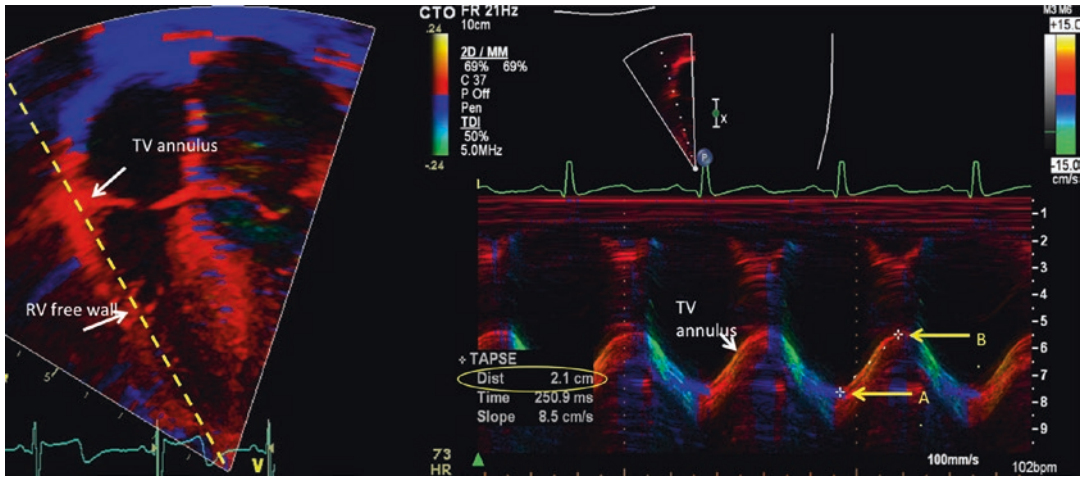

Fig. 9.6 Tricuspid Annular Planar Systolic Excursion (TAPSE) can be measured using the RV-centric apical 4-chamber view. Place the cursor parallel to the RV free wall and activate TDI colour mapping. Activate M-mode and obtain a tracing of the TV annulus. Measure TAPSE from the end-diastolic point (A) to the maximal excursion point at end-systole (B). TAPSE is the distance between A and B in centimeters. The use of TDI colour mapping, though not required, helps define the systolic timing (transition *blue-red* is start systole; transition *red-blue* is end systole. TAPSE is measured between the two points

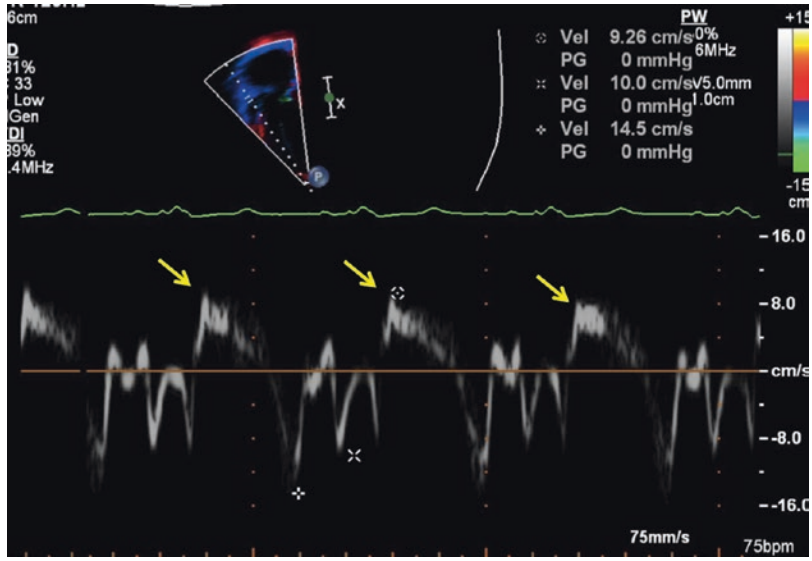

Fig. 9.7 Tissue Doppler imaging of the tricuspid lateral annulus. Peak systolic velocity is measured (*arrows*). This patient after tetralogy of Fallot repair had preserved s' but reduced RV EF (35%) as measured by MRI. This is likely related to the effect of RVOT dysfunction on global EF

regional parameter assessing RV longitudinal function. In the case of global RV dysfunction, s' can be reduced but is influenced by cardiac translation, tricuspid regurgitation, ventricular interactions and loading conditions (changes in preload and afterload). Typically after cardiac surgery RV s'-values are reduced and remain reduced during follow-up while FAC often normalizes. This is possibly related to reduced cardiac translation after opening the pericardium and the effect of adhesions on RV longitudinal motion. When regional dysfunction is present, s' also does not correlate well with global RVEF. This was nicely demonstrated in patients after tetralogy of Fallot repair where the relationship between s' and RVEF as measured by MRI was influenced by RVOT function [28]. All these factors have to be taken into consideration when interpreting RV s'-values. RV s'-velocities have been reported to be reduced after cardiac surgery and heart transplantation while RV ejection fraction is within normal range [29]. In these conditions RV s' does not seem to represent global RV function.

RV longitudinal strain and strain rate can be measured from the apical 4-chamber view using speckle-tracking echocardiography. Typically RV strain and strain rate are calculated in the RV free wall as the interventricular septal values are generally used for LV longitudinal strain values although the septum should be considered an important interface between RV and LV (Fig. 9.8). Typically end-systolic strain values in the RV basal, mid and apical RV free wall segments are measured. Most strain software applications are not specifically designed to measure RV strain, and differences between values obtained using different vendors have been documented. In adults average lateral wall end-systolic longitudinal strain values < -20 are considered normal. As the negative value can be confusing, this corresponds to an absolute value of >20. Limited normal RV strain data are available in children. Using the apical RV 2-chamber and 3-chamber views, RV longitudinal strain values can also be obtained in the RV inferior and posterior walls [30, 31]. The anterior wall and right ventricular outflow tract are more difficult to track and feasibility of obtaining strain measurements in these RV segments is low even in children with good imaging windows. Thus a 'global RV strain' value is more difficult to obtain although different wall segments can be evaluated.

RV longitudinal strain measurements have been investigated in different diseases and have been proven to add additional prognostic information in patients with heart failure [32, 33], pulmonary hypertension in adults [34–36] and also in children [37], ischemic heart disease [38–40] and aortic stenosis [32, 41]. In congenital heart dis-

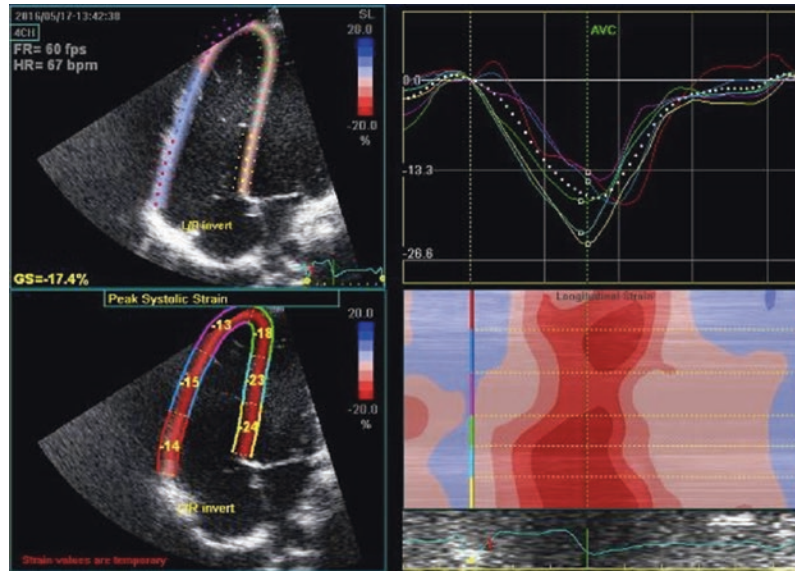

Fig. 9.8 Longitudinal RV strain measured by speckle-tracking echocardiography in patient after TOF repair. The RV is significantly dilated and longitudinal strain values are significantly reduced in the RV lateral wall. Average RV longitudinal strain value is −14 while an average value <−20 is normal

ease, different studies have looked at RV longitudinal function using strain imaging. After tetralogy of Fallot repair, RV longitudinal strain and strain rate are reduced with the RV apical segments more significantly affected compared to the RV basal parts. The reduction in RV longitudinal strain is associated with exercise capacity in children [42–46] and both RV and LV longitudinal strain values were demonstrated to have prognostic value in adults after TOF repair [47, 48]. Right bundle branch block is common after tetralogy of Fallot repair and causes dyssynchronous RV contraction with early septal activation and delayed RV lateral wall contraction [49]. In adults, biventricular pacing has been suggested to be potentially beneficial in post-operative tetralogy patients with RV dysfunction and right bundle branch block [50–52]. Strain imaging has also been proven to provide additional prognostic information for assessment of systemic RV function such as after atrial switch for transposition of the great arteries [53] and after palliative surgery for hypoplastic left heart syndrome [54]. In both conditions it was observed that adequate RV remodelling and adaptation involved a transition in RV mechanics from a predominantly longitudinal to a more circumferential contraction pattern [55]. Further standardization and optimization of RV strain measurements are required for routine clinical utilization but it can be expected to become part of routine RV functional assessment for selected patient groups. More recently three-dimensional strain methods have been proposed for assessing RV global longitudinal strain [56–58]. These methods could provide simultaneous assessment of RV volumes, ejection fraction and mechanics.

Assessment of RV Diastolic Function

Assessment of RV diastolic function is even more challenging than assessment of LV diastolic function. Guideline recommendations include assessment of IVC diameter and collapse with respiration, tricuspid inflow patterns, tricuspid annulus tissue Doppler velocities (e') and E/e'-ratio [2]. Restrictive RV physiology is suggested by late antegrade flow in the pulmonary artery during atrial contraction. This can be measured by pulsed wave velocity with a sample volume placed midway between the pulmonary valve and the bifurcation of the main pulmonary artery and assessing for the presence of late

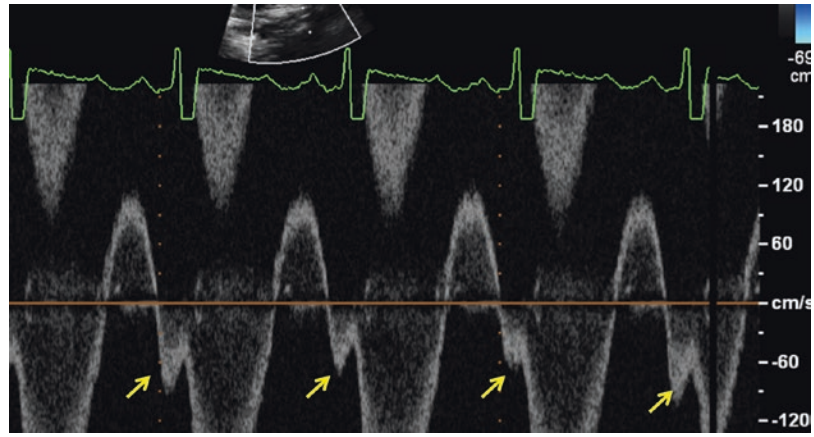

Fig. 9.9 Restrictive RV physiology in post-operative tetralogy of Fallot patient. Pulsed wave spectral Doppler trace is obtained between the pulmonary valve leaflets. Late diastolic antegrade forward flow is observed throughout respiration suggestive of RV end-diastolic pressure exceeding pulmonary diastolic pressure

diastolic antegrade flow thoughout inspiration and expiration (Fig. 9.9). There is poor validation of RV diastolic functional assessment especially in the pediatric age group.

Conclusion

Quantitative assessment of RV size and function should be part of every echocardiographic examination performed in patients in whom RV function can be affected, especially in patients with pulmonary hypertension or patients with congenital heart disease affecting the RV. Two-dimensional measurements of dimensions and RV areas provide simple tools for screening. More accurate assessment of RV size can be performed using three-dimensional echocardiography with the caveat that echocardiographic volumes are lower compared to MRI volumes. For functional RV assessment, measurement of FAC, TAPSE and s' wave velocity also are good screening tools. Improvements in echocardiographic equipment and analysis software will hopefully result in 3-D and RV strain imaging becoming more easily accessible techniques for the assessment of RV size and function.

References

1. Lang RM, Badano LP, Mor-Avi V, Afilalo J, Armstrong A, Ernande L, et al. Recommendations for cardiac chamber quantification by echocardiography in adults: an update from the American Society of Echocardiography and the European Association of Cardiovascular Imaging. Eur Heart J Cardiovasc Imaging. 2015;16(3):233–70.
2. Rudski LG, Lai WW, Afilalo J, Hua L, Handschumacher MD, Chandrasekaran K, et al. Guidelines for the echocardiographic assessment of the right heart in adults: a report from the American Society of Echocardiography endorsed by the European Association of Echocardiography, a registered branch of the European Society of Cardiology, and the Canadian Society of Echocardiography. J Am Soc Echocardiogr. 2010;23(7):685–713. quiz 86–8.
3. Ling LF, Obuchowski NA, Rodriguez L, Popovic Z, Kwon D, Marwick TH. Accuracy and interobserver concordance of echocardiographic assessment of right ventricular size and systolic function: a quality control exercise. J Am Soc Echocardiogr. 2012;25(7):709–13.
4. Bellsham-Revell HR, Simpson JM, Miller OI, Bell AJ. Subjective evaluation of right ventricular systolic function in hypoplastic left heart syndrome: how accurate is it? J Am Soc Echocardiogr. 2013;26(1):52–6.
5. Mertens LL, Friedberg MK. Imaging the right ventricle—current state of the art. Nat Rev Cardiol. 2010;7(10):551–63.
6. Helbing WA, Bosch HG, Maliepaard C, Rebergen SA, van der Geest RJ, Hansen B, et al. Comparison of echocardiographic methods with magnetic resonance imaging for assessment of right ventricular function in children. Am J Cardiol. 1995;76(8):589–94.
7. Sheehan FH, Ge S, Vick GW 3rd, Urnes K, Kerwin WS, Bolson EL, et al. Three-dimensional shape analysis of right ventricular remodeling in repaired tetralogy of Fallot. Am J Cardiol. 2008;101(1):107–13.
8. Lang RM, Bierig M, Devereux RB, Flachskampf FA, Foster E, Pellikka PA, et al. Recommendations for chamber quantification: a report from the American Society of Echocardiography's Guidelines and Standards Committee and the Chamber Quantification Writing Group, developed in conjunction with the European Association of Echocardiography, a branch of the European Society of Cardiology. J Am Soc Echocardiogr. 2005;18(12):1440–63.

9. Lopez L, Colan SD, Frommelt PC, Ensing GJ, Kendall K, Younoszai AK, et al. Recommendations for quantification methods during the performance of a pediatric echocardiogram: a report from the Pediatric Measurements Writing Group of the American Society of Echocardiography Pediatric and Congenital Heart Disease Council. J Am Soc Echocardiogr. 2010;23(5):465–95. quiz 576–7.
10. Zervan K, Male C, Benesch T, Salzer-Muhar U. Ventricular interaction in children after repair of tetralogy of Fallot: a longitudinal echocardiographic study. Eur J Echocardiogr. 2009;10(5):641–6.
11. Lai WW, Gauvreau K, Rivera ES, Saleeb S, Powell AJ, Geva T. Accuracy of guideline recommendations for two-dimensional quantification of the right ventricle by echocardiography. Int J Cardiovasc Imaging. 2008;24(7):691–8.
12. Greutmann M, Tobler D, Biaggi P, Mah ML, Crean A, Oechslin EN, et al. Echocardiography for assessment of right ventricular volumes revisited: a cardiac magnetic resonance comparison study in adults with repaired tetralogy of Fallot. J Am Soc Echocardiogr. 2010;23(9):905–11.
13. Alghamdi MH, Grosse-Wortmann L, Ahmad N, Mertens L, Friedberg MK. Can simple echocardiographic measures reduce the number of cardiac magnetic resonance imaging studies to diagnose right ventricular enlargement in congenital heart disease? J Am Soc Echocardiogr. 2012;25(5):518–23.
14. Jain A, Mohamed A, El-Khuffash A, Connelly KA, Dallaire F, Jankov RP, et al. A comprehensive echocardiographic protocol for assessing neonatal right ventricular dimensions and function in the transitional period: normative data and z scores. J Am Soc Echocardiogr. 2014;27(12):1293–304.
15. Khoo NS, Young A, Occleshaw C, Cowan B, Zeng IS, Gentles TL. Assessments of right ventricular volume and function using three-dimensional echocardiography in older children and adults with congenital heart disease: comparison with cardiac magnetic resonance imaging. J Am Soc Echocardiogr. 2009;22(11):1279–88.
16. Dragulescu A, Grosse-Wortmann L, Fackoury C, Mertens L. Echocardiographic assessment of right ventricular volumes: a comparison of different techniques in children after surgical repair of tetralogy of Fallot. Eur Heart J Cardiovasc Imaging. 2012;13(7):596–604.
17. Grewal J, Majdalany D, Syed I, Pellikka P, Warnes CA. Three-dimensional echocardiographic assessment of right ventricular volume and function in adult patients with congenital heart disease: comparison with magnetic resonance imaging. J Am Soc Echocardiogr. 2010;23(2):127–33.
18. van der Zwaan HB, Geleijnse ML, McGhie JS, Boersma E, Helbing WA, Meijboom FJ, et al. Right ventricular quantification in clinical practice: two-dimensional vs. three-dimensional echocardiography compared with cardiac magnetic resonance imaging. Eur J Echocardiogr. 2011;12(9):656–64.
19. Dragulescu A, Grosse-Wortmann L, Fackoury C, Riffle S, Waiss M, Jaeggi E, et al. Echocardiographic assessment of right ventricular volumes after surgical repair of tetralogy of Fallot: clinical validation of a new echocardiographic method. J Am Soc Echocardiogr. 2011;24(11):1191–8.
20. Anavekar NS, Gerson D, Skali H, Kwong RY, Yucel EK, Solomon SD. Two-dimensional assessment of right ventricular function: an echocardiographic-MRI correlative study. Echocardiography. 2007;24(5):452–6.
21. Koestenberger M, Nagel B, Avian A, Ravekes W, Sorantin E, Cvirn G, et al. Systolic right ventricular function in children and young adults with pulmonary artery hypertension secondary to congenital heart disease and tetralogy of Fallot: tricuspid annular plane systolic excursion (TAPSE) and magnetic resonance imaging data. Congenit Heart Dis. 2012;7(3):250–8.
22. Koestenberger M, Nagel B, Ravekes W, Urlesberger B, Raith W, Avian A, et al. Systolic right ventricular function in preterm and term neonates: reference values of the tricuspid annular plane systolic excursion (TAPSE) in 258 patients and calculation of Z-score values. Neonatology. 2011;100(1):85–92.
23. Koestenberger M, Ravekes W, Everett AD, Stueger HP, Heinzl B, Gamillscheg A, et al. Right ventricular function in infants, children and adolescents: reference values of the tricuspid annular plane systolic excursion (TAPSE) in 640 healthy patients and calculation of z score values. J Am Soc Echocardiogr. 2009;22(6):715–9.
24. Hauck A, Guo R, Ivy DD, Younoszai A. Tricuspid annular plane systolic excursion is preserved in young patients with pulmonary hypertension except when associated with repaired congenital heart disease. Eur Heart J Cardiovasc Imaging. 2016;18(4):459–66.
25. Kassem E, Humpl T, Friedberg MK. Prognostic significance of 2-dimensional, M-mode, and Doppler echo indices of right ventricular function in children with pulmonary arterial hypertension. Am Heart J. 2013;165(6):1024–31.
26. Dallaire F, Slorach C, Hui W, Sarkola T, Friedberg MK, Bradley TJ, et al. Reference values for pulse wave Doppler and tissue Doppler imaging in pediatric echocardiography. Circ Cardiovasc Imaging. 2015;8(2):e002167.
27. Eidem BW, McMahon CJ, Cohen RR, Wu J, Finkelshteyn I, Kovalchin JP, et al. Impact of cardiac growth on Doppler tissue imaging velocities: a study in healthy children. J Am Soc Echocardiogr. 2004;17(3):212–21.
28. Kutty S, Zhou J, Gauvreau K, Trincado C, Powell AJ, Geva T. Regional dysfunction of the right ventricular outflow tract reduces the accuracy of Doppler tissue imaging assessment of global right ventricular systolic function in patients with repaired tetralogy of Fallot. J Am Soc Echocardiogr. 2011;24(6):637–43.
29. Raina A, Vaidya A, Gertz ZM, Susan C, Forfia PR. Marked changes in right ventricular contractile pattern after cardiothoracic surgery: implications for post-surgical assessment of right ventricular function. J Heart Lung Transplant. 2013;32(8):777–83.

30. Forsha D, Risum N, Kropf PA, Rajagopal S, Smith PB, Kanter RJ, et al. Right ventricular mechanics using a novel comprehensive three-view echocardiographic strain analysis in a normal population. J Am Soc Echocardiogr. 2014;27(4):413–22.
31. Rajagopal S, Forsha DE, Risum N, Hornik CP, Poms AD, Fortin TA, et al. Comprehensive assessment of right ventricular function in patients with pulmonary hypertension with global longitudinal peak systolic strain derived from multiple right ventricular views. J Am Soc Echocardiogr. 2014;27(6):657–65. e3
32. Galli E, Guirette Y, Feneon D, Daudin M, Fournet M, Leguerrier A, et al. Prevalence and prognostic value of right ventricular dysfunction in severe aortic stenosis. Eur Heart J Cardiovasc Imaging. 2015;16(5):531–8.
33. Motoki H, Borowski AG, Shrestha K, Hu B, Kusunose K, Troughton RW, et al. Right ventricular global longitudinal strain provides prognostic value incremental to left ventricular ejection fraction in patients with heart failure. J Am Soc Echocardiogr. 2014;27(7):726–32.
34. Haeck ML, Scherptong RW, Marsan NA, Holman ER, Schalij MJ, Bax JJ, et al. Prognostic value of right ventricular longitudinal peak systolic strain in patients with pulmonary hypertension. Circ Cardiovasc Imaging. 2012;5(5):628–36.
35. Park JH, Park MM, Farha S, Sharp J, Lundgrin E, Comhair S, et al. Impaired global right ventricular longitudinal strain predicts long-term adverse outcomes in patients with pulmonary arterial hypertension. J Cardiovasc Ultrasound. 2015;23(2):91–9.
36. van Kessel M, Seaton D, Chan J, Yamada A, Kermeen F, Butler T, et al. Prognostic value of right ventricular free wall strain in pulmonary hypertension patients with pseudo-normalized tricuspid annular plane systolic excursion values. Int J Cardiovasc Imaging. 2016;32(6):905–12.
37. Okumura K, Humpl T, Dragulescu A, Mertens L, Friedberg MK. Longitudinal assessment of right ventricular myocardial strain in relation to transplant-free survival in children with idiopathic pulmonary hypertension. J Am Soc Echocardiogr. 2014;27(12):1344–51.
38. Antoni ML, Scherptong RW, Atary JZ, Boersma E, Holman ER, van der Wall EE, et al. Prognostic value of right ventricular function in patients after acute myocardial infarction treated with primary percutaneous coronary intervention. Circ Cardiovasc Imaging. 2010;3(3):264–71.
39. Chang WT, Liu YW, Liu PY, Chen JY, Lee CH, Li YH, et al. Association of decreased right ventricular strain with worse survival in non-acute coronary syndrome angina. J Am Soc Echocardiogr. 2016;29(4):350–8.e4.
40. Park SJ, Park JH, Lee HS, Kim MS, Park YK, Park Y, et al. Impaired RV global longitudinal strain is associated with poor long-term clinical outcomes in patients with acute inferior STEMI. JACC Cardiovasc Imaging. 2015;8(2):161–9.
41. Dahou A, Clavel MA, Capoulade R, Bartko PE, Magne J, Mundigler G, et al. Right ventricular longitudinal strain for risk stratification in low-flow, low-gradient aortic stenosis with low ejection fraction. Heart. 2016;102(7):548–54.
42. Weidemann F, Eyskens B, Mertens L, Dommke C, Kowalski M, Simmons L, et al. Quantification of regional right and left ventricular function by ultrasonic strain rate and strain indexes after surgical repair of tetralogy of Fallot. Am J Cardiol. 2002;90(2):133–8.
43. Eyskens B, Brown SC, Claus P, Dymarkowski S, Gewillig M, Bogaert J, et al. The influence of pulmonary regurgitation on regional right ventricular function in children after surgical repair of tetralogy of Fallot. Eur J Echocardiogr. 2010;11(4):341–5.
44. Dragulescu A, Grosse-Wortmann L, Redington A, Friedberg MK, Mertens L. Differential effect of right ventricular dilatation on myocardial deformation in patients with atrial septal defects and patients after tetralogy of Fallot repair. Int J Cardiol. 2012;168(2):803–10.
45. Alghamdi MH, Mertens L, Lee W, Yoo SJ, Grosse-Wortmann L. Longitudinal right ventricular function is a better predictor of right ventricular contribution to exercise performance than global or outflow tract ejection fraction in tetralogy of Fallot: a combined echocardiography and magnetic resonance study. Eur Heart J Cardiovasc Imaging. 2013;14(3):235–9.
46. Friedberg MK, Fernandes FP, Roche SL, Slorach C, Grosse-Wortmann L, Manlhiot C, et al. Relation of right ventricular mechanics to exercise tolerance in children after tetralogy of Fallot repair. Am Heart J. 2013;165(4):551–7.
47. Diller GP, Kempny A, Liodakis E, Alonso-Gonzalez R, Inuzuka R, Uebing A, et al. Left ventricular longitudinal function predicts life-threatening ventricular arrhythmia and death in adults with repaired tetralogy of fallot. Circulation. 2012;125(20):2440–6.
48. Orwat S, Diller GP, Kempny A, Radke R, Peters B, Kuhne T, et al. Myocardial deformation parameters predict outcome in patients with repaired tetralogy of Fallot. Heart. 2016;102(3):209–15.
49. Hui W, Slorach C, Dragulescu A, Mertens L, Bijnens B, Friedberg MK. Mechanisms of right ventricular electromechanical dyssynchrony and mechanical inefficiency in children after repair of tetralogy of fallot. Circ Cardiovasc Imaging. 2014;7(4):610–8.
50. Thambo JB, Dos Santos P, De Guillebon M, Roubertie F, Labrousse L, Sacher F, et al. Biventricular stimulation improves right and left ventricular function after tetralogy of Fallot repair: acute animal and clinical studies. Heart Rhythm. 2010;7(3):344–50.
51. Thambo JB, De Guillebon M, Dos Santos P, Xhaet O, Ploux S, Iriart X, et al. Electrical dyssynchrony and resynchronization in tetralogy of Fallot. Heart Rhythm. 2011;8(6):909–14.
52. Thambo JB, De Guillebon M, Xhaet O, Dos Santos P, Roubertie F, Labrousse L, et al. Biventricular pac-

ing in patients with Tetralogy of Fallot: non-invasive epicardial mapping and clinical impact. Int J Cardiol. 2013;163(2):170–4.
53. Kalogeropoulos AP, Deka A, Border W, Pernetz MA, Georgiopoulou VV, Kiani J, et al. Right ventricular function with standard and speckle-tracking echocardiography and clinical events in adults with D-transposition of the great arteries post atrial switch. J Am Soc Echocardiogr. 2012;25(3):304–12.
54. Khoo NS, Smallhorn JF, Kaneko S, Kutty S, Altamirano L, Tham EB. The assessment of atrial function in single ventricle hearts from birth to Fontan: a speckle-tracking study by using strain and strain rate. J Am Soc Echocardiogr. 2013;26(7):756–64.
55. Pettersen E, Helle-Valle T, Edvardsen T, Lindberg H, Smith HJ, Smevik B, et al. Contraction pattern of the systemic right ventricle shift from longitudinal to circumferential shortening and absent global ventricular torsion. J Am Coll Cardiol. 2007;49(25):2450–6.
56. Atsumi A, Seo Y, Ishizu T, Nakamura A, Enomoto Y, Harimura Y, et al. Right ventricular deformation analyses using a three-dimensional speckle-tracking echocardiographic system specialized for the right ventricle. J Am Soc Echocardiogr. 2016;29(5):402–11.e2.
57. Ryo K, Goda A, Onishi T, Delgado-Montero A, Tayal B, Champion HC, et al. Characterization of right ventricular remodeling in pulmonary hypertension associated with patient outcomes by 3-dimensional wall motion tracking echocardiography. Circ Cardiovasc Imaging. 2015;8(6):pii: e003176.
58. Smith BC, Dobson G, Dawson D, Charalampopoulos A, Grapsa J, Nihoyannopoulos P. Three-dimensional speckle tracking of the right ventricle: toward optimal quantification of right ventricular dysfunction in pulmonary hypertension. J Am Coll Cardiol. 2014;64(1):41–51.

Magnetic Resonance Assessment of RV Remodeling and Function

10

Lars Grosse-Wortmann and Adam L. Dorfman

Abstract

Cardiac magnetic resonance imaging (CMR) provides unique opportunities for the assessment of right ventricular (RV) geometry, function, and myocardial structure. These allow CMR to play a pivotal role in diagnosis, monitoring, and decision-making in pediatric and congenital cardiology. CMR is the reference standard for quantification of RV volume, ejection fraction and mass. Phase contrast flow velocity mapping by CMR offers an accurate measurement of pulmonary blood flow and of the degree of pulmonary regurgitation in the presence of pulmonary valvar insufficiency, for example after Tetralogy of Fallot repair. More recently, CMR has been employed for the quantification of RV strain, rotation, and torsion. CMR allows for the complete visualization of the RV as compared to echocardiography, but is hampered by inferior temporal resolution, particular for the assessment of diastolic function. Scar imaging with late gadolinium enhancement CMR is established as a risk predictor in certain types of congenital and acquired heart disease, although it can be difficult to detect scarring with certainty in the thin walled RV myocardium. For the same reason, the assessment of diffuse myocardial fibrosis in the RV by CMR T1 mapping is challenging.

In this chapter we describe the technical underpinnings of CMR for the RV, outline its utility and limitations in pediatric and congenital heart disease, and provide examples on how CMR contributes to clinical decision making.

Electronic Supplementary Material The online version of this chapter (doi:10.1007/978-3-319-67096-6_10) contains supplementary material, which is available to authorized users.

L. Grosse-Wortmann (✉)
Paediatric Cardiology, Labatt Family Heart Centre, Hospital for Sick Children, 555 University Ave, Toronto, ON M1G 1X8, Canada
e-mail: lars.grosse-wortmann@sickkids.ca

A.L. Dorfman
University of Michigan, Congenital Heart Center, Department of Pediatrics, C.S. Mott Children's Hospital, University of Michigan, 1540 E. Hospital Drive, Ann Arbor, MI 48109, USA

M.K. Friedberg, A.N. Redington (eds.), *Right Ventricular Physiology, Adaptation and Failure in Congenital and Acquired Heart Disease*, https://doi.org/10.1007/978-3-319-67096-6_10

Keywords

Right ventricle • Cardiac magnetic resonance imaging • Ventricular volume • Contractility • Myocardial deformation imaging • Right ventricular outflow tract • Tissue characterization • Myocardial fibrosis

Introduction

One of the pivotal strengths of cardiac magnetic resonance imaging (CMR) is the ability to accurately and reproducibly quantify the size and function of the right ventricle (RV) [1]. Using techniques that include standard cine imaging, myocardial deformation and tissue characterization, CMR affords novel insights into the structure, myocardial composition, and function of the RV. In clinical practice, CMR has become the gold standard for quantification of RV volumes and ejection fraction. This asset is of enormous clinical importance in the care of patients with congenital as well as acquired pediatric heart disease. For example, in repaired tetralogy of Fallot (rTOF) and pulmonary hypertension (PHTN), RV size, ejection fraction, and mass by CMR have been linked to outcomes and aid in clinical decision-making [2–4].

Imaging Techniques for Assessing RV Size and Ejection Fraction

The current CMR technique of choice for the quantification of RV size and systolic function is by cine imaging using steady state free precession techniques (SSFP, Fig. 10.1; Videos 10.1a and 10.1b). A variety of modifications, including

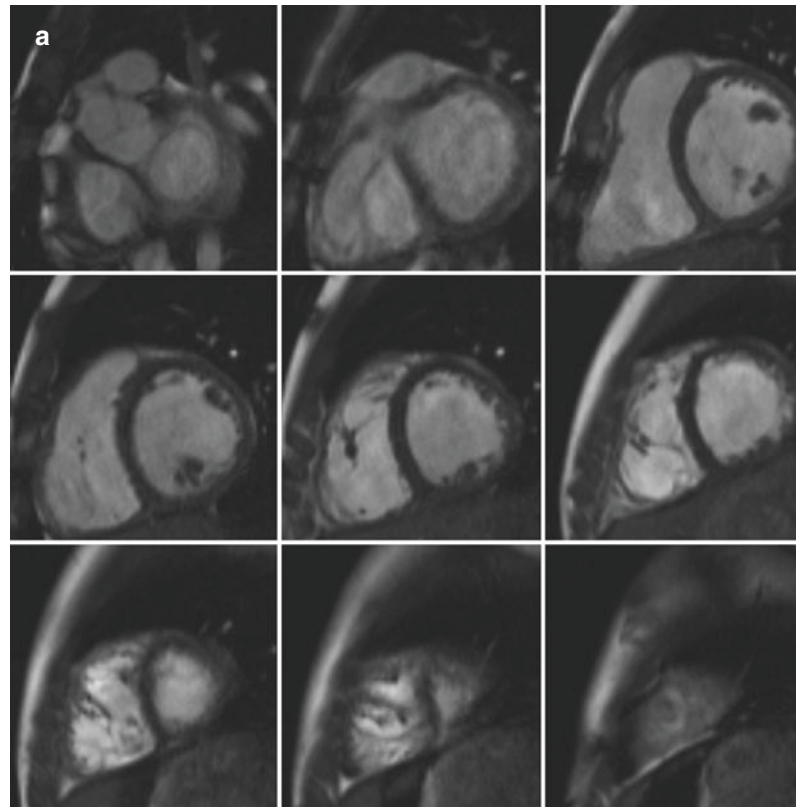

Fig. 10.1 Short axis (**a**) and axial stack (**b**) of steady state free precession images at end-diastole in a patient with Tetralogy of Fallot. See also Videos 10.1a and 10.1b

Fig. 10.1 (continued)

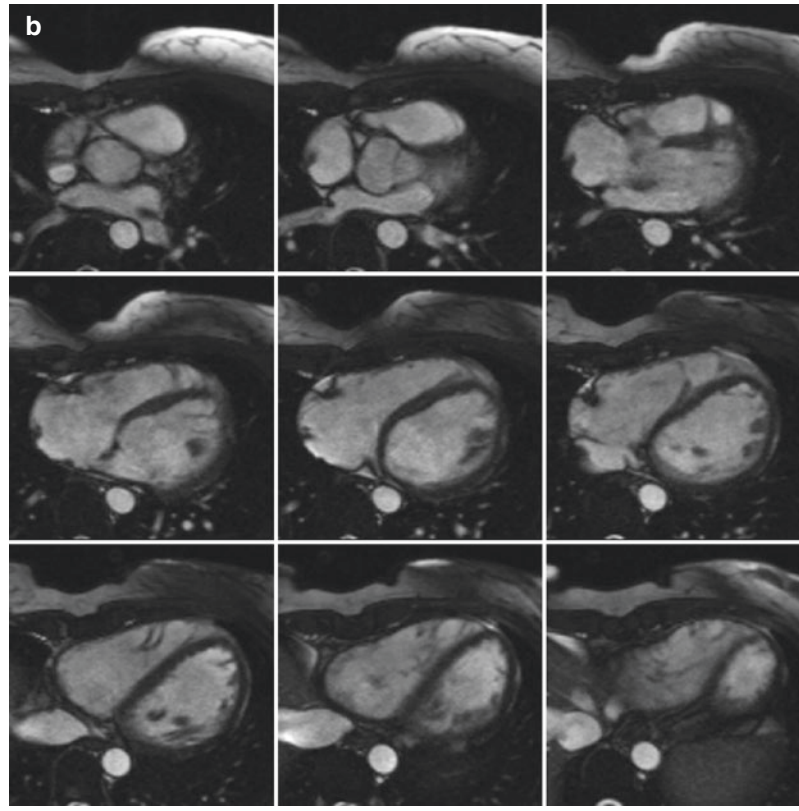

parallel imaging and partial Fourier imaging, are routinely applied to accelerate the imaging acquisition, allowing for shorter breathhold durations. The temporal resolution should be adjusted to allow for at least 20–25 true images per cardiac cycle, not through interpolation. Decreasing temporal resolution results in faster imaging time but risks missing the true maximum and minimum ventricular volumes at end- diastole and -systole, respectively.

For RV volumetry, a stack of parallel slices is acquired that cover the ventricle. Theoretically, this can be done in any plane, as long as the entire ventricle is included. In clinical practice, the RV is measured from either a short axis stack or an axial stack of images. Some studies have found that measuring the RV in the axial plane has better reproducibility [5] while others showed no significant difference between the orientations [6], and both approaches remain in wide clinical use. In contrast to ventricular volume measurements by echocardiography, cine CMR is not a real time technique; end-systole and end-diastole are not defined based on ECG, but on the smallest and largest ventricular sizes, respectively. By this definition, in patients with rTOF, who typically have complete right bundle branch block, RV end-systole often occurs later than LV end-systole due to delayed RV activation.

During post-processing, the area encompassed by the RV endocardium is quantified in each slice, by manually tracing the endocardial-blood pool border. This area is multiplied by the sum of the slice thickness and gap between slices, using the method of disks. No assumptions are made about the RV luminal area, as opposed to Simpson's method in echocardiography, which is based on the RV diameter in one or two dimensions. However, contouring the endocardial-blood border in the heavily trabeculated RV can be challenging (Fig. 10.2a), as numerous muscle bundles cannot practically be excluded from the blood pool and are therefore included in the ventricular volume rather than in its mass. Alternatively, it is

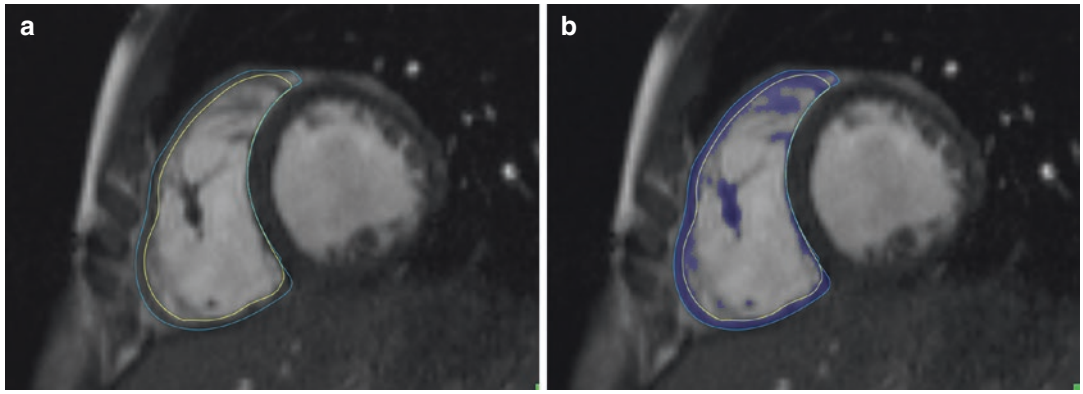

Fig. 10.2 Postprocessing of right ventricular volume and mass in short axis at end-diastole. The endocardial border can be defined either by contouring (**a**, *yellow line*) or by thresholding (**b**). Note how by thresholding the trabeculations in the right ventricular cavity are included in the muscle mass

possible to detect myocardium by applying 'thresholding' (Fig. 10.2b), via signal intensity differences between the blood pool and the myocardium. Using this approach, even complex trabeculations are readily included in the ventricular mass. However, measurements performed with thresholding differ from published normative data, most of which were generated using the classic contouring techniques, so that new normative data sets are necessary.

The greatest variability in the quantification of RV volumes is introduced by contouring slices around the tricuspid and pulmonary valve annuli. A cine stack in the axial orientation is more 'vulnerable' to inaccuracies around the pulmonary valve, while it is more difficult to identify the border between atrium and ventricle in the short axis orientation. Neither the tricuspid nor the pulmonary valve annulus is entirely 'flat' and, therefore, part of the imaging slice will be on the 'ventricular side' while part will be on the 'atrial side'. Nonetheless, in the short axis orientation the imaging plane should be prescribed as parallel to the valve annulus as possible, using the double oblique technique [6, 7]. In addition, most quantification software packages offer a cross-referencing function, in which the location of the short axis slice can be visualized in the vertical and horizontal long axis cine images and vice versa. Identifying the location of the pulmonary valve annulus can be particularly difficult in individuals with rTOF, particularly after transannular patch repair when there is little residual pulmonary valve tissue to visualize. In this case, knowledge of the anatomy, including the expected location of the pulmonary annulus, is helpful in obtaining accurate measurements.

There are several published sets of normative data for RV size and ejection fraction [8–11]. However, all such data in children are limited by low sample sizes. For smaller children who typically require sedation or anesthesia for MRI scanning normal values are nearly absent [9]. When using a normative dataset for comparison, it is important to ensure that scanning and postprocessing techniques are similar (e.g.; axial vs. short axis imaging for RV volumetry, use of sedation, contouring vs. thresholding) and that the patient population is consistent with that in the reference used (e.g.; age, gender).

In general, 2-D echo measurements of the RV do not correlate well with volume measurements by CMR [12]. There are a number of reasons for this discrepancy, including the fact that most echocardiographic metrics of RV systolic function are based on longitudinal shortening in the inlet and apical trabecular portions. Many patients with rTOF, for example, have a dysfunctional infundibulum, which these methods do not capture (Fig. 10.3). 3-D echo has been more promising, with better correlation but consistent underestimation of right ventricular volume compared to CMR, both in congenital heart disease and other disease states [13, 14]. Knowledge-

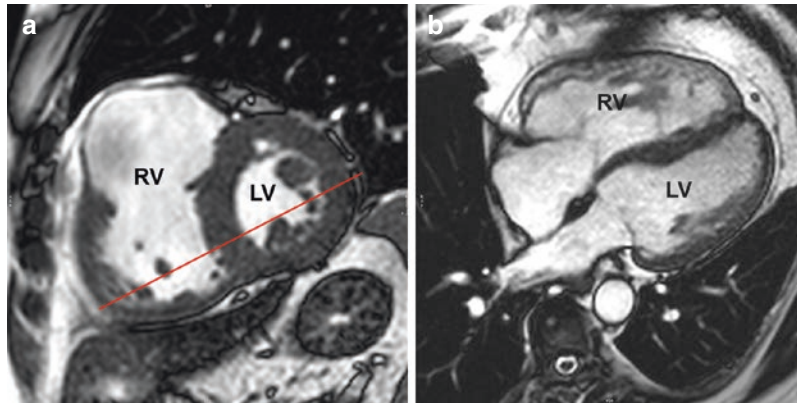

Fig. 10.3 Cardiac magnetic resonance steady state free precession image of the right and left ventricles in short axis (**a**) and four chamber view (**b**). The right ventricle is dilated. Note the dilated and thin anterior wall of the infundibulum. The *red line* on the short axis image delineates the four chamber plane. Note that the four chamber view does not include the dyskinetic infundibulum. *LV* left ventricle, *RV* right ventricle

based reconstruction of 2-D echo data into a 3-D data set, using pre-defined landmarks and a 'library' of lesion-specific RV shapes, has been compared to CMR in rTOF patients with good reproducibility and good correlation of volume measurements [15].

Exact quantification of RV size and volumes is important in a variety of congenital heart lesions, most commonly in TOF, where RV volumes feature prominently both in risk prediction and in decision making regarding timing of pulmonary valve replacement [16–19]. Other types of congenital heart disease in which CMR volumetry is commonly applied include functionally single ventricles with a dominant RV [20], subsystemic RVs in transposition of the great arteries [21] and Ebstein's anomaly of the tricuspid valve [22]. In addition, CMR measurement of RV ejection fraction in pediatric pulmonary hypertension is predictive of survival [3]. In arrhythmogenic right ventricular cardiomyopathy, RV ejection fraction and end-diastolic volume are criteria in the diagnostic score [23, 24].

Regional and Compartmental Function of the Right Ventricle

While ejection fraction provides a useful gauge for global systolic function, regional variations in contractility have pathophysiological, diagnostic, and even prognostic significance. In ARVC for example [24], a positive imaging criterion is conditional on the presence of regional wall motion abnormalities (RWMAs) within the RV. In a recent study of children under investigation for ARVC [23], patients with greater certainty for ARVC as per the revised Task Force Criteria [24] were not only more likely to have RWMAs, but also had more severe RWMAs. Diagnosing subtle RWMAs, even with the superior visualization of the anterior wall of the RV provided by CMR, is challenging, with considerable interobserver variability [23].

The abilities of CMR to cover the entire heart and depict RV geometry and function without geometric assumptions make it an ideal tool for the description of RV compartmental function. The normal RV is composed of an inlet portion, an apical trabecular portion, and an outlet. Global RV dysfunction can be the result of (1) homogenous hypocontractility of all of these segments, (2) hypo- or akinesia of one of the segments, or (3) dyssynchrony. Conversely, RV ejection fraction can be preserved even in the presence of dysfunction of one of its components. In contrast to the left ventricle, there is no universally accepted method for segmentation of the RV. Wald et al. proposed to divide the RV into ten segments [25], although the segment boundaries are not well established by anatomical landmarks in their model. Zhong and co-workers [26] introduced a 13-segment model of the RV. Most

studies, however, particularly in TOF, do not use a segmental approach, but merely differentiate an outlet or infundibular portion from the remainder of the RV, sometimes referred to as the RV sinus. As pointed out above, the distal RV outflow tract in rTOF is often grossly dilated and dyskinetic, while the inferior wall and inlet portions of the RV contract normally [27, 28]. The resultant ejection fraction of an RV with aneurysmal outflow tract can be the same as that of a ventricle with global dysfunction and normal sized outflow tract. In patients with a very dyskinetic RVOT, global RV ejection fraction measured by CMR can be up to 25% lower as compared to a normally functioning RVOT [29]. Most rTOF patients in the current surgical era have preserved RV function outside of the outflow tract. Whether or not the function of the RVOT or that of the remainder of the RV is of greater significance for the patient's clinical status after TOF repair is under debate. Wald et al. found that RVOT ejection fraction was the only RV parameter that was associated with aerobic capacity as a surrogate of clinical well-being [25]. In contrast, Bove and Alghamdi and their respective co-workers described a closer association between ejection fraction of the RV 'sinus' portion [30] and RV longitudinal shortening [29] and peak oxygen uptake (VO_{2max}) during exercise than between global RV or RVOT ejection fraction and VO_{2max}.

In Ebstein anomaly of the tricuspid valve, RV longitudinal function is typically preserved and sometimes even supranormal [31]. As compared to a normal heart, the apical region contributes relatively more to global systolic function.

Imaging Techniques for Assessing Pulmonary Regurgitation

Pulmonary flow and regurgitation are measured using phase contrast (PC MRI) flow velocity mapping in the main pulmonary artery. Quantification of pulmonary regurgitation is part of the routine CMR examination in patients with repaired rTOF. The authors suggest PC MRI be performed during free breathing, since breath holding can alter pulmonary blood flow [32]. Pulmonary regurgitation can be expressed as a percentage of systolic forward flow, or "regurgitant fraction" (Fig. 10.4), or as an absolute volume of retrograde flow per beat or per minute. Pulmonary regurgitant volume appears to be a better correlate of RV volume than regurgitant fraction [33, 34].

There are important pitfalls to PC MRI: For example, turbulent flow from RV outflow tract obstruction can result in underestimation of volume and velocity of flow [35]. Newer 4-D PC MRI sequences allow for flexibility in choosing an area of the vessel that has less turbulence and lower velocity of flow. Currently a research tool, it is expected that 4D PC MRI sequences will be part of the clinical armamentarium in the near future (Fig. 10.5; Video 10.2). Underestimation of flow volume in dilated pulmonary arteries is a widely recognized problem. This may be in part due to helical flow patterns and vortex formation [36] and to translational motion of the main pulmonary artery through the imaging plane in the presence of significant pulmonary regurgitation. In some situations it may be more accurate to measure flows in both branch pulmonary arteries and use their sum as a proxy for main pulmonary artery flow, unless there is isolated unilateral PA flow reversal [37].

Imaging Techniques for Assessing Myocardial Deformation

Myocardial strain, measures the local change in length or thickness of a myocardial segment through the cardiac cycle, expressed as a percentage change. The components of strain include circumferential, longitudinal and radial deformation. If the myocardium shortens from diastole to systole, as occurs in the circumferential and longitudinal directions, the strain is described as a negative number, with a higher

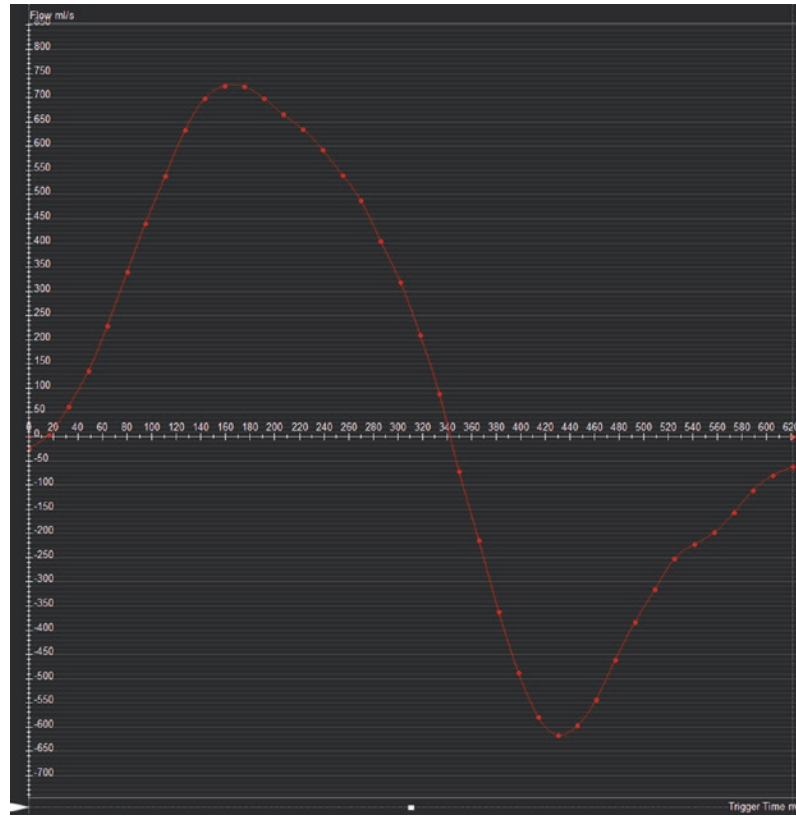

Fig. 10.4 Flow curve obtained from phase contrast imaging through the main pulmonary artery. This patient has severe pulmonary regurgitation, as evidenced by the negative flow seen after 340 ms on the x-axis

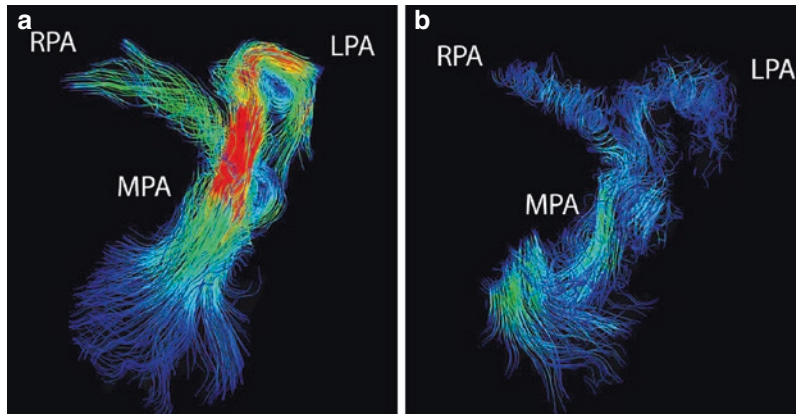

Fig. 10.5 Four-dimensional phase contrast imaging in a patient with Tetralogy of Fallot, depicting the streamlines of flow during systole (**a**) and diastole (**b**). Note the flow acceleration in the right ventricular outflow tract during systole and flow reversal during diastole (images and movie courtesy of M. Rose, M. Markl, J. Robinson, C. Rigsby, Northwestern University, Chicago, IL). *LPA* left pulmonary artery, *MPA* main pulmonary artery, *RPA* right pulmonary artery. See also Video 10.2

magnitude equating to greater strain. In the radial direction, the myocardium thickens in systole, leading to a positive strain value. Strain can be described from a Lagrangian or Eulerian perspective. While an extended discussion of this concept is beyond the scope of this chapter, the values differ and it is important to recognize which type of data is being measured by a given software package.

The right ventricle poses particular challenges, mostly related to the thin free wall and the more complex geometry, compared to the bullet-shaped, thicker walled, LV. There are several CMR-based techniques for measuring myocardial strain in either the right or left ventricle. These approaches can be compared to tissue Doppler and speckle-tracking strain imaging by echocardiography. In general, these techniques offer better temporal resolution than CMR. However, echo remains dependent on acoustic windows, and CMR offers more consistent and superior visualization of all segments of the heart, especially the RV [38, 39].

The most established method for measuring myocardial strain by CMR is with tagged images. This is accomplished with a sequence using spatial modulation of magnetization (SPAMM), resulting in a grid that is laid on top of the myocardium (Fig. 10.6; Video 10.3). This grid deforms with the myocardium throughout the cardiac cycle. Post-processing software is used track this deformation to obtain measurements of strain. Short axis images are used to analyze circumferential and radial strain, and long axis images to analyze longitudinal strain. However, the tag line spacing is typically at least 6–8 mm, making this technique of limited use for analyzing the thin RV free wall.

Sensitivity-encoded MRI (SENC) is another tagging-based sequence for measurement of strain that has been used more successfully for analysis of the RV [40, 41]. Unlike traditional tagging sequences, the SENC tags are generated in the through-plane, so that short axis images are used to measure longitudinal strain, and long axis images to measure circumferential strain. The spatial resolution for strain analysis is the same as the imaging voxel size, which is why SENC is a more viable technique for RV strain analyses.

In DENSE (displacement encoding with stimulated echoes), as for traditional tagging, SPAMM is used to encode the position of myocardium throughout the cardiac cycle. However, DENSE provides phase-reconstructed images that encode displacement at a voxel-level resolution of strain data (Fig. 10.7) [42]. A 3D DENSE sequence has been developed more recently, which may be of additional benefit for measuring the complex deformation patterns of the right ventricle [43].

As for SPAMM-based tagging sequences, both SENC and DENSE require the acquisition of specific sequences while the patient is in the scanner. Feature-tracking, on the other hand, generates strain data using SSFP cine images. Thus, no additional sequences are required and data can be analyzed retrospectively, using the short axis

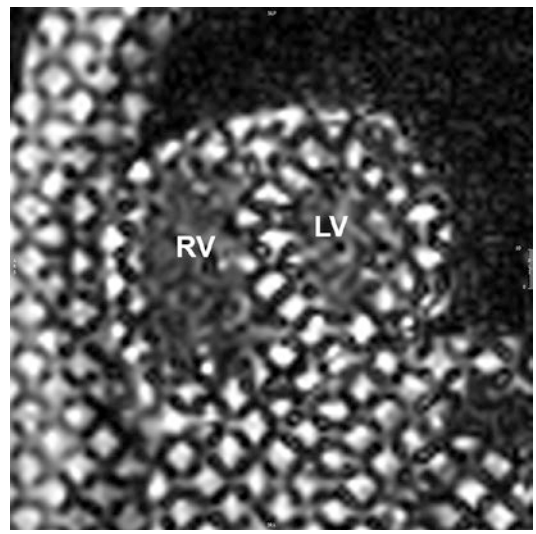

Fig. 10.6 Tagged short axis CMR image. The grid superimposed on the heart deforms with the myocardium through the cardiac cycle. Note that the spacing between the tag lines is wider than the free wall of the right ventricle, limiting the use of CMR tagging for analysis of right ventricular mechanics. *LV* left ventricle, *RV* right ventricle. See also Video 10.3

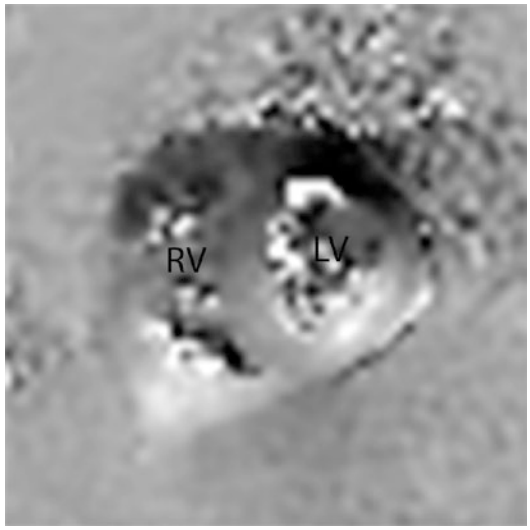

Fig. 10.7 Two-dimensional cine displacement-encoded MR (DENSE) phase image in the short axis plane. Displacement is encoded into the phase of each voxel, providing high spatial resolution that is necessary for measuring RV strain (image courtesy of M. Fogel, Philadelphia, PA). *LV* left ventricle, *RV* right ventricle

stack that was acquired for ventricular volumetry (for circumferential and radial strain) as well as two- and four-chamber cine sequences (for longitudinal strain) (Fig. 10.8) [44].

Right ventricular myocardial deformation imaging with the techniques described above (tagging, SENC, DENSE, feature tracking) has been applied predominantly in the rTOF population, in the hope that changes in strain may be an earlier finding of compromised RV 'health' than size or ejection fraction, providing an opportunity for more timely pulmonary valve replacement before irreversible damage to the RV occurs [45–47]. Right ventricular longitudinal strain has been shown to be a predictor of adverse outcome in this population, independent of ventricular size or ejection fraction [48].

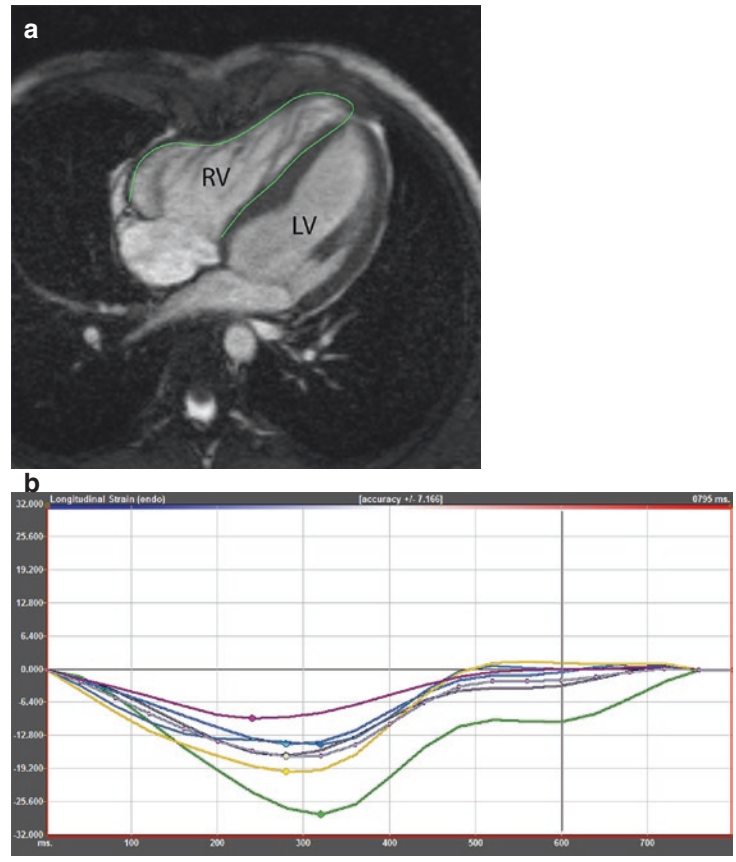

Fig. 10.8 Cardiac magnetic resonance feature tracking analysis in a patient with repaired tetralogy of Fallot, based on routine steady state free precession cine images (**a**), similar to Figure 10.3. Using the endocardial contour throughout the cardiac cycle and a proprietary analysis algorithm, the software derives segmental RV longitudinal strain curves (**b**). LV=left ventricle, RV=right ventricle. See supplemental material for movie file

Imaging Techniques for Assessing Myocardial Scarring and Fibrosis

Detection and Quantification of Fibrosis with CMR

The detection and quantification of myocardial scar and diffuse fibrosis is one of the unique assets of CMR. Discrete scars surrounded by relatively healthy myocardium are detected by late gadolinium enhancement (LGE) imaging. Late gadolinium enhancement CMR is based on different wash in and washout kinetics of gadolinium contrast in healthy vs. scarred myocardium: In the absence of scarring, gadolinium is rapidly taken up, but also quickly cleared from the myocardium, within a matter of minutes. In scarred tissue, gadolinium becomes trapped within the fibrous strands of the extracellular matrix. Similar to chronic scars, acute necrosis, either through infarction or inflammation, also produces LGE, presumably due to gadolinium trapping within necrotic tissue and ruptured myocytes [49]. LGE sequences are T1 weighted, showing gadolinium deposits as signal intense regions. The size of these regions can be quantified and expressed as a percentage of the total myocardium.

Importantly, LGE relies on a critical scar size for detection as well as on the contrast between healthy and diseased myocardium. Hence, if the myocardium is uniformly fibrosed or if the scars are very small, LGE imaging may be falsely reassuring as this technique is 'blind' to diffuse fibrosis. T1 relaxometry, often referred to as 'T1 mapping,' is a quantitative approach which exploits the differences in tissue specific longitudinal relaxation (or T1 recovery) kinetics (Fig. 10.9; Video 10.4). Fibrosed myocardium has higher T1 times as compared to healthy myocardium. Using pre- and post-contrast T1 time measurements, as well as the patient's hematocrit, the extracellular volume (ECV) can be quantified as an approximation of the patient's extracellular matrix, relative to the total myocardial volume (within an imaging voxel). It must be noted that the overlap of native T1 times and of ECV between health and disease is significant, limiting its use in identifying pathology.

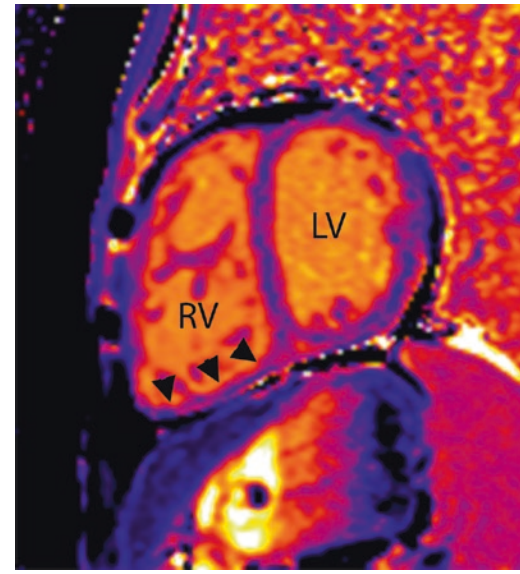

Fig. 10.9 Non-contrast T1 map in a patient with repaired tetralogy of Fallot. Each color encodes for a specific T1 time. Higher T1 times are found in fibrotic myocardium. Note the thin RV diaphragmatic (arrowheads) and free walls, making it difficult to draw a region of interest that excludes the blood pool as well as epicardial fat. *LV* left ventricle, *RV* right ventricle

Nevertheless, T1 relaxometry has provided important insights into pathophysiology and is expected to become useful during serial monitoring when followed within the same patient.

While a wealth of science and clinical experience is available on LV fibrosis imaging using LGE and T1 relaxometry, the understanding of RV fibrosis and its significance is limited. The reasons for the paucity of data include not only a scientific focus on the LV, particularly in acquired heart disease, but also the technical challenges of 'fibrosis imaging' in the RV. The finite spatial resolution of LGE CMR sequences and partial volume effects (combining the signal properties of two adjacent tissues) with blood and epicardial fat render scar imaging in the RV challenging [50]. In fact, in cases of confirmed RV infarction the sensitivity of LGE to identify necrotic myocardium was only 16% [51]. Some experts advocate for the acquisition of LGE at end-systole when the myocardium is thicker and the LGE less prone to partial volume effects between myocardium and blood. The accuracy of CMR

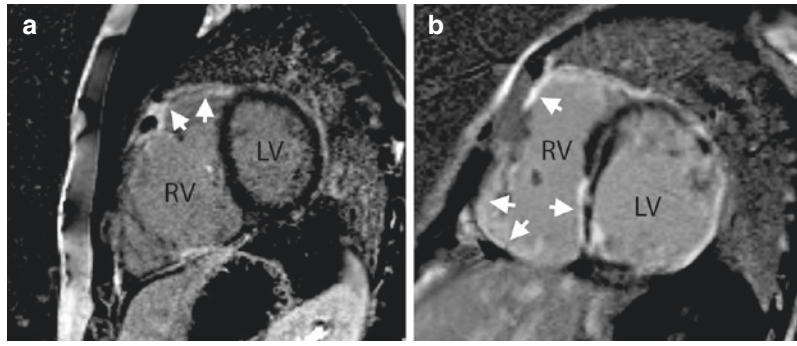

Fig. 10.10 Late gadolinium enhancement imaging in short axis orientation in (**a**) a patient with Ebstein anomaly of the tricuspid valve and (**b**) a patient with arrhythmogenic right ventricular cardiomyopathy with severe biventricular involvement. Arrows denote areas of right ventricular scarring, as evidenced by the retention of gadolinium, giving high signal intensity on T1 weighted imaging. *LV*=left ventricle, *RV*=right ventricle

sequences for native T1 and ECV measurements in the RV is a topic of debate. One of the challenges of T1 relaxometry is that the maximum spatial resolution of most sequences approaches the myocardial thickness of the RV. As each 'T1 map' contains the composite information from several (typically 5–11) 'source' images, T1 quantification also relies on the co-registration of these images. Both the limited spatial resolution relative to the RV thickness and imperfect image registration can lead to partial volume effects between myocardium and blood. As a result, measurements of the myocardium are 'contaminated' by blood falsely elevating T1 and ECV. Nevertheless, a recent T1 mapping study in patients after TOF repair reported values in the RV inferior wall and outflow tract with reasonable reproducibility [52]. Experimental approaches using segmented k-space sampling, i.e. collecting the imaging data over multiple heartbeats, rather than single shot techniques which use the information from a single heart beat to reconstruct the entire image, have shown promise in measuring RV T1 times [53].

Overall, evidence is accumulating that RV myocardial fibrosis, both diffuse and patchy, is present in many patients with congenital heart disease (Figure 10.10a), particularly in those with increased afterload such as pulmonary hypertension [54] and in RV hypoplasia [55]. There is early evidence that surgical factors play a role in the development of fibrosis [56]. Residual lesions also seem to be important [52]. However, we do not yet understand the exact pathophysiological triggers, nor do we know when fibrosis manifests and how it progresses. Some patients with congenital heart disease appear to have a profibrotic milieu, with an augmented collagen metabolism, which is associated with greater degrees of RV LGE by CMR [57]. A certain genetic make-up and epigenetic phenomena also appear to promote fibrosis [58].

In a study of adults after atrial redirection surgery for transposition of the great arteries, half had myocardial scarring by LGE in their systemic right ventricles [59, 60]. The presence of LGE was associated with electromechanical delay and ventricular dyssynchrony, as well as with atrial arrhythmias. One patient had progression in the amount of LGE during follow-up, suggesting that scarring is not static, but can worsen over time. Adults after the atrial switch procedure also have increased ECV within the interventricular septum, although the clinical significance of this finding has yet to be demonstrated [61]. Although the long-term cardiac health after the arterial switch operation appears to be better than with the atrial switch procedures, T1 mapping data in children and adolescents after arterial switch suggests an increased level of diffuse myocardial fibrosis (Grotenhuis, *unpublished data*).

Patchy scarring within the RVOT is an inevitable consequence of surgical RV reconstruction as part of the TOF repair. Not surprisingly, LGE

within the RVOT is associated with dyskinesia of that compartment of the RV [25]. The ventricular septal defect patch also enhances routinely. In a study of 92 TOF patients, Babu-Narayan et al. found LGE in these regions in nearly every patient [62]. However, one fourth also had LGE outside of the patch and the RVOT. The mechanism of LGE in these locations is less clear and has been interpreted as a sign of chronic remodeling rather than surgical trauma. These patients were older, had later repair, and had higher RV end-systolic volume. Patients with a greater RV LGE extent were more likely to experience arrhythmias and have decreased exercise tolerance. In another study, Park et al. showed that the extent of RV LGE was associated with fragmentation of the electrocardiogram QRS complex, which signifies conduction abnormalities and predisposes to arrhythmias [63]. Importantly, most patients in these two studies had been operated in the 1970s and 1980s. Clinical experience indicates that for patients who underwent operation in the current surgical era, LGE outside of the predilection sites is rare, suggesting overall healthier RV myocardium.

Two recent studies in adults with TOF found elevated RV ECV in patients with TOF as compared to controls [52, 64]. In one of them, greater RV ECV was associated with female gender and lower RV mass-to-volume ratio. Patients with predominant RV volume overload as opposed to pressure overload had higher ECV. A subsequent study in children, using native T1 as a CMR marker of fibrosis, also found evidence of increased RV fibrosis in TOF patients and confirmed the associations with volume overload [65].

An increased degree of myocardial fibrosis and RV wall thinning [66] has also been recognized in cardiomyopathic diseases (Figure 10.10b). In arrhythmogenic right ventricular cardiomyopathy (ARVC), for example, fibrofatty replacement diagnosed by histology during endomyocardial biopsy or pathology is part of the revised Task Force Criteria for the diagnosis of this condition. CMR, using LGE and T2 weighted turbo spin echo sequences, has been proposed as a noninvasive tool for the detection of fibrotic changes and fatty remodeling of RV myocardium. However, the ability of RV LGE to detect scarring in ARVC has been questioned in clinical practice. In a study of 142 pediatric patients who were evaluated for ARVC, including 23 with ‘definite’ ARVC, only three patients had evidence of RV scarring by LGE [23]. Importantly, all three had other signs of myocardial pathology, including global and regional RV dysfunction so that the added clinical benefit from a positive LGE result was incremental.

Myocardial Viability

Healthy myocardium contracts and thickens with every heartbeat. With the exception of intrinsic myopathic processes (not covered in detail here), reduced myocardial contractility reflects an imbalance between myocardial substrate demand and supply. This imbalance manifests in coronary ischemia, most often as a result of coronary artery stenosis, compression, or thromboembolism; or caused by low cardiac output or inadequate blood pressure. Reduced myocardial contractility at rest is a sign of severely compromised myocardial perfusion. In patients with preserved contractility at rest, a supply/demand deficit may be unmasked by increasing the myocardial oxygen requirement. This is accomplished with either exercise [67] or pharmacological ‘stress’, most often using dobutamine. The physiologic response to both exercise and dobutamine administration is an increase in heart rate, ejection fraction, and stroke volume, via a decrease in RV end-systolic volume.

An abnormal RV stress CMR is often characterized by a less than normal decrease in RV end-systolic volume, resulting in a blunted increase in ejection fraction. Such a response to exercise can identify endurance athletes who are at risk for ventricular arrhythmias [68]. In some patients after TOF repair, the RV end-systolic volume by CMR during dobutamine infusion fails to

decrease, or even increases; this pathologic finding is usually not predictable from examination at rest [69]. Similarly, many patients after TOF repair do not respond to exercise with an increase in RV ejection fraction [70]. A weaker increase in RV ejection fraction with dobutamine predicts a steeper decline in exercise tolerance during follow-up [71]. Fontan patients, and especially those with dominant RVs, respond with an increase in ejection fraction to low dose dobutamine stress [72].

'Stress CMR' also provides clues to the presence of RV diastolic dysfunction: In TOF, an infusion of low dose dobutamine at a concentration of 7.5mcg/kg/min reveals abnormal RV relaxation. In a study of patients after atrial switch operation for transposition of the great arteries, an infusion of dobutamine leads to an increase in RV contractility, but not to an augmentation in cardiac output [73]. The authors concluded that RV filling did not increase enough to provide the preload necessary to support an increase in cardiac output. Interestingly, patients after atrial switch do not increase their RV ejection fraction with exercise and experience regional wall motion abnormalities at rest and exercise [74].

First pass gadolinium perfusion CMR is widely used to assess LV myocardial viability in coronary artery disease, but also in patients with anomalous coronary artery origins, after coronary artery transfer, or with Kawasaki disease. In conjunction with myocardial deformation and LGE it can help differentiate between scarred (impaired contractility, reduced perfusion, positive LGE), hibernating (impaired contractility, reduced perfusion, but no LGE), and stunned myocardium (impaired contractility, normal perfusion, no LGE). However, the evaluation of first pass perfusion of the thin-walled subpulmonic RV with CMR is challenging due to the limited spatial resolution of commercially available sequences and not undertaken in clinical practice. First pass perfusion of the hypertrophied systemic RV may be more feasible, but no published data are available.

References

1. Mooij CF, de Wit CJ, Graham DA, Powell AJ, Geva T. Reproducibility of MRI measurements of right ventricular size and function in patients with normal and dilated ventricles. J Magn Reson Imaging. 2008;28(1):67–73.
2. Geva T. Repaired tetralogy of Fallot: the roles of cardiovascular magnetic resonance in evaluating pathophysiology and for pulmonary valve replacement decision support. J Cardiovasc Magn Reson. 2011;13:9.
3. Moledina S, Pandya B, Bartsota M, et al. Prognostic significance of cardiac magnetic resonance imaging in children with pulmonary hypertension. Circ Cardiovasc Imaging. 2013;6(3):407–14.
4. Valente AM, Gauvreau K, Assenza GE, et al. Contemporary predictors of death and sustained ventricular tachycardia in patients with repaired tetralogy of Fallot enrolled in the INDICATOR cohort. Heart. 2014;100(3):247–53.
5. Clarke CJ, Gurka MJ, Norton PT, Kramer CM, Hoyer AW. Assessment of the accuracy and reproducibility of RV volume measurements by CMR in congenital heart disease. JACC Cardiovasc Imaging. 2012;5(1):28–37.
6. D'Errico L, Lamacie MM, Jimenez Juan L, et al. Effects of slice orientation on reproducibility of sequential assessment of right ventricular volumes and ejection fraction: short-axis vs transverse SSFP cine cardiovascular magnetic resonance. J Cardiovasc Magn Reson. 2016;18(1):60.
7. Grosse-Wortmann L, Lee W, Yoo SJ. Magnetic resonance imaging and computed tomography. In: Anderson R, Baker E, Penny D, Redington A, Rigby M, Wernovsky G, editors. Paediatric cardiology. Philadelphia, PA: Churchill-Livingstone; 2009. p. 363–78.
8. Alfakih K, Plein S, Thiele H, Jones T, Ridgway JP, Sivananthan MU. Normal human left and right ventricular dimensions for MRI as assessed by turbo gradient echo and steady-state free precession imaging sequences. J Magn Reson Imaging. 2003;17(3):323–9.
9. Buechel EV, Kaiser T, Jackson C, Schmitz A, Kellenberger CJ. Normal right- and left ventricular volumes and myocardial mass in children measured by steady state free precession cardiovascular magnetic resonance. J Cardiovasc Magn Reson. 2009;11:19.
10. Robbers-Visser D, Boersma E, Helbing WA. Normal biventricular function, volumes, and mass in children aged 8 to 17 years. J Magn Reson Imaging. 2009;29(3):552–9.
11. Sarikouch S, Peters B, Gutberlet M, et al. Sex-specific pediatric percentiles for ventricular size and mass as reference values for cardiac MRI: assessment by steady-state free-precession and phase-contrast MRI flow. Circ Cardiovasc Imaging. 2010;3(1):65–76.

12. Lai WW, Gauvreau K, Rivera ES, Saleeb S, Powell AJ, Geva T. Accuracy of guideline recommendations for two-dimensional quantification of the right ventricle by echocardiography. Int J Cardiovasc Imaging. 2008;24(7):691–8.
13. Crean AM, Maredia N, Ballard G, et al. 3D Echo systematically underestimates right ventricular volumes compared to cardiovascular magnetic resonance in adult congenital heart disease patients with moderate or severe RV dilatation. J Cardiovasc Magn Reson. 2011;13:78.
14. Nagata Y, Wu VC, Kado Y, et al. Prognostic value of right ventricular ejection fraction assessed by transthoracic 3d echocardiography. Circ Cardiovasc Imaging. 2017;10(2):pii: e005384.
15. Dragulescu A, Grosse-Wortmann L, Fackoury C, et al. Echocardiographic assessment of right ventricular volumes after surgical repair of tetralogy of Fallot: clinical validation of a new echocardiographic method. J Am Soc Echocardiogr. 2011;24(11):1191–8.
16. Buechel ER, Dave HH, Kellenberger CJ, et al. Remodelling of the right ventricle after early pulmonary valve replacement in children with repaired tetralogy of Fallot: assessment by cardiovascular magnetic resonance. Eur Heart J. 2005;26(24):2721–7.
17. Knauth AL, Gauvreau K, Powell AJ, et al. Ventricular size and function assessed by cardiac MRI predict major adverse clinical outcomes late after tetralogy of Fallot repair. Heart. 2008;94(2):211–6.
18. Oosterhof T, van Straten A, Vliegen HW, et al. Preoperative thresholds for pulmonary valve replacement in patients with corrected tetralogy of Fallot using cardiovascular magnetic resonance. Circulation. 2007;116(5):545–51.
19. Therrien J, Provost Y, Merchant N, Williams W, Colman J, Webb G. Optimal timing for pulmonary valve replacement in adults after tetralogy of Fallot repair. Am J Cardiol. 2005;95(6):779–82.
20. Rathod RH, Prakash A, Kim YY, et al. Cardiac magnetic resonance parameters predict transplantation-free survival in patients with fontan circulation. Circ Cardiovasc Imaging. 2014;7(3):502–9.
21. van der Bom T, Winter MM, Bouma BJ, et al. Effect of valsartan on systemic right ventricular function: a double-blind, randomized, placebo-controlled pilot trial. Circulation. 2013;127(3):322–30.
22. Hosch O, Sohns JM, Nguyen TT, et al. The total right/left-volume index: a new and simplified cardiac magnetic resonance measure to evaluate the severity of Ebstein anomaly of the tricuspid valve: a comparison with heart failure markers from various modalities. Circ Cardiovasc Imaging. 2014;7(4):601–9.
23. Etoom Y, Govindapillai S, Hamilton R, et al. Importance of CMR within the Task Force Criteria for the diagnosis of ARVC in children and adolescents. J Am Coll Cardiol. 2015;65(10):987–95.
24. Marcus FI, McKenna WJ, Sherrill D, et al. Diagnosis of arrhythmogenic right ventricular cardiomyopathy/dysplasia: proposed modification of the task force criteria. Circulation. 2010;121(13):1533–41.
25. Wald RM, Haber I, Wald R, Valente AM, Powell AJ, Geva T. Effects of regional dysfunction and late gadolinium enhancement on global right ventricular function and exercise capacity in patients with repaired tetralogy of Fallot. Circulation. 2009;119(10):1370–7.
26. Zhong L, Gobeawan L, Su Y, et al. Right ventricular regional wall curvedness and area strain in patients with repaired tetralogy of Fallot. Am J Physiol Heart Circ Physiol. 2012;302(6):H1306–16.
27. Lytrivi ID, Ko HH, Srivastava S, et al. Regional differences in right ventricular systolic function as determined by cine magnetic resonance imaging after infundibulotomy. Am J Cardiol. 2004;94(7):970–3.
28. Bodhey NK, Beerbaum P, Sarikouch S, et al. Functional analysis of the components of the right ventricle in the setting of tetralogy of Fallot. Circ Cardiovasc Imaging. 2008;1(2):141–7.
29. Alghamdi MH, Mertens L, Lee W, Yoo SJ, Grosse-Wortmann L. Longitudinal right ventricular function is a better predictor of right ventricular contribution to exercise performance than global or outflow tract ejection fraction in tetralogy of Fallot: a combined echocardiography and magnetic resonance study. Eur Heart J Cardiovasc Imaging. 2013;14(3):235–9.
30. Bove T, Vandekerckhove K, Devos D, et al. Functional analysis of the anatomical right ventricular components: should assessment of right ventricular function after repair of tetralogy of Fallot be refined? Eur J Cardiothorac Surg. 2014;45(2):e6–12.
31. Lee CM, Sheehan FH, Bouzas B, Chen SS, Gatzoulis MA, Kilner PJ. The shape and function of the right ventricle in Ebstein's anomaly. Int J Cardiol. 2013;167(3):704–10.
32. Johansson B, Babu-Narayan SV, Kilner PJ. The effects of breath-holding on pulmonary regurgitation measured by cardiovascular magnetic resonance velocity mapping. J Cardiovasc Magn Reson. 2009;11:1.
33. Gorter TM, van Melle JP, Freling HG, et al. Pulmonary regurgitant volume is superior to fraction using background-corrected phase contrast MRI in determining the severity of regurgitation in repaired tetralogy of Fallot. Int J Cardiovasc Imaging. 2015;31(6):1169–77.
34. Wald RM, Redington AN, Pereira A, et al. Refining the assessment of pulmonary regurgitation in adults after tetralogy of Fallot repair: should we be measuring regurgitant fraction or regurgitant volume? Eur Heart J. 2009;30(3):356–61.
35. O'Brien KR, Cowan BR, Jain M, Stewart RA, Kerr AJ, Young AA. MRI phase contrast velocity and flow errors in turbulent stenotic jets. J Magn Reson Imaging. 2008;28(1):210–8.
36. Burk J, Blanke P, Stankovic Z, et al. Evaluation of 3D blood flow patterns and wall shear stress in the normal and dilated thoracic aorta using flow-sensitive 4D CMR. J Cardiovasc Magn Reson. 2012;14:84.
37. Rutz T, Meierhofer C, Naumann S, et al. Comparison of MR flow quantification in peripheral and main pulmonary arteries in patients after right ventricular outflow tract surgery: A retrospective study. J Magn

Reson Imaging. 2017. doi: https://doi.org/10.1002/jmri.25701 [Epub ahead of print].
38. Pedrizzetti G, Claus P, Kilner PJ, Nagel E. Principles of cardiovascular magnetic resonance feature tracking and echocardiographic speckle tracking for informed clinical use. J Cardiovasc Magn Reson. 2016;18(1):51.
39. Tee M, Noble JA, Bluemke DA. Imaging techniques for cardiac strain and deformation: comparison of echocardiography, cardiac magnetic resonance and cardiac computed tomography. Expert Rev Cardiovasc Ther. 2013;11(2):221–31.
40. Ohyama Y, Ambale-Venkatesh B, Chamera E, et al. Comparison of strain measurement from multimodality tissue tracking with strain-encoding MRI and harmonic phase MRI in pulmonary hypertension. Int J Cardiol. 2015;182:342–8.
41. Shehata ML, Harouni AA, Skrok J, et al. Regional and global biventricular function in pulmonary arterial hypertension: a cardiac MR imaging study. Radiology. 2013;266(1):114–22.
42. Kim D, Gilson WD, Kramer CM, Epstein FH. Myocardial tissue tracking with two-dimensional cine displacement-encoded MR imaging: development and initial evaluation. Radiology. 2004;230(3):862–71.
43. Auger DA, Zhong X, Epstein FH, Spottiswoode BS. Mapping right ventricular myocardial mechanics using 3D cine DENSE cardiovascular magnetic resonance. J Cardiovasc Magn Reson. 2012;14:4.
44. Hor KN, Baumann R, Pedrizzetti G, et al. Magnetic resonance derived myocardial strain assessment using feature tracking. J Vis Exp. 2011;(48):pii: 2356.
45. Kempny A, Fernandez-Jimenez R, Orwat S, et al. Quantification of biventricular myocardial function using cardiac magnetic resonance feature tracking, endocardial border delineation and echocardiographic speckle tracking in patients with repaired tetralogy of Fallot and healthy controls. J Cardiovasc Magn Reson. 2012;14:32.
46. Lu JC, Ghadimi Mahani M, Agarwal PP, Cotts TB, Dorfman AL. Usefulness of right ventricular free wall strain to predict quality of life in "repaired" tetralogy of Fallot. Am J Cardiol. 2013;111(11):1644–9.
47. Moon TJ, Choueiter N, Geva T, Valente AM, Gauvreau K, Harrild DM. Relation of biventricular strain and dyssynchrony in repaired tetralogy of fallot measured by cardiac magnetic resonance to death and sustained ventricular tachycardia. Am J Cardiol. 2015;115(5):676–80.
48. Orwat S, Diller GP, Kempny A, et al. Myocardial deformation parameters predict outcome in patients with repaired tetralogy of Fallot. Heart. 2016;102(3):209–15.
49. Mahrholdt H, Wagner A, Judd RM, Sechtem U. Assessment of myocardial viability by cardiovascular magnetic resonance imaging. Eur Heart J. 2002;23(8):602–19.
50. Grosse-Wortmann L, Macgowan CK, Vidarsson L, Yoo SJ. Late gadolinium enhancement of the right ventricular myocardium: is it really different from the left? J Cardiovasc Magn Reson. 2008;10:20.
51. Larose E, Ganz P, Reynolds HG, et al. Right ventricular dysfunction assessed by cardiovascular magnetic resonance imaging predicts poor prognosis late after myocardial infarction. J Am Coll Cardiol. 2007;49(8):855–62.
52. Chen CA, Dusenbery SM, Valente AM, Powell AJ, Geva T. Myocardial ecv fraction assessed by CMR is associated with type of hemodynamic load and arrhythmia in repaired tetralogy of Fallot. JACC Cardiovasc Imaging. 2016;9(1):1–10.
53. Mehta BB, Chen X, Bilchick KC, Salerno M, Epstein FH. Accelerated and navigator-gated look-locker imaging for cardiac T1 estimation (ANGIE): development and application to T1 mapping of the right ventricle. Magn Reson Med. 2015;73(1):150–60.
54. Hartke LP, Gilkeson RC, O'Riordan MA, Siwik ES. Evaluation of right ventricular fibrosis in adult congenital heart disease using gadolinium-enhanced magnetic resonance imaging: initial experience in patients with right ventricular loading conditions. Congenit Heart Dis. 2006;1(5):192–201.
55. Kim H, Park EA, Lee W, et al. Magnetic resonance imaging findings of isolated right ventricular hypoplasia. Int J Cardiovasc Imaging. 2012;28(Suppl 2):149–52.
56. Riesenkampff E, Messroghli DR, Redington AN, Grosse-Wortmann L. Myocardial T1 mapping in pediatric and congenital heart disease. Circ Cardiovasc Imaging. 2015;8(2):e002504.
57. Chen CA, Tseng WY, Wang JK, et al. Circulating biomarkers of collagen type I metabolism mark the right ventricular fibrosis and adverse markers of clinical outcome in adults with repaired tetralogy of Fallot. Int J Cardiol. 2013;167(6):2963–8.
58. Jeewa A, Manickaraj AK, Mertens L, et al. Genetic determinants of right-ventricular remodeling after tetralogy of Fallot repair. Pediatr Res. 2012;72(4):407–13.
59. Rydman R, Gatzoulis MA, Ho SY, et al. Systemic right ventricular fibrosis detected by cardiovascular magnetic resonance is associated with clinical outcome, mainly new-onset atrial arrhythmia, in patients after atrial redirection surgery for transposition of the great arteries. Circ Cardiovasc Imaging. 2015;8(5):pii: e002628.
60. Babu-Narayan SV, Goktekin O, Moon JC, et al. Late gadolinium enhancement cardiovascular magnetic resonance of the systemic right ventricle in adults with previous atrial redirection surgery for transposition of the great arteries. Circulation. 2005;111(16):2091–8.
61. Plymen CM, Sado DM, Taylor AM, et al. Diffuse myocardial fibrosis in the systemic right ventricle of patients late after Mustard or Senning surgery: an equilibrium contrast cardiovascular magnetic resonance study. Eur Heart J Cardiovasc Imaging. 2013;14(10):963–8.
62. Babu-Narayan SV, Kilner PJ, Li W, et al. Ventricular fibrosis suggested by cardiovascular magnetic resonance in adults with repaired tetralogy of fallot and its relationship to adverse markers of clinical outcome. Circulation. 2006;113(3):405–13.

63. Park SJ, On YK, Kim JS, et al. Relation of fragmented QRS complex to right ventricular fibrosis detected by late gadolinium enhancement cardiac magnetic resonance in adults with repaired tetralogy of fallot. Am J Cardiol. 2012;109(1):110–5.
64. Broberg CS, Chugh SS, Conklin C, Sahn DJ, Jerosch-Herold M. Quantification of diffuse myocardial fibrosis and its association with myocardial dysfunction in congenital heart disease. Circ Cardiovasc Imaging. 2010;3(6):727–34.
65. Yim D, Riesenkampff E, Caro-Dominguez P, Yoo SJ, Seed M, Grosse-Wortmann L. Assessment of diffuse ventricular myocardial fibrosis using native t1 in children with repaired tetralogy of Fallot. Circ Cardiovasc Imaging. 2017;10(3):e005695.
66. Sato Y, Kato K, Hashimoto M, et al. Localized right ventricular structural abnormalities in patients with idiopathic ventricular fibrillation: magnetic resonance imaging study. Heart Vessel. 1996;11(2):100–3.
67. Roest AA, Kunz P, Lamb HJ, Helbing WA, van der Wall EE, de Roos A. Biventricular response to supine physical exercise in young adults assessed with ultrafast magnetic resonance imaging. Am J Cardiol. 2001;87(5):601–5.
68. La Gerche A, Claessen G, Dymarkowski S, et al. Exercise-induced right ventricular dysfunction is associated with ventricular arrhythmias in endurance athletes. Eur Heart J. 2015;36(30):1998–2010.
69. Parish V, Valverde I, Kutty S, et al. Dobutamine stress MRI in repaired tetralogy of Fallot with chronic pulmonary regurgitation: a comparison with healthy volunteers. Int J Cardiol. 2013;166(1):96–105.
70. Roest AA, Helbing WA, Kunz P, et al. Exercise MR imaging in the assessment of pulmonary regurgitation and biventricular function in patients after tetralogy of fallot repair. Radiology. 2002;223(1):204–11.
71. Luijnenburg SE, Mekic S, van den Berg J, et al. Ventricular response to dobutamine stress relates to the change in peak oxygen uptake during the 5-year follow-up in young patients with repaired tetralogy of Fallot. Eur Heart J Cardiovasc Imaging. 2014;15(2):189–94.
72. Robbers-Visser D, Jan Ten Harkel D, Kapusta L, et al. Usefulness of cardiac magnetic resonance imaging combined with low-dose dobutamine stress to detect an abnormal ventricular stress response in children and young adults after fontan operation at young age. Am J Cardiol. 2008;101(11):1657–62.
73. Tulevski II, Lee PL, Groenink M, et al. Dobutamine-induced increase of right ventricular contractility without increased stroke volume in adolescent patients with transposition of the great arteries: evaluation with magnetic resonance imaging. Int J Card Imaging. 2000;16(6):471–8.
74. Tops LF, Roest AA, Lamb HJ, et al. Intraatrial repair of transposition of the great arteries: use of MR imaging after exercise to evaluate regional systemic right ventricular function. Radiology. 2005;237(3):861–7.

Pulmonary Hypertension in Chronic Neonatal Lung Disease: Mechanisms and Targets

11

Robert P. Jankov and A. Keith Tanswell

Abstract

Chronic neonatal lung disease is a common complication of preterm birth for which no effective preventive or rescue therapies currently exist. This condition has been and remains associated with serious pulmonary and neurological sequelae that have major lifelong health implications. Pulmonary hypertension is a common and important associated phenomenon, contributing to high mortality. Considerable gaps in knowledge exist, particularly with respect to pathogenesis, natural history, mechanisms contributing to right ventricular failure and the role, if any, of pulmonary vasodilators. Addressing these gaps will require careful prospective study of at-risk infants and improved understanding of pathophysiological mechanisms employing relevant animal models.

Keywords

Neonate • Prematurity • Extremely-low birth weight • Chronic lung disease • Bronchopulmonary dysplasia • Pulmonary hypertension • Nitric oxide • Rho-kinase

R.P. Jankov, MBBS, PhD, FRACP (✉)
Neonatologist, Children's Hospital of Eastern Ontario (CHEO), The Ottawa Hospital, Ottawa, ON K1H 8L6, Canada

Associate Professor, Department of Pediatrics, University of Ottawa, Ottawa, ON K1H 8L6, Canada

Senior Scientist, CHEO Research Institute, Ottawa, ON K1H 8L6, Canada
e-mail: robert.jankov@sickkids.ca

A.K. Tanswell
Neonatology, Translational Medicine, The Hospital for Sick Children, 555 University Ave, Toronto, ON M1G 1X8 Canada
e-mail: keithtanswell@aol.com

Bronchopulmonary Dysplasia

Positive pressure ventilation for the treatment of respiratory distress syndrome in prematurely-born infants was introduced into clinical practice in the mid-1960s [1]. Shortly thereafter, a chronic neonatal lung disease (CNLD), termed bronchopulmonary dysplasia (BPD), was first described by Northway and colleagues [2]. The affected infants were generally born preterm (the average postmenstrual age in Northway's cohort was 32 weeks) and all had severe respiratory failure, were ventilated with high O_2 concentrations and

M.K. Friedberg, A.N. Redington (eds.), *Right Ventricular Physiology, Adaptation and Failure in Congenital and Acquired Heart Disease*, https://doi.org/10.1007/978-3-319-67096-6_11

required high inflation pressures. The development of respiratory failure was accompanied by a classical sequence of radiological changes evolving from an initial "white-out", which cleared to reveal multiple cystic lesions. If infants survived this stage, a streaky pattern consistent with pulmonary fibrosis and/or distended lymphatics predominated. The mortality was very high at approximately 60% [2]. At autopsy there was evidence of both atelectasis and emphysematous changes, pulmonary fibrosis, marked proximal airway injury and vascular remodeling indicative of severe pulmonary hypertension (PHT) [2]. While the term BPD has been preserved over the intervening 50 years, the clinical, radiological and pathological features of CNLD have dramatically changed. The affected population is now much more immature at birth, the illness during the neonatal period is generally less severe, the classic sequence of radiological changes is no longer apparent, and proximal airway injury and fibrosis are no longer common pathological features.

CNLD in the Present Era

Advances in neonatal care over the past 25 years have had a major impact on the survival of infants born ≤1000 g (known as extremely low birth weight (ELBW) infants, coinciding with ≤28 weeks' postmenstrual age at birth). CNLD now arises predominantly in ELBW infants with an overall incidence of around 50% [3, 4], leading to more than 10,000 new cases per year in the United States alone [5]. This incidence has not changed over the last 15 years, and in Canada has possibly even increased [4], despite advances in many aspects of neonatal care. CNLD has been and remains associated with serious pulmonary [6, 7] and neurological [8] sequelae that have major lifelong health implications.

Since the increasing use of antenatal corticosteroids and the advent of exogenous surfactant therapy in the early 1990s, the early respiratory course of ELBW infants has been generally characterized by minimal respiratory distress and little or no initial requirement for O_2 supplementation or ventilatory support. A subgroup will subsequently go on to have a progressive deterioration in respiratory function, requiring an increase in inspired O_2 and occasionally invasive or prolonged non-invasive respiratory support. The radiographic picture in these infants generally evolves from initial homogeneous hazy pulmonary opacities to a generalized coarse interstitial pattern [3]. The most widely used clinical definition of CNLD has been an O_2-dependency at 36 weeks' postmenstrual age. The use of this definition has limitations, in that it does not differentiate between mildly and severely affected infants. This has led to the development of a classification scheme which differentiates between three levels of severity (mild, moderate, severe) based on degree of supplemental O_2 requirement and need for respiratory support at 36 weeks' postmenstrual age [9]. A minority of ELBW infants will develop severe CNLD with significant and prolonged need for invasive ventilation and O_2 supplementation. Severe CNLD may be heralded during the first 2 weeks of life by a limited initial response to surfactant and/or deteriorations associated with development of air leaks, a hemodynamically significant patent ductus arteriosus and/or sepsis.

Although ELBW is the most common factor associated with development of CNLD, there is significant variability in the severity of lung disease amongst infants born at the same weight and gestational age, to which genetic factors are likely major contributors. Indeed, polymorphisms in tumor necrosis factor-α, toll-like receptor −10 and vascular endothelial growth factor are all suggested to play a role [10], as are single nucleotide polymorphisms in the fibroblast growth factor receptor-4 [11]. The barely understood complexity of a genetic contribution to CNLD is evident from a recent whole genome study in which there were alterations in expression of almost 10% of the genome [12].

Pathological Features of CNLD

Five distinct stages of lung development have been defined: embryonic, pseudoglandular, canalicular, saccular and alveolar [13–16]. These stages are conserved among mammalian species

but with differing timing in relation to gestation, which has important implications for the relevance of experimental models recapitulating CNLD [17]. Preterm infants most as risk of developing CNLD are born during the transition between the late canalicular and early saccular phases, which are characterized by formation of primitive large distal airspaces, differentiation of Type I and Type II pneumocytes and expansion and thinning of the airway-capillary interface to an extent that is sufficient to support life. In humans, the alveolar stage, characterized by ingrowth of secondary crests into larger precursor saccules, commences in late gestation and continues well into childhood [18, 19]. The major pathological features of severe CNLD in the current era are an inhibition, or arrest, of alveolar formation, thickening of the interstitium and pulmonary inflammation [5, 20]. Hypoplastic, dysmorphic pulmonary microvasculature is also evident [21], resulting in reduced vascular surface area. Failure of alveolarization appears to last into adult life [22].

Pulmonary Hypertension and CNLD

PHT is a common finding in patients with CNLD [23]. Available studies estimate the incidence of echocardiographic signs of PHT at between 17 and 43% of CNLD cases overall [24–27]. The incidence and severity generally increases in parallel with lung disease, being present in as many as 60% of severe CNLD [24]. Given the retrospective nature of the majority of published data, lack of long-term follow-up data, and the predominant reliance on echocardiography for diagnosis, the true incidence, severity and prevalence of PHT in formerly-premature infants is likely much greater than is currently appreciated. Other than the degree of prematurity, additional risk factors for PHT that are evident at birth include maternal pre-eclampsia, prolonged oligohydramnios and being born small for gestational age [28]. While genetic factors almost certainly contribute to the development of CNLD, no specific loci have yet been consistently associated with increased risk for PHT in this population.

As described above, the presence of evolving CNLD is usually evident within the first several weeks of life with respiratory deterioration (or lack of improvement) and persistent radiological abnormalities. Echocardiographic signs of PHT are frequently evident at this early stage and chronicity of PHT is generally established by 34–36 weeks' postmenstrual age [27]. Pathological contributors to PHT include sustained pulmonary vasoconstriction, exaggerated vasoreactivity (often precipitated by hypoxemic episodes), vascular hypoplasia and arterial wall remodeling due to smooth muscle hyperplasia and distal extension of smooth muscle into normally non-muscular arteries [29]. The extent to which the latter two structural features contribute to a "fixed" (i.e., non-reversible) form of chronic PHT is unknown. Since PHT is usually clinically silent, screening is recommended for all high-risk infants. It remains unclear whether the severity of PHT is simply a marker of CNLD severity or contributes to adverse outcomes in its own right. However, the diagnosis of PHT imposes a far greater burden of illness, resulting in lengthened hospital stay, prolongation of need for O_2 therapy, and a four-fold increase in mortality during the NICU stay [26]. Co-morbidities that worsen or inhibit recovery of lung function will also exacerbate PHT, including the persistence of left-to-right shunts that increase pulmonary blood flow (patent ductus arteriosus or large systemic-pulmonary collateral vessels) [30], airway abnormalities (subglottic stenosis, tracheomalacia, distal airway obstruction), gastro-esophageal reflux and factors contributing to poor growth, such as suboptimal nutrition and prolonged or repeated courses of corticosteroid therapy. The presence of pulmonary vein stenosis is an occasional finding in ex-preterm infants that heralds an extremely poor prognosis, especially in late-onset cases [31].

Long-Term Outcome of PHT in CNLD

Retrospective data suggest that the majority of infants with CNLD-associated PHT will demonstrate gradual improvement in hemodynamic parameters during the first year of life, as lung

growth and function improves [30]. However, prospective long-term cohort data on these patients is lacking, and there is no knowledge regarding the (presumably high) potential for reappearance of PHT later in life [32]. For those patients with severe CNLD, progression of PHT is common, ultimately leading to right ventricular (RV) failure and early death, in most cases within 1 year of diagnosis [24]. Pulmonary hypertensive crises and cardiac arrest are also common [26], frequently precipitated by worsening hypercapnia and/or systemic hypotension in the settings of improperly-applied mechanical ventilation, anesthesia, sedation or intercurrent infection.

Long-term survival in progressive PHT is dependent upon an ability of the right ventricle to maintain adequate output in the face of increased pressure load, yet this aspect of disease has only recently been considered as a distinct therapeutic target [33, 34]. RV adaptation to increased pressure load evolves from a compensated (hypertrophied) state to a decompensated (dilated) state, in which a progressive decline in contractile function heralds imminent death [35]. The available evidence suggests that this evolution proceeds more rapidly in infants than in older children and adults [36]. Earlier dogma held that RV failure simply represented a mechanical response to increased pressure, which could be corrected by pulmonary vasodilators. Recent evidence has challenged this belief [33, 34, 37], indicating that discrete right ventricle-specific and/or pressure load-independent mechanisms may be responsible for RV contractile dysfunction. At this time, there is no specific knowledge on the pathogenesis of right heart failure in formerly premature infants.

Current Therapies for Established CNLD and Associated PHT

The current mainstays of therapy for established CNLD with or without associated PHT include adequate nutrition, diuretics, prevention of infection, supplemental O_2 and correction of comorbidities (as described above) that may further contribute to lung injury. Optimizing nutrition in ELBW infants may impact the risk of CNLD [38], as under nutrition has been demonstrated in animal models to impair lung growth and to enhance lung injury [39]. Loop and thiazide diuretics are commonly used as therapy for CNLD [40]. Their use frequently leads to short-term improvements in oxygenation and requirement for respiratory support; however, there is no consensus on the dose, type or duration of diuretic therapy that is optimal or safe and no data suggesting any sustained or long-term benefits to their use [41].

Supplemental O_2, while necessary to avoid hypoxemia, can be directly cytotoxic to the lung due to increased reactive oxygen species (ROS) produced by mitochondria in direct proportion to the PO_2 to which the lung is exposed. Maturation of enzymatic antioxidants is gestation dependent [42, 43], and it has long been assumed that the ELBW infant is particularly at risk from ROS-mediated injury due to reduced antioxidant defenses [44]. That pulmonary toxicity due to supplemental O_2 occurs in ELBW infants has been demonstrated in trials comparing different target O_2 saturations in which the high target group ($SaO_2 \geq 96\%$) had more adverse pulmonary outcomes [45, 46], while low O_2 saturation targets ($SaO_2 < 90\%$) may lead to increased mortality [47]. These observations limit and render uncertain the O_2 saturation range that is available for safe clinical use. What is clear is that hyperoxia ($PaO_2 > 80$ mmHg) provides no further reduction to pulmonary vascular resistance (PVR) in excess of normoxia (PaO_2 60–80 mmHg) [48] and may in fact further increase vasoreactivity [49].

PHT in CNLD is a dynamic phenomenon and its severity at any given time is strongly influenced by factors such as pH, PaO_2 and state of lung distension. The importance of these factors is generally underappreciated by clinicians. While pulmonary vasodilation with inhaled nitric oxide (iNO) has been used as rescue therapy for refractory hypoxemia in severe CNLD, often producing short-term improvements in oxygenation [50, 51], there is no data on long-term effects. Other therapies leading to improved outcomes in older children and adults with pulmonary arterial

hypertension [52] are unsupported by good quality clinical data in patients with CNLD and are suggested to be of doubtful value in this context [53]. Such therapies include Sildenafil (phosphodiesterase 5 inhibitor), Bosentan (endothelin receptor antagonist) or Epoprostenol (prostacyclin analogue), given either alone or in combination [54–58]. Sildenafil may have additional benefits on systolic function of the hypertrophied right ventricle [59, 60], aside from its vasodilator effects. Concerns regarding these agents relate to the potential for systemic hypotension, hepatotoxicity (Bosentan) and hypoxemia due to worsened ventilation-perfusion mismatch. Ideally, any consideration of long-term treatment with these agents should be accompanied by comprehensive evaluation of cardiopulmonary hemodynamics by cardiac catheterization, which allows for accurate determination of PHT severity, evaluation of acute vasodilator responsiveness and definitive exclusion of major collateral vessels, pulmonary vein stenosis and left heart disease as contributing factors [61].

Prevention of CNLD and Associated PHT

The most effective way of preventing the development of CNLD would be to avoid prematurity. Given the current absence of any effective interventions targeting premature delivery, preventive therapy for CNLD and associated PHT must be directed at the contributing factors that lead to lung and cardiac injury, and their underlying mechanisms of action. Despite numerous trials of pharmacological treatments [62, 63], only three preventive agents have been convincingly demonstrated to reduce the incidence of CNLD: caffeine [64], Vitamin A [65] and early postnatal Dexamethasone [66]. The mechanism by which caffeine exerts its effects is unclear. Despite residual concerns surrounding the potential for increased mortality [67] or gut complications [necrotizing enterocolitis [68]] with caffeine, its prophylactic use is now common practice in North America, Europe and Australasia [69]. Vitamin A prophylaxis, which is modestly effective and shown to be safe [65, 70], has not been widely adopted. This likely relates to whether the small reduction in incidence of CNLD is seen to justify a prolonged course of intramuscular injections. Greater acceptance will likely depend on the results of ongoing trials assessing intravenous delivery. While certainly effective, early (within the first 7 days of life) postnatal Dexamethasone is not recommended due to high potential for adverse neurodevelopmental effects [66, 71]. Dexamethasone also reversed established PHT in adult rats [72], yet prolonged treatment of neonatal rats caused permanent lung hypoplasia, and augmented the severity of hypoxia-induced PHT when pups reached maturity [73]. Benefits of alternative strategies, such as systemic use of a less potent steroid, hydrocortisone, or inhaled steroids to reduce systemic side-effects remain unproven [63].

Experimental Therapies

Nitric Oxide (NO)

NO is a readily diffusible and highly-reactive free radical gas, first identified as the "endothelium-derived relaxing factor" in 1987. NO mediates smooth muscle relaxation via activation of soluble guanylate cyclase (sGC), leading to cyclic guanosine monophosphate (cGMP)-dependent calcium desensitization. NO-mediated signaling is critical to the rapid decrease in PVR following birth [74]. Properties of NO on the lung that are protective of experimental injury also include anti-inflammatory [75], antioxidant [76], anti-(smooth muscle) proliferative [77] and cytoprotective [78] effects. Abundant experimental evidence implicates deficient NO signaling as critical to the pathogenesis of CNLD and associated PHT [79–82]. Augmentation of NO signaling has also been shown to reverse sustained vasoconstriction, inhibit smooth muscle proliferation, and stimulate angiogenesis and alveolarization in experimental animals [83–88]. In neonates, iNO is employed as a short-acting pulmonary vasodilator, limiting hypoxemia by matching perfusion to ventilation and decreasing

right-to-left shunting. Unfortunately, despite promising preclinical studies [83, 85], iNO has proven ineffective as a preventive therapy for human CNLD [89–91]. Other than providing short-term improvement in oxygenation, iNO also does not appear to improve or slow the progression of CNLD-associated PHT [51, 92].

Assuming that the biological rationale for NO-based therapy in the prevention of neonatal lung and pulmonary vascular injury is sound, there are several possible explanations for the disappointing results of human studies despite strong supportive preclinical data. Firstly, that the beneficial effects of exogenous NO are counterbalanced by adverse ones and secondly, that inhalation of NO gas is a suboptimal means of providing NO to tissues in which endogenous production is deficient. Circulating and tissue-bound *S*-nitrosothiols (SNOs) contribute importantly to NO-cGMP signalling [93] and cause reversible post-translational regulation of protein function in a manner akin to phosphorylation. iNO has been shown inferior as a means of improving tissue NO function in experimental animals, when compared to SNO-based (ethyl nitrite) therapy [94]. In pilot human studies, inhaled ethyl nitrite improved oxygenation and hemodynamics in term infants with hypoxemic respiratory failure due to PHT [95]. No studies have been carried out to date in preterm infants. Another potential means to boost the potential benefits of exogenous NO may be as combination therapy with other agents known to improve lung growth and decrease lung injury, such as Vitamin A [96]. Treatment with Sildenafil, a PDE 5 inhibitor which, like NO, enhances cGMP signaling, attenuates both the PHT and the impairment of alveologenesis in experimental CNLD [84, 87]. Unfortunately, a recent pilot study of sildenafil for prevention of CNLD also proved disappointing [97].

Strategies to Limit Adverse NO-Mediated Reactions

A biochemical barrier to effective NO-based therapy, that has yet to be overcome, relates to the high reactivity of NO (which is a free radical)—the dominant reaction depending upon the milieu in which NO is provided or generated (see Fig. 11.1). Physiological signaling of NO is regulated by reaction with heme proteins and reversible nitrosylation [98] of cysteine thiols, producing SNOs [93] either directly or following oxidation to nitrite anion. Under pathological conditions (e.g. oxidative stress, inflammation), NO will preferentially react with supra-physiological levels of O_2 or superoxide to produce reactive nitrogen species (RNS), nitrogen dioxide and peroxynitrite, respectively. Nitrogen dioxide is an important source of RNS in inflammatory states, where neutrophil-derived peroxidases and hydrogen peroxide are present in abundance [99]. These molecules cause nitration of tyrosine residues [100] that irreversibly inhibits protein function by forming 3-nitrotyrosine [101–104]. Nitration is linked to numerous disease states by triggering cellular responses ranging from pathological alterations in cell sig-

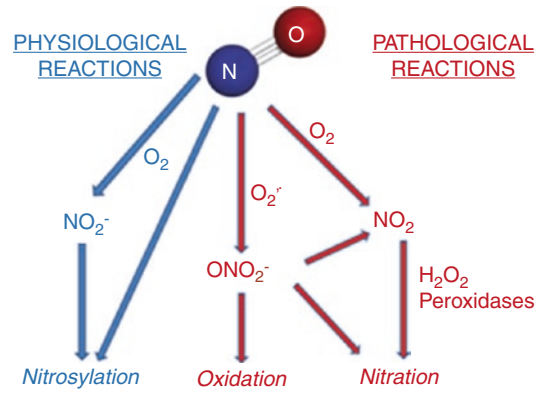

Fig. 11.1 Reactions of nitric oxide (NO). Physiological effects of NO are mediated by *direct or indirect* (via oxidation to nitrite (NO_2^-)) *nitrosylation* reactions with divalent metal-based heme proteins, including soluble guanylate cyclase and hemoglobin, leading to alterations in cell signaling pathways and vascular function. Pathological reactions of NO are mediated by reaction with supraphysiological levels of molecular oxygen (O_2) to produce nitrogen dioxide (NO_2) or with superoxide ($O_2^{\bullet-}$) to produce peroxynitrite (ONO_2^-). Peroxynitrite is a potent oxidant and causes protein (tyrosine) *nitration*. This reaction may be direct, or via decomposition of ONO_2^- to NO_2, which can mediate nitration reactions under inflammatory conditions in which hydrogen peroxide (H_2O_2) and heme peroxidases (such as myeloperoxidase) are present in abundance

naling to abnormal proliferation or cell death [105]. In human infants with CNLD, 3-nitrotyrosine levels from circulating and lung-derived proteins are a direct marker of disease severity [106, 107].

The reaction of NO with superoxide to form peroxynitrite occurs at the fastest rate constant known in biology (1.9×10^{10} M^{-1} s^{-1}), such that the two molecules will always react when in proximity [108]. Peroxynitrite is both a nitrating agent [103, 109] and a potent oxidant [108, 110], leading to both tyrosine nitration [101–104] and cysteine oxidation [111]. Peroxynitrite also plays specific roles in the pathogenesis of experimental neonatal PHT, causing pulmonary vasoconstriction [112], vascular remodeling [113, 114] and RV dysfunction [115]. Inflammatory cell-derived RNS are also critical to hyperoxia-induced experimental CNLD [114]. Peroxynitrite decomposition catalysts that cause peroxynitrite to decompose to nitrate, rather than the toxic hydroxyl radical generated by spontaneous decomposition [108], have been employed with success by our group as preventive agents in experimental models of CNLD and PHT [113–115]. Unfortunately, currently available peroxynitrite decomposition catalysts are metalloporphyrin (iron or manganese-based) compounds which are potentially toxic, especially to the immature liver. This makes translation of the current generation of such compounds in ELBW infants highly unlikely.

Antioxidant Therapies

Other than the direct cytotoxic effects of ROS on the lung discussed earlier, oxidative stress limits NO bioavailability (by steering NO toward production of RNS), limits the sensitivity of sGC to NO [116] and increases hydrolysis of cGMP via increased expression and activity of PDE 5 [117, 118]. Pharmacological therapy with broad spectrum antioxidants (e.g., Lazaroids or Tempol) is effective at limiting experimental chronic neonatal PHT [119]. However, our group has reported that a major adverse effect of effective antioxidant therapy in neonatal rats was inhibited lung cellular proliferation and decreased somatic growth [119], in keeping with a known critical role for low endogenous levels of ROS in normal growth and development [120]. A potentially safer alternative strategy is to supplement deficient antioxidant enzymes [such as superoxide dismutase (SOD)] or their co-factors. Unfortunately, clinical trials examining preventive effects of recombinant human SOD or selenium (co-factor for glutathione peroxidase) have not shown any impact on the incidence of CNLD [121, 122]. Similarly, preventive treatment with N-acetylcysteine, a glutathione precursor, was of no benefit [123]. The above highlights the challenges inherent in developing antioxidant therapies for the newborn that are both safe and effective [120]. The possibility must also be considered that, despite ample evidence of increased oxidative markers in the lungs of infants with evolving and established CNLD, increased ROS may not play a uniformly pathological role.

Strategies to Improve Endogenous NO Function

Endogenous endothelial NO production by endothelial nitric oxide synthase (eNOS) requires an adequate supply of substrate, L-arginine, and arginine precursors, including L-citrulline. In the absence of sufficient substrate, "uncoupling" of eNOS results in a shift from NO to superoxide production. Up-regulation of arginases are an important cause of substrate deficiency directly contributing to inflammation and lung injury, which is preventable by hypercapnic acidosis in hypoxia-exposed neonatal rats [124] or by arginase-specific inhibitors in LPS-exposed Guinea pigs [125]. Supplementation of L-citrulline has also been shown to inhibit arginase and to prevent hyperoxia-induced lung injury in neonatal rats [88]. Tetrahydrobiopterin (BH4) is an important cofactor for eNOS to remain in a coupled state. Newborn mice haploinsufficient for GTP cyclohydrolase I, a rate-limiting enzyme in BH4 synthesis, spontaneously develop PHT [126]. eNOS function may be restored by treatment with L-sepiapterin, which serves as a substrate for BH4 synthesis [86].

Alternative NO-Based Therapies

Nitrite was until recently considered a physiologically inert by-product of NO oxidation. It is now apparent that circulating nitrite is recycled in tissues to form NO, thereby acting as a stable endocrine pool for "NO-like" bioactivity that is complementary to endogenous NOS [127]. Systemic or inhaled inorganic nitrite possesses many theoretical advantages over other forms of NO-based therapy in that tachyphylaxis does not occur with chronic dosing, effects are of relatively rapid onset and last many hours and (sodium) nitrite is inexpensive and stable. Protective effects of sodium nitrite on adult experimental models of PHT have been reported [127–131] but no studies have been reported to date in neonatal animals.

Rho-Kinase (ROCK) Inhibitors

Activation of the small GTPase, RhoA, by G-protein-coupled receptor ligands, and its downstream effector, ROCK [132–135], is a key pathway leading to sustained vasoconstriction and vascular remodeling in experimental chronic neonatal PHT [118, 136–140]. In neonatal rats with bleomycin-induced lung injury, ROCK is critical to inhibited pulmonary angiogenesis, possibly via up-regulation of anti-angiogenic thrombospondin (TSP)-1 [140]. ROCK mediates smooth muscle contraction by causing calcium sensitization [141, 142]. NO-mediated reversal of vasoconstriction is in part mediated through attenuating effects on RhoA expression [143] and activation [144–146], or through direct inhibitory effects on ROCK activity [147–149]. Hence, therapies which enhance cGMP signaling also suppress RhoA/ROCK activation [150, 151, 152].

The above insights have developed largely from experimental use of two kinase inhibitors, Y-27632 [153] and Fasudil (HA-1077) [154], which possess high specificity toward ROCK. Numerous animal studies [155] [136] and pilot reports using single doses or brief infusions of Fasudil in human adults [156, 157] and children [158] have confirmed an efficacy that is equal or superior to existing vasodilators. In addition to modulating vascular smooth muscle tone, evidence also indicates that ROCK regulates the expression of key mediators which modify smooth muscle phenotype, including actin polymerisation through LIM domain kinase-induced inhibition of cofilin [159] and changes in expression of mediators leading to increased proliferation and inhibited apoptosis of vascular smooth muscle, including platelet-derived growth factors [138, 160] and endothelin-1 [86, 113, 115, 137, 138, 161–166]. ROCK inhibitors are also effective when given by inhalation [157]. In addition, ROCK appears to play a role in cardiac failure with benefits of ROCK inhibition on the failing left ventricle being well-described [167–169]. Recent work in adult animals has also identified a direct role for ROCK in experimental RV hypertrophy and dysfunction [170]. Neonatal rat pups chronically exposed to hypoxia develop significant RV systolic dysfunction, secondary to afterload-independent mechanisms that involve up-regulated RV ROCK activity [171]. No studies employing ROCK inhibitors have been conducted to date in human neonates.

Cell-Based Therapy

Endogenous endothelial and mesenchymal progenitor cells appear to play a role in normal lung development and in repair from lung injury [172–180]. Treatment with mesenchymal [181, 182] or endothelial [177] progenitor cells prevents experimental CNLD. These effects appear to be mediated by secreted factors [176, 181, 183], which as yet remain unidentified. A phase 1 study examining safety of intra-tracheal delivery of allogeneic umbilical cord blood-derived mesenchymal stem cells in preterm infants has been recently reported [184].

Therapies Targeting Specific Growth Factors or Cytokines

Antagonizing growth factors or cytokines which are up-regulated during injury is another promising therapeutic approach. A candidate for which there is abundant supportive evidence is transforming growth factor (TGF)β1. Increased TGFβ is observed in lung tissue at autopsy of infants with CNLD [185] and bronchoalveolar lavage (BAL)

fluid of human preterm infants destined to develop CNLD [186]. Blockade of TGFβ1 signalling prevents vascular remodeling [187, 188] and inhibited alveolarization [189] in experimental animals. Interestingly, protective effects of attenuated ROCK signalling [190, 191] and peroxisome proliferator-activated receptor agonism [192–194] on the lung and heart may at least partially result from inhibition of TGFβ1 signalling. Another rational target is interleukin (IL)-1. Increased BAL and serum IL-1β is evident in infants developing CNLD [195, 196]. Transgenic mice over-expressing IL-1β develop a lung injury similar to CNLD, with lack of alveolar septation, and impaired vascular development of the lung, which may be mediated through effects on the retinoic acid pathway [197]. They also have inflammation mediated by the increased expression of neutrophil and macrophage chemokines [197]. Antagonism of IL-1β receptor signalling protects against hyperoxia-induced lung injury [198] and iNO-induced RV systolic dysfunction in neonatal rats [199].

Conclusions

CNLD remains an important and unresolved health issue in infants born extremely preterm. If major therapeutic inroads are to be made in the future, it will need to be through novel pharmacologic interventions based on mechanistic insights derived from relevant animal models. Such studies ideally should: (1) examine for toxicity and dose-response in multiple models, (2) incorporate reversal of established disease as well as prevention as therapeutic strategies and (3) include evaluation of sex differences, functional effects (exercise capacity, airway and vascular reactivity) and longevity of effects into adult life.

With respect to understanding the determinants of PHT in CNLD, there are a number of barriers to improving upon our currently poor understanding of pathogenesis and natural history in human infants. Diagnosis of PHT and right heart dysfunction is problematic. Clinical signs are unreliable and catheterization is often not feasible until well after term corrected age, leading to a sole reliance on echocardiography. Performance of echocardiography can be challenging, especially for evaluation of the right heart due to the thin chest walls of premature infants and frequent presence of lung hyperinflation. Echocardiography-derived parameters indicating raised pulmonary arterial pressure, such as triscuspid regurgitant jet velocity, are not measurable in all patients, and when present have been shown to correlate poorly with pulmonary arterial pressure measured by catheter [61]. In addition, there are no agreed upon echocardiography-based definitions for diagnosis of PHT in neonates, and certainly none for evaluation of right heart function. Systematic study of echocardiographic parameters of RV function that are useful in newborns is required, incorporating new methodologies, including tissue Doppler and strain imaging, that have shown potential in older children and adults [200, 201]. Finally, lung or heart-lung transplantation, the only "curative" option for end-stage disease, is rarely feasible in CNLD-associated PHT, which contributes to a paucity of high quality human tissue available for study and a consequently much greater reliance on mechanistic and therapeutic insights from preclinical models [17].

While improved understanding of pathophysiological mechanisms will certainly facilitate the development of new therapies, challenges to clinical translation remain significant and include the inherent variability in phenotype and risk for CNLD and the development of associated PHT, the relatively low numbers of patients available for study and the uniquely high potential of this vulnerable population for off-target drug effects. Such considerations also have important implications for adoption of existing therapies employed in older children and adults.

References

1. Delivoria-Papadopoulos M, Levison H, Swyer PR. Intermittent positive pressure respiration as a treatment in severe respiratory distress syndrome. Arch Dis Child. 1965;40(213):474–9.
2. Northway WH Jr, Rosan RC, Porter DY. Pulmonary disease following respirator therapy of hyaline-membrane disease. Bronchopulmonary dysplasia. N Engl J Med. 1967;276(7):357–68.

3. Jain D, Bancalari E. Bronchopulmonary dysplasia: clinical perspective. Birth Defects Res A Clin Mol Teratol. 2014;100(3):134–44.
4. Shah PS, Sankaran K, Aziz K, Allen AC, Seshia M, Ohlsson A, et al. Outcomes of preterm infants <29 weeks gestation over 10-year period in Canada: a cause for concern? J Perinatol. 2012;32(2):132–8.
5. Bhandari V. Postnatal inflammation in the pathogenesis of bronchopulmonary dysplasia. Birth Defects Res A Clin Mol Teratol. 2014;100(3):189–201.
6. Bhandari A, Panitch HB. Pulmonary outcomes in bronchopulmonary dysplasia. Semin Perinatol. 2006;30(4):219–26.
7. Gough A, Spence D, Linden M, Halliday HL, McGarvey LP. General and respiratory health outcomes in adult survivors of bronchopulmonary dysplasia: a systematic review. Chest. 2012;141(6):1554–67.
8. Anderson PJ, Doyle LW. Neurodevelopmental outcome of bronchopulmonary dysplasia. Semin Perinatol. 2006;30(4):227–32.
9. Jobe AH, Bancalari E. Bronchopulmonary dysplasia. Am J Respir Crit Care Med. 2001;163(7):1723–9.
10. Mailaparambil B, Krueger M, Heizmann U, Schlegel K, Heinze J, Heinzmann A. Genetic and epidemiological risk factors in the development of bronchopulmonary dysplasia. Dis Markers. 2010;29(1):1–9.
11. Rezvani M, Wilde J, Vitt P, Mailaparambil B, Grychtol R, Krueger M, et al. Association of a FGFR-4 gene polymorphism with bronchopulmonary dysplasia and neonatal respiratory distress. Dis Markers. 2013;35(6):633–40.
12. Pietrzyk JJ, Kwinta P, Wollen EJ, Bik-Multanowski M, Madetko-Talowska A, Gunther CC, et al. Gene expression profiling in preterm infants: new aspects of bronchopulmonary dysplasia development. PLoS One. 2013;8(10):e78585.
13. Thurlbeck WM. Lung growth and alveolar multiplication. Pathobiol Annu. 1975;5:1–34.
14. Thurlbeck WM. Postnatal growth and development of the lung. Am Rev Respir Dis. 1975;111(6):803–44.
15. Kotecha S. Lung growth: implications for the newborn infant. Arch Dis Child Fetal Neonatal Ed. 2000;82(1):F69–74.
16. Hislop AA. Airway and blood vessel interaction during lung development. J Anat. 2002;201(4):325–34.
17. Hilgendorff A, Reiss I, Ehrhardt H, Eickelberg O, Alvira CM. Chronic lung disease in the preterm infant. Lessons learned from animal models. Am J Respir Cell Mol Biol. 2014;50(2):233–45.
18. Zeltner TB, Caduff JH, Gehr P, Pfenninger J, Burri PH. The postnatal development and growth of the human lung. I. Morphometry. Respir Physiol. 1987;67(3):247–67.
19. Zeltner TB, Burri PH. The postnatal development and growth of the human lung. II. Morphology. Respir Physiol. 1987;67(3):269–82.
20. Coalson JJ. Pathology of chronic lung disease of early infancy. In: Bland RD, Coalson JJ, editors. Chronic lung disease in early infancy. New York: Marcel Dekker; 2000. p. 85–124.
21. Bhatt AJ, Pryhuber GS, Huyck H, Watkins RH, Metlay LA, Maniscalco WM. Disrupted pulmonary vasculature and decreased vascular endothelial growth factor, Flt-1, and TIE-2 in human infants dying with bronchopulmonary dysplasia. Am J Respir Crit Care Med. 2001;164(10 Pt 1):1971–80.
22. Wong PM, Lees AN, Louw J, Lee FY, French N, Gain K, et al. Emphysema in young adult survivors of moderate-to-severe bronchopulmonary dysplasia. Eur Respir J. 2008;32(2):321–8.
23. Mourani PM, Abman SH. Pulmonary vascular disease in bronchopulmonary dysplasia: pulmonary hypertension and beyond. Curr Opin Pediatr. 2013;25(3):329–37.
24. An HS, Bae EJ, Kim GB, Kwon BS, Beak JS, Kim EK, et al. Pulmonary hypertension in preterm infants with bronchopulmonary dysplasia. Korean Circ J. 2010;40(3):131–6.
25. Khemani E, McElhinney DB, Rhein L, Andrade O, Lacro RV, Thomas KC, et al. Pulmonary artery hypertension in formerly premature infants with bronchopulmonary dysplasia: clinical features and outcomes in the surfactant era. Pediatrics. 2007;120(6):1260–9.
26. Slaughter JL, Pakrashi T, Jones DE, South AP, Shah TA. Echocardiographic detection of pulmonary hypertension in extremely low birth weight infants with bronchopulmonary dysplasia requiring prolonged positive pressure ventilation. J Perinatol. 2011;31(10):635–40.
27. Bhat R, Salas AA, Foster C, Carlo WA, Ambalavanan N. Prospective analysis of pulmonary hypertension in extremely low birth weight infants. Pediatrics. 2012;129(3):e682–9.
28. Kim DH, Kim HS, Choi CW, Kim EK, Kim BI, Choi JH. Risk factors for pulmonary artery hypertension in preterm infants with moderate or severe bronchopulmonary dysplasia. Neonatology. 2012;101(1):40–6.
29. Thibeault DW, Truog WE, Ekekezie II. Acinar arterial changes with chronic lung disease of prematurity in the surfactant era. Pediatr Pulmonol. 2003;36(6):482–9.
30. Del Cerro MJ, Sabate Rotes A, Carton A, Deiros L, Bret M, Cordeiro M, et al. Pulmonary hypertension in bronchopulmonary dysplasia: Clinical findings, cardiovascular anomalies and outcomes. Pediatr Pulmonol. 2014;49(1):49–59.
31. Drossner DM, Kim DW, Maher KO, Mahle WT. Pulmonary vein stenosis: prematurity and associated conditions. Pediatrics. 2008;122(3):e656–61.
32. Sartori C, Allemann Y, Trueb L, Delabays A, Nicod P, Scherrer U. Augmented vasoreactivity in adult life associated with perinatal vascular insult. Lancet. 1999;353(9171):2205–7.
33. Voelkel NF, Quaife RA, Leinwand LA, Barst RJ, McGoon MD, Meldrum DR, et al. Right ventricular function and failure: report of a National Heart,

Lung, and Blood Institute working group on cellular and molecular mechanisms of right heart failure. Circulation. 2006;114(17):1883–91.
34. Bogaard HJ, Abe K, Vonk Noordegraaf A, Voelkel NF. The right ventricle under pressure: cellular and molecular mechanisms of right-heart failure in pulmonary hypertension. Chest. 2009;135(3):794–804.
35. Haddad F, Doyle R, Murphy DJ, Hunt SA. Right ventricular function in cardiovascular disease, part II: pathophysiology, clinical importance, and management of right ventricular failure. Circulation. 2008;117(13):1717–31.
36. van Loon RL, Roofthooft MT, Delhaas T, van Osch-Gevers M, ten Harkel AD, Strengers JL, et al. Outcome of pediatric patients with pulmonary arterial hypertension in the era of new medical therapies. Am J Cardiol. 2010;106(1):117–24.
37. Bogaard HJ, Natarajan R, Henderson SC, Long CS, Kraskauskas D, Smithson L, et al. Chronic pulmonary artery pressure elevation is insufficient to explain right heart failure. Circulation. 2009;120(20):1951–60.
38. Ehrenkranz RA. Nutrition, growth and clinical outcomes. World Rev Nutr Diet. 2014;110:11–26.
39. Frank L. Antioxidants, nutrition, and bronchopulmonary dysplasia. Clin Perinatol. 1992;19(3):541–62.
40. Slaughter JL, Stenger MR, Reagan PB. Variation in the use of diuretic therapy for infants with bronchopulmonary dysplasia. Pediatrics. 2013;131(4):716–23.
41. Segar JL. Neonatal diuretic therapy: furosemide, thiazides, and spironolactone. Clin Perinatol. 2012;39(1):209–20.
42. Yam J, Frank L, Roberts RJ. Age-related development of pulmonary antioxidant enzymes in the rat. Proc Soc Exp Biol Med. 1978;157(2):293–6.
43. Tanswell AK, Freeman BA. Pulmonary antioxidant enzyme maturation in the fetal and neonatal rat. I. Developmental profiles. Pediatr Res. 1984;18(7):584–7.
44. Saugstad OD. Oxygen radical disease in neonatology. Semin Neonatol. 1998;3(3):229–38.
45. The STOP-ROP Study Group. Supplemental Therapeutic Oxygen for Prethreshold Retinopathy Of Prematurity (STOP-ROP), a randomized, controlled trial. I: primary outcomes. Pediatrics. 2000;105(2):295–310.
46. Boost-II Collaborative Groups. Oxygen saturation and outcomes in preterm infants. N Engl J Med. 2013;368(22):2094–104.
47. Bancalari E, Claure N. Oxygenation targets and outcomes in premature infants. JAMA. 2013;309(20):2161–2.
48. Lakshminrusimha S, Swartz DD, Gugino SF, Ma CX, Wynn KA, Ryan RM, et al. Oxygen concentration and pulmonary hemodynamics in newborn lambs with pulmonary hypertension. Pediatr Res. 2009;66(5):539–44.
49. Lakshminrusimha S, Russell JA, Steinhorn RH, Ryan RM, Gugino SF, Morin FC 3rd, et al. Pulmonary arterial contractility in neonatal lambs increases with 100% oxygen resuscitation. Pediatr Res. 2006;59(1):137–41.
50. Mourani PM, Ivy DD, Gao D, Abman SH. Pulmonary vascular effects of inhaled nitric oxide and oxygen tension in bronchopulmonary dysplasia. Am J Respir Crit Care Med. 2004;170(9):1006–13.
51. Banks BA, Seri I, Ischiropoulos H, Merrill J, Rychik J, Ballard RA. Changes in oxygenation with inhaled nitric oxide in severe bronchopulmonary dysplasia. Pediatrics. 1999;103(3):610–8.
52. Ivy DD, Abman SH, Barst RJ, Berger RM, Bonnet D, Fleming TR, et al. Pediatric pulmonary hypertension. J Am Coll Cardiol. 2013;62(25 Suppl):D117–26.
53. Kulik TJ, Rhein LM, Mullen MP. Pulmonary arterial hypertension in infants with chronic lung disease: will we ever understand it? J Pediatr. 2010;157(2):186–90.
54. Nyp M, Sandritter T, Poppinga N, Simon C, Truog WE. Sildenafil citrate, bronchopulmonary dysplasia and disordered pulmonary gas exchange: any benefits? J Perinatol. 2012;32(1):64–9.
55. Wardle AJ, Wardle R, Luyt K, Tulloh R. The utility of sildenafil in pulmonary hypertension: a focus on bronchopulmonary dysplasia. Arch Dis Child. 2013;98(8):613–7.
56. Krishnan U, Krishnan S, Gewitz M. Treatment of pulmonary hypertension in children with chronic lung disease with newer oral therapies. Pediatr Cardiol. 2008;29(6):1082–6.
57. Rugolotto S, Errico G, Beghini R, Ilic S, Richelli C, Padovani EM. Weaning of epoprostenol in a small infant receiving concomitant bosentan for severe pulmonary arterial hypertension secondary to bronchopulmonary dysplasia. Minerva Pediatr. 2006;58(5):491–4.
58. McIntyre CM, Hanna BD, Rintoul N, Ramsey EZ. Safety of epoprostenol and treprostinil in children less than 12 months of age. Pulm Circ. 2013;3(4):862–9.
59. Borgdorff MA, Bartelds B, Dickinson MG, Boersma B, Weij M, Zandvoort A, et al. Sildenafil enhances systolic adaptation, but does not prevent diastolic dysfunction, in the pressure-loaded right ventricle. Eur J Heart Fail. 2012;14(9):1067–74.
60. Nagendran J, Archer SL, Soliman D, Gurtu V, Moudgil R, Haromy A, et al. Phosphodiesterase type 5 is highly expressed in the hypertrophied human right ventricle, and acute inhibition of phosphodiesterase type 5 improves contractility. Circulation. 2007;116(3):238–48.
61. Mourani PM, Sontag MK, Younoszai A, Ivy DD, Abman SH. Clinical utility of echocardiography for the diagnosis and management of pulmonary vascular disease in young children with chronic lung disease. Pediatrics. 2008;121(2):317–25.
62. McEvoy CT, Jain L, Schmidt B, Abman S, Bancalari E, Aschner JL. Bronchopulmonary dysplasia: NHLBI workshop on the primary prevention of chronic

lung diseases. Ann Am Thorac Soc. 2014;11(Suppl 3):S146–53.
63. Ghanta S, Leeman KT, Christou H. An update on pharmacologic approaches to bronchopulmonary dysplasia. Semin Perinatol. 2013;37(2):115–23.
64. Schmidt B, Roberts RS, Davis P, Doyle LW, Barrington KJ, Ohlsson A, et al. Caffeine therapy for apnea of prematurity. N Engl J Med. 2006;354(20):2112–21.
65. Tyson JE, Wright LL, Oh W, Kennedy KA, Mele L, Ehrenkranz RA, et al. Vitamin A supplementation for extremely-low-birth-weight infants. National Institute of Child Health and Human Development Neonatal Research Network. N Engl J Med. 1999;340(25):1962–8.
66. Doyle LW, Ehrenkranz RA, Halliday HL. Dexamethasone treatment in the first week of life for preventing bronchopulmonary dysplasia in preterm infants: a systematic review. Neonatology. 2010;98(3):217–24.
67. Dobson NR, Patel RM, Smith PB, Kuehn DR, Clark J, Vyas-Read S, et al. Trends in caffeine use and association between clinical outcomes and timing of therapy in very low birth weight infants. J Pediatr. 2014;164(5):992–8. e3
68. Taha D, Kirkby S, Nawab U, Dysart KC, Genen L, Greenspan JS, et al. Early caffeine therapy for prevention of bronchopulmonary dysplasia in preterm infants. J Matern Fetal Neonatal Med. 2014. https://doi.org/10.3109/14767058.2014.885941.
69. Kreutzer K, Bassler D. Caffeine for apnea of prematurity: a neonatal success story. Neonatology. 2014;105(4):332–6.
70. Guimaraes H, Guedes MB, Rocha G, Tome T, Albino-Teixeira A. Vitamin A in prevention of bronchopulmonary dysplasia. Curr Pharm Des. 2012;18(21):3101–13.
71. Doyle LW, Ehrenkranz RA, Halliday HL. Early (< 8 days) postnatal corticosteroids for preventing chronic lung disease in preterm infants. Cochrane Database Syst Rev. 2014;5:CD001146.
72. Price LC, Montani D, Tcherakian C, Dorfmuller P, Souza R, Gambaryan N, et al. Dexamethasone reverses monocrotaline-induced pulmonary arterial hypertension in rats. Eur Respir J. 2011;37(4):813–22.
73. Le Cras TD, Markham NE, Morris KG, Ahrens CR, McMurtry IF, Abman SH. Neonatal dexamethasone treatment increases the risk for pulmonary hypertension in adult rats. Am J Physiol Lung Cell Mol Physiol. 2000;278(4):L822–9.
74. Ziegler JW, Ivy DD, Kinsella JP, Abman SH. The role of nitric oxide, endothelin, and prostaglandins in the transition of the pulmonary circulation. Clin Perinatol. 1995;22(2):387–403.
75. Kang JL, Park W, Pack IS, Lee HS, Kim MJ, Lim CM, et al. Inhaled nitric oxide attenuates acute lung injury via inhibition of nuclear factor-kappa B and inflammation. J Appl Physiol. 2002;92(2):795–801.
76. Stenger MR, Rose MJ, Joshi MS, Rogers LK, Chicoine LG, Bauer JA, et al. Inhaled nitric oxide prevents 3-nitrotyrosine formation in the lungs of neonatal mice exposed to >95% oxygen. Lung. 2010;188(3):217–27.
77. Thomae KR, Nakayama DK, Billiar TR, Simmons RL, Pitt BR, Davies P. The effect of nitric oxide on fetal pulmonary artery smooth muscle growth. J Surg Res. 1995;59(3):337–43.
78. Tang JR, Seedorf G, Balasubramaniam V, Maxey A, Markham N, Abman SH. Early inhaled nitric oxide treatment decreases apoptosis of endothelial cells in neonatal rat lungs after vascular endothelial growth factor inhibition. Am J Physiol Lung Cell Mol Physiol. 2007;293(5):L1271–80.
79. Zachary I, Gliki G. Signaling transduction mechanisms mediating biological actions of the vascular endothelial growth factor family. Cardiovasc Res. 2001;49(3):568–81.
80. Thebaud B, Abman SH. Bronchopulmonary dysplasia: where have all the vessels gone? Roles of angiogenic growth factors in chronic lung disease. Am J Respir Crit Care Med. 2007;175(10):978–85.
81. Bachiller PR, Cornog KH, Kato R, Buys ES, Roberts JD Jr. Soluble guanylate cyclase modulates alveolarization in the newborn lung. Am J Physiol Lung Cell Mol Physiol. 2013;305(8):L569–81.
82. Tonelli AR, Haserodt S, Aytekin M, Dweik RA. Nitric oxide deficiency in pulmonary hypertension: Pathobiology and implications for therapy. Pulm Circ. 2013;3(1):20–30.
83. Bland RD, Albertine KH, Carlton DP, Macritchie AJ. Inhaled nitric oxide effects on lung structure and function in chronically ventilated preterm lambs. Am J Respir Crit Care Med. 2005;172(7):899–906.
84. Ladha F, Bonnet S, Eaton F, Hashimoto K, Korbutt G, Thebaud B. Sildenafil improves alveolar growth and pulmonary hypertension in hyperoxia-induced lung injury. Am J Respir Crit Care Med. 2005;172(6):750–6.
85. Tourneux P, Markham N, Seedorf G, Balasubramaniam V, Abman SH. Inhaled nitric oxide improves lung structure and pulmonary hypertension in a model of bleomycin-induced bronchopulmonary dysplasia in neonatal rats. Am J Physiol Lung Cell Mol Physiol. 2009;297(6):L1103–11.
86. Teng RJ, Du J, Xu H, Bakhutashvili I, Eis A, Shi Y, et al. Sepiapterin improves angiogenesis of pulmonary artery endothelial cells with in utero pulmonary hypertension by recoupling endothelial nitric oxide synthase. Am J Physiol Lung Cell Mol Physiol. 2011;301(3):L334–45.
87. Park HS, Park JW, Kim HJ, Choi CW, Lee HJ, Kim BI, et al. Sildenafil alleviates bronchopulmonary dysplasia in neonatal rats by activating the hypoxia-inducible factor signaling pathway. Am J Respir Cell Mol Biol. 2013;48(1):105–13.
88. Vadivel A, Aschner JL, Rey-Parra GJ, Magarik J, Zeng H, Summar M, et al. L-citrulline attenuates

arrested alveolar growth and pulmonary hypertension in oxygen-induced lung injury in newborn rats. Pediatr Res. 2010;68(6):519–25.
89. Raffay TM, Martin RJ, Reynolds JD. Can nitric oxide-based therapy prevent bronchopulmonary dysplasia? Clin Perinatol. 2012;39(3):613–38.
90. Askie LM, Ballard RA, Cutter GR, Dani C, Elbourne D, Field D, et al. Inhaled nitric oxide in preterm infants: an individual-patient data meta-analysis of randomized trials. Pediatrics. 2011;128(4):729–39.
91. Cole FS, Alleyne C, Barks JD, Boyle RJ, Carroll JL, Dokken D, et al. NIH Consensus Development Conference Statement: inhaled nitric-oxide therapy for premature infants. Pediatrics. 2011;127(2):363–9.
92. Day RW, Lynch JM, White KS, Ward RM. Acute response to inhaled nitric oxide in newborns with respiratory failure and pulmonary hypertension. Pediatrics. 1996;98(4 Pt 1):698–705.
93. Gaston B, Singel D, Doctor A, Stamler JS. S- nitrosothiol signaling in respiratory biology. Am J Respir Crit Care Med. 2006;173(11):1186–93.
94. Auten RL, Mason SN, Whorton MH, Lampe WR, Foster WM, Goldberg RN, et al. Inhaled ethyl nitrite prevents hyperoxia-impaired postnatal alveolar development in newborn rats. Am J Respir Crit Care Med. 2007;176(3):291–9.
95. Moya MP, Gow AJ, Califf RM, Goldberg RN, Stamler JS. Inhaled ethyl nitrite gas for persistent pulmonary hypertension of the newborn. Lancet. 2002;360(9327):141–3.
96. Gadhia MM, Cutter GR, Abman SH, Kinsella JP. Effects of early inhaled nitric oxide therapy and vitamin A supplementation on the risk for bronchopulmonary dysplasia in premature newborns with respiratory failure. J Pediatr. 2014;164(4):744–8.
97. Konig K, Barfield CP, Guy KJ, Drew SM, Andersen CC. The effect of sildenafil on evolving bronchopulmonary dysplasia in extremely preterm infants: a randomised controlled pilot study. J Matern Fetal Neonatal Med. 2014;27(5):439–44.
98. Thomas DD, Miranda KM, Colton CA, Citrin D, Espey MG, Wink DA. Heme proteins and nitric oxide (NO): the neglected, eloquent chemistry in NO redox signaling and regulation. Antioxid Redox Signal. 2003;5(3):307–17.
99. Thomas DD, Espey MG, Vitek MP, Miranda KM, Wink DA. Protein nitration is mediated by heme and free metals through Fenton-type chemistry: an alternative to the NO/O2- reaction. Proc Natl Acad Sci U S A. 2002;99(20):12691–6.
100. van der Vliet A, Eiserich JP, O'Neill CA, Halliwell B, Cross CE. Tyrosine modification by reactive nitrogen species: a closer look. Arch Biochem Biophys. 1995;319(2):341–9.
101. Gole MD, Souza JM, Choi I, Hertkorn C, Malcolm S, Foust RF 3rd, et al. Plasma proteins modified by tyrosine nitration in acute respiratory distress syndrome. Am J Physiol Lung Cell Mol Physiol. 2000;278(5):L961–7.
102. Peluffo G, Radi R. Biochemistry of protein tyrosine nitration in cardiovascular pathology. Cardiovasc Res. 2007;75(2):291–302.
103. Souza JM, Peluffo G, Radi R. Protein tyrosine nitration--functional alteration or just a biomarker? Free Radic Biol Med. 2008;45(4):357–66.
104. Turko IV, Murad F. Protein nitration in cardiovascular diseases. Pharmacol Rev. 2002;54(4):619–34.
105. Pacher P, Beckman JS, Liaudet L. Nitric oxide and peroxynitrite in health and disease. Physiol Rev. 2007;87(1):315–424.
106. Sheffield M, Mabry S, Thibeault DW, Truog WE. Pulmonary nitric oxide synthases and nitrotyrosine: findings during lung development and in chronic lung disease of prematurity. Pediatrics. 2006;118(3):1056–64.
107. Banks BA, Ischiropoulos H, McClelland M, Ballard PL, Ballard RA. Plasma 3-nitrotyrosine is elevated in premature infants who develop bronchopulmonary dysplasia. Pediatrics. 1998;101(5):870–4.
108. Beckman JS, Beckman TW, Chen J, Marshall PA, Freeman BA. Apparent hydroxyl radical production by peroxynitrite: implications for endothelial injury from nitric oxide and superoxide. Proc Natl Acad Sci U S A. 1990;87(4):1620–4.
109. Zou M, Martin C, Ullrich V. Tyrosine nitration as a mechanism of selective inactivation of prostacyclin synthase by peroxynitrite. Biol Chem. 1997;378(7):707–13.
110. Beckman JS, Koppenol WH. Nitric oxide, superoxide, and peroxynitrite: the good, the bad, and ugly. Am J Phys. 1996;271(5 Pt 1):C1424–37.
111. Quijano C, Alvarez B, Gatti RM, Augusto O, Radi R. Pathways of peroxynitrite oxidation of thiol groups. Biochem J. 1997;322(Pt 1):167–73.
112. Belik J, Jankov RP, Pan J, Tanswell AK. Peroxynitrite inhibits relaxation and induces pulmonary artery muscle contraction in the newborn rat. Free Radic Biol Med. 2004;37(9):1384–92.
113. Belik J, Stevens D, Pan J, McIntyre BA, Kantores C, Ivanovska J, et al. Pulmonary vascular and cardiac effects of peroxynitrite decomposition in newborn rats. Free Radic Biol Med. 2010;49(8):1306–14.
114. Masood A, Belcastro R, Li J, Kantores C, Jankov RP, Tanswell AKA. peroxynitrite decomposition catalyst prevents 60% O_2-mediated rat chronic neonatal lung injury. Free Radic Biol Med. 2010;49(7):1182–91.
115. Jankov RP, Lewis P, Kantores C, Ivanovska J, EZ X, Van Vliet T, et al. Peroxynitrite mediates right-ventricular dysfunction in nitric oxide-exposed juvenile rats. Free Radic Biol Med. 2010;49(9):1453–67.
116. Mingone CJ, Gupte SA, Ali N, Oeckler RA, Wolin MS. Thiol oxidation inhibits nitric oxide-mediated pulmonary artery relaxation and guanylate cyclase stimulation. Am J Physiol Lung Cell Mol Physiol. 2006;290(3):L549–57.
117. Farrow KN, Groh BS, Schumacker PT, Lakshminrusimha S, Czech L, Gugino SF, et al. Hyperoxia increases phosphodiesterase 5 expression

and activity in ovine fetal pulmonary artery smooth muscle cells. Circ Res. 2008;102(2):226–33.
118. Peng G, Ivanovska J, Kantores C, Van Vliet T, Engelberts D, Kavanagh BP, et al. Sustained therapeutic hypercapnia attenuates pulmonary arterial Rho-kinase activity and ameliorates chronic hypoxic pulmonary hypertension in juvenile rats. Am J Physiol Heart Circ Physiol. 2012;302(12):H2599–611.
119. Jankov RP, Kantores C, Pan J, Belik J. Contribution of xanthine oxidase-derived superoxide to chronic hypoxic pulmonary hypertension in neonatal rats. Am J Physiol Lung Cell Mol Physiol. 2008;294(2):L233–45.
120. Jankov RP, Negus A, Tanswell AK. Antioxidants as therapy in the newborn: Some words of caution. Pediatr Res. 2001;50(6):681–7.
121. Davis JM, Rosenfeld WN, Richter SE, Parad MR, Gewolb IH, Spitzer AR, et al. Safety and pharmacokinetics of multiple doses of recombinant human CuZn superoxide dismutase administered intratracheally to premature neonates with respiratory distress syndrome. Pediatrics. 1997;100(1):24–30.
122. Darlow BA, Winterbourn CC, Inder TE, Graham PJ, Harding JE, Weston PJ, et al. The effect of selenium supplementation on outcome in very low birth weight infants: a randomized controlled trial. The New Zealand Neonatal Study Group. J Pediatr. 2000;136(4):473–80.
123. Ahola T, Lapatto R, Raivio KO, Selander B, Stigson L, Jonsson B, et al. N-acetylcysteine does not prevent bronchopulmonary dysplasia in immature infants: a randomized controlled trial. J Pediatr. 2003;143(6):713–9.
124. Belik J, Stevens D, Pan J, Shehnaz D, Ibrahim C, Kantores C, et al. Chronic hypercapnia downregulates arginase expression and activity and increases pulmonary arterial smooth muscle relaxation in the newborn rat. Am J Physiol Lung Cell Mol Physiol. 2009;297(4):L777–84.
125. Pera T, Zuidhof AB, Smit M, Menzen MH, Klein T, Flik G, et al. Arginase inhibition prevents inflammation and remodeling in a Guinea pig model of chronic obstructive pulmonary disease. J Pharmacol Exp Ther. 2014;349(2):229–38.
126. Belik J, McIntyre BA, Enomoto M, Pan J, Grasemann H, Vasquez-Vivar J. Pulmonary hypertension in the newborn GTP cyclohydrolase I-deficient mouse. Free Radic Biol Med. 2011;51(12):2227–33.
127. Bueno M, Wang J, Mora AL, Gladwin MT. Nitrite signaling in pulmonary hypertension: mechanisms of bioactivation, signaling, and therapeutics. Antioxid Redox Signal. 2013;18(14):1797–809.
128. Zuckerbraun BS, Shiva S, Ifedigbo E, Mathier MA, Mollen KP, Rao J, et al. Nitrite potently inhibits hypoxic and inflammatory pulmonary arterial hypertension and smooth muscle proliferation via xanthine oxidoreductase-dependent nitric oxide generation. Circulation. 2010;121(1):98–109.
129. Zuckerbraun BS, George P, Gladwin MT. Nitrite in pulmonary arterial hypertension: therapeutic avenues in the setting of dysregulated arginine/nitric oxide synthase signalling. Cardiovasc Res. 2011;89(3):542–52.
130. Baliga RS, Milsom AB, Ghosh SM, Trinder SL, Macallister RJ, Ahluwalia A, et al. Dietary nitrate ameliorates pulmonary hypertension: cytoprotective role for endothelial nitric oxide synthase and xanthine oxidoreductase. Circulation. 2012;125(23):2922–32.
131. Pankey EA, Badejo AM, Casey DB, Lasker GF, Riehl RA, Murthy SN, et al. Effect of chronic sodium nitrite therapy on monocrotaline-induced pulmonary hypertension. Nitric Oxide. 2012;27(1):1–8.
132. Matsui T, Amano M, Yamamoto T, Chihara K, Nakafuku M, Ito M, et al. Rho-associated kinase, a novel serine/threonine kinase, as a putative target for small GTP binding protein Rho. EMBO J. 1996;15(9):2208–16.
133. Somlyo AP, Somlyo AV. Signal transduction by G-proteins, Rho-kinase and protein phosphatase to smooth muscle and non-muscle myosin II. J Physiol. 2000;522(Pt 2):177–85.
134. Seasholtz TM, Majumdar M, Brown JH. Rho as a mediator of G protein-coupled receptor signaling. Mol Pharmacol. 1999;55(6):949–56.
135. Scherer EQ, Herzog M, Wangemann P. Endothelin-1-induced vasospasms of spiral modiolar artery are mediated by rho-kinase-induced Ca(2+) sensitization of contractile apparatus and reversed by calcitonin gene-related Peptide. Stroke. 2002;33(12):2965–71.
136. McNamara PJ, Murthy P, Kantores C, Teixeira L, Engelberts D, van Vliet T, et al. Acute vasodilator effects of Rho-kinase inhibitors in neonatal rats with pulmonary hypertension unresponsive to nitric oxide. Am J Physiol Lung Cell Mol Physiol. 2008;294(2):L205–13.
137. Xu EZ, Kantores C, Ivanovska J, Engelberts D, Kavanagh BP, McNamara PJ, et al. Rescue treatment with a Rho-kinase inhibitor normalizes right ventricular function and reverses remodeling in juvenile rats with chronic pulmonary hypertension. Am J Physiol Heart Circ Physiol. 2010;299(6):H1854–64.
138. Ziino AJ, Ivanovska J, Belcastro R, Kantores C, Xu EZ, Lau M, et al. Effects of rho-kinase inhibition on pulmonary hypertension, lung growth, and structure in neonatal rats chronically exposed to hypoxia. Pediatr Res. 2010;67(2):177–82.
139. Enomoto M, Gosal K, Cubells E, Escobar J, Vento M, Jankov RP, et al. Sex-dependent changes in the pulmonary vasoconstriction potential of newborn rats following short-term oxygen exposure. Pediatr Res. 2012;72(5):468–78.
140. Lee AH, Dhaliwal R, Kantores C, Ivanovska J, Gosal K, McNamara PJ, et al. Rho-kinase inhibitor prevents bleomycin-induced injury in neonatal rats independent of effects on lung inflammation. Am J Respir Cell Mol Biol. 2014;50(1):61–73.
141. Feng J, Ito M, Ichikawa K, Isaka N, Nishikawa M, Hartshorne DJ, et al. Inhibitory phosphorylation site for Rho-associated kinase on smooth muscle myosin phosphatase. J Biol Chem. 1999;274(52):37385–90.

142. Somlyo AP, Somlyo AV. Ca^{2+} sensitivity of smooth muscle and nonmuscle myosin II: modulated by G proteins, kinases, and myosin phosphatase. Physiol Rev. 2003;83(4):1325–58.
143. Sauzeau V, Rolli-Derkinderen M, Marionneau C, Loirand G, Pacaud P. RhoA expression is controlled by nitric oxide through cGMP-dependent protein kinase activation. J Biol Chem. 2003;278(11):9472–80.
144. Murthy KS, Zhou H, Grider JR, Makhlouf GM. Inhibition of sustained smooth muscle contraction by PKA and PKG preferentially mediated by phosphorylation of RhoA. Am J Physiol Gastrointest Liver Physiol. 2003;284(6):G1006–16.
145. Sawada N, Itoh H, Yamashita J, Doi K, Inoue M, Masatsugu K, et al. cGMP-dependent protein kinase phosphorylates and inactivates RhoA. Biochem Biophys Res Commun. 2001;280(3):798–805.
146. Sauzeau V, Le Jeune H, Cario-Toumaniantz C, Smolenski A, Lohmann SM, Bertoglio J, et al. Cyclic GMP-dependent protein kinase signaling pathway inhibits RhoA-induced Ca^{2+} sensitization of contraction in vascular smooth muscle. J Biol Chem. 2000;275(28):21722–9.
147. Jernigan NL, Walker BR, Resta TC. Chronic hypoxia augments protein kinase G-mediated Ca^{2+} desensitization in pulmonary vascular smooth muscle through inhibition of RhoA/Rho kinase signaling. Am J Physiol Lung Cell Mol Physiol. 2004;287(6):L1220–9.
148. Wooldridge AA, MacDonald JA, Erdodi F, Ma C, Borman MA, Hartshorne DJ, et al. Smooth muscle phosphatase is regulated in vivo by exclusion of phosphorylation of threonine 696 of MYPT1 by phosphorylation of Serine 695 in response to cyclic nucleotides. J Biol Chem. 2004;279(33):34496–504.
149. Gao Y, Portugal AD, Liu J, Negash S, Zhou W, Tian J, et al. Preservation of cGMP-induced relaxation of pulmonary veins of fetal lambs exposed to chronic high altitude hypoxia: role of PKG and Rho kinase. Am J Physiol Lung Cell Mol Physiol. 2008;295(5):L889–96.
150. Guilluy C, Sauzeau V, Rolli-Derkinderen M, Guerin P, Sagan C, Pacaud P, et al. Inhibition of RhoA/Rho kinase pathway is involved in the beneficial effect of sildenafil on pulmonary hypertension. Br J Pharmacol. 2005;146(7):1010–8.
151. Hemnes AR, Zaiman A, Champion HC. PDE5A inhibition attenuates bleomycin-induced pulmonary fibrosis and pulmonary hypertension through inhibition of ROS generation and RhoA/Rho kinase activation. Am J Physiol Lung Cell Mol Physiol. 2008;294(1):L24–33.
152. Chung HH, Dai ZK, BN W, Yeh JL, Chai CY, Chu KS, et al. The xanthine derivative KMUP-1 inhibits models of pulmonary artery hypertension via increased NO and cGMP-dependent inhibition of RhoA/Rho kinase. Br J Pharmacol. 2010;160(4):971–86.
153. Ishizaki T, Uehata M, Tamechika I, Keel J, Nonomura K, Maekawa M, et al. Pharmacological properties of Y-27632, a specific inhibitor of Rho-associated kinases. Mol Pharmacol. 2000;57(5):976–83.
154. Sasaki Y, Suzuki M, Hidaka H. The novel and specific Rho-kinase inhibitor (S)-(+)-2-methyl-1-[(4-methyl-5-isoquinoline)sulfonyl]-homopiperazine as a probing molecule for Rho-kinase-involved pathway. Pharmacol Ther. 2002;93(2–3):225–32.
155. McMurtry IF, Abe K, Ota H, Fagan KA, Oka M. Rho kinase-mediated vasoconstriction in pulmonary hypertension. Adv Exp Med Biol. 2010;661:299–308.
156. Ishikura K, Yamada N, Ito M, Ota S, Nakamura M, Isaka N, et al. Beneficial acute effects of Rho-kinase inhibitor in patients with pulmonary arterial hypertension. Circ J. 2006;70(2):174–8.
157. Nagaoka T, Fagan KA, Gebb SA, Morris KG, Suzuki T, Shimokawa H, et al. Inhaled Rho kinase inhibitors are potent and selective vasodilators in rat pulmonary hypertension. Am J Respir Crit Care Med. 2005;171(5):494–9.
158. Li F, Xia W, Yuan S, Sun R. Acute inhibition of Rho-kinase attenuates pulmonary hypertension in patients with congenital heart disease. Pediatr Cardiol. 2009;30(3):363–6.
159. Zeidan A, Javadov S, Karmazyn M. Essential role of Rho/ROCK-dependent processes and actin dynamics in mediating leptin-induced hypertrophy in rat neonatal ventricular myocytes. Cardiovasc Res. 2006;72(1):101–11.
160. Jankov RP, Kantores C, Belcastro R, Yi S, Ridsdale RA, Post M, et al. A role for platelet-derived growth factor β-receptor in a newborn rat model of endothelin-mediated pulmonary vascular remodeling. Am J Physiol Lung Cell Mol Physiol. 2005;288(6):L1162–70.
161. Jankov RP, Kantores C, Belcastro R, Yi M, Tanswell AK. Endothelin-1 inhibits apoptosis of pulmonary arterial smooth muscle in the neonatal rat. Pediatr Res. 2006;60(3):245–51.
162. Yi SL, Kantores C, Belcastro R, Cabacungan J, Tanswell AK, Jankov RP. 8-Isoprostane-induced endothelin-1 production by infant rat pulmonary artery smooth muscle cells is mediated by Rho-kinase. Free Radic Biol Med. 2006;41(6):942–9.
163. Dou D, Ma H, Zheng X, Ying L, Guo Y, Yu X, et al. Degradation of leucine zipper-positive isoform of MYPT1 may contribute to development of nitrate tolerance. Cardiovasc Res. 2010;86(1):151–9.
164. Keller RL, Tacy TA, Hendricks-Munoz K, Xu J, Moon-Grady AJ, Neuhaus J, et al. Congenital diaphragmatic hernia: endothelin-1, pulmonary hypertension, and disease severity. Am J Respir Crit Care Med. 2010;182(4):555–61.
165. Lu Z, Xu X, Hu X, Lee S, Traverse JH, Zhu G, et al. Oxidative stress regulates left ventricular PDE5 expression in the failing heart. Circulation. 2010;121(13):1474–83.
166. Ma H, He Q, Dou D, Zheng X, Ying L, Wu Y, et al. Increased degradation of MYPT1 contributes to the development of tolerance to nitric oxide in porcine

pulmonary artery. Am J Physiol Lung Cell Mol Physiol. 2010;299(1):L117–23.
167. Hamid SA, Bower HS, Baxter GF. Rho kinase activation plays a major role as a mediator of irreversible injury in reperfused myocardium. Am J Physiol Heart Circ Physiol. 2007;292(6):H2598–606.
168. Kobayashi N, Horinaka S, Mita S, Nakano S, Honda T, Yoshida K, et al. Critical role of Rho-kinase pathway for cardiac performance and remodeling in failing rat hearts. Cardiovasc Res. 2002;55(4):757–67.
169. Lin G, Craig GP, Zhang L, Yuen VG, Allard M, McNeill JH, et al. Acute inhibition of Rho-kinase improves cardiac contractile function in streptozotocin-diabetic rats. Cardiovasc Res. 2007;75(1):51–8.
170. Ikeda S, Satoh K, Kikuchi N, Miyata S, Suzuki K, Omura J, et al. Crucial role of rho-kinase in pressure overload-induced right ventricular hypertrophy and dysfunction in mice. Arterioscler Thromb Vasc Biol. 2014;34(6):1260–71.
171. Gosal K, Dunlop K, Ivanovska J, Kantores C, Jain A, McNamara PJ, et al. Right-ventricular systolic dysfunction is mediated by cardiac up-regulation of Rho-kinase activity in juvenile rats with chronic hypoxic pulmonary hypertension. Washington, DC: Pediatric Academic Societies; 2013.
172. Balasubramaniam V, Mervis CF, Maxey AM, Markham NE, Abman SH. Hyperoxia reduces bone marrow, circulating, and lung endothelial progenitor cells in the developing lung: implications for the pathogenesis of bronchopulmonary dysplasia. Am J Physiol Lung Cell Mol Physiol. 2007;292(5):L1073–84.
173. Marsboom G, Pokreisz P, Gheysens O, Vermeersch P, Gillijns H, Pellens M, et al. Sustained endothelial progenitor cell dysfunction after chronic hypoxia-induced pulmonary hypertension. Stem Cells. 2008;26(4):1017–26.
174. Baker CD, Ryan SL, Ingram DA, Seedorf GJ, Abman SH, Balasubramaniam V. Endothelial colony-forming cells from preterm infants are increased and more susceptible to hyperoxia. Am J Respir Crit Care Med. 2009;180(5):454–61.
175. Fadini GP, Avogaro A, Ferraccioli G, Agostini C. Endothelial progenitors in pulmonary hypertension: new pathophysiology and therapeutic implications. Eur Respir J. 2010;35(2):418–25.
176. Baker CD, Seedorf GJ, Wisniewski BL, Black CP, Ryan SL, Balasubramaniam V, et al. Endothelial colony-forming cell conditioned media promote angiogenesis in vitro and prevent pulmonary hypertension in experimental bronchopulmonary dysplasia. Am J Physiol Lung Cell Mol Physiol. 2013;305(1):L73–81.
177. Alphonse RS, Vadivel A, Fung M, Shelley WC, Critser PJ, Ionescu L, et al. Existence, functional impairment, and lung repair potential of endothelial colony-forming cells in oxygen-induced arrested alveolar growth. Circulation. 2014;129(21):2144–57.
178. Ortiz LA, Gambelli F, McBride C, Gaupp D, Baddoo M, Kaminski N, et al. Mesenchymal stem cell engraftment in lung is enhanced in response to bleomycin exposure and ameliorates its fibrotic effects. Proc Natl Acad Sci U S A. 2003;100(14):8407–11.
179. Patel KM, Crisostomo P, Lahm T, Markel T, Herring C, Wang M, et al. Mesenchymal stem cells attenuate hypoxic pulmonary vasoconstriction by a paracrine mechanism. J Surg Res. 2007;143(2):281–5.
180. Borghesi A, Massa M, Campanelli R, Bollani L, Tzialla C, Figar TA, et al. Circulating endothelial progenitor cells in preterm infants with bronchopulmonary dysplasia. Am J Respir Crit Care Med. 2009;180(6):540–6.
181. Aslam M, Baveja R, Liang OD, Fernandez-Gonzalez A, Lee C, Mitsialis SA, et al. Bone marrow stromal cells attenuate lung injury in a murine model of neonatal chronic lung disease. Am J Respir Crit Care Med. 2009;180(11):1122–30.
182. van Haaften T, Byrne R, Bonnet S, Rochefort GY, Akabutu J, Bouchentouf M, et al. Airway delivery of mesenchymal stem cells prevents arrested alveolar growth in neonatal lung injury in rats. Am J Respir Crit Care Med. 2009;180(11):1131–42.
183. Ionescu L, Byrne RN, van Haaften T, Vadivel A, Alphonse RS, Rey-Parra GJ, et al. Stem cell conditioned medium improves acute lung injury in mice: in vivo evidence for stem cell paracrine action. Am J Physiol Lung Cell Mol Physiol. 2012;303(11):L967–77.
184. Chang YS, Ahn SY, Yoo HS, Sung SI, Choi SJ, Oh WI, et al. Mesenchymal stem cells for bronchopulmonary dysplasia: phase 1 dose-escalation clinical trial. J Pediatr. 2014;164(5):966–72. e6
185. Toti P, Buonocore G, Tanganelli P, Catella AM, Palmeri ML, Vatti R, et al. Bronchopulmonary dysplasia of the premature baby: an immunohistochemical study. Pediatr Pulmonol. 1997;24(1):22–8.
186. Been JV, Debeer A, van Iwaarden JF, Kloosterboer N, Passos VL, Naulaers G, et al. Early alterations of growth factor patterns in bronchoalveolar lavage fluid from preterm infants developing bronchopulmonary dysplasia. Pediatr Res. 2010;67(1):83–9.
187. Markewitz BA, Farrukh IS, Chen Y, Li Y, Michael JR. Regulation of endothelin-1 synthesis in human pulmonary arterial smooth muscle cells. Effects of transforming growth factor-beta and hypoxia. Cardiovasc Res. 2001;49(1):200–6.
188. Sturrock A, Cahill B, Norman K, Huecksteadt TP, Hill K, Sanders K, et al. Transforming growth factor-beta1 induces Nox4 NAD(P)H oxidase and reactive oxygen species-dependent proliferation in human pulmonary artery smooth muscle cells. Am J Physiol Lung Cell Mol Physiol. 2006;290(4):L661–L73.
189. Nakanishi H, Sugiura T, Streisand JB, Lonning SM, Roberts JD Jr. TGF-beta-neutralizing antibodies improve pulmonary alveologenesis and vasculogenesis in the injured newborn lung. Am J Physiol Lung Cell Mol Physiol. 2007;293(1):L151–61.

190. Bei Y, Hua-Huy T, Duong-Quy S, Nguyen VH, Chen W, Nicco C, et al. Long-term treatment with fasudil improves bleomycin-induced pulmonary fibrosis and pulmonary hypertension via inhibition of Smad2/3 phosphorylation. Pulm Pharmacol Ther. 2013;26(6):635–43.
191. Zhang YM, Bo J, Taffet GE, Chang J, Shi J, Reddy AK, et al. Targeted deletion of ROCK1 protects the heart against pressure overload by inhibiting reactive fibrosis. FASEB J. 2006;20(7):916–25.
192. Gong K, Xing D, Li P, Aksut B, Ambalavanan N, Yang Q, et al. Hypoxia induces downregulation of PPAR-γ in isolated pulmonary arterial smooth muscle cells and in rat lung via transforming growth factor-β signaling. Am J Physiol Lung Cell Mol Physiol. 2011;301(6):L899–907.
193. Sakurai R, Villarreal P, Husain S, Liu J, Sakurai T, Tou E, et al. Curcumin protects the developing lung against long-term hyperoxic injury. Am J Physiol Lung Cell Mol Physiol. 2013;305(4):L301–11.
194. Ichihara S, Obata K, Yamada Y, Nagata K, Noda A, Ichihara G, et al. Attenuation of cardiac dysfunction by a PPAR-alpha agonist is associated with down-regulation of redox-regulated transcription factors. J Mol Cell Cardiol. 2006;41(2):318–29.
195. Rindfleisch MS, Hasday JD, Taciak V, Broderick K, Viscardi RM. Potential role of interleukin-1 in the development of bronchopulmonary dysplasia. J Interf Cytokine Res. 1996;16(5):365–73.
196. Koksal N, Kayik B, Cetinkaya M, Ozkan H, Budak F, Kilic S, et al. Value of serum and bronchoalveolar fluid lavage pro- and anti-inflammatory cytokine levels for predicting bronchopulmonary dysplasia in premature infants. Eur Cytokine Netw. 2012;23(2):29–35.
197. Bry K, Whitsett JA, Lappalainen U. IL-1beta disrupts postnatal lung morphogenesis in the mouse. Am J Respir Cell Mol Biol. 2007;36(1):32–42.
198. Johnson BH, Yi M, Masood A, Belcastro R, Li J, Shek S, et al. A critical role for the IL-1 receptor in lung injury induced in neonatal rats by 60% O_2. Pediatr Res. 2009;66(3):260–5.
199. Dunlop K, Gosal K, Kantores C, Ivanovska J, Dhaliwal R, Desjardins JF, et al. Therapeutic hypercapnia prevents inhaled nitric oxide-induced right-ventricular systolic dysfunction in juvenile rats. Free Radic Biol Med. 2014;69C:35–49.
200. Mertens LL, Friedberg MK. Imaging the right ventricle – current state of the art. Nat Rev Cardiol. 2010;7(10):551–63.
201. Banerjee D, Haddad F, Zamanian RT, Nagendran J. Right ventricular failure: a novel era of targeted therapy. Curr Heart Fail Rep. 2010;7(4):202–11.

Right Ventricular Function in Ebstein's Malformation

12

Jan Marek, Marina L. Hughes, and Victor Tsang

Abstract

Ebstein's anomaly is a developmental anomaly of the tricuspid valve that primarily involves failure of delamination of the leaflets. However this label encompasses a huge range of valve and ventricular components, in terms of morphology, cellular composition and function, and therefore a great spectrum of haemodynamic situations. On pathologic analysis, increased fibrosis of the right and left ventricular myocardium is a common finding. This is related to intrinsic disease and is progressive, resulting from the abnormal loading conditions for both ventricles. Assessing the underlying function of the RV myocardium is confounded by the loading conditions, and the load-dependency of all conventional echocardiographic and cardiac MRI parameters. Surgical repair of the tricuspid valve, with procedures such as the cone reconstruction, promises to improve TV function and ventricular mechanics. Prudent case selection for this type of surgical repair is crucial and long-term comparative outcome is not yet available, but this type of intervention offers a unique opportunity to examine RV function within the complex haemodynamics of this valve and ventricular anomaly.

Keywords

Ebstein anomaly • Tricuspid valve • Cone reconstruction • Echocardiography Magnetic resonance

Introduction

Ebstein's anomaly (EA) is a rare congenital heart disease occurring in 1 per 200,000 live births and accounting for approximately 1% of all congenital cardiac abnormalities [1]. EA may present at any age and has a variable natural history,

J. Marek (✉) • M.L. Hughes
Paediatric Cardiology, Hospital for Sick Children, Great Ormond St, London WC13JH, UK
e-mail: jan.marek@gosh.nhs.uk

V. Tsang
Cardiothoracic Surgery, Hospital for Sick Children, Great Ormond St, London WC13JH, UK

M.K. Friedberg, A.N. Redington (eds.), *Right Ventricular Physiology, Adaptation and Failure in Congenital and Acquired Heart Disease*, https://doi.org/10.1007/978-3-319-67096-6_12

primarily related to the severity of the lesion (Fig. 12.1). These variations have important consequences on the functional interaction of the right atrium, functional right ventricle (RV), pulmonary circulation and the left ventricle [2]. Because of tricuspid regurgitation, the two ventricular myocardial components separated by the tricuspid valve leaflets are exposed to abnormal physiology with prenatally high preload and high afterload and postnatally with high preload and low afterload. Understanding biventricular myocardial and circulatory function in abnormal loading conditions remains challenging and existing data are sparse, but a better understanding of myocardial mechanics may have direct impact on patient's management by optimizing timing of referral for surgical repair.

Morphological and Pathophysiological Considerations

Ebstein's anomaly is characterized by (1) adherence of the septal and posterior leaflets to the underlying myocardium (failure of delamination); (2) downward (apical) displacement of the functional annulus; (3) dilation of the "atrialised" portion of the right ventricle, with various degrees of hypertrophy and thinning of the wall; (4) redundancy, fenestrations, and tethering of the anterior leaflet; and (5) dilation of the right atrioventricular junction. Variations of displacement are very wide, in extreme forms the effective orifice "spirals" towards the RV outflow tract with chordal attachments of the anterosuperior leaflet that can be connected in the RV outflow tract towards the pulmonary annulus [3] resulting in severely diminished effective RV volume (Fig. 12.2).

While tricuspid valve morphology has been described in detail by several authors, understanding the morphology of the atrialised and functional right ventricular myocardium enables a better understanding of the mechanisms of right ventricular failure. Ebstein's anomaly is associated with right ventricular dilatation, which may be extreme. It may involve not only the right ventricular wall proximal to the tricuspid valve (atrialized ventricle) but also the right ventricle distal to the valve (functional right ventricle), including the right ventricular infundibulum. In some cases, right ventricular dilatation is so marked that the ventricular septum bulges leftward, compressing the left ventricular chamber [4].

A morphometric and histological study performed on ten hearts with EA and ten normal age-matched controls demonstrated that dilatation of the right ventricle in Ebstein's anomaly was associated not only with thinning of the wall

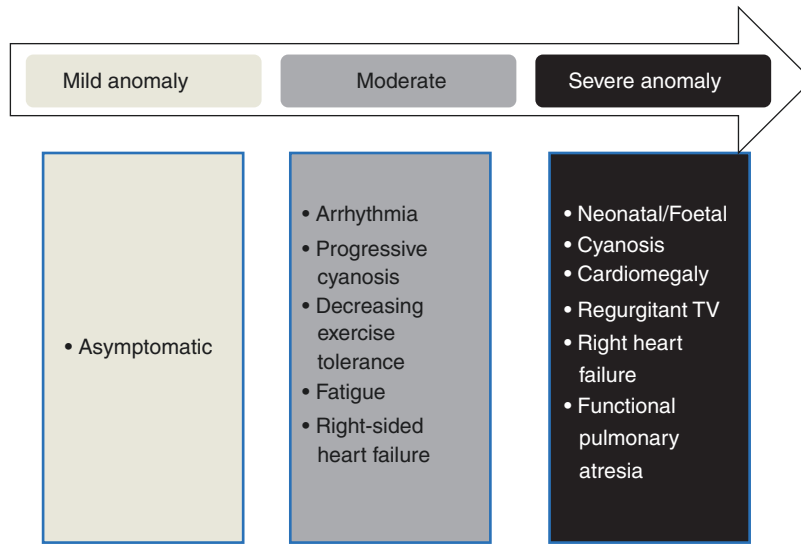

Fig. 12.1 Clinical presentation of patients with Ebstein anomaly of tricuspid valve based on severity of disease

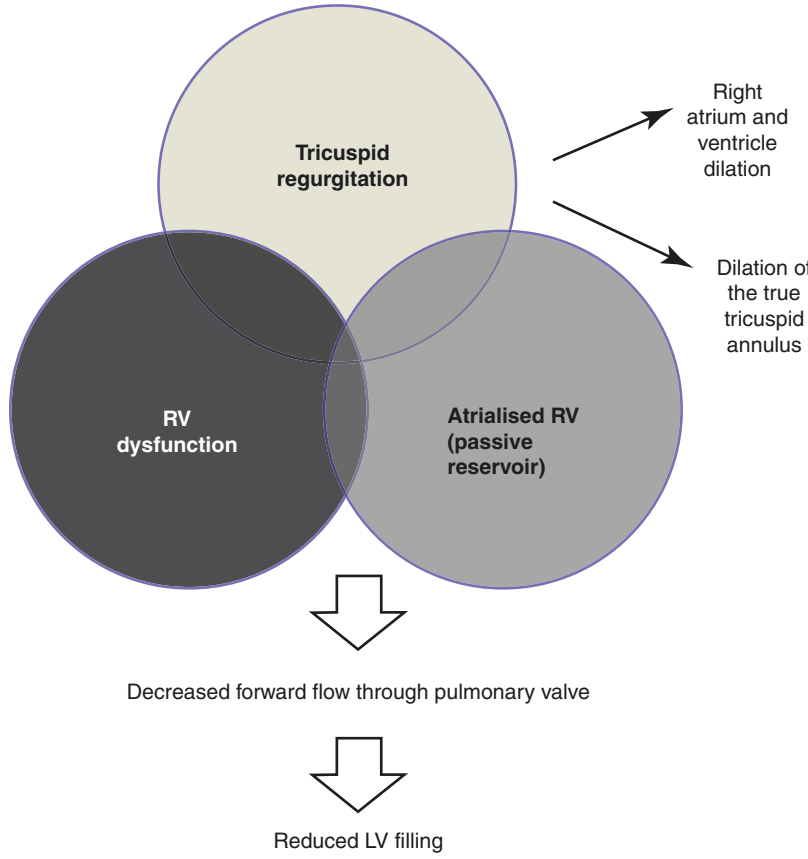

Fig. 12.2 Schematic drawing of pathophysiology of Ebstein anomaly

but also with an absolute decrease in the number of myocardial fibers counted through the full thickness of the wall from endocardium to epicardium [5, 6]. The same group studied 15 well-preserved autopsy specimens. Enlargement of the right atrioventricular (A-V) junction and malalignment of the giant and sometimes muscularised anterior leaflet of the tricuspid valve were found consistently. In addition, massive aneurysmal dilation of the right ventricle was present in almost two thirds of the hearts suggesting the possibility of primary abnormal embryonic development of the right A-V junction that leads to malformation of the tricuspid valve apparatus.

Furthermore, Celermajer et al.'s [3] histologic study of six neonates who died postnatally revealed significant thinning of the right ventricular free wall distal to the tricuspid valve. There was reduced right ventricular fiber size compared to controls whilst the fibrous tissue content of both right and left ventricular free walls was increased. The posterior wall of the atrialised right ventricle was typically aneurysmal with sparse muscle fibers. Indeed, in two hearts it was devoid of any muscle and composed entirely of fibrous tissue. In an excellent study [7] assessing myocardial fibrosis in 27 hearts from fetuses, children and adults with EA and tricuspid valve dysplasia, micromorphometry revealed that endocardial thickening develops in perinatal life, and in patients with Ebstein's malformation, the interstitial fibrosis develops later in life. Although these right ventricular abnormalities might be explained by hemodynamic stress in utero, the frequent co-existence of abnormalities of the left ventricular free wall suggest that either genetic or non-hemodynamic environmental factors are involved in the morphogenesis of this condition.

Increased right and left ventricular fibrosis may contribute to the poor early outcome in this group and may predispose to late complications, such as subnormal exercise performance,

hemodynamic deterioration or late sudden death that may occur in patients with Ebstein's anomaly who survive the neonatal period. A potential explanation of the late histological changes in the right ventricle is overload of the right ventricle caused by tricuspid regurgitation. The left ventricular histological changes may be related to functional impairment of the left ventricle, which has been shown in Ebstein's malformation. Paradoxical motion of the interventricular septum and right heart dilatation, which is seen in Ebstein's anomaly, both in utero and in postnatal life, and bowing of the septum into the left ventricle in tricuspid valvar dysplasia, may affect left ventricular diastolic and systolic function by altering left ventricular geometry. Although the septum and ventricles activate simultaneously, it appears that in EA the septum does not always move synchronously particularly where mid-septal segments interact with the functionally right atrium. Normally, just prior to the onset of systole, atrial contraction completes the filling of both ventricles and the augmented trans-septal pressure gradient pushes the septum to the right [8]. In Ebstein's patients, increased RA pressure due to significant tricuspid regurgitation and right atrial hypertrophy, exceeds LV end-diastolic pressure resulting in the ventricular septum moving towards the left ventricle. At the onset of LV contraction, the septum moves back towards low-pressure right atrial pressure chamber (anatomic RA and atrialized RV).

In adult patients with unoperated EA, recent MRI derived 3D models suggest that LV has preserved volume but exhibits basal narrowing, modest apical dilation and global hypokinesis [9]. Additionally, LV EF and percent LV length change were reduced in Ebstein's patients compared to normal, and the authors suggested that the apparent basal septal dyskinesis observed in most patients is likely attributable to anterior cardiac translation rather than true paradoxical motion.

Electrical conduction abnormalities have been well described and may relate to functional abnormalities. The ECG shows right atrial hypertrophy, a prolonged PR interval, right bundle branch block, and small QRS voltages over the right chest leads. Left bundle branch block and atrioventricular block are also common. The reported association of pre-excitation syndromes ranges between 10 and 23%, and most of the accessory pathways identified thus far are located around the orifice of the malformed tricuspid valve. The accessory muscular pathways, often multiple in the same patient, are thought to be caused by faulty formation of the insulating tissues at the atrioventricular junctions [10–13].

The relationship between QRS duration and RV volume and function was studied in a group of 63 patients [14]. Prolonged RV conduction was present in 45 patients (71%). The QRS duration correlated with anatomic RV diastolic volume and inversely with RV ejection fraction. The presence of QRS fractionation predicted greater atrialized RV volume, while normal QRS duration was associated with smaller anatomic RV diastolic volume, higher RV ejection fraction, higher oxygen consumption (VO_2) at cardiopulmonary exercise testing and lower incidence of oxygen desaturation with exercise [14]. Although 60% of these patients were older than 18 years, it appears that RV EDV was strongly associated with the QRS duration regardless of age.

The impact of EA, in terms of mortality extends from the fetal period, into adult life. A recent multicenter study of 243 prenatally diagnosed fetuses reported a total perinatal mortality of 45% [15]. These studies revealed that the most powerful predictors of poor outcome include the lack of antegrade flow across the pulmonary valve, retrograde duct flow, and the presence of pulmonary regurgitation [16]. In the context of severe tricuspid regurgitation, lack of antegrade flow across the pulmonary valve leads to retrograde duct flow, which increases afterload on the RV. Because tricuspid regurgitation favors the high-capacitance systemic venous feto-placental circuit, inadequate filling forces subsequently diminishes RV preload. Reduced RV preload and high afterload reduce RV contractile reserve with further increase of central venous pressure and low biventricular cardiac

output due to poor RV function and an under-filled LV. Pulmonary regurgitation, either pre-existing or induced by interventions (usually in the setting of associated valvar atresia), is particularly egregious as it serves as the final component of a circular shunt, leading to systemic steal, reduced systemic cardiac output, diminished endorgan perfusion, acidosis, and ultimately, demise in the fetus or newborn.

Extreme cardiac dilatation in early fetal life compromises development of lungs resulting in low lung volume and further compromises pulmonary flow and resistance postnatally.

Finally, in addition to these circulatory mechanism of RV failure, the myocardium in EA patients may be abnormal secondary to a MYH7 gene mutation, known to be linked to LV non-compaction cardiomyopathy. Sabine Classen's group [17] analysed 141 unrelated probands with EA, and among 8 mutation-positive patients, 6 had LV non-compaction cardiomyopathy, whereas among 133 mutation-negative probands, none showed evidence of LV non-compaction. The frequency of *MYH7* mutations was significantly different between patients with and without LVNC accompanying Ebstein anomaly.

In summary, it seems obvious that there is no common denominator of mechanism of ventricular impairment in patients with EA. The natural history is guided by combination of early ("congenital") and late ("acquired") intrinsic myocardial changes, genetically modified myocardium, morphology of tricuspid valve, severity of tricuspid regurgitation, volume of functional RV and abnormal inter-ventricular interactions.

Surgical Treatment Options

A retrospective review of surgical procedures performed on 498 patients with a primary diagnosis of Ebstein's malformation in The Society of Thoracic Surgeons Congenital Heart Surgery Database between 2002 and 2009, confirmed a large variety of procedures, with high numbers of palliative procedures in neonates. Tricuspid valve surgery was performed in 32% of neonates, 54.5% children and 68.8% in adults [18]. In-hospital mortality was highest in neonates (23.4%), compared with infants (4.1%), children (0.7%), and adults (1.1%). Several repair techniques have been advocated. These include vertical plication as described initially by Carpentier, and TV replacement [19, 20]. In 2007 da Silva [21] described Carpentier's modificiation of tricuspid valve repair known as the cone reconstruction technique. This involves delamination and rotation of the detached TV antero-superior leaflet and the use of the remnant of the septal and inferior leaflets to create a Cone, the vertex of which faces the RV apex (Fig. 12.3). With sufficient valve tissue, this technique promotes the full coaptation of valve leaflets, with a more physiological distribution of stresses and the creation of a central blood stream through the new TV. This recently introduced method consistently improved the functional anatomy of the right ventricular inflow and had a hospital mortality of 2.5%. The TR grade reduced from 3.6 ± 0.5 pre-operatively to 1.2 ± 0.4 post-operatively and there was improved NYHA functional class from 2.6 ± 0.7 to 1.2 ± 0.4 ($P < 0.0001$) [21].

These early encouraging results have also been supported by surgical series from Boston and the Mayo clinic [22–24] suggesting that cone operation can be performed with low early mortality and excellent durability at short-term follow-up in children and young adults with Ebstein anomaly. They conclude that cone operation represents an important surgical option for young patients. It is applicable to patients with a broad range of anatomic variability and avoids valve replacement in the vast majority. This operation should be considered prior to the deleterious effects of chronic right ventricular volume overload and the development of systolic dysfunction, which hamper long-term prognosis, however longer follow-up is essential to determine late durability of cone reconstruction. Despite the good early outcomes, data on postoperative RV and LV adaptation, and objective cardiopulmonary testing are lacking.

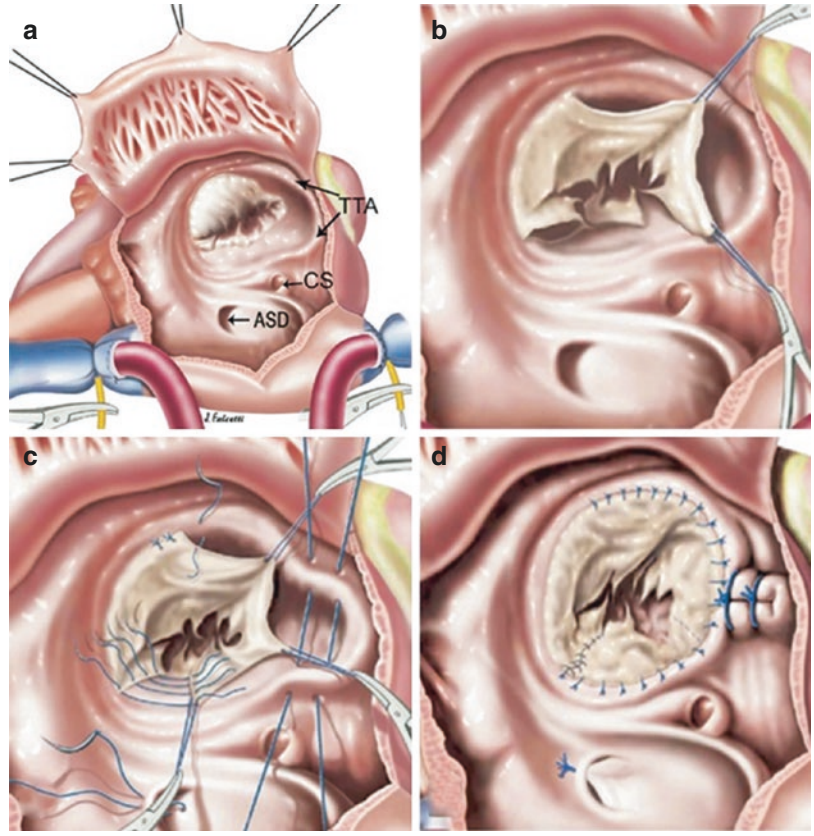

Fig. 12.3 Cone operation. Operative steps for Ebstein's anomaly repair. (**a**) Opened right atrium showing displacement of the tricuspid valve. *TTA* true tricuspid annulus, *ASD* atrial septal defect, *CS* coronary sinus. (**b**) Detached part of the anterior and posterior leaflet forming a single piece. (**c**) Clockwise rotation of the posterior leaflet edge to be sutured to the anterior leaflet septal edge and plication of the true tricuspid annulus. (**d**) Complete valve attachment to the true tricuspid annulus and valved closure of the atrial septal defect With permission from Da Silva JP et al, J Thorac Cardiovasc Surg 2007;133:215-23 © Elsevier 2007 [21]

Assessment of the Right Ventricular Function in Ebstein's Anomaly

Transthoracic Echocardiography

Transthoracic conventional echocardiographic studies are performed from multiple subcostal, apical 2-chamber and 4-chamber and parasternal long- and short-axis views to obtain images of the tricuspid valve, atrial and ventricular chambers, and right ventricular outflow tract and pulmonary valve. The presence of an atrial communication is best assessed from multiple views using color flow mapping. Tricuspid valve systolic and pulmonary valve diastolic regurgitation flow profiles are identified and velocities are measured in order to estimate pulmonary arterial and right ventricular pressures. Systolic pulmonary flow is typically very low velocity, pulmonary regurgitation is often result of "atonic" infundibulum rather than pulmonary annular dilatation. In most severe forms of EA with impaired RV function we observed significant pulmonary regurgitation due to incomplete pulmonary valve closure in cases with elevated end-diastolic pressure. Rapid diastolic pressure equilibrium at the beginning of diastole in case of impaired RV relaxation does not allow the pulmonary valve (although anatomically normal) to close completely.

Tricuspid regurgitation is measured semi-quantitatively by color flow mapping of flow conversion area, width of vena contracta and extension of regurgitant jet(s) within the right atrium. Measurements of cardiac chamber size includes BSA indexed anatomic right atrial area (aRAa), atrialised right ventricle area (aRVa), functional right ventricular area (fRVa), left atrial area (LAa) and left ventricular area (LVa). The right atrial index (aRAa + aRVa/fRVa + LAa + LVa) described by Celermajer [10]

can be used to stratify patients at risk for poor outcome.

Several functional parameters can be used in assessing ventricular function in Ebstein's anomaly. All parameters used have their advantages and limitations, and no parameter is load independent. Furthermore, the validity of some indices has not been established. For example, while widely used to assess RV performance in other conditions, the role of TAPSE and the myocardial performance index are not well established in EA.

Right Ventricular Ejection Fraction (RVEF) and Right Ventricular Fractional Area Change (FAC)

These measurements can be applied only in a small proportion of patients with EA; those with well-developed inlet portion of the functional RV. In many cases, the functional RV is displaced towards the right ventricular outflow tract, and is not visible in standard views. Nonetheless, the 4-chamber view typically displays a dilated anatomical right atrium, true tricuspid annulus (right AV groove) and the atrialised right ventricle.

Tissue Velocity, Strain, and Strain Rate

Systolic tissue Doppler velocities of the tricuspid annulus reflect longitudinal RV function [25, 26], although there are significant limitations to this approach in EA patients. However, in a recent study of 49 unoperated patients with EA (mean age of 32 ± 18 years) [26], tricuspid annular plane systolic excursion, tissue Doppler myocardial velocities (peak S and IVA) and 2D strain and strain rate measures for the RV were compared with CMR-derived EF. Only 2D global longitudinal strain showed a weak, although statistically significant correlation with CMR-derived EF.

Cardiac Magnetic Resonance

CMR is fast becoming the technique of choice in assessing EA patients. Evaluation of ventricular and valve function is achieved using retrospectively gated, breath-held, balanced, steady-state free-precession cine images (SSFP). The TV leaflet attachments and the margins of right atrium and right ventricle are visualized and analyzed throughout the cardiac cycle in multiple planes.

Net flow through the pulmonary valve and aortic valve can be measured using phase contrast flow mapping. During postprocessing, ventricular volumes are measured by manually tracing the blood-endocardium boundary for each slice at end-diastole and end-systole. From these data ventricular stroke volumes and ejection fraction can be calculated. TV regurgitant fraction is calculated by subtracting the pulmonary forward flow stroke volume from the RV stroke volume, and expressing the remainder as a percentage of the RV stroke volume. Tissue characterization techniques have also been used in the detection of myocardial fibrosis in patients with Ebstein's anomaly using delayed contrast enhancement techniques, however the thinned RV myocardial wall challenges the spatial resolution capacity of conventional MRI techniques.

Prognostic Indices in Patients with Ebstein's Anomaly

In 1992 the Great Ormond Street Hospital (GOSH) team led by David Celermajer established the right atrial index as an ECHO derived grading of severity of neonatal Ebstein anomaly. It is expressed as the ratio of the combined area of the right atrium and atrialized right ventricle to that of the combined area of the functional right ventricle, left atrium and left ventricle in a four-chamber view at end-diastole ($Index = RA + aRV/fRV + LA + LV$). This ratio was used to define four grades of increasing severity: grade 1; ratio <0.5; grade 2; 0.5−0.99; grade 3; 1.0−1.49; and grade 4; ≥1.5, and was shown to relate to outcomes.

Tobler et al. described a correlation of the CMR-derived functional right ventricular (fRV) end-diastolic volume (EDV) and a ratio of fRV EDV/left ventricular EDV (from transversal steady state free precession (SSFP) cine images with several cardiopulmonary exercise measures ($Index = fRV\ EDV/LV\ EDV$). Defining the fRV in SSFP cine images is tedious because of strong interindividual variations of TV morphology

and TV offset. Most recently, a prospective multicenter study [27, 28] of 24 patients described the total right/left-volume index, defined from end-diastolic volume measurements: *Index = (RA + aRV + fRV)/(LA + LV)*. Mean total right/left-volume index was 2.6 ± 1.7 (normal values: 1.1 ± 0.1). The total right/left-volume index correlated with almost all clinically used biomarkers of heart failure: brain natriuretic peptide (r = 0.691; P = 0.0003), QRS (r = 0.432; P = 0.039), peak oxygen consumption/kg (r = −0.479; P = 0.024), ventilatory response to carbon dioxide production at anaerobic threshold (r = 0.426; P = 0.048), the severity of tricuspid regurgitation (r = 0.692; P = 0.009), tricuspid valve offset (r = 0.583; P = 0.004), and tricuspid annular plane systolic excursion (r = 0.554; P = 0.006). Previously described severity indices ([*RA + aRV*]/[*fRV + LA + LV*]) and *fRV/LV* end-diastolic volume corresponded only to some parameters (Table 12.1).

Ventricular Function Before and After Cone Reconstruction

We investigated the adaptation of right and left ventricles to change in loading conditions after Cone reconstruction in 27 patients prospectively examined and retrospectively analysed before and after operation using cross-sectional imaging, ECG and cardiopulmonary exercise testing [35]. All patients were symptomatic preoperatively. Four patients required pacemaker insertion (3 for new complete heart block). Patients median age was 15.8 years (22 days – 56.9 years), median follow-up was 2.7 ± 1.5 years. Postoperatively, there were no deaths and there was significant improvement in clinical status and there was significant improvement in peak oxygen uptake. The cone TV functioned well in all but 1 patient with late dehiscence of inferior annuloplasty sutures that were subsequently repaired. Echocardiographic and MRI data obtained postoperatively showed significantly reduced size of the TV annulus, anatomical right atrium and RA/LA ratio while LV size and volume significantly increased (Table 12.2). The right atrial index was significantly reduced by both ECHO and CMR measurement (Fig. 12.4). RV end-diastolic and end-systolic volumes and ejection fraction calculated using CMR did not change following surgery. Interestingly, data from the Munich group found RV volumes and ejection fraction reduced postoperatively [36], perhaps because

Table 12.1 Severity indices of EA using echocardiography and CMR

		Severity index 4CV	Severity index 4CV	fRV/LV index	Severity index volume	Total right/left-volume index
Study by		Celermajer et al [10]	Yalonetsky et al. [29]	Tobler et al. [30]	Hosch et al. [28]	Hosch et al. [28]
Modality		TTE	CMR	CMR	CMR	CMR
Measure		Area	Area	Volume	Volume	Volume
Calculation		(RA + aRV)/ fRV + LA + LV)	(RA + aRV)/ (fRV + LA + LV)	fRV EDV/ LV EDV	(RA + aRV)/ (fRV + LA + LV)	(RA + aRV + fRV)/ LA + LV)
Results	n					
10–18 years	10	0.7 ± 0.6	0.6 ± 0.4	1.5 ± 0.6	0.6 ± 0.6	2.6 ± 1.8
>18 years	15	0.7 ± 0.4	0.6 ± 0.2	1.7 ± 1.4	0.5 ± 0.1	2.6 ± 1.6
All	25	0.7 ± 0.5	0.6 ± 0.3	1.7 ± 1.1	0.5 ± 0.4	2.6 ± 1.7
Reference[a]				1.1 ± 0.1		1.1 ± 0.1

Values are mean ±SD. 4CV indicates 4-chamber view; *aRV* atrialized right ventricle, *CMR* cardiac magnetic resonance, *EA* Ebstein anomaly, *EDV* end diastolic volume, *fRV* functional right ventricle, *LA* left atrium, *LV* left ventricle, *RA* right atrium, *TTE* transthoracic echocardiography

With permission from Hoesch O, Circ Cardiovasc Imaging. 2014;7:601–609 © Wolters Kluwer 2014 [28]

[a]Reference values from the literature, calculated in healthy subjects [31–34]. Reference results for children and adults are equal

Table 12.2 Echocardiographic and MRI data of cardiac dimensions before and after cone operation

Parameters	Before operation	After operation	P value
TV annular diameter Z score	13.50 ± 3.15	0.05 ± 0.14	<0.001
Anatomical RA area Z score	16.10 ± 5.92	(−)0.20 ± 1.19	<0.001
Anatomical LA area Z score	(−)3.45 ± 0.78	(−)0.50 ± 1.40	0.001
RA/LA areas ratio	2.95 ± 0.76	0.90 ± 0.26	<0.001
Diastolic LV diameter Z score	(−)2.35 ± 1.07	(−)0.80 ± 0.60	0.002
Systolic LV diameter Z score	(−)0.75 ± 1.07	(−)0.10 ± 0.64	0.054
IVS Z score	0.00 ± 0.48	0.10 ± 0.10	0.541
LVPW Z score	(−)0.45 ± 0.51	0.65 ± 0.65	0.016
Diastolic eccentricity index	0.50 ± 0.24	0.70 ± 0.22	0.527
Systolic eccentricity index	0.65 ± 0.28	0.50 ± 0.24	0.467
RV End-diastolic index (ml/m^2)	112.1 ± 80.6	91.0 ± 45.3	0.54
RV End-systolic index (ml/m^2)	166.0 ± 66.3	145.9 ± 56.1	0.24
LV End-diastolic index (ml/m^2)	19.8 ± 8.9	22.4 ± ± 10.4	0.25
LV End-systolic index (ml/m^2)	49.4 ± 14.4	60.1 ± 14.5	0.006

TV tricuspid valve, *RA* right atrium, *LA* left atrium, *LV* left ventricle, *IVS* ventricular septum, *LVPW* left ventricular posterior wall (GOSH data)

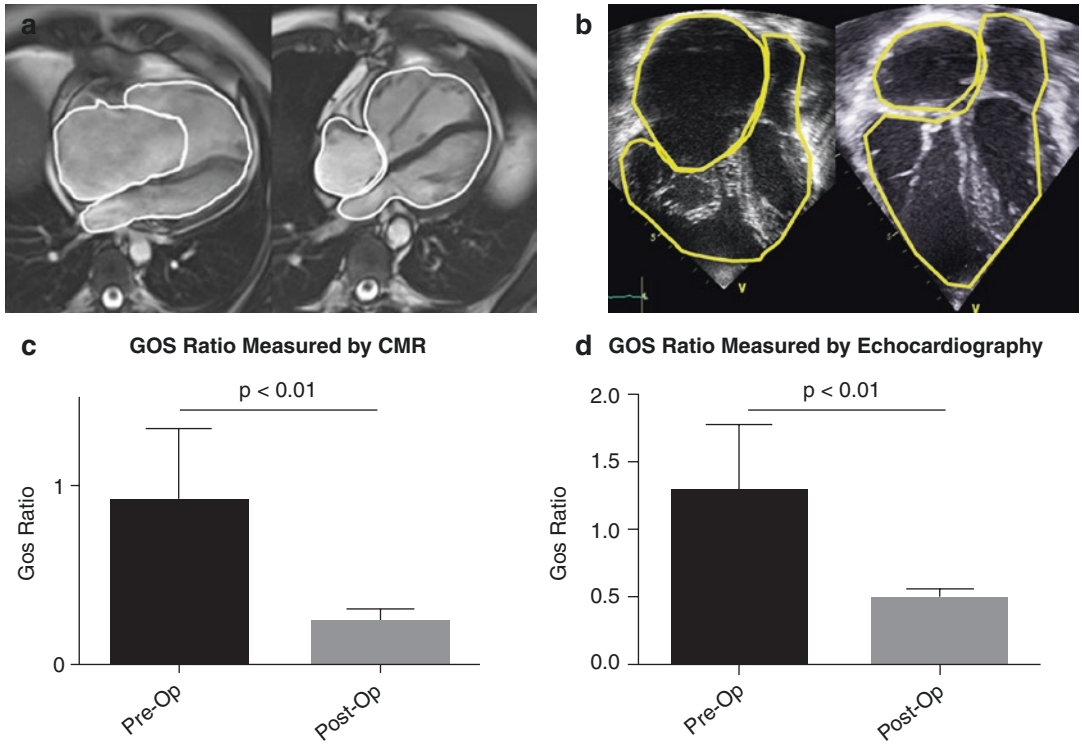

Fig. 12.4 Change of GOSH Index before and after Cone operation. Tracing of cardiac contours on cine MRI (**a**) and 2D ECHO (**b**) images. Significant change in results documented on MRI (**c**) and 2D ECHO (**d**) before (Pre-OP) and after (Post-OP) cone operation (**c**). *Pre-Op* before operation, *post-Op* after operation

of their older patients in the Munich group, or shorter follow up. Both studies however confirmed significantly increased indexed forward flow in main pulmonary artery (Fig. 12.5). Our ECHO data however confirmed significantly reduced RV function on subjective assessment, TAPSE and RV fractioning area change (Fig. 12.6).

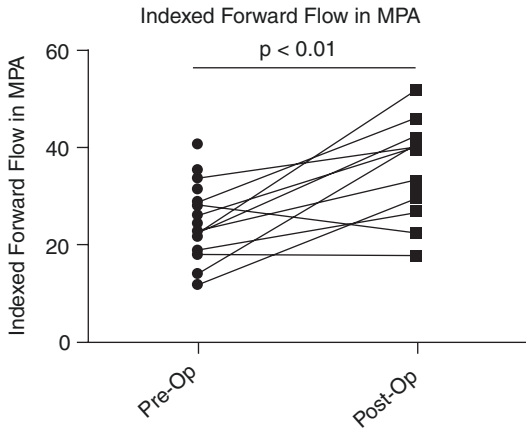

Fig. 12.5 Indexed forward net flow measured before and after cone operation by MRI. *Pre-Op* before operation, *post-Op* after operation

Global LV function measured by biplane Simpson and fractional shortening remained unchanged and within normal limits in our patients, although none had echocardiographic appearances of non-compacted myocardium. Our recent data [37] on LV function measured by advanced 2D Strain deformation imaging revealed that although LV size and volume increases after cone reconstruction, LV longitudinal function appeared reduced but tended to recover with time (Fig. 12.7). We also did not confirm significant systolic LV mechanical dyssynchrony by measuring change of global LV time to systolic peak corrected by HR (Fig. 12.8). This is in agreement with MRI study [9] suggesting that apparent basal septal dyskinesis observed

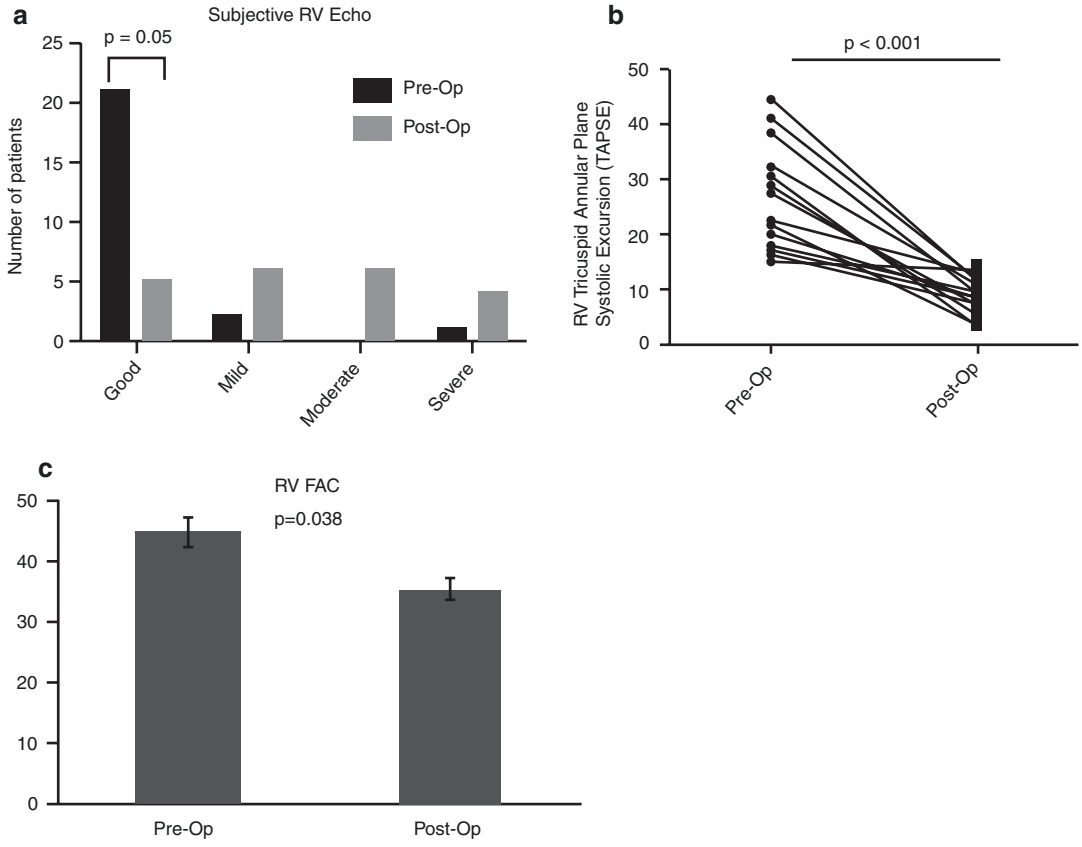

Fig. 12.6 Assessments of RV function by conventional ECHO techniques. Almost a half of patients did have significant RV impairment assessed subjectively (*upper panel*), significant impairment was demonstrated by tricuspid annular plane systolic excursion (TAPSE; *left lower panel*) and RV fractional area of change (RV FAC; *right lower panel*). *Pre-Op* before operation, *post-Op* after operation

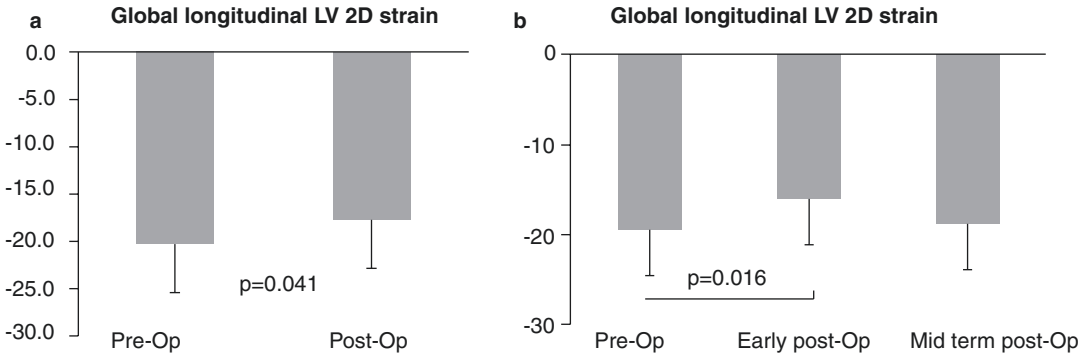

Fig. 12.7 Assessment of LV function by 2D Strain deformation technique. Global longitudinal 2D Strain before (pre-Op) and after (post-Op) cone operation (**a**). Global longitudinal 2D Strain assessed before (pre op), immediately after (early post-Op) and later (mid term post-Op) after cone operation (**b**)

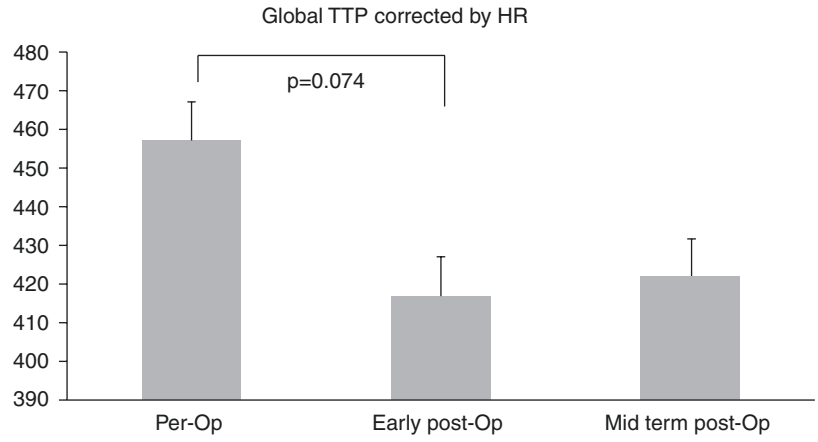

Fig. 12.8 Left ventricular global time-to-peak change (TTP) corrected by heart rate (HR) measured by 2D Strain. *Pre-Op* before operation, *early post-Op* early after operation, *mid term post-OP* later after operation

in most patients is likely due to cardiac translation rather than true myocardial dyskinesis.

In summary, the cone reconstruction is the most anatomically natural of all repairs described and although prudent case selection may be crucial, and robust parameters have yet to be defined, the procedure can be applied at all ages and across a wide range of valve morphology. It offers a unique opportunity to further investigate response to acute change of loading conditions and to examine potential for improved myocardial growth and contractility. More serial data and the results of longterm follow up are awaited.

References

1. Attenhofer Jost CH, Connolly HM, Dearani JA, Edwards WD, Danielson GK. Ebstein's anomaly. Circulation. 2007;115:277–85.
2. Celermajer DS, Bull C, Till JA, Cullen S, Vassillikos VP, Sullivan ID, Allan L, Nihoyannopoulos P, Somerville J, Deanfield JE. Ebsteim's anomaly: presentation and outcome from fetus to adult. J Am Coll Cardiol. 1994;23(1):170–6.
3. Schreiber C, Cook A, Ho SY, Augustin N, Anderson RH. Morphologic spectrum of Ebstein's malformation: revisitation relative to surgical repair. J Thorac Cardiovasc Surg. 1999;117:148–55.
4. Edwards WD. Embryology and pathologic features of Ebstein's anomaly. Prog Pediatr Cardiol. 1993;2:5–15.

5. Anderson KR, Lie JT. Pathologic anatomy of Ebstein's anomaly of the heart revisited. Am J Cardiol. 1978;41:739–45.
6. Anderson KR, Zuberbuhler JR, Anderson RH, Becker AE, Lie JT. Morphologic spectrum of Ebstein's anomaly of the heart: a review. Mayo Clin Proc. 1979;54:174–80.
7. Lee AH, Moore IE, Fagg NL, Cook AC, Kakadekar AP, Allan LD, Keeton BR, Anderson RH. Histological changes in the left and right ventricle in hearts with Ebstein's malformation and tricuspid valvar dysplasia: A morphometric study of patients dying in the fetal and perinatal periods. Cardiovasc Pathol. 1995;4:19–24.
8. Luo C, Ware DL, Zwischenberger JB, Clark JW Jr. A mechanical model of the human heart relating septal function to myocardial work and energy. Cardiovasc Eng. 2008;8:174–84.
9. Goleski PJ, Sheehan FH, Chen SSM, Kilner PJ, Gatyoulis MA. The shape and function of the left ventricle in Ebstein's anomaly. Int J Cardiol. 2014;171:404–12.
10. Celermajer DS, Cullen S, Sullivan ID, Spiegelhalter DJ, Wyse RK, Deanfield JE. Outcome in neonates with Ebstein's anomaly. J Am Coll Cardiol. 1992;19:1041–6.
11. Yater WM, Shapiro MJ. Congenital displacement of the tricuspidvalve (Ebstein's disease): review and report of a case with electrocardiographic abnormalities and detailed histologic study of the conduction system. Ann Intern Med. 1937;11:1043–62.
12. Rossi L, Thiene G. Mild Ebstein's anomaly associated with supraventricular tachycardia and sudden death: clinicomorphologic features in 3 patients. Am J Cardiol. 1984;53:332–4.
13. Chauvaud SM, Brancaccio G, Alain F, Carpentier AF. Cardiac arrhythmia in patients undergoing surgical repair of Ebstein's anomaly. Ann Thorac Surg. 2001;71:1547–5.
14. Assenza GE, Valente AM, Geva T, Graham D, Pluchinotta FR, Sanders SP, Autore C, Volpe M, Landzberg MJ, Cecchin F. QRS duration and QRS fractionation on surface electrocardiogram are markers of right ventricular dysfunction and atrialization in patients with Ebstein anomaly. Eur Heart J. 2013;34:191–200.
15. Freud LR, Escobar-Diaz MC, Kalish BT, Komarlu R, Puchalski MD, Jaeggi ET, Szwast AL, Freire G, Levasseur SM, Kavanaugh-McHugh A, Michelfelder EC, Moon-Grady AJ, Donofrio MT, Howley LW, Tierney ES, Cuneo BF, Morris SA, Pruetz JD, van der Velde ME, Kovalchin JP, Ikemba CM, Vernon MM, Samai C, Satou GM, Gotteiner NL, Phoon CK, Silverman NH, McElhinney DB, Tworetzki W. Outcomes and predictors of perinatal mortality in fetuses with Ebstein anomaly or tricuspid valve dysplasia in the current era: a multicenter study. Circulation. 2015;132:481–9.
16. McElhinney DB, Salvin JW, Colan SD, Thiagarajan R, Crawford EC, Marcus EN, del Nido PJ, Tworetzky W. Improving outcomes in fetuses and neonates with congenital displacement (Ebstein's malformation) or dysplasia of the tricuspid valve. Am J Cardiol. 2005;96:582–6.
17. Postma AV, van Engelen K, van de Meerakker J, Rahman T, Probst S, Baars MJH, Bauer U, Pickardt T, Sperling SR, Berger F, Moorman AFM, Mulder BJM, Thierfelder L, Keavney B, Goodship J, Klaassen S. Mutations in the sarcomere gene MYH7 in Ebstein anomaly. Circ Cardiovasc Genet. 2011;4:43–50.
18. Davies RR, Pasquali SK, Jacobs ML, Jacobs JJ, Wallace AS, Pizarro C. Current spectrum of surgical procedures performed for Ebstein's malformation: An Analysis of The Society of Thoracic Surgeons Congenital Heart Surgery Database. Ann Thorac Surg. 2013;96:1703–10.
19. Danielson GK, Fuster V. Surgical repair of Ebstein's anomaly. Ann Surg. 1982;196:499–504.
20. Carpentier A, Chauvaud S, Mace L, Relland J, Mihaileanu S, Marino JP, Abry B, Buibourt P. A new reconstructive operation for Ebstein's anomaly of the tricuspid valve. J Thorac Cardiovasc Surg. 1988;96:92–101.
21. da Silva JP, Baumgratz JF, da Fonseca L, Franchi SM, Lopes LM, Tavares GM, Soares AM, Moreira LF, Barbero-Marcial M. The cone reconstruction of the tricuspid valve in Ebstein's anomaly. The operation: early and midterm results. J Thorac Cardiovasc Surg. 2007;133:215–23.
22. Anderson HN, Dearani JA, Said SM, Norris MD, Pundi KN, Miller AR, et al. Cone reconstruction in children with Ebstein anomaly: the Mayo Clinic experience. Congenit Heart Dis. 2014;9:266–71.
23. Dearani JA, Said SM, O'Leary PW, Burkhart HM, Barnes RD, Cetta F. Anatomic repair of Ebstein's malformation: lessons learned with cone reconstruction. Ann Thorac Surg. 2013;95:220–6. Discussion 6–8.
24. Vogel M, Marx GR, Tworetzky W, Cecchin F, Graham D, Mayer JE, et al. Ebstein's malformation of the tricuspid valve: short-term outcomes of the "cone procedure" versus conventional surgery. Congenit Heart Dis. 2012;7:50–8.
25. Kostenburger J, Everett AD, Stueger HP, Heinzl B, Gamillscheg A, Cvirn G, Boysen A, Fandl A, Nagel B. Right ventricular function in infants, children and adolescents: reference values of the tricuspid annular plane systolic excursion (TAPSE) in 640 Healthy Patients and Calculation of z Score Values. Am Soc Echocardiogr. 2009;22:715–9.
26. Mertens LL, Friedberg MK. Imaging the right ventricle-current state of the art. Nat Rev Cardiol. 2010;7:551–63.
27. Kühn A, Meierhofer C, Rutz T, Rondak IC, Röhling C, Schreiber C, Fratz S, Ewert P, Vogt M. Non-volumetric echocardiographic indices and qualitative assessment of right ventricular systolic function in Ebstein's anomaly: comparison with CMR-derived

ejection fraction in 49 patients. Eur Heart J Cardiovasc Imaging. 2016;17(8):930–5.
28. Hosch O, Sohns JM, Nguyen T-T, Lauerer P, Rosenberg C, Kowallick JT, Kutty S, Unterberg C, Schuster A, Martin Fashauer M, Staab W, Paul T, Lotz J, Steinmetz M. The total right/left-volume index: a new and simplified cardiac magnetic resonance measure to evaluate the severity of Ebstein anomaly of the tricuspid valve. A comparison with heart failure markers from various modalities. Circ Cardiovasc Imaging. 2014;7:601–9.
29. Yalonetsky S, Tobler D, Greutmann M, Crean AM, Wintersperger BJ, Nguyen ET, Oechslin EN, Silversides CK, Wald RM. Cardiac magneticresonance imaging and the assessment of Ebstein anomaly in adults. Am J Cardiol. 2011;107:767–73.
30. Tobler D, Yalonetsky S, Crean AM, Granton JT, Burchill L, Silversides CK, Wald RM. Right heart characteristics and exercise parameters in adults with Ebstein anomaly: new perspectives from cardiac magnetic resonance imaging studies. Int J Cardiol. 2013;165:146–50.
31. Hudsmith LE, Petersen SE, Francis JM, Robson MD, Neubauer S. Normal human left and right ventricular and left atrial dimensions using steady state free precession magnetic resonance imaging. J Cardiovasc Magn Reson. 2005;7:775–82.
32. Sievers B, Addo M, Breuckmann F, Barkhausen J, Erbel R. Reference right atrial function determined by steady-state free precession cardiovascular magnetic resonance. J Cardiovasc Magn Reson. 2007;9:807–14.
33. Sarikouch S, Peters B, Gutberlet M, Leismann B, Kelter-Kloepping A, Koerperich H, Kuehne T, Beerbaum P. Sex-specific pediatric percentiles for ventricular size and mass as reference values for cardiac MRI: assessment by steady-state free-precession and phase-contrast MRI flow. Circ Cardiovasc Imaging. 2010;3:65–76.
34. Sarikouch S, Koerperich H, Boethig D, Peters B, Lotz J, Gutberlet M, Beerbaum P, Kuehne T. Reference values for atrial size and function in children and young adults by cardiac MR: a study of the German competence network congenital heart defects. J Magn Reson Imaging. 2011;33:1028–39.
35. Ibrahim M, Tsang VT, Caruana M, Hughes ML, Jenkyns S, Perdreau E, Giardini A, Marek J. Cone reconstruction for Ebstein's anomaly: patient outcomes, biventricular function, and cardiopulmonary exercise capacity. J Thorac Cardiovasc Surg. 2015;149:1144–50.
36. Lange R, Burri M, Eschenbach LK, Badiu CC, da Silva JP, Nagdyman N, Fratz S, Hörer J, Kühn A, Schreiber C, Vogt MO. Da Silvaś cone repair for Ebsteon's anomaly: effect on right ventricular size and function. Eur J Cardiothorac Surg. 2015;48(2):316–20. Discussion 320–1.
37. Perdreau E, Tsang V, Hughes M, Ibrahim M, Kataria S, Janagarajan K, Iriart X, Khambadkone S, Marek J. Change in biventricular function after cone repair of Ebstein's anomaly: an echocardiographic study. Eur Heart J Cardiovasc Imaging. 2017; July 31. doi:10.1093/ehjci/jex186.

Ebstein's Malformation: Does Echocardiographic Assessment Determine Surgical Repair?

13

Norman H. Silverman

Abstract

Ebstein's malformation is a complex lesion whose spectrum varies from the serious, when there is marked valvar dysplasia and deformity, to being relatively benign in nature. It is, therefore, impossible to provide a single option for treatment without understanding both the developmental aspects of this lesion and the fetal and neonatal presentations affecting not only the heart, but also other organs such as the lungs. An echocardiographer approaching this condition must take cognizance of many issues that are of critical importance when approaching the echocardiogram, which, while it cannot determine the repair on its own, is certainly a major determinant in deciding the type of repair needed.

Keywords

Ultrasound • Preoperative evaluation

Introduction

Ebstein's malformation is a complex lesion whose spectrum varies from the serious, when there is marked valvar dysplasia and deformity, to being relatively benign in nature. It is, therefore, impossible to provide a single option for treatment without understanding both the developmental aspects of this lesion and the fetal and neonatal presentations affecting not only the heart, but also other organs such as the lungs. In a previous volume in this series, I described the echocardiographic features of this condition [1].

An echocardiographer approaching this condition must take cognizance of many issues that

Electronic Supplementary Material The online version of this chapter (doi:10.1007/978-3-319-67096-6_13) contains supplementary material, which is available to authorized users.

N.H. Silverman, MD DSc (Med) FACC, FASE, FAHA
Division of Pediatric Cardiology, Stanford University, Stanford, CA 94305, USA

Division of Pediatric Cardiology, University of California, San Francisco, Box 0544, 550, 15th street, 5th Floor, San Francisco, CA 94143, USA
e-mail: norm.silverman@stanford.edu

M.K. Friedberg, A.N. Redington (eds.), *Right Ventricular Physiology, Adaptation and Failure in Congenital and Acquired Heart Disease*, https://doi.org/10.1007/978-3-319-67096-6_13

are of critical importance when approaching the echocardiogram, which, while it cannot determine the repair on its own, is certainly a major determinant in deciding the type of repair needed, as shown below [1–12].

Pathological Considerations for Echocardiography

The tricuspid valvar abnormality in Ebstein's malformation describes the proximal displacement of the tricuspid valve from its proper position at the right atrioventricular junction (Fig. 13.1) This displacement is not uniform. The anterior leaflet is usually attached normally, with progressive displacement of the septal leaflet from its junctional position across the septum to its junction with the mural (or inferior) leaflet, thus creating two divisions within the right ventricle: an "atrialized" portion of the right ventricle and a functional (or true part) of the right ventricle, distal to the tricuspid attachment to the underlying right ventricular myocardium (Fig. 13.2). This displacement comes about because normal apoptosis, which brings the tricuspid valve into its usual position, does not occur during development.

The degree of displacement is variable, leading to a variety of situations from mild to severe valvar displacement, and even to the obliteration of the right ventricular outflow tract, producing pulmonary atresia (Fig. 13.3).

It is important to understand the condition's developmental aspects, because the lesion is modified by the secondary consequences of fetal cardiovascular development, particularly by the effects on the developing right ventricle. In addition to the displacement of the valve from its intended proximal attachment, there is also a change in the tricuspid valve that is deformed in many ways. There are often verrucae on the valvar surfaces. The valve appears to be thickened in some regions and thinned in others (Fig. 13.3). The tendinous cords may be visible through some parts of the valve and the edges of the valve are thickened and rolled. Adherence of the valve to the wall of the ventricle, particularly the mural and septal leaflets, is part of the fundamental morphology of this lesion (Fig. 13.1). The distal attachments of the valvar leaflets to the tendinous cords and papillary muscles and, indeed, to the underlying ventricle, is fundamental and important to surgical liberation of the valve. The attachment of the valve to the underlying myocardium

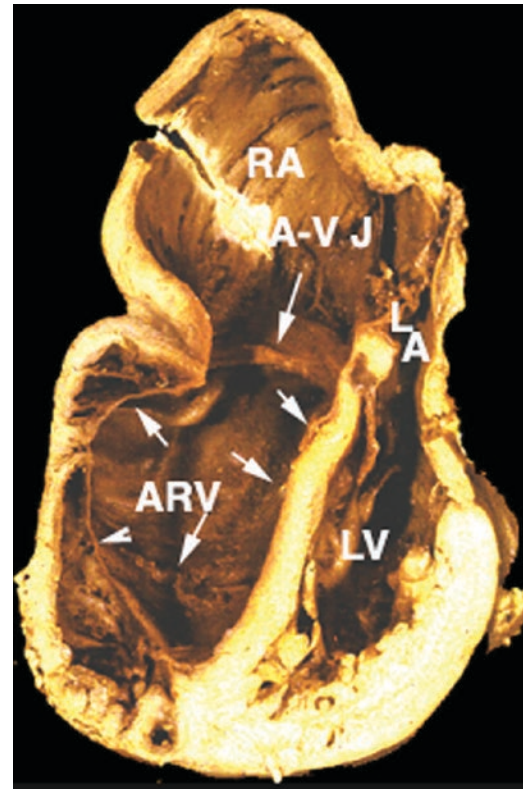

Fig. 13.1 This pathological specimen is cut to simulate and apical four-chamber view with enlarged right atrium (RA) and right ventricle. The anterior leaflet is seen with its normal cordal attachment to the underlying inferior tricuspid wall. The rest of the mural leaflet is seen lying deep within the ventricle toward the apex (*arrows*) plastered down from that point to the atrioventricular junction posteriorly (A-V J). The displacement of the valve from the atrioventricular junction (*arrows*), delimit the "atrialized" portion of the right ventricle from the rest of the right ventricle. The tricuspid septal leaflet is on the ventricular septum but is displaced apically as well when compared to the mitral leaflet lying within the left ventricle LV. Other abbreviations; *LA* left atrium. With permission from Silverman NH. Anatomic Definition and Imaging of Ebstein's Malformation. In: Reddington AN, Van Arsdell GS, and Anderson RH, eds. Congenital Diseases of the Right Heart. Springer-Verlag, London 2009 [1]

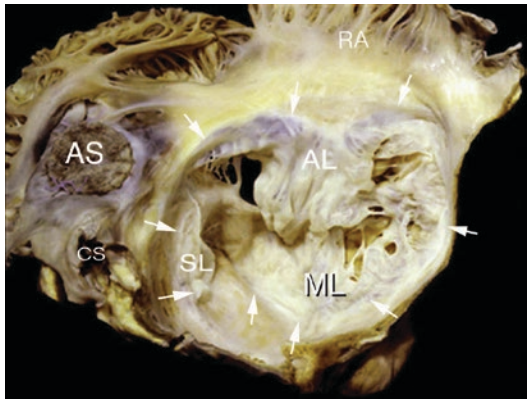

Fig. 13.2 A pathological view of the valve from an 8-year-old boy who died after the atrial septal defect patch (AS) was placed. The right atrium (RA) has been opened and the tricuspid valve is exposed from this chamber. The three leaflets of the tricuspid valve are labeled. The anterior leaflet (AL) is large and sail-like. The *arrows* show normal attachment of the leaflet to the underlying atrioventricular junction. The septal leaflet (SL) is not delaminated from the underlying ventricular septal myocardium and the hinge point of the valve (*arrow* becomes progressively more displaced from the atrioventricular junction). At the junction with the mural leaflet (ML), which is difficult to define clearly in this specimen and may indicate fusion of these two leaflets, the displacement reaches a maximum point away from the right atrioventricular junction (compare this to Fig. 13.1) The mural leaflet in this specimen is largely adhering to the underlying myocardium. It then makes its way back to the atrioventricular junction on its lateral surface. On this specimen note also the abnormal distal attachments of the valve via the abnormal chordae tendiniae as well as the thickening of the valve itself. Other abbreviations; CS coronary sinus orifice. With permission from Silverman NH. Anatomic Definition and Imaging of Ebstein's Malformation. In: Reddington AN, Van Arsdell GS, and Anderson RH, eds. Congenital Diseases of the Right Heart. Springer-Verlag, London 2009 [1]

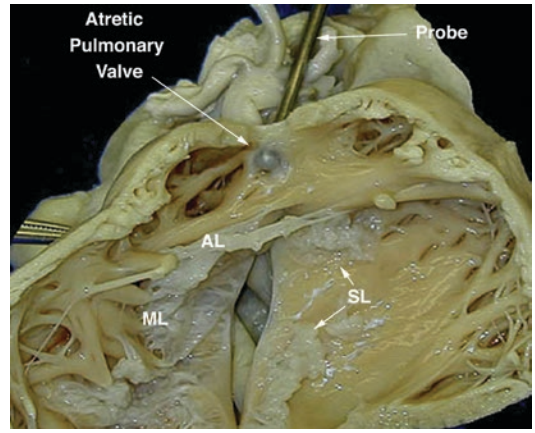

Fig. 13.3 This figure shows the morbid anatomy from a fetus that died at 38 weeks of gestational age. The heart is viewed from the anterior aspect of the right ventricle. The features of Ebstein's malformation of the tricuspid valve are noted with a normal anterior leaflet (AL), a moderately sized mural leaflet (ML) and plastered down (nondelaminated) septal leaflet of the tricuspid valve.(SL). At 20 weeks of gestation this patient's fetal echocardiogram of the pulmonary valve showed the valve to be patent, but in the course of the next 16 weeks when we last examined this fetus echocardiographically, the pulmonary valve was motionless. The fetus died 2 weeks later. On the specimen a probe has been placed in the main pulmonary artery and shows a thin but atretic pulmonary valve, which had no cusp formation noted on it

or papillary muscle, particularly of the anterior leaflet, may be linear, hyphenated (through a series of abnormally thickened tendinous cords), or through abnormal or normally attached cords. In some specimens the anterior leaflet can be muscularized (Fig. 13.4).

In addition to the valvar pathology, other defects of morphological concern are important to the surgeon. The papillary muscles are often elongated and attenuated, and the myocardium is often abnormal in several areas (Fig. 13.4). Because of fetal tricuspid regurgitation the atrium is enlarged and surprisingly thinned. The "atrialized" portion of the right ventricle may also be thinned, sometimes demonstrating replacement fibrosis, and the rest of the ventricle may be thinned as well. Due to the lack of propulsive forward flow across the right ventricular outflow tract the outflow area may not develop well and may become narrowed.

The pulmonary valve plays a unique part in the ongoing development of Ebstein's malformation (Fig. 13.3). Because tricuspid regurgitation in the fetus is at levels of systemic systolic pressure, and pulmonary arterial pressure transmitted via the arterial duct is also at systemic systolic pressure, the pulmonary valve may be held in a closed position interfering with its development, leading to pulmonary atresia, stenosis or insufficiency (Fig. 13.4). Physiologically this leads to the development of a reversed circuit within the

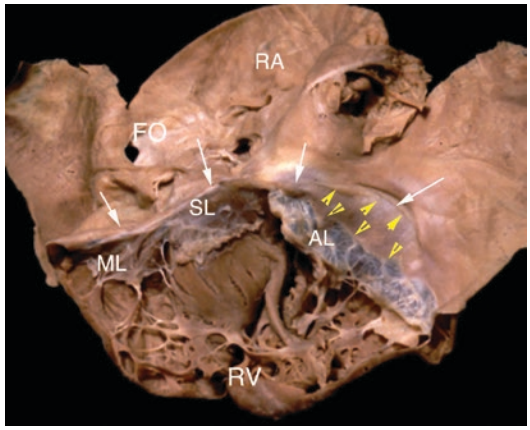

Fig. 13.4 This morbid anatomic example of Ebstein's malformation from a neonate shows an extremely large right atrium (RA). The patent fossa ovalis (FO can be identified. The mural (ML), septal (SL) and anterior leaflets (AL) of the tricuspid valves are all identified. *White arrows* highlight the atrioventricular junction. The septal leaflet is only minimally delaminated at its leaflet tips. The anterior leaflet is muscularized (*yellow arrowheads*). The muscular structures of the right ventricle (RV) are abnormal with thinned trabeculations and papillary muscles supporting the leaflets

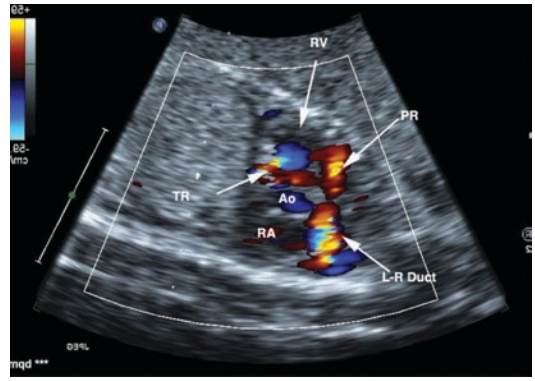

Fig. 13.5 This fetal echocardiogram was taken from a fetus near term and shows features of the so-called circular shunt. This Doppler color flow superimposition on a cross-sectional image shows tricuspid regurgitation (TR). With ineffective forward flow from the right ventricle, pulmonary blood flow is derived from the ductus shunting left-to-right (L-R Duct). Because the pressure in the pulmonary artery is systemic and the pulmonary valve is not functioning well, there is pulmonary regurgitation (PR). Other abbreviations are (Ao) aorta (RA) right atrium

right heart, from left-to-right shunting at arterial duct level through pulmonary regurgitation, tricuspid regurgitation and atrial right-to-left shunting. These features are important both for neonatal management and for surgery. Future fetal therapy may involve administering oxygen to the mother in an attempt to increase fetal oxygen tensions, thereby lowering fetal pulmonary vascular resistance when fetal pulmonary arterioles become sensitive to oxygen in the last trimester. Additionally, prostaglandin synthetase inhibitors such as Indomethacin or ibuprophen can close the ductus in utero, thereby lowering pulmonary arterial pressure, may play a part in allowing affected fetuses to be delivered in a healthier state.

Fetal Echocardiographic Considerations

In a recent collaborative multi-institutional study of a cohort of 264 fetuses, Freud et al. showed a persistently high mortality, both for fetuses and neonates with this condition [13]. This study reported that fetuses have a 40% prenatal demise and neonates have a 35% mortality rate. Of the 72% live-born infants only 68% survived through discharge from the nursery. Although there has been some improvement in the statistics, the prognosis for symptomatic fetal survival still appears poor [14–17].

Recognition of fetal disorders begins early. We have recorded frank anomalies as early as 16 weeks, and the changes are progressive, relating to developing physiologic abnormalities. It is the degree of tricuspid regurgitation that tends to hold the pulmonary valve in the closed and functionless position (Fig. 13.3). Consequently, pulmonary valvar maldevelopment either causes atresia, stenosis or regurgitation that can be observed by fetal echocardiography (Fig. 13.5; Video 13.1). With progressive increase in systemic pressure and increased afterload the amount of tricuspid regurgitation worsens, because the valve is functionally maldeveloped and the annulus of the valve dilates as right atrial and right ventricular volumes increase (Fig. 13.6; Videos 13.2a and 13.2b). This leads to enlargement of the right heart structures and to the fetal

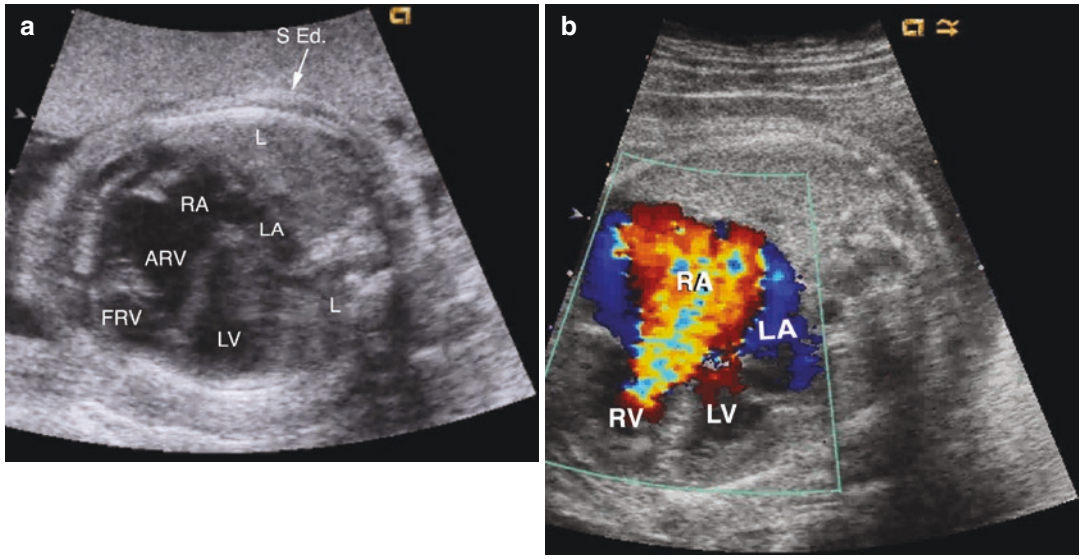

Fig. 13.6 (**a**) A four-chamber view in a 33-week-old fetus with Ebstein's malformation and early hydrops fetalis as evidenced by the early skin edema (S Ed). The heart is enlarged, occupying about 70% of the area for the cardiothoracic cavity, due to enlargement of the right heart chambers, the right atrium (RA) and the right ventricle (RV). The lungs (L) are correspondingly small. The left atrium LA and left ventricle (LV) is not enlarged. (**b**) A corresponding four-chamber view with superimposed Doppler color flow imaging indicates the marked degree of tricuspid regurgitation

scoring of Roberson and, later, Celermajer and his colleagues, involving the ratio of the area of the right atrium and atrialized right ventricle to the area of the rest of the heart in the four-chamber view (Figs. 13.7, 13.8, and 13.9; Videos 13.3a, 13.3b, 13.3c, and 13.3d) [3, 5, 8].

Survival stat istics are available for fetuses and infants with this classification [8]. When pulmonary insufficiency occurs and blood flows backward, this is an ominous sign that my students have termed the "circle of death" (Fig. 13.5). The left heart is also affected, with evidence that the left ventricle contracts poorly because there is no support for the upper ventricular septum against the stress of a systemic right ventricle. Tissue Doppler abnormalities have also been reported [17]. All these features lead to a dilated right heart. The degree of cardiomegaly can be profound, and an increase in the cardiothoracic ratio over 65% leads to an ominous prognosis (Fig. 13.10) [5, 15]. When the circulation is over-

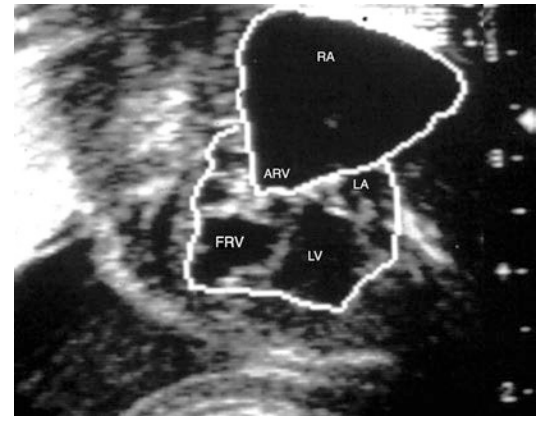

Fig. 13.7 This frame is from a fetus with Ebstein's malformation where the right atrium (RA) and atrialized right ventricle (ARV) are planimitered separately from the left atrium (LA), left ventricle (LV) and the functional right ventricle (FRV). A ratio of >1:1 is a poor prognostic sign. Celermajer and his colleagues expanded this index. With permission from Roberson DA, Silverman NH. Ebstein's anomaly: echocardiographic and clinical features in the fetus and neonate. J Am Coll Cardiol 1989; 14:1300–7 © Elsevier 1989 [3]

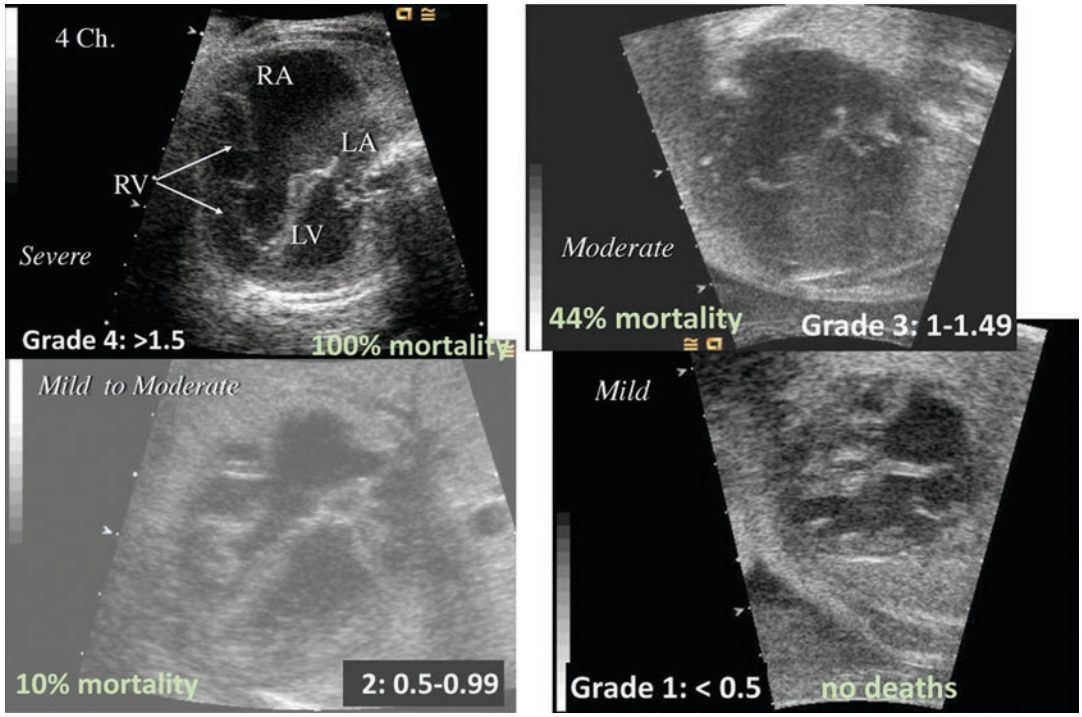

Fig. 13.8 This is a series of four-chamber images in the fetus with varying severities, from the most severe *top left*) to the mildest (*bottom right*). The variations on the Celermajer index [7] are shown in white lettering at the *bottom part* of each frame and the mortality as per these indices are shown in green at the *bottom right corner* of each image

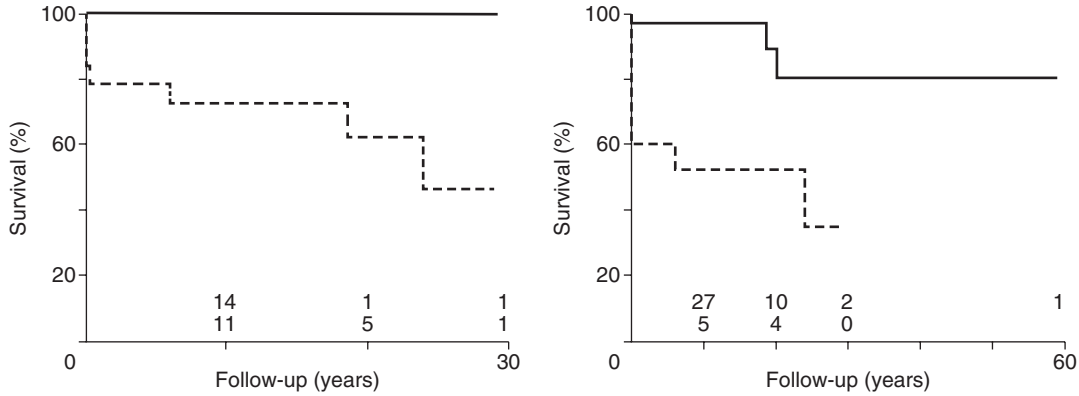

Fig. 13.9 These are Celermajer plottings of Kaplan-Meier survival curves, cases with fetal or neonatal diagnosis from Arizmendi et al. [5] The left-hand graph shows a dark line representing cases with Celermajer index of Grade 1 or 2 (*continuous line*), and cases with Grade 3 or 4 (*broken line*). The *right-hand panel* represents patients with fetal or neonatal Ebstein's malformation with cardiothoracic index less than 65% (*continuous line*) and cases with index equal or greater than 65% (*broken line*). With permission from Arizmendi AF, Pineda LF, Jiménez, CQ, Azcárate MJM, Sarachaga IH, Urroz E, de León JP, Moya JL, Jiménez MQ. The clinical profile of Ebstein's malformation as seen from the fetus to the adult in 52 patients. Cardiol Young 2004; 14: 55–63 © Cambridge University Press 2004 [5]

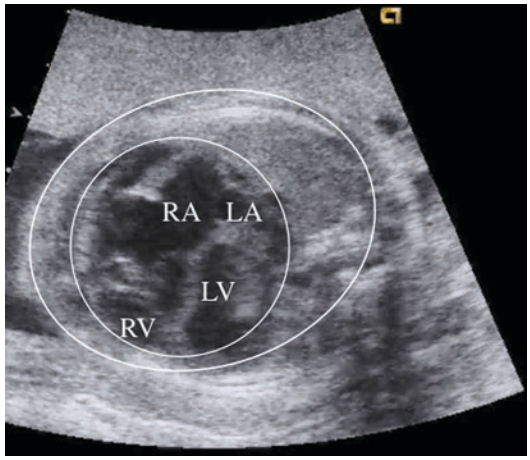

Fig. 13.10 This is a diagrammatic tracing of the cardiothoracic cavity at the four-chamber level (*outer circle*) and the outline of the heart (*inner circle*) from the patient in Fig. 13.6 left. The heart is markedly enlarged and would only fill the area of the thoracic cavity less than twice, whereas it should fill the cavity three times. The cardiac enlargement is due to right heart enlargement

come hydrops fetalis develops, because increased permeability of fetal capillaries and low fetal colloid oncotic pressure fail to draw fluid back from the interstitium in the vascular system. As fluid accumulates in the pleural and pericardial spaces lung development is compromised, thereby contributing to postnatal mortality. In some measure hydrops, increased heart size, and the serous cavity component of hydrops all compromise cardiac filling and contribute to diastolic dysfunction.

Prenatal echocardiography provides clues as to how the lesion might be handled surgically and which medical and surgical techniques might be considered [18, 19].

Surgical Considerations

As an echocardiographer one has to know what the surgical options for this lesion are. There are many options, because of the marked variability in the expression of the lesion (Fig. 13.11). Echocardiography can help in deciding which treatment algorithms are relevant. These algorithms can be divided into the one-ventricle repair option (shunt + tricuspid exclusion and/or pulmonary arterial exclusion), one-and-a-half ventricle repair (with a Glenn shunt) or a two-ventricle repair (tricuspid valvar repair plus tricuspid valvar annuloplasty and atrial septal defect closure). Finally, one has to consider the option of cardiac transplantation. The time of presentation of the anomaly may determine the treatment options. Should the fetus present with a severe form of the disease, for example when hydrops is present, the options are limited. If, for example, there is a small left ventricle that would have difficulty supporting a greater part of the circulation, options are a one-ventricle repair or transplant. The fetal option may, however, be modified by medical management such as early delivery for the severer forms of this malformation (Tworetzky W, personal communication) has used Indomethacin in the hope of decreasing pulmonary pressure by closing the arterial duct, just as Wald et al. [20] achieved in the postnatal situation with a group of neonates presenting with a severe form of the disease. Kohl [18] has suggested, in addition, using maternal hyperoxia in the third trimester fetus in the hope that, should pulmonary vascular resistance fall, right ventricular forward flow may increase (personal communication). These suggestions are currently anecdotal. In the neonate, the treatment algorithm allows several options, as have been espoused by Dearani and his colleagues [21] from the Mayo Clinic (Fig. 13.8) and Bove and his colleagues from the University of Michigan (Fig. 13.9) [22]. If there is antegrade flow in the right heart with a good anterior leaflet as defined echocardiographically, the patient is put on a path toward a two-ventricle repair, which can be delayed to later infancy. If there is anatomic pulmonary atresia and the pulmonary arteries are hypoplastic, their approach is to use the one-ventricle route for repair. If there is *functional* pulmonary atresia with a hypoplastic left ventricle, or if the left ventricle functions poorly and cannot support the systemic circulation and part or all of the pulmonary circulation, the only option for survival is

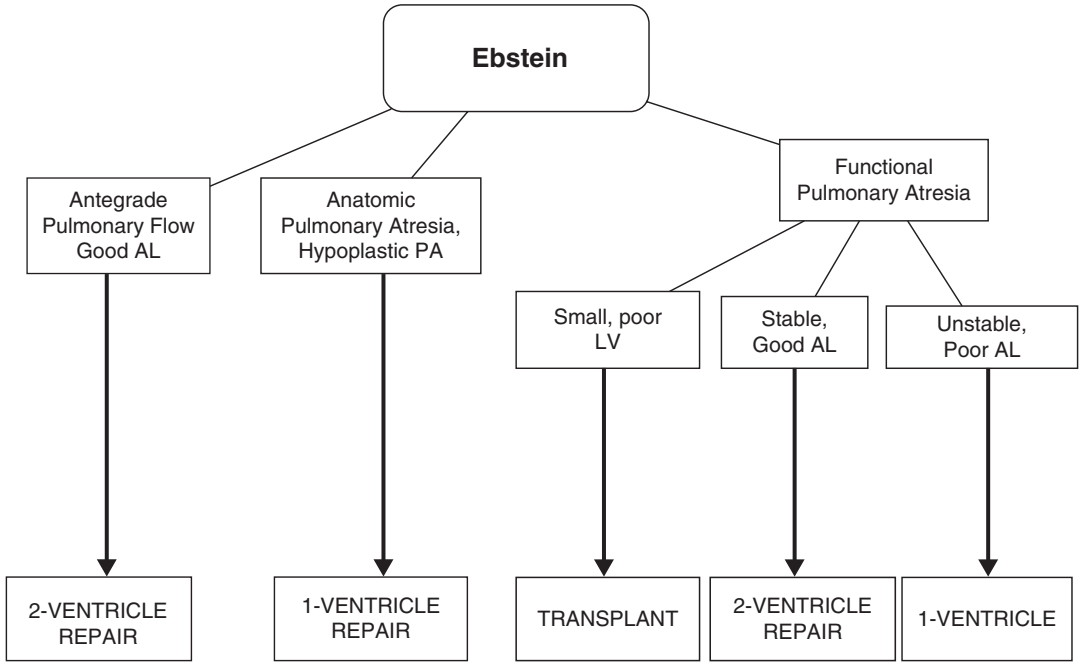

Fig. 13.11 This Logic diagram is modified from the method of Joseph Dearani and the Mayo Clinic. With permission from Dearani JA, Said SM, Burkhart HM, Pike RB, O'Leary PW, Cetta F., Strategies for Tricuspid Re-Repair in Ebstein Malformation Using the Cone Technique. Ann Thorac Surg. 2013J;96):202–8 © Elsevier 2013 [21]

heart transplantation. If there is functional pulmonary atresia aggressive lowering of the pulmonary arterial pressure by means of oxygen and nitric oxide, and the attempt to close the ductus with indomethacin, as described by Wald and colleagues, should be attempted before surgery is undertaken [20].

The treatment algorithm for single ventricle repair has been successfully used by Starnes et al. and involves an aortopulmonary shunt with closure of the tricuspid and the pulmonary valve [23–27]. These choices depend both on the surgeon's intuitive operative preferences and on the combined opinion and skill of the medical team. Bove et al. [22] offer an approach in the neonate (Fig. 13.9). In their opinion, repair or replacement of the valve is best avoided in the neonate but may be utilized selectively when the morphology of the valve and the RV function are favorable. If the cyanosis does not abate and there is additional heart failure due to fetal hydrops, the Starnes approach is used [22] When there is cyanosis without heart failure they suggest a shunt alone. If the neonate cannot be weaned from the prostaglandin infusion on the first or second attempt, the patient is on-track for a single ventricle operation, ultimately involving the Fontan procedure, or one-and-a-half ventricle repair. The single ventricle repair track is also chosen if tricuspid closure with a shunt is needed. If the patient can be weaned from pharmacological and ventilation support, no further treatment is offered in the neonatal period.

A decision about a two-ventricle or one-and-a-half ventricle repair, or a total cavopulmonary connection approach can be made at a later date. If there is a later presentation after the neonatal period, or when the neonate successfully recovers from the period of transitional circulation, some form of biventricular repair can be offered.

When there is additional left ventricle compromise in addition to the Ebstein's malforma-

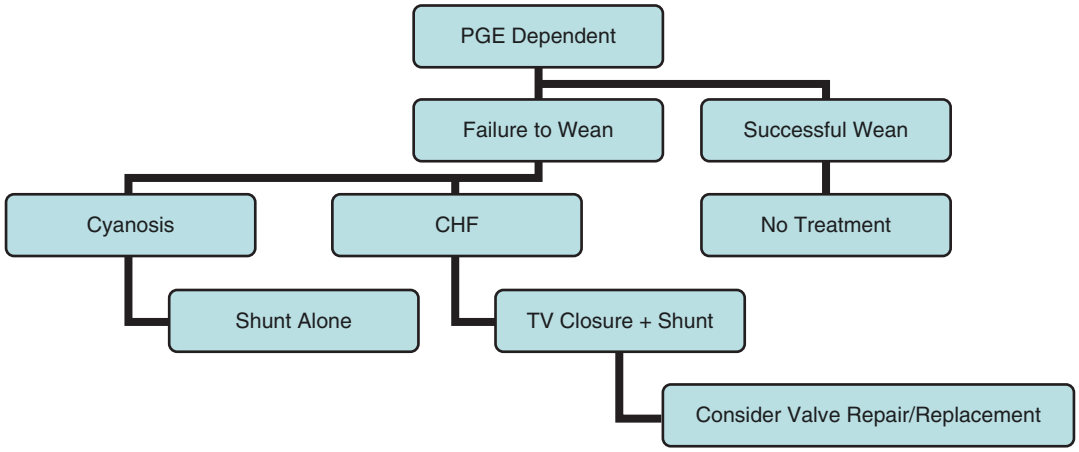

Fig. 13.12 This diagram of the treatment protocol for Ebstein's anomaly in the neonate is modified from Bove EL, Hirsch JC, Ohye RG, Devaney EJ. How I Manage Neonatal Ebstein's Anomaly Semin Thorac Cardiovasc Surg Pediatr Card Surg Ann 2009;12:63–65, with permission © Elsevier 2009 [22]

tion, heart transplant remains a plausible and viable option. This option is also indicated if the anterior leaflet of the tricuspid valve is poor or unstable. In some cases where there is left ventricular dysfunction, such as in conditions associated with spongy myocardium, or where there is bad function of the ventricles, heart transplant remains the only viable option. We had a two-day-old neonate with a poor left ventricle due to spongy myocardium with Ebstein's malformation who was successfully transplanted (Figs. 13.12 and 13.13; Videos 13.4a and 13.4b).

There are several operative techniques involved when considering a two-ventricle repair. Carpentier and Chavaud described the first approach [27–30]. This approach involves repair of the tricuspid valve, atrial reduction and tricuspid annuloplasty. Knott-Craig, and most recently da Silva and Dearani, have reported modification of the approach in what has now been termed the "Cone" procedure (Figs. 12.3 and 13.14) [21, 31–33]. In this procedure, the antero-superior and posterior tricuspid valve leaflets are detached from the right ventricle, the cut edge of this complex is rotated clockwise and re-sutured to the septal border of the anterior leaflet (thus creating a cone), the vertex of which remains fixed at the right ventricular apex and the base of which is sutured to the true tricuspid valve annulus level. The septal leaflet is incorporated into the cone of tissue whenever possible, even incorporating a pericardial addition to the circumference of the cone. A folding or excision of the redundant tissue accomplishes reduction in the atrial size and the atrialized portion of the right ventricle, and the atrial septal defect is closed in a "valved" fashion. The results have been excellent and have been successfully completed in very young infants, as young as 5 days of age [33].

There is a preference by some surgeons for performing a bidirectional Glenn when operating on age-appropriate babies in order to assist the right ventricle in its recovery and pulmonary perfusion. This is often done when there is an enlarged and dysfunctional right ventricle, when the right atrial pressure is 1.5 times greater than the left atrial pressure after separation from cardiopulmonary bypass, and when the repaired tricuspid orifice is small. It also has the advantage of reducing tension on the repair, facilitating a tighter tricuspid annuloplasty [34, 35].

Still in favor is the atrial reduction and valve annuloplasty described by Danielson [30, 35] a very successful procedure with long-lasting

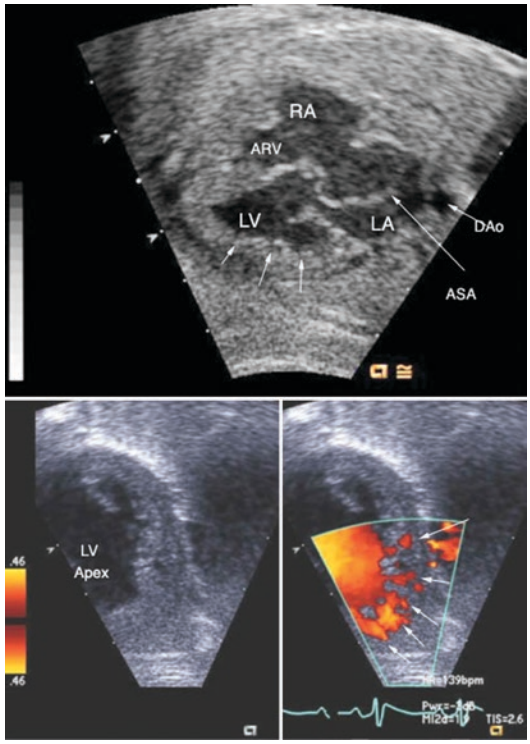

Fig. 13.13 *Top*. A Four-chamber image in a 36-week-old fetus with marked enlargement of the right atrium (RA) and an atrial septum which is aneurysmal (ASA), bulging into the left atrium (LA) The left ventricle (LV) demonstrates numerous trabeculations characteristic of spongy myocardium. Only the atrialized portion of the right ventricle is seen in this four-chamber cut because the tricuspid valve was displaced into the right ventricular outflow area. The descending aortic (Dao) lies posterior to the left atrium. *Bottom*: An immediate postnatal echocardiogram demonstrating the spongy trabeculations lying within the apical portion of the left ventricle in this color-compare apical magnified four-chamber cut

favorable results. These authors also perform a moderate apical ventricular reduction and an aggressive annular reduction down to an area of 2.5 cm^2/m^2 BSA [35].

Other options for the worst tricuspid pathology include replacement of the tricuspid valve with a prosthesis.

Attention to associated disease such as ventricular septal defects, or right ventricular outflow problems such as subpulmonary obstruction, pulmonary valvar repair or replacement, repair of supravalvar stenosis, atrial septal defect and partial vein anomaly repair, or electro-physiological operations, are all part of the repair strategy [35].

Echocardiography

What can ultrasound do to define the lesion for the surgeon? As is the case with atrioventricular canal defects, the surgeon who deals with Ebstein's malformation has to define what can best be done by assessing the valve visually. Ultrasound certainly plays a part in this assessment, but visual inspection of the valve is of the utmost importance. We described the echocardiographic features of this malformation in a previous volume from this symposium so will concentrate on the key features of what echocardiography can currently provide for the surgical repair [1].

The Four-Chamber View

The apical four-chamber view first demonstrated the downward displacement of the septal leaflet of the tricuspid valve and the area of the atrialized right ventricle (Fig. 13.15; Videos 13.5a and 13.5b) [2]. The degree of displacement roughly parallels the degree of tricuspid regurgitation and, therefore, the severity of the disease. Because the valve in this condition is displaced anteriorly there may well be patients with more severe forms of this malformation in whom the valve is not seen in the classical four-chamber view at all. A craniad tilt of the transducer on the cardiac apex brings the imaging plane of the transducer to lie antero-superiorly, defining the tricuspid valve lying in the outflow tract.

It is important to recognize attachments of the anterior leaflet, which can be identified in this view, to the underlying myocardium (Figs. 13.15 and 13.16; Video 13.6). Indeed, it is possible

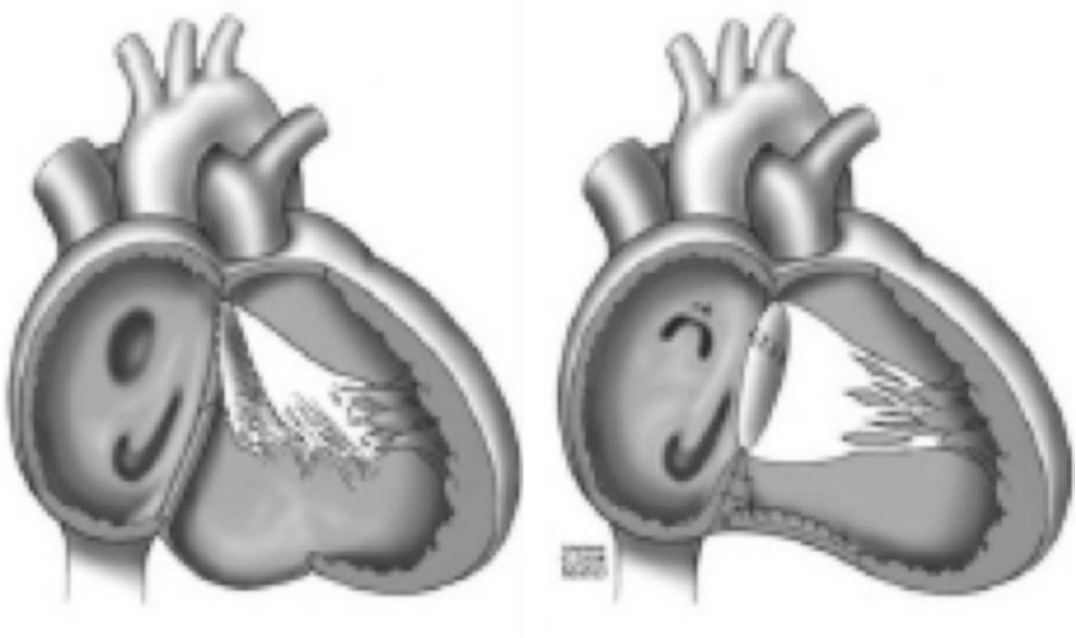

Fig. 13.14 A view of the Cone reconstruction of Ebstein anomaly. The main principle includes complete surgical delamination of the tricuspid valve septal leaflet, which is mobilized and then rotated and reattached at the true atrioventricular junction, followed by leaflet-to-leaflet attachment, creating a "leaflet cone." Fig. 12.3 also depicts the Cone operation as defined by Da Silva [32]

using this view to define distal attachment of the valve to the underlying myocardium. The attachment may be normal, hyphenated or linear to the underlying myocardium, and these features are important in planning the type of procedure contemplated. The valve leaflets may be thickened in parts, thinned in other parts and a degree of tethering with tendinous cords or attachment to the underlying myocardium can be assessed in this view. Systolic prolapse of the leaflets may be observed on real-time imaging. The displacement of the septal leaflet can be defined, and has been used to define this disorder echocardiographically [2, 11]. The four-chamber view has also demonstrated the mobility of the septal leaflet and how much redundancy of the valvar leaflets is present, which is important for the modern Cone procedure (Fig. 13.16).

The degree of tricuspid regurgitation may be determined echocardiographically, and the index described by Celermajer may be used to define the outcome of this disorder (Fig. 13.17) [7]. Modern techniques of management, both medical and surgical, have improved the outcomes and blurred the distinctions of Celermajer's original description [24].

From the apical four-chamber view the associated size of the mitral and tricuspid annuli may be measured. It is well known that annular dilation may be a poor prognostic sign, which, at direct surgical inspection of the valve, may be as large as 6 cm/m^2 of body surface area [35]. Marked dilation, as well as multiple jets of tricuspid regurgitation, are poor prognostic signs of successful repair.

Although one has to concede that echocardiography is limited in its ability to predict right ventricular function, it does provide a visual index of how poor the function is and where thinning of the myocardium exists. At

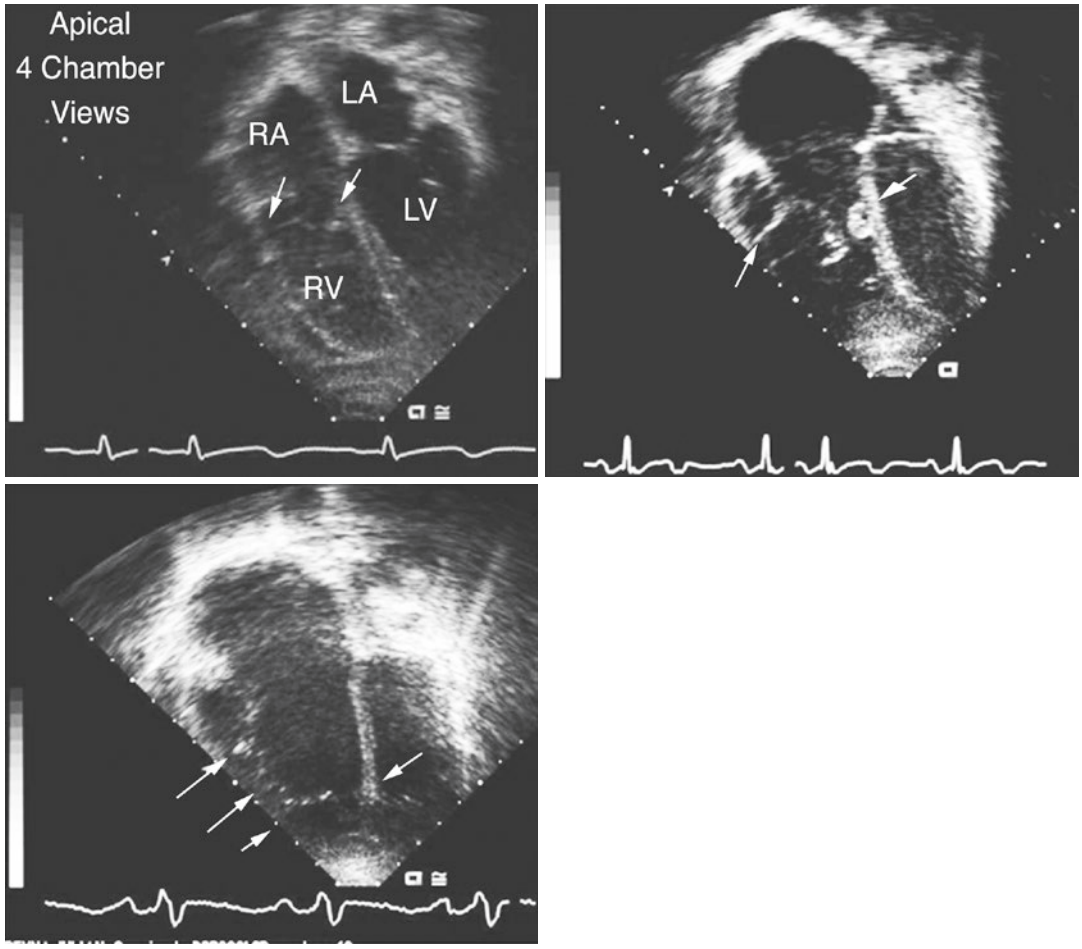

Fig. 13.15 This series of apical four-chamber images shows the progressive displacement of the tricuspid septal leaflet with progressive severity of the disease. In this view the anterior and septal leaflets are demonstrated. *Top Frame*: The right atrium (RA) in the top frame is minimally enlarged, as is the right ventricle. Note the attachment of the anterior leaflet is normal in all of these frames. The lateral *arrows* indicate the chordae tendiniae, attached to the right ventricular wall. The medial *arrows* indicate the septal attachment of the tricuspid valve. The mitral valve for comparison lies between the left atrium (LA) and left ventricle (LV). *Middle Frame*: This shows a moderated degree of displacement of the septal leaflet of the tricuspid valve (*Medial arrow*). The lateral *arrow* indicates thin attachment of the tendinous cords underneath the anterior leaflet. The medial *arrow* shows the septal leaflet of the tricuspid valve, which is thickened and rolled. The right atrium is moderately enlarged and encroaches on the left atrium, which is small. The right ventricle is also much larger than its fellow. *Bottom Frame*: This shows a severe degree of displacement of the septal leaflet of the tricuspid valve (*medial arrow*). The lateral *arrows* again demonstrate tendinous cordal attachment of the anterior leaflet of the tricuspid valve to the underlying right ventricle. Compared to the middle frame, the right heart chambers are proportionally larger. When these images were seen with Doppler color flow the degree of tricuspid regurgitation paralleled the displacement of the valve and the chamber enlargement too

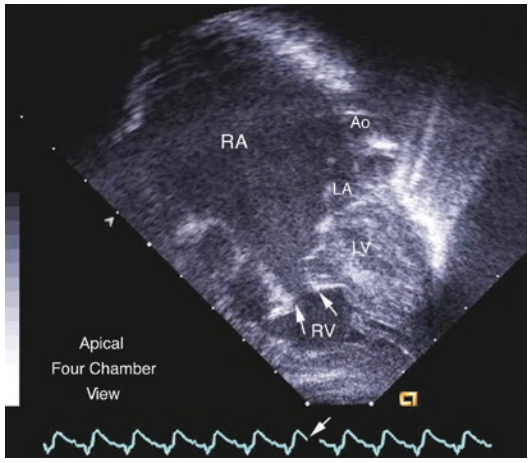

Fig. 13.16 This four-chamber image shows an infant with severe Ebstein's malformation without systolic coaptation of a thickened and restrictive tricuspid valve (*arrows*). The electrocardiogram indicates the frame is taken in late systole. The right atrium is enlarged far beyond the descending aorta (Dao), which usually delimits the posterior extent of the heart in this view. The functional right ventricle (RV) is small. The left atrium (LA) and left ventricle (LV) appear small

the same time, from the four-chamber view, the left ventricle can be assessed for function and dyskinetic contraction. These techniques have now been enhanced by speckle tracking and Tissue Doppler indices for assessing cardiac function [36].

The Subcostal View

This transducer location provides a most important complement to the four-chamber view as can be seen from the diagram popularized by Chauvaud and Carpentier, which can be matched exactly with that seen by echocardiography (Figs. 13.18 and 13.19; Videos 13.7a, 13.7b, 13.7c, and 13.7d) [28]. Even in the adult it is possible to obtain views in this location or they may be obtained by transgastric imaging using transesophageal echocardiography.

In the subcostal coronal view the anterior and mural leaflets are seen, permitting all the

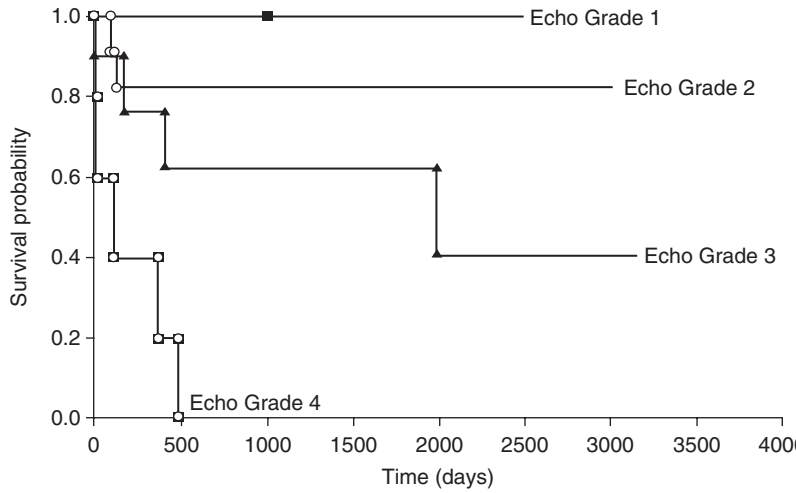

Fig. 13.17 This figures shows the Kaplan-Meier Survival curves for 28 patients with echocardiographic grading of the severity of their disorder as reported by Celermajer et al. [7]. The ratio of the atrialized right ventricle and the right atrium to the rest of the heart in the four-chamber view was shown previously in Fig. 13.8. With permission from Celermajer DS, Dodd SM, Greenwald SE, et al. Morbid Anatomy in Neonates with Ebstein's anomaly of the Tricuspid Valve: Pathophysiological and Clinical Implications. J Am Coll Cardiol 1992;19: 1049–53 © Elsevier 1992 [7]

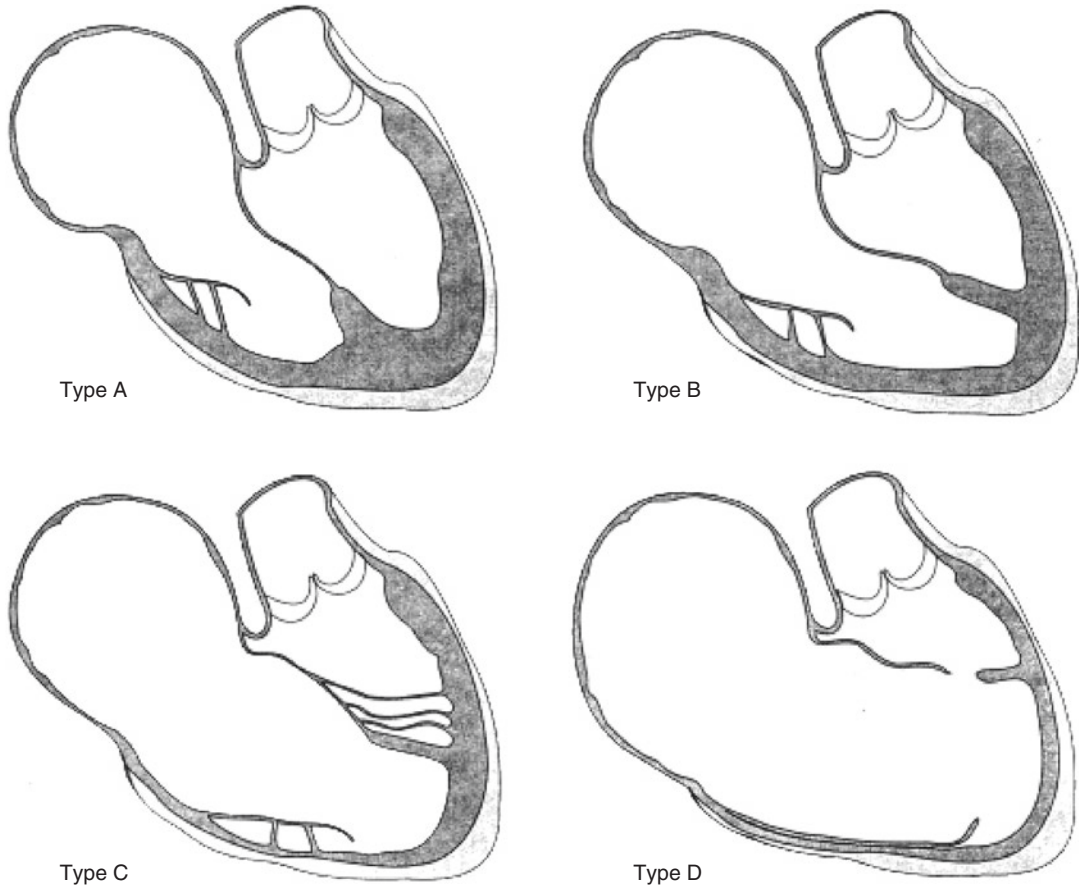

Fig. 13.18 This figure is a diagrammatic classification of Ebstein's malformation using the classification of types. [27] Type A shows minimal displacement of the attachment of the septal leaflet to the underlying myocardium and the small size of the atrialized right ventricle. Type B shows moderate displacement of the septal leaflet with a large atrialized right ventricle. Type C shows important displacement of the septal and postero-inferior leaflet associated with a non-or dyskinetic atrialized right ventricle, and restricted anterior leaflet motion with short cords. Note also the thinning of the inferior wall of the atrialized portion of the right ventricle at its acute margin. Type D is termed the tricuspid sack. Based on this classification various treatment options can be planned

valve leaflets to be assessed. The subcostal coronal view provides the echocardiographic equivalent of what Carpentier and Chauvaud describe in their classification of patients for surgical repair (Figs. 13.18, 13.19, 13.20, and 13.21) [27–29]. The view, which is shown diagrammatically (Fig. 13.18), defines another important aspect of leaflet pathology that can be seen on the subcostal coronal echocardiographic cut, which shows mural leaflet displacement from its usual position. Normally, the Eustachian valve and the entrance of the inferior vena cava into the right atrium mark the position of the mural leaflet. In Ebstein's malformation the mural leaflet is markedly displaced (Fig. 13.19). The position of the anterior leaflet is also defined in this lesion. In the mildest forms the leaflet is minimally displaced and the atrialized portion of the right ventricle can be gauged to be small whereas, when the mural leaflets are maximally displaced, the leaflets can be seen in the right ventricular outflow

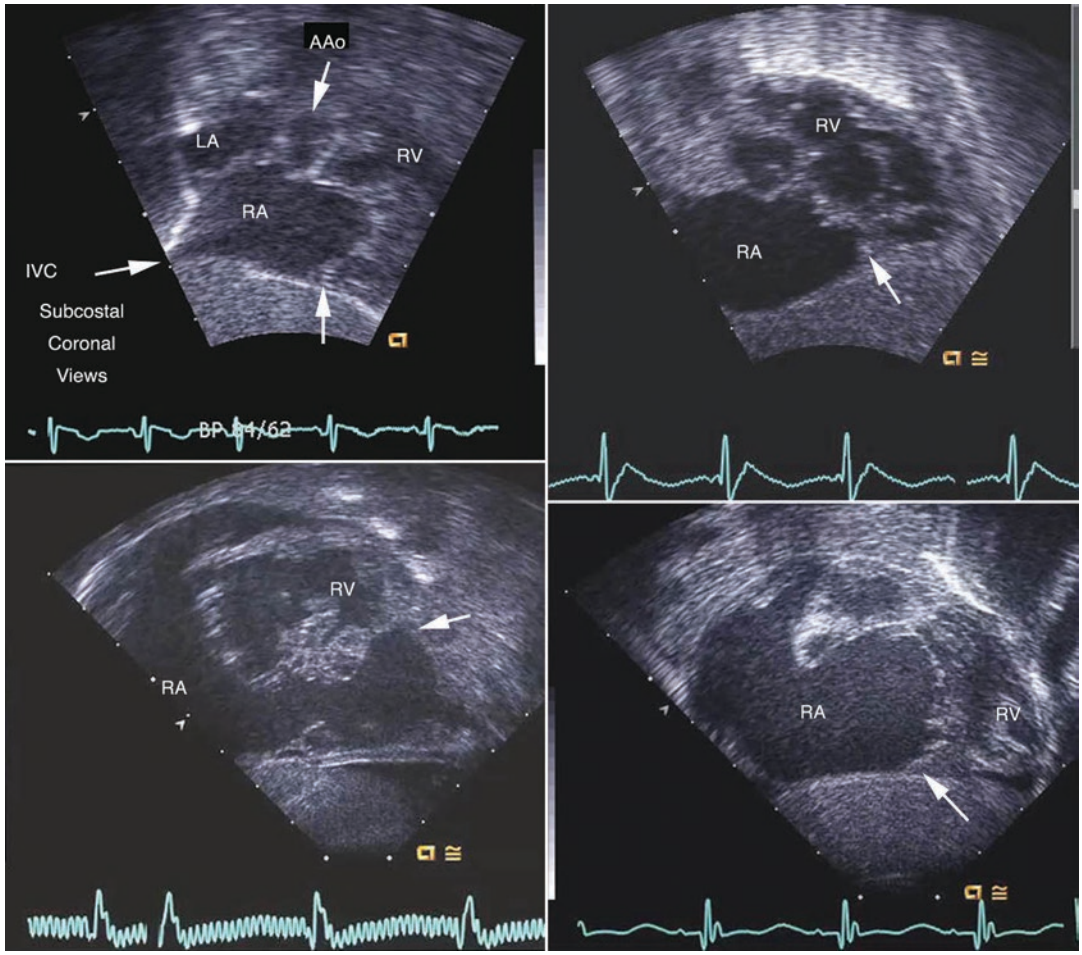

Fig. 13.19 These subcostal coronal images demonstrate the same leaflet pathology as shown in Fig. 13.18 and indicate how echocardiography can fit into a surgical classification for treatment. The lesions are mild in the *top left frame*, more severe in the *top right frame*, worse in the bottom left frame and the worst in the bottom right frame. The rotation of the inferior leaflet (*arrow*) shows progressive displacement from the functional tricuspid annulus. *AAo* ascending aorta, *LA* left atrium, *RA* right atrium, *RV* right ventricle. These images were matched with the images show in Fig. 13.18

tract. The direction of the jet of tricuspid regurgitation as directed with Doppler color flow is altered depending on the place where apposition of the valvar leaflets occurs, varying from mild displacement inferiorly from the atrial posterior wall toward the diaphragm in the milder forms of this anomaly, to a position directed toward the inferior wall of the atrialized right ventricle (Fig. 13.20). This occurs because the plane of the valvar closure plane is rotated into the right ventricular outflow, as shown in the diagrammatic images of Schreiber et al. (Fig. 13.21). As the direction of the jet is most frequently axial to that plane, the direction of the tricuspid regurgitation jet is altered, as shown in Fig. 13.20. With progressive valvar rotation toward the outflow tract, the direction of the jet moves perpendicular to the place of the valve indicating the plane of functional apposition of the valvar leaflets.

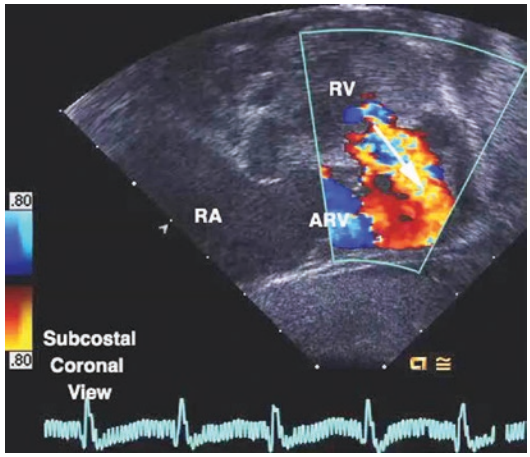

Fig. 13.20 This figure is the color information for Fig. 13.18 (bottom left). The tricuspid regurgitation from the diminutive right ventricle (RV) is directed inferiorly toward the diaphragm and the apex of the right ventricle, which is substantially "atrialized" (ARV). The right atrium (RA) is also enlarged

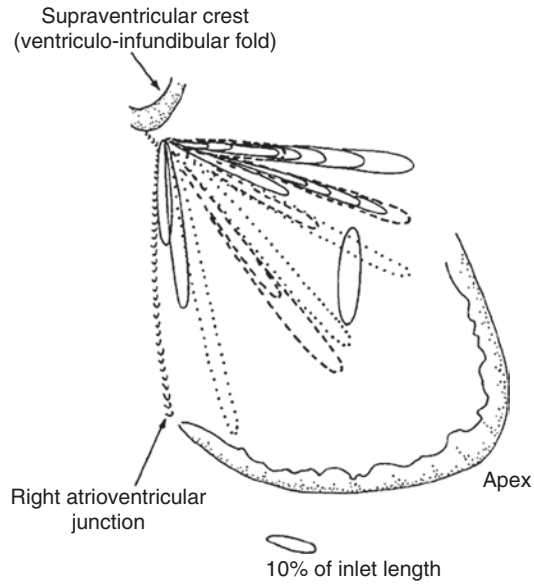

Fig. 13.21 This is a stylized representation of the angle of tilt of the effective valvar orifice (*ellipses*) as estimated from the 23 morbid anatomical specimens from the work of Schreiber et al. [4] which also mirrors our experience using echocardiography. The *solid lines* represent the cases with linear attachment; the *ellipses* with *dotted lines* and *broken lines* represent hearts with focal and hyphenated attachment of the antero-superior leaflet, respectively. The vertical ellipse represents the solitary case with the orifice parallel to the atrioventricular junction. The scale represents the maximal width of the orifice as a percentage of the distance between the atrioventricular junction and the apex of the right ventricle measured along the acute margin. With permission from Schreiber, C, Cook A, Ho S-Y, Augustin N,. Anderson RH, Morphologic Spectrum of Ebstein's malformation: Revisitation Relative to Surgical Repair. J Thorac Cardiovasc Surg 1999;117: 148–55 © Elsevier [4]

Mobility and thickening of the leaflets, as well as lack of apposition in systole, can be defined from this view. Cordal attachments of the anterior and mural leaflets of the valve to the underlying myocardium can also be defined from this view (Figs. 13.22, 13.23, and 13.24; Videos 13.8, 13.9, and 13.10).

Using this view, and its orthogonal equivalent the subcostal sagittal view, a volume assessment of the right ventricular size may be made by biplane two-dimensional echocardiography. The orthogonal subcostal view and the sagittal view are invaluable for defining the degree of right ventricular outflow narrowing, the quality of contraction of the functional right ventricle and the degree of pulmonary regurgitation (Figs. 13.22, 13.23, and 13.24). In the neonate these subcostal views define the presence of a ductus and, most importantly, the degree of pulmonary and tricuspid regurgitation and the sites of origin of these jets. The two subcostal views in the coronal and sagittal planes are used together to define the size of the tricuspid valve and to provide a much better appreciation of the valvar function, as well as the size of the right atrioventricular junction and the true right ventricle.

Parasternal Short Axis View

The parasternal short axis view is particularly valuable for surgical decision in older patient as it provides complementary views of the tri-

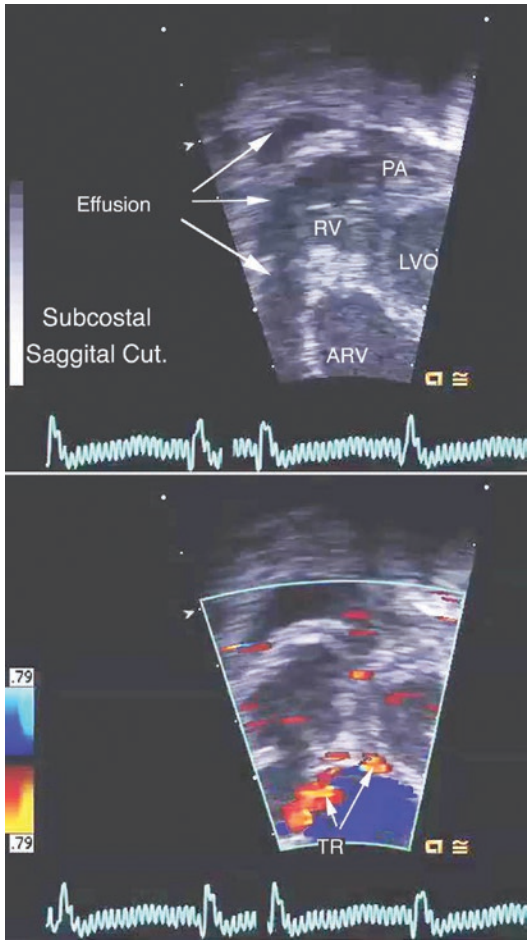

Fig. 13.22 This subcostal sagittal-cut image series shows gray scale images above with Doppler color flow superimposition below. These are the orthogonal images, taken from Fig. 13.18 top right, and show how small the true right ventricle can be when imaged together from these orthogonal views. Anterior to the right ventricle is a pericardial effusion. The tricuspid leaflets are thickened and rolled, and divide the right ventricle into an atrialized portion (ARV) and a functional portion (RV). The pulmonary valvar leaflets are also thickened and were held closed on the real-time image with blood flow supplied to the pulmonary arteries exclusively from the arterial duct. *The bottom color frame* shows two jets of tricuspid regurgitation (TR and *arrows*) arising from different coaptation points of the tricuspid valve

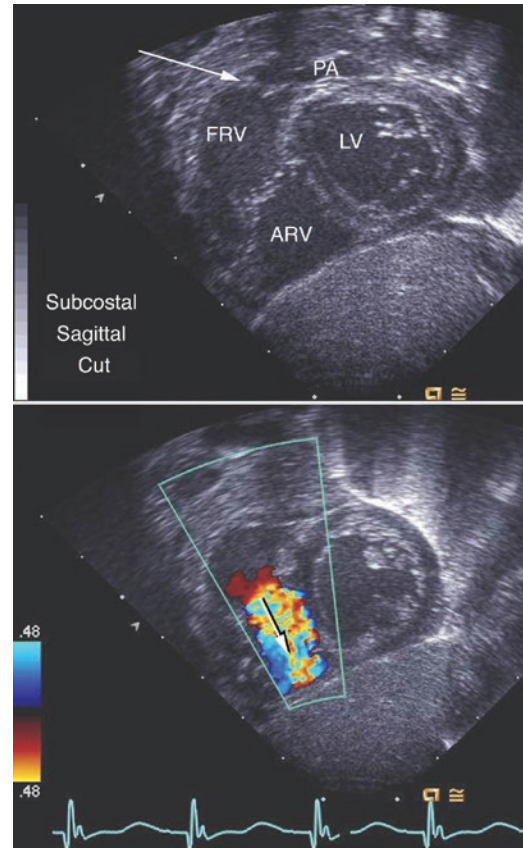

Fig. 13.23 This subcostal sagittal cut shows a series of images in gray scale above with Doppler color flow superimposition below in a milder form of this anomaly. In this example the functional right ventricle (FRV) is larger and the pulmonary artery (PA) more prominent. The atrialized right ventricle (ARV) lies on the diaphragmatic or acute marginal surface of the heart. The tricuspid jet in the bottom frame is directed toward the diaphragm. *LV* left ventricle

cuspid valve and the atrial septum as well as pulmonary valvar stenosis, atresia or regurgitation, and the presence of a patent arterial duct (Fig. 13.25; Video 13.11). The view is also used for assessing the atrial septum, and permits important assessment of the sizes of the main and branch pulmonary arteries. It also permits assessment of ventricular "pancaking" and the attachment of the tricuspid valvar leaflets and their attachment to the underlying myocardium (Fig. 13.26; Videos 13.12a and 13.12b).

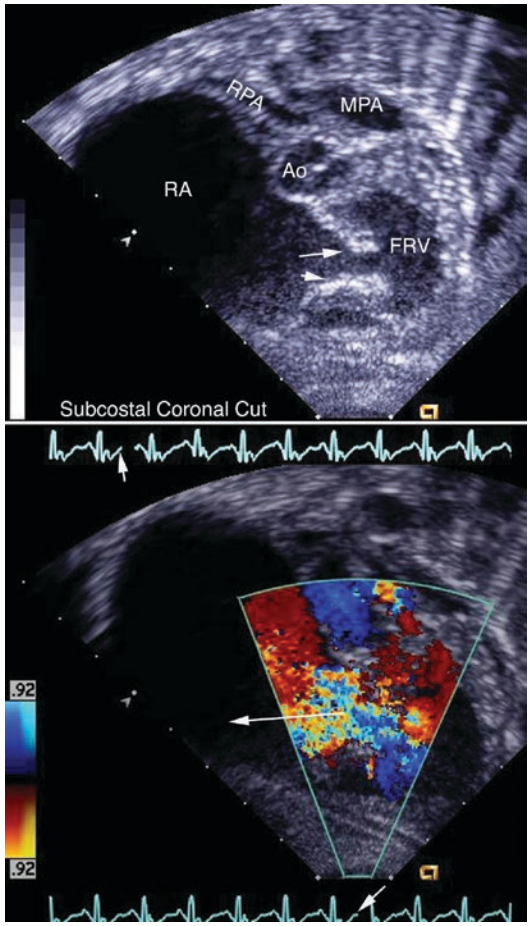

Fig. 13.24 In this example of severe neonatal Ebstein's malformation taken in the subcostal coronal view in *gray scale* above and with color below, there is no coaptation of the abnormally thickened and deformed tricuspid valvar leaflets in systole as indicated by *arrows* on the electrocardiogram. The functional right ventricle is small, as are the main (MPA) and right pulmonary arteries (RPA). The point of junction between the atrialized right ventricle and the right atrium is not shown in this example that concentrates on the valvar leaflets and the tricuspid regurgitation. The *arrow* shows the direction of the jet on the color flow image

Right Ventricular Long Axis View

In many adult patients it may be difficult to identify the mural leaflet. Parasternal imaging is helpful in this regard as, when one angulates the transducer medially on the other side of the ventricular septum, one can define the coronary sinus and the mural leaflet of the tricuspid valve (Fig. 13.27; Video 13.13). This view provides the surgeon with the opportunity to assess cordal attachments to the underlying myocardium on the anterior leaflet and a similar view can also be obtained by transesophageal echocardiography.

The Suprasternal Views

Suprasternal views provide information about the patency of the arterial duct (Fig. 13.28; Video 13.14). Arch morphology, as well as information about the size of the branch pulmonary arteries, is also available from these views.

Additional Defects

Additional defects of surgical importance may also be present in this anomaly, and a thorough search for these defects needs to be made. We have found a number of patients with ventricular septal defects (Fig. 13.29; Video 13.15). Bicuspid aortic valves and, more important for the patient who requires urgent therapy in the neonatal period, aortic coarctation has also been noted.

Three-Dimensional Echocardiography

Three-dimensional echocardiography affords a tremendous opportunity for defining issues related to surgical repair, including a true picture of leaflet mobility that the surgeon will not be able to emulate, as well as orifice size and points of origin of valvar insufficiency (Figs. 13.30 and 13.31; Videos 13.16 and 13.17). The technique provides useful definition in adult patients with tricuspid valvar

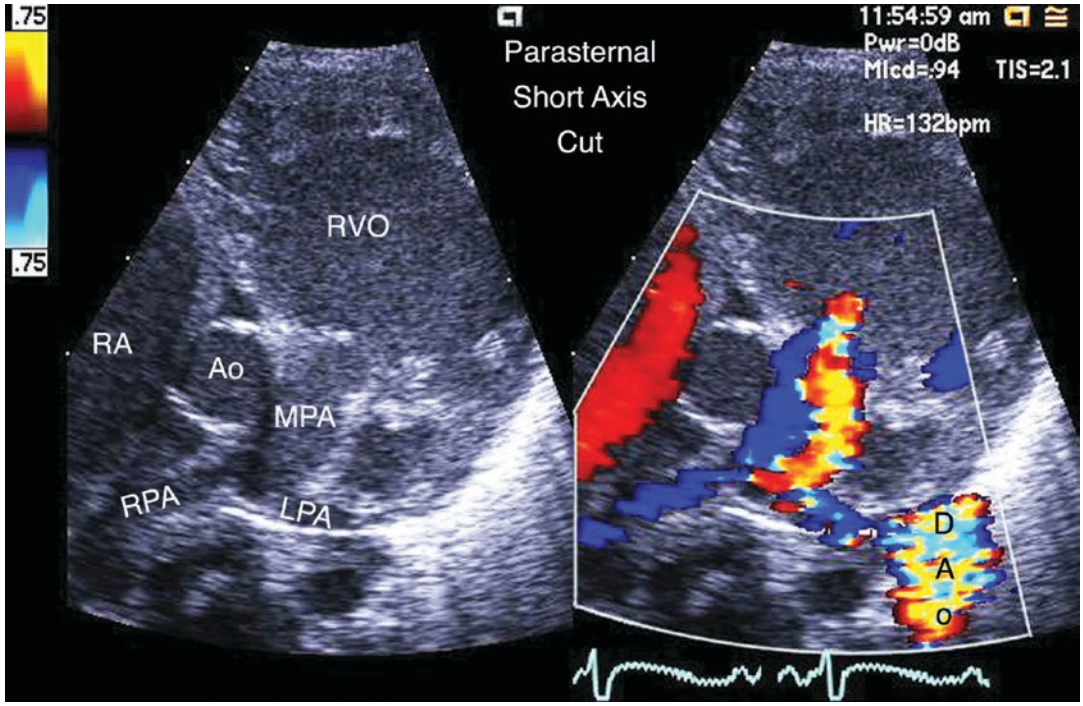

Fig. 13.25 This figure, taken in the parasternal short axis cut at the level of the great arteries, is a gray scale and Doppler color flow simultaneous recording in late diastole in an infant. The main (MPA) and left and right branch pulmonary arteries (LAP, RPA) are small and there is some regurgitation into the right ventricular outflow indicating pulmonary insufficiency. There is also a ductus left-to-right shunt noted by the *red* and *yellow* stream coming toward the pulmonary valve in the main pulmonary artery, and the majority of this flow is reflected off the pulmonary valve and returns back into the main pulmonary artery indicated by the blue signal, also seen entering the small pulmonary arterial branches. The Doppler color flow also indicates disturbed flow from the descending aorta (DAO). Other abbreviations: *Ao* Aortic root, *RA* right atrium

dysplasia as opposed to Ebstein's malformation [37]. The technique provides a view of the tricuspid leaflets in their entirety and images of the leaflets, which cannot be seen surgically because they are viewed from the right ventricular outflow tract (Fig. 13.30). Currently three-dimensional imaging is not able to reproduce the fine attachment of the tendinous cords to the underlying valvar commissures or to the papillary muscles.

In imaging the tricuspid valve from the three-dimensional dataset it is important to make the viewpoint from the inferior right ventricular wall

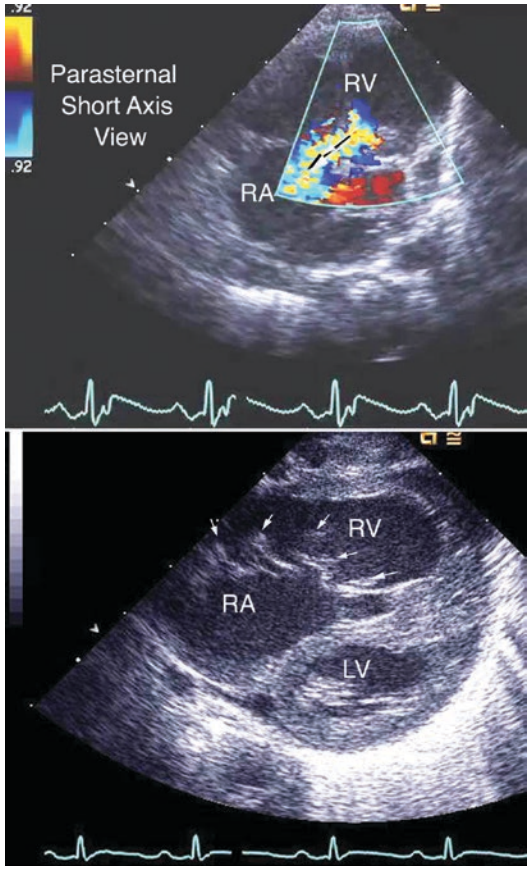

Fig. 13.26 This parasternal short axis view taken at the level of the ventricles shows the Doppler color flow image above and the gray scale image below. The right atrium (RA) right and left ventricles (RV and LV) are shown. The enlargement of the right ventricle pushes the ventricular septum backward, diminishing the size of the left ventricle. In the *top frame*, the direction of the tricuspid regurgitant jet is from the displaced apposition of the valve as shown by a highlighted *arrow*. In the *bottom frame*, small *arrows* show the attachments of the chordae tendiniae to the tricuspid valve

toward the displaced valve especially if the displacement is marked, where it cannot be seen from the conventional right atrial viewpoint. It is also important to image the valve from the right ventricular apex or anterior wall, looking backward to image the three leaflets and their distal attachments (Fig. 13.30).

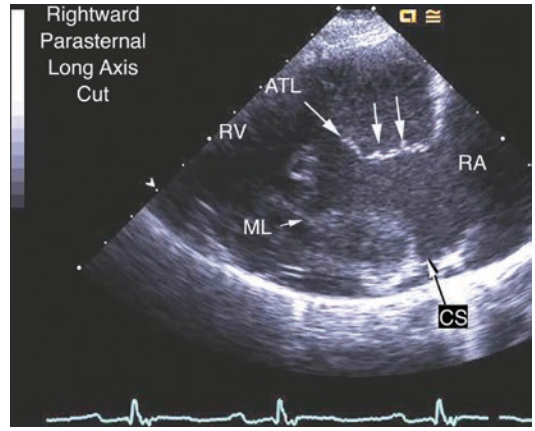

Fig. 13.27 This parasternal long axis cut with medial angulation brings the right heart into view. The plane passes through the right ventricle (RV) anteriorly and the right atrium (RA) posteriorly. The coronary sinus (CS, highlighted *arrow*) is identified. The leaflets seen in this view are the anterior (ATL) and the mural (ML) tricuspid leaflets. The *small arrows* indicate the attachments of the tendinous cords in the anterior leaflet. The mural leaflet is displaced from the coronary sinus orifice demarcating the length of the displacement for the atrialized portion of the right ventricle

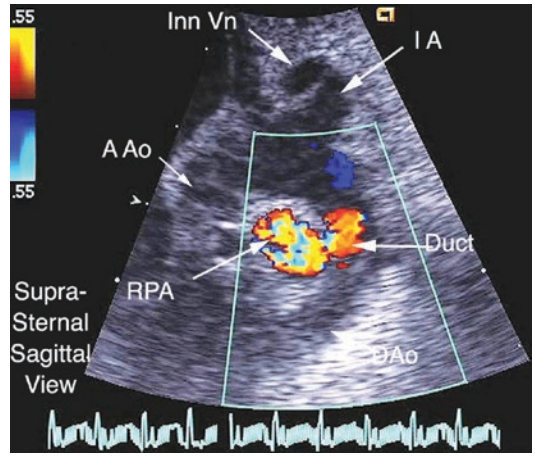

Fig. 13.28 This suprasternal sagittal plane cut in the plane of the aortic arch in an infant shows the presence of a patent arterial duct (Duct) shunting left to right on this Doppler color flow image. The flow disturbance carries out into the right pulmonary artery (RPA). Other abbreviations: *AAo* ascending aorta, *INN Vn* innominate vein, *IA* innominate artery, *DAo* descending aorta

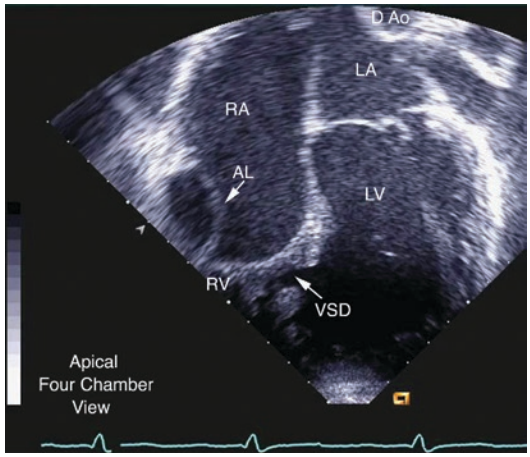

Fig. 13.29 This four-chamber cut in an older child shows the presence of severe Ebstein's malformation with only a small part of the anterior leaflet of the valve identified (AL). The tricuspid valve has become plastered down to the underlying myocardium of the right ventricle. A small ventricular septal defect is identified (VSD, *arrow*) to the functional right ventricle as the only source of pulmonary blood flow. Other Abbreviations: *D Ao* descending aorta, *LA* left atrium, *LV* left ventricle, *RA* right atrium, *RV* right ventricle

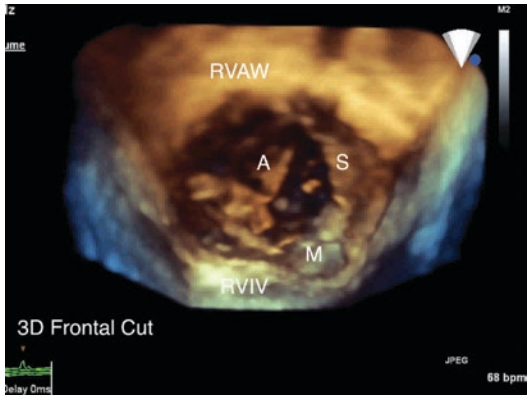

Fig. 13.30 This 3-dimensional full volume rendering of a child with Ebstein's malformation is cut from the anterior aspect of the right ventricle and shows the displaced valvar leaflets at its apex with the anterior (A), septal (S), and mural leaflet (M) seen. The right ventricular anterior (RVAW) and inferior (RVIW) walls are noted

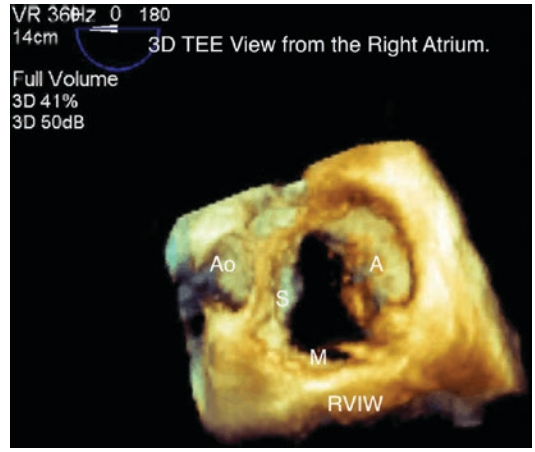

Fig. 13.31 This transesophageal example was made using a full volume technique. The image has been cut from the atrial aspect. The aorta (Ao) is also sliced medially in the image. The anterior (A) septal (S) and mural leaflets (M), are shown and the right ventricular inferior wall (RVIW) is noted. This image is courtesy of Dr. David Roberson

Conclusion

Echocardiography provides a unique and important addition to the pre-operative assessment of Ebstein's malformation. The ability to see valve motion, attachment to the wall of the ventricle, cordal attachments, attachments to the underlying myocardium and the degree of thickening and mal-coaptation of the valve are unrivalled by other imaging modalities. Echocardiography also provides an assessment of the areas of tricuspid valve leakage, as well as functional capacity of the right and left ventricles. These attributes persist in the operating room, immediately after repair and in post-operative assessment when the patient has had an operative repair. This view is second only to the exquisite view available to the experienced surgeon performing the repair.

References

1. Silverman NH. Anatomic definition and imaging of Ebstein's malformation. In: Reddington AN, Van Arsdell GS, Anderson RH, editors. Congenital diseases of the right heart. London: Springer; 2009.
2. Ports TA, Silverman NH, Schiller NB. Two-dimensional assessment of Ebstein's anomaly. Circulation. 1978;58:336.
3. Roberson DA, Silverman NH. Ebstein's anomaly: echocardiographic and clinical features in the fetus and neonate. J Am Coll Cardiol. 1989;14:1300–7.
4. Schreiber C, Cook A, Ho S-Y, Augustin N, Anderson RH. Morphologic spectrum of Ebstein's malformation: revisitation relative to surgical repair. J Thorac Cardiovasc Surg. 1999;117:148–55.
5. Arizmendi AF, Pineda LF, Jiménez CQ, Azcárate MJM, Sarachaga IH, Urroz E, de León JP, Moya JL, Jiménez MQ. The clinical profile of Ebstein's malformation as seen from the fetus to the adult in 52 patients. Cardiol Young. 2004;14:55–63.
6. Attenhofer-Jost CJ, Connolly HM, Edwards WD, Hayes D, Warnes CA, Danielson GK. Ebstein's anomaly- review of a multifaceted congenital cardiac lesion. Swiss Med Weekly. 2005;135:269–81.
7. Celermajer DS, Dodd SM, Greenwald SE, et al. Morbid anatomy in neonates with Ebstein's anomaly of the tricuspid valve: pathophysiological and clinical implications. J Am Coll Cardiol. 1992;19:1049–53.
8. Celermajer DS, Cullen S, Sullivan ID, Spiegelhalter DJ, Wyae KH, Deanfield JE. Outcome in neonates with Ebstein's anomaly. J Am Coll Cardiol. 1992;19:1041–6.
9. Celermajer DS, Bull C, Till JA, Cullen S, Vassillikos VP, Sullivan ID, Allan L, N Annopoulos P, Sommerville J, Deanfield JE. Ebstein's anomaly: presentation and outcome from fetus to adult. J Am Coll Cardiol. 1994;23(1):170–6.
10. Hornberger LK, Sahn DJ, Kleinman CS, Copel JA, Reed KL. Tricuspid valve disease with significant tricuspid insufficiency in the fetus: diagnosis and outcome. J Am Coll Cardiol. 1991;17:167–73.
11. Shiina A, Seward JB, Edwards WD, Hagler DJ, Tajik AJ. Two-dimensional echocardiographic spectrum of Ebstein's anomaly: detailed anatomic assessment. J Am Coll Cardiol. 1984;3:356–70.
12. Shiina A, Seward JB, Tajik AJ, Hagler DJ, Danielson GK. Two dimensional echocardiographic-surgical correlation in Ebstein's malformation: preoperative determination of patients requiring tricuspid valve application vs. replacement. Circulation. 1983;68:534–44.
13. Freud LR, Escobar-Diaz M, Kalish B, et al. Perinatal outcomes after fetal diagnosis of Ebstein anomaly or tricuspid valve dysplasia in the current era: a multicenter study. J Am Coll Cardiol. 2014;12(63):A473.
14. Lee AHS, Moore IE, Nuala LK, Fagg NLK, Cook AC, Kakadekar AP, Allan LD, Keeton BL, Anderson RH. Histological changes in the left and right ventricle in hearts with Ebstein's malformation and tricuspid valvar dysplasia: a morphometric study of patients dying in the fetal and perinatal periods. Cardiovascu Path. 1995;4:19–24.
15. Andrews RE, Tibby SM Sharland G Simpson JM. Prediction of outcome of tricuspid valve malformations diagnosed during fetal life. Cardiol Young. 2006;16(Suppl):6–19.
16. McElhinney DB, Salvin JA, Colan SD, Thiagarajan R, Crawford EC, Marcus EN, del Nido Pedro J, Tworetzky W. Improving outcomes in fetuses and neonates with congenital displacement (Ebstein's malformation) or dysplasia of the tricuspid valve. Am J Cardiol. 2005;96:582–6.
17. Inamura N, Taketazu M, Smallhorn JF, Hornberger LK. Left ventricular myocardial performance in the fetus with severe tricuspid valve disease and tricuspid insufficiency. Am J Perinatol. 2005;22:91–7.
18. Kohl T. Chronic intermittent materno-fetal hyperoxygenation in late gestation may improve on hypoplastic cardiovascular structures associated with cardiac malformations in human fetuses. Pediatr Cardiol. 2010;31:250–63.
19. Rasanen J, Wood DC, Debbs RH, Cohen J, Weiner S, James C, Huhta JC. Reactivity of the human fetal pulmonary circulation to maternal hyperoxygenation increases during the second half of pregnancy. a randomized study. Circulation. 1998;97: 257–62.
20. Wald RM, Adatia I, Glen S, Van Arsdell Glen S, Hornberger LK. Relation of limiting ductal patency to survival in neonatal Ebstein's anomaly. Am J Cardiol. 2005;96:851–6.
21. Dearani JA, Said SM, Burkhart HM, Pike RB, O'Leary PW, Cetta F. Strategies for tricuspid re-repair in Ebstein malformation using the cone technique. Ann Thorac Surg. 2013;96:202–8.
22. Bove EL, Hirsch JC, Ohye RG, Devaney EJ. How I manage neonatal Ebstein's anomaly. Semin Thorac Cardiovasc Surg Pediatr Card Surg Ann. 2009;12:63–5.
23. Starnes VA, Pitlick PT, Bernstein D, Griffin ML, Choy M, Shumway NE. Ebstein's malformation appearing in the neonate. A new surgical approach. J Thorac Cardiovasc Surg. 1991;101:1082–7.
24. Reemtsen BL, Fagan BT, Wells WJ, Starnes VA, Current MD. surgical therapy for Ebstein anomaly in neonates. J Thorac Cardiovasc Surg. 2006;132:1285–90.
25. Watanabe M, Harada Y, Takeuchi T, Satomi G, Yasukouchi S. Modified starnes operation for neonatal Ebstein's anomaly. Ann Thorac Surg. 2002;74: 917–9.
26. Pflaumer A, Eicken A, Augustin N, Hess J. Symptomatic neonates with Ebstein anomaly. J Thorac Cardiovasc Surg. 2004;127:1208–9.
27. Carpentier A, Chauvaud S, Mace L, et al. A new reconstructive operation for Ebstein anomaly of the tricuspid valve. J Thorac Cardiovasc Surg. 1988;96:92–101.
28. Chavaud S, Fuzellier JF, Berrebi A, et al. Bi-directional cavopulmonary shunt associated with ventriculo

and valvuloplasty in Ebstein's malformation: benefits in high risk patients. Eur J Cardiothorac Surg. 1998;13:514–9.
29. Chauvaud SM, Mihaileanu SA, Gaer JAR, Carpentier AC. Surgical treatment of Ebstein's malformation—the "Hôpital Broussais" experience. Cardiol Young. 1996;6:4–11.
30. Brown ML, Dearani JA, Danielson GK, Cetta F, Connolly HM, Warnes CA, Li Z, Hodge DO, Driscoll DJ. The outcomes of operations for 539 patients with Ebstein anomaly. J Thorac Cardiovasc Surg. 2008;135(5):1120–36.
31. Knott-Craig CJ, Overholt ED, Ward KE, Ringewald JM, Baker SS, Razook JD. Repair of Ebstein's malformation in the symptomatic neonate: an evolution of technique with 7-year follow-up. Ann Thorac Surg. 2002;73:1786–92.
32. da Silva JP, José Francisco Baumgratz JF, da Fonseca L, Franchi SM, Lopes LM, Tavares GMP, Soares AM, Moreira LF, Barbero-Marcial MD. The cone reconstruction of the tricuspid valve in Ebstein's anomaly. The operation: early and midterm results. J Thorac Cardiovasc Surg. 2007;133:215–23.
33. Anderson HN, Dearani JA, Said SM, Norris MD, Pundi KN, Miller AR, Cetta ML, Eidem BW, O'Leary PW, Cetta F. Cone reconstruction in children with Ebstein anomaly: the mayo clinic experience. Congenit Heart Dis. 2014;9(3):266–71.
34. Marianeschi SM, McElhinney DB, Reddy VM, Silverman NH, Hanley FL. Alternative approach to the repair of Ebstein's malformation: intracardiac repair with ventricular unloading. Ann Thorac Surg. 1998;66:1546–50.
35. Malhotra SP, Petrosian E, Reddy VM, Qui M, Maeda K, Suleman S, McDonald M, Reinhartz O, Hanley F. Selective right ventricular unloading and novel concepts in Ebtein's anomaly. Ann Thorac Surg. 2009;88:1975–81.
36. Eidem BW, Tei C, O'Leary PW, Cetta F, Seward JB. Non-geometric quantitative assessment of right and left ventricular function: myocardial performance index in normal children and patients with Ebstein's anomaly. J Am Soc Echocardiogr. 1998;11:849–56.
37. Bharucha T, Anderson RH, Lim ZS, Vettukatti JJ. Multiplanar review of three-dimensional echocardiography gives new insights into the morphology of Ebstein's Malformation. Cardiol Young. 2010;20:49–53.

Single Right Ventricular Function and Failure in the Fontan Circulation

14

Andrew N. Redington

Abstract

The Fontan procedure generates a unique human circulation, relying on a functionally single ventricle to pump blood around the systemic and pulmonary circulations, in series. If ever the frailty of a particular ventricular morphology were to be exposed, one might imagine that it would be the case for the Fontan circulation. In this chapter we will review the evidence for and against the right ventricle being more susceptible when acting as a functionally singular ventricle.

Keywords

Fontan procedure • Right ventricle • Systolic function • Diastolic dysfunction

Introduction

Although debatable under all circumstances, if the dogma regarding the right ventricle being inherently the "weaker" ventricle is correct, then it could argued that that dogma would be no better illustrated within the functionally single ventricle circulation. Even when part of a biventricular circulation, the ability of the right ventricle to perform as a systemic ventricle in the long-term (for example in congenitally corrected transposition or after the atrial switch procedure) has been questioned repeatedly, albeit with relatively little scientific justification. Given the fragility of the Fontan circulation, relying on its singular ventricle, one might expect even modest differences in ventricular performance, when the morphologic left and right ventricles are compared, would playout to a much greater degree in terms of either symptoms or survival. In this chapter we will discuss the available data in regard to both.

Functionally Single Right Ventricle as Risk Factor for Mortality After the Fontan Procedure

Today, the majority of patients with a functionally single ventricle are patients that have gone through staged palliation for hypoplastic left

A.N. Redington
Heart Institute, Cincinnati Children's Hospital Medical Center, 3333 Burnet Ave, Cincinnati, OH 45229, USA
e-mail: andrew.redington@cchmc.org

M.K. Friedberg, A.N. Redington (eds.), *Right Ventricular Physiology, Adaptation and Failure in Congenital and Acquired Heart Disease*, https://doi.org/10.1007/978-3-319-67096-6_14

heart syndrome (HLHS), and few would argue that HLHS is a risk factor for survival by comparison to other morphologic substrates that have 'single ventricle physiology'. However, much of the mortality risk in HLHS is concentrated around the time of the Norwood procedure, and while ventricular morphology may play its part, the surgical mortality for the Norwood procedure performed in lesions other than HLHS (e.g. Double inlet left ventricle or tricuspid atresia with discordant ventriculo-arterial connections) appears not to be significantly different [1]. Consequently, if we are to appropriately examine the inherent properties of the right ventricle as the systemic ventricle in the Fontan circulation it will necessarily be part of a conditional survival analysis of patients having survived to the point of Fontan surgery. This question has been examined in several publications over the past two decades. In 1997 Gentles et al. [2] examined the probability of late survival with a Fontan circulation categorized by ventricular morphology. They grouped patients with a systemic left ventricle and normally related great arteries and patients with a functionally single right ventricle as the systemic ventricle together as there was no difference in outcomes between those two subgroups. Perhaps surprisingly, given the dogma alluded to previously, this combined group of patients had substantially better survival than patients with all other diagnoses, a large proportion of whom had a systemic left ventricle. It should be noted however that their analysis excluded patients with a functionally single right ventricle in the setting of heterotaxy syndromes and HLHS. The issue of whether the systemic RV in HLHS was a risk factor was addressed indirectly by the Philadelphia Group 2 years later [3]. Asking the question 'Is Hypoplastic left heart syndrome a risk factor for poor outcome after the Fontan operation', the answer was a resounding no. Examining outcomes in a cohort of 332 patients operated on between 1992 and 1999, systemic ventricular morphology had no effect on early mortality, when these patients were compared with all other Fontan patients, although the HLHS patients had a longer duration of postoperative effusions and a prolonged hospital stay. Similarly, in a review of Fontan outcomes from the Heart Centre in Munich [4] those patients with a functionally single right ventricle had prolonged hospital stay, but no difference in either early or late mortality compared to those with a systemic left ventricle. Perhaps paradoxically, Becker Rencoret et al. [5] showed a slightly superior survival (albeit non-significant statistically) at 10 years for those patients with HLHS (88 percent survival at 10 years) compared with all other patients, the vast majority of whom has a systemic left ventricle (81 percent survival at 10 years) in their series of 100 consecutive patients undergoing the Fontan procedure in Chile between 1996 and 2014. Finally, in the largest of the single center reports, the Mayo Clinic showed 10, 20 and 30-year conditional survival after the Fontan procedure of 74, 61 and 43 percent respectively in their huge series of 1052 patients [6]. Several perioperative and physiologic parameters were associated with poor long-term outcomes, but long-term survival was unaffected by ventricular morphology.

These consistent observations regarding the utility of the right ventricle in the Fontan circulation from single center reports has recently been confirmed (at least partially) in a multinational multi-center study. In an extraordinary, population-based analysis of long-term survival after the Fontan from Australia and New Zealand, the 25-year follow-up of 1089 patients was reported [7]. Regression analysis revealed several risk factors associated with late mortality, including age at Fontan and prolonged early postoperative plural effusions, but ventricular morphology was not associated with worse survival. This study does however provide tantalizing evidence that there may be more subtle events at play, in regard to the impact of ventricular morphology. The analysis also included Fontan failure as an endpoint. Once again, and consistent with that discussed previously, ventricular morphology per se, was not associated with a higher incidence of late Fontan failure. However when those with HLHS were analyzed separately, they were more likely to experience Fontan failure compared to those with a systemic left ventricle or a systemic right ventricle in a setting other than HLHS. This

data begs the questions as to whether the right ventricle may ultimately be exposed as a long-term risk factor, particularly when subjected to significant additional hemodynamic burdens (such as multiple palliative procedures, atrioventricular valve regurgitation, etc.). To fully explore this question, an analysis of the fundamental characteristics of the Fontan circulation, and how those may be affected by ventricular morphology and hemodynamic burden, is required.

Ventricular Adaptation to the Fontan Circulation

Systolic Function While there can be no doubt that the myocardial architecture, cavity geometry, and the contraction pattern and ejection fraction of the right ventricle is substantially different from that of the normal left ventricle, the evidence to suggest that systolic performance is a key driver of Fontan outcomes is essentially lacking. Indeed, when studied, the systemic ventricle (no matter whether right or left) after the Fontan operation appears to be hypercontractile, and relatively well coupled to the increased vascular elastance [8], reflective of the increased systemic vascular resistance [9] and decreased arterial compliance [10], seen in these patients. For example, when measured indirectly using tissue Doppler-derived isovolumic acceleration (a relatively load independent index of contractility), the force-frequency relationships of the systemic ventricle, a measurement of contractile reserve, is consistently supra normal whether the systemic ventricle is a right ventricle or a left ventricle after the Fontan operation [11]. When measured directly, ventricular elastance has consistently been found to be increased in the systemic ventricle of Fontan patients, although some have questioned whether the increase in ventricular elastance is fully compensatory to the increased vascular elastance [12]. This may be important if one considers potential treatment, for example with systemic vasodilators, to reduce or slow progression to failure. However, not only is this a theoretically flawed argument (as systolic dysfunction is a relatively rare component of reduced Fontan circulatory performance or failure), but when tested, the role of afterload reduction has failed to produce benefit. Even when purported to provide physiologic advantage, as in a potentially elegant invasive study of the use of dobutamine to improve ventriculo-arterial coupling, a critical analysis of the data shows no benefit, at least in terms of an acute change in cardiac output that could be related to reduced afterload. More chronic afterload reduction has also been tested in the Fontan circulation. In a double blinded, cross-over study examining the effect of 10 weeks of enalapril therapy or placebo [13], there was no convincing benefit with vasodilator therapy in terms of echo-Doppler assessment of ventricular function or resting cardiac output, and on formal exercise testing the exercise-induced increase in cardiac output was *lower* during the enalapril treatment period. While clearly not something that can be disregarded completely given the relative paucity of data, modification of ventricular systolic performance therefore is unlikely to provide the answer to late Fontan failure in the majority patients. Perhaps more worthy of investigation is diastolic performance.

Diastolic Function Acute volume unloading associated with either a primary Fontan procedure [14], or at the time of bidirectional Glenn during staged palliation [15], is associated with predictable changes in ventricular geometry and wall thickness. In the setting of preserved ventricular systolic function and (acutely at least) a constant myocardial mass, reduction of ventricular preload with its consequent reduction in cavity volume will lead to a predictable increase in mass-volume ratio. This is manifest as an abrupt increase in ventricular wall thickness. This 'acquired hypertrophy' is a consistent feature early after the volume-unloading procedure and more contemporary data now suggests that it is a long lasting legacy of the Fontan operation. Indeed, several studies have shown that there is failure to "renormalize" ventricular mass-volume ratio in these patients [16, 17]. While it is compelling to imagine that increased ventricular wall thickness, and an increase in mass volume ratio may be associated with poorer ventricular

compliance, this is not the case, at least in the early years after the procedure. In fact, the diastolic abnormalities that these changes impose, appear to be related to early relaxation [14, 18, 19]. There is an acute and early increase in tau [19], the time constant of isovolumic relaxation, a prolongation of the isovolumic relaxation time, and a reduction in early rapid filling measured by trans atrioventricular valve Doppler flow studies. These changes, characteristic of the early phase of ventricular hypertrophy seen under other circumstances, seems to be predicated by an acute development of incoordinate ventricular wall motion [18]. This is typified by post systolic shortening of some ventricular wall segments (particularly basal) and as a result, given that blood is incompressible, there is reciprocal outward motion of other segments during isovolumic relaxation. This phenomenon can be observed in up to three-quarters of patients, and has been demonstrated using multiple imaging strategies, including detailed analysis of ventriculograms obtained at cardiac catheterization [18], the finding of intraventricular isovolumic flow (Fig. 14.1) within the ventricle by colour and spectral Doppler studies [19], and a particularly elegant cardiac magnetic resonance study [20, 21] showed some segments of the ventricular wall to be essentially 180 degrees out of phase with the rest of the ventricle (i.e. some segments in systole while the majority of the ventricle is in diastole, and vice versa). The impact of these abnormalities has only been studied only relatively recently. For example, Border et al. [22] showed a highly significant, and linear relationship between the ventricular time constant of relaxation and postoperative hospital stay after the Fontan procedure. This, of course, begs the question as to whether electrical resynchronization of this incoordinate wall motion might benefit the patient in the early post-operative period. This hypothesis was test by Bacha et al. [23], who performed multi-site pacing in 26 single ventricle patients (including patients with systemic right ventricle) undergoing various forms of surgery. They were able to show a consistent reduction in QRS dura-

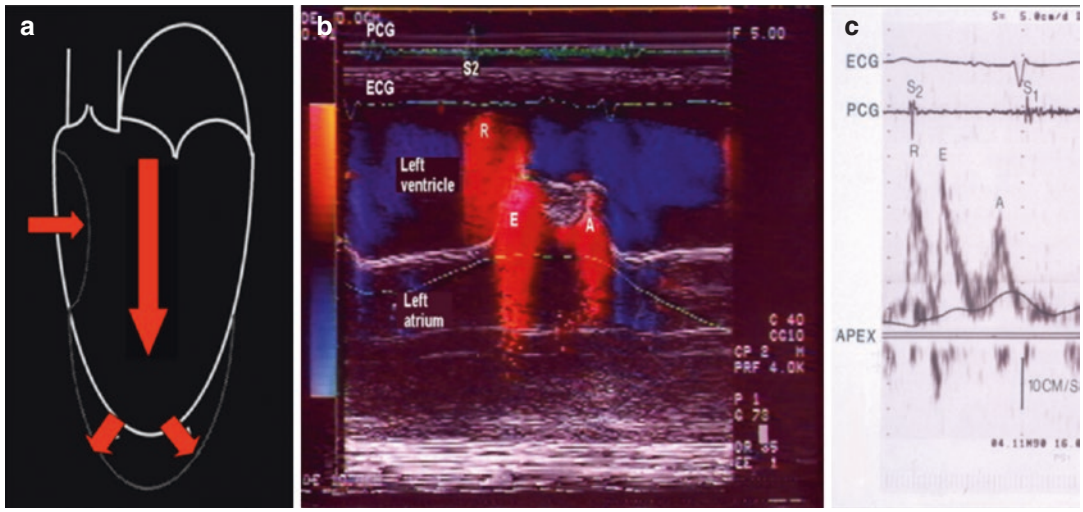

Fig. 14.1 Incoordinate diastolic relaxation after the Fontan procedure. Panel (**a**) shows a diagram to explain the effects of post-systolic shortening of basal segments during isovolumic relaxation (seen in approximately 75% of patients after the Fontan procedure). Because blood is incompressible, inward motion at the base leads to reciprocal outward motion of the apical segments, and produces the intraventricular flow phenomena illustrated in panels (**b**, **c**). Panel (**b**) shows a colour M-mode recording across the atrioventricular valve of a patient with tricuspid atresia. Note the intraventricular isovolumic relaxation flow (R) that precedes the usual atrioventricular flow that occurs across the valve in early (E) and late (A) diastole. Panel (**c**) shows a spectral Doppler example of the same phenomenon. There is a prominent wave of flow in isovolumic relaxation (R) prior to the transmitral flow. *ECG* electrocardiogram, *PCG* phonocardiogram

tion, improved systolic blood pressure and an increase in cardiac output in 21 of 22 patients in whom it was measured (3.2 vs. 3.7 liters per minute/liters, $p < 0.001$). While rarely required as a therapeutic strategy, this study emphasizes the potential impact of these early relaxation abnormalities, at least in the short term after Fontan procedures. The long-term implications are less well understood. However persistence of relaxation abnormalities has been demonstrated up to 8 years after the Fontan operation [24] and the less direct assessments of Fontan diastolic physiology are supportive of a persisting relaxation abnormality, and will be discussed later.

However, if we accept that the Fontan ventricle is inherently incoordinate with impaired early relaxation, the superimposition of worsening late diastolic compliance could be particularly profound. Already impaired ventricular filling during early diastole would be substantially compounded by worsening filling during atrial systole, and cardiac output will necessarily fall. Again, early postoperative data seems to support this concept. In a study of perioperative ventricular stiffness measured by intraoperative transesophageal echo general pressure-area loops [25], those patients with increased ventricular stiffness had increased CT tube drainage and prolonged length of hospital stay. There is also emerging evidence to suggest that this combination of a relaxation abnormality, and the development of reduced late diastolic compliance, is a relatively consistent feature. In the study by Cheung et al. diastolic performance was assessed in post Fontan patients over an 8-year period [24]. Evidence of impaired incoordinate relaxation was manifest by intraventricular isovolumic relaxation flow in 70% of the patients in the later studies, unchanged from the immediate postoperative period. Interestingly there was a shortened isovolumic relaxation time at the 8-year study and faster e-wave deceleration, suggesting that even over this relatively short period there was evidence of worsening ventricular compliance. While this data is interesting, the relatively small numbers of patients studied, makes it difficult to interpret definitively. Although limited by the fact that it is a cross sectional study, the data from the Pediatric Heart network (PHN) Cross Sectional Fontan study [26] provides important corroborative evidence regarding the changes in diastolic function seen after the Fontan procedure. Over 500 patients were included in this echo Doppler assessment of function. Interestingly the ejection fraction was normal in three-quarters of the subjects, but normal diastolic function was seen in under one third. The data reinforce all that has been discussed previously. As a group, patients had a persistently increased mass volume ratio, a persistently higher Tei index, the peak early diastolic velocity was consistently lower, and the E/E' ratio consistently higher, the latter two indices suggesting persistent relaxation abnormalities and possible worsening late diastolic compliance.

Is the Right Ventricle the More Susceptible to Diastolic Disease than the Left Ventricle After the Fontan?

The aforementioned cross sectional study performed by the Pediatric Heart Network [26], also analyzed the influence of systemic ventricular morphology on cardiac function. Unsurprisingly, ejection fraction was somewhat lower in the systemic right ventricle compared with the left (56 vs. 60%), but again very few patients fell into the abnormal range. Interestingly, there was no difference in mass-volume ratio z-score for systemic left or right ventricles (although both were highly abnormal by comparison to normal values), but those with mixed morphology (presumably biventricular hearts unsuitable for Fontan procedure) had an even more markedly increased mass-volume ratio, compared with the other Fontan groups. The left and right ventricle started to separate themselves in terms of diastolic performance. There was a significantly lower E' tissue Doppler velocity in the systemic right ventricle and the E/E' ratio significantly higher in the systemic right ventricle. Furthermore, as can be seen in Fig. 14.2, significantly more patients in the systemic right ventricle group were outliers in terms of their diastolic performance. It should

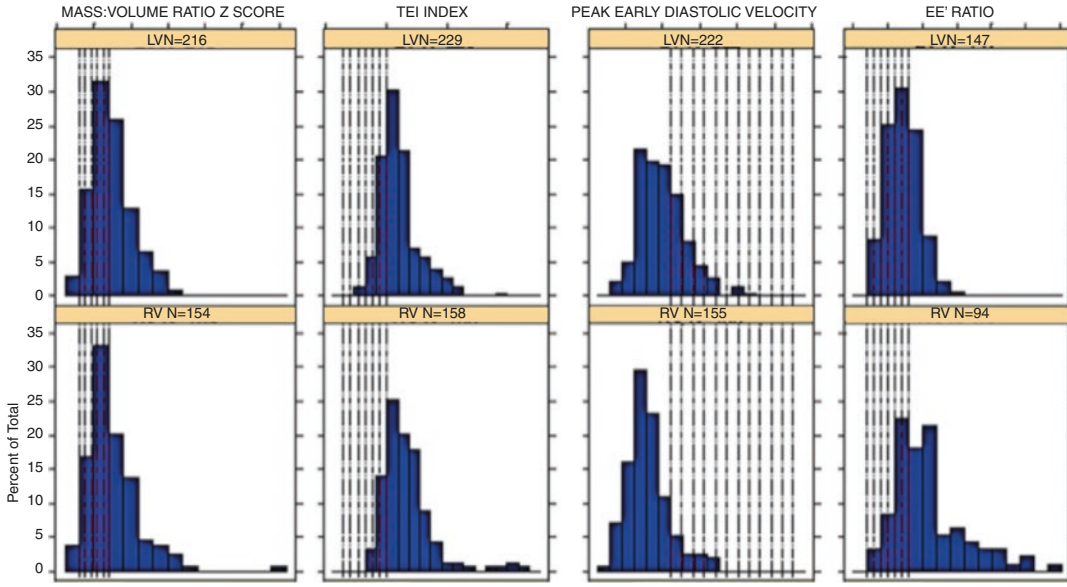

Fig. 14.2 Adapted figure from PHN Network cross-sectional Fontan study [26]. These histograms show echo-Doppler data for patients stratified as to systemic ventricular morphology (*LV* left ventricle, *RV* right ventricle). The shaded areas show the 95% confidence intervals for normal. Note how the Fontan patients consistently have increased mass:Volume ratio, increased Tei index, reduced early filling velocities, and increased E:E' ratio. See text for discussion

be noted however, that the patients with a systemic right ventricle were also more likely to have additional hemodynamic burdens. There was a significantly higher incidence and grade of atrial ventricular valve regurgitation for example. This study is also interesting in another way. A relatively small number of patients also underwent cardiac MRI and some of the data showed inconsistencies between echo Doppler finding and MRI findings. For example the mass-volume ratio measured by MRI, while again markedly increased compared to normal, was no different amongst the subgroups. Similarly, the ejection fraction was not statistically different when measured by MRI. Clearly MRI assessment of diastolic function is less sensitive than echo and no attempt was made to measure any other diastolic parameters in this part of the study. Finally, when analyzed in terms of exercise performance a systemic right ventricle was associated with worse exercise function. The percent predicted peak VO_2 at maximal exercise was lower (66 ± 17 vs. 63 ± 16 for left and right ventricles respectively, $p < 0.05$), although clearly no causal relationship between indices of ventricular dysfunction and exercise capacity could be ascertained. Exercise function was not measured in an extremely detailed assessment of post-Fontan ventricular systolic and diastolic function, published by the Edmonton Group more recently in 2012 [27]; however, the underlying trends in this more contemporary cohort were similar to those reported by the PHN network. Comparing systemic left and right ventricles, there was essentially no difference in tissue Doppler assessment of ventricular systolic performance when right and left ventricles were compared. Interestingly, peak E wave velocity was significantly higher in the systemic right ventricle compared to the systemic left ventricle, perhaps suggesting superior early-diastolic function, but those with systemic right ventricles had a profoundly abnormal E/E' ratio of 14.7 (10.3–38.3) compared to those with a systemic left ventricle, where the ratio for the group was close to normal at 6.7 (5.1–10.9). This may be evidence that abnormalities of late-diastolic right compliance may be accelerated or increased in frequency in the RV, particularly in cohorts

where HLHS (and its association with early Norwood staged palliation) is the underlying lesion, as is the case in more contemporary cohorts.

Summary

The limitations of the Fontan circulation are not unique to either systemic right or left ventricles. Indeed, many of the adaptations appear to be generic and occur irrespective of underlying ventricular morphology. That is not to underplay the importance of the abnormal diastolic function observed so frequently in these patients no matter whether they have a systemic right or left ventricle. The available data hint at a trend toward the systemic right ventricle being more severely affected in terms of its diastolic performance, than the left ventricle although the super added effects of associated abnormalities of the atrial ventricular valves and semi-lunar valves, make interpretation of this on the basis of ventricular morphology alone, difficult. Nonetheless, efforts either to modify the persistent incoordinate relaxation, or to blunt the progression of late diastolic changes in ventricular stiffness with time, both may be worthy therapeutic targets.

References

1. Hansen JH, Petko C, Bauer G, Voges I, Kramer HH, Scheewe J. Fifteen-year single-center experience with the Norwood operation for complex lesions with single-ventricle physiology compared with hypoplastic left heart syndrome. J Thorac Cardiovasc Surg. 2012;144(1):166–72.
2. Gentles TL, Mayer JE Jr, Gauvreau K, Newburger JW, Lock JE, Kupferschmid JP, Burnett J, Jonas RA, Castañeda AR, Wernovsky G. Fontan operation in five hundred consecutive patients: factors influencing early and late outcome. J Thorac Cardiovasc Surg. 1997;114(3):376–91.
3. Gaynor JW, Bridges ND, Cohen MI, Mahle WT, Decampli WM, Steven JM, Nicolson SC, Spray TL. Predictors of outcome after the Fontan operation: is hypoplastic left heart syndrome still a risk factor? J Thorac Cardiovasc Surg. 2002;123(2):237–45.
4. Ono M, Kasnar-Samprec J, Hager A, Cleuziou J, Burri M, Langenbach C, Callegari A, Strbad M, Vogt M, Hörer J, Schreiber C, Lange R. Clinical outcome following total cavopulmonary connection: a 20-year single-centre experience. Eur J Cardiothorac Surg. 2016;50(4):632–41.
5. Becker Rencoret P, Besa Bandeira S, Riveros González S, Frangini Sanhueza P, Springmüller Pinto D, González Foretic R, Urcelay Montecinos G. Comparative results of Fontan surgery in patients with and without hypoplastic left heart syndrome. Rev Chil Pediatr. 2016;87(5):366–72.
6. Pundi KN, Johnson JN, Dearani JA, Pundi KN, Li Z, Hinck CA, Dahl SH, Cannon BC, O'Leary PW, Driscoll DJ, Cetta F. 40-year follow-up after the Fontan operation: long-term outcomes of 1,052 patients. J Am Coll Cardiol. 2015;66(15):1700–10.
7. d'Udekem Y, Iyengar AJ, Galati JC, Forsdick V, Weintraub RG, Wheaton GR, Bullock A, Justo RN, Grigg LE, Sholler GF, Hope S, Radford DJ, Gentles TL, Celermajer DS, Winlaw DS. Redefining expectations of long-term survival after the Fontan procedure: twenty-five years of follow-up from the entire population of Australia and New Zealand. Circulation. 2014;130(11 Suppl 1):S32–8.
8. Tanoue Y, Sese A, Ueno Y, Joh K, Hijii T. Bidirectional Glenn procedure improves the mechanical efficiency of a total cavopulmonary connection in high-risk Fontan candidates. Circulation. 2001;103(17):2176–80.
9. Akagi T, Benson LN, Gilday DL, Ash J, Green M, Williams WG, Freedom RM. Influence of ventricular morphology on diastolic filling performance in double-inlet ventricle after the Fontan procedure. J Am Coll Cardiol. 1993;22(7):1948–52.
10. Myers KA, Leung MT, Terri Potts M, Potts JE, Sandor GG. Noninvasive assessment of vascular function and hydraulic power and efficiency in pediatric Fontan patients. J Am Soc Echocardiogr. 2013;26(10):1221–7.
11. Cheung MM, Smallhorn JF, McCrindle BW, Van Arsdell GS, Redington AN. Non-invasive assessment of ventricular force-frequency relations in the univentricular circulation by tissue Doppler echocardiography: a novel method of assessing myocardial performance in congenital heart disease. Heart. 2005;91(10):1338–42.
12. Senzaki H, Masutani S, Kobayashi J, Kobayashi T, Sasaki N, Asano H, Kyo S, Yokote Y, Ishizawa A. Ventricular afterload and ventricular work in fontan circulation: comparison with normal two-ventricle circulation and single-ventricle circulation with blalock-taussig shunts. Circulation. 2002;105(24):2885–92.
13. Kouatli AA, Garcia JA, Zellers TM, Weinstein EM, Mahony L. Enalapril does not enhance exercise capacity in patients after Fontan procedure. Circulation. 1997;96(5):1507–12.
14. Penny DJ, Lincoln C, Shore DF, Rigby ML, Redington AN. the early response of the systemic ventricle during transition to the Fontan circulation: an acute hypertrophic cardiomyopathy? Cardiol Young. 1992;2:78–84.

15. Rychik J, Jacobs ML, Norwood WI Jr. Acute changes in left ventricular geometry after volume reduction operation. Ann Thorac Surg. 1995;60(5):1267–73.
16. Fogel MA, Weinberg PM, Chin AJ, Fellows KE, Hoffman EA. Late ventricular geometry and performance changes of functional single ventricle throughout staged Fontan reconstruction assessed by magnetic resonance imaging. J Am Coll Cardiol. 1996;28(1):212–21.
17. Rathod RH, Prakash A, Kim YY, Germanakis IE, Powell AJ, Gauvreau K, Geva T. Cardiac magnetic resonance parameters predict transplantation-free survival in patients with fontan circulation. Circ Cardiovasc Imaging. 2014;7(3):502–9.
18. Penny DJ, Redington AN. Angiographic demonstration of incoordinate motion of the ventricular wall after the Fontan operation. Br Heart J. 1991;66(6):456–9.
19. Penny DJ, Rigby ML, Redington AN. Abnormal patterns of intraventricular flow and diastolic filling after the Fontan operation: evidence for incoordinate ventricular wall motion. Br Heart J. 1991;66(5):375–8.
20. Penny DJ, Redington AN. Diastolic ventricular function after the Fontan operation. Am J Cardiol. 1992;69(9):974–5.
21. Fogel MA, Gupta KB, Weinberg PM, Hoffman EA. Regional wall motion and strain analysis across stages of Fontan reconstruction by magnetic resonance tagging. Am J Phys. 1995;269(3 Pt 2):H1132–52.
22. Border WL, Syed AU, Michelfelder EC, Khoury P, Uzark KC, Manning PB, Pearl JM. Impaired systemic ventricular relaxation affects postoperative short-term outcome in Fontan patients. J Thorac Cardiovasc Surg. 2003;126(6):1760–4.
23. Bacha EA, Zimmerman FJ, Mor-Avi V, Weinert L, Starr JP, Sugeng L, Lang RM. Ventricular resynchronization by multisite pacing improves myocardial performance in the postoperative single-ventricle patient. Ann Thorac Surg. 2004;78(5):1678–83.
24. Cheung YF, Penny DJ, Redington AN. Serial assessment of left ventricular diastolic function after Fontan procedure. Heart. 2000;83(4):420–4.
25. Garofalo CA, Cabreriza SE, Quinn TA, Weinberg AD, Printz BF, Hsu DT, Quaegebeur JM, Mosca RS, Spotnitz HM. Ventricular diastolic stiffness predicts perioperative morbidity and duration of pleural effusions after the Fontan operation. Circulation. 2006;114(1 Suppl):I56–61.
26. Anderson PA, Sleeper LA, Mahony L, Colan SD, Atz AM, Breitbart RE, Gersony WM, Gallagher D, Geva T, Margossian R, McCrindle BW, Paridon S, Schwartz M, Stylianou M, Williams RV, Clark BJ 3rd. Pediatric Heart Network Investigators. Contemporary outcomes after the Fontan procedure: a Pediatric Heart Network multicenter study. J Am Coll Cardiol. 2008;52(2):85–98.
27. Kaneko S, Khoo NS, Smallhorn JF, Tham EB. Single right ventricles have impaired systolic and diastolic function compared to those of left ventricular morphology. J Am Soc Echocardiogr. 2012;25(11):1222–30.

Right Ventricular Dysfunction Post-Heart Transplantation

15

Jacob Mathew and Anne I. Dipchand

Abstract

Right ventricular dysfunction is prevalent following orthotopic heart transplantation. The sequential insults of donor brain death, cardioplegia, ischemia, reperfusion injury and cardiopulmonary bypass interact together with raised recipient pulmonary vascular resistance to produce this common complication. Early recognition is important because the principles of management, which hinge on avoiding volume overload, inappropriate inotropic support, and the maintenance of adequate blood pressure to maintain coronary perfusion, differ substantially from other forms of acute heart failure. With improved management, and in particular, the availability of selective pulmonary vasodilators and advances in mechanical circulatory support, the prognosis has improved considerably within the last two decades.

Keywords

Right ventricle • Right ventricular failure • Primary graft failure • Heart failure • Catecholamine cardiotoxicity • Brain death • Orthotopic Heart Transplantation • Pulmonary hypertension

Introduction

Since the earliest heart transplantation series, right ventricular (RV) dysfunction has been a recognized component of primary graft failure (PGF) and an important contributor to early mortality [1]. In 1992, Costard-Jäckle reported a 6.6% incidence of RV failure (RVF) in the Stanford adult experience in the cyclosporine era, and found a 50% early mortality in patients with RVF [2]. Cosío Carmena reported a 22% incidence of PGF, with RV dysfunction predom-

J. Mathew
Department of Cardiology, The Royal Children's Hospital, Melbourne, Australia

A.I. Dipchand (✉)
Paediatric Cardiology, Labatt Family Heart Centre, Hospital for Sick Children, 555 University Ave., Toronto, ON M5G 1X8, Canada
e-mail: anne.dipchand@sickkids.ca

M.K. Friedberg, A.N. Redington (eds.), *Right Ventricular Physiology, Adaptation and Failure in Congenital and Acquired Heart Disease*, https://doi.org/10.1007/978-3-319-67096-6_15

inating in 45% and contributing to a further 47% of cases. Patients with PGF experienced a 90-day mortality of 53% in this series [3]. Similarly, pediatric heart transplant series report a 4.2% [4] to 27.2% [5] early mortality, with PGF comprising 2.1% [4] to 20% [6]. Where explicitly stated, early mortality attributed to pulmonary hypertension or right ventricular failure ranged from 2.3% [7] to 8.3% of transplants [8].

Tracking the incidence of RV dysfunction after transplantion has been hampered by the absence of a consensus definition of PGF until recently [9]. As a result, within clinical registries, this important outcome is subsumed under the categories of "primary graft failure," "pulmonary hypertension," and "ventricular failure," which prevents consistent identification of patients retrospectively. This limits accurate estimation of the incidence of RVF, outcomes, predictive factors, and how the impact of these factors has changed over time. Nonetheless, understanding of the predisposing factors and the physiology of this complication has improved in the last three decades. This, together with the availability of more selective pulmonary vasodilators and advances in mechanical circulatory support, has better equipped clinicians to pre-empt and manage this complication.

This clinical scenario is uniquely prevalent following heart transplant because of the requirement for an "untrained" donor right ventricle to meet the afterload imposed by increased recipient pulmonary vascular resistance (PVR). Further, the donor heart bares the sequential insults of donor brain death, cardioplegia and ischemia-reperfusion injury, processes that impair the contractility of both ventricles, though seem to affect right ventricular contractility disproportionately. The graft is further impaired by the adverse effects of cardiopulmonary bypass on myocardial contractility, PVR and systemic vascular resistance (SVR), as well as the loss of chronotropic reserve that follows denervation.

This chapter reviews the physiological underpinnings, clinical recognition and principles of management of post-transplant right ventricular failure.

Physiology of Acute RV Failure in the Post-Transplant Setting

A Working Clinical Definition of Systolic RV Failure

Attempts to formulate a definition of RVF in terms of absolute hemodynamic values have been confounded by the poor reliability of these measures in defining patients with disproportionate systolic RV function. Further, the echocardiographic assessment of RV size and function is limited. In practice, a combination of clinical and echocardiographic findings is utilized, together with clinical judgment, to recognize this complication (Table 15.1).

Table 15.1 Features supporting a diagnosis of systolic right heart failure

Low Cardiac Output State with relatively preserved LV systolic function plus:
Elevated right ventricular filling pressures
• Elevated CVP or CVP: pulmonary artery wedge pressure ratio
• Dilated IVC with absent respiratory variation
• Paradoxical worsening of hemodynamics with increased preload
Diminished Right Ventricular Contractility
• Reduced Fractional Area Change
• Reduced TAPSE
Right ventricular dilatation
• Increased RV 4-chamber diastolic area
Abnormal septal geometry
Increasing tricuspid regurgitation
Diminished LV volume
• M-mode, Biplane EDV, 3D EDV
Relatively Preserved LV systolic function
• Biplane or 3D EF >45%

LV left ventricle, *RV* right ventricle, *CVP* central venous pressure, *IVC* inferior vena cava, *TAPSE* tricuspid annular plane systolic excursion, *EDV* end diastolic volume, *EF* ejection fraction

RVF is typically recognized by the occurrence of a low cardiac output state in the presence of *elevated RV filling pressures* and typically *diminished preload response*, or even paradoxical hemodynamic deterioration in the face of volume challenge. This is accompanied by *RV dilatation*, *RV systolic dysfunction*, often increased *tricuspid regurgitation* secondary to annular dilatation and septal displacement and *variably elevated RV systolic pressure* on echocardiography. The latter may not be markedly elevated even in the face of substantially increased PVR where RV systolic function is reduced and the RV is unable to generate a high pressure.

Limits of RV Adaptation to Volume and Pressure Loading

Clinical experience with patients with a morphological RV in the sub-aortic position, as well as those with pulmonary arterial hypertension establishes that a chronically pressure-loaded RV can sustain systemic systolic pressures for an extended period of time, albeit with an elevated risk of attrition due to RV failure and tricuspid regurgitation [10]. Experimentally this adaptation can be reproduced by slowly progressive pulmonary arterial constriction in animals [11]. On the other hand, experience with adult patients who have been exposed acutely to substantial RV afterload, commonly after pulmonary embolism, demonstrates that the acutely pressure loaded RV cannot generate systemic systolic pressures outside the neonatal period, a fact that is recapitulated in numerous animal models [12–14].

The initial response to acutely increased RV afterload is increased stroke volume associated with increased RV systolic pressure, which is effected in part by an increase in end-diastolic volume via the Frank-Starling mechanism, also known as *heterometric regulation*. However, after several minutes an increase in intrinsic RV contractility is also seen, representing an example of *homeometric regulation* (Anrep effect) [14–17].

When the limits of these adaptive mechanisms are exceeded, acute RVF ensues, being marked by progressive RV dilatation with increased filling pressures and diminished RV cardiac output, which is in turn associated with reduced LV filling, reduced LV cardiac output and hypotension [18–20]. Figure 15.1 illustrates these effects in representative experiment from a leporine PA banding model, in which the RV has begun to fail [14]. When RV afterload is abruptly increased, the onset of RVF can be rapid. With intermediate pressure load, an initial compensatory response is seen, though one that cannot be sustained over several hours of continued loading [21]. When such ventricles are unloaded again, residual impairment of systolic function may be seen [22].

The mechanisms underlying this failure are incompletely understood, though *relative ischemia* has long been recognized as a contributing factor. In an important early paper, Brooks confirmed the previous identified failure of RV adaptation to acute pressure loading in a canine RV pressure load model. They also described an increase in right coronary flow, which was likely due to coronary vasodilatation given that the perfusion pressure was reduced by elevated RV pressure and later systemic hypotension. With more substantial increments in RV afterload however, RCA flow declined, at a point coinciding with the onset of overt RV failure. Further, extrinsic perfusion of the RCA with supra-physiological flow rates permitted partial recovery of RV function and delayed the onset of RV failure [13]. Other groups have also documented diminished or exhausted coronary vasodilator reserve prior to the onset of RV failure [19, 23].

Using radioactive tracers (the microsphere method), Gold found evidence of relative subendocardial ischemia despite increased myocar-

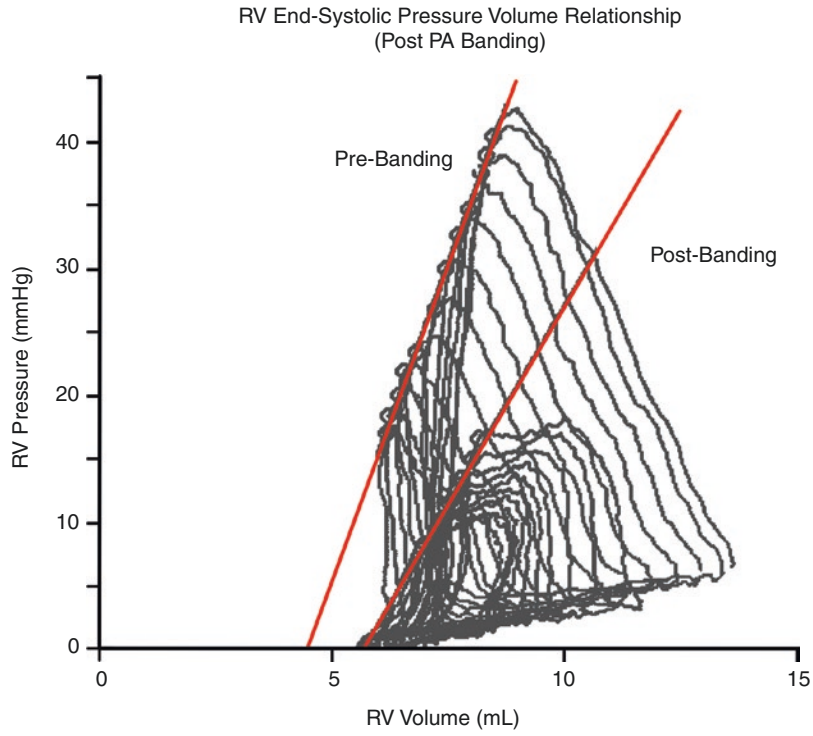

Fig. 15.1 Alteration of the end-systolic pressure volume relationship (ESPVR) in an ovine PA banding experiment is depicted. The reduced ESPVR slope, or RV Ees, is a relatively load-independent indicator of diminished RV contractility after PA banding. PA: Pulmonary Artery. *RV* Right Ventricle. With permission from Hon JK, Steendijk P, Khan H, Wong K, Yacoub M. Acute effects of pulmonary artery banding in sheep on right ventricle pressure-volume relations: relevance to the arterial switch operation. Acta Physiol Scand. 2001;172(2):97–106 © John Wiley and Sons [14]

dial blood flow, in a canine pressure-loading model. He further noted that restoration of systemic blood pressure to control levels, by aortic constriction, reversed both the RV systolic dysfunction together with subendocardial ischemia, a finding that was attributed to improved coronary perfusion pressure [20]. Others have documented similar improvement of RV function following exposure to increased left ventricular afterload in models of both acute [24] and chronic RV [25] failure due to pressure overload, as well as in models of intrinsic dysfunction [26]. As with the left ventricle, this perfusion-supply mismatch is exacerbated by conditions which increase RV systolic wall tension [27].

Calpain is an intracellular protease activated by calcium influx. Greyson observed that treatment with a calpain inhibitor was able to attenuate RV pressure-load induced RVF in pigs. The effect did not appear to be mediated by degradation of common calpain targets such as spectrin, desmin, troponin-I or SERCA2 [28]. A later report from his group suggested that the adhesion protein talin may be target of calpain's action in this setting [29].

Taken together the above studies demonstrated that (1) the naive non-neonatal RV cannot generate systemic systolic pressures in response to an acute pressure load and experiences acute systolic failure if it meets substantial afterload, (2) RV dysfunction induced by excessive pressure load may persist after the stimulus is removed, (3) the incidence of such dysfunction may be related to the peak systolic wall tension, and is mediated by relative ischemia, particularly of the

subendocardium, (4) calpain-mediated degradation of proteins such as talin may be an important mediator of this failure. The latter two points suggest that optimization of RV loading conditions such as to minimize wall tension, measures to optimize coronary perfusion pressure and perhaps inhibition of calpain may prove to be viable therapeutic modalities in the future.

Sequelae of Brain Death and its Impact on Graft Function

Hemodynamic perturbations have long been recognized following acute intracranial hypertension and brain death itself. The resulting injury contributes to primary myocardial dysfunction of the donor heart following transplantation, and as will be seen below, disproportionately affects the RV independently of the other hemodynamic insults that yet are in store for it.

Cardiovascular Responses to Brain Death in the Donor

Experiments by Novitsky in the chacma baboon described the stereotyped response to induction of brain death by acute intracranial hypertension [30], extending the description of Cushing over 80 years earlier [31]. These findings were corroborated by others in canine [32, 33], porcine [34, 35], feline [36] and murine [37, 38] models.

Typically in these experiments, acute intracranial hypertension was followed by concomitant vagal discharge and sympathetic discharge producing systemic hypertension in association with sinus bradycardia, often with conduction abnormalities (Cushing response). After this brief phase, vagal tone diminishes and a dramatic *hyperdynamic state* ensues, which is driven by both neural [39] and humoral [17, 30, 32, 33, 40] release of catecholamines. This phase is associated with sinus tachycardia, frequent atrial and ventricular ectopy and variable ST segment changes, and attenuates within the first 15 min following brain death. By 30–60 min, the sympathetic discharge abates, and a low cardiac output state associated with hypotension ensues. This early constellation of events has been described as an "*autonomic storm*" [30, 37]. A similar sequence is seen clinically following the onset of brain death in a potential organ donor.

When examined, animal hearts which have been subjected to this process display characteristic histological features including *myocardial contraction band necrosis*, which is considered to be the pathological hallmark, together with myocytolysis, coagulative necrosis, variable subendocardial hemorrhage, a monocytic infiltrate and contraction bands in the media of the epicardial coronaries. Electron microscopic features include electron dense material in the mitochondria, which exhibit disrupted cristae [41]. Similar features have been observed in potential human organ donors who had suffered brain death [42], those of patients who had died of acute intracranial hemorrhage [43], and following exposure to large doses of catecholamines [44, 45].

Shivalkar described the differential impacts of abrupt and gradual escalation of intracranial pressure in dogs, by comparison to a non-brain death group. The elevation in blood catecholamine hormone concentrations, intensity of the acute hyperdynamic response and extent of histological ischemic injury were each greatest in the abrupt brain death group, intermediate in the gradual escalation group, and absent in the non-brain death group [33]. In contrast, Bruinsma, however, did not find any association between the extent of histological injury and hemodynamic profile following brain death in a feline model [36].

Following the initial hyperdynamic response, the subsequent hypotension and low cardiac output state appears to be driven by a reduction in contractility and SVR. In order to differentiate the contribution of intrinsic myocardial dysfunction from that of the grossly deranged loading conditions in these experiments, Bittner reported the influence of brain death on the preload-recruitable stroke work (PRSW) relationship, a relatively load insensitive measure of contractility, in a canine model. He demonstrated a substantial reduction in the slope of the PRSW

relationship, which was present by 2 h, and sustained to at least 4 h following brain-death, indicating a decrease in contractility during this time. Interestingly RV function was, in relative terms, affected to a greater degree than that of the LV (34% vs. 22% reduction in PRSW gradient compared to baseline values) [46–48]. Panadali reported similar findings in pigs [49]. Examination of RV end-systolic elastance (RV Ees) in human donors has shown diminished RV function by comparison to patients undergoing coronary revascularization, and further, that RV Ees was lower in non-survivors than in survivors, 1 year after transplantation [50].

Szabó found that dogs subjected to PA constriction after brain death exhibited RV dilatation, and right-shifted stroke-work: RVEDP and regional pressure: length relationships, by comparison to control dogs. These animals were able to maintain RV stroke work, but the above results imply that RV performance was maintained by heterometric regulation, and that the ventricles of these dogs could not exploit homeometric regulation to adapt to the increased afterload [17].

Despite these various insults borne by the donor heart, with optimal hemodynamic management and 12–48 h of observation, a significant proportion may recover sufficiently to permit transplantation [51, 52].

Mechanisms and Modifiers of Post Brain-death Injury

The association of catecholamine hormone concentrations with the intensity of the hyperdynamic phase and severity of histological injury, together with the histological similarities between these hearts and those exposed to large concentrations of exogenous catecholamines led naturally to the hypothesis that the latter were causative. In support, Pilati demonstrated that massive sympathetic discharge induced in rabbits by injection of veratrine into the cisterna magna was associated with a reduction in Ees but that this was reversible with treatment with propranolol or phentolamine [53]. The failure of adrenalectomy to forestall histologically apparent injuries following brain death found in Novitzky's experiments, together with the prevention of the same following bilateral cardiac sympathectomy, suggested that neurological mechanisms may predominate [54, 55]. This was confirmed by Galiñanes' murine experiments, wherein replacement of the entire blood volume of brain-dead rats with that from control rats did not offer protection from the hemodynamic compromise induced by brain death, and conversely, transfusion of blood from acutely brain-dead rats into control rats did not induce hemodynamic compromise [38].

D'Amico [56], White [57], Owen [58] and Pandalai [49] have reported a reduction in stimulated adenylate cyclase activity in association with post brain-death dysfunction, implying an uncoupling of downstream adrenergic signaling. However, others found no variation in expression or affinity of adrenergic receptors after experimental brain death. [58, 59]. A further report from Pandali's group found that in addition to preventing systolic dysfunction post brain-death, β blockade preserves β-adrenoceptor signaling [60]. Owen suggested that this uncoupling is mediated by upregulation of an inhibitory G protein, Gi-α [58]. Contradicting these studies, Bittner et al reported an up regulation of β-adrenoceptors on canine myocardium post brain-death, which was associated with increased stimulated adenylate cyclase activity [61].

Calcium overload is assumed to play a central role in the pathophysiology of catecholamine-mediated toxicity, being associated with direct disruption to mitochondrial membranes and function, as well as potentiation of oxidative stress [45, 62]. Novitky and colleagues explored the impact of calcium channel blockade and reported that pretreatment of baboons with verapamil before brain-death modified the hemodynamic response and prevented the typically associated histological changes [63].

As with pressure-load induced myocardial dysfunction, oxygen supply-demand mismatch is thought to be a significant contributor to catecholamine-mediated toxicity, though the data are inconsistent [45, 62]. Early studies reported ST segment changes and increased myocardial lactate production during the acute hyperdynamic reaction [64]. However the former is inconsistent,

and the latter does not extend beyond the first 1–2 h post brain death [35], whilst myocardial dysfunction, as described above, does. Though some studies had postulated vascular spasm in response to catecholamines as a potential mechanism of injury [37], others found evidence of reactive vasodilatation which rose in tandem with measures of myocardial workload [65]. Further, measurement of myocardial high energy phosphates by biochemical assay [61] or magnetic-resonance spectroscopy (MRS) [66] showed no derangement following brain death implying that this auto regulatory response kept up with demand, and that ischemia was not the etiology of myocardial dysfunction in these studies. In contrast, Pinelli's experiments on pigs however did show diminished intracellular ATP, by MRS, following brain-death [35]. Szabó documented in dogs that hypotension due to low SVR and diminished coronary perfusion pressure accompanied the myocardial dysfunction that follows brain death, and that this dysfunction could be reversed in a cross-circulation model where myocardial loading conditions could be separated from coronary perfusion, and the latter restored to control levels. Further the relationship between maximal elastance (Emax) and the coronary perfusion pressure was identical in both the brain-dead and control animals, supporting the notion that it is hypotension related to reduced SVR, and not direct myocardial toxicity that mediates post brain-death dysfunction [67].

Brain death is accompanied by substantial dysregulation of inflammatory cytokines in many organs, with elevated IL-6, IL-6R, IL-1β and TGF-β levels in a porcine model [68]. In a study of human donors, Birks et al demonstrated elevated myocyte IL-6 and TNF-α mRNA, myocyte TNF-α protein expression and serum TNF-α concentration in unused donor hearts, by comparison to that in transplanted hearts [69]. Interestingly, the same group also observed that expression of TNF-α in a pre-transplant RV biopsy predicted the development of post-transplant RV failure [70].

Combined, the above data suggest that, (1) catecholamine mediated toxicity is likely to contribute to post-brain death RV dysfunction, (2) the latter is marked by a decrease in contractility and inability to exploit the homeometric response to increased afterload, (3) this may be mediated by uncoupling of β-adrenergic receptors from adenylate cyclase and by calcium overload, (4) whilst evidence of failed coronary autoregulation is inconsistent, a substantial component of myocardial dysfunction in this setting may be driven by diminished afterload and its impact on coronary perfusion pressure, and that (5) dysregulated inflammatory mediators at the time of transplant may contribute to RV dysfunction.

Impact of Ischemia, Graft Preservation, Bypass and Reperfusion

The detrimental impact of graft ischemia, ischemia-reperfusion injury and cardiopulmonary bypass on donor heart function has long been recognized and much planning in the peri-transplant period goes toward mitigating the effects of these variables.

Van Trigt and colleagues explored the impact of cold ischemia on graft function. They described a 43% reduction in the slope of the RV preload recruitable stroke work (PRSW) relationship following orthotopic heart transplant (OHT) from a non-brain dead canine donor, after a mean of 85 min of cold ischemic storage, whilst there was no impairment in LV contractility, implying a failure of RV myocardial protection during preservation. This is of a similar magnitude to the 37% reduction in PRSW gradient seen in the RV of animals who had undergone brain death pre-explantation [46], as described previously. The same group later described that the RV PRSW slope of grafts from brain dead donors was further diminished (by an additional 28%) after transplantation following 4 h of cold preservation, by comparison to those organs transplanted without preservation [71].

Further, Mankad described a time-dependent deterioration of biventricular diastolic function and LV systolic function following preservation of porcine hearts [72]. In contrast, hearts from porcine donors who did not undergo brain death

or extended cold ischemia had a preserved PRSW relationship, and further could increase contractility as evidenced by an increased PRSW slope, when transplanted to recipients with elevated PVR (almost twice the PVR faced by control and brain-dead animals). This increase in contractility presumably reflects a preserved capacity to exploit the Anrep mechanism in hearts that have not been insulted by brain death and preservation, and suggests that the impacts of brain death, cold ischemia and increased afterload on donor RV dysfunction are additive.

Though ischemic time remains a risk factor for PGF [3, 73, 74] and early mortality [75–80] in the present era, there are few clinical studies relating this to RVF specifically and in single center studies the association was negative [81]. In a small cohort, Ahlgren described a reduction in RV circumferential and longitudinal systolic function, which correlated with both warm and cold ischemic times [82]. Similarly Mastouri found diminished RV longitundinal contractility to be associated with total ischemic time in another small cohort [83].

Ventricular Interdependence in the Setting of Systolic RV Failure

Responding appropriately to this clinical syndrome mandates an appreciation of the manifestations and mechanisms of ventricular interdependence. Where RV systolic failure predominates, the response of left ventricular cardiac output to administration of volume and to variation in pulmonary and systemic resistance differs substantially from that seen in the more familiar clinical syndrome of acute decompensated left heart failure, and therapeutic maneuvers that are commonly employed in the latter situation may exacerbate the hemodynamics of a patient with the former.

Ventricular interdependence has been recognized in a number of clinical contexts, and such interactions stem from the co-location of both ventricles within a noncompliant pericardial space (a factor however, which does not generally apply post-transplant), a shared ventricular septum [84], together with the fact that the stroke volume of one ventricle determines the preload of the other: a corollary of their being connected in series and pumping at the same rate. Further, it has long been clear to cardiac histologists that the ventricles are mechanically interdependent not only on account of the shared septum, but due to shared superficial myocardial fibers [85]. This is further supported by recent findings using diffusion tensor imaging [86].

The presence of a shared septum links the diastolic filling of one ventricle to that of the other, particularly in the presence of a pericardium, representing a form of *diastolic interaction*. By implication, volume loading of the RV such as occurs during acute RV systolic dysfunction, causes diastolic septal displacement toward the left ventricle, which impairs filling, so lowering LV stroke volume [87–91]. Berisha demonstrated that excessive preload in the setting of acute RV myocardial infarction was associated with decreased RV stroke-work, presumably reflecting responses beyond the peak of their Starling curves [92]. Some of the LV unloading that occurs in this situation is due to reduced RV cardiac output as well as direct diastolic interaction. Such interactions have been recognized to occur in the context of pure right sided volume loading lesions [93, 94] as well as in acute pulmonary embolism [95] and chronic pulmonary hypertension [96] wherein the RV adapts in part by dilatation in order to exploit heterometric regulation. Similarly, Belenkie demonstrated reduced LV stroke work following volume loading in acute pulmonary hypertension due to experimental pulmonary embolism; in this model phlebotomy was associated with significantly improved LV preload and stroke work [97].

The occurrence of *systolic ventricular interaction* stems in large part from the fact that the left ventricle contributes to the pressure-volume work done by the RV [98]; the contribution ranges from about one quarter of its total stroke-work at rest [99] to over a third under conditions of increased RV afterload [100]. The converse is not true under normal conditions [101], but may be relevant under conditions of left heart systolic failure [102] as has recently been exploited by Schranz in the treatment of dilated cardiomyopathy [103].

Given that the LV contribution to RV stroke-work persisted in the presence of an artificial, non-contractile, RV free wall in Hoffman's experiments it follows that a combination of septal contraction and force transmission mediates this contribution [100].

An important form of systolic ventricular interaction from a transplant perspective is the impact of RV dilatation and systolic dysfunction on LV systolic function, which was most clearly demonstrated by Brookes in an in-vivo porcine model. Here, RCA occlusion was associated with a reduction in RV dilatation, septal flattening and reduced LV contractility as defined by the diminished slope of the LV PRSW:EDV relationship. In this model, pericardiectomy was associated with diminished septal shift which coincided with recovered LV contractility [104]. In Hoffman's experiments, the presence of a more capacious and redundant non-contractile RV free wall diminished the LV contribution to RV stroke-work, which may represent a further mechanism by which a dilated non-functional RV can further impair total cardiac output [100]. Takagaki found that, in the setting of marked RV dilatation and dysfunction, predominantly due to Ebstein's anomaly, RV excision and establishment of a Glenn circulation was associated with a dramatic improvement in LV volumes and contractility [105]. Davis [106] and Amà [107] demonstrated a reduction in LV contractility by load independent measures following moderate experimental RV hypertension in animal models.

An intriguing set of interactions, with respect to the possibilities for treatment, is the increase in RV contractility seen with increased LV afterload in the setting of RV systolic failure. Evidence for this phenomenon includes the experiments of Gold described previously, as well as the leporine models of Pinsky [108] and Apitz [24] wherein acute afterload-induced RV dysfunction was reversible by aortic constriction. The latter study also found that noradrenaline had a similar effect to aortic banding. The same authors intriguingly demonstrated, in a chronic leporine PA banding model, that mild aortic constriction could increase the RV ESPVR slope, whilst also improving multiple histological and cytokine markers of adverse remodeling in the RV [25]. Previous authors had attributed such effects to increased coronary flow, which may well be a contributory factor [13], but Belenkie and colleges demonstrated a similar response to aortic banding in a canine RV pressure overload model, whilst maintaining RCA perfusion at baseline levels via artificial perfusion. It is therefore possible that some of this effect is mediated by a combination of increased LV contractility via the Anrep effect, combined with left-to-right systolic interaction via the mechanisms suggested above. A more mechanically favorable septal position may also play a role [26].

Viewed as a whole, this body of experimental and, as-yet, limited clinical evidence, yields strong support for the concept that RV systolic dysfunction negatively influences LV systolic function, especially in the setting of RV volume overload, and the interesting possibility that the contribution of LV contraction to RV stroke-work might be exploited clinically by moderately increasing LV afterload in the setting of acute RV failure.

Risk Factors for Post-Transplant RV Failure

Impact of Recipient Pulmonary Hypertension

Recipient pulmonary hypertension has been the most consistently reported risk factor for RV dysfunction following heart transplantation [109] and has been recognized as such since the earliest transplants [110]. Increasing recognition of this association, ability to stratify risk, and the availability of more targeted therapies seem to have substantially altered the prognostic implications of this risk factor in the current era.

Early in the adult heart transplant experience, Greipp reported the results of the Stanford program's first 26 transplantation procedures, noting that three of these recipients died from RVF and pulmonary hypertension. Further, he observed that these patients had a substantially increased mean pulmonary vascular resistance (PVR) by comparison to other patients [1, 110].

Griepp's findings were further substantiated by multiple reports in the 1980s and early 1990s which reaffirmed an association between recipient pulmonary hypertension and PGF due to RV dysfunction [111–114], though some did not [115]. Many of these reports analyzed the impact of PVR as a categorical, rather than continuous, variable, which has led various authors to propose cutoff values of PVR (>4–6 Wood units), or transpulmonary gradient (TPG; >12–15 mmHg), beyond which pulmonary hypertension was felt to be a relative contraindication to transplantation [116–118]. Data from reports such as Kirklin's [119] however, seemed to suggest the absence of such a clear threshold. PVR as a risk factor was first analyzed in the ISHLT registry dataset in 2000, which confirmed a linear relationship between PVR and the odds ratio for 1-year mortality (Fig. 15.2) [109].

It has long been controversial as to which measure of pulmonary vascular impedance best describes the risk associated with transplantation. Early reports by Addonizio in a mixed adult and pediatric population advocated for use of pulmonary vascular resistance index (PVRI) given its correction for body size. These authors found that a PVRI greater than 6 Wood units.m^2 (WU.m^2) better predicted the incidence of RVF and death in their cohort, than a PVR greater than 6 WU.m^2 [111]. Kirklin reported similar findings [119]. Others found the TPG to be a more robust predictor of relevant outcomes in their cohorts at varying cutoffs [113, 121].

When PVR, PVRI and TPG were subjected to receiver-operating characteristic (ROC) analysis in an adult population by Chen, each of the measures was found to have similar areas under the ROC curve, and hence discriminating ability [114]. In fact, all are imperfect measures of pulmonary impedance and provide complementary information. The pulmonary vasculature is distensible and endothelium dependent dilatation of resistance vessels occurs in the presence of shear stress at higher flow rates, meaning that resistance is not independent of flow, and this is particularly so in disease states. Use of the PVR as a static measure of pulmonary impedance ignores this fact and it may be misleading in conditions

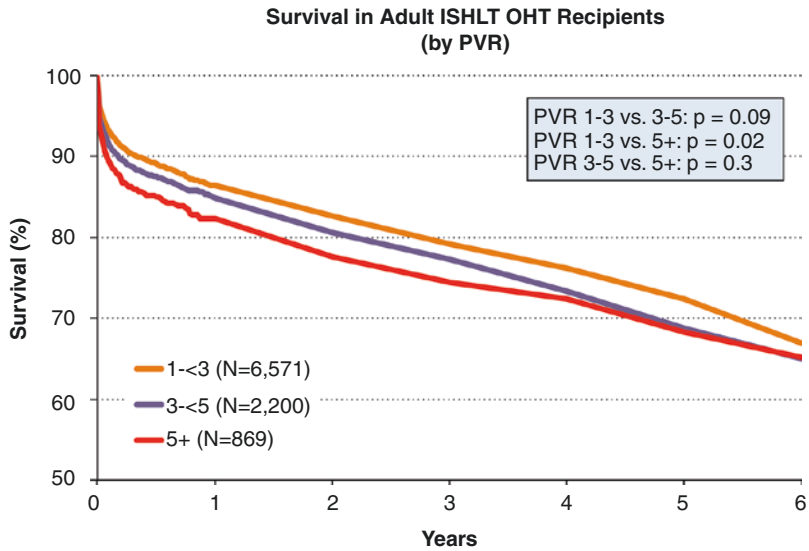

Fig. 15.2 The impact of pulmonary vascular resistance on mortality in ISHLT adult orthotopic heart transplant recipients between 1996 and 2002 is depicted. The greatest impact on mortality hazard is apparent early in the postoperative course. OHT: orthotopic heart transplantation. *PVR* pulmonary vascular resistance. With permission from Taylor DO, Edwards LB, Boucek MM, Trulock EP, Keck BM, Hertz MI. The Registry of the International Society for Heart and Lung Transplantation: twenty-first official adult heart transplant report—2004. J Heart Lung Transplant. 2004 Jul;23(7):796–803 © Elsevier [120]

of low flow [122]. Similarly, TPG is not truly independent of LA pressure, even under conditions of constant flow [123]. In keeping with this, Murali noted that the combination of a TPG >15 mmHg and a PVR >5 Wood units acted synergistically to influence early mortality [121]. These were similar to the findings of Gorlitzer a decade later (Fig. 15.3) [124].

An important modulator of the risk imparted by pulmonary hypertension, however it is defined, appears to be the capacity of the pulmonary vascular bed to reduce impedance in response to increased blood flow, or exogenous vasodilators, a phenomenon known as reactivity. A number of early authors found that the presence of vascular reactivity reduced the early hazard that is otherwise associated with fixed, or irreversible, elevation of PVR [111, 125–128]. Others found that the presence of vascular reactivity did not significantly alter early mortality hazard or that the mortality in such reactive recipients was still substantially greater than in patients without pulmonary hypertension [114, 129, 130]. The issue is further clouded by the lack of a common definition for what agents should be used to test for reactivity, which of the above hemodynamic parameters reactivity should be measured and how much of a response constitutes reactivity. The definition of the latter varies greatly between studies and differs from that proposed in pulmonary arterial hypertension guidelines [131, 132]. Complicating things further is the observation that though PVR is "fixed," in the face of an acute vasodilator challenge, it cannot be inferred that it is *irreversibly elevated*. Even in patients with non-reactive pulmonary hypertension, a substantial component of the pulmonary hypertension is passive, due to pulmonary venous hypertension. In this setting pulmonary pressure and resistance has been found to drop rapidly after support with a ventricular assist device [133–135] or indeed, transplantation [136–138].

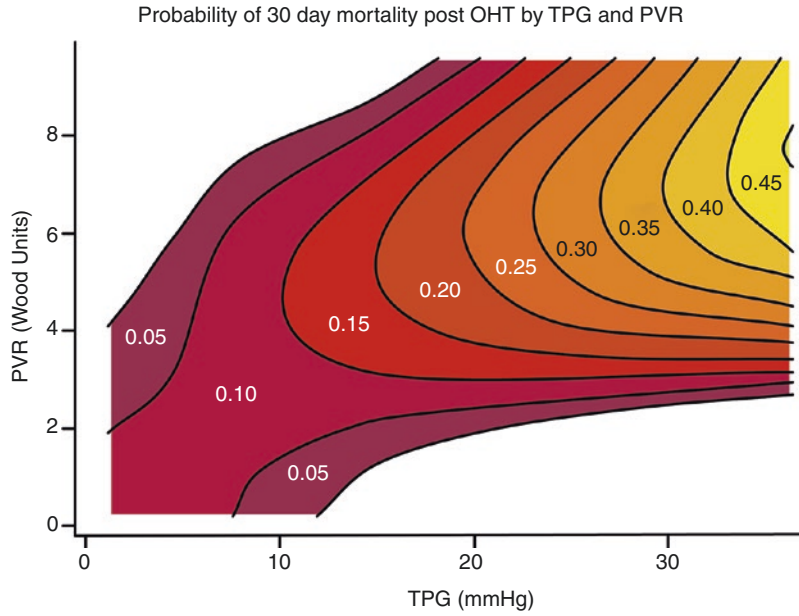

Fig. 15.3 The risk of 30-day mortality is depicted as a function of pulmonary vascular resistance in Wood Units and the transpulmonary gradient in mmHg is depicted, reflecting the experience of 718 adult heart recipients at the General Hospital, Vienna, between 1984 and 2001. Image has been redrawn [124] *OHT* orthotopic heart transplantation, *PVR* pulmonary vascular resistance, *TPG* transpulmonary gradient. With permission from Gorlitzer M, Ankersmit J, Fiegl N, Meinhart J, Lanzenberger M, Unal K, et al. Is the transpulmonary pressure gradient a predictor for mortality after orthotopic cardiac transplantation? Transpl Int Off J Eur Soc Organ Transplant. 2005 Apr;18(4):390–5 © John Wiley and Sons [124]

Interaction with Other Risk Factors for Primary Graft Failure

Multiple other risk factors have been described for primary graft failure and early mortality following heart transplantation and it is reasonable to assume that these may interact with the risk of RV failure, particularly given that some studies explicitly include RVF in their definition of PGF. Such risk factors are listed in (Table 15.2) [139–141].

Donor-recipient size match is a point of interest. Authors of early reports had speculated that larger donors may be useful to compensate for the elevated pulmonary resistance [111, 112]. Adult ISHLT data do not suggest a benefit to oversizing donors in this setting (Fig. 15.4) [142], and some pediatric reports find an increased risk of delayed sternal closure, pulmonary complications, graft failure and mortality [143]. Conversely, while analysis of the United Network for Organ Sharing (UNOS) registry data has not found associated poorer outcomes with size mismatch, in general, undersizing (ratio <0.8) is associated with greater mortality in the subset of patients with a PVR >4 WU [144]. This is consistent with an increase in early graft dysfunction that has been found in other studies [145, 146].

Table 15.2 Risk factors for primary graft dysfunction [139–141]

Increasing donor age
Recipient-donor size mismatch
Prolonged total and warm ischemic times
Increased recipient pulmonary vascular resistance
Previous recipient cardiac surgery
Recipient congenital heart disease diagnosis
Impaired recipient renal function
Recipient waiting list status at time of transplantation
Inpatient status at time of transplantation
Inotropes at time of transplantation
Ventilation at time of transplantation
Mechanical circulatory support at time of transplantation
Hemodialysis at time of transplantation

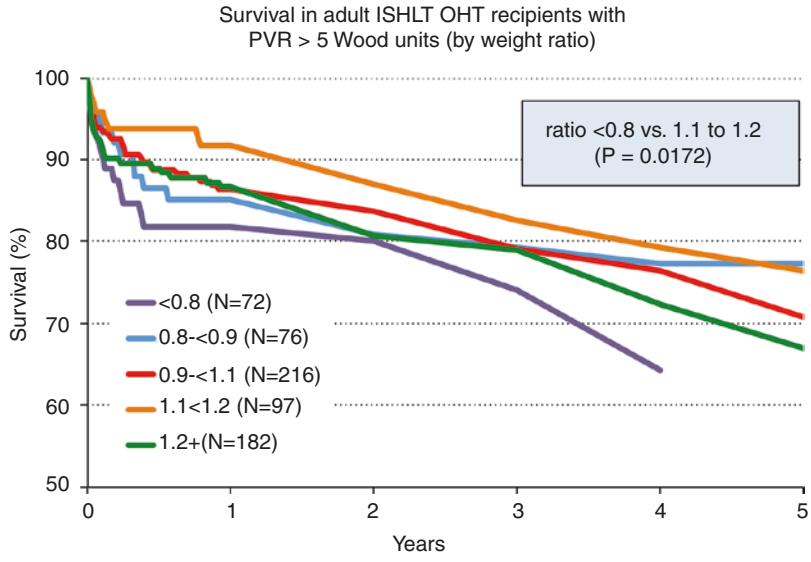

Fig. 15.4 The actuarial survival of adult heart transplant recipients with a pre-transplant pulmonary vascular resistance (PVR) >5 Wood Units, stratified by donor-recipient weight ratio, is shown. Oversizing of donors (ratio >1.2) was not associated with a mortality advantage, but undersizing (ratio <0.8) was associated with the lowest survival, being significantly reduced by comparison to the group with a ratio between 1.1 and 1.2. *OHT* orthotopic heart transplantation, *PVR* pulmonary vascular resistance. With permission from Stehlik J, Edwards LB, Kucheryavaya AY, Benden C, Christie JD, Dobbels F, et al. The Registry of the International Society for Heart and Lung Transplantation: Twenty-eighth Adult Heart Transplant Report—2011. J Heart Lung Transplant. 2011 Oct;30(10):1078–94 © Elsevier [142]

A Changing Landscape

Over time, a substantial reduction in early mortality has been seen following transplantation in general, and this has also been the case for recipients with pulmonary hypertension [109, 142]. An interesting contrast emerges when the hazard associated with pulmonary hypertension in adult recipients in the ISHLT registry up to 2000 is contrasted with a more recent analysis between 2003 and 2008 (Fig. 15.5) [142]. In the latter period, PVR remains an independent risk factor for 1-year mortality, but the hazard ratio for any given PVR has dramatically reduced. One may speculate that this is due to improved recognition of this clinical problem, early, and in some cases, preemptive vasodilator therapy and increasing experience with mechanical circulatory support.

Management

Optimal management of acute RV dysfunction in the post-transplant setting necessitates pre-empting its occurrence in higher risk scenarios, early recognition and institution of appropriate therapeutic interventions. Appropriate management of acute systolic RV failure differs significantly from that employed in predominant LV systolic dysfunction. Priorities in management include optimization of preload, reduction of PVR, and avoiding inappropriate inotropic support and reduction in LV afterload.

Preemptive Management

A number of approaches have been described to mitigate risk, particularly in patients with pulmonary hypertension.

First, given the interaction with other PGF risk factors as described above, potentially modifiable risk factors such as donor:recipient size match, and minimization of ischemic time must be considered in peri-operative decision making.

An important tool in the setting of adult systolic heart failure with fixed, elevated PVR has been the use of *ventricular assist devices* as a "*bridge to candidacy*." Such use has been

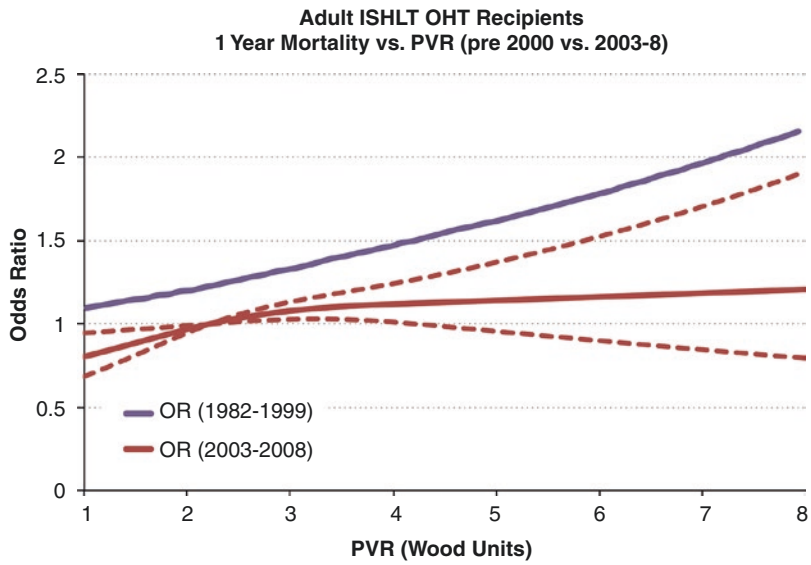

Fig. 15.5 The impact of pulmonary vascular resistance, in multivariable analysis, on 1-year mortality is compared between two eras: 1984–2000 [109] and 2000–2005. A clear difference between the two eras, with respect to mortality hazard imposed by a given degree of pulmonary hypertension, is seen. *OHT* orthotopic heart transplantation, *PVR* pulmonary vascular resistance. With permission from Stehlik J, Edwards LB, Kucheryavaya AY, Benden C, Christie JD, Dobbels F, et al. The Registry of the International Society for Heart and Lung Transplantation: Twenty-eighth Adult Heart Transplant Report—2011. J Heart Lung Transplant. 2011 Oct;30(10):1078–94 © Elsevier [142]

associated with pulmonary vascular remodeling and reversal of the previously "fixed" elevated PVR, with such patients experiencing a similar risk of post-transplant mortality to recipients without pulmonary hypertension at baseline [134, 135]. In pediatric centers VAD has not generally been employed for this indication alone in the absence of medically unmanageable decompensated heart failure, primarily because of the increased morbidity and mortality associated with current VAD options in children [147] and improving outcomes of patients with pulmonary hypertension as noted above.

There are also preliminary data suggesting that pulmonary vascular remodeling can occur with the use of pulmonary vasodilators such as bosentan and sildenafil [148–150], but more data are required given the potential risks of pulmonary vasodilators in the setting of left heart disease.

In light of the previously discussed data, we do not oversize donors in the setting of confirmed or suspected elevated PVR but avoid under-sizing (weight ratio >0.9).

Heterotopic transplantation was proposed as a way to retain the recipient's already conditioned RV in recipients with pulmonary hypertension [151]. However, it was associated with increased mortality due to pulmonary complications related to mass effect, and the retention of a failing LV which contributes to death by arrhythmia and systemic thromboembolism [129]. More recent registry analyses however [152], suggest that these complications may be lower in well-selected candidates, though it is not clear what place, if any, this therapeutic option has in the current era and it remains a low volume activity accounting for 0.2% of all transplant in the ISHLT registry in 2012 [153].

Domino transplantation, involving the retrieval of a donor heart from a patient with pulmonary hypertension who is undergoing heart-lung transplantation for a heart transplant recipient has been employed successfully [154]. However, broader application is limited by small numbers of end stage PAH patients undergoing transplantation, and the no longer routine preference for heart-lung transplantation as opposed to lung transplantation only in these recipients.

Heart-lung transplantation remains an option for candidates with associated respiratory failure, non-cardiac PAH (WHO Group II) and perhaps for some patients with markedly elevated, fixed, PVR. This strategy, however, is limited by the poorer graft survival in lung transplantation [155, 156].

Optimizing Volume Status

The acutely failing RV is sensitive to excessive volume and optimization of volume status is an important goal of therapy. Generally in the peri-operative period volume overload, rather than hypovolemia, is the rule and such ventricles may be operating at or beyond the peak of their Starling curve, with pejorative effects on overall cardiac output that are exacerbated by the complex inter-ventricular interactions described above [157].

Clues to this physiological state are hypotension or evidence of a low cardiac output state and central venous pressure, which is elevated, often to more than 15 cmH_2O, with non-response or even adverse hemodynamic response to volume challenge. Pulse pressure variability (and its echocardiographic correlates) is often maintained in this setting and is a misleading marker of volume status in this clinical context [158, 159]. Frequently echocardiography will show progressive RV dilatation and increasing tricuspid regurgitation.

While the published data are sparse, our clinical experience suggests that aggressive measures to effect control of volume are warranted in this scenario [159]. In the face of diuretic resistance or rapidly worsening clinical parameters, we have found that phlebotomy of 2–5 mL/kg can result in substantial hemodynamic improvement.

Minimizing RV Afterload

Minimizing RV afterload remains an important goal in the peri-operative setting. It is to be reemphasized that patients with RV failure may have hemodynamically significant elevation of PVR

without a marked elevation of measured or estimated RVSP.

As with all cardiac ICU patients, optimization of ventilation with a view to minimizing both derecruitment and atelectasis, and overinflation, is important. Additionally, hypoxia, hypercarbia and acidosis should be minimized. In unstable patients the adverse response to noxious stimuli may be abrogated by analgesia, sedation and, where necessary, paralysis.

Selective pulmonary vasodilators are employed to decrease PVR whilst maintaining or increasing the SVR. In this regard nitric oxide has seen common use [160–162] and, given its direct respiratory route of administration, effects pulmonary vasodilatation with minimal systemic effects and less tendency to potentiate V:Q mismatch and worsen hypoxemia than parenteral agents. Other vasodilators including inhaled iloprost, prostaglandin E1, prostacyclin, sildenafil and sodium nitroprusside have been reported though their effects are less specific to the pulmonary circulation [160, 163–165]. It is likely that pre-emptive initiation of selective pulmonary vasodilators, particularly nitric oxide, in high risk patients whilst weaning from cardiopulmonary bypass may diminish the risk of associated RV failure [166, 167], and this is our current practice.

Optimizing Inotropic Support

Agents used in this setting historically have included isoproterenol and dobutamine, each of which couples chronotropic and inotropic effects with systemic and pulmonary vasodilatation, thus optimizing ventriculovascular coupling. However vasodilation may limit use in hypotensive states and epinephrine may be preferred in this setting [168].

Phosphodiesterase inhibitors, including milrinone and enoximone have been found to have similar inodilator properties, with the theoretical advantage that they operate downstream of the adrenergic receptor and adenylate cyclase, which are often dysregulated in the transplant setting. They are felt to have a synergistic effect when combined with catecholaminergic drugs [169].

Levosimendan acts via a calcium sensitizing mechanism, with physiological effects that are comparable to the above inodilator agents. It was reportedly useful in the management of preoperative RV dysfunction and PGF post transplant [170, 171], though late follow-up of such patients was less encouraging [172].

The response to inotropic support, particularly with catecholaminergic agents, is subdued in the context of PGF and this may be disproportionately the case for RV dysfunction. Inappropriate inotropic therapy may exacerbate both systemic and pulmonary vasoconstriction, which may in turn compromise cardiac output to a greater degree than any incremental improvement in contractility.

Maintenance of Systemic Blood Pressure

Though the published clinical data in support are again limited, maintenance of systemic blood pressure is felt to be an important therapeutic goal, given the previously described favorable effects on RV performance via improved coronary perfusion, mechanically advantageous septal position and exploitation of beneficial systolic ventricular interaction. There is little data to guide how this is best achieved, although norepinephrine, vasopressin and intra-aortic balloon pump (IABP) usage have all been reported [173]. Tolerance of vasopressors in this setting is contingent on adequate LV systolic function, which may not always be the case with primary graft failure.

Mechanical Circulatory Support

Mechanical support options for post transplant graft dysfunction include IABP, various centrifugal LVAD, RVAD or BiVAD options, and central or peripheral ECMO. Despite a favorable early report of IABP in 5 patients with post transplant RVF [173], it has been displaced by other modalities in adult practice, and experience is negligible in pediatric centers. Early reports of pulsatile

and centrifugal LVAD usage for PGF were marked by extremely low survival [174–177] and other centers have commented on a similarly disappointing experience with RVAD for predominant RV dysfunction [178, 179].

In contrast, ECMO presents a cheaper, less surgically traumatic option with improved reported survival. Marasco reported a 66% survival following mechanical circulatory support of varying modalities for refractory primary graft failure (their definition included patients with RVF) [179]. In a subsequent article she reported a 39 patient series of ECMO cannulation for PGF (again including RVF); 74% survived to hospital discharge [180]. Similarly, d'Alessandro reported a 50% survival to discharge in a large early graft failure series, and Listijono reported an 82% 30-day survival in the adult population [178, 181]. Some pediatric centers have also presented similar results [143, 182], though others reported less favorable outcomes [183]. Given the adult experience and the far more extensive experience with postoperative ECMO than RVAD, it seems likely that ECMO is the current support modality of choice for RV dysfunction post transplant in children also.

Prognosis and Long-term Outcome

Perioperative Mortality and Morbidity

As noted in the introductory section, the morbidity and mortality attributable to post-transplant RV dysfunction is difficult to track due to marked variation in definition and non-inclusion of this variable in registry datasets.

It seems likely, however, that whilst the occurrence of RV dysfunction continues [3], the attributable mortality in many reports has decreased over time, even in patients who would previously have been considered high risk [184]. Some component of this is due to early and even pre-emptive use of pulmonary vasodilators [3]. and improvements in mechanical circulatory support have also played a large role [178, 180]. These improvements may in fact constitute a large part of the dramatic reduction in early mortality documented in registry datasets since their inception [185].

Longer-term Pulmonary Vascular and RV Remodeling

Serial evaluation of PVR over time has found evidence of continued vascular remodeling post heart transplantation. Indeed, a majority of patients with elevated PVR due to left atrial hypertension will experience normalization of PVR by 2 weeks post transplantation [129, 136, 186, 187], despite histologically apparent muscularization of pulmonary arterioles at the time transplant in many such patients [188, 189].

When compared to the non-transplanted normal population, evidence of adverse RV remodeling with RV dilatation [136], reduced longitudinal systolic function [83] and tricuspid regurgitation are seen over the medium term [136]. The impact of these findings is unclear, as, both in high risk subsets such as patients with pulmonary hypertension, and in patients with overt RVF, the difference in mortality appears generally to occur early, with no difference in late hazard [3, 178, 180].

Conclusions

In the present era, with increasing complexity of transplantation and increasing use of marginal donors, post-transplant RV dysfunction remains prevalent: its occurrence is not always predictable and certainly not avoidable. Recent standardization of nomenclature should, in time, contribute to clarifying these temporal trends in incidence and outcome.

It remains an important source of morbidity and mortality, though with improving recognition and preoperative management, including the availability of selective pulmonary vasodilators and improvements in mechanical circulatory support, improvements in early outcome are being seen.

References

1. Griepp RB, Stinson EB, Clark DA, Shumway NEA. Two-year experience with human heart transplantation. Calif Med. 1970;113(2):17.
2. Costard-Jäckle A, Fowler MB. Influence of preoperative pulmonary artery pressure on mortality after heart transplantation: testing of potential reversibility of pulmonary hypertension with nitroprusside is useful in defining a high risk group. J Am Coll Cardiol. 1992;19(1):48–54.
3. Cosío Carmena DG, Bueno MG, Almenar L, Delgado JF, Arizón JM, Vilchez FG, et al. Primary graft failure after heart transplantation: characteristics in a contemporary cohort and performance of the RADIAL risk score. J Heart Lung Transplant. 2013;32(12):1187–95.
4. Kanter KR, Tam VK, Vincent RN, Cuadrado AR, Raviele AA, Berg AM. Current results with pediatric heart transplantation. Ann Thorac Surg. 1999;68(2):527–30.
5. Hehrlein FW, Netz H, Moosdorf R, Dapper F, Scheld HH, Bauer J, et al. Pediatric heart transplantation for congenital heart disease and cardiomyopathy. Ann Thorac Surg. 1991;52(1):112–7.
6. Mavroudis C, Harrison H, Klein JB, Gray LA, Ganzel BL, Wellhausen SR, et al. Infant orthotopic cardiac transplantation. J Thorac Cardiovasc Surg. 1988;96(6):912–24.
7. Bailey LL, Wood M, Razzouk A, Van Arsdell G, Gundry S. Heart transplantation during the first 12 years of life. Arch Surg. 1989;124(10):1221–6.
8. Starnes VA, Oyer PE, Bernstein D, Baum D, Gamberg P, Miller J, et al. Heart, heart-lung, and lung transplantation in the first year of life. Ann Thorac Surg. 1992;53(2):306–10.
9. Kobashigawa J, Zuckermann A, Macdonald P, Leprince P, Esmailian F, Luu M, et al. Report from a consensus conference on primary graft dysfunction after cardiac transplantation. J Heart Lung Transplant. 2014;33(4):327–40.
10. Graham TP, Bernard YD, Mellen BG, Celermajer D, Baumgartner H, Cetta F, et al. Long-term outcome in congenitally corrected transposition of the great arteries: a multi-institutional study. J Am Coll Cardiol. 2000;36(1):255–61.
11. Lange PE, Nürnberg JH, Sievers HH, Onnasch DGW, Bernhard A, Heintzen PH. Response of the right ventricle to progressive pressure loading in pigs. Basic Res Cardiol. 1985 Jul 1;80(4):436–44.
12. Guyton AC, Lindsey AW, Gilluly JJ. The limits of right ventricular compensation following acute increase in pulmonary circulatory resistance. Circ Res. 1954 Jul 1;2(4):326–32.
13. Brooks H, Kirk ES, Vokonas PS, Urschel CW, Sonnenblick EH. Performance of the right ventricle under stress: relation to right coronary flow. J Clin Invest. 1971;50(10):2176–83.
14. Hon JK, Steendijk P, Khan H, Wong K, Yacoub M. Acute effects of pulmonary artery banding in sheep on right ventricle pressure-volume relations: relevance to the arterial switch operation. Acta Physiol Scand. 2001;172(2):97–106.
15. Karunanithi MK, Michniewicz J, Copeland SE, Feneley MP. Right ventricular preload recruitable stroke work, end-systolic pressure-volume, and dP/dtmax-end-diastolic volume relations compared as indexes of right ventricular contractile performance in conscious dogs. Circ Res. 1992;70(6):1169–79.
16. De Vroomen M, Cardozo RH, Steendijk P, van Bel F, Baan J. Improved contractile performance of right ventricle in response to increased RV afterload in newborn lamb. Am J Physiol Heart Circ Physiol. 2000;278(1):H100–5.
17. Szabó G, Sebening C, Hagl C, Tochtermann U, Vahl CF, Hagl S. Right ventricular function after brain death: response to an increased afterload. Eur J Cardiothorac Surg. 1998;13(4):449–58.
18. Spotnitz HM, Berman MA, Epstein SE. Pathophysiology and experimental treatment of acute pulmonary embolism. Am Heart J. 1971;82(4):511–20.
19. Vlahakes GJ, Turley K, Hoffman JI. The pathophysiology of failure in acute right ventricular hypertension: hemodynamic and biochemical correlations. Circulation. 1981;63(1):87–95.
20. Gold FL, Bache RJ. Transmural right ventricular blood flow during acute pulmonary artery hypertension in the sedated dog. Evidence for subendocardial ischemia despite residual vasodilator reserve. Circ Res. 1982;51(2):196–204.
21. Schmitto JD, Doerge H, Post H, Coulibaly M, Sellin C, Popov AF, et al. Progressive right ventricular failure is not explained by myocardial ischemia in a pig model of right ventricular pressure overload. Eur J Cardiothorac Surg. 2009 Feb 1;35(2):229–34.
22. Greyson C, Xu Y, Cohen J, Schwartz GG. Right ventricular dysfunction persists following brief right ventricular pressure overload. Cardiovasc Res. 1997 May 1;34(2):281–8.
23. Schwartz GG, Steinman S, Garcia J, Greyson C, Massie B, Weiner MW. Energetics of acute pressure overload of the porcine right ventricle. In vivo 31P nuclear magnetic resonance. J Clin Invest. 1992;89(3):909–18.
24. Apitz C, Honjo O, Friedberg M, Assad R, Van Arsdell G, Humpl T, et al. Beneficial effects of vasopressors on right ventricular function in experimental acute right ventricular failure in a Rabbit model. Thorac Cardiovasc Surg. 2012;60(01):017–23.
25. Apitz C, Honjo O, Humpl T, Li J, Assad RS, Cho MY, et al. Biventricular structural and functional responses to aortic constriction in a rabbit model of chronic right ventricular pressure overload. J Thorac Cardiovasc Surg. 2012;144(6):1494–501.
26. Belenkie I, Horne SG, Dani R, Smith ER, Tyberg JV. Effects of aortic constriction during experimental acute right ventricular pressure loading further insights into diastolic and systolic ventricular interaction. Circulation. 1995 Aug 1;92(3):546–54.

27. Greyson C, Xu Y, Lu L, Schwartz GG. Right ventricular pressure and dilation during pressure overload determine dysfunction after pressure overload. Am J Physiol—Heart Circ Physiol. 2000 May 1;278(5):H1414–20.
28. Greyson CR, Schwartz GG, Lu L, Ye S, Helmke S, Xu Y, et al. Calpain inhibition attenuates right ventricular contractile dysfunction after acute pressure overload. J Mol Cell Cardiol. 2008;44(1):59–68.
29. Ahmad HA, Lu L, Ye S, Schwartz GG, Greyson CR. Calpain inhibition preserves talin and attenuates right heart failure in acute pulmonary hypertension. Am J Respir Cell Mol Biol. 2012;47(3):379–86.
30. Novitzky D, Wicomb WN, Cooper DKC, Rose AG, Fraser RC, Barnard CN. Electrocardiographic, haemodynamic and endocrine changes occuring during experimental brain death in the Chacma baboon. J Heart Transplant. 1984;4(1):63–9.
31. Cushing H. Some experimental and clinical observations concerning states of increased intracranial tension. Am J Med Sci. 1902;124(3):375–400.
32. Bittner HB, Kendall SW, Campbell KA, Montine TJ, Van Trigt PA. valid experimental brain death organ donor model. J Heart Lung Transplant. 1995;14(2):308–17.
33. Shivalkar B, Van Loon J, Wieland W, Tjandra-Maga TB, Borgers M, Plets C, et al. Variable effects of explosive or gradual increase of intracranial pressure on myocardial structure and function. Circulation. 1993;87(1):230–9.
34. Mertes PM, el Abassi K, Jaboin Y, Burtin P, Pinelli G, Carteaux JP, et al. Changes in hemodynamic and metabolic parameters following induced brain death in the pig. Transplantation. 1994;58(4):414–8.
35. Pinelli G, Mertes PM, Carteaux JP, Jaboin Y, Escanye JM, Brunotte F, et al. Myocardial effects of experimental acute brain death: evaluation by hemodynamic and biological studies. Ann Thorac Surg. 1995;60(6):1729–34.
36. Bruinsma GJ, Nederhoff MG, Geertman HJ, van Huffelen AC, Slootweg PJ, Ferrari R, et al. Acute increase of myocardial workload, hemodynamic instability, and myocardial histological changes induced by brain death in the cat. J Surg Res. 1997 Feb 15;68(1):7–15.
37. Shanlin RJ, Sole MJ, Rahimifar M, Tator CH, Factor SM. Increased intracranial pressure elicits hypertension, increased sympathetic activity, electrocardiographic abnormalities and myocardial damage in rats. J Am Coll Cardiol. 1988;12(3):727–36.
38. Galiñanes M, Hearse DJ. Brain-death-induced cardiac contractile dysfunction: studies of possible neurohormonal and blood-borne mediators. J Mol Cell Cardiol. 1994;26(4):481–98.
39. Mertes PM, Carteaux JP, Jaboin Y, Pinelli G, el Abassi K, Dopff C, et al. Estimation of myocardial interstitial norepinephrine release after brain death using cardiac microdialysis. Transplantation. 1994;57(3):371–7.
40. Sebening C, Hagl C, Szabo G, Tochtermann U, Strobel G, Schnabel P, et al. Cardiocirculatory effects of acutely increased intracranial pressure and subsequent brain death. Eur J Cardio-Thorac Surg Off J Eur Assoc Cardio-Thorac Surg. 1995;9(7):360–72.
41. Novitzky D. Detrimental effects of brain death on the potential organ donor. Transplant Proc. 1997;29(8):3770–2.
42. Dujardin KS, McCully RB, Wijdicks EFM, Tazelaar HD, Seward JB, McGregor CGA, et al. Myocardial dysfunction associated with brain death: clinical, echocardiographic, and pathologic features. J Heart Lung Transplant. 2001 Mar 1;20(3):350–7.
43. Kolin A, Norris JW. Myocardial damage from acute cerebral lesions. Stroke. 1984 Nov 1;15(6):990–3.
44. Todd GL, Baroldi G, Pieper GM, Clayton FC, Eliot RS. Experimental catecholamine-induced myocardial necrosis. I. Morphology, quantification and regional distribution of acute contraction band lesions. J Mol Cell Cardiol. 1985;17(4):317–38.
45. Rona G. Catecholamine cardiotoxicity. J Mol Cell Cardiol. 1985;17(4):291–306.
46. Van Trigt P, Bittner HB, Kendall SW, Milano CA. Mechanisms of transplant right ventricular dysfunction. Ann Surg. 1995;221(6):666–76.
47. Bittner HB, Chen EP, Craig D, Van Trigt P. Preload-recruitable stroke work relationships and diastolic dysfunction in the brain-dead organ donor. Circulation. 1996 Nov 1;94(9 Suppl):II320–5.
48. Kendall SW, Bittner HB, Peterseim DS, Campbell KA, Van Trigt P. Right ventricular function in the donor heart. Eur J Cardio-Thorac Surg Off J Eur Assoc Cardio-Thorac Surg. 1997;11(4):609–15.
49. Pandalai PK, Lyons JM, Duffy JY, McLean KM, Wagner CJ, Merrill WH, et al. Role of the beta-adrenergic receptor kinase in myocardial dysfunction after brain death. J Thorac Cardiovasc Surg. 2005;130(4):1183–9.
50. Stoica SC, Satchithananda DK, White PA, Parameshwar J, Redington AN, Large SR. Noradrenaline use in the human donor and relationship with load-independent right ventricular contractility. Transplantation. 2004 Oct 27;78(8):1193–7.
51. Zaroff JG, Babcock WD, Shiboski SC, Solinger LL, Rosengard BR. Temporal changes in left ventricular systolic function in heart donors: results of serial echocardiography. J Heart Lung Transplant. 2003;22(4):383–8.
52. Casartelli M, Bombardini T, Simion D, Gaspari MG, Procaccio F. Wait, treat and see: echocardiographic monitoring of brain-dead potential donors with stunned heart. Cardiovasc Ultrasound. 2012;10:25.
53. Pilati CF, Bosso FJ, Maron MB. Factors involved in left ventricular dysfunction after massive sympathetic activation. Am J Phys. 1992;263(3 Pt 2):H784–91.
54. Novitzky D, Wicomb WN, Cooper DKC, Rose a G, Reichart B. Prevention of myocardial injury during brain death by total cardiac sympathectomy in the Chacma Baboon. Ann Thorac Surg. 1986;41(5):520–4.

55. Novitzky D, Rose AG, Cooper DK. Injury of myocardial conduction tissue and coronary artery smooth muscle following brain death in the baboon. Transplantation. 1988;45(5):964–6.
56. D'Amico TA, Meyers CH, Koutlas TC, Peterseim DS, Sabiston DC, Van Trigt P, et al. Desensitization of myocardial beta-adrenergic receptors and deterioration of left ventricular function after brain death. J Thorac Cardiovasc Surg. 1995;110(3):746–51.
57. White M, Wiechmann RJ, Roden RL, Hagan MB, Wollmering MM, Port JD, et al. Cardiac β-adrenergic neuroeffector systems in acute myocardial dysfunction related to brain injury evidence for catecholamine-mediated myocardial damage. Circulation. 1995 Oct 15;92(8):2183–9.
58. Owen VJ, Burton PBJ, Michel MC, Zolk O, Bohm M, Pepper JR, et al. Myocardial dysfunction in donor hearts: a possible etiology. Circulation. 1999;99(19):2565–70.
59. Seguin C, Devaux Y, Aubert N, Siaghy EM, Zannad F, Burlet C, et al. Consequences of labetalol administration on myocardial beta adrenergic receptors in the brain dead pig. Ann Transplant Q Pol Transplant Soc. 2000;5(4):54–60.
60. McLean KM, Pandalai PK, Pearl JM, Bulcao CF, Lyons JM, Wagner CJ, et al. Beta-adrenergic receptor antagonism preserves myocardial function after brain death in a porcine model. J Heart Lung Transplant. 2007;26(5):522–8.
61. Bittner HB, Chen EP, Milano CA, Kendall SWH, Jennings RB, Sabiston DC, et al. Myocardial β-adrenergic receptor function and high-energy phosphates in brain death—related cardiac dysfunction. Circulation. 1995 Nov 1;92(9):472–8.
62. Liaudet L, Calderari B, Pacher P. Pathophysiological mechanisms of catecholamine and cocaine-mediated cardiotoxicity. Heart Fail Rev. 2014 Jan 8;19:1–10.
63. Novitzky D, Cooper DK, Rose AG, Reichart B. Prevention of myocardial injury by pretreatment with verapamil hydrochloride prior to experimental brain death: efficacy in a baboon model. Am J Emerg Med. 1987;5(1):11–8.
64. Novitzky D, Cooper DK, Morrell D, Isaacs S. Change from aerobic to anaerobic metabolism after brain death, and reversal following triiodothyronine therapy. Transplantation. 1988;45(1):32–6.
65. Herijgers P, Leunens V, Tjandra-Maga TB, Mubagwa K, Flameng W. Changes in organ perfusion after brain death in the rat and its relation to circulating catecholamines. Transplantation. 1996 Aug 15;62(3):330–5.
66. Bruinsma GJ, Nederhoff MGJ, van de Kolk CWA, de Groot MCH, Slootweg PJ, Bredée JJ, et al. Bioenergetic response of the heart to dopamine following brain death–related reduced myocardial workload: a phosphorus-31 magnetic resonance spectroscopy study in the cat. J Heart Lung Transplant. 1999;18(12):1189–97.
67. Szabó G, Hackert T, Sebening C, Vahl CF, Hagl S. Modulation of coronary perfusion pressure can reverse cardiac dysfunction after brain death. Ann Thorac Surg. 1999;67(1):18–25. discussion 25–6
68. Skrabal CA, Thompson LO, Potapov EV, Southard RE, Joyce DL, Youker KA, et al. Organ-specific regulation of pro-inflammatory molecules in heart, lung, and kidney following brain death. J Surg Res. 2005;123(1):118–25.
69. Birks EJ, Burton PB, Owen V, Mullen AJ, Hunt D, Banner NR, et al. Elevated tumor necrosis factor-alpha and interleukin-6 in myocardium and serum of malfunctioning donor hearts. Circulation. 2000 Nov 7;102(19 Suppl 3):III352–8.
70. Birks EJ, Owen VJ, Burton PBJ, Bishop AE, Banner NR, Khaghani A, et al. Tumor necrosis factor-α is expressed in donor heart and predicts right ventricular failure after human heart transplantation. Circulation. 2000 Jul 18;102(3):326–31.
71. Bittner HB, Chen EP, Biswas SS, Van Trigt P, Davis RD. Right ventricular dysfunction after cardiac transplantation: primarily related to status of donor heart. Ann Thorac Surg. 1999;68(5):1605–11.
72. Mankad PS, Yacoub MH. Systolic and diastolic function of both ventricles after prolonged cardioplegic arrest. Ann Thorac Surg. 1993;55(4):933–9.
73. Marasco SF, Esmore DS, Richardson M, Bailey M, Negri J, Rowland M, et al. Prolonged cardiac allograft ischemic time ? no impact on long-term survival but at what cost? Clin Transpl. 2007;21(3):321–9.
74. Chen J-W, Chen Y-S, Chi N-H, Huang S-C, H-Y Y, Chou N-K, et al. Risk factors and prognosis of patients with primary graft failure after heart transplantation: An asian center experience. Transplant Proc. 2014;46(3):914–9.
75. Lund LH, Edwards LB, Kucheryavaya AY, Dipchand AI, Benden C, Christie JD, et al. The Registry of the International Society for heart and lung transplantation: Thirtieth Official Adult Heart Transplant Report—2013; focus theme: age. J Heart Lung Transplant. 2013;32(10):951–64.
76. Davies RR, Russo MJ, Mital S, Martens TM, Sorabella RS, Hong KN, et al. Predicting survival among high-risk pediatric cardiac transplant recipients: an analysis of the United Network for Organ Sharing database. J Thorac Cardiovasc Surg. 2008;135(1):147–55. 155.e1–2
77. Banner NR, Thomas HL, Curnow E, Hussey JC, Rogers CA, Bonser RS. The importance of cold and warm cardiac ischemia for survival after heart transplantation. Transplantation. 2008;86(4):542–7.
78. Dipchand AI, Kirk R, Edwards LB, Kucheryavaya AY, Benden C, Christie JD, et al. The Registry of the International Society for heart and lung transplantation: Sixteenth Official Pediatric Heart Transplantation Report—2013; focus theme: age. J Heart Lung Transplant. 2013;32(10):979–88.
79. Conway J, Chin C, Kemna M, Burch M, Barnes A, Tresler M, et al. Donors' characteristics and impact on outcomes in pediatric heart transplant recipients. Pediatr Transplant. 2013;17(8):774–81.

80. Ford MA, Almond CS, Gauvreau K, Piercey G, Blume ED, Smoot LB, et al. Association of graft ischemic time with survival after heart transplant among children in the United States. J Heart Lung Transplant. 2011;30(11):1244–9.
81. Hoskote A, Carter C, Rees P, Elliott M, Burch M, Brown K. Acute right ventricular failure after pediatric cardiac transplant: predictors and long-term outcome in current era of transplantation medicine. J Thorac Cardiovasc Surg. 2010;139(1):146–53.
82. Ahlgren B, Puskas F, Seres T. Total ischemia time alters the longitudinal and circumferential shortening of the right ventricle in transplanted hearts. Seminars in cardiothoracic and vascular anesthesia [Internet]. Sage Publications; 2011 [cited 2014 Oct 25]. p. 163–8. http://scv.sagepub.com/content/15/4/163.short
83. Mastouri R, Batres Y, Lenet A, Gradus-Pizlo I, O'Donnell J, Feigenbaum H, et al. Frequency, time course, and possible causes of right ventricular systolic dysfunction after cardiac transplantation: a single center experience. Echocardiography. 2013;30(1):9–16.
84. Weyman AE, Wann S, Feigenbaum H, Dillon JC. Mechanism of abnormal septal motion in patients with right ventricular volume overload: a cross-sectional echocardiographic study. Circulation. 1976 Aug 1;54(2):179–86.
85. Pettigrew JB. On the arrangement of the muscular fibres in the ventricles of the vertebrate heart, with physiological remarks. Philos Trans R Soc Lond. 1864;154:445–500.
86. Froeling M, Strijkers GJ, Nederveen AJ, Chamuleau SA, Luijten PR. Diffusion tensor MRI of the heart—in Vivo Imaging of myocardial fiber architecture. Curr Cardiovasc Imaging Rep. 2014 Jul 1;7(7):1–11.
87. Bemis CE, Serur JR, Borkenhagen D, Sonnenblick EH, Urschel CW. Influence of right ventricular filling pressure on left ventricular pressure and dimension. Circ Res. 1974 Apr 1;34(4):498–504.
88. Brinker JA, Weiss JL, Lappé DL, Rabson JL, Summer WR, Permutt S, et al. Leftward septal displacement during right ventricular loading in man. Circulation. 1980 Mar 1;61(3):626–33.
89. Taylor RR, Covell JW, Sonnenblick EH, J Ross J. Dependence of ventricular distensibility on filling of the opposite ventricle. Am J Physiol: Leg Content. 1967 Sep 1;213(3):711–8.
90. Janicki JS, Weber KT. The pericardium and ventricular interaction, distensibility, and function. Am J Physiol—Heart Circ Physiol. 1980 Apr 1;238(4):H494–503.
91. Goldstein JA, Vlahakes GJ, Verrier ED, Schiller NB, Tyberg JV, Ports TA, et al. The role of right ventricular systolic dysfunction and elevated intrapericardial pressure in the genesis of low output in experimental right ventricular infarction. Circulation. 1982 Mar 1;65(3):513–22.
92. Berisha S, Kastrati A, Goda A, Popa Y. Optimal value of filling pressure in the right side of the heart in acute right ventricular infarction. Br Heart J. 1990;63(2):98–102.
93. Graham TP, Jarmakani JM, Canent RV. Left heart volume characteristics with a right ventricular volume overload total anomalous pulmonary venous connection and large atrial septal defect. Circulation. 1972 Feb 1;45(2):389–96.
94. Popio KA, Gorlin R, Teichholz LE, Cohn PF, Bechtel D, Herman MV. Abnormalities of left ventricular function and geometry in adults with an atrial septal defect: ventriculographic, hemodynamic and echocardiographic studies. Am J Cardiol. 1975;36(3):302–8.
95. Jardin F, Dubourg O, Guéret P, Delorme G, Bourdarias J-P. Quantitative two-dimensional echocardiography in massive pulmonary embolism: emphasis on ventricular interdependence and leftward septal displacement. J Am Coll Cardiol. 1987;10(6):1201–6.
96. Boxt LM, Katz J, Kolb T, Czegledy FP, Barst RJ. Direct quantitation of right and left ventricular volumes with nuclear magnetic resonance imaging in patients with primary pulmonary hypertension. J Am Coll Cardiol. 1992;19(7):1508–15.
97. Belenkie I, Dani R, Smith ER, Tyberg JV. Effects of volume loading during experimental acute pulmonary embolism. Circulation. 1989;80(1):178–88.
98. Yamaguchi S, Harasawa H, Li KS, Zhu D, Santamore WP. Comparative significance in systolic ventricular interaction. Cardiovasc Res. 1991;25(9):774–83.
99. Farrar DJ, Woodard JC, Chow E. Pacing-induced dilated cardiomyopathy increases left-to-right ventricular systolic interaction. Circulation. 1993 Aug 1;88(2):720–5.
100. Hoffman D, Sisto D, Frater RW, Nikolic SD. Left-to-right ventricular interaction with a noncontracting right ventricle. J Thorac Cardiovasc Surg. 1994;107(6):1496–502.
101. Damiano RJ, La Follette P, Cox JL, Lowe JE, Santamore WP. Significant left ventricular contribution to right ventricular systolic function. Am J Phys. 1991;261(5 Pt 2):H1514–24.
102. Farrar DJ, Chow E, Brown CD. Isolated systolic and diastolic ventricular interactions in pacing-induced dilated cardiomyopathy and effects of volume loading and pericardium. Circulation. 1995 Sep 1;92(5):1284–90.
103. Schranz D, Rupp S, Müller M, Schmidt D, Bauer A, Valeske K, et al. Pulmonary artery banding in infants and young children with left ventricular dilated cardiomyopathy: a novel therapeutic strategy before heart transplantation. J Heart Lung Transplant. 2013;32(5):475–81.
104. Brookes C, Ravn H, White P, Moeldrup U, Oldershaw P, Redington A. Acute right ventricular dilatation in response to ischemia significantly impairs left ventricular systolic performance. Circulation. 1999 Aug 17;100(7):761–7.
105. Takagaki M, Ishino K, Kawada M, Ohtsuki S, Hirota M, Tedoriya T, et al. Total right ventricular exclusion improves left ventricular function in patients with end-stage congestive right ventricular failure. Circulation. 2003 Sep 9;108(10 suppl 1):II – 226–9.

106. Davis KL, Mehlhorn U, Laine GA, Allen SJ. Myocardial edema, left ventricular function, and pulmonary hypertension. J Appl Physiol. 1995 Jan 1;78(1):132–7.
107. Amà R, Leather HA, Segers P, Vandermeersch E, Wouters PF. Acute pulmonary hypertension causes depression of left ventricular contractility and relaxation. Eur J Anaesthesiol. 2006;23(10):824–31.
108. Pinsky MR, Perlini S, Luigi Solda P, Pantaleo P, Calciati A, Bernardi L. Dynamic right and left ventricular interactions in the rabbit: Simultaneous measurement of ventricular pressure-volume loops. J Crit Care. 1996;11(2):65–76.
109. Hosenpud JD, Bennett LE, Keck BM, Boucek MM, Novick RJ. The Registry of the International Society for heart and lung transplantation: seventeenth official report—2000. J Heart Lung Transplant. 2000;19(10):909–31.
110. Griepp RB, Stinson EB, Dong E, D a C, Shumway NE. Determinants of operative risk in human heart transplantation. Am J Surg. 1971;122(2):192–7.
111. Addonizio LJ, Gersony WM, Robbins RC, Drusin RE, Smith CR, Reison DS, et al. Elevated pulmonary vascular resistance and cardiac transplantation. Circulation. 1987;76:V52–5.
112. Kirklin JK, Naftel DC, Kirklin JW, Blackstone EH, White-Williams C, Bourge RC. Pulmonary vascular resistance and the risk of heart transplantation. J Heart Transplant. 1988;7(5):331–6.
113. Erickson KW, Costanzo-Nordin MR, O'Sullivan EJ, Johnson MR, Zucker MJ, Pifarré R, et al. Influence of preoperative transpulmonary gradient on late mortality after orthotopic heart transplantation. J Heart Transplant. 1990;9(5):526–37.
114. Chen JM, Levin HR, Michler RE, Prusmack CJ, Rose EA, Aaronson KD. Reevaluating the significance of pulmonary hypertension before cardiac transplantation: determination of optimal thresholds and quantification of the effect of reversibility on perioperative mortality. J Thorac Cardiovasc Surg. 1997;114(4):627–34.
115. Espinoza C, Manito N, Roca J, Castells E, Mauri J, Ribas M, et al. Reversibility of pulmonary hypertension in patients evaluated for orthotopic heart transplantation: importance in the postoperative morbidity and mortality. Transplant Proc. 1999;31(6):2503–4.
116. Costanzo MR, Augustine S, Bourge R, Bristow M, O'Connell JB, Driscoll D, et al. Selection and treatment of candidates for heart transplantation a statement for health professionals from the Committee on Heart Failure and Cardiac Transplantation of the Council on Clinical Cardiology, American Heart Association. Circulation. 1995 Dec 15;92(12):3593–612.
117. O'Connell JB, Bourge RC, Costanzo-Nordin MR, Driscoll DJ, Morgan JP, Rose EA, et al. Cardiac transplantation: recipient selection, donor procurement, and medical follow-up. A statement for health professionals from the Committee on Cardiac Transplantation of the Council on Clinical Cardiology, American Heart Association. Circulation. 1992 Sep 1;86(3):1061–79.
118. Mudge GH, Goldstein S, Addonizio LJ, Caplan A, Mancini D, Levine TB, et al. 24th Bethesda conference: Cardiac transplantation. Task Force 3: Recipient guidelines/prioritization. J Am Coll Cardiol. 1993;22(1):21–31.
119. Kirklin JK, Naftel DC, McGlffin DC, McVay RF, Blackstone EH, Karp RB. Analysis of morbid events and risk factors for death after cardiac transplantation. J Am Coll Cardiol. 1988;11(5):917–24.
120. Taylor DO, Edwards LB, Boucek MM, Trulock EP, Keck BM, Hertz MI. The Registry of the International Society for Heart and Lung Transplantation: twenty-first official adult heart transplant report—2004. J Heart Lung Transplant. 2004;23(7):796–803.
121. Murali S, Kormos RL, Uretsky BF, Schechter D, Reddy PS, Denys BG, et al. Preoperative pulmonary hemodynamics and early mortality after orthotopic cardiac transplantation: the Pittsburgh experience. Am Heart J. 1993;126(4):896–904.
122. Brimioulle S, Maggiorini M, Stephanazzi J, Vermeulen F, Lejeune P, Naeije R. Effects of low flow on pulmonary vascular flow–pressure curves and pulmonary vascular impedance. Cardiovasc Res. 1999;42(1):183–92.
123. Naeije R, Vachiery J-L, Yerly P, Vanderpool R. The transpulmonary pressure gradient for the diagnosis of pulmonary vascular disease. Eur Respir J. 2013;41(1):217–23.
124. Gorlitzer M, Ankersmit J, Fiegl N, Meinhart J, Lanzenberger M, Unal K, et al. Is the transpulmonary pressure gradient a predictor for mortality after orthotopic cardiac transplantation? Transpl Int Off J Eur Soc Organ Transplant. 2005;18(4):390–5.
125. Iberer F, Wasler A, Tscheliessnigg K, Petutschnigg B, Auer T, Müller H, et al. Prostaglandin E1-induced moderation of elevated pulmonary vascular resistance. Survival on waiting list and results of orthotopic heart transplantation. J Heart Lung Transplant. 1993;12(2):173–8.
126. Zales VR, Pahl E, Backer CL, Crawford S, Mavroudis C, Benson DW. Pharmacologic reduction of pretransplantation pulmonary vascular resistance predicts outcome after pediatric heart transplantation. J Heart Lung Transplant. 1993;12(6 Pt 1):965–72. discussion 972–3
127. Klotz S, Deng MC b, Hanafy D, Schmid C, Stypmann J, Schmidt C, et al. Reversible pulmonary hypertension in heart transplant candidates—Pretransplant evaluation and outcome after orthotopic heart transplantation. Eur J Heart Fail. 2003;5(5):645–53.
128. Drakos SG, Kfoury AG, Gilbert EM, Horne BD, Long JW, Stringham JC, et al. Effect of reversible pulmonary hypertension on outcomes after heart transplantation. J Heart Lung Transplant. 2007;26(4):319–23.
129. Kawaguchi A, Gandjbakhch I, Pavie A, Bors V, Muneretto C, Leger P, et al. Cardiac transplant recipients with preoperative pulmonary hypertension. Evolution of pulmonary hemodynamics and surgical options. Circulation. 1989;80(5 Pt 2):III90–6.

130. Butler J, Stankewicz MA, Wu J, Chomsky DB, Howser RL, Khadim G, et al. Pre-transplant reversible pulmonary hypertension predicts higher risk for mortality after cardiac transplantation. J Heart Lung Transplant. 2005;24(2):170–7.
131. Galiè N, Hoeper MM, Humbert M, Torbicki A, Vachiery J-L, Barbera JA, et al. Guidelines for the diagnosis and treatment of pulmonary hypertension The Task Force for the Diagnosis and Treatment of Pulmonary Hypertension of the European Society of Cardiology (ESC) and the European Respiratory Society (ERS), endorsed by the International Society of Heart and Lung Transplantation (ISHLT). Eur Heart J. 2009 Oct 1;30(20):2493–537.
132. McLaughlin VV, Archer SL, Badesch DB, Barst RJ, Farber HW, Lindner JR, et al. ACCF/AHA 2009 Expert Consensus Document on Pulmonary Hypertension A Report of the American College of Cardiology Foundation Task Force on Expert Consensus Documents and the American Heart Association: Developed in Collaboration With the American College of Chest Physicians, American Thoracic Society, Inc., and the Pulmonary Hypertension Association. Circulation. 2009 Apr 28;119(16):2250–94.
133. Adamson RM, Dembitsky WP, Jaski BE, Daily PO, Moreno R, Kim JC, et al. Left ventricular assist device support of medically unresponsive pulmonary hypertension and aortic insufficiency ASAIO. J Am Soc Artif Intern Organs 1992. 1997;43(4):365–9.
134. Alba AC, Rao V, Ross HJ, Jensen AS, Sander K, Gustafsson F, et al. Impact of fixed pulmonary hypertension on post-heart transplant outcomes in bridge-to-transplant patients. J Heart Lung Transplant. 2010;29(11):1253–8.
135. Kutty RS, Parameshwar J, Lewis C, Catarino PA, Sudarshan CD, Jenkins DP, et al. Use of centrifugal left ventricular assist device as a bridge to candidacy in severe heart failure with secondary pulmonary hypertension. Eur J Cardio-Thorac Surg Off J Eur Assoc Cardio-Thorac Surg. 2013;43(6):1237–42.
136. Bhatia SJ, Kirshenbaum JM, Shemin RJ, Cohn LH, Collins JJ, Di Sesa VJ, et al. Time course of resolution of pulmonary hypertension and right ventricular remodeling after orthotopic cardiac transplantation. Circulation. 1987;76(4):819–26.
137. Gajarski RJ, J a T, Bricker JT, Radovancevic B, Frazier OH, Price JK, et al. Intermediate follow-up of pediatric heart transplant recipients with elevated pulmonary vascular resistance index. J Am Coll Cardiol. 1994;23(7):1682–7.
138. Kimberling MT, Balzer DT, Hirsch R, Mendeloff E, Huddleston CB, Canter CE. Cardiac transplantation for pediatric restrictive cardiomyopathy: presentation, evaluation, and short-term outcome. J Heart Lung Transplant. 2002;21(4):455–9.
139. Russo MJ, Iribarne A, Hong KN, Ramlawi B, Chen JM, Takayama H, et al. Factors associated with primary graft failure after heart transplantation. Transplantation. 2010;90:444–50.
140. Iyer A, Kumarasinghe G, Hicks M, Watson A, Gao L, Doyle A, et al. Primary graft failure after heart transplantation. J Transp Secur. 2011;2011:175768.
141. Kirk R, Dipchand AI, Edwards LB, Kucheryavaya AY, Benden C, Christie JD, et al. The Registry of the International Society for Heart and Lung Transplantation: fifteenth pediatric heart transplantation report—2012. J Heart Lung Transplant. 2012;31(10):1065–72.
142. Stehlik J, Edwards LB, Kucheryavaya AY, Benden C, Christie JD, Dobbels F, et al. The Registry of the International Society for Heart and Lung Transplantation: Twenty-eighth Adult Heart Transplant Report—2011. J Heart Lung Transplant. 2011;30(10):1078–94.
143. Huang J, Trinkaus K, Huddleston CB, Mendeloff EN, Spray TL, Canter CE. Risk factors for primary graft failure after pediatric cardiac transplantation: importance of recipient and donor characteristics. J Heart Lung Transplant. 2004;23(6):716–22.
144. Patel ND, Weiss ES, Nwakanma LU, Russell SD, Baumgartner WA, Shah AS, et al. Impact of donor-to-recipient weight ratio on survival after heart transplantation analysis of the United Network for organ sharing database. Circulation. 2008 Sep 30;118(14 suppl 1):S83–8.
145. Costanzo-Nordin MR, Liao YL, Grusk BB, O'Sullivan EJ, Cooper RS, Johnson MR, et al. Oversizing of donor hearts: beneficial or detrimental? J Heart Lung Transplant. 1991;10(5 Pt 1):717–30.
146. Tamisier D, Vouhé P, Le Bidois J, Mauriat P, Khoury W, Leca F. Donor-recipient size matching in pediatric heart transplantation: a word of caution about small grafts. J Heart Lung Transplant. 1996;15(2):190–5.
147. Fraser CD, Jaquiss RDB, Rosenthal DN, Humpl T, Canter CE, Blackstone EH, et al. Prospective trial of a pediatric ventricular assist device. N Engl J Med. 2012 Aug 9;367(6):532–41.
148. Perez-Villa F, Farrero M, Sionis A, Castel A, Roig E. Therapy with sildenafil or bosentan decreases pulmonary vascular resistance in patients ineligible for heart transplantation because of severe pulmonary hypertension. J Heart Lung Transplant. 2010;29(7):817–8.
149. Perez-Villa F, Farrero M, Cardona M, Castel MA, Tatjer I, Penela D, et al. Bosentan in heart transplantation candidates with severe pulmonary hypertension: efficacy, safety and outcome after transplantation. Clin Transpl. 2013;27(1):25–31.
150. De Santo LS, Romano G, Maiello C, Buonocore M, Cefarelli M, Galdieri N, et al. Pulmonary artery hypertension in heart transplant recipients: how much is too much? Eur J Cardiothorac Surg. 2012 Nov 1;42(5):864–70.
151. Losman JG, Barnard CN. Heterotopic heart transplantation: a valid alternative to orthotopic transplantation: results, advantages, and disadvantages. J Surg Res. 1982;32(4):297–312.

152. Jahanyar J, Koerner MM, Ghodsizad A, Loebe M, Noon GP. Heterotopic heart transplantation: the United States experience. Heart Surg Forum. 2014;17(3):E132–40.
153. Stehlik J, Edwards LB, Kucheryavaya AY, Benden C, Christie JD, Dipchand AI, et al. The Registry of the International Society for Heart and Lung Transplantation: 29th official adult heart transplant report—2012. J Heart Lung Transplant. 2012;31(10):1052–64.
154. Birks EJ, Yacoub MH, Anyanwu A, Smith RR, Banner NR, Khaghani A. Transplantation using hearts from primary pulmonary hypertensive donors for recipients with a high pulmonary vascular resistance. J Heart Lung Transplant. 2004;23(12):1339–44.
155. Benden C, Edwards LB, Kucheryavaya AY, Christie JD, Dipchand AI, Dobbels F, et al. The Registry of the International Society for Heart and Lung Transplantation: Sixteenth Official Pediatric Lung and Heart-Lung Transplantation Report—2013; Focus Theme: Age. J Heart Lung Transplant. 2013;32(10):989–97.
156. Yusen RD, Christie JD, Edwards LB, Kucheryavaya AY, Benden C, Dipchand AI, et al. The Registry of the International Society for Heart and Lung Transplantation: Thirtieth Adult Lung and Heart-Lung Transplant Report—2013; Focus Theme: age. J Heart Lung Transplant. 2013;32(10):965–78.
157. Greyson CR. Right heart failure in the intensive care unit. Curr Opin Crit Care. 2012;18:424–31.
158. Daudel F, Tuller D, Krahenbuhl S, Jakob SM, Takala J. Pulse pressure variation and volume responsiveness during acutely increased pulmonary artery pressure: an experimental study. Crit Care. 2010;14(3):R122.
159. Von Ballmoos MW, Takala J, Roeck M, Porta F, Tueller D, Ganter CC, et al. Pulse-pressure variation and hemodynamic response in patients with elevated pulmonary artery pressure: a clinical study. Crit Care Lond Engl. 2010;14(3):R111.
160. Kieler-Jensen N, Lundin S, Ricksten SE. Vasodilator therapy after heart transplantation: effects of inhaled nitric oxide and intravenous prostacyclin, prostaglandin E1, and sodium nitroprusside. J Heart Lung Transplant. 1995;14(3):436–43.
161. Auler Júnior JO, Carmona MJ, Bocchi EA, Bacal F, Fiorelli AI, Stolf NA, et al. Low doses of inhaled nitric oxide in heart transplant recipients. J Heart Lung Transplant. 1996;15(5):443–50.
162. Rajek A, Pernerstorfer T, Kastner J, Mares P, Grabenwöger M, Sessler DI, et al. Inhaled nitric oxide reduces pulmonary vascular resistance more than prostaglandin E1 during heart transplantation. Anesth Analg. 2000;90(3):523–30.
163. Sablotzki A, Hentschel T, Gruenig E, Schubert S, Friedrich I, Mühling J, et al. Hemodynamic effects of inhaled aerosolized iloprost and inhaled nitric oxide in heart transplant candidates with elevated pulmonary vascular resistance. Eur J Cardiothorac Surg. 2002 Nov 1;22(5):746–52.
164. Vincent JL, Carlier E, Pinsky MR, Goldstein J, Naeije R, Lejeune P, et al. Prostaglandin E1 infusion for right ventricular failure after cardiac transplantation. J Thorac Cardiovasc Surg. 1992;103(1):33–9.
165. Maruszewski M, Zakliczyński M, Przybylski R, Kucewicz-Czech E, Zembala M. Use of sildenafil in heart transplant recipients with pulmonary hypertension may prevent right heart failure. Transplant Proc. 2007;39(9):2850–2.
166. Bauer J, Dapper F, Demirakça S, Knothe C, Thul J, Hagel KJ. Perioperative management of pulmonary hypertension after heart transplantation in childhood. J Heart Lung Transplant. 1997;16(12):1238–47.
167. Ardehali A, Hughes K, Sadeghi A, Esmailian F, Marelli D, Moriguchi J, et al. Inhaled nitric oxide for pulmonary hypertension after heart transplantation. Transplantation. 2001;72(4):638–41.
168. Wagner F. Monitoring and management of right ventricular function following cardiac transplantation. Appl Cardiopulm Pathophysiol. 2011;15:220–9.
169. Stobierska-Dzierzek B, Awad H, Michler RE. The evolving management of acute right-sided heart failure in cardiac transplant recipients. J Am Coll Cardiol. 2001;38(4):923–31.
170. Weis F, Beiras-Fernandez A, Kaczmarek I, Sodian R, Kur F, Weis M, et al. Levosimendan: a new therapeutic option in the treatment of primary graft dysfunction after heart transplantation. J Heart Lung Transplant. 2009;28(5):501–4.
171. Pérez Vela JL, Corres Peiretti MA, Rubio Regidor M, Hernández Tejedor A, Renes Carreño E, Arribas López P, et al. Levosimendan for postoperative ventricular dysfunction following heart transplantation. Rev Esp Cardiol Engl Ed. 2008;61(5):534–9.
172. Beiras-Fernandez A, Kur F, Kaczmarek I, Frisch P, Weis M, Reichart B, et al. Levosimendan for primary graft failure after heart transplantation: a 3-year follow-up. Transplant Proc. 2011;43(6):2260–2.
173. Arafa OE, Geiran OR, Andersen K, Fosse E, Simonsen S, Svennevig JL. Intraaortic balloon pumping for predominantly right ventricular failure after heart transplantation. Ann Thorac Surg. 2000;70(5):1587–93.
174. Ibrahim M, Hendry P, Masters R, Rubens F, Lam B-K, Ruel M, et al. Management of acute severe perioperative failure of cardiac allografts: a single-centre experience with a review of the literature. Can J Cardiol. 2007;23(5):363–7.
175. Tenderich G, Koerner MM, Stuettgen B, Minami K, El-Banayosy A, Arusoglu L, et al. Mechanical circulatory support after orthotopic heart transplantation. Int J Artif Organs. 1998;21(7):414–6.
176. Minev PA, El-Banayosy A, Minami K, Körtke H, Kizner L, Körfer R. Differential indication for mechanical circulatory support following heart transplantation. Intensive Care Med. 2001;27(8):1321–7.
177. Thomas HL, Dronavalli VB, Parameshwar J, Bonser RS, Banner NR. Incidence and outcome of Levitronix CentriMag support as rescue therapy for early cardiac allograft failure: a United Kingdom

national study. Eur J Cardiothorac Surg. 2011 Dec 1;40(6):1348–54.
178. D'Alessandro C, Aubert S, Golmard JL, Praschker BL, Luyt CE, Pavie A, et al. Extra-corporeal membrane oxygenation temporary support for early graft failure after cardiac transplantation. Eur J Cardiothorac Surg. 2010 Feb 1;37(2):343–9.
179. Marasco SF, Esmore DS, Negri J, Rowland M, Newcomb A, Rosenfeldt FL, et al. Early institution of mechanical support improves outcomes in primary cardiac allograft failure. J Heart Lung Transplant. 2005;24(12):2037–42.
180. Marasco SF, Vale M, Pellegrino V, Preovolos A, Leet A, Kras A, et al. Extracorporeal membrane oxygenation in primary graft failure after heart transplantation. Ann Thorac Surg. 2010;90:1541–6.
181. Listijono DR, Watson A, Pye R, Keogh AM, Kotlyar E, Spratt P, et al. Usefulness of extracorporeal membrane oxygenation for early cardiac allograft dysfunction. J Heart Lung Transplant. 2011;30(7):783–9.
182. Bando K, Konishi H, Komatsu K, Fricker FJ, del Nido PJ, Francalancia NA, et al. Improved survival following pediatric cardiac transplantation in high-risk patients. Circulation. 1993;88(5 Pt 2):II218–23.
183. Kirshbom PM, Bridges ND, Myung RJ, Gaynor JW, Clark BJ, Spray TL b. Use of extracorporeal membrane oxygenation in pediatric thoracic organ transplantation. J Thorac Cardiovasc Surg. 2002;123(1):130–6.
184. Goland S, Czer LSC, Kass RM, De Robertis MA, Mirocha J, Coleman B, et al. Pre-existing pulmonary hypertension in patients with end-stage heart failure: impact on clinical outcome and hemodynamic follow-up after orthotopic heart transplantation. J Heart Lung Transplant. 2007;26(4):312–8.
185. Stehlik J, Edwards LB, Kucheryavaya AY, Aurora P, Christie JD, Kirk R, et al. The Registry of the International Society for Heart and Lung Transplantation: Twenty-seventh official adult heart transplant report—2010. J Heart Lung Transplant. 2010;29(10):1089–103.
186. Bourge RC, Kirklin JK, Naftel DC, White C, Mason DA, Epstein AE. Analysis and predictors of pulmonary vascular resistance after cardiac transplantation. J Thorac Cardiovasc Surg. 1991;101(3):432–44. discussion 444–5
187. Lindelöw B, Andersson B, Waagstein F, Bergh CH. High and low pulmonary vascular resistance in heart transplant candidates. A 5-year follow-up after heart transplantation shows continuous reduction in resistance and no difference in complication rate. Eur Heart J. 1999;20(2):148–56.
188. Delgado JF, Conde E, Sánchez V, López-Ríos F, Gómez-Sánchez MA, Escribano P, et al. Pulmonary vascular remodeling in pulmonary hypertension due to chronic heart failure. Eur J Heart Fail. 2005;7(6):1011–6.
189. Gläser S, Meyer R, Opitz CF, Hetzer R, Ewert R. Pulmonary interstitial and vascular abnormalities following cardiac transplantation. Transplant Proc. 2008;40(10):3585–9.

Medical Therapy for Chronic Right Ventricular Failure in Congenital Heart Disease

16

S. Lucy Roche

Abstract

The clinical importance of right ventricular (RV) function has been increasingly recognised in populations with and without congenital heart disease (CHD). CHD patients most at risk of chronic RV failure are those with repaired tetralogy of Fallot (TOF), atrial baffle redirection procedures for transposition of the great arteries (TGA-baffle), congenitally corrected transposition of the great arteries (ccTGA), Ebstein anomaly of the tricuspid valve or a Fontan circulation with a dominant RV. This chapter considers medical management options that might be beneficial in these groups. It reviews current literature and guidelines, offers opinions based on clinical experience and discusses potential avenues for future research.

Keywords

Congenital heart disease • Heart failure • Right ventricle • Pharmacological therapy

Introduction

Whether there is benefit to be derived from the medical treatment of chronic heart failure (HF) in patients with congenital heart disease (CHD) remains unproven. While outcome data from HF medication studies in CHD patients have been underwhelming, anatomical, electrical and physiological dissimilarities restrict confident application of evidence or guidelines in non-CHD populations. There is particular need for pause when contemplating the use of medical therapies of known benefit in systolic left ventricular (LV) failure for CHD patients whose primary problem is a failing right ventricle (RV). A failing RV in patients with CHD may have been subject to surgical incision, decades of exposure to abnormal loading conditions and/or the effects of chronic pacing; any of which could induce significant divergence from the pathophysiological pathways seen in acquired HF. In addition, a RV has an inherently different myocardial fibre arrange-

S.L. Roche
The Peter Munk Cardiac Center, University Health Network, Toronto Congenital Cardiac Center for Adults, 5N-521, 585 University Avenue, Toronto, ON, Canada, M5G 2N2
e-mail: lucy.roche@uhn.ca

M.K. Friedberg, A.N. Redington (eds.), *Right Ventricular Physiology, Adaptation and Failure in Congenital and Acquired Heart Disease*, https://doi.org/10.1007/978-3-319-67096-6_16

ment and geometry from a LV and this too may affect its processes and mechanisms of failure. This chapter reviews what is known about medical therapy for chronic RV failure in patients with CHD, considers the available data and its quality and draws on the author's clinical experience of caring for these patients as children and adults. Underpinning the narrative is an assumption that potentially reversible causes of RV dysfunction (arrhythmia, valve disease, baffle leaks, volume loading due to arterial-venous collaterals, dyssynchronous pacing and the potential to improve hemodynamics by surgical revision) have been already addressed.

Medical Therapy for Symptom Control

In CHD, patients with quite severe RV dysfunction often remain well compensated for many years. Symptoms usually arise relatively late in the "natural" history and may first be recognised when something additional occurs to tip the balance: arrhythmia, inter-current infection, surgery or development of pulmonary hypertension. The symptoms and signs of chronic RV failure in CHD depend in part on the RV's position (subaortic or subpulmonary) as well as on the type of circulation (biventricular or single ventricle physiology) and perhaps also on whether the main problem is systolic or diastolic dysfunction.

Fluid overload affects most CHD patients with a failing RV, albeit to different extents and with different patterns of symptoms. Patients with a failing subpulmonary RV (TOF, Ebstein anomaly, unrepaired ASDs, Eisenmenger syndrome) or a failing single RV in a Fontan circulation tend to manifest classic features of "right-sided HF" with elevated jugular venous pressures, hepatic enlargement, peripheral edema and ascites. These symptoms and signs are less prevalent in patients with a failing systemic RV in a biventricular circulation, but so also are clasisic "left-sided HF" manifestations, at least until the later stages of disease. In patients with ccTGA or TGA-baffle and a failing RV, fluid overload can be difficult to detect clinically, existing as hemodynamic-congestion, only evident on cardiac catheterisation. Somewhat arbitarily, our group routinely performs cardiac catheterisation in ccTGA and TGA-baffle patients once they reach the age of 40 years, because we have noted elevated filling and pulmonary artery pressures are so difficult to detect by any other means.

While it forms a keystone of most HF self-care behaviour advice, in fact sodium and fluid restriction in HF remains a much-debated topic. All contemporary general adult and paediatric HF guidelines recommend some degree of fluid and sodium intake restriction (Table 16.1). These recommendations are based on population data that excessive sodium adversely affects cardiovascular outcomes [1], an understanding that maladaptive activation of the renin-angiotensin-aldosterone system leads to sodium and water retention [2] and from recognition that fluid overload is very often the stimulus for HF hospitalizations [3]. Nevertheless, the evidence available from clinical studies fails to support an aggressive approach. Travers et al. conducted the first randomised trial of fluid restriction versus free fluids in patients with acute decompensated HF in 2007 [4]. This study of 67 patients showed that fluid restriction to 1 L per day had no impact on time to discontinuation of intravenous therapy or markers of clinical and biochemical stability [4]. Paterna et al.'s 2008 study of 232 outpatients with stable chronic HF, compared the impact of a normal (120 mmol) and low (80 mmol) sodium diet [5]. During 180 days of follow-up, the low sodium diet was associated with adverse neurohormonal effects and increased risk of hospital admission [5]. In 2013, Aliti and colleagues published the results of a randomised clinical trial conducted in 75 patients with acute HF and found that at 3 days after hospital admission, aggressive sodium and fluid restriction (<800 mL and <800 mg per day) had no effect on weight loss or clinical stability [6]. This somewhat counterintuitive data has led to several reviews articles that discuss how we should counsel patients with HF about sodium and fluid restriction [7–9]. Most authorities support mild to moderate fluid and

Table 16.1 Recommendations regarding sodium and fluid restriction in heart failure

Reference	Body	Patients	Daily Na intake		Daily fluid intake	
			Amount	Class/level	Volume	Class/level
Can J Cardiol 2006;22:23–45	Canadian Cardiovascular Society	Adults	2–3 g with reduction to 1–2 g in advanced HF	Class 1 Level C	1.5–2 L in all with uncontrolled fluid overload or those with renal dysfunction or hyponatremia	Class 1 Level C
J Card Fail 2010;16:475–539	Heart failure Society of America	Adults	2–3 g and <2 g in severe HF	Level C	<2 L if Na <130 mEq/L. Should be considered when difficult to control fluid overload	Level C
Eur Heart J 2012 33:1787–847	European society of Cardiology	Adults	Na restriction may help control symptoms and signs	Not provided	1.5–2 L may be considered in severe HF. Routine restriction in all patients probably not of benefit	Not provided
Circulation 2013;128:e240–e327	American Heart Association	Adults	1.5 g for stage A&B, consider some degree (<3 g) for stage C&D	Class IIa Level C	Not discussed	–
Can J Cardiol 2013;29:1535–1552	Canadian Cardiovascular Society	Children	Not discussed	–	Restriction to 80% of basal requirements may be necessary in some patients	–
ISHLT monograph series Volume 8 published 2014	International Society of Heart and Lung Transplantation	Children with acute heart failure	Fluid restriction is reasonable for patients with acute heart failure regardless of serum sodium	Class IIa Level C	A low sodium diet is reasonable for hospitalized patients	Class IIa Level C

sodium restriction in patients with HF and suggest that stricter restriction less likely to be beneficial and may indeed carry some risk. There is no data on this subject specific to patients with CHD. Until further evidence becomes available it seems reasonable to suggest mild to moderate restriction for CHD patients with RV failure and in clinical practice this approach generally reduces symptoms.

Although their effects on disease progression and mortality remain uncertain, diuretics are the pharmacological mainstay of treatment for symptoms of HF related to hypervolemia [10, 11]. They are recommended for symptom relief in general adult and paediatric HF guidelines [12–16] and appear clinically successful at relieving symptoms and improving hemodynamics in CHD patients with RV failure. Diuretics have different mechanisms of action, but for the most part function by blocking sodium reabsorption from different parts of the renal tubules. Furosemide is the most familiar diuretic used in the management of heart failure. It is a loop diuretic, acting at the ascending limb

of the loop of Henle and distal tubule, impairing reabsorption of sodium, potassium and chloride. Metolazone, a thiazide-like diuretic that works in the distal tubule, can be a useful addition in some patients, but care must be taken to monitor electrolytes for hypokalemia. Potassium-sparing aldosterone antagonists and potassium supplementation are often required. Patients with hepatic involvement may gain particular benefit from spironolactone, which is recommended, as the drug of choice in the initial treatment of ascites due to cirrhosis [17, 18]. We have noted clinical improvement after addition of high dose spironolactone (100 mg or more) to the diuretic regimen of failing adult Fontan patients or those with Ebstein anomaly, again careful monitoring of serum electrolytes is essential. When trying to make rational decisions about medical therapy for chronic RV failure in CHD, it is also important to be aware that aldosterone antagonists have been identified as drugs with potential anti-fibrotic properties [19]. Given the growing evidence that fibrosis plays an important role in the pathophysiology of HF in CHD, particularly in conditions such as TOF [20, 21] and TGA-baffle [22, 23] these drugs may have theoretical benefits beyond their role in symptom control.

Diuretic doses may need frequent adjustment in the initial stages of therapy and blood pressure and electrolytes should be monitored closely after any medication change. Further adjustments may be needed as a patient's HF progresses. The aim should be to identify and maintain a euvolaemic state in which the patient has minimal symptoms or signs of fluid overload. If patients are listed for cardiac transplant we perform frequent (3–6 monthly depending on the diagnosis) invasive hemodynamic studies and adjust diuretics according to intra-cardiac and pulmonary pressures so as to maintain optimum clinical condition for as long as possible while on the waiting list.

Without measures that improve cardiac output, it is difficult to tackle the lethargy, decreased exercise capacity and general malaise from which patients with a failing subaortic RV (ccTGA, TGA-baffle) frequently suffer. However, exercise training [21], lifestyle modification and addressing systemic issues such as anaemia [24–26] and thyroid disorders [27] may have benefit.

Potential Disease-Modifying Medications

The neurohormonal hypothesis is a key reason that HF advances, even in instances where the initial activating injury has ceased and its direct effects on the myocardium have ended. Neurohormonal activation is a maladaptive response to cardiac injury/stress that both exacerbates hemodynamic abnormalities and has independent, direct toxic effects on cardiac cells. A wealth of mechanistic evidence supports this hypothesis and therapies targeted against neurohormonal activation are proven to reduce mortality and hospital admissions in non-CHD adult HF patients with systolic dysfunction. On the strength of this evidence the 2013 American College of Cardiology Foundation/American Heart Association guideline for the management of heart failure recommends an angiotensin converting enzyme inhibitor (ACEi) and sympathetic beta-receptor antagonist (β-blocker) in all patients without contraindications who have reduced ejection fraction and current or prior symptoms of HF [12]. They recommend that patients who cannot take ACEi be prescribed an angiotensin receptor blocker (ARB) [12]. In addition, and with some additional specified criteria, these guidelines recommend aldosterone receptor antagonists in patients with New York Heart Association (NYHA) class II-IV HF and an LV ejection fraction of <35% [12]. All adult HF guidelines from other major bodies carry similar advice [13, 14, 28]. The 2013 ACC/AHA guidelines unambiguously state that they do not address HF in the setting of CHD [12]. This is not made explicit in the European Society of Cardiology [13] or Heart Failure Society of America [28] guidelines but since CHD is not included in the former's list of causes of HF or the latter's section on special populations, one can assume the documents were not intended for direct application to this patient group.

Adults and children with CHD also exhibit biochemical evidence of neurohormonal activation [29, 30]; although there is much individual variation with levels highly dependent on age and underlying hemodynamic substrate [30–32]. One of the largest studies of neurohormonal activation in patients with CHD considered levels of NT-proBNP in 475 adult outpatients with a broad cross-section of repaired lesions [31]. This 2013 study by Eindhoven et al. found that NT-proBNP levels correlated with NYHA functional class and some echocardiographic parameters [31]. The investigators reported NT-proBNP levels >3 times above their laboratory upper reference range value of 14 pmol/L in 28% of Mustard patients, 55% of ccTGA and 18% of TOF patients [31]. Again in a mixed CHD population, Giannakoulas et al. found neurohormonal activation to be prevalent [33]. This was the first study to document an association between BNP level and mortality adults with CHD and of the 49 patients included 18 (37%) had TOF and 6 (12%) had a systemic RV [33]. The cut-off identified in this unselected population of consecutive patients recruited from ambulatory ACHD clinics was 78 pg/mL [33]. In our own ACHD/HF clinic, which includes only patients with identified HF or referred for transplant assessment; there are very few patients with BNP levels below this. Most patients having levels in the mid-hundreds to thousands (unpublished data) and we therefore find it challenging to apply this cut-off as means of stratifying risk. Plymen et al. investigated NT-proBNP levels and their relationship to ECG and MRI indices in 35 adults with Mustard or Senning repairs of TGA [34]. This group found modest but statistically significant correlations between NT-proBNP and QRS duration, RV volumes and ejection fraction as measured by magnetic resonance imaging (MRI) [34]. There are several other, mostly small-scale, studies looking at NT-proBNP or BNP in children and adults with repaired TOF [32–36]. In general, their findings suggest that patients with repaired TOF also exhibit neurohormonal activation and that the degree of this activation may correspond to RV size, dysfunction and exercise capacity [35–39].

The studies discussed in the preceding paragraph lend support to the hypothesis that patients with CHD including those with failing RVs exhibit neurohormonal activation and suggest that while individual variability exists, there is some correlation between this activation and worsening clinical, hemodynamic and/or RV contractile status. However in the main, investigations of RV failure in CHD have studied only BNP or NT-proBNP and it remains true that little is yet known about activation of the renin-angiotensin aldosterone or sympathetic nervous system in this patient group, or even in the wider population of RV failure without CHD [40]. Nothing is understood about the extent to which maladaptive compensatory mechanisms might control evolution of RV failure in CHD. It is entirely possible that the prominence of other issues (such as abnormal atrioventricular coupling, chronic tricuspid or pulmonary regurgitation, decades of abnormal electromechanical interaction or ventricular fibrosis) may completely eclipse neurohormonal activation as a driver of HF progression in these specific patients. If so, neurohormonal activation might simply be the wrong pathophysiological focus [41]. It is however important to review the data that exists regarding clinical uses of these agents for RV failure in CHD and what the CHD guidelines currently recommend.

There have been several small studies and randomised, controlled trials of ACEi/ARBs and β-blockers in patients with subaortic RVs, which are summarised in Table 16.2. Studies looking at the role of neurohormonally active medications in patients with a Fontan circulation or TOF are summarized in Table 16.3. The results of ACEi/ARB studies in patients with a systemic RV have thus far been disappointing with no signal these medications are likely to be of clinical benefit in this population, despite several randomised, placebo-controlled trials. Data regarding β-blockade are a little more encouraging, but the quality of these data is less impressive and those relating specifically to RV failure are smaller-scale and in the main, retrospective or observational in design. Data regarding the role

of these medications in patients with a Fontan circulation and dominant RV is sparse, but that which exists also suggests no benefit. A similar story is seen in studies regarding neurohormonal therapy in patients with TOF. One double-blind randomized, placebo-controlled trial of ramipril vs. placebo in 72 patients with repaired TOF did find improvement in RV long-axis shortening in those who were treated with ramipril for 6 months, although RVEF did not improve [42].

Published guidelines addressing the management of pediatric HF have been published and sections relevant to this discussion. The 2014 Canadian Cardiovascular Society guidelines on presentation, diagnosis and management of heart failure in children suggest use of an ACEi is indicated in children with primary heart muscle disease of a systemic LV and that β-blockers might be indicated in treatment of moderate to severe systolic LV dysfunction [15], but the role of these medications in children with primary RV failure is not directly addressed [15]. The International Society of Heart and Lung Transplantation's (ISHLT) monograph series includes the 2014 publication: ISHLT Guidelines for the Management of Pediatric Heart Failure [16]. Chapter 6: Pharmacological treatment of chronic heart failure with reduced systolic ejection fraction, provides recommendations regarding neurohormonally active medications that are similar to those of general adult HF guidelines, but specifies these relate only to patients with systemic LV systolic failure [16]. Chapter 12 of the monograph discusses special pediatric HF populations and specifically addresses RV failure in the setting of CHD [16]. The section on systemic RV failure in a biventricular circulation (which in children will almost always mean ccTGA) states that there is no evidence to support prophylactic use of ACEi or ARBs but these medications might be reasonably considered once RV dysfunction is evident (Class IIa, level of evidence C) [16]. No recommendations are made either for or against use of β-blockers [16]. The section relating to chronic single ventricle failure cites data from the Pediatric Heart Network Infant Single Ventricle Trial [43] and makes a Class IIb recommendation against routine use of ACEi in single ventricle patients with preserved ejection fraction but again states that ACEi can reasonably be considered in those with systemic ventricular dysfunction [16]. Here no reference is made to ventricular morphology. They state there is not enough data to make a recommendation regarding use of β-blockers in children with failing single ventricles [16].

Physicians must thus make therapeutic decisions on an individual patient basis, reflecting on the potential benefits and risks of medication and reasonable arguments and experience rather than definite evidence. ACHD patients with chronic RV failure often experience coexisting complications of atrial or ventricular tachyarrhythmia [44–43] and sudden cardiac death is a particular concern for patients with failing subaortic RVs or with RV failure after TOF repair [44–48]. With this in mind, it is reasonable to develop an argument in favour of prescribing β-blockers to patients with severe subaortic RV dysfunction or RV dysfunction in the setting of repaired TOF, especially if there is evidence of biventricular failure. If prescribing a β-blocker, it seems sensible to choose one with demonstrated mortality efficacy in general adult systolic HF trials (bisoprolol, sustained release metoprolol or carvedilol) as data suggest benefit from β-blockade in HF cannot be considered a class effect [12]. For patients with a failing subpulmonary RV with any suggestion of coexisting subaortic LV failure or evidence that chronic ischemia might be a contributor, arguments in favor of ACEi/ARB prescription carry significant sway. The role of these medications in patients with a subaortic RV is much less certain and in fact the evidence summarized in Table 16.2 suggests ACEi/ARB may have no benefit at all in this population. It is the author's observation that adult Mustard, Senning and ccTGA patients with severe, symptomatic RV dysfunction are often hypotensive, with systolic blood pressure in the 80–95 mmHg range and associated dizziness and pre-syncope. By the time they are referred to our ACHD/HF clinic these patients have usually been taking an ACEi or ARB for a number of years. In most cases, gradually reducing and then stopping these

Table 16.2 Studies of neurohormonal modulation in patients with a subaortic right Ventricle

Reference	Population	Drug	Study Design	N	Therapy duration	Outcome
Am J Cardiol 2001;88:1314–16	Mustard or Senning patients aged >13 years. who had never taken ACEi	Losartan	Randomized placebo controlled crossover	7	8 weeks	Improved exercise duration, reduced TR
Am J Cardiol 2001;87:660–663	Mustard adults	ACEi	Observational retrospective	14	2 years	No difference in exercise capacity or MRI measured ejection fraction
Circulation 2005;112:2411–2416	Adults with subaortic RV (Mustard/ Senning/ccTGA)	Losartan	Multicenter randomized double-blind placebo-controlled	29	15 weeks	No improvement in exercise capacity or NT-proBNP levels
Inj J Cardiol 2008;129:187–192	Mustard or Senning adults	Ramipril	Randomized double-blind placebo-controlled	17	1 year	No benefit in RV function as assessed by MRI or exercise capacity
Circulation 2013;127:322–330	Adults with subaortic RV (Mustard/ Senning/ccTGA)	Valsartan	Multicenter randomized double-blind placebo-controlled	88	3 years	No benefit in RV function assessed by MRI, exercise capacity, TR, Q of L or neurohormonal activation
Can J Cardiol 2006;22;769–772	Mustard or Senning adults with impaired RV function who were taking a β-blocker	Any β-blocker	Case series	8	3 years	Drugs well-tolerated and associated with a trend towards improved symptoms, less TR and improved functional status
Int J Cardiol 2007;114:241–246	Adults with subaortic RV (Mustard/ Senning/cc/TGA) and RV dysfunction, no pacemakers	Carvedilol	Prospective with patients studied before and after treatment	8	12 months	Drug safe and target dose achieved in 5/8 patients. RVEF and LVEF improved, exercise duration increased, VO_{2peak} unchanged

(continued)

Table 16.2 (continued)

Reference	Population	Drug	Study Design	N	Therapy duration	Outcome
Am J Cardiol 2007;99:704–706	Mustard or Senning adults	Any β-blocker: Carvedilol n = 15 Metoprolol n = 16	Retrospective chart review	60	4 months	Significant improvement in NYHA functional class if treated with β-blocker but effect seen only in those with pacemakers
JAMA 2007;298:1171–1179	Children and adolescents with symptomatic systolic heart failure. 43 patients with a subaortic ventricle that was not an LV	Carvedilol	Multicenter, randomized, double-blind, placebo controlled trial	161	8 months	No difference in composite endpoint Non-beneficial trend in those CHD patients whose subaortic ventricle was not an LV (included Fontan)
Cardiol Young 2010;20:615–619	Adults with subaortic RV (Mustard/ Senning/ccTGA)	Bisoprolo n = 13 Carvedilol n = 1	Prospective with patients studied before and after treatment	14	13 months	RNA measured RVEF improved but change in RVEF as measured by MRI not significant, NYHA class improved, No change VO_{2peak} or NT-proBNP

Table 16.3 Studies of neurohormonal modulation in patients with Fontan palliation or Tetralogy of Fallot

Reference	Population	N	Number with RV dominant anatomy	Drug	Study design	Therapy duration	Outcome
Circulation 1997;96:1507–1512	Children and young adults after a Fontan procedure	18	Not clear but probably only 2	Enalapril	Randomized, double-blind, placebo-controlled crossover trial	10 weeks	No benefit in exercise performance, systemic vascular resistance or resting cardiac index
Circulation 2010;122:333–340	Infants <45 days old with single ventricle physiology	230	Not provided but 127 had hypoplastic left heart syndrome	Enalapril	Multicenter, randomized, double-blind, placebo-conrtrolled trial	Followed until 14 months of age	No improvement in growth, ventricular function or heart failure severity
Cardiol Young 2007;17:372–379	Adults with repaired tetralology of Fallot	33		Bisoprolol	Randomized, double-blind, placebo-controlled trial	6 months	No beneficial effect on NT-proBNP exercise capacity or ventricular function as measured by MRI
Int J Cardiol 2012;154:299–305	Adults with repaired tetralology of Fallot	64		Ramipril	Randomized, double-blind, placebo-controlled trial	6 months	No difference in MRI-measured RV ejection function. RV and LV long axis shortening improved in treatment group. No changes in NT-proBNP or exercise capacity

medications seems to improve blood pressure and alleviates dizziness. This strategy usually permits up-titration of a β-blocker, which as already discussed, is of value in these patients to reduce their poorly tolerated intermittent atrial and ventricular arrhythmias.

Medical Treatment of Pulmonary Hypertension

Pulmonary hypertension should be considered as both a potential cause of and an adverse effect from chronic RV failure in patients with CHD. The medical treatment of pulmonary vascular disease may play an important role when it is a cause of subpulmonary RV failure. It is important to appreciate that patients with TGA are particularly vulnerable to the development of pulmonary hypertension and pulmonary vascular disease. This is an increasing problem for Mustard and Senning patients who have developed subaortic RV failure and subsequent elevation of left atrial pressure. In many instances this complication has been considered a contraindication to heart-only transplantation, resulting in referral for heart-lung transplantation, which has inferior long-term outcomes. Our group has found that aggressive diuresis in TGA-baffle patients with failing subaortic RVs and pulmonary hypertension can significantly improve baseline hemodynamics, even in patients without overt clinical signs of fluid overload. In some cases, with careful progressive and carefully monitored increases in diuretic doses, we have been able to reduce previously highly elevated pulmonary artery pressures and trans-pulmonary gradients into a range acceptable for heart-only transplantation. This usually takes several weeks, requires the addition of potassium sparing diuretics or supplements and weekly (sometimes more frequent) follow-up visits to our ACHD/HF clinic. It remains to be seen how long this improvement can be maintained and it seems likely that if we are to continue to pursue heart-only transplant, some of our patients will require subaortic RV assist devices to support them during the wait for a suitable donor organ.

Future Directions: RV Specific Therapies

Although they are interlinked, from the earliest stages of fetal development there are also fundamental differences between the right and left ventricles of the heart [49]. The orientation of RV myofibrils is unlike the arrangement seen in the LV [50] and this produces differences in RV [51, 52] and LV [53] contractile properties which are essential for efficient movement of blood through two such geometrically distinct chambers. The two ventricles have different myocardial oxygen demand/supply balances [54] and responses to ischemia [55–57] and other stressors. In a subpulmonary position, the RV usually operates against a low resistance system and it tolerates rapid increases in afterload poorly. However, in a subaortic position, the RV can function against a chronically high afterload. It seems to adapt through hypertrophy, dilatation and with increased circumferential shortening [58–60]. However, in the absence of a middle circular layer of muscle fibres [50] a subaortic RV remains unable to produce the highly efficient smooth wringing/unwringing motion that would be generated by a subaortic LV [58, 60]. Given these distinctions, and the growing suspicion that drugs successful in treating LV systolic dysfunction may not be effective (or as effective) in chronic RV failure in CHD, we perhaps ought to seek more specific RV therapies.

The ideal RV specific drug might have the following properties: Increase RV inotropy, reduce RV fibrosis, promote RV reverse remodelling and dilate the pulmonary vasculature while having few effects on the systemic circulation. Ideally, this drug's efficacy could be monitored noninvasively, since it would cause an improvement in RV ejection fraction, reduce RV size and diminish tricuspid regurgitation and these positive effects would lead to measurable improvements in exercise capacity, clinical status and reduce the risk of both arrhythmia and mortality. Sadly, at the moment no such drug exists. However, there are some interesting potential candidates.

Phosphodiesterase type 5 (PDE5) inhibitors, typically known for their vascular smooth muscle relaxation properties, have to date primarily been

used in situations where this is the desired effect (pulmonary arterial hypertension, erectile dysfunction). In 1999 an expert consensus document stated that due to absence of PDE5 expression in cardiac myocytes, sildenafil lacked direct effects on the myocardium; although it did mention the drug had not been extensively studied in patients with heart failure [61] As it turns out, PDE5 can be expressed by cardiac myocytes, but only in hypertrophied myocardium, something which could potentially be turned to therapeutic advantage [62] In 2007, Nagendran et al. studied surgical specimens from nine patients, seven of whom had RV hypertrophy (three as a result of TOF and one with hypoplastic left heart syndrome), one with LV hypertrophy and one without any ventricular hypertrophy [62]. PDE5 expression was markedly up-regulated in the hypertrophied RV and LV myocardium but not seen in the normal ventricles [62]. In the patient with a hypertrophied LV but normal RV, PED5 was only expressed in the LV [62]. These investigators also studied the isolated perfused hearts and cardiomyocytes from an animal model of RV hypertrophy [62]. They found significant PDE5 expression occurred in only in the hypertrophied RV chambers and that PDE5 inhibition increased RV contractility in those specimens [62]. The authors hypothesised that PDE5 inhibitors might have an important role in cardiac conditions where RV hypertrophy and failure predominate, both for their direct myocardial and pulmonary vasculature effects [62].

Goldberg et al. conducted a randomized, double-blind, placebo-controlled cross over trial looking at oral sildenafil in 28 children and young adults with a Fontan circulation [63]. Fifteen of the patients included in this study had a single ventricle of RV morphology [63]. After 6 weeks of oral sildenafil subjects demonstrated improvement in their myocardial performance index and in the product of the velocity time integral of the dominant outflow tract [64] although cardiovascular exercise performance measures (particularly in those with a dominant RV) were not improved [63]. Tunks et al. studied the hemodynamic effects of a single dose of iv sildenafil in 9 children with a Fontan (6/9 with a single RV) [65]. They found that stroke volume and cardiac output improved, with no change in heart rate and a fall in both systemic and pulmonary vascular resistance [65]. Van De Bruaene et al. performed MRIs at rest and during exercise before and after a single dose of oral sildenafil in 10 adult patients with a Fontan (2/10 had a single RV) and measured pulmonary artery pressures with a central venous catheter [66]. This group found sildenafil improved cardiac index during exercise, with an increase in stroke work index and a fall in pulmonary vascular index [66]. These studies were designed to examine whether pharmacological pulmonary vasodilation might be advantageous in a Fontan circulation and not specifically to look at the potential inotropic effects of PDE5 inhibition in patients with systemic RVs. Nonetheless they provide an interesting signal of benefit and further investigation might well prove valuable.

Metabolic modulators are another group of drugs with potential promise as an RV-specific therapy, primarily in situations that result in RV hypertrophy. Better known as anti-angina drugs, trimetazidine and ranolazine are inhibitors of fatty acid oxidation (FAO) that act within mitochondria to modify the pathways of cellular energy (ATP) generation, altering the balance of carbohydrate and fat metabolism [67, 68]. Owing to its reciprocal relationship with carbohydrate metabolism [69], inhibiting FAO results in an increase in pyruvate oxidation and shifting the balance towards glucose as the primary source of acetyl coenzyme A (and hence ATP) production. An additional effect of this switch is less reduction of pyruvate and less anaerobic glycolysis. This is relevant because hearts with RV hypertrophy demonstrate a mitochondrial metabolic adaptation favouring anaerobic glycolysis [70], which is associated with impaired RV contractility, decreased cardiac output and adverse electrical remodelling [71, 72]. In experimental models of RV hypertrophy, forcing a shift (for example by inhibiting FAO) away from anaerobic glycolysis and towards pyruvate oxidation improves RV performance [72]. In patients whose RV hypertrophy is in some part related to pulmonary vasculature disease inhibitors of FAO may prove particularly useful because these drugs also seem to beneficially affect metabolism in the pulmo-

nary arteries [73]. Thus far the RV effects of FAO inhibition have been tested only in animal models and it is likely the first human trials will be in patients with pulmonary hypertension, rather than those with CHD. However FAO inhibitors and other potential metabolic modulators remain intriguing avenues for further research into the management of chronic RV failure.

Conclusions

Medical management of fluid overload experienced by CHD patients with chronic RV failure can be achieved and is a valid endeavour. But heart failure is not a static disease; it progresses and many survivors of CHD will find themselves in dire need of treatments that interrupt their specific underlying pathophysiology. Currently, there is insufficient data to be able to recommend any medical option with confidence; which is not to say that we will never have a good treatment or that those we have now are certainly useless. It is just that presently, few signs indicate that therapies developed for treatment of systolic HF in the adult general population address targets germane to RV failure in CHD. It is self-evident that more and better research is needed. Given the lack of certainty in medication's ability to improve outcomes or slow disease progression, it is important that while treating symptoms and up-titrating heart failure medication, we keep sight of the bigger picture. This is because in CHD patients with chronic RV failure, if one exists, the window of opportunity for definitive management (usually surgical revision or transplantation) may be relatively small.

References

1. He FJ, Burnier M, Macgregor GA. Nutrition in cardiovascular disease: salt in hypertension and heart failure. Eur Heart J. 2011;32(24):3073–80.
2. Schrier RW, Abraham WT. Hormones and hemodynamics in heart failure. N Engl J Med. 1999;341(8):577–85.
3. Devroey D, Van Casteren V. Symptoms and clinical signs associated with hospital admission and mortality for heart failure. Cent Eur J Public Health. 2010;18(4):209–14.
4. Travers B, O'Loughlin C, Murphy NF, Ryder M, Conlon C, Ledwidge M, et al. Fluid restriction in the management of decompensated heart failure: no impact on time to clinical stability. J Card Fail. 2007;13(2):128–32.
5. Paterna S, Gaspare P, Fasullo S, Sarullo FM, Di Pasquale P. Normal-sodium diet compared with low-sodium diet in compensated congestive heart failure: is sodium an old enemy or a new friend? Clin Sci. 2008;114(3):221.
6. Aliti GB, Rabelo ER, Clausell N, Rohde LE, Biolo A, Beck-da-Silva L. Aggressive fluid and sodium restriction in acute decompensated heart failure. Am Med Assoc. 2013;173(12):1058–64.
7. Weiss BD. Sodium restriction in heart failure: how low should you go? Am Fam Physician. 2014;89(7):508–10.
8. Cheitlin MD. Counterintuitive evidence concerning salt and water restriction in acute decompensated heart failure patients: comment on "aggressive fluid and sodium restriction in acute decompensated heart failure". JAMA Intern Med Am Med Assoc. 2013;173(12):1064–6.
9. Lennie TA, Chung ML, Moser DK. What should we tell patients with heart failure about sodium restriction and how should we counsel them? Curr Heart Fail Rep. 2013;10(3):219–26.
10. Roush GC, Kaur R, Ernst ME. Diuretics: a review and update. J Cardiovasc Pharmacol Ther. 2014;19(1):5–13.
11. Voelkel NF, Quaife RA, Leinwand LA, Barst RJ, McGoon MD, Meldrum DR, et al. Right ventricular function and failure: report of a national heart, lung, and blood institute working group on cellular and molecular mechanisms of right heart failure. Circulation. 2006;114(17):1883–91.
12. Stevenson WH, Tsai EJ, Wilkoff BL. 2013 ACCF/AHA guideline for the management of heart failure: a report of the american college of cardiology foundation/American Heart Association task force on practice guidelines. Circulation. 2013;128:e240–327.
13. McMurray JJV, Adamopoulos S, Anker SD, Auricchio A, Böhm M, Dickstein K, et al. ESC Guidelines for the diagnosis and treatment of acute and chronic heart failure 2012: The Task Force for the Diagnosis and Treatment of Acute and Chronic Heart Failure 2012 of the European Society of Cardiology. Developed in collaboration with the Heart Failure Association (HFA) of the ESC. Eur Heart J. 2012;33(14):1787–847.
14. Arnold JMO, Liu P, Demers C, Dorian P, Giannetti N, Haddad H, et al. Canadian Cardiovascular Society consensus conference recommendations on heart failure 2006: diagnosis and management. Can J Cardiol. 2006;22(1):23–45.
15. Kantor PF, Lougheed J, Dancea A, McGillion M. Presentation, diagnosis, and medical management of heart failure in children: Canadian Cardiovascular Society Guidelines. Can J Cardiol. 2013;29:1535–52.
16. ISHLT. Guidelines for the management of pediatric heart failure. 1st ed. Dipchand AI, Rosenthal DN, (null), editors. Birmingham; 2014.

17. Moore KP, Aithal GP. Guidelines on the management of ascites in cirrhosis. Gut. 2006;55:vi1–12.
18. Biecker E. Diagnosis and therapy of ascites in liver cirrhosis. World J Gastroenterol. 2011;17(10):1237–48.
19. Brown RD, Ambler SK, Mitchell MD, Long CS. The cardiac fibroblast: therapeutic target in myocardial remodeling and failure. Annu Rev Pharmacol Toxicol. 2005;45(1):657–87.
20. Wald RM, Haber I, Wald R, Valente AM, Powel AJ, Geva T. Effects of regional dysfunction and late gadolinium enhancement on global right ventricular function and exercise capacity in patients with repaired tetralogy of Fallot. Circulation. 2009;119:1370–7.
21. Babu-Narayan SV, Kilner PJ, Li W, Moon JC, Giktekin O, Davlouros PA, et al. Ventricular fibrosis suggested by cardiovascular magnetic resonance in adults with repaired tetralogy of Fallot and its relationship to adverse markers of clinical outcome. Circulation. 2006;116:405–13.
22. Babu-Narayan SV, Goketekin O, Moon JC, Broberg CS, Pantley G, Pennel DJ, et al. Late gadolinum enhancement cardiovascular magnetic resonance of the systemic right ventricle in adults with previous atrial redirection surgery for transposition of the great arteries. Circulation. 2005;111:2091–8.
23. Plymen CM, Sado DM, Taylor AM, Bolger AP, Lambiase PD, Hughes M, et al. Diffuse myocardial fibrosis in the systemic right ventricle of patients late after Mustard or Senning surgery: an equilibrium contrast cardiovascular magnetic resonance study. Eur Heart J Cardiovasc Imaging. 2013;14(10):963–8.
24. Winter MM, van der Bom T, de Vries LCS, Balducci A, Bouma BJ, Pieper PG, et al. Exercise training improves exercise capacity in adult patients with a systemic right ventricle: a randomized clinical trial. Eur Heart J. 2012;33(11):1378–85.
25. Groenveld HF, Januzzi JL, Damman K, van Wijngaarden J, Hillege HL, van Veldhuisen DJ, et al. Anemia and mortality in heart failure patients a systematic review and meta-analysis. J Am Coll Cardiol. 2008;52(10):818–27.
26. Dimopoulos K, Diller GP, Giannakoulas G, Petraco R, Chamaidi A, Karaoli E, et al. Anemia in adults with congenital heart disease relates to adverse outcome. J Am Coll Cardiol. 2009;54(22):2093–100.
27. Klein I, Danzi S. Thyroid disease and the heart. Circulation. 2007;116(15):1725–35.
28. Heart Failure Society of America. Executive summary: HFSA 2010 comprehensive heart failure practice guideline. J Card Fail. 2010;16(6):475–539.
29. Bolger AP, Sharma R, Li W, Leenarts M, Kalra PR, Kemp M, et al. Neurohormonal activation and the chronic heart failure syndrome in adults with congenital heart disease. Circulation. 2002;106(1):92–9.
30. Cantinotti M, Giovannini S, Murzi B, Clerico A. Diagnostic, prognostic and therapeutic relevance of B-type natriuretic hormone and related peptides in children with congenital heart diseases. Clin Chem Lab Med. 2011;49(4):567–80.
31. Eindhoven JA, van den Bosch AE, Ruys TPE, Opić P, Cuypers JAAE, McGhie JS, et al. N-terminal pro-B-type natriuretic peptide and its relationship with cardiac function in adults with congenital heart disease. J Am Coll Cardiol. 2013;62(13):1203–12.
32. Cantinotti M, Clerico A, Emdin M. Amino terminal fragment of pro-B-type natriuretic peptide for complex congenital heart diseases: one for all, all for one? J Am Coll Cardiol. 2014;63(13):1342–3.
33. Giannakoulas G, Dimopoulos K, Bolger AP, Tay EL, Inuzuka R, Bedard E, et al. Usefulness of natriuretic peptide levels to predict mortality in adults with congenital heart disease. Am J Cardiol. 2010;105(6):869–73.
34. Plymen CM, Hughes ML, Picaut N, Panoulas VF, Macdonald ST, Cullen S, et al. The relationship of systemic right ventricular function to ECG parameters and NT-proBNP levels in adults with transposition of the great arteries late after Senning or Mustard surgery. Heart. 2010;96(19):1569–73.
35. Norozi K, Buchhorn R, Kaiser C, Hess G, Grunewald RW, Binder L, et al. Plasma N-terminal pro-brain natriuretic peptide as a marker of right ventricular dysfunction in patients with tetralogy of Fallot after surgical repair. Chest. 2005;128(4):2563–70.
36. Khositseth A, Manop J, Khowsathit P, Siripornpitak S, Pornkul R, Lolekha P, et al. N-terminal pro-brain natriuretic peptide as a marker in follow-up patients with tetralogy of Fallot after total correction. Pediatr Cardiol. 2007;28(5):333–8.
37. Cheung EWY, Lam WWM, Chiu CSW, Chau AKT, Cheung SCW, Cheung Y-F. Plasma brain natriuretic peptide levels, right ventricular volume overload and exercise capacity in adolescents after surgical repair of tetralogy of Fallot. Int J Cardiol. 2007;121(2):155–62.
38. Festa P, Ait-Ali L, Prontera C, De Marchi D, Fontana M, Emdin M, et al. Amino-terminal fragment of pro-brain natriuretic hormone identifies functional impairment and right ventricular overload in operated tetralogy of Fallot patients. Pediatr Cardiol. 2007;28(5):339–45.
39. Koch AME, Zink S, Glöckler M, Seeliger T, Dittrich S. Plasma levels of B-type natriuretic peptide in patients with tetralogy of Fallot after surgical repair. Int J Cardiol Elsevier. 2010;143(2):130–4.
40. Kurzyna M, Torbicki A. Neurohormonal modulation in right ventricular failure. Eur Heart J Suppl. 2007;9:H35–40.
41. Roche SL, Redington AN. Right ventricle: wrong targets?: another blow for pharmacotherapy in congenital heart diseases. Circulation. 2013;127(3):314–6.
42. Babu-Narayan SV, Uebing A, Davlouros PA, Kemp M, Davidson S, Dimopoulos K, et al. Randomised trial of ramipril in repaired tetralogy of Fallot and pulmonary regurgitation. Int J Cardiol. 2012;154(3):299–305.
43. Hsu DT, Zak V, Mahony L, Sleeper LA, Atz AM, Levine JC, et al. Enalapril in infants with single ventricle: results of a multicenter randomized trial. Circulation. 2010;122(4):333–40.

44. Khairy P, Aboulhosn J, Gurvitz MZ, Opotowsky AR, Mongeon F-P, Kay J, et al. Arrhythmia burden in adults with surgically repaired tetralogy of Fallot: a multi-institutional study. Circulation. 2010;122(9):868–75.
45. Schwerzmann M, Salehian O, Harris L, Siu SC, Williams WG, Webb GD, et al. Ventricular arrhythmias and sudden death in adults after a Mustard operation for transposition of the great arteries. Eur Heart J. 2009;30(15):1873–9.
46. Brown ML, Dearani JA, Danielson GK, Cetta F, Connolly HM, Warnes CA, et al. Functional status after operation for ebstein anomaly. J Am Coll Cardiol. 2008;52(6):460–6.
47. Valente AM, Gauvreau K, Assenza GE, Babu-Narayan SV, Schreier J, Groenink M, et al. Contemporary predictors of death and sustained ventricular tachycardia in patients with repaired tetralogy of Fallot enrolled in the INDICATOR cohort. Heart. 2014;100(3):247–53.
48. Gatzoulis MA, Balaji S, Webber SA, Siu SC, Hokanson JS, Poile C, et al. Risk factors for arrhythmia and sudden cardiac death late after repair of tetralogy of Fallot: a multicentre study. Lancet. 2000;356(9234):975–81.
49. Srivastava D. Making or breaking the heart: from lineage determination to morphogenesis. Cell. 2006;126(6):1037–48.
50. Sanchez-Quintana D, Anderson RH, Ho SY. Ventricular myoarchitecture in tetralogy of Fallot. Heart. 1996;76(3):280–6.
51. Meier GD, Bove AA, Santamore WP, Lynch PR. Contractile function in canine right ventricle. Am J Phys. 1980;239(6):H794–804.
52. Klein SS, Graham TP, Lorenz CH. Noninvasive delineation of normal right ventricular contractile motion with magnetic resonance imaging myocardial tagging. Ann Biomed Eng. 1998;26(5):756–63.
53. Sengupta PP, Tajik AJ, Chandrasekaran K, Khandheria BK. Twist mechanics of the left ventricle: principles and application. JACC Cardiovasc Imaging. 2008;1(3):366–76.
54. Zong P, Tune JD, Downey HF. Mechanisms of oxygen demand/supply balance in the right ventricle. Exp Biol Med (Maywood). 2005;230(8):507–19.
55. Goldstein JA. Pathophysiology and management of right heart ischemia. J Am Coll Cardiol. 2002;40(5):841–53.
56. Cadete VJJ, Lin H-B, Sawicka J, Wozniak M, Sawicki G. Proteomic analysis of right and left cardiac ventricles under aerobic conditions and after ischemia/reperfusion. Proteomics. 2012;12(14):2366–77.
57. Quaglietta D, Belanger MP, Wittnich C. Ventricle-specific metabolic differences in the newborn piglet myocardium in vivo and during arrested global ischemia. Pediatr Res. 2008;63(1):15–9.
58. Fogel MA, Weinberg PM, Fellows KE, Hoffman EA. A study in ventricular-ventricular interaction. Single right ventricles compared with systemic right ventricles in a dual-chamber circulation. Circulation. 1995;92(2):219–30.
59. Khoo NS, Smallhorn JF, Kaneko S, Myers K, Kutty S, Tham EB. Novel insights into RV adaptation and function in hypoplastic left heart syndrome between the first 2 stages of surgical palliation. JACC Cardiovasc Imaging. 2011;4(2):128–37.
60. Pettersen E, Helle-Valle T, Edvardsen T, Lindberg H, Smith H-J, Smevik B, et al. Contraction pattern of the systemic right ventricle: shift from longitudinal to circumferential shortneing and absent global ventricular torsion. J Am Coll Cardiol. 2007;49:2450–6.
61. Cheitlin MD, Hutter AM, Brindis RG, Ganz P, Kaul S, Russell RO, et al. ACC/AHA expert consensus document. Use of sildenafil (Viagra) in patients with cardiovascular disease. American College of Cardiology/American Heart Association. J Am Coll Cardiol. 1999;33(1):273–82.
62. Nagendran J, Archer SL, Soliman D, Gurtu V, Moudgil R, Haromy A, et al. Phosphodiesterase type 5 is highly expressed in the hypertrophied human right ventricle, and acute inhibition of phosphodiesterase type 5 improves contractility. Circulation. 2007;116(3):238–48.
63. Goldberg DJ, French B, Mcbride MG, Marino BS, Mirarchi N, Hanna BD, et al. Impact of oral sildenafil on exercise performance in children and young adults after the fontan operation: a randomized, double-blind, placebo-controlled, crossover trial. Circulation. 2011;123(11):1185–93.
64. Goldberg DJ, French B, Szwast AL, McBride MG, Marino BS, Mirarchi N, et al. Impact of sildenafil on echocardiographic indices of myocardial performance after the Fontan operation. Pediatr Cardiol. 2012;33(5):689–96.
65. Tunks RD, Barker PCA, Benjamin DK Jr, Cohen-Wolkowiez M, Fleming GA, Laughon M, et al. Sildenafil exposure and hemodynamic effect after fontan surgery. Pediatr Crit Care Med. 2014;15(1):28–34.
66. Van De Bruaene A, La Gerche A, Claessen G, De Meester P, Devroe S, Gillijns H, et al. Sildenafil improves exercise hemodynamics in fontan patients. Circ Cardiovasc Imaging. 2014;7(2):265–73.
67. Hara A, Matsumura H, Maruyama K, Hashizume H, Ushikubi F, Abiko Y. Ranolazine: an antiischemic drug with a novel mechanism of action. Cardiovasc Drug Rev. 1999;17(1):58–74.
68. Kantor PF, Lucien A, Kozak R, Lopaschuk GD. The antianginal drug trimetazidine shifts cardiac energy metabolism from fatty acid oxidation to glucose oxidation by inhibiting mitochondrial long-chain 3-ketoacyl coenzyme a thiolase. Circ Res. 2000;86(5):580–8.
69. Randle PJ, Priestman DA, Mistry SC, Halsall A. Glucose fatty acid interactions and the regulation of glucose disposal. J Cell Biochem. 1994;55(Suppl):1–11.

70. Piao L, Marsboom G, Archer SL. Mitochondrial metabolic adaptation in right ventricular hypertrophy and failure. J Mol Med. 2010;88(10):1011–20.
71. Piao L, Fang Y-H, Cadete VJJ, Wietholt C, Urboniene D, Toth PT, et al. The inhibition of pyruvate dehydrogenase kinase improves impaired cardiac function and electrical remodeling in two models of right ventricular hypertrophy: resuscitating the hibernating right ventricle. J Mol Med. 2009;88(1):47–60.
72. Fang Y-H, Piao L, Hong Z, Toth PT, Marsboom G, Bache-Wiig P, et al. Therapeutic inhibition of fatty acid oxidation in right ventricular hypertrophy: exploiting Randle's cycle. J Mol Med. 2011;90(1):31–43.
73. Archer S, Fang Y-H, Ryan J, Piao L. Metabolism and bioenergetics in the right ventricle and pulmonary vasculature in pulmonary hypertension. Pulm Circ. 2013;3(1):144.

Transcatheter Pulmonary Valve Replacement: Impact on Management

17

Harsimran S. Singh and Lee Benson

Abstract

Transcatheter valve therapeutics has revolutionized interventional cardiology in the twenty-first century. When Bonhoeffer and colleagues performed the first-in-man percutaneous pulmonary valve implantation (PPVI) in 2000, it changed the treatment paradigm of what we can offer patients with congenital heart disease (CHD). In the span of this chapter, we will discuss the underlying burden of pulmonary valve disease in the CHD population and the current indications for surgical pulmonary valve replacement. We will outline the PPVI procedure from procedural and technologic perspective and then review the state of the evidence regarding clinical outcomes, risks & benefits, and potential future perspectives.

Keywords

Transcatheter pulmonary valve replacement • Surgical pulmonary valve replacement • Percutaneous pulmonary valve replacement • Valve systems

Introduction

Transcatheter valve therapeutics has revolutionized interventional cardiology in the twenty-first century. When Bonhoeffer and colleagues performed the first-in-man percutaneous pulmonary valve implantation (PPVI) in 2000, it changed the treatment paradigm of what we can offer patients with congenital heart disease (CHD). In the span of this chapter, we will discuss the underlying burden of pulmonary valve disease in the CHD population and the current indications for surgical pulmonary valve replacement. We will out-

H.S. Singh
Weill Cornell Medicine—New York Presbyterian Hospital, Internal Medicine and Pediatrics, 520 E. 70th St. Starr 4, Cardiology-Weill Cornell Medicine, New York, NY 10021, USA

L. Benson (✉)
Paediatric Cardiology, Labatt Family Heart Center Hospital for Sick Children, Toronto, Ontario, Canada
e-mail: lee.benson@sickkids.ca

M.K. Friedberg, A.N. Redington (eds.), *Right Ventricular Physiology, Adaptation and Failure in Congenital and Acquired Heart Disease*, https://doi.org/10.1007/978-3-319-67096-6_17

line the PPVI procedure from procedural and technologic perspective and then review the state of the evidence regarding clinical outcomes, risks & benefits, and potential future perspectives.

Pulmonary Valve Disease Burden

The majority of pulmonary valve pathology is either congenital or a consequence of surgery or intervention. Native pulmonary valve stenosis or right ventricular outflow tract (RVOT) obstruction occurs in ~25% of patients with CHD, in isolation or in association with other congenital syndromes such as Tetralogy of Fallot (TOF). The majority of isolated congenital pulmonary stenosis (PS) is valvular; while patients with TOF or Williams syndrome can present with PS at the subvalvular, valvular, and supravalvular anatomic levels. Depending on the patient's age and the degree of obstruction to pulmonary blood flow, PS can lead to variable clinical presentations. In the case of severe fetal PS or pulmonary atresia, a neonate may present with ductal-dependent physiology requiring emergent intervention. Children with mild or moderate valvular PS may be asymptomatic; but symptoms can develop or progress in severity later in life. Worsening PS can lead to secondary RV hypertrophy, decreased compliance, and elevated diastolic filling pressures. Patients may seek medical attention with exertional dyspnea, dysrhythmias, or rarely congestive heart failure.

Pulmonary regurgitation (PR) is a common finding in CHD patients especially in those with repaired conotruncal abnormalities. While significant PR may be present as an isolated congenital condition, it is typically iatrogenic from cardiac surgery or intervention. PR can develop after surgical valvotomy or balloon valvuloplasty performed for valvular pulmonary stenosis. After surgical TOF repair, PR is a near universal finding especially when a transannular patch is inserted. It can develop as a consequence of valve dysplasia, bilateral pulmonary artery (PA) stenosis, or with significant pulmonary hypertension. Adding to disease prevalence, with the passage of time, nearly all surgical implanted homografts, monocusps or bioprosthetic valves in the pulmonary position will develop some combination of PS and/or PR.

Historically severe PR was considered benign as it can be tolerated for many years. However, by the third or fourth decade, many patients will notice changes in exertional capacity or other symptoms. Chronic RV volume loading will lead to RV dilation, secondary decrease in LV filling volumes, and reduction in biventricular efficiency and cardiac output. Changes in RV compliance and dimensions can further lead to fibrosis, reduced ejection fraction in both ventricles, secondary tricuspid regurgitation, an increased preponderance for dysrhythmias and electrical instability. In addition to dyspnea/fatigue with exertion, patients may present with palpitations, syncope, edema, hepatic congestion, and sudden cardiac death.

Surgical Pulmonary Valve Replacement

Up until the start of this century, the only definitive therapy available for pulmonary valve disease was surgical replacement. Surgical PVR has been the gold standard in the treatment of severe PR, mixed native PS or PR, or failure of a prior surgical bioprosthetic valve, homograft, monocusp or conduit implants. In patients who develop symptomatic PV disease, including changes in functional status, the decision to offer surgery is relatively straightforward (Table 17.1). The more controversial question has been when to offer surgical PVR to the "asymptomatic patient" with severe PR—given the inherent procedural risks associated with open heart surgery and the limited durability of most valve prosthesis. Several observation studies have suggested cut offs of RV-end diastolic volume index (RVEDVI) of >150 to >170 ml/m^2 to offer asymptomatic patients surgical PVR [1–4] in addition to objective findings on formal exercise testing and Holter monitoring. Most adult congenital heart disease (ACHD) specialists use a holistic, individualized approach combining RV

Table 17.1 Suggested Indications for Pulmonary Valve Replacement

Figiola et al. [1]
• Significant PR (PR fraction ≥35% on MRI) with progressive RV dilation and dysfunction. RV/LV end-diastolic ratio ≥ 1.5 in symptomatic patients
• RV/LV end-diastolic ratio ≥ 2 in asymptomatic patients
• Reduced exercise capacity with or without documented arrhythmias
Geva et al. [2]
• Moderate or severe PR (PR fraction ≥25% on MRI) and 2 or more of the following:
• RV end-diastolic volume index ≥150 ml/m^2 (z score >4)
• RV end-systolic volume index ≥80 ml/m^2
• LV end-diastolic volume index ≥65 ml/m^2
• RV ejection fraction ≤47%
• RV outflow tract aneurysm
Clinical criteria: exercise intolerance, symptoms and signs of heart failure, cardiac medications, syncope, sustained ventricular tachycardia
• Presence of other hemodynamically significant lesions
• Patients who underwent TOF repair at age ≥ 3 years, PVR may be indicated sooner and in the presence of less severe RV dilation and dysfunction due to higher risk of adverse clinical outcomes

PVR pulmonary valve replacement, *PR* pulmonary regurgitation, *MRI* magnetic resonance imaging, *RV* right ventricular, *LV* left ventricular, *TOF* tetralogy of Fallot

size and function, LV function, functional status and disease burden in deciding when to offer surgical PVR.

Isolated surgical PVR is an effective therapy with low perioperative mortality (~1–2%) and relatively little perioperative morbidity [5]. There remain a variety of surgical approaches in performing PVR that depend on the choice of prosthesis, reduction of prior RVOT surgical patch, and the need for any additional repairs (e.g. tricuspid valve repair, RA MAZE procedure, pulmonary arterioplasty). The majority of PVR operations are performed with cardiopulmonary bypass, though off-bypass PVR has been described. The choice of prosthesis should take into account the patient's age, potential for growth and the need for future reoperations or interventions. In general, mechanical valves have not been implanted in the pulmonary position due largely to theoretical concerns of valve thrombosis in a low pressure system [6–8]. Homografts are commonly used in the children with complex RVOT obstruction because of the availability of smaller diameters [9]. Bioprosthetic implants are xenograft based valves (porcine, bovine, or equine) either animal valves or reconstructed pericardium encased in a metallic ring/stent or using a "stentless" design. Finally monocusp valves are constructed individually by the surgeon to fit the patient's anatomy using pericardial tissue or polytetrafluoroethylene (PTFE) [10].

Prospective comparisons between these surgical options are limited. Most retrospective series suggest ~50–80% 10-year freedom from redo-PVR, regardless of chosen valve type [5, 11–14]. Valve degradation over time is conjectured to occur from exaggerated fibrosis and calcification of valve leaflets related to the chemical cryopreservative used for the valves and possibly exacerbated by an autoimmune response. In general, it appears that most patients after surgical PVR will require a repeat operation ~5–15 years after implantation.

Percutaneous Pulmonary Valve Replacement

While surgical PVR remains a success story in congenital cardiac disease, there are many clinical scenarios in which surgery is high risk or contraindicated. Young patients undergoing RVOT reconstruction will likely require multiple sternotomies throughout their lives. Each subsequent surgery adds surgical risk and higher perioperative mortality from adhesions, scar tissue, and anatomic disruption [15]. Each subsequent ventriculotomy theoretically increases the possibility of scar related VT from the healed incision. Some patients are poor surgical candidates due to comorbidities including physical or mental challenges that can complicate post-op recovery. The desire to find alternatives to open heart surgery also stems from the drive to minimize risk. Our patients demand the least invasive means of

accomplishing the medical task—in order to minimize procedural risk. Patients intuitively seek out approaches that will minimize discomfort and recovery times. Likewise, cosmetic concerns related to sternotomies, wound healing, complications related to cardiopulmonary bypass all come into play.

After overcoming multiple technologic hurdles of developing compressible valves that can be delivered through catheter-based systems, the first-in-man percutaneous PVR was performed by Dr. Philipp Bonhoeffer in 2000 [16]. Since then, thousands of pulmonary valves have been implanted worldwide using primarily the Medtronic Melody® valve (Minneapolis, MN) and Edwards SAPIEN®, Sapien XT® and Sapien 3® valves (Edwards Life Sciences, Irvine, CA).

Indications

PPVI has become an alternative to surgical pulmonary valve replacement (PVR) in patients with dysfunctional bioprosthetic pulmonary valves, homografts, or conduits with intermediate-to-long-term follow-up [17, 18]. Severe PR, progressive symptoms, exercise intolerance, arrhythmias, RV dilation and dysfunction are all (in various combinations) considered criteria for replacement or implantation of a pulmonary valve (see Table 17.1) [19]. Patient selection is important and as in all congenital heart disease should be performed using a multidisciplinary construct using echo and MRI assessment of outflow tract morphology and PR severity, cardiopulmonary exercise testing (as a measure of exercise capacity), serial assessment of change in symptoms, and cardiac catheterization to confirm findings, assess PA pressures, and examine the coronary arteries. One must ensure that there is no subvalvular or supravalvular (including PA) obstruction that requires treatment with stents prior to PPVI. In patients for whom additional repairs are needed such as atrial arrhythmia treatment (MAZE) or with significant tricuspid valve regurgitation and requires direct repair, surgery remains a preferred strategy over PPVI.

The Valve Systems

The two valve systems with greatest worldwide experience for percutaneous PVI are the Melody® valve and Ensemble® delivery system (Medtronic Inc) and the Edwards Sapien® Pulmonic Transcatheter valve (Edwards Lifesciences) and the Edwards RetroFlex III® transfemoral delivery system. Newer generation valves from Edwards (Sapien XT® and Sapien 3®) and newer delivery systems (Novoflex® and Commander®) have also been used in the pulmonic position.

The Melody® valve and corresponding Medtronic Ensemble® delivery system (Fig. 17.1) were approved in Canada and Europe in 2006 and by the U.S. Federal Drug Administration (FDA) in 2010. The Melody® valve consists of a harvested valve bovine jugular vein that is sutured into a 28 mm long, 18 mm in diameter platinum/iridium stent frame. The valve is preserved in a proprietary mixture of glutaraldehyde and alcohol and must be manually crimped onto a 22 Fr. balloon-in-balloon catheter (BIB, NuMED Inc., Hopkinton, New York) with available balloon diameters of 18, 20 and 22 mm (stent-valve outer diameter up to 24 mm on the 22 mm balloon). The Ensemble® delivery system allows the valve to remain sheathed until positioned in the landing zone, achieving the correct position at the pulmonary annulus.

The original Sapien® valve consisted of bovine pericardial leaflets with a proprietary Thermafix® treatment to prevent calcification, sewn into a balloon expandable stainless steel platform. The Sapien XT® and Sapien 3® use a cobalt chromium alloy in place of stainless steel and the Sapien 3® adds a polyethylene terephthalate outer skirt to minimize paravalvar leak. The Sapien 3® is available in 20 mm, 23 mm, 26 mm, and 29 mm sizes—and given its lower profile with improved stent design is expected to supplant prior valve generations. The Commander® delivery system requires an Edwards eSheath® that is 14 Fr. for smaller valve sizes and 16 Fr. for the 29 mm valve (that expands to 18 and 20 Fr. outer diameter—allowing delivery in vasculature $\geq$5.5 mm and $\geq$6 mm in diameter respectively).

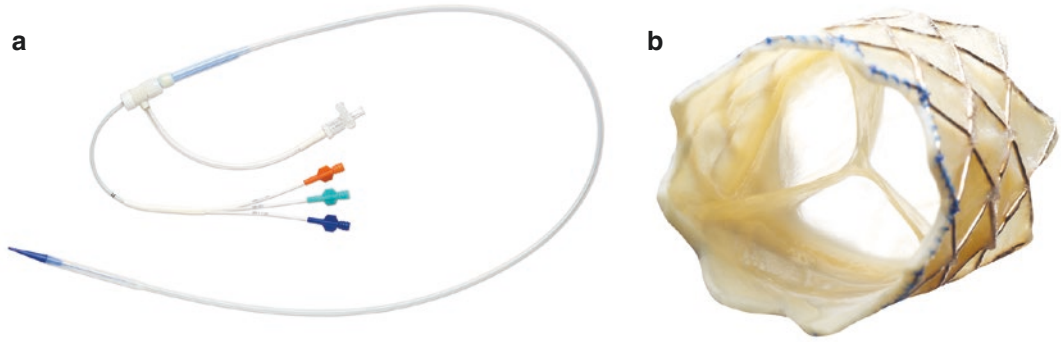

Fig. 17.1 The Medtronic Melody® Transcatheter Pulmonary Valve and Ensemble® Delivery System. *Panel A*. The Medtronic Melody® Valve which is a harvested bovine jugular vein valve that is sewn onto a 28 mm long platinum/iridium stent. *Panel B*. Medtronic Ensemble® delivery system is 22 Fr. delivery system with an integrated sheath designed for Melody® valve via the femoral or internal jugular veins. The Ensemble® delivery system comes with expandable balloon sizes of 18, 20, and 22 mm. Images published with permission—Melody® and Ensemble® systems are trademarks of Medtronic

Table 17.2 Approved valves in North America used for PPVI

	Medtronic melody® valve	Edwards SAPIEN XT® valve
Valve sizes	*Initial diameter:* 18 mm	16, 17, 20, 22 mm
	Crimped diameter: 6 mm	*Specialized crimper*
	Final diameter: 16–22 mm	20, 23, 26, 29 mm[a]
Valve type	Bovine jugular	Bovine pericardial
Balloon	BiB – 18, 20, 22 mm	Semi-compliant 23 or 26 mm
Stent platform	Platinum/iridium	Cobalt chromium
Sheath size	22 Fr.	22 or 24 Fr. (outer diameter 25 or 28 Fr.)
Delivery catheter	Ensemble® delivery system	Retroflex 3® system
	Nose cone sheath	Deflectable nose cone

PPVI percutaneous pulmonary valve implantation, *BIB* balloon in balloon
[a]The final diameters for the Melody® valve is the inner diameter, for the Sapien® it is the outer diameter, depending on balloon size for the Melody® vale. The Sapien XT® valve comes in four different sizes

Procedural Summary

PPVI should be conducted under general anesthesia to minimize movement and patient discomfort during valve delivery. Biplane or multi-angle single plane angiography will delineate the anatomy and confirm measurements made with non-invasive imaging. The lateral projection or a shallow RAO projection will usually provide optimal views of the conduit. Both the Melody® and Sapien 3® valves use balloon expandable delivery systems. Occasionally, rapid right ventricular pacing may be used to assure valve stabilization at the target zone. In the pulmonary (or tricuspid valve-in-valve) position, access is usually from the femoral or internal jugular vein—which should be of adequate size to accommodate the delivery sheath. In addition, periventricular valve delivery has been described using hybrid approach with direct surgical RV ventriculotomy [20]. The Edwards 26 and 29 mm valves allow for implantation in larger RVOTs than the Melody® valve (Table 17.2; Fig. 17.2). Beyond considerations of annulus size, there are several differences between these two valve platforms that should be considered when choosing one over the other. It is optimal for an ACHD cath lab to have access to both valve choices if performing PPVI.

Table 17.3 summarizes a procedural guide for performing a PPVI. A stiff exchange length

Fig. 17.2 Edwards SAPIEN® transcatheter heart valve and transfemoral delivery A. Edwards SAPIEN® Valve—Consists of bovine pericardial leaflets sewn into a balloon expandable cobalt chromium platform. Currently available in 23 mm and 26 mm sizes B. RetroFlex 3® delivery system—transfemoral delivery catheter used for the Edwards SAPIEN® valve. Images published with permission—Edwards, Edwards SAPIEN, Edwards SAPIEN XT, RetroFlex®, RetroFlex 2®, RetroFlex 3®, and SAPIEN® are trademarks of Edwards Lifesciences Corporation)

wire should be positioned in the pulmonary artery, preferably the left PA when coming from a femoral approach. PA position should initially be achieved via a balloon tipped catheter to avoid catheter entanglement at later stages with the tricuspid valve apparatus. Prior to valve implantation, compression coronary angiography must be performed to assess for coronary impingement. Using simultaneous non-compliant balloon inflation in RVOT to similar sizes as expected with the pulmonary valve implant, coronary angiography of the left and right coronary arteries should be performed obtained for evidence of coronary compression (see Fig. 17.3). This phenomenon can occur in 1–4% of patients and is more common in ToF with anomalous coronary origins, pulmonary homografts and valves after the Ross procedure [21].

Pre-stenting is generally recommended in all implants using the Melody valve to reduce the incidence of stent fracture [22] and in most implant situation with the Edwards valve other than valve-in-valve into bioprosthetic rings. Where available we recommend using a covered stent, i.e., the Cheatham-Platinum (CP) covered stents® (NuMED Inc., Hopkinton, New York) for homograft or conduit preparation. This accounts for any possible dissection or rupture that calcified homografts and conduits can be

Table 17.3 Basic procedural steps leading up to valve implantation

• Time-out—check list of equipment, personnel, and patient
• General anesthesia—patient is sedated and intubated for the procedure
– valve implantation can be painful and relies on precise placement
• Large caliber venous access (22–24 Fr.)
– consider preclose technique using a suture mediated closure device
– Prostar XL® (Abbott Vascular, Santa Clara, CA) and Perclose ProGlide® (Abbott Vascular)
• Bail out equipment for femoral, iliac, or inferior vena cava stenting
– e.g. Bard Fluency stent
• 5–6 Fr. arterial access for pressure monitoring and coronary injections
– frequent catheter flushing, heparin 100 U/kg to goal ACT ~250; perioperative antibiotic dose 1 h prior to procedure
• Diagnostic evaluation:
– right heart catheterization—use balloon tipped catheter to enter PA (avoid tricuspid apparatus), confirm no associated branch or peripheral PA stenosis that must be addressed
– Use stiff exchange wire (e.g. Amplatz Ultrastiff® or Lunderquist®) with shaped end for positioning
– L-PA preferable to R-PA for easier valve delivery
• RVOT angiographic assessment via 6 or 7 Fr. Multi-track® catheter
– keep distal wire position while allowing for both pull back pressure measurements and angiography
– Balloon predilation—use non-compliant balloon sized to valve (~22 mm) with full inflation and simultaneous coronary injections.
– ensure that coronaries are distant from implant site—otherwise an abrupt coronary occlusion can be a lethal (and avoidable) complication
• Pre-stenting—choose stent size, type, and number
– availability of covered stents; number of stents planned
– sequential angiographic and hemodynamic assessment
• Placement of percutaneous pulmonary valve
– Melody® or SAPIEN® valve and their corresponding delivery systems
– final angiograms and pressure measurements

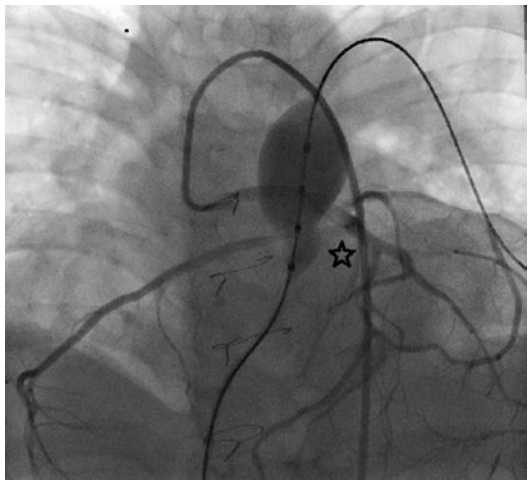

Fig. 17.3 Selective angiogram in a child with a single coronary artery during balloon occlusion of a right ventricular to pulmonary artery conduit. Note (*star*) area of obstructed flow in the coronary during balloon inflation

prone to [23]. In addition, Palmaz XL® series (J&J Interventional Systems Co., Warren, NJ) stents and Andrastent XL® or XLL® series (Andramed, Reutlingen, Germany) are bare metal stent options when placing a covered stent is unfavorable. It is important to receive full stent expansion at this stage without residual gradient.

For both Melody® and SAPIEN® valves, positioning and catheter stability are the crucial tenets during implantation. Once the Melody® valve is in position, the sheath is pulled back unveiling the valve. The Edwards valve is brought directly up to position. Slow inflation with either the BiB® or Edwards balloon allows time to make micro-adjustments in the event of device slippage. Once the valve is in place, post-inflation is occasionally needed to achieve full stent-valve expansion.

Evidence and Outcomes of PPVI

With nearly two decades of experience, PPVI implantation can be achieved with high procedural success and overall good procedural safety. PPVI achieves clinical results similar to surgical PVR. In the treatment of PR, there is reverse remodeling with a reduction in RV size and improvement in RV function over time. PPVI achieves increases in LV end diastolic volumes with subsequent improvement in early diastolic filling, decreased RV wall stress, and more balanced intraventicular septal interaction [24, 25]. When treatment is performed for PS, PPVI leads to reduction in RV systolic pressure and improved hemodynamics that is sustained in intermediate and long-term follow-up [26].

Periprocedural Outcomes

The largest published evidence pool in the pulmonary position rests with the Melody® valve. The U.S. Melody Transcatheter Pulmonary Valve study is a prospective, nonrandomized trial designed to assess safety, procedural success, and short-term efficacy of the Melody® valve in patients with dysfunctional RVOT conduits, following patients up to 7 years after their procedure [17]. This US Investigational Device Exemption trial enrolled 171 pediatric and adult patients at a median age of 19 years. Of the 148 patients who received a valve and were discharged were followed for a median of 4.5 years (range, 0.4–7 years). Thirty-two patients underwent right ventricular outflow tract re-intervention for obstruction ($n = 27$, with stent fracture in 22), endocarditis ($n = 3$, 2 with stenosis and 1 with pulmonary regurgitation), or right ventricular dysfunction ($n = 2$). Eleven patients had the Melody® valve explanted as an initial or second re-intervention. Five-year freedom from re-intervention and explantation was 76 ± 4% and 92 ± 3%, respectively. Conduits that were prestented and those with a lower right ventricular outflow tract gradient at hospital discharge had longer freedoms from re-intervention. Of 113 patients who were alive and re-intervention free, the follow-up gradient (median, 4.5 years after implantation) was unchanged from early after valve implantation, and all but 1 patient had mild or less pulmonary regurgitation. Almost all patients were in New York Heart Association class I or II. More severely impaired baseline spirometry was associated with a lower likelihood of improvement in exercise function after TPV replacement. In a similar study of consecutive patients from both a pediatric and adult congenital heart disease program, cardiac MRI, echocardiography, metabolic exercise testing, chest radiography, and hemodynamics before intervention were compared with repeated follow-up measurements to assess changes over time. Fifty-one patients (including 23 patients <16 years old) were followed for a mean 4.5 ± 1.9 (0.9–6.9) years after Melody® valve implantation. Freedom from any re-intervention was 87% and 68% at 3 and 5 years, and freedom from surgery was 90% at 5 years. For every decade younger at implantation, there was an increase of 3.9% ± 1.0% in cardiac MRI left ventricular ejection fraction ($p < 0.001$) and 2.4 ± 0.9 ml/kg/min in maxVO_2 ($P = 0.005$) and a decrease of 0.7 ± 0.2 cm in RV end-diastolic dimension ($p < 0.001$) after intervention. Younger patients displayed an additional decline in the RV/left ventricular end-diastolic volume ratio ($p = 0.05$) and trended toward improved RV ejection fraction in late follow-up (50% ± 7% versus 41% ± 12%, $p = 0.07$) [27].

With regards to the Edwards SAPIEN® and Sapien XT® valves, these valves have been in clinical use for RVOT lesions since 2011. The COMPASSION trial (COngenital Multicenter trial of Pulmonic vAlve regurgitation Studying the SAPIEN interventIONal) is a prospective, nonrandomized multicenter study that uses the SAPIEN® valve in the treatment of dysfunctional RV-to-PA conduits with moderate to severe PR or with PS. The FDA Phase I results were reported on 36 patients with the SAPIEN® valve resulting in an acute reduction in RV pressure to a median of 42 mm Hg and a reduction in peak gradients across the RVOT to a median of 12 mm Hg. There was trace or no PR in 31 of 33 patients on post-procedure angiography [18]. In a similar single centre 'real world' study from Toronto [28], 25 patients (70% male, mean age 34 ± 8.9 years) with an

underlying diagnosis of Fallot's tetralogy in 15, after a Ross procedure in 5, and 5 miscellaneous RVOT surgeries underwent either a Sapien® or Sapien XT® valve implant. The RV outflow tract characteristics included: 16 biological valve and 9 homografts. Technical success was 96%. One patient required an elective surgical pulmonary valve replacement for a high residual gradient. Pre-stenting was performed in all cases (half with covered stents). Valve sizes were 23 mm in 8, 26 mm in 15), and 29 mm in 2 patients. Acute hemodynamics noted a decrease in the mean RV-to-systemic pressure ratio ($p < 0.001$) and RV-to-PA gradient ($p < 0.001$). No patient had clinically significant PR. At a mean follow-up of 3.5 ± 2.1 years (range 0.3–7.2 years), there were no deaths with 1 patient requiring re-intervention for severe PR at 1 year having a valve-in-valve procedure. There were no episodes of endocarditis and no stent fractures and there was preserved valve function during follow-up with no change in RV-to-PA gradient nor PR severity.

While percutaneous valve implantation in the pulmonary position has been a 'game changer' in the management of the patient with congenital heart disease, less than a quarter of patients with RVOT dysfunction have conduits. Rather, the majority of patients in need of a competent pulmonary valve have undergone surgical modification of the RVOT with some form of RVOT patch with or without crossing the annulus. As a result PR is the dominant lesion that must be addressed. As the Sapien® series has a 29 mm diameter valve, a number of investigators have implanted this valve into the RVOT of patients with transannular patch RVOT reconstructions in the 26 mm diameter range [29–36].

Long-term Outcomes

In long-term prospective studies, PPVI has been found to be an effective therapy to achieve a competent PV without significant regurgitation. There has been no direct randomized comparison with surgical PVR—however, studies examining equivalent populations have suggested similar clinical outcomes. Published follow-up after Melody® PPVI has been reported up to 7 years. Overall freedom from reintervention/reoperation are reported at 90–95% at 1 year, 85–90% at 2 years [37] and freedom from RVOT re-intervention 95% at 1 year and 88% at 2 years. A smaller Toronto series examined PPVI performed in an adolescent population and found freedom from transcatheter reintervention to be 91%, 80%, and 80%, at 12, 24, and 36 months, respectively [38]. Eicken et al. have published their 2-institution clinical experience 102 patients receiving PPVI between 2006 and 2010 [39]. Pre-stenting was routinely performed, and they report one procedural death secondary to coronary compression. At a median of 1 year clinical follow-up, 1 valve (1%) was removed secondary to endocarditis; 8 valves (8%) required repeat dilation for residual gradients from which 4 led to repeat valve-in-valve procedures.

With regards to stent fractures after PPVI, clinical series have reported 1-year rates ranging as low as 5% to as high as 40%, likely depending on case mix, incidence of pre-stenting, and the rigor of follow-up [37, 39–41]. At a mean of 13 months follow-up, Nordmeyer et al. reports a 21% rate of stent fracture with fracture free survival of 85.1% at 1 year, 74.5% at 2 years, and 69.2% at 3 years [40]. with most events occurring in the first 400 days. The Melody® Transcatheter Pulmonary Valve study has also reported stent fracture rates of 22% at 14 months follow-up. There are considerably fewer PPVI patients who have received a SAPIEN® compared to Melody® valves; however, there were no reported stent fractures at 6 months in the phase I of the COMPASSION trial [18]. Whether this finding will hold up over longer term and with increased patient numbers is unknown.

Published studies have consistently shown an improvement in New York Heart Association (NYHA) class after PPVI [42]. There are hemodynamic differences after PPVI seen between lesions treated for predominantly RVOT obstruction vs. significant PR [26, 43]. Reduction of RV afterload leads to improvement in RV functional parameters and functional capacity as seen on peak oxygen uptake during cardiopulmonary exercise testing, while this has not been found with resolution of pulmonary regurgitation alone [43]. The majority of the improvement in systolic RV function after PPVI for obstructive lesions

occurs early, and little additional improvement has been noted on sequential MRI evaluations beyond 1 year [25].

In the cohort treated for severe PR, Plymen et al. found a statistically significant decrease in QRS duration and in QT_c dispersion after PPVI, akin to observations after surgical PVR [44]. The decrease in QRS duration was not statistically significant for the PPVI cohort treated for RVOT obstruction. To date there is no evidence correlating improvement in ECG parameters after PPVI with any reduction in clinical arrhythmia burden; however, it is hypothesized that increased homogeneity in repolarization is a sign of favorable electrical remodeling.

Recent studies have identified an increased risk of endocarditis in patients receiving bovine jugular vein implants to the RVOT compared to homograft implants [45–49]. Precise risk factors have yet to be determined, although the effect of a residual outflow gradient, turbulence in the valve sinuses, and the development of layered thrombus within the valve have been considered. Data are incomplete as to the endocarditis risk with a Sapien® valve, as the numbers of implants in the RVOT and length of follow up have been limited although endocarditis on the valve in the RVOT has been reported [50].

Up and Coming Pulmonary Valve Technologies

While PPVI has emerged as an alternative to surgical valve implantation, the diameters of the existing commercially available valves limits their application to surgically placed conduits, or those patients with small (26–27 mm) outflows as noted above. However, the majority (over three-quarters) of patients with congenital heart disease who undergo management of right ventricular outflow tract lesions have post operatively in longer-term follow up, large patulous outflows not amenable to existing transcatheter therapies [51]. As such, treatment of PR in this setting has traditionally been limited to surgical valve replacement. New techniques and technologies are being developed to facilitate valve insertion in such cases. Outflow tract reducers [52], valves placed in a hybrid manner (with simultaneous plication of the outflow) (Fig. 17.4) [53], and large diameter valve implants are currently under investigation (Fig. 17.5) [54–56]. Successful completion of these clinical trial will significantly alter the management options for the patient with CHD, the timing of interventions and ultimately indications.

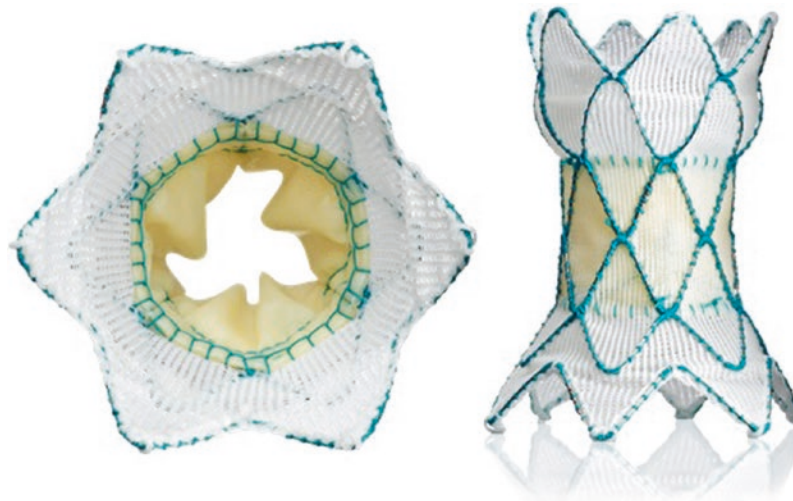

Fig. 17.4 The Harmony® self-expanding valve (Medtronic Inc. Minneapolis MN) is a 22 mm bovine pericardial valve (seen in the mid-portion of the *right panel*), shown into a Dacron® tube supported by a Nitinol® framework. *Left panel* shows the inflow portion of the implant. This implant has undergone an Early Feasibility FDA approved study and now in an early multicenter clinical trial

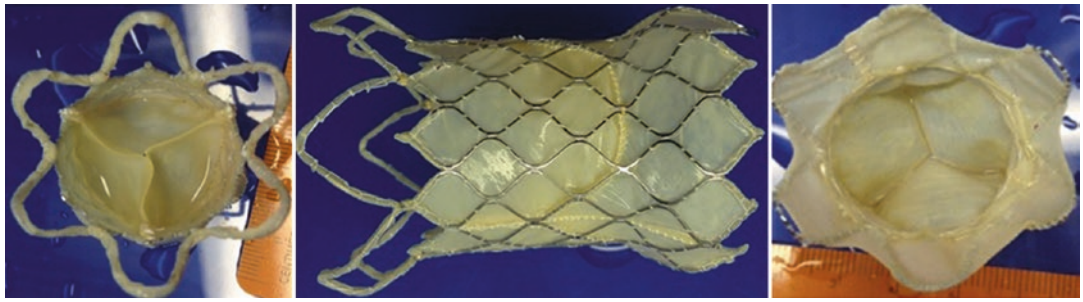

Fig. 17.5 The Venus P-valve® (Venus MedTech Inc., Hangzhou, China) is a Nitinol® self-expanding stent valve with leaflets made from porcine pericardium. *Left* and *right panels* show the outflow and inflow portions of the valve, the middle panel the Nitinol framework. Courtesy of Dr. S Qureshi

References

1. Frigiola A, Giamberti A, Chessa M, Di Donato M, Abella R, Foresti S, Carlucci C, Negura D, Carminati M, Buckberg G, Menicanti L. RESTORE group. Right ventricular restoration during pulmonary valve implantation in adults with congenital heart disease. Eur J Cardiothorac Surg. 2006;29:S279–85.
2. Geva T. Repaired tetralogy for Fallot: the roles of cardiovascular magnetic resonance in evaluating pathophysiology and for pulmonary valve replacement decision support. J Cardiovasc Magn Reson. 2011;13:9–32.
3. Buechel ER, Dave HH, Kellenberger CJ, Dodge-Khatami A, Pretre R, Berger F, Bauersfeld U. Remodelling of the right ventricle after early pulmonary valve replacement in children with repaired tetralogy of Fallot: assessment by cardiovascular magnetic resonance. Eur Heart J. 2005;26:2721–7.
4. Therrien J, Provost Y, Merchant N, Williams W, Colman J, Webb G. Optimal timing for pulmonary valve replacement in adults after tetralogy of Fallot repair. Am J Cardiol. 2005;95:779–82.
5. Lee C, Park CS, Lee CH, Kwak JG, Kim SJ, Shim WS, Song JY, Choi EY, Lee SY. Durability of bioprosthetic valves in the pulmonary position: long-term follow-up of 181 implants in patients with congenital heart disease. J Thorac Cardiovasc Surg. 2011;142:351–8.
6. Ilbawi MN, Lockhart CG, Idriss FS, DeLeon SY, Muster AJ, Duffy CE, Paul MH. Experience with St. Jude Medical valve prosthesis in children. A word of caution regarding right-sided placement. J Thorac Cardiovasc Surg. 1987;93:73–9.
7. Miyamura H, Kanazawa H, Hayashi J, Eguchi S. Thrombosed St. Jude Medical valve prosthesis in the right side of the heart in patients with tetralogy of Fallot. J Thorac Cardiovasc Surg. 1987;94:148–50.
8. Waterbolk TW, Hoendermis ES, den Hamer IJ, Ebels T. Pulmonary valve replacement with a mechanical prosthesis. Promising results of 28 procedures in patients with congenital heart disease. Eur J Cardiothorac Surg. 2006;30:28–32.
9. Gulbins H, Kreuzer E, Reichart B. Homografts: a review. Expert Rev. Cardiovasc Ther. 2003;1:533–9.
10. Turrentine MW, McCarthy RP, Vijay P, Fiore AC, Brown JW. Polytetrafluoroethylene monocusp valve technique for right ventricular outflow tract reconstruction. Ann Thorac Surg. 2002;74:2202–5.
11. Oosterhof T, Meijboom FJ, Vliegen HW, Hazekamp MG, Zwinderman AH, Bouma BJ, van Dijk AP, Mulder BJ. Long-term follow-up of homograft function after pulmonary valve replacement in patients with tetralogy of Fallot. Eur Heart J. 2006;27(12):1478–84.
12. Brown JW, Ruzmetov M, Vijay P, Rodefeld MD, Turrentine MW. Right ventricular outflow tract reconstruction with a polytetrafluoroethylene monocusp valve: a twelve-year experience. J Thorac Cardiovasc Surg. 2007;133(5):1336–43.
13. Discigil B, Dearani JA, Puga FJ, Schaff HV, Hagler DJ, Warnes CA, Danielson GK. Late pulmonary valve replacement after repair of tetralogy of Fallot. J Thorac Cardiovasc Surg. 2001;121(2):344–51.
14. Yemets IM, Williams WG, Webb GD, Harrison DA, McLaughlin PR, Trusler GA, Coles JG, Rebeyka IM, Freedom RM. Pulmonary valve replacement late after repair of tetralogy of Fallot. Ann Thorac Surg. 1997;64(2):526–30.
15. Holst KA, Dearani JA, Burkhart HM, Connolly HM, Warnes CA, Li Z, Schaff HV. Risk factors and early outcomes of multiple reoperations in adults with congenital heart disease. Ann Thorac Surg. 2011;92(1):122–30.
16. Bonhoeffer P, Boudjemline Y, Saliba Z, Merckx J, Aggoun Y, Bonnet D, Acar P, Le Bidois J, Sidi D,

Kachaner J. Percutaneous replacement of pulmonary valve in a right-ventricle to pulmonary-artery prosthetic conduit with valve dysfunction. Lancet. 2000;356(9239):1403–5.
17. Cheatham JP, Hellenbrand WE, Zahn EM, Jones TK, Berman DP, Vincent JA, McElhinney DB. Clinical and hemodynamic outcomes up to 7 years after transcatheter pulmonary valve replacement in the US melody valve investigational device exemption trial. Circulation. 2015;131(22):1960–70.
18. Kenny D, Hijazi ZM, Kar S, Rhodes J, Mullen M, Makkar R, Shirali G, Fogel M, Fahey J, Heitschmidt MG, Cain C. Percutaneous implantation of the Edwards SAPIEN transcatheter heart valve for conduit failure in the pulmonary position: early phase 1 results from an international multicenter clinical trial. J Am Coll Cardiol. 2011;58(21):2248–56.
19. Warnes CA, et al. ACC/AHA 2008 Guidelines for the Management of Adults with Congenital Heart Disease: a report of the American College of Cardiology/American Heart Association Task Force on Practice Guidelines (writing committee to develop guidelines on the management of adults with congenital heart disease). Circulation. 2008;118:e714–833.
20. Simpson KE, Huddleston CB, Foerster S, Nicholas R, Balzer D. Successful subxyphoid hybrid approach for placement of a Melody percutaneous pulmonary valve. Catheter Cardiovasc Interv. 2011;78(1):108–11.
21. Morray BH, McElhinney DB, Cheatham JP, Zahn EM, Berman DP, Sullivan PM, Lock JE, Jones TK. Risk of coronary artery compression among patients referred for transcatheter pulmonary valve implantation: a multicenter experience. Circ Cardiovasc Interv. 2013;6(5):535–42.
22. Nordmeyer J, Lurz P, Khambadkone S, Schievano S, Jones A, McElhinney DB, Taylor AM, Bonhoeffer P. Pre-stenting with a bare metal stent before percutaneous pulmonary valve implantation: acute and 1-year outcomes. Heart. 2010;97(2):118–23.
23. Hainstock MR, Marshall AC, Lock JE, McElhinney DB. Angioplasty of obstructed homograft conduits in the right ventricular outflow tract with ultra-noncompliant balloons: assessment of therapeutic efficacy and conduit tears. Circ Cardiovasc Interv. 2013;6(6):671–9.
24. Lurz P, Puranik R, Nordmeyer J, Muthurangu V, Hansen MS, Schievano S, Marek J, Bonhoeffer P, Taylor AM. Improvement in left ventricular filling properties after relief of right ventricle to pulmonary artery conduit obstruction: contribution of septal motion and interventricular mechanical delay. Eur Heart J. 2009;30(18):2266–74.
25. Lurz P, Nordmeyer J, Giardini A, Khambadkone S, Muthurangu V, Schievano S, Thambo JB, Walker F, Cullen S, Derrick G, Taylor AM, Bonhoeffer P. Early versus late functional outcome after successful percutaneous pulmonary valve implantation: are the acute effects of altered right ventricular loading all we can expect? J Am Coll Cardiol. 2011;57(6):724–31.
26. Coats L, Khambadkone S, Derrick G, Hughes M, Jones R, Mist B, Pellerin D, Marek J, Deanfield JE, Bonhoeffer P, Taylor AM. Physiological consequences of percutaneous pulmonary valve implantation: the different behaviour of volume- and pressure-overloaded ventricles. Eur Heart J. 2007;28(15):1886–93.
27. Borik S, Crean A, Horlick E, Osten M, Lee KJ, Chaturvedi R, Friedberg MK, McCrindle BW, Manlhiot C, Benson L. Percutaneous pulmonary valve implantation: 5 years of follow-up: does age influence outcomes? Circ Cardiovasc Interv. 2015;8(2):e001745.
28. Wilson WM, Benson LN, Osten MD, Shah A, Horlick EM. Transcatheter pulmonary valve replacement with the Edwards Sapien System: The Toronto experience. JACC Cardiovasc Interv. 2015;8(14):1819–27.
29. Momenah TS, El Oakley R, Al Najashi K, Khoshhal S, Al Qethamy H, Bonhoeffer P. Extended application of percutaneous pulmonary valve implantation. J Am Coll Cardiol. 2009;53(20):1859–63.
30. Boudjemline Y, Brugada G, Van-Aerschot I, Patel M, Basquin A, Bonnet C, Legendre A, Bonnet D, Iserin L. Outcomes and safety of transcatheter pulmonary valve replacement in patients with large patched right ventricular outflow tracts. Arch Cardiovasc Dis. 2012;105(8–9):404–13.
31. Guccione P, Milanesi O, Hijazi ZM, Pongiglione G. Transcatheter pulmonary valve implantation in native pulmonary outflow tract using the Edwards SAPIEN™ transcatheter heart valve. Eur J Cardiothorac Surg. 2012;41(5):1192–4.
32. Boshoff DE, Cools BL, Heying R, Troost E, Kefer J, Budts W, Gewillig M. Off-label use of percutaneous pulmonary valved stents in the right ventricular outflow tract: time to rewrite the label? Catheter Cardiovasc Interv. 2013;81(6):987–95.
33. Demkow M, Rużyłło W, Biernacka EK, Kalińczuk Ł, Spiewak M, Kowalski M, Sitkowska E, Kuśmierczyk M, Różanski J, Banaś S, Chmielak Z, Hoffman P. Percutaneous Edwards SAPIEN(™) valve implantation for significant pulmonary regurgitation after previous surgical repair with a right ventricular outflow patch. Catheter Cardiovasc Interv. 2014;83(3):474–81.
34. Malekzadeh-Milani S, Ladouceur M, Cohen S, Iserin L, Boudjemline Y. Results of transcatheter pulmonary valvulation in native or patched right ventricular outflow tracts. Arch Cardiovasc Dis. 2014;107(11):592–8.
35. Meadows JJ, Moore PM, Berman DP, Cheatham JP, Cheatham SL, Porras D, Gillespie MJ, Rome JJ, Zahn EM, McElhinney DB. Use and performance of the Melody Transcatheter Pulmonary Valve in native and postsurgical, nonconduit right ventricular outflow tracts. Circ Cardiovasc Interv. 2014;7(3):374–80.
36. Cools B, Brown SC, Heying R, Jansen K, Boshoff DE, Budts W, Gewillig M. Percutaneous pulmonary valve implantation for free pulmonary regurgitation following conduit-free surgery of the right ventricular outflow tract. Int J Cardiol. 2015;186:129–35.

37. McElhinney DB, Hellenbrand WE, Zahn EM, Jones TK, Cheatham JP, Lock JE, Vincent JA. Short- and medium-term outcomes after transcatheter pulmonary valve placement in the expanded multicenter US melody valve trial. Circulation. 2010;122(5):507–16. 44
38. Vezmar M, Chaturvedi R, Lee KJ, Almeida C, Manlhiot C, McCrindle BW, Horlick EM, Benson LN. Percutaneous pulmonary valve implantation in the young 2-year follow-up. JACC Cardiovasc Interv. 2010;3(4):439–48.
39. Eicken A, Ewert P, Hager A, Peters B, Fratz S, Kuehne T, Busch R, Hess J, Berger F. Percutaneous pulmonary valve implantation: two-centre experience with more than 100 patients. Eur Heart J. 2011;32(10):1260–5.
40. Nordmeyer J, Khambadkone S, Coats L, Schievano S, Lurz P, Parenzan G, Taylor AM, Lock JE, Bonhoeffer P. Risk stratification, systematic classification, and anticipatory management strategies for stent fracture after percutaneous pulmonary valve implantation. Circulation. 2007;115(11):1392–7.
41. Nordmeyer J, Coats L, Lurz P, Lee TY, Derrick G, Rees P, Cullen S, Taylor AM, Khambadkone S, Bonhoeffer P. Percutaneous pulmonary valve-in-valve implantation: a successful treatment concept for early device failure. Eur Heart J. 2008;29(6):810–5.
42. Lurz P, Coats L, Khambadkone S, Nordmeyer J, Boudjemline Y, Schievano S, Muthurangu V, Lee TY, Parenzan G, Derrick G, Cullen S, Walker F, Tsang V, Deanfield J, Taylor AM, Bonhoeffer P. Percutaneous pulmonary valve implantation: impact of evolving technology and learning curve on clinical outcome. Circulation. 2008;117(15):1964–72.
43. Lurz P, Giardini A, Taylor AM, Nordmeyer J, Muthurangu V, Odendaal D, Mist B, Khambadkone S, Schievano S, Bonhoeffer P, Derrick G. Effect of altering pathologic right ventricular loading conditions by percutaneous pulmonary valve implantation on exercise capacity. Am J Cardiol. 2010;105(5):721–6.
44. Plymen CM, Bolger AP, Lurz P, Nordmeyer J, Lee TY, Kabir A, Coats L, Cullen S, Walker F, Deanfield JE, Taylor AM, Bonhoeffer P, Lambiase PD. Electrical remodeling following percutaneous pulmonary valve implantation. Am J Cardiol. 2011;107(2):309–14.
45. Van Dijck I, Budts W, Cools B, Eyskens B, Boshoff DE, Heying R, Frerich S, Vanagt WY, Troost E, Gewillig M. Infective endocarditis of a transcatheter pulmonary valve in comparison with surgical implants. Heart. 2015;101(10):788–93.
46. McElhinney DB, Benson LN, Eicken A, Kreutzer J, Padera RF, Zahn EM. Infective endocarditis after transcatheter pulmonary valve replacement using the Melody valve: combined results of 3 prospective North American and European studies. Circ Cardiovasc Interv. 2013;6(3):292–300.
47. Buber J, Bergersen L, Lock JE, Gauvreau K, Esch JJ, Landzberg MJ, Valente AM, Sandora TJ, Marshall AC. Bloodstream infections occurring in patients with percutaneously implanted bioprosthetic pulmonary valve: a single-center experience. Circ Cardiovasc Interv. 2013;6(3):301–10.
48. Mery CM, Guzmán-Pruneda FA, De León LE, Zhang W, Terwelp MD, Bocchini CE, Adachi I, Heinle JS, McKenzie ED, Fraser CD Jr. Risk factors for development of endocarditis and reintervention in patients undergoing right ventricle to pulmonary artery valved conduit placement. J Thorac Cardiovasc Surg. 2016;151(2):432–9. 441.e1–2
49. Hascoet S, Mauri L, Claude C, Fournier E, Lourtet J, Riou JY, Brenot P, Petit J. infective endocarditis risk after percutaneous pulmonary valve implantation with the Melody and Sapien Valves. JACC Cardiovasc Interv. 2017;10(5):510–7.
50. Vollroth M, Daehnert I, Kostelka M, Wagner R. First case of blood-culture proven Staphylococcus aureus endocarditis of a Sapien® XT valve after percutaneous pulmonary valve implantation. Eur J Cardiothorac Surg. 2015;48(6):e124–5.
51. Schievano S, Coats L, Migliavacca F, Norman W, Frigiola A, Deanfield J, Bonhoeffer P, Taylor AM. Variations in right ventricular outflow tract morphology following repair of congenital heart disease: implications for percutaneous pulmonary valve implantation. J Cardiovasc Magn Reson. 2007;9(4):687–95.
52. Schievano S, Taylor AM, Capelli C, Coats L, Walker F, Lurz P, Nordmeyer J, Wright S, Khambadkone S, Tsang V, Carminati M, Bonhoeffer P. First-in-man implantation of a novel percutaneous valve: a new approach to medical device development. EuroIntervention. 2010;5(6):745–50.
53. Phillips AB, Nevin P, Shah A, Olshove V, Garg R, Zahn EM. Development of a novel hybrid strategy for transcatheter pulmonary valve placement in patients following transannular patch repair of tetralogy of fallot. Catheter Cardiovasc Interv. 2016;87(3):403–10.
54. Husain J, Praichasilchai P, Gilbert Y, Qureshi SA, Morgan GJ. Early European experience with the Venus P-valve®: filling the gap in percutaneous pulmonary valve implantation. EuroIntervention. 2016;12(5):e643–51.
55. Promphan W, Prachasilchai P, Siripornpitak S, Qureshi SA, Layangool T. Percutaneous pulmonary valve implantation with the Venus P-valve: clinical experience and early results. Cardiol Young. 2016;26(4):698–710.
56. Garay F, Pan X, Zhang YJ, Wang C, Springmuller D. Early experience with the Venus p-valve for percutaneous pulmonary valve implantation in native outflow tract. Neth Heart J. 2017;25(2):76–81.

18 Can Surgeons Preserve Right Ventricular Function in Hypoplastic Left Heart Syndrome?

Christoph Haller and Christopher A. Caldarone

Abstract

The systemic right ventricle in hypoplastic left heart syndrome commonly shows gradually declining function after initial palliation. It is therefore crucial to optimally preserve myocardial performance. Decisions in the operating room can have long term impact on systemic right ventricular function. For example, the choice of surgical procedures, shunt types, myocardial protection strategies, techniques used to reconstruct the hypoplastic aorta, and tricuspid valve procedures may all play an important role in the preservation of myocardial function. We herein discuss assets and drawbacks of surgical decisions with regard to right ventricular function in hypoplastic left heart syndrome, summarize currently available data, and give a perspective on contemporary and future therapy.

Keywords

HLHS • Systemic right ventricle • Right ventricular function • Norwood operation • Arch obstruction • Recoarctation • Tricuspid valve • Blalock-taussig shunt • Right ventricle to pulmonary artery conduit • Hybrid procedure • Stage II palliation • Fontan completion

Introduction

"It is as if the heart were constituted for the sake of the left ventricle, with some thin heart substance attached to the right side of the septum in order to make the right ventricle" [1]. It was Andreas Vesalius' unprecedented work "De humani corporis fabrica" in 1543 that paved the way for modern cardiac surgery. Exceptionally detailed and accurate, he described distinct anatomic features of both ventricles, and even

C. Haller • C.A. Caldarone (✉)
Cardiovascular Surgery, The Hospital for Sick Children, 555 University Ave, Toronto, ON, Canada, M5G 1X8
e-mail: christopher.caldarone@sickkids.ca

M.K. Friedberg, A.N. Redington (eds.), *Right Ventricular Physiology, Adaptation and Failure in Congenital and Acquired Heart Disease*, https://doi.org/10.1007/978-3-319-67096-6_18

delineated the right ventricle's (RV) close relationship to the lung. For centuries the RV was regarded as less important or even neglectable. 440 years after Vesalius' groundbreaking publication, Norwood et al. laid the foundation of palliation in hypoplastic left heart syndrome (HLHS), bringing the RV back into surgery's focus [2].

The RV is an extraordinary and complex structure. From a developmental standpoint, the RV's crucial role manifests in its function as the systemic ventricle during normal fetal circulation. In HLHS the fetal RV is not only fundamentally different from its left-sided counterpart but also significantly different from the normal RV, as it shows signs of antenatal diastolic dysfunction, lower cardiac output and altered contraction pattern [3–5].

RV dysfunction is a common but poorly understood problem after initial palliation of HLHS. Although some studies failed to link preoperative RV function with early mortality [6–9], parameters that are surrogates of RV performance (e.g. atrioventricular valve regurgitation, postoperative shock, and extracorporeal support) have been clearly identified as risk factors for in-hospital and interstage mortality [9–11]. Acute postoperative failure aside, functional deterioration can occur gradually, late after initial palliation, with a considerable delay and arises from a multitude of causes [12, 13]. Since ventricular function is not only a reflection of myocardial contractility but also the result of preload, afterload, ventricular macroscopic structure, myofiber architecture, valve function, heart rhythm and synchrony, as well as ventricular interdependence and many dynamic processes [14–16], the surgeon's approach in preserving RV function in HLHS has to take all these factors into account. Nevertheless, the surgeon has a limited set of variables, which can be manipulated to prevent RV dysfunction. These variables include the selection of the initial palliative strategy, technique of myocardial protection, technique of aortic reconstruction, and timing and type of tricuspid valve (TV) interventions.

Choice of Surgical Strategy

Obviously, the surgical strategy is one of the key points in single ventricle palliation as it provides the basis for the subsequent course. Many different options are on hand for each palliative step, ranging from timing of procedures to technical surgical aspects.

Stage I

If the patient's condition can be stabilized after birth, timing of stage I surgical palliation in HLHS aims at postpartum maturation and adaptation to extrauterine life on the one hand and avoiding pulmonary overflow or systemic malperfusion on the other hand. Older age has been identified as a risk factor for mortality [17, 18]. Analysis of the Single Ventricle Reconstruction trial did not show an association of age at the Norwood procedure with interstage mortality [9]. At least in the short term, right ventricular function is not necessarily affected by age at stage I [17].

Strategic aspects of stage I comprise the use of a modified Blalock-Taussig (BT) shunt, the implantation of an RV to pulmonary artery (RVPA) conduit, or the placement of an arterial duct stent as part of a hybrid approach.

Most of the studies addressing the type of shunt have a retrospective design and small patient numbers. In contrast, the Single Ventricle Reconstruction Trial is a prospective, randomized, multicenter trial comparing BT-Shunt palliation with RVPA conduit placement in HLHS, and gives valuable insights into the effect on right ventricular function. The ejection fraction after the initial procedure was significantly greater with an RVPA conduit, but insignificantly different at 14 months. RV volumes were lower in the RVPA group before stage II palliation, but again showed no difference at 14 months. Tricuspid valve regurgitation as an indirect measure of RV performance demonstrated no difference after 14 months. In a separate analysis focusing on echocardiographic parameters of ventricular function, RV ejection fraction, percent area

change and myocardial performance index after the Norwood procedure were all significantly higher with an RVPA conduit [19]. Again, no differences in functional ventricular indices could be shown. Indirect parameters of RV function such as TV size and degree of regurgitation were not influenced by shunt type. Follow-up data after 3 years, showed significantly lower pre-Fontan RV ejection fraction in the RVPA conduit group [20]. Furthermore, RVPA conduit patients showed a significant decline in ventricular function from 14 months to the pre-Fontan assessment [21]. Global RV function remained stable irrespective of initial shunt type. This analysis may be confounded by the measurement technique which does not include the right ventricular outflow tract (RVOT). The RVOT could be adversely affected by the RV incision used for placement of the RVPA conduit. Possibly, the deterioration of RV ejection fraction suggests impaired RV remodeling in patients treated with an RVPA conduit. It remains important to see if this decrease is ongoing or plateaus during follow-up [22].

RVPA conduits are considered beneficial for patients at high risk for a Norwood procedure, such as preterm and low-birth-weight patients. Surprisingly, no beneficial effect on survival could be found in this patient group during the interstage period in the SVR trial [9]. Few pathological studies have addressed the impact of the RV incision. The ensuing myocardial changes have been studied on specimens after palliation with either BT shunt or RVPA conduit [23]. Differences in remote myocardial scarring indicating coronary perfusion deficits could not be detected. However, myocardial thinning and scarring was noted at the site of the ventriculotomy. This correlated to previously assessed echocardiography, that detected signs of decreased segmental myocardial deformation at the ventriculotomy and increased deformation at the opposing site in the RVPA group, as a sign of mechanical dyssynchrony [23, 24]. In turn, mechanical dysynchrony has been associated with decreased diminished ventricular function in HLHS.

Several studies highlight the aspects of stage I palliation with regard to hybrid palliation with bilateral pulmonary artery banding and ductal stenting. The advantage of the latter is due to the postponement of major surgery with the use of cardiopulmonary bypass, cardiac and circulatory arrest from the neonatal period to several months of age. In a retrospective analysis of patients at the Hospital for Sick Children, BT shunt, RVPA conduit and hybrid palliation were compared and analyzed beyond stage II palliation [25]. Although diminished ventricular function was associated with mortality, none of the palliative approaches were associated with superior RV function or atrioventricular valve function 3 and 6 months after initial palliation. Other comparisons of hybrid palliation and classic Norwood operations with implantation of a BT shunt could not identify any difference in ventricular function between groups [26, 27]. Therefore, available clinical data shows neither a beneficial nor detrimental effect of hybrid palliation on RV function. Mathematical modeling as a means of theoretically understanding hemodynamic effects in hybrid palliation compared to BT shunt, and RVPA conduit revealed negative effects such as lower RV ejection fraction, lower mechanical efficiency, higher stroke work and higher afterload with reduced coronary and cerebral perfusion in patients after hybrid palliation [28].

In conclusion, a BT shunt seems to have a favorable (or the least detrimental effect) of the three palliative strategies on RV function—with the caveat that long-term comparative data for hybrid palliation is not yet available.

Stage II

The palliated circulation established with the Norwood operation leads to a gradual increase in RV volumes and a decrease in RV function before stage II palliation [29, 30]. After the Norwood procedure the RV has to generate up to 280% of normal cardiac output [31]. After completion of stage II palliation significant decreases in RV volumes were found [30]. Therefore, unloading of the RV at stage II is considered beneficial for preservation of RV function [32, 33].

With regard to timing of stage II, earlier operation offers earlier volume unloading of the systemic ventricle. Available data gives no conclusive statement on the best point in time to proceed to stage II. Although it is feasible to create a cavopulmonary anastomosis as early as 8 weeks, patients may show signs of limited pulmonary blood flow irrespective of preoperatively assessed pulmonary vascular resistance. There is little data to support the notion that early ventricular unloading with a cavopulmonary shunt results in improved RV function. A higher incidence of postoperative cardiac complications, such as cardiopulmonary resuscitation and arrhythmias in patients undergoing cavopulmonary shunt younger than 4 months has been reported [34]. Younger patients had a higher rate of severely impaired RV function pre- and postoperatively. Patients with an RVPA conduit are more susceptible to volume overload than patients with a BT shunt and may especially benefit from an earlier stage II operation [35].

Bidirectional cavopulmonary anastomosis or hemi-Fontan reduces the volume overload of the systemic RV in HLHS, and it seems plausible that this affects RV function positively. Despite a reduction in RV volume, RV ejection fraction and mass-to-volume ratio remained unchanged 14 months after stage II [30]. Assessment of RV functional parameters using two-dimensional speckle tracking detected no changes in global function after stage II [36]. MRI data demonstrated preserved indexed stroke volume and increased RV ejection fraction but decreased RV index [37]. Furthermore, the decreased RV volume did not result in a reduction of TV regurgitation [30]. Although TV annulus size decreases after stage II palliation, TV regurgitation does not demonstrate a commensurate improvement [32, 34, 37–39]. Diverging observations have been reported concerning TV repair at stage II palliation, with some groups advocating a rather conservative approach and other suggesting early intervention [32, 34, 39].

The effects of stage II palliation are therefore not reflected in a substantial improvement of RV function, but significant unloading and RV remodeling. The latter may contribute to improved diastolic dysfunction in the long term [40].

Fontan Completion

Stage III palliation, as the final separation of pulmonary and systemic circulation, can contribute to further ventricular volume unloading [40, 41] through prevention or reduction in systemic-pulmonary collateral development or intrapulmonary arteriovenous malformations. Little is known about special considerations for preservation of myocardial function with regard to type and timing of Fontan completion. Management has been widely derived from mixed single ventricle patient groups.

While it is well-established that an atriopulmonary connection is associated with atrial arrhythmia, sinus node dysfunction and thromboembolic events, there is little data on ventricular function favoring lateral tunnels over extracardiac conduits and vice versa. Extracardiac conduits have the advantage that they can be constructed without cardioplegic arrest and lesser manipulation of atrial tissue. Although this may theoretically be beneficial for the RV, we lack evidence on whether this actually reflects in better preservation of ventricular function. The better exercise capacity seen in extracardiac Fontan patients compared to those palliated with a lateral tunnel may indicate a beneficial effect [42]. Lateral tunnels can increase in size and can therefore be performed earlier than extracardiac conduits. Earlier conversion to a Fontan circulation did not show significant changes with regard to ventricular volumes and ejection fraction, but had a significantly better age-adjusted Tei-index, indicating less ventricular dysfunction.

Myocardium

Adequate myocardial protection is crucial to ensure good long-term function of the hypertrophied systemic ventricle. This can be achieved by ensuring optimal myocardial perfusion, by addressing any inherent anatomical coronary

problems, and by optimal myocardial protection during cardioplegic cardiac arrest.

It is important to consider anatomic features of the native hypoplastic aorta, which functions as a single coronary. Small ascending aortas as seen in aortic atresia subtypes can be technically challenging and pose the risk of pre-coronary stenosis during reconstruction of the aortic arch. On the other hand, thrombus formation in relatively large aortic roots with low flow or stasis has been reported [43, 44]. The surgical technique has to ensure an unobstructed, wide opening to the reconstructed part of the ascending aorta. Common techniques to achieve this surgical objective include longitudinal proximal incision of the native aorta and the corresponding pulmonary artery wall, patch augmentation of the contralateral aortic wall, and division with reattachment of the diminutive ascending aorta into the neoaortic root [45].

Anatomic studies have reported no relevant increase in coronary artery abnormalities in HLHS, but a higher rate of ventriculocoronary connections [43, 46]. Left coronary dominance was higher than in the normal population [43]. Flow reserve in patients with a systemic right ventricle has been examined in other patient populations. For example, patients with transposition of the great arteries after atrial switch have impairment of myocardial flow reserve [47, 48]. Compared to patients with a systemic left ventricle, a disproportionately lower perfusion of the systemic myocardium in HLHS has been reported suggesting higher vulnerability to malperfusion and cardioplegic arrest [49]. Although the systemic RV seems to be susceptible to malperfusion, most of the underlying mechanisms are surgically not modifiable.

Cardioplegia regimes vary between institutions and we lack objective data on advantages and disadvantages in pediatric patients. A survey among members of the Congenital Heart Surgeons' Society illustrated the multitude of cardioplegia techniques used [50]. Nevertheless, no conclusions on optimal cardioplegia and myocardial preservation in HLHS can be drawn from existing data. Strategies have been developed to avoid cardioplegic arrest completely, showing non-inferiority compared to conventional regimes in small series [51].

The use of an RVPA conduit has the theoretical advantage of maintaining higher diastolic arterial pressures and avoiding coronary steal when compared to palliation with a BT shunt. The diastolic runoff seen in patients with a systemic to pulmonary artery shunt reduces coronary perfusion. As discussed above, an RVPA conduit improves early postoperative mortality and this in turn may be the reflection of a better coronary perfusion. Nevertheless, it does not affect long-term outcome and results in decreased RV function after 3 years [20, 52]. Retrograde aortic arch malperfution with impaired coronary flow is a feared complication in hybrid palliation which may be prevented or treated with a reverse BT shunt [53, 54].

Although there may be several important aspects of myocardial protection, there is only little evidence for an optimal strategy with regard to cardioplegia or shunt type.

Aortic Arch

The extensive reconstruction of the aortic arch is one of the key points in palliation of HLHS. The close interrelationship between the systemic RV and the neoaorta, also known as ventriculoarterial coupling, has been studied extensively, showing not only the deleterious effects of recoarctation on ventricular function but also the negative impact of altered mechanical properties of the reconstructed aorta [55–60]. An unobstructed reconstruction, a favorable geometric shape, minimal turbulent flow, and avoidance of recurrence of coarctation are all required to optimize ventricular function.

The right ventricle is sensitive to changes in afterload [15, 61]. Patients with HLHS are particularly vulnerable to increased systemic vascular resistance due to the associated myocardial work and O_2 consumption [62]. Increased afterload leads to RV hypertrophy and functional deterioration. The surgeon faces a wide array of geometric options when reconstructing the aortic arch—and the selection of these options can

have a favorable or unfavorable effect on postoperative RV function. Suboptimal reconstruction, leading to coronary malperfusion, neoaortic obstruction and ventricular failure has been identified as major cause of death [63]. Because of the need to ensure ongoing growth while avoiding arch obstruction, surgically reconstructed aortic diameters are larger than diameters in single ventricle patients with a native aorta [12, 57, 59]. A wide anastomosis and a smooth shape of the aorta ensure maximal reduction in RV workload [64]. Nevertheless a disproportionately large reconstruction may not achieve the intended effects, as an inverse relationship between neoaortic diameter and wave energy could be shown [59].

Acute angles, stenosis, or folds cause turbulence, altered blood flow and pooling in the reconstructed aorta. Many surgical techniques have been developed, ranging from an interdigitating technique to avoid recoarctation, different uses of preshaped or custom-made bovine pericardium, division and reconfiguration of the ascending aorta to an entirely patch-free reconstruction [65–69]. Different techniques of aortic arch reconstruction can result in alterations in flow patterns and subsequent effects on RV performance.

As an example, in techniques avoiding any additional patch material, the pulmonary trunk is anastomosed to the concavity of the arch, shifting the pulmonary trunk closer to the descending aorta. This creates a relatively direct inflow to the aortic arch vessels but a very sharp angle with the descending aorta [66, 70]. Quantification of the impact of arch geometry is relatively difficult to assess. Computational fluid dynamics form an interesting new approach to evaluate the blood flow. Although computational models can only provide an approximation of the biological changes in this setting, they give valuable insights [28, 64, 71–74]. Calculated streamlines, energy loss and wall shear stress show that up to 15% of the energy generated by the systemic RV is lost depending on the neoaortic configuration [64]. To minimize energy loss and wall shear stress, a wide anastomosis and a smooth angle of the reconstructed arch have to be achieved.

It is not only the arch geometry that affects ventricular function, but also the mechanical properties of the arch material including stiffness and distensibility [55, 57, 59]. Most of the neoaortic arch is usually comprised of the augmenting patch. Native tissue can only be found on the outer curvature and its circumferential extent depends on the hypoplastic aorta's original size. Aortic arch growth in HLHS is predominantly due to growth of the native segment with no significant increase of the homograft patch [12].

Correlation of the mechanical properties of patch material and ventricular function is not well studied. Most commonly the reconstruction is performed with pulmonary artery homograft, but bovine pericardium, autologous pericardium and alternative patch material have been used as well. While some report good results with bovine pericardium [67], others consider it a major risk factor for recoarctation [75]. Even the abandonment of any patch material failed to significantly improve the incidence of reinterventions [76]. Wave intensity calculated from MRI data as a reflection of ventricular function, was significantly lower in HLHS patients, although they had no signs of malconfiguration of the reconstructed arch. An increase of arterial elastance in palliated HLHS has been associated with impaired RV diastolic but not systolic function [77]. To date, no surgical approach can significantly improve the unfavorable wall properties of the reconstructed aorta.

The incidence of coarctation of the reconstructed aorta is high with freedom from recoarctation as low as 52% at 5 years [75]. Recoarctation has an unfavorable influence on ventricular performance, RV fractional area change, atrioventricular valve function and systemic-to-pulmonary blood flow balance [56]. An unobstructed aortic arch is therefore essential to optimize and preserve RV function. At the Hospital for Sick Children, we utilize an interdigitating technique [66]. After complete excision of the periductal area, the descending aorta is incised longitudinally at the anterior and posterior wall. The posterior portion of the proximal and distal aortic arch are then anastomosed in a manner similar to an extended end-to-end coarctation repair leav-

ing the anterior portion of the anastomosis open to receive a pulmonary homograft patch. The patch augments the proximal aortic arch and extends distally to the end of the incision which was made in the anterior wall of the descending aorta. This interdigitating technique removes all periductal tissue and creates a wide unobstructed anastomosis with the descending aorta. The anterior and posterior incision thereby lead to a non-circular anastomosis, avoiding circumferential constriction. The technique showed superiority compared to classic and autologous arch reconstruction with regard to recoarctation.

The optimal hypoplastic arch repair has yet to be defined. It is vital to create a neo-aorta that provides mechanical characteristics, geometry and growth as natural as possible. This can be achieved best with wide anastomotic sites, smooth angles, and generous removal of ductal tissue.

Tricuspid Valve

Tricuspid regurgitation (TR) is a risk factor for mortality after the Norwood operation and associated with poor survival [78–81]. Up to 23% of all palliated HLHS patients have to face TV procedures within 10 years [82]. A bimodal time course has been reported with failure relatively early after diagnosis and late failure after more than 5 years [82].

No other pathology unveils its relation to RV function as openly as that of the TV. Therefore, a thorough understanding of TV dysfunction and its surgical therapy cannot be achieved without considering RV characteristics. Changes in RV contraction pattern can already be seen in the fetal circulation in HLHS [3–5], but further adaptive responses have been shown in systemic RVs after birth and the respective palliative steps [83, 84]. The ventricle in single ventricle patients has to generate output that is approximately 2.3 times higher in utero and even up to 2.8 times higher after shunt construction, than in normally developed hearts [31]. The ventricle responds with myocardial hypertrophy, especially of the middle layer, geometric reformation with a septal shift to the left, forming a more cylindrical shape, and a rather circumferential than longitudinal contraction pattern [83–85]. Ventricular dilatation, annulus dilatation, papillary muscle displacement and TV tethering are triggered by these changes and reflect gradual ventricular dysfunction. TV dysfunction may cause further RV functional decline and vice versa.

With regard to ventricular function, surgical strategies have to address any inherent or developing pathology of the TV. The annulus in a normal TV has a complex three-dimensional shape with two anteroposteriorly opposing high and two mediolaterally opposing low points [84, 86]. In patients with functional TR, this geometry deforms and the tricuspid annulus becomes larger and adopts a more circular and flattened shape. Annular dilation occurs in an anteroposterior direction along the free RV wall in patients with two ventricles [86] and in HLHS [84]. Additionally leaflet tethering with papillary muscle displacement and prolapse is associated with significant TR and myocardial dysfunction due to increased myocardial mass, afterload or coronary supply-demand mismatch [82, 84]. It remains inconclusive if ventricular interdependence has a relevant effect on TV function [16, 87, 88]. Most reports confirm the findings of anterior leaflet prolapse, septal leaflet tethering and annular dilatation in HLHS [32, 89–91]. These underlying mechanisms have to be considered in TV repair in HLHS.

TV repair is frequently undertaken for patients with moderate or severe TR. Partial annuloplasty, commissural closure, tricuspid ring annuloplasty, chordal shortening, papillary muscle relocation, and leaflet resuspension have been reported as useful surgical techniques [79, 81, 90, 92, 93]. The necessary combination of valve repair techniques remains individualized for each patient depending on the anatomic and functional contributors to the TR. Success depends on the underlying pathology and surgeon's experience. Posterior leaflet obliteration can be used to form a functional bicuspid valve with favorable results [79, 81]. Because a regurgitation jet along the anteroseptal commissure is found in 68% of patients undergoing TV repair, closure of that

commissure can be utilized [90]. Furthermore papillary muscle relocation forms a promising approach, as it restores ventricular geometry and eliminates an underlying mechanism of insufficient coaptation [90, 94]. RV function in patients with sustained successful TV repair remains better than in those with a failing valve. This can be a result of the repair itself, but may also be biased by a persisting RV function that influences the TV positively [81]. Most likely, both are true and it is impossible to quantify the respective impact.

Results of TV repair in the course of HLHS palliation are fortunately good. Freedom from TV replacement of 97% has been reported [90]. After a median follow-up period of 38.2 months after initial TV intervention 15% of patients showed recurrence of significant TR and 21% had RV dysfunction. TV repair if initially successful, is likely to have lasting results on follow-up [79]. In contrast, even initially successful TV repairs often fail in those patients with persistently poor RV function, highlighting the close interaction of RV and TV. Outcome is significantly associated with TV or RV function respectively [79]. Our experience showed excellent outcome and long-term consistency of TV repair as well [82]. After repair, TR remained stable or declined after a median of 5.1 years of follow-up. RV function was lower directly after the operation but showed non-significant differences compared to patients without the need for TV repair in the long-term. The postoperative decline in RV function can be caused by a preoperatively masked RV dysfunction, that becomes apparent after the operation [89]. The latter along with the reassuring results in this patient group is indicative for a low threshold for TV repair. The reported higher risk with younger and smaller patients should not be interpreted as a reason to delay therapy but as associated with more severe disease [79, 82].

Evolving Concepts

The complexity of HLHS and the impact of staged palliation have led to several attempts to reduce the surgical burden. Intermediate-term results of fetal intervention in a well-selected subset of patients with severe midgestation aortic stenosis have been reported recently, demonstrating the feasibility of biventricular repair [95]. Despite good results in the biventricular group, the concept has to be weighed with the associated risks for the patient and the mother in mind. Furthermore, the biventricular repair strategy preselects less critical patients, as compared to those facing univentricular palliation.

The use of routine postoperative mechanical support shows encouraging results [96]. Facing the risk of low cardiac output or unbalanced pulmonary to systemic perfusion and the possibility of impaired neurological outcome after stage I palliation, the concept aims at initial stabilization. Although this strategy has good hospital survival, it comes with the associated risks of mechanical support and less cost-effectiveness.

At our institution, an interesting new concept was introduced, that created a primary in-series circulation [97, 98]. Since cavopulmonary anastomosis in neonates has deleterious results, due to high pulmonary vascular resistance, palliation delays the connection of the superior caval vein with the pulmonary artery until four to six months of age. To avoid the risks of shunt-dependent in-parallel circulation, the concept of mechanical cavopulmonary assist establishes stable hemodynamics as the mechanical support ensures pulmonary blood flow despite high pulmonary resistance. First promising results still need to find their way from bench to bedside, but the ongoing rapid progress in mechanical circulatory support may open up exciting possibilities in the near future.

Cell based therapies have been developed to reduce RV failure or improve RV function. After years of research on myocardial recovery with autologous stem cells in adults, mainly with ischemic heart diseases, first clinical reports have shown the safety and efficacy of autologous stem cell therapy in children with HLHS [99, 100].

Conclusion

Preserving RV function in HLHS is a challenging task for all involved disciplines. Certainly, the way from the neonate to the adult is paved with endless options and decisions that finally may reflect in myocardial

performance. Nevertheless some of the surgical strategies at hand are well established and can preserve the fragile systemic RV's function. The use of a modified BT-shunt seems to be favorable in the long-term. Earlier conversion to a cavopulmonary shunt may decelerate functional decline. Unobstructed coronary perfusion, wide anastomoses and smooth angles of the reconstructed aorta, as well as techniques to avoid recoarctation are essential for the RV. Early TV repair addressing the underlying mechanisms of regurgitation can further preserve ventricular function.

Although many other aspects of HLHS palliation have been identified as contributors to RV functional decline, we still seek optimal combinations of surgical strategies to preserve RV function and promote patient survival.

References

1. Vesalius A, Richardson WF, Carman JB. On the fabric of the human body: Book VI the heart and associated organs, Book VII the brain. Norman Pub.; 2009. 1–413 p. (Lww, Handbook of Signs & Symptoms).
2. Norwood WI, Lang P, Hansen DD. Physiologic repair of aortic atresia-hypoplastic left heart syndrome. N Engl J Med. 1983;308(1):23–6.
3. Brooks PA, Khoo NS, Mackie AS, Hornberger LK. Right ventricular function in fetal hypoplastic left heart syndrome. J Am Soc Echocardiogr. 2012;25(10):1068–74.
4. Natarajan S, Szwast A, Tian Z, McCann M, Soffer D, Rychik J. Right ventricular mechanics in the fetus with hypoplastic left heart syndrome. J Am Soc Echocardiogr. 2013;26(5):515–20.
5. Szwast A, Tian Z, McCann M, Donaghue D, Rychik J. Right ventricular performance in the fetus with hypoplastic left heart syndrome. Ann Thorac Surg. 2009;87(4):1214–9.
6. Helton JG, Aglira BA, Chin AJ, Murphy JD, Pigott JD, Norwood WI. Analysis of potential anatomic or physiologic determinants of outcome of palliative surgery for hypoplastic left heart syndrome. Circulation. 1986;74(3 Pt 2):I70–6.
7. Altmann K, Printz BF, Solowiejczyk DE, Gersony WM, Quaegebeur J, Apfel HD. Two-dimensional echocardiographic assessment of right ventricular function as a predictor of outcome in hypoplastic left heart syndrome. Am J Cardiol. 2000;86(9):964–8.
8. Stasik CN, Goldberg CS, Bove EL, Devaney EJ, Ohye RG, Gelehrter S, et al. Current outcomes and risk factors for the Norwood procedure. J Thorac Cardiovasc Surg. 2006;131(2):412–7.
9. Ghanayem NS, Allen KR, Tabbutt S, Atz AM, Clabby ML, Cooper DS, et al. Interstage mortality after the Norwood procedure: results of the multicenter Single Ventricle Reconstruction trial. J Thorac Cardiovasc Surg. 2012;144(4):896–906.
10. Tabbutt S, Ghanayem N, Ravishankar C, Sleeper LA, Cooper DS, Frank DU, et al. Risk factors for hospital morbidity and mortality after the Norwood procedure: a report from the Pediatric Heart Network Single Ventricle Reconstruction trial. J Thorac Cardiovasc Surg. 2012;144(4):882–95.
11. Shamszad P, Gospin TA, Hong BJ, McKenzie ED, Petit CJ. Impact of preoperative risk factors on outcomes after Norwood palliation for hypoplastic left heart syndrome. J Thorac Cardiovasc Surg. 2014;147(3):897–901.
12. Mahle WT, Rychik J, Weinberg PM, Cohen MS. Growth characteristics of the aortic arch after the Norwood operation. J Am Coll Cardiol. 1998;32(7):1951–4.
13. Feinstein JA, Benson DW, Dubin AM, Cohen MS, Maxey DM, Mahle WT, et al. Hypoplastic left heart syndrome: current considerations and expectations. J Am Coll Cardiol. 2012;59(1 Suppl):S1–42.
14. Voelkel NF, Quaife RA, Leinwand LA, Barst RJ, McGoon MD, Meldrum DR, et al. Right ventricular function and failure: report of a National Heart, Lung, and Blood Institute working group on cellular and molecular mechanisms of right heart failure. Circulation. 2006;114(17):1883–91.
15. Haddad F, Hunt SA, Rosenthal DN, Murphy DJ. Right ventricular function in cardiovascular disease, part I: anatomy, physiology, aging, and functional assessment of the right ventricle. Circulation. 2008;117(11):1436–48.
16. Walsh MA, McCrindle BW, Dipchand A, Manlhiot C, Hickey E, Caldarone CA, et al. Left ventricular morphology influences mortality after the Norwood operation. Heart. 2009;95(15):1238–44.
17. Hehir DA, Dominguez TE, Ballweg JA, Ravishankar C, Marino BS, Bird GL, et al. Risk factors for interstage death after stage 1 reconstruction of hypoplastic left heart syndrome and variants. J Thorac Cardiovasc Surg. 2008;136(1):94–9. 99–3.
18. Alsoufi B, Manlhiot C, Al-Ahmadi M, Al-Halees Z, McCrindle BW, Mousa AY, et al. Older children at the time of the Norwood operation have ongoing mortality vulnerability that continues after cavopulmonary connection. J Thorac Cardiovasc Surg. 2011;142(1):142–147.e2.
19. Frommelt PC, Guey LT, Minich LL, Bhat M, Bradley TJ, Colan SD, et al. Does initial shunt type for the Norwood procedure affect echocardiographic measures of cardiac size and function during infancy? The Single Ventricle Reconstruction trial. Circulation. 2012;125(21):2630–8.
20. Newburger JW, Sleeper LA, Frommelt PC, Pearson GD, Mahle WT, Chen S, et al. Transplantation-free survival and interventions at 3 years in the

single ventricle reconstruction trial. Circulation. 2014;129(20):2013–20.
21. Frommelt PC, Gerstenberger E, Cnota JF, Cohen MS, Gorentz J, Hill KD, et al. Impact of initial shunt type on cardiac size and function in children with single right ventricle anomalies before the Fontan procedure: the single ventricle reconstruction extension trial. J Am Coll Cardiol. 2014;64(19):2026–35.
22. Shenoy RU, Parness IA. Hypoplastic left heart syndrome: looking back, looking forward. J Am Coll Cardiol. 2014;64(19):2036–8.
23. Menon SC, Erickson LK, McFadden M, Miller DV. Effect of ventriculotomy on right-ventricular remodeling in hypoplastic left heart syndrome: a histopathological and echocardiography correlation study. Pediatr Cardiol. 2013;34(2):354–63.
24. Menon SC, Minich LL, Casper TC, Puchalski MD, Hawkins JA, Tani LY. Regional myocardial dysfunction following Norwood with right ventricle to pulmonary artery conduit in patients with hypoplastic left heart syndrome. J Am Soc Echocardiogr. 2011;24(8):826–33.
25. Chetan D, Kotani Y, Jacques F, Poynter JA, Benson LN, Lee K-J, et al. Surgical palliation strategy does not affect interstage ventricular dysfunction or atrioventricular valve regurgitation in children with hypoplastic left heart syndrome and variants. Circulation. 2013;128(11 Suppl 1):S205–12.
26. Honjo O, Benson LN, Mewhort HE, Predescu D, Holtby H, Van Arsdell GS, et al. Clinical outcomes, program evolution, and pulmonary artery growth in single ventricle palliation using hybrid and Norwood palliative strategies. Ann Thorac Surg. 2009;87(6):1885–92.
27. Brescia AA, Jureidini S, Danon S, Armbrecht E, Fiore AC, Huddleston CB. Hybrid versus Norwood procedure for hypoplastic left heart syndrome: contemporary series from a single center. J Thorac Cardiovasc Surg. 2014;147(6):1777–82.
28. Hsia T-YY, Cosentino D, Corsini C, Pennati G, Dubini G, Migliavacca F. Use of mathematical modeling to compare and predict hemodynamic effects between hybrid and surgical Norwood palliations for hypoplastic left heart syndrome. Circulation. 2011;124(11 Suppl):S204–10.
29. Kutty S, Graney BA, Khoo NS, Li L, Polak A, Gribben P, et al. Serial assessment of right ventricular volume and function in surgically palliated hypoplastic left heart syndrome using real-time transthoracic three-dimensional echocardiography. J Am Soc Echocardiogr. 2012;25(6):682–9.
30. Marx GR, Shirali G, Levine JC, Guey LT, Cnota JF, Baffa JM, et al. Multicenter study comparing shunt type in the norwood procedure for single-ventricle lesions: three-dimensional echocardiographic analysis. Circ Cardiovasc Imaging. 2013;6(6):934–42.
31. Hijazi ZM, Fahey JT, Kleinman CS, Kopf GS, Hellenbrand WE. Hemodynamic evaluation before and after closure of fenestrated Fontan. An acute study of changes in oxygen delivery. Circulation. 1992;86(1):196–202.
32. Kasnar-Samprec J, Kühn A, Hörer J, Vogt M, Cleuziou J, Lange R, et al. Unloading of right ventricle by bidirectional superior cavopulmonary anastomosis in hypoplastic left heart syndrome patients promotes remodeling of systemic right ventricle but does not improve tricuspid regurgitation. J Thorac Cardiovasc Surg. 2012;144(5):1102–8.
33. Mahle WT, Wernovsky G, Bridges ND, Linton AB, Paridon SM. Impact of early ventricular unloading on exercise performance in preadolescents with single ventricle fontan physiology. J Am Coll Cardiol. 1999;34(5):1637–43.
34. Hansen JH, Uebing A, Furck AK, Scheewe J, Jung O, Fischer G, et al. Risk factors for adverse outcome after superior cavopulmonary anastomosis for hypoplastic left heart syndrome. Eur J Cardiothorac Surg. 2011;40(1):e43–9.
35. Rüffer A, Arndt F, Potapov S, Mir TS, Weil J, Cesnjevar RA. Early stage 2 palliation is crucial in patients with a right-ventricle-to-pulmonary-artery conduit. Ann Thorac Surg. 2011;91(3):816–22.
36. Petko C, Hoffmann U, Möller P, Scheewe J, Kramer H-H, Uebing A. Assessment of ventricular function and dyssynchrony before and after stage 2 palliation of hypoplastic left heart syndrome using two-dimensional speckle tracking. Pediatr Cardiol. 2010;31(7):1037–42.
37. Bellsham-Revell HR, Tibby SM, Bell AJ, Witter T, Simpson J, Beerbaum P, et al. Serial magnetic resonance imaging in hypoplastic left heart syndrome gives valuable insight into ventricular and vascular adaptation. J Am Coll Cardiol. 2013;61(5):561–70.
38. Michelfelder EC, Kimball TR, Pearl JM, Manning PB, Beekman RH. Effect of superior cavopulmonary anastomosis on the rate of tricuspid annulus dilation in hypoplastic left heart syndrome. Am J Cardiol. 2002;89(1):96–8.
39. Mahle WT, Cohen MS, Spray TL, Rychik J. Atrioventricular valve regurgitation in patients with single ventricle: impact of the bidirectional cavopulmonary anastomosis. Ann Thorac Surg. 2001;72(3):831–5.
40. Grattan M, Mertens L. Mechanics of the functionally univentricular heart-how little do we understand and why does it matter? Can J Cardiol. 2015;32(8):1033.e11–8.
41. Fogel MA, Weinberg PM, Chin AJ, Fellows KE, Hoffman EA. Late ventricular geometry and performance changes of functional single ventricle throughout staged fontan reconstruction assessed by magnetic resonance imaging. J Am Coll Cardiol. 1996;28(1):212–21.
42. Anderson PAW, Sleeper LA, Mahony L, Colan SD, Atz AM, Breitbart RE, et al. Contemporary outcomes after the Fontan procedure a Pediatric Heart Network multicenter study. J Am Coll Cardiol. 2008;52(2):85–98.

43. Hansen JH, Uebing A, Scheewe J, Kramer H-H, Fischer G. Angiographic evaluation of the coronary artery anatomy in patients with hypoplastic left heart syndrome. Eur J Cardiothorac Surg. 2012;41(3):561–8.
44. Brennan TV, Rodefeld MD, Tacy TA, Reddy VM, Hanley FL. Late thrombosis of the native aortic root after Norwood reconstruction for hypoplastic left heart syndrome. J Thorac Cardiovasc Surg. 2001;121(3):580–2.
45. Gaynor JW, Mahle WT, Cohen MI, Ittenbach RF, DeCampli WM, Steven JM, et al. Risk factors for mortality after the Norwood procedure. Eur J Cardiothorac Surg. 2002;22(1):82–9.
46. Baffa JM, Chen S-L, Guttenberg ME, Norwood WI, Weinberg PM. Coronary artery abnormalities and right ventricular histology in hypoplastic left heart syndrome. J Am Coll Cardiol. 1992;20(2):350–8.
47. Singh TP, Humes RA, Muzik O, Kottamasu S, Karpawich PP, Di Carli MF. Myocardial flow reserve in patients with a systemic right ventricle after atrial switch repair. J Am Coll Cardiol. 2001;37(8):2120–5.
48. Lubiszewska B, Gosiewska E, Hoffman P, Teresińska A, Różański J, Piotrowski W, et al. Myocardial perfusion and function of the systemic right ventricle in patients after atrial switch procedure for complete transposition: long-term follow-up. J Am Coll Cardiol. 2000;36(4):1365–70.
49. Donnelly JP, Raffel DM, Shulkin BL, Corbett JR, Bove EL, Mosca RS, et al. Resting coronary flow and coronary flow reserve in human infants after repair or palliation of congenital heart defects as measured by positron emission tomography. J Thorac Cardiovasc Surg. 1998;115(1):103–10.
50. Kotani Y, Tweddell J, Gruber P, Pizarro C, Austin EH, Woods RK, et al. Current cardioplegia practice in pediatric cardiac surgery: a North American multiinstitutional survey. Ann Thorac Surg. 2013;96(3):923–9.
51. Turek JW, Hanfland RA, Davenport TL, Torres JE, Duffey DA, Patel SS, et al. Norwood reconstruction using continuous coronary perfusion: a safe and translatable technique. Ann Thorac Surg. 2013;96(1):219–23.
52. Ohye RG, Sleeper LA, Mahony L, Newburger JW, Pearson GD, Lu M, et al. Comparison of shunt types in the Norwood procedure for single-ventricle lesions. N Engl J Med. 2010;362(21):1980–92.
53. Stoica SC, Philips AB, Egan M, Rodeman R, Chisolm J, Hill S, et al. The retrograde aortic arch in the hybrid approach to hypoplastic left heart syndrome. Ann Thorac Surg. 2009;88(6):1939–46.
54. Baba K, Honjo O, Chaturvedi R, Lee K-J, Van Arsdell G, Caldarone CA, et al. "Reverse Blalock-Taussig shunt": application in single ventricle hybrid palliation. J Thorac Cardiovasc Surg. 2013;146(2):352–7.
55. Cardis BM, Fyfe DA, Mahle WT. Elastic properties of the reconstructed aorta in hypoplastic left heart syndrome. Ann Thorac Surg. 2006;81(3):988–91.
56. Larrazabal LA, Tierney ESS, Brown DW, Gauvreau K, Vida VL, Bergersen L, et al. Ventricular function deteriorates with recurrent coarctation in hypoplastic left heart syndrome. Ann Thorac Surg. 2008;86(3):869–74.
57. Voges I, Jerosch-Herold M, Hedderich J, Westphal C, Hart C, Helle M, et al. Maladaptive aortic properties in children after palliation of hypoplastic left heart syndrome assessed by cardiovascular magnetic resonance imaging. Circulation. 2010;122(11):1068–76.
58. Porras D, Brown DW, Marshall AC, Del Nido P, Bacha EA, McElhinney DB. Factors associated with subsequent arch reintervention after initial balloon aortoplasty in patients with Norwood procedure and arch obstruction. J Am Coll Cardiol. 2011;58(8):868–76.
59. Biglino G, Schievano S, Steeden JA, Ntsinjana H, Baker C, Khambadkone S, et al. Reduced ascending aorta distensibility relates to adverse ventricular mechanics in patients with hypoplastic left heart syndrome: noninvasive study using wave intensity analysis. J Thorac Cardiovasc Surg. 2012;144(6):1307–13.
60. Biglino G, Giardini A, Ntsinjana HN, Schievano S, Hsia T-Y, Taylor AM. Ventriculoarterial coupling in palliated hypoplastic left heart syndrome: Noninvasive assessment of the effects of surgical arch reconstruction and shunt type. J Thorac Cardiovasc Surg. 2014;148(4):1526–33.
61. MacNee W. Pathophysiology of cor pulmonale in chronic obstructive pulmonary disease. Part One. Am J Respir Crit Care Med. 1994;150(3):833–52.
62. Wright GE, Crowley DC, Charpie JR, Ohye RG, Bove EL, Kulik TJ. High systemic vascular resistance and sudden cardiovascular collapse in recovering norwood patients. Ann Thorac Surg. 2004;77(1):48–52.
63. Bartram U, Grünenfelder J, Van Praagh R. Causes of death after the modified norwood procedure: a study of 122 postmortem cases. Ann Thorac Surg. 1997;64(6):1795–802.
64. Itatani K, Miyaji K, Qian Y, Liu JL, Miyakoshi T, Murakami A, et al. Influence of surgical arch reconstruction methods on single ventricle workload in the Norwood procedure. J Thorac Cardiovasc Surg. 2012;144(1):130–8.
65. Gargiulo G, Napoleone CP, Solinas M, Frascaroli G, Pierangeli A. A new patch for the Norwood procedure. Ann Thorac Surg. 1999;68:1873–4.
66. Burkhart HM, Ashburn DA, Konstantinov IE, De Oliveira NC, Benson L, Williams WG, et al. Interdigitating arch reconstruction eliminates recurrent coarctation after the Norwood procedure. J Thorac Cardiovasc Surg. 2005;130(1):61–5.
67. Morell VO, Wearden PA. Experience with bovine pericardium for the reconstruction of the aortic arch in patients undergoing a Norwood procedure. Ann Thorac Surg. 2007;84(4):1312–5.

68. Boye FJ, Pigula FA. Arch reconstruction in hypoplastic left heart syndrome: handling the diminutive aorta. World J Pediatr Congenit Heart Surg. 2013;2013:198–200.
69. Fraser CD, Mee RB. Modified Norwood procedure for hypoplastic left heart syndrome. Ann Thorac Surg. 1995;60(6 Suppl):S546–9.
70. Ishino K, Stümper O, De Giovanni JJV, Silove ED, Wright JGC, Sethia B, et al. The modified Norwood procedure for hypoplastic left heart syndrome: Early to intermediate results of 120 patients with particular reference to aortic arch repair. J Thorac Cardiovasc Surg. 1999;117(5):920–30.
71. Bove EL, Migliavacca F, de Leval MR, Balossino R, Pennati G, Lloyd TR, et al. Use of mathematic modeling to compare and predict hemodynamic effects of the modified Blalock-Taussig and right ventricle-pulmonary artery shunts for hypoplastic left heart syndrome. J Thorac Cardiovasc Surg. 2008;136(2):312–320.e2.
72. Migliavacca F, Yates R, Pennati G, Dubini G, Fumero R, de Leval MR. Calculating blood flow from Doppler measurements in the systemic-to-pulmonary artery shunt after the Norwood operation: a method based on computational fluid dynamics. Ultrasound Med Biol. 2000;26(2):209–19.
73. Qian Y, Liu JL, Itatani K, Miyaji K, Umezu M. Computational hemodynamic analysis in congenital heart disease: simulation of the Norwood procedure. Ann Biomed Eng. 2010;38(7):2302–13.
74. Ceballos A, Argueta-Morales IR, Divo E, Osorio R, Caldarone CA, Kassab AJ, et al. Computational analysis of hybrid Norwood circulation with distal aortic arch obstruction and reverse Blalock-Taussig shunt. Ann Thorac Surg. 2012;94(5):1540–50.
75. Ashcraft TM, Jones K, Border WL, Eghtesady P, Pearl JM, Khoury PR, et al. Factors affecting long-term risk of aortic arch recoarctation after the norwood procedure. Ann Thorac Surg. 2008;85(4):1397–402.
76. Griselli M, McGuirk SP, Stümper O, Clarke AJB, Miller P, Dhillon R, et al. Influence of surgical strategies on outcome after the Norwood procedure. J Thorac Cardiovasc Surg. 2006;131(2):418–26.
77. Schlangen J, Fischer G, Petko C, Hansen JH, Voges I, Rickers C, et al. Arterial elastance and its impact on intrinsic right ventricular function in palliated hypoplastic left heart syndrome. Int J Cardiol. 2013;168(6):5385–9.
78. Barber G, Helton JG, Aglira BA, Chin AJ, Murphy JD, Pigott JD, et al. The significance of tricuspid regurgitation in hypoplastic left-heart syndrome. Am Heart J. 1988;116(6):1563–7.
79. Ohye RG, Gomez CA, Goldberg CS, Graves HL, Devaney EJ, Bove EL. Tricuspid valve repair in hypoplastic left heart syndrome. J Thorac Cardiovasc Surg. 2004;127(2):465–72.
80. Hickey EJ, Caldarone CA, Blackstone EH, Lofland GK, Yeh T, Pizarro C, et al. Critical left ventricular outflow tract obstruction: The disproportionate impact of biventricular repair in borderline cases. J Thorac Cardiovasc Surg. 2007;134(6):1429–36.
81. Dinh DC, Gurney JG, Donohue JE, Bove EL, Hirsch JC, Devaney EJ, et al. Tricuspid valve repair in hypoplastic left heart syndrome. Pediatr Cardiol. 2011;32(5):599–606.
82. Elmi M, Hickey EJ, Williams WG, Van Arsdell G, Caldarone CA, McCrindle BW. Long-term tricuspid valve function after Norwood operation. J Thorac Cardiovasc Surg. 2011;142(6):1341–7.e4.
83. Pettersen E, Helle-Valle T, Edvardsen T, Lindberg H, Smith H-J, Smevik B, et al. Contraction pattern of the systemic right ventricle shift from longitudinal to circumferential shortening and absent global ventricular torsion. J Am Coll Cardiol. 2007;49(25):2450–6.
84. Takahashi K, Inage A, Rebeyka IM, Ross DB, Thompson RB, Mackie a S, et al. Real-time 3-dimensional echocardiography provides new insight into mechanisms of tricuspid valve regurgitation in patients with hypoplastic left heart syndrome. Circulation. 2009;120(12):1091–8.
85. Stamm C, Anderson RH, Ho SY. The morphologically tricuspid valve in hypoplastic left heart syndrome. Eur J Cardiothorac Surg. 1997;12(4):587–92.
86. Ton-Nu T-T, Levine RA, Handschumacher MD, Dorer DJ, Yosefy C, Fan D, et al. Geometric determinants of functional tricuspid regurgitation: insights from 3-dimensional echocardiography. Circulation. 2006;114(2):143–9.
87. Schlangen J, Fischer G, Steendijk P, Petko C, Scheewe J, Hart C, et al. Does left ventricular size impact on intrinsic right ventricular function in hypoplastic left heart syndrome? Int J Cardiol. 2013;167(4):1305–10.
88. Wisler J, Khoury PR, Kimball TR. The effect of left ventricular size on right ventricular hemodynamics in pediatric survivors with hypoplastic left heart syndrome. J Am Soc Echocardiogr. 2008;21(5):464–9.
89. Ugaki S, Khoo NS, Ross DB, Rebeyka IM, Adatia I. Tricuspid valve repair improves early right ventricular and tricuspid valve remodeling in patients with hypoplastic left heart syndrome. J Thorac Cardiovasc Surg. 2013;145(2):446–50.
90. Bautista-Hernandez V, Brown DW, Loyola H, Myers PO, Borisuk M, Del Nido PJ, et al. Mechanisms of tricuspid regurgitation in patients with hypoplastic left heart syndrome undergoing tricuspid valvuloplasty. J Thorac Cardiovasc Surg. 2014;148(3):832–40.
91. Bharucha T, Honjo O, Seller N, Atlin C, Redington A, Caldarone CA, et al. Mechanisms of tricuspid valve regurgitation in hypoplastic left heart syndrome: a case-matched echocardiographic-surgical comparison study. Eur Heart J Cardiovasc Imaging. 2013;14(2):135–41.
92. Reyes A, Bove EL, Mosca RS, Kulik TJ, Ludomirsky A. Tricuspid valve repair in children with hyepoplastic left heart syndrome during staged surgical recon-

struction. Circulation. 1997;96(9 Suppl):II-341-3; discussion II-344-5.
93. Tsang VT, Raja SG. Tricuspid valve repair in single ventricle: timing and techniques. Semin Thorac Cardiovasc Surg Pediatr Card Surg Annu. 2012;15(1):61–8.
94. Nii M, Guerra V, Roman KS, Macgowan CK, Smallhorn JF. Three-dimensional tricuspid annular function provides insight into the mechanisms of tricuspid valve regurgitation in classic hypoplastic left heart syndrome. J Am Soc Echocardiogr. 2006;19(4):391–402.
95. Freud LR, McElhinney DB, Marshall AC, Marx GR, Friedman KG, Del Nido PJ, et al. Fetal aortic valvuloplasty for evolving hypoplastic left heart syndrome: postnatal outcomes of the first 100 patients. Circulation. 2014;130(8):638–45.
96. Ungerleider RM, Shen I, Yeh T, Schultz J, Butler R, Silberbach M, et al. Routine mechanical ventricular assist following the Norwood procedure—improved neurologic outcome and excellent hospital survival. Ann Thorac Surg. 2004;77(1):18–22.
97. Honjo O, Merklinger SL, Poe JB, Guerguerian A-M, Alghamdi AA, Takatani S, et al. Mechanical cavopulmonary assist maintains pulmonary and cerebral blood flow in a piglet model of a bidirectional cavopulmonary shunt with high pulmonary vascular resistance. J Thorac Cardiovasc Surg. 2009;137(2):355–61.
98. Merklinger SL, Honjo O, Al-Radi OO, Poe J, Wang J, Oka N, et al. Primary in-series palliation of hypoplastic left heart syndrome with mechanical lung assist in neonatal pigs. ASAIO J. 2009;55(6):620–5.
99. Ishigami S, Ohtsuki S, Tarui S, Ousaka D, Eitoku T, Kondo M, et al. Intracoronary autologous cardiac progenitor cell transfer in patients with hypoplastic left heart syndrome: the TICAP prospective phase 1 controlled trial. Circ Res. 2015;116(4):653–64.
100. Burkhart HM, Qureshi MY, Peral SC, O'Leary PW, Olson TM, Cetta F, et al. Regenerative therapy for hypoplastic left heart syndrome: first report of intraoperative intramyocardial injection of autologous umbilical-cord blood-derived cells. J Thorac Cardiovasc Surg. 2015;149(3):e35–7.

Index

M.K. Friedberg, A.N. Redington (eds.), *Right Ventricular Physiology, Adaptation and Failure in Congenital and Acquired Heart Disease*, https://doi.org/10.1007/978-3-319-67096-6